ROSEMAR BATISTA DA SILVA

PERFORMANCE OF DIFFERENT CUTTING TOOL MATERIALS IN FINISH TURNING OF Ti-6Al-4V ALLOY WITH HIGH PRESSURE COOLANT SUPPLY TECHNOLOGY

UNIVERSIDADE FEDERAL DE UBERLÂNDIA
FACULDADE DE ENGENHARIA MECÂNICA

2006

ROSEMAR BATISTA DA SILVA

PERFORMANCE OF DIFFERENT CUTTING TOOL MATERIALS IN FINISH TURNING OF Ti-6Al-4V ALLOY WITH HIGH PRESSURE COOLANT SUPPLY TECHNOLOGY

Tese apresentada ao Programa de Pós-Graduação em Engenharia Mecânica da Universidade Federal de Uberlândia - modalidade Sanduíche no Exterior realizado com a London South Bank University – Londres, Reino Unido, como parte dos requisitos para a obtenção do título de DOUTOR EM ENGENHARIA MECÂNICA.

Área de Concentração: Materiais e Processos de Fabricação

Orientadores:
- Prof. Dr. Alisson Rocha Machado (Brasil)
- Prof. Dr. Emmanuel Okechukwu Ezugwu (Inglaterra)

UBERLÂNDIA – MG

2006

To my parents, Mrs. Rosalina Batista and Mr. Antônio Caetano,
and sisters
Ms. Rejaine Inês, Ms. Jeane Inês, Ms. Josiane Inês
for their encouragements and love.
To the memory of Mr. Jovino Batista da Fonseca,
my unforgettable grandfather.

DECLARATION

The research presented in this thesis is the original work of the author except where otherwise specified by references, or where acknowledgements are made. The project was carried out at the Machining Research Centre, Faculty of Engineering Science and the Built Environment (England), and Laboratory of Teaching and Research in Machining, Faculty of Mechanical Engineering of Federal University of Uberlândia (Brazil) under the supervision of Professor E. O. Ezugwu and Professor A.R. Machado, respectively. This work is being submitted for the degree of Doctor of Philosophy – Ph.D. jointly to London South Bank University (UK) and Universidade Federal de Uberlândia – Brazil.

ACKNOWLEDGEMENTS

The author, R.B. Da Silva, wishes to thank:

- Professor E.O. Ezugwu (my British Supervisor) for his magnificent supervision, encouragement, enormous patience, support, specialised advice, professionalism and constructive suggestions throughout the developing of this research work and for carefully reviewing the manuscripts.
- Professor A. R. Machado (my Brazilian Supervisor), a special person to whom I am in debt for the rest of my life because he believed in myself and gave me the opportunity to know and work with Prof. Ezugwu. His dedication, excellent supervision, professionalism, guidance, encouragement and contributions will be always remembered.
- Dr. J. Bonney, a friend and colleague who I also consider my Supervisor, for his patience, assistance, invaluable help on machining trials and valuable suggestions throughout the development of this research work.
- Conselho Nacional de Desenvolvimento Científico e Tecnológico – CNPq and Instituto Fábrica do Milênio, both in Brazil, for their financial support throughout the course of this research work.
- Rolls-Royce plc for funding this study providing workpiece materials and the cutting tools employed for the research project. Sincere thanks should go to Mr. I. Baker and Mr. J. Watkins (retired) both from Rolls-Royce, whose superb project management and leadership skills as well as persistent encouragements led to successful conclusion of the JSF GAF project.
- Mr. A. R. Shabbazz Nelson, a dear friend whose knowledge is greatly admired, for his help in English Language study and invaluable advices.
- Technical staff of the Faculty of Engineering, Science and the Built Environment, especially to Mr. J. Heyndyk and Mr. B. Hopday-Pepper who contributed to this work. Sincere thanks to Mr. W. Winter who prepared the chemical etchants for Ti-6Al-4V alloy workpiece samples.
- Postgraduate Programme of Faculdade de Engenharia Mecânica da Universidade Federal de Uberlândia for providing the necessary research facilities and allowing me to go this thesis.
- My Brazilian colleagues from Faculdade de Engenharia Mecânica (FEMEC-UFU) in particular Dr. M.B da Silva, Dr. A.M. Reis, Dr. E.S. Costa, Mr. F.J. da Silva, Mr. F. Neto, Mr.

P.R. Mota, Mr. U.B. Souto, Ms. D. O. Almeida, Mr. I. L. Siqueira, Mr. N. E. Luiz and Mr. R. Viana for their help, consideration and friendship.

- Finally my parents, Mrs. Rosalina Batista and Mr. Antônio Caetano, and sisters Ms. Rejaine Inês, Ms. Jeane Inês for their prayers, encouragements, support and trust. In particular I am very grateful to my youngest sister Ms. Josiane Inês who left her activities in Brazil to help and support me in London.

Da Silva, R.B. Performance of Different Cutting Tool Materials in Finish Turning of Ti-6Al-4V Alloy with High Pressure Coolant Supply Technology, 2006, 299 f. Ph.D. Thesis, Universidade Federal de Uberlândia, Uberlândia.

ABSTRACT

This study investigated the machinability of Ti-6Al-4V alloy with newly developed cutting tools such as uncoated (T1 and T3) and coated (T2 and T4) cemented carbides, Polycrystalline Diamond (PCD) – T5 and T6 inserts, Cubic Boron Nitride (CBN) – T7,T8,T9 inserts, SiC Whiskers Reinforced Ceramic (T10) insert, and Al_2O_3 base (T11) and Si_3N_4 base nano-grain size ceramic (T12) inserts using various cooling environments such as high pressure coolant supplies at pressures of 7 MPa, 11 MPa and 20.3 MPa, argon enriched environment and conventional coolant flow at high speed machining conditions typical of finish turning operation. Tool life and failure modes, wear mechanisms, component forces generated, surface integrity, surface finish and chip form data were used to assess the performance of the different cutting tools and cooling environments investigated. PCD and carbide inserts gave the best performance, in terms of tool life, when machining Ti-6Al-4V alloy. In general coarser (T1 and T4) grain size carbides and PCD (T5) inserts gave the best overall performance in terms of lower wear rate hence longer tool life compared to finer grain (T2,T3 and T6) grades. Encouraging tool life can be achieved when machining with high pressure coolant supply relative to conventional coolant flow and in the presence of argon. Tool lives generally increased with increasing coolant pressure due to the ability of the high coolant pressure to reduce the tool-chip contact length/area and to lift the chip, thereby providing adequate lubrication at the tool-chip interface with consequent reduction in friction. Machining with T1, T4 and T10 inserts in presence of argon was only able to prevent chip ignition with no improvement in tool life, due probably to the suppression of the cooling and/or lubrication characteristics of argon gas when machining at cutting conditions investigated. Up to 8 fold improvement in tool life were achieved when machining with PCD inserts relative to carbide inserts under conventional coolant flow. All the grades of CBN inserts gave poor performance during machining due to accelerated nose wear and, in some cases, severe chipping of the cutting edge associated with a relatively high diffusion wear rate that tends to weaken the bond strength of the tool substrate. An increase in the CBN content tends to accelerate notch wear rate, consequently diminishing tool life under the cutting conditions investigated. Micron and nano-grain size ceramics did not demonstrate satisfactory performance in terms of tool wear rate and tool life, due to severe abrasive wear and chipping of the cutting edge, hence the poor machined surfaces generated. Nose wear was the dominating tool failure mode when machining with carbide, PCD and CBN (T7) inserts due to a reduction in tool-chip and tool-workpiece contact lengths and the consequent increase in both normal and shear stresses and temperature at the tool tip, while severe notching and chipping occurred when machining with CBN (T8 and T9) and micron grain size ceramics. Severe notching also occurred when machining with nano-grain ceramic inserts, often leading to catastrophic tool failure at speeds in excess of 110 m min^{-1}. Machining with PCD tools gave lower cutting forces than carbides inserts. Surface roughness values generated with carbides, PCD and CBN inserts were generally within the 1.6 μm rejection criterion for finish machining and above 2 μm when machining with all grades of ceramics employed. Micrographs of the machined surfaces show that micro-pits are the main damage to the machined surfaces. Microhardness of the machined surfaces when machining with carbides varied randomly around the hardness values of the workpiece material prior to machining. Machining with PCD tools generally led to softening of machined surfaces. Increase in cutting speed generally led to increased hardness when machining with the larger grain size PCD (T5) tool using conventional coolant flow and with coolant pressures up to 11 MPa. No evidence of plastic deformation was observed on the machined surfaces and the surface integrity of the finish machined surfaces is generally in agreement with Rolls–Royce CME 5043 specification.

Keywords: Titanium alloy, High Coolant Pressure, Various cutting tools, Tool life, Surface integrity

DA SILVA, R.B. Desempenho de diferentes Materiais de Ferramentas de Corte no Torneamento de Acabamento da liga de titânio Ti-6Al-4V com a Tecnologia de Aplicação de Fluido de Corte à Alta Pressão, 2006, 299 f. Tese de Doutorado, Universidade Federal de Uberlândia, Uberlândia.

RESUMO

Este estudo visa avaliar a usinabilidade da liga de titânio Ti-6Al-4V utilizando várias classes de diferentes materiais de ferramentas de corte tais como metal duro sem revestimento (insertos T1 e T3) e com revestimento (insertos T2 e T4), PCD – insertos: T5 e T6, CBN – insertos: T7,T8 e T9, cerâmicas Whiskers (inserto T10), e nano-cerâmicas à base de alumina (inserto T11) e à base de nitreto de silício (inserto T12) em diferentes atmosferas de usinagem (fluido de corte aplicado a altas pressões (HPC) de 7 MPa; 11 MPa and 20,3 MPa, argônio e aplicação de fluido de corte convencional) e em elevadas condições de corte típicas de acabamento (velocidade de corte de 100 m min^{-1} a 500 m min^{-1}, com avanço de 0,15 mm $volta^{-1}$ e profundidade de corte de 0,5 mm constantes). Foram monitorados a vida das ferramentas bem como os mecanismos e tipos de desgaste, as forças de usinagem, a integridade superficial, a rugosidade das superfícies usinadas, a circularidade e os tipos e classes de cavacos produzidos. Os resultados foram utilizados para avaliar a eficiência das diferentes ferramentas de corte e atmosferas de usinagem empregadas na usinagem da liga Ti-6Al-4V. Os resultados mostraram que as ferramentas de PCD e metal duro tiveram o melhor desempenho, em termos de vida de ferramenta, que as demais ferramentas testadas. Em geral, as ferramentas com tamanho de grãos maior, metal duro (T1 e T4) e PCD (T5), apresentaram o melhor desempenho, em termos baixa taxa de desgaste e, consequentemente, vida mais longa, comparada com as ferramentas com tamanho de grãos menores (classes T2,T3 e T6). A utilização da técnica HPC mostrou ser eficiente na usinagem da liga Ti-6Al-4V, em termos de aumento de vida da ferramenta e, consequentemente, de aumento de produtividade, em relação à técnica de aplicação de fluido de corte convencional e com utilização de argônio nas condições investigadas. Em geral, a vida das ferramentas aumentaram com o aumento da pressão de aplicação de fluido de corte devido à sua capacidade de reduzir a área de contato cavaco-ferramenta e de quebrar o cavaco mais eficientemente e, portanto, propiciando uma melhor condição de lubrificação na interface cavaco-ferramenta com conseqüente redução de atrito. A utilização do argônio na usinagem com as ferramentas T1, T4 e T10 nas condições investigadas apenas evitou com que o centelhamento e ignição do titânio ocorresse, além de não propiciar aumento de vida da ferramenta, provavelmente devido à supressão das características de refrigeração e lubrificação que o argônio tem. As ferramentas de PCD apresentaram uma vida cerca de 8 vezes maior que as ferramentas de metal duro quando empregadas com aplicação de fluido de corte convencional. Todas as classes de ferramentas de CBN, em geral, apresentaram baixo desempenho em termos de vida de ferramenta devido ao acelerado desgaste na ponta da ferramenta e, em certos casos, lascamentos da aresta de corte que estão associados com a relativa alta taxa de difusão que ocorre durante a usinagem com titânio, que tende a diminuir a forças de ligações entre os átomos do substrato. Todas as ferramentas de cerâmicas testadas não demonstraram desempenho satisfatório em termos de desgaste e de vida ferramenta durante a usinagem da liga Ti-6Al-4V por causa da ocorrência de desgaste abrasivo e de lascamento da aresta de corte, como também da produção de superfícies usinadas com pobre acabamento superficial. O desgaste de ponta foi o tipo de desgaste predominante durante a usinagem com as ferramentas de metal duro, PCD e CBN (T7) devido à redução da área de contato cavaco-ferramenta e, consequentemente, ao aumento das tensões atuantes e aumento da temperatura na ponta da ferramenta. Já o desgaste de entalhe e lascamento ocorreram durante a usinagem com as ferramentas de CBN (T8 and T9) e com cerâmicas convencionais. O desgaste de entalhe também ocorreu de forma mais acentuada nas ferramentas de nano-cerâmicas, o que levou à falha catastrófica de tais ferramentas quando empregadas em velocidades de corte superiores a 110 m min^{-1}. A usinagem com ferramentas de PCD geraram baixas forças de corte em relação às ferramentas de metal duro. Os valores de rugosidade superficial produzidos com as ferramentas de metal duro, PCD e CBN em geral ficaram abaixo do valor estipulado para critério de rejeição para torneamento de acabamento de 1.6 μm, enquanto que todas as ferramentas de cerâmicas produziram valores de rugosidade acima de 2 μm. A análise metalográfica das superfícies usinadas permitiu identificar pequenas marcas que não comprometeram as superfícies produzidas. A usinagem com ferramentas de metal duro produziu valores de dureza que variam aleatoriamente dentro dos limites inferior e superior de dureza da peça medidos antes da usinagem. Nenhuma evidência de deformação plástica nas superfícies de titânio usinadas com todas as ferramentas e condições testadas. Em geral, a integridade superficial das superfícies usinadas atendem à norma Rolls–Royce CME 5043.

Palavras-chave: Liga de titânio, Fluido de corte à alta pressão, Várias ferramentas de corte, Vida de ferramenta, Integridade superficial.

TABLE OF CONTENTS

FIGURES……..			xv
TABLES ……..…...			xxvi
LIST OF SYMBOLS ...…….…...			xxvii
Chapter I	INTRODUCTION ……...		1
1.1	Aims of the Thesis		4
Chapter II	LITERATURE SURVEY		6
2.1	Historical Background of Machining		6
2.2	Overview of Aerospace Alloys		8
	2.2.1	Aero-Engine Alloys	9
2.3	Superalloys		14
	2.3.1	Titanium Superalloys in the Aerospace Industry	15
2.4	Machining Operations		23
	2.4.1	Terminology used in Metal Cutting	24
	2.4.2	Nomenclature of Cutting Tools	28
2.5	Chip Formation Process		30
2.6	Classes of Chips		33
2.7	Forces in Metal Cutting		36
2.8	Stress and Strain Distribution in Machining		39
	2.8.1	Stress Distribution	39
	2.8.2	Strain Distribution	40
2.9	Heat Generation During Machining Operation		42
	2.9.1	Effect of Cutting Parameters On Temperature Generated During Machining	43
	2.9.2	Heat Generation and Cutting Temperature when Machining Titanium Alloy	45
2.10	Tool Failure Modes		47
2.11	Tool Wear Mechanisms		49
2.12	Titanium Machinability		51
2.13	Tool Materials for Machining Titanium Alloys		53

2.13.1 Tool Materials Requirements 55
2.13.2 High Speed Steel (HSS) Tools 56
2.13.3 Cemented Carbide Tools 59
2.13.3.1 Uncoated Carbide Tools 62
2.13.3.2 Coated Carbide Tools 67
2.13.4 Ultrahard (Superabrasive) Tool Materials 72
2.13.4.1 Polycrystalline Diamond (PCD) Tools 73
2.13.4.2 Cubic Boron Nitride (CBN) Tools 76
2.13.5 Ceramic Tools 80
2.13.5.1 Pure Oxide Ceramics 81
2.13.5.2 Mixed Oxide Ceramics 81
2.13.5.3 Whisker Reinforced Alumina Ceramics 82
2.13.5.4 Silicon Nitride-base Ceramics 82
2.13.5.5 Nano-grain Ceramics 84
2.14 Cutting Fluids 86
2.14.1 Classification of Cutting Fluids 88
2.14.2 Directions of Application of Cutting Fluids 92
2.15 Cutting Environments and Techniques Employed when Machining Titanium Alloys 94
2.15.1 Dry Machining 94
2.15.2 Conventional Coolant Supply 99
2.15.3 High Pressure and Ultra Pressure Coolant Supplies 100
2.15.4 Minimum Quantity of Lubrication (MQL) 106
2.15.5 Cryogenic Machining 108
2.15.6 Other Atmospheres 111
2.15.7 Ledge Cutting Tools 114
2.15.8 Rotary Tools 115
2.15.9 Ramping Technique 117
2.15.10 Hot Machining / Hybrid Machining 118
2.16 Surface Integrity 121
2.16.1 Surface Finish and Texture 121
2.16.2 Subsurface Changes 124

Chapter III	EXPERIMENTAL PROCEDURE	126
3.1	Introduction	126
3.2	Work Material	127
3.3	Machine Tool	127
3.4	Cutting Fluid	128
3.5	High Pressure Unit	128
3.6	Argon Delivery System	130
3.7	Tool Material and Machining Procedure	131
3.8	Cutting Conditions	135
3.9	Tool Life Criteria	137
3.10	Tool Wear Measurement	137
3.11	Component Force Measurement	138
3.12	Surface Roughness Measurement	139
3.13	Runout Measurement	141
3.14	Tool and Workpiece Specimen Preparation	141
3.15	Microhardness Measurements Below the Machined Surface	143
Chapter IV	EXPERIMENTAL RESULTS	145
4.1	Benchmark trials - Machining of Ti-6Al-4V alloy with Uncoated Carbide (883 grade) inserts	145
4.2	Machining of Ti-6Al-4V alloy with various carbide tool grades (uncoated and coated tools) under various machining environments	146
4.2.1	Tool life	146
4.2.2	Tool wear when machining Ti-6Al-4V alloy with various carbide insert grades	149
4.2.3	Component forces when machining with various carbide insert grades	159
4.2.4	Surfaces roughness and runout values when machining with various carbide insert grades	161
4.2.5	Surfaces generated after machining with various carbide insert grades	163
4.2.6	Surface hardness after machining with various carbide tool grades	167
4.2.7	Subsurface micrographs after machining Ti-6Al-4V alloy with various carbide insert grades	175
4.2.8	Chips shapes	180
4.3	Machining of Ti-6Al-4V alloy with different grades of PCD tools under various coolant supply pressures	182
4.3.1	Tool life	182

	4.3.2	Tool wear when machining Ti-6Al-4V alloy with different grades of PCD tools	184
	4.3.3	Component forces when machining with different grades of PCD tools	190
	4.3.4	Surfaces roughness and roundness values when machining with different grades of PCD tools	192
	4.3.5	Surface alteration after machining with different grades of PCD tools	194
	4.3.6	Surface hardness after machining with different grades of PCD tools	197
	4.3.7	Subsurface alteration after machining Ti-6Al-4V alloy with different grades of PCD tools	200
	4.3.8	Chips shapes	203
4.4	Machining of Ti-6Al-4V alloy with different grades of CBN tools under various coolant supply pressures		204
	4.4.1	Tool life	204
	4.4.2	Tool wear when machining Ti-6Al-4V alloy with different grades of CBN tools	206
	4.4.3	Component forces	211
	4.4.4	Surfaces roughness and runout values	212
	4.4.5	Surface hardness and subsurface alteration	214
	4.4.6	Chips shapes	216
4.5	Machining of Ti-6Al-4V alloy with whisker reinforced ceramic cutting tools under various machining environments		217
	4.5.1	Wear rate and tool life	217
	4.5.2	Component forces	222
	4.5.3	Surfaces roughness	223
	4.5.4	Surface hardness and subsurface alterations	224
	4.5.5	Chips shapes	226
4.6	Machining of Ti-6Al-4V alloy with Nano-ceramic cutting tools		227
	4.6.1	Wear rate and tool life	227
	4.6.2	Component forces	230
	4.6.3	Surfaces roughness and runout values	230
	4.6.4	Chips shapes	232
Chapter V	DISCUSSIONS		233
5.1	Introduction		233
5.2	Tool performance when machining Ti-6Al-4V alloy with different grades of carbide, PCD, CBN and ceramic tools		233

5.2.1 Carbides tools 233

5.2.2 PCD tools 237

5.2.3 CBN tools 239

5.2.4 Micron-grain ceramic tools 240

5.2.5 Nanoceramic tools 241

5.3 Tool failure modes and wear mechanisms when machining Ti-6Al-4V alloy with different grades of carbide, PCD, CBN and ceramic tools 242

5.3.1 Carbide tools 242

5.3.2 PCD tools 246

5.3.3 CBN tools 248

5.3.4 Micron-grain ceramic tools 251

5.3.5 Nano-grain ceramic tools 253

5.4 Components forces when machining Ti-6Al-4V alloy with different grades of carbide, PCD, CBN and ceramic tools 254

5.5 Surfaces roughness and runout values when machining Ti-6Al-4V alloy with different grades of carbide, PCD, CBN and ceramic tools 258

5.6 Surface generated of Ti-6Al-4V after machining with carbide and PCD tools 260

5.7 Surface hardness after machining Ti-6Al-4V alloy with different grades of carbide, PCD, CBN and ceramic tools 261

5.8 Subsurface micrographs after machining Ti-6Al-4V alloy with different grades of carbide, PCD, CBN and ceramic tools 265

5.9 Chips shapes 266

Chapter VI CONCLUSIONS 269

Chapter VII RECOMMENDATIONS FOR FURTHER WORK 272

Chapter VIII REFERENCES 274

APPENDIX 298

LIST OF PUBLICATIONS FROM THIS STUDY 298

Refereed Journals 298

Refereed Conferences 299

FIGURES

Figure 2.1 - (a) A typical jet engine and its main parts (Pratt and Whitney F100 jet engine) (BENSON, 2002); (b) typical jet engine (Trent 700) manufactured by Rolls-Royce plc (ROLLS-ROYCE PLC, 2003) 10
Figure 2.2 - Trends in turbine inlet temperature in areo-engines (OHNABE et al., 1999) 11
Figure 2.3 - Improvements in aero-engine performance (BENSON, 2002) 11
Figure 2.4 - Maximum service temperature of various materials (LOVATT; SHERCLIFF, 2002) 12
Figure 2.5 - Trend of materials usage in aero-engines (MILLER, 1996) 12
Figure 2.6 - Typical applications of titanium: (a) modular femoral components (prostheses manufactured in titanium-base, Ti-6Al-4V, alloy, (b) valves and (c) screw (TIG, 2002) 20
Figure 2.7 - Phases of titanium product life cycle in the U.S. (ASM HANDBOOK, 1998) 20
Figure 2.8 - Metal cutting diagram (WATERS, 2000) 23
Figure 2.9 - Basic machining operation and important parameters (KALPAKJIAN; SCHMID, 2000) 25
Figure 2.10 - Schematic illustration of typical single-point cutting tool with the tool angles (KALPAKJIAN; SCHMID, 2000) 26
Figure 2.11 - Workpiece-tool-machine system for turning operation 26
Figure 2.12 - Form-milling operation with gangs of side and face milling cutters (AB SANDVIK COROMANT, 1994) 27
Figure 2.13 - Cutting tool planes: (a) *"tool-in-hand"* planes and (b) *"tool-in-use"* planes (BOOTHROYD; KNIGHT, 1989) 29
Figure 2.14 - Tool angles for a single-point tool according to the ISO: tool cutting edge angle (k_r), tool minor cutting edge angle (k'_r), tool included angle (ε_r), tool cutting edge inclination angle (λ_s), tool normal rake angle (γ_n), tool normal clearance angle (α_n) and tool normal wedge angle (β_n) (BOOTHROYD; KNIGHT, 1989) 30
Figure 2.15 - Metal cutting diagram - the chip formation (TRENT; WRIGHT, 2000) 32
Figure 2.16 - Metal cutting diagram illustrating the primary and secondary shear zones (THE METALS HANDBOOK, 1989) 32
Figure 2.17 - Classes of chips: (a) Continuous chip, (b) Continuous chip with BUE, (c) Discontinuous chip, (d) Serrated chips (TRENT; WRIGHT (2000), MACHADO; WALLBANK (1990), KALPAKJIAN; SCHMID (2000)) 35
Figure 2.18 - Cutting forces a) Three components forces acting on the cutting tool (DE GARMO; BLACK; KOHSER, 1999) and b) Merchant´s circle (TRENT; WRIGHT, 2000) 38
Figure 2.19 - The Zorev´s model of stress distribution on the rake face of a cutting tool in orthogonal cutting where σ_{fmax}= maximum normal stress, σ_f = normal stress, τ_f = shear stress, τ_{st} = shear strength of chip material in the sticking region (BOOTHROYD; KNIGHT, 1989) 40
Figure 2.20 - The shear strain in the shear plane (SHAW, 1984) 41
Figure 2.21 - Zones of heat generation during machining: (a) schematic diagram, (b) isothermal lines for dry orthogonal cutting of free machining steel with carbide tool ($\alpha = 20^o$) obtained from a finite element technique, at a cutting speed of 155.4 m min^{-1} 43

and a feed rate of 0.274 mm rev^{-1} [adapted from (SHAW, 1984)]
Figure 2.22 - Distribution of thermal load when machining titanium-base, Ti-6Al-4V and steel Ck 45 [adapted from (DEARNLEY; GREARSON, 1986) 46
Figure 2.23 - Influence of cutting speed on the cutting temperature when machining titanium and its alloys [adapted from (MOTONISHI et al., 1987)] 46
Figure 2.24 - Regions of wear on a cutting tool (DEARNLEY; TRENT, 1985) 47
Figure 2.25 - The main wear mechanisms on a cutting tool [adapted from (TRENT; WRIGHT, 2000)] 50
Figure 2.26 - Influence of temperature on hot hardness of some tool materials (ALMOND, 1981) 56
Figure 2.27 - Flow stress measured at 0.6% strain during three point bending tests at a constant strain rate in WC-11wt.%Co (MARI; GONSETH, 1993) 60
Figure 2.28 - Tool live when turning Ti-6242 alloy with mixed uncoated carbide tools with different grain sizes of substrates: 0.68 μm (890 grade) and 1.0 μm (883 grade) (JAWAID; CHE-HARON; ABDULLAH, 1999) 61
Figure 2.29 - Average crater wear rates of various tool materials in turning of Ti-6Al-4V alloy at a cutting speed of 61 m min^{-1} for 10 minutes (HARTUNG; KRAMER, 1982) 64
Figure 2.30 - SEM micrograph of exposed mixed cemented carbide substrate after fracture of the welded junction (NABHANI, 2001b) 65
Figure 2.31 - Flank face of a worn uncoated straight carbide tool showing abrasion by carbide grains after turning titanium base, Ti-6242, alloy under dry condition (JAWAID; CHE-HARON; ABDULLAH, 1999) 65
Figure 2.32 - Evidence of adhesion of the chips on the nose of a mixed ((Ta,Nb)C) uncoated straight carbide tool after machining Ti-6Al-4V alloy with conventional coolant supply at a speed of 100 m min^{-1}, a feed rate of 0.15 mm rev^{-1} and a depth of cut of 0.5 mm (EZUGWU et al., 2005) 67
Figure 2.33 - Flank wear curves when machining Ti-6Al-4V alloy with coated (CrN and TiCN) and a straight uncoated carbide tools (TURLEY, 1981) 71
Figure 2.34 - Worn surface of a multilayer (TiC/TiCN/TiN) coated mixed cemented carbide tool showing remains of adherent metal layer (a) and enlarged view of the crater wear showing smooth ridges with fine scoring in direction of chip flow (b) after machining titanium base, Ti-5Al-4Mo-(2-2.5)Sn-(6-7)Si alloy (NABHANI, 2001b) 71
Figure 2.35 - Coating delamination of PVD coated (TiN) carbide tool, grinding marks and adhered material observed after 10 s (a) and adhesion of work material onto the flank face, plastic deformation and cracks at the cutting edge after 20 s; (b) after face milling Ti-6Al-4V alloy at cutting speeds of 100 m min^{-1} and 50 m min^{-1} and feed rates of 0.15 mm per tooth and 0.1 mm per tooth, respectively (JAWAID; SHARIF; KOKSAL, 2000) 72
Figure 2.36 - The performance of various grades of PCD tools when milling ceramic impregnated surface of a flooring board (HPL) (COOK; BOSSOM, 2000) 75
Figure 2.37 - Formation of strongly adherent layer on the rake face of a PCD tool after machining titanium base, Ti-5Al-4Mo-2Sn-6Si alloy under dry condition (NABHANI, 2001b) 76
Figure 2.38 - (a) Section through ‘quick-stop’ specimen showing part of CBN tool adhering to underside of chip (100x), (b) close-up view of Fig. 2.38(a) (200x) (NABHANI, 2001a) 78
Figure 2.39 - (a) A typical scanning electron micrographs of worn-out edges: (a) cutting temperature of 734ºC, (b) cutting temperature of 900ºC (ZOYA; KRISHNAMURTHY, 2000) 80

Figure 2.40 - Variation in uniform flank wear with cutting time for the turning of Ti-6Al-4V (hardness, 36 HRC), showing reduced tool wear with the new geometry (cutting speed, 122 m min^{-1}; feed rate, 0.23 mm rev^{-1} unless otherwise indicated; depth of cut, 1.52 mm; tool SNG432 (SCEA, 15º): curve A, SIALON (Kyon 2000) with clearance angles of 17º (localised wear, 0.889 mm; edge fracture; crater) and 5º (localized wear, 1.321 mm; fracture; crater); curve B, SIALON (Kyon 2000) with a clearance angle of 5º and a feed rate of 0.127 mm rev^{-1}; curves C and D, cemented carbide (Carboloy grade 999) with clearance angles of 5º and 17º, respectively (KOMANDURI; REED JR, 1983) 84
Figure 2.41 - TEM micrograph of HIPed (Hot Isostatic Pressing) nanophase SiC sample with a density of 97% TD (Theoretical density) (VAβEN; STÖVER, 1999) 85
Figure 2.42 - Schematic illustration of the possible directions of application of cutting fluids 93
Figure 2.43 - Schematic illustration of a tool holder used for machining with high pressure coolant supply (SECO TOOLS, 2002b) 100
Figure 2.44 - Pressure distribution from the jet momentum action on the chip. (a) Cutting in tube with single straight edge; (b) pressure distribution (2D) at longitudinal turning (DAHLMAN, 2000). 102
Figure 2.45 - Schematic illustration of nozzle orientation for localized LN2 delivery (HONG; DING; JEONG, 2001) 109
Figure 2.46 - A schematic representation of the cryogenic cooling concepts (MAZURKIEWICZ; KUBALA; CHOW, 1989) 110
Figure 2.47 -The tool assembly, nozzles and LN2 flowing out of the nozzle (MAZURKIEWICZ; KUBALA; CHOW, 1989) 110
Figure 2.48 - Ledge tool (after KOMANDURY; LEE, 1984)) 115
Figure 2.49 - Schematic representation of principle of rotary cutting action (WANG; EZUGWU; GUPTA, 1998) 116
Figure 2.50 - Schematic representation of a hot machining technique design (ÖZLER; ÍNAN; ÖZEL, 2001) 120
Figure 2.51 - Standard terminology and symbols of the elements of surface texture (μin) (KALPAKJIAN; SCHMID, 2000) 122
Figure 2.52 - Schematic illustration of the determination of some amplitude parameters of surface texture (SHOUCKRY; 1982) 123
Figure 2.53 - Form tolerances for machined surfaces in turning operations: (a) Roundness, (b) Cylindricity (DE GARMO; BLACK; KOHSER, 1999) 126
Figure 2.54 - Production and cost curves versus cutting speed (GORCZYCA, 1987) 128
Figure 3.1 - Colchester Electronic MASTIFF CNC lathe 128
Figure 3.2 - The high pressure pumping coolant system - Chipblaster (CV26-3000) 129
Figure 3.3 - Special tool holder and a cutting fluid jet-pressure of 7 MPa supply. 130
Figure 3.4 - Argon gas delivery system: (a) cylinder and (b) close-up view of the valve and the hose. 131
Figure 3.5 - Cutting tools used in the machining trials: uncoated carbides: T1 (883 grade), T2 (890 grade), coated carbides T3 (CP 200), T4 (CP 250 grade); PCD: T5 (20 grade with grain size of 10 μm), T6 (20 grade with grain size < 10 μm); CBN: T7 (10 grade), T8 (300 grade), T9 (300-P grade); silicon carbide (SiC_w) whisker reinforced alumina ceramic inserts (WG300): T10 (rhomboid shaped) and T11 (square shaped); nano-grain ceramic inserts: T12 (Al_2O_3 grade) and T13 (Si_3N_4 grade). 132

Figure 3.6 - Tool holders used in the machining trials: (a) designation PCLNR2525-M12 used for carbide tools (T1,T2,T3,T4); (b) designation SCLCR2525-M12 used for PCD tools (T5,T6); (c) designation DCLNR2525-M12 used for CBN and ceramic tools (T7,T8, T9 and T10); (d) designation MSLNR-252512 used for square tools: micron-grain and nano-grain size ceramics (T11,T12,T13). 134

Figure 3.7 - Mitutoyo tool maker´s microscope. 138

Figure 3.8 - (a) Kistler dynamometer for capturing forces generated during machining and (b) Oscilloscope with charge amplifier. 139

Figure 3.9 - (a) Surtronic-10 portable stylus type used for surface roughness measurement; (b) dial indicator Shockproof – BATY used for roundness measurement. 140

Figure 3.10 - (a) Hitachi (S530) Scanning Electron Microscope; (b) Nicon Metallurgical Optical Microscope (OPTIPHOT-100) with computerised image system. 142

Figure 3.11 - (a) Buehler Automatic Mounting Press (Simplimet 2000); (b) Automatic Grinding/Polishing Equipment (Metaserv 2000). 143

Figure 3.12 - Mitutoyo (MVK – VL) Vickers micro-hardness tester machine. 144

Figure 4.1 - Average flank wear of uncoated carbide (T1) insert at various cutting speeds with conventional coolant supply during 15 minutes machining time (benchmark trials) 146

Figure 4.2 - Figure 4.2 - Tool life recorded when machining Ti-6Al-4V alloy with different cemented carbide insert grades with conventional coolant flow (CCF), high coolant pressures of 7 MPa, 11 MPa and 20.3 MPa and in argon enriched environment at various speed conditions. 147

Figure 4.3 - Nose wear rate curves of different cemented carbide insert grades when machining Ti-6Al-4V alloy with conventional coolant flow (CCF), high coolant pressures of 7 MPa, 11 MPa and 20.3 MPa and in argon enriched environment, at a feed rate of 0.15 mm rev^{-1} and a depth of cut of 0.5 mm. 150

Figure 4.4 - Nose wear curves when finish machining with cemented carbide (T1 and T4) inserts at a cutting speed of 110 m $min^{-1.}$ 151

Figure 4.5 - Nose wear curves when finish machining with cemented carbide (T2 and T3) inserts at a cutting speed of 110 m min^{-1}. 151

Figure 4.6 - Worn T1 insert after machining Ti-6Al-4V alloy with conventional coolant supply at a speed of (a) 100 m min^{-1} and (b) 130 m $min^{-1.}$ 152

Figure 4.7 - Wear generated at the cutting edge of uncoated carbide T1 insert after machining Ti-6Al-4V alloy with a coolant pressure of 7MPa at a speed of 110 m $min^{-1.}$ 153

Figure 4.8 -Wear generated at the cutting edge of uncoated carbide T1 insert after machining Ti-6Al-4V alloy with a coolant pressure of 11MPa at a speed of 120 m min^{-1}. 153

Figure 4.9 - Worn cutting edge of uncoated carbide T1 insert after machining Ti-6Al-4V alloy with a coolant pressure of 20.3 MPa at a speed of 130 m min^{-1}. 154

Figure 4.10 - Worn cutting edge of uncoated carbide T1 insert after machining Ti-6Al-4V alloy in argon enriched environment at a speed of 130 m min^{-1}. 154

Figure 4.11 - Flank and nose wears at the cutting edge of uncoated carbide T2 insert grade after machining Ti-6Al-4V alloy with conventional coolant supply at a speed of 130 m min^{-1}, a feed rate of 0.15 mm rev^{-1} and a depth of cut of 0.5 mm. 155

Figure 4.12 - Wear generated at the cutting edge of uncoated carbide T2 insert after machining Ti-6Al-4V alloy with a coolant pressure of 11 MPa at a speed of (a) 110 m min^{-1} and (b) 130 m $min^{-1.}$ 155

Figure 4.13 - Wear generated at the cutting edge of uncoated carbide T2 insert after machining Ti-6Al-4V alloy with a coolant pressure of 20.3 MPa at a speed of 130 m min^{-1}. 156

Figure 4.14 - Worn cutting edge of T3 coated carbide insert when machining with conventional coolant supply at a speed of (a) 110 m min-1 and (b) 130 m min^{-1}. 156
Figure 4.15 - Flank and nose wears a the cutting edge of T3 coated carbide insert after machining Ti-6Al-4V alloy with a coolant pressure of 11 MPa at a speed of 110 m min^{-1}. 157
Figure 4.16 - Flank and nose wears at the cutting edge of T3 coated carbide insert after machining Ti-6Al-4V alloy with a coolant pressure of 20.3 MPa at a speed of (a) 110 m min^{-1} and (b) 130 m min^{-1}. 157
Figure 4.17 - Worn cutting edge of T4 coated carbide insert after machining Ti-6Al-4V alloy with conventional coolant supply at a speed of 130 m min^{-1}. 158
Figure 4.18 - Adhesion of work material on a worn T4 coated carbide insert after machining Ti-6Al-4V alloy with a coolant pressure of 11 MPa at a speed of 110 m min^{-1}. 158
Figure 4.19 - Nose wear at the cutting edge of T4 coated carbide insert after machining Ti-6Al-4V alloy with a coolant pressure of 20.3 MPa at a speed of (a) 110 m min^{-1} and (b) 120 m min^{-1}. 159
Figure 4.20 - Wear at the cutting edge of T4 coated carbide insert after machining Ti-6Al-4V alloy in argon enriched environment at a speed of (a) 100 m min^{-1} and (b) 120 m min^{-1}. 159
Figure 4.21 - Cutting forces (F*c*) recorded at the beginning of cut when machining Ti-6Al-4V alloy with different cemented carbide grades with various cutting conditions. 160
Figure 4.22 - Feed forces (F_f) recorded at the beginning of cut when machining Ti-6Al-4V alloy with different cemented carbide grades under various cutting conditions. 161
Figure 4.23 - Surface roughness values recorded at the beginning of cut when machining Ti-6Al-4V alloy with different cemented carbide grades under various cutting conditions. 162
Figure 4.24 - Roundness variation recorded at the end of cut when machining Ti-6Al-4V alloy with different cemented carbide grades under various cutting conditions. 163
Figure 4.25 - Surfaces generated after machining with uncoated carbide T1 tool with conventional coolant supply at cutting speeds of (a) 110 m min^{-1} and (b) 130 m min^{-1}. 163
Figure 4.26 - Surfaces generated after machining with uncoated carbide T1 tool with a coolant pressure of 7 MPa at cutting speeds of (a) 100 m min^{-1} and (b) 130 m min^{-1}. 164
Figure 4.27 - Surfaces generated after machining with uncoated carbide T1 tool with a coolant pressure of 11 MPa at cutting speeds of (a) 110 m min^{-1} and (b) 120 m min^{-1}. 164
Figure 4.28 - Surfaces generated after machining with uncoated carbide T1 tool with a coolant pressure of 20.3 MPa at cutting speeds of (a) 120 m min^{-1} and (b) 130 m min^{-1}. 164
Figure 4.29 - Surfaces generated after machining with uncoated carbide T1 tool in an argon enriched environment at cutting speeds of (a) 110 m min^{-1} and (b) 120 m min^{-1}. 165
Figure 4.30 - Surfaces generated after machining with uncoated carbide T2 tool with coolant pressures of (a) 11 MPa and (b) 20.3 MPa at a cutting speedsof (a) 110 m min^{-1}. 165
Figure 4.31 - Surfaces generated after machining with coated carbide T3 tool with coolant pressures of (a) 11 MPa and (b) 20.3 MPa at a cutting speed of 110 m min^{-1}. 166
Figure 4.32 - Surfaces generated after machining with coated carbide T4 tool with (a) conventional coolant supply, (b) in argon enriched environment, (c) coolant pressure of 11 MPa and (d) 20.3 MPa at a cutting speed of 120 m min^{-1}. 167
Figure 4.33 - Hardness variation after machining Ti-6Al-4V alloy with uncoated carbide (T1) insert grade with conventional coolant supply. 169
Figure 4.34 - Hardness variation after machining Ti-6Al-4V alloy with uncoated carbide (T1) insert grade with 7 MPa coolant pressure. 169

Figure 4.35 - Hardness variation after machining Ti-6Al-4V alloy with uncoated carbide (T1) insert grade with 11MPa coolant pressure. 170
Figure 4.36 - Hardness variation after machining Ti-6Al-4V alloy with uncoated carbide (T1) insert grade with 20.3 MPa coolant pressure. 170
Figure 4.37 - Hardness variation after machining Ti-6Al-4V alloy with uncoated carbide (T1) insert grade in argon-enriched environment. 171
Figure 4.38 - Hardness variation after machining Ti-6Al-4V alloy with uncoated carbide (T2) insert grade with various cutting conditions. 172
Figure 4.39 - Hardness variation after machining Ti-6Al-4V alloy with coated carbide (T3) insert grade with various cutting conditions. 172
Figure 4.40 - Hardness variation after machining Ti-6Al-4V alloy with coated carbide (T4) insert grade with conventional coolant. 173
Figure 4.41 - Hardness variation after machining Ti-6Al-4V alloy with coated carbide (T4) insert grade with 11MPa coolant pressure. 174
Figure 4.42 - Hardness variation after machining Ti-6Al-4V alloy with coated carbide (T4) insert grade with 20.3 MPa coolant pressure. 174
Figure 4.43 - Microstructure of Ti-6Al-4V alloy after machining with uncoated carbide T1 inserts with conventional coolant supply at cutting speeds of (a) 110 m min^{-1} and (b) 130 m min^{-1}. 175
Figure 4.44 - Microstructure of Ti-6Al-4V alloy after machining with uncoated carbide T1 inserts with a coolant pressure of 7 MPa at cutting speeds of (a) 100 m min^{-1} and (b) 120 m min^{-1}. 175
Figure 4.45 - Microstructure of Ti-6Al-4V alloy after machining with uncoated carbide T1 inserts with a coolant pressure of 11 MPa at cutting speeds of (a) 110 m min^{-1} and (b) 120 m min^{-1}. 176
Figure 4.46 - Microstructure of Ti-6Al-4V alloy after machining with uncoated carbide T1 insert with a coolant pressure of 20.3 MPa at cutting speeds of (a) 120 m min^{-1} and (b) 130 m min^{-1}. 176
Figure 4.47 - Microstructure of Ti-6Al-4V alloy after machining with uncoated carbide T1 inserts in an argon enriched environment at cutting speeds of (a) 110 m min^{-1} and (b) 120 m min^{-1}. 176
Figure 4.48 - Microstructure of Ti-6Al-4V alloy after machining with uncoated carbide T2 inserts with conventional coolant supply at a cutting speed of (a) 110 m min^{-1} and (b) 130 m min^{-1}. 177
Figure 4.49 - Microstructure of Ti-6Al-4V alloy after machining with uncoated carbide T2 inserts with a coolant pressure of 11 MPa at cutting speeds of (a) 110 m min^{-1} and (b) 130 m min^{-1}. 177
Figure 4.50 - Microstructure of Ti-6Al-4V alloy after machining with uncoated carbide T2 tools with a coolant pressure of 20.3 MPa at cutting speeds of (a) 110 m min^{-1} and (b) 130 m min^{-1}. 177
Figure 4.51 - Microstructure of Ti-6Al-4V alloy after machining with coated carbide T3 inserts with conventional coolant supply at a cutting speed of (a) 110 m min^{-1} and (b) 130 m min^{-1}. 178
Figure 4.52 - Microstructure of Ti-6Al-4V alloy after machining with coated carbide T3 tools with a coolant pressure of 11 MPa at cutting speeds of (a) 110 m min^{-1} and (b) 130 m min^{-1}. 178
Figure 4.53 - Microstructure of Ti-6Al-4V alloy after machining with coated carbide T3 tools with a coolant pressure of 20.3 MPa at cutting speeds of (a) 110 m min^{-1} and (b) 130 m min^{-1}. 178
Figure 4.54 - Microstructure of Ti-6Al-4V alloy after machining with coated carbide T4 tools with conventional coolant supply at cutting speeds of (a) 100 m min^{-1} and (b) 120 m min^{-1}. 179

Figure 4.55 - Microstructure of Ti-6Al-4V alloy after machining with coated carbide T4 tools with a coolant pressure of 11 MPa at cutting speeds of (a) 120 m min^{-1} and (b) 130 m min^{-1}. 179
Figure 4.56 - Microstructure of Ti-6Al-4V alloy after machining with coated carbide T4 tools with a coolant pressure of 20.3 MPa at cutting speeds of (a) 110 m min^{-1} and (b) 130 m min^{-1}. 179
Figure 4.57 - Microstructure of Ti-6Al-4V alloy after machining with coated carbide T4 tools in an argon enriched environment at cutting speeds of (a) 120 m min^{-1} and (b) 130 m min^{-1}. 180
Figure 4.58 - Chips generated when machining Ti-6Al-4V alloy with different carbide tool grades under various cutting conditions: (a) continuous tubular chip; (b), (f), (h) and (k) continuous and snarled chips, (c), (g) and (i) partially segmented chips, (d), (e) and (l) segmented C-shaped chips. 181
Figure 4.59 - Tool life recorded when machining Ti-6Al-4V alloy with PCD-STD (T5) and PCD MM (T6) tool grades with conventional coolant flow (CCF) and high coolant pressures of 7 MPa, 11 MPa and 20.3 MPa at various cutting speed conditions. 183
Figure 4.60 - Nose wear rate when machining Ti-6Al-4V alloy with PCD inserts with conventional coolant flow and high coolant pressures of 7 MPa, 11 MPa and 20.3 MPa at various cutting speed conditions. 185
Figure 4.61 - Nose wear when finish machining with PCD-STD (T5) and PCD-MM insert grades (T6) at a cutting speed of 175 m min^{-1}. 186
Figure 4.62 - Wear observed on T5 insert after machining Ti-6Al-4V alloy with conventional coolant supply at a speed of (a) 140 m min^{-1} and (b) 200 m min^{-1}. 187
Figure 4.63 - Worn T5 insert after machining Ti-6Al-4V alloy with a 7MPa coolant pressure and at a speed of (a) 175 m min^{-1} and (b) 230 m min^{-1}. 187
Figure 4.64 - Worn T5 insert after machining Ti-6Al-4V alloy with 11 MPa coolant pressure at a speed of (a) 175 m min^{-1} and (b) 230 m min^{-1}. 188
Figure 4.65 - Wear observed on a T5 insert after machining Ti-6Al-4V alloy with 20.3 MPa coolant pressure at a speed of (a) 200 m min^{-1} and (b) 250 m min^{-1}. 188
Figure 4.66 - Wear observed on a T6 insert after machining Ti-6Al-4V alloy with conventional coolant supply at a speed of 175 m min^{-1}. 189
Figure 4.67 - Worn T6 insert after machining Ti-6Al-4V alloy with 11MPa coolant pressure at a speed of (a) 175 m min^{-1} and (b) 230 m min^{-1}. 189
Figure 4.68 - Worn T6 insert after machining Ti-6Al-4V alloy with 20.3 MPa coolant pressure at a speed of (a) 175 m min^{-1} and (b) 230 m min^{-1}. 190
Figure 4.69 - Cutting forces (Fc) recorded at the beginning of cut when machining Ti-6Al-4V alloy with PCD-STD (T5) and PCD-MM insert grades (T6) at various cutting conditions. 191
Figure 4.70 - Feed forces (Ff) recorded at the beginning of cut when machining Ti-6Al-4V alloy with PCD-STD (T5) and PCD-MM insert grades (T6) at various cutting conditions. 191
Figure 4.71 - Surface roughness values recorded at the beginning of cut when machining Ti-6Al-4V alloy with T5 and T6 inserts at various cutting conditions. 193
Figure 4.72 - Roundness values recorded at the end of cut after machining Ti-6Al-4V alloy with T5 and T6 insert grades at various cutting conditions. 193
Figure 4.73 - Surfaces generated after machining with PCD (T5) inserts with conventional coolant supply at a cutting speed of (a) 175 m min^{-1} and (b) 200 m min^{-1}. 195
Figure 4.74 - Surfaces generated after machining with PCD (T5) inserts with a coolant pressure of 7 MPa at a cutting speed of (a) 175 m min^{-1} and (b) 200 m min^{-1}. 195

Figure 4.75 - Surfaces generated after machining with PCD (T5) inserts with a coolant pressure of 11 MPa at a cutting speed of (a) 200 m min^{-1} and (b) 250 m min^{-1}. 195
Figure 4.76 - Surfaces generated after machining with PCD (T5) inserts with a coolant pressure of 20.3 MPa at a cutting speed of (a) 175 m min^{-1} and (b) 200 m min^{-1}. 196
Figure 4.77 - Surfaces generated after machining with PCD (T6) inserts with conventional coolant supply at a cutting speed of (a) 175 m min^{-1} and (b) 200 m min^{-1}. 196
Figure 4.78 - Surfaces generated after machining with PCD (T6) inserts with a coolant pressure of 11 MPa at a cutting speed of (a) 175 m min-1 and (b) 230 m min-1. 196
Figure 4.79 - Surfaces generated after machining with PCD (T6) inserts with a coolant pressure of 20.3 MPa at a cutting speed of (a) 175 m min^{-1} and (b) 200 m min^{-1}. 197
Figure 4.80 - Hardness variation after machining Ti-6Al-4V alloy with PCD (T5) insert with conventional coolant supply. 197
Figure 4.81 - Hardness variation after machining Ti-6Al-4V alloy with PCD (T5) insert with 7 MPa coolant pressure supply. 198
Figure 4.82 - Hardness variation after machining Ti-6Al-4V alloy with PCD (T5) insert with 11 MPa coolant pressure supply. 198
Figure 4.83 - Hardness variation after machining Ti-6Al-4V alloy with PCD (T5) insert with 20.3 MPa coolant pressure supply. 199
Figure 4.84 - Hardness variation after machining Ti-6Al-4V alloy with PCD (T6) insert with conventional coolant supply. 199
Figure 4.85 - Hardness variation after machining Ti-6Al-4V alloy with PCD (T6) insert with 11 MPa coolant pressure supply. 200
Figure 4.86 - Hardness variation after machining Ti-6Al-4V alloy with PCD (T6) insert with 20.3 MPa coolant pressure supply. 200
Figure 4.87 - Microstructure of Ti-6Al-4V alloy after machining with PCD (T5) insert with conventional coolant supply at a cutting speed of (a) 140 m min^{-1} and (b) 230 m min^{-1}. 201
Figure 4.88 - Microstructure of Ti-6Al-4V alloy after machining with PCD (T5) insert with a coolant pressure of 7 MPa at a cutting speed of (a) 175 m min^{-1} and (b) 250 m min^{-1}. 201
Figure 4.89 - Microstructure of Ti-6Al-4V alloy after machining with PCD (T5) insert with a coolant pressure of 11 MPa at a cutting speed of (a) 175 m min^{-1} and (b) 230 m min^{-1}. 202
Figure 4.90 - Microstructure of Ti-6Al-4V alloy after machining with PCD (T5) insert with a coolant pressure of 20.3 MPa at a cutting speed of (a) 200 m min^{-1} and (b) 230 m min^{-1}. 202
Figure 4.91 - Microstructure of Ti-6Al-4V alloy after machining with PCD (T6) insert with conventional coolant supply at a cutting speed of (a) 140 m min^{-1} and (b) 200 m min^{-1}. 202
Figure 4.92 - Microstructure of Ti-6Al-4V alloy after machining with PCD (T6) insert with a coolant pressure of 11 MPa at a cutting speed of (a) 175 m min^{-1} and (b) 230 m min^{-1}. 203
Figure 4.93 - Microstructure of Ti-6Al-4V alloy after machining with PCD (T6) insert with a coolant pressure of 20.3 MPa at a cutting speed of (a) 175 m min^{-1} and (b) 230 m min^{-1}. 203
Figure 4.94 - Chips generated when machining Ti-6Al-4V alloy with different grades of PCD under various cutting conditions: (a): snarled chip; (e): long continuous chip, (b), (c), (d), (f) and (g): segmented C-shaped chips. 204
Figure 4.95 - Tool life recorded when machining Ti-6Al-4V alloy with different CBN 205

tools (T6, T7 and T8) grades with conventional coolant flow (CCF), high coolant pressures of 11 MPa and 20.3 MPa at various cutting speed conditions.
Figure 4.96 - Wear rate curves of different CBN tools when machining Ti-6Al-4V alloy with conventional coolant flow and high pressures coolant supplies at various speed conditions. 207
Figure 4.97 - Worn CBN 10 (T7) inserts after machining Ti-6Al-4V alloy using conventional coolant supply at a speed of (a) 150 m min^{-1} and (b) 200 m min^{-1}. 207
Figure 4.98 - Worn CBN 10 (T7) inserts after machining Ti-6Al-4V alloy with 11 MPa coolant pressure at a speed of (a) 150 m min^{-1} and (b) 250 m min^{-1}. 208
Figure 4.99 - Worn CBN 10 (T7) inserts after machining Ti-6Al-4V alloy with 20.3 MPa coolant pressure at a speed of (a) 150 m min^{-1} and (b) 250 m min^{-1}. 208
Figure 4.100 - Worn CBN 300 (T8) inserts after machining Ti-6Al-4V alloy using conventional coolant supply at a speed of 150 m min^{-1}. 209
Figure 4.101 - (a) Worn CBN 300 (T8) insert after machining Ti-6Al-4V alloy with 11 MPa coolant pressure at a speed of 150 m min^{-1} and (b) enlarged section of worn surface. 209
Figure 4.102 - Worn CBN 300 (T8) inserts machining Ti-6Al-4V alloy with 20.3 MPa coolant pressure at a speed of (a) 200 m min^{-1} and (b) 250 m min^{-1}. 210
Figure 4.103 - Worn CBN 300-P (T9) inserts after machining Ti-6Al-4V alloy with conventional coolant supply at a speed of (a) 150 m min^{-1} and (b) with 11 MPa coolant pressure at a speed of 250 m min^{-1}. 210
Figure 4.104 - Worn CBN 300-P (T9) inserts after machining Ti-6Al-4V alloy with 20.3 MPa coolant pressure at a speed of (a) 150 m min^{-1} and (b) 200 m min^{-1}. 210
Figure 4.105 - Cutting forces (F*c*) recorded at the beginning of cut when machining Ti-6Al-4V alloy with different CBN inserts at various cutting conditions. 211
Figure 4.106 - Feed forces (F*f*) recorded at the beginning of cut when machining Ti-6Al-4V alloy with different CBN inserts at various cutting conditions. 212
Figure 4.107 - Surface roughness values recorded at the beginning of cut when machining Ti-6Al-4V alloy with CBN inserts at various cutting conditions. 213
Figure 4.108 - Roundness variation recorded at end of cut when machining Ti-6Al-4V alloy with CBN inserts using conventional coolant flow and high coolant supply pressures at a speed of 150 m min^{-1}. 213
Figure 4.109 - Hardness variation after machining Ti-6Al-4V alloy with CBN 10 (T7) tools with conventional coolant flow and high coolant supply pressures at a speed of 150 m min^{-1}. 214
Figure 4.110 - Hardness variation after machining Ti-6Al-4V alloy with CBN 300 (T8) tools with conventional coolant flow and high coolant supply pressures at a speed of 150 m min^{-1}. 214
Figure 4.111 - Hardness variation after machining Ti-6Al-4V alloy with CBN 300-P (T9) tools with conventional coolant flow and high coolant supply pressures at a speed of 150 m min^{-1}. 215
Figure 4.112 - Microstructure of Ti-6Al-4V alloy after machining with CBN 10 (T7) tools with (a) conventional coolant flow and (b) high coolant pressure of 20.3 MPa at a cutting speed of 150 m min^{-1}. 215
Figure 4.113 - Microstructure of Ti-6Al-4V alloy after machining with CBN 300 (T8) tools at (a) 11 MPa and (b) 20.3 MPa coolant pressure at a cutting speed of 150 m min-1. 216
Figure 4.114 - Microstructure of Ti-6Al-4V alloy after machining with CBN 300-P (T9) tools at (a) 11 MPa and (b) 20.3 MPa coolant pressure at a cutting speed of 216

150 m min^{-1}.
Figure 4.115 - Chips generated when machining Ti-6Al-4V alloy with CBN tools with various coolant supplies at a cutting speed of 150 m min^{-1}. 217
Figure 4.116 - Nose wear curves of silicon carbide (SiCw) whisker reinforced alumina ceramic - rhomboid-shaped (T10) and square-shaped (T11) - inserts after machining Ti-6Al-4V at various cutting conditions. 218
Figure 4.117 - Tool life recorded when machining Ti-6Al-4V alloy with silicon carbide (SiCw) whisker reinforced alumina ceramic - rhomboid-shaped (T10) and square-shaped (T11) - inserts at various cutting conditions. 219
Figure 4.118 - Wear observed on rhomboid-shaped SiCw alumina ceramic (T10 grade) insert after machining Ti-6Al-4V alloy with conventional coolant supply at a speed of (a) 140 m min^{-1}; coolant pressure of 11 MPa at speeds of (b) 140 m min^{-1} and (c) 400 m min^{-1}, coolant pressure of 20.3 MPa at a speed of (d) 140 m min^{-1}, and in an argon enriched environment at speeds of (e) 200 m min^{-1} and (f) 400 m min^{-1}. 221
Figure 4.119 - Wear observed on square-shaped SiCw alumina ceramic (T11 grade) insert after machining Ti-6Al-4V alloy with conventional coolant supply at speeds of (a): 130 m min^{-1} and (b): 200 m min^{-1}. 222
Figure 4.120 - Cutting forces (Fc) recorded at the beginning of cut when machining Ti-6Al-4V alloy with SiCw alumina ceramic (T10 and T11) inserts at various cutting conditions. 223
Figure 4.121 - Feed forces (Ff) recorded at the beginning of cut when machining Ti-6Al-4V alloy with SiCw alumina ceramic inserts (T10 and T11) at various cutting conditions. 223
Figure 4.122 - Surface roughness values recorded at the beginning of cut when machining Ti-6Al-4V alloy with SiCw alumina ceramic inserts (T10 and T11) at various cutting conditions. 224
Figure 4.123 - Hardness variation after machining Ti-6Al-4V alloy with rhomboid-shaped SiCw alumina ceramic insert (T10 grade) at various environments and at a speed of 140 m min^{-1}. 225
Figure 4.124 - Microstructure of Ti-6Al-4V alloy after machining with SiCw alumina ceramic tool (T10 grade) with: (a) conventional coolant flow, (b) high coolant pressure of 11 MPa and (c) high coolant pressure of 20.3 MPa at a cutting speed of 140 m min^{-1}. 226
Figure 4.125 - Chips generated when machining Ti-6Al-4V alloy with SiCw alumina ceramic inserts: T10 grade at a cutting speed of 140 m min^{-1} with: (a) conventional coolant flow, (b) argon enriched environment, (c) coolant pressure of 11 MPa; T11 grade with conventional coolant flow at cutting speeds of: (d) 130 m min^{-1} and (e) 200 m min^{-1}. 227
Figure 4.126 - Notch wear rate when machining Ti-6Al-4V alloy with T12 and T13 nano-grain size ceramics tools, Al_2O_3 and Si_3N_4 base respectively, with conventional coolant flow and at various speed conditions 228
Figure 4.127 - Recorded tool life when machining Ti-6Al-4V alloy with nano-grain size ceramics tools (T12 and T13) with conventional coolant flow and at various cutting speeds. 228
Figure 4.128 - Wear observed on nano-ceramic tools after machining with Ti-6Al-4V alloy at different cutting speeds: T12 (a: 130 m min^{-1}), (b: 200 m min^{-1}); T13 (c: 110 m min^{-1}) and (d: 200 m min^{-1}). 229
Figure 4.129 - Component forces (cutting forces: Fc and feed forces: Ff) recorded at the beginning of cut when machining Ti-6Al-4V alloy with T12 and T13 tools with conventional coolant flow. 230

Figure 4.130 - Surface roughness values at the beginning of cut when machining Ti-6Al-4V alloy with nano-ceramic (T12 and T13) tools with conventional coolant flow. 231
Figure 4.131 - Roundness values recorded at the end of cut when machining Ti-6Al-4V alloy cut with nano-ceramic (T12 and T13) tools with conventional coolant flow. 231
Figure 4.132 - Chips generated when machining Ti-6Al-4V alloy with nano-ceramic tools: T12 (a): 110 m min^{-1}, b: 130 m min^{-1} and c: 200 m min^{-1}); T13 (d: 200 m min^{-1}) 232
Figure 5.1 - Variation of reactive component forces with coolant pressure supply before machining Ti-6Al-4V alloy. 255

TABLES

Table 2.1 - Classification of aerospace materials (FIELD, 1968). 13
Table 2.2 - Application of aerospace alloys (FIELD, 1968). 14
Table 2.3 - Nominal chemical composition (wt.%) of various commercially available pure-titanium and titanium-base alloys (ASM HANDBOOK, 1998). 18
Table 2.4 - Properties of Ti-6Al-4V alloy compared with a medium carbon steel, AISI 1045 (MACHADO; WALLBANK, 1990) 22
Table 2.5 - Softening points of tool materials (KRAMER, 1987). 56
Table 2.6 - Tool materials properties and cost (ABRÃO, 1995). 91
Table 3.1 - Nominal chemical composition of Ti-6Al-4V alloy (wt. %). 127
Table 3.2 - Physical properties of Ti-6Al-4V alloy. 127
Table 3.3 - Specification, chemical and mechanical properties of the cutting tool materials used in the machining trials. 133
Table 3.4 - Mechanical properties and chemical composition (wt. %) of nano-ceramic tools material (square shape inserts). 133
Table 3.5 - Summary of the experimental tests carried out when finish turning of Ti-6Al-4V alloy at a constant feed rate of 0.15 mm rev-1 and a depth of cut of 0.5 mm. 136
Table 4.1 - Percentage improvement in tool life relative to conventional coolant supply after machining Ti-6Al-4V alloy with different grades of carbides. 149
Table 4.2 - Percentage improvement in tool life relative to conventional coolant supply after machining Ti-6Al-4V alloy with PCD inserts (STD and MM grades). 183

LIST OF SYMBOLS

ϕ	Shear plane angle
ρ	Angle for chip friction
μ	Coefficient of friction
δ	Shear strain at the primary shear plane
σ_f	Normal stress component
τ_f	Shear stress component
σ_{fma}	Maximum normal stress
γ_n	Tool normal rake angle
α_n	Tool normal clearance angle
β_n	Tool normal wedge angle
ε_r	Tool included angle
λ_s	Tool cutting edge inclination angle
τ_{st}	Shear strength of chip material
Al_2O_3	Alumina oxide
ANOVA	Analysis of Variance: a statistical assessment of sample data to decide if differences exist between various groups of data.
C.I.	Confidence Interval of 99% for distribution.
C_2H_5OH	Ethanol vapour
CBN	Cubic Nitride Boron
CCF	Conventional Cooling Flow delivery system
CCl_4	Tetrachloromethane
DOC	Depth of Cut (mm)
DOC	Depth of Cut (mm)
EP	Extreme Pressure
f	Feed rate (mm rev^{-1})
HfC	Hafnium carbide
HfN	Hafnium nitride
HIPed	Hot Isostatic Pressing
HPC	High Pressure Coolant delivery system
HV	Hardness Vickers
ISO	International Standardisation Organisation
k	Constant for the work material
k'_r	Tool minor cutting edge angle
k_r	Tool cutting edge angle
m	meter
Max.	Maximum value of a measured hardness
MgO	Magnesium oxide
Min.	Minimum value of a measured hardness
MM	Multi-Modal Grade of Polycrystalline Diamond insert
MMC	Metal Removal Rate (cm^3 min^{-1})
MQL	Minimum Quantity Lubrication
n	Spindle Speed (rev min^{-1})
PCD	Polycrystalline Diamond
Pn	Cutting edge normal plane
Pr	Tool reference plane

Pre	Working reference plane
Ps	Tool cutting edge plane
Pse	Working cutting edge plane
r	Chip thickness ratio
Ra	Average Surface Roughness
SIALON	Silicon aluminium oxynitride
Si_3N_4	Silicon nitride
STD	Standard Grade of Polycrystalline Diamond insert
T1	Uncoated carbide insert – 883 designation
t_1	Underformed chip thickness
t_1	Actual chip thickness
T1	Uncoated carbide insert – 883 designation
T2	Uncoated carbide insert – 890 designation
T3	Coated carbide insert – CP 200 designation
T4	Coated carbide insert – CP 250 designation
T5	PCD insert – STD designation
T6	PCD insert – MM designation
T7	CBN insert – 10 designation
T8	Solid CBN insert –300 designation
T9	Solid Coated CBN insert – 300-P designation
T10	Silicon carbide whisker reinforced alumina ceramic insert – micron-grain size - WG 300 designation – rhomboid-shaped geometry
T11	Silicon carbide whisker reinforced alumina ceramic insert – micron-grain size - designation WG 300 – squared-shaped geometry
T12	Alumina base nano-grain size ceramic insert – SAZT2 designation
T13	Silicon nitride base nano-grain size ceramic insert – SNCTN1 designation
TaC	Tantalum carbide
TD	Theoretical Density
TiB_2	Titanium diboride
TiC	Titanium carbide
TiN	Titanium nitride
TiAlN	Titanium aluminium nitride
TiZrN	Titanium zirconium nitride
TiO_2	Titanium oxide
T_M	Cutting temperature
V	Cutting Speed (m min^{-1})
Vc	Chip Velocity (m min^{-1})
WC	Tungsten carbide
Y_2O_3	Yttria
ZrO_2	Zirconium oxide

CHAPTER I

INTRODUCTION

The machinability of titanium alloys is generally considered to be poor due to their inherent properties such as chemical reactivity, consequently their tendency to weld onto the cutting tool during machining leading to excessive chipping and/or premature tool failure. The low thermal conductivity of titanium alloys increases temperature generated at the tool-workpiece interface, adversely affecting tool life. They also exhibit tendency to form localised shears bands (ASPINWALL et al., 2003) and work-harden during machining. Additionally, their high strength maintained at elevated temperature and their low modulus of elasticity further impair their machinability. These pose considerable problems in manufacturing hence titanium-alloys have poor machinability (MILLER (1996), EZUGWU; WANG (1997), VIGNEAU (1997), GATTO; IULIANO (1997)). The poor machinability of titanium alloys have prompted many large companies (e.g. Rolls-Royce and General Electrics) to invest large sums of money in developing techniques to minimise machining and overall processing costs (EZUGWU; WANG, 1997). The best tool material is one that will maximise the efficiency and ensure accuracy at the lowest cost, in other words, one that will satisfy the requirements of a specific workpiece material (OKEKE, 1999). A cutting tool must possess high resistance to abrasion in order to withstand changes in dimensions by rubbing action; hot-hardness to maintain a sharp and consistent cutting edge when machining at elevated temperature conditions; chemical stability (lack of affinity between the tool and workpiece) in order to avoid the formation of a built-up edge; high resistance to thermal shock in order to withstand continuous heating and cooling cycles (typical in milling operation) and high toughness which allows the insert to absorb the forces and shock loads during machining. If a machine tool is not sufficiently tough, then induced shock load alone can cause the edge to chatter.

Despite the developments in cutting tool materials for the machining of difficult-to-machine materials at higher metal removal rates, they tend to be ineffective in machining titanium-alloys because of their high chemical affinity. Also, recent developments in coating technology seem to demonstrate only marginal improvement when machining titanium-alloys, despite additional cost of the coated inserts. Ceramics and Cubic Boron Nitride (CBN)/Polycrystalline Cubic Boron Nitride (PCBN) tools are not usually recommended for machining titanium-alloys because of their poor performance due to excessive wear rates as a result of the high reactivity of titanium-alloys to the tool materials in addition to their relatively high cost (HONG; MARKUS; JEONG, 2001). Cutting tools used for machining titanium alloys generally exhibit accelerated wear as a result of extreme thermal and mechanical stresses close to the cutting edge. An ideal cutting tool for machining titanium should have, among others, a hot hardness property to withstand elevated temperatures generated at relatively high speed conditions. Reduction of hot hardness at elevated temperature conditions lead to the weakening of the inter-particle bond strength and the consequent acceleration of tool wear. In addition to that, the machining environment plays a very important role in order to improve the machinability of titanium alloys.

Aero-engine alloys, particularly titanium alloys, cannot be effectively machined without cooling. There is excessive concentration of temperature at the cutting interfaces when machining titanium alloys because of their poor thermal conductivity. In addition to that, practically all the energy consumed in machining is converted into thermal energy. Cutting fluids are used to minimise problems associated with the high temperature and high stresses generated at the cutting edge of the tool during machining. Titanium alloys are generally machined using conventional coolant flow. Also, there is other technique to deliver coolant in variable quantities at high/ultra high pressures, generally within the range 0.5 – 360 MPa (SECO TOOLS (2002a)). This technique has been employed when machining mainly nickel alloys. One of the benefits of using high pressure coolant supply is because it acts as a chip-breaker. Additionally, the temperature gradient is reduced by penetration of the high-energy jet into the tool-chip interface and consequently eliminating the seizure effect (MAZURKIEWICZ; KUBALA; CHOW, 1989), thereby providing adequate lubrication at the tool-chip interface with a significant reduction in friction (EZUGWU; BONNEY; YAMANE, 2003). These combined with high velocity coolant flow causes the breakage of the continuous-type chips into very small segments. Because the tool-chip contact time is shorter, the tool is less susceptible to dissolution wear caused by chemical reaction with newly

generated chips, especially titanium-alloy chips (LINDEKE; SCHOENIG; KHAN, 1991). Increase in productivity has been noticed using high pressure coolant delivery relative to the conventional methods of coolant delivery when machining nickel and titanium alloys at lower speed conditions. Other cooling technique like the minimum quantity of lubrication (MQL) has shown considerably improvement in the machinability of aerospace alloys compared to conventional coolant flow and looks promising for machining titanium alloys in order to improve the tribological processes present at the tool-workpiece interface and at the same time eliminate environmental damages as well as minimizing some serious problems regarding the health and safety of operators (SOKOVIC; MIJANOVIC (2001), DA SILVA; BIANCHI (2000), LI et al. (2000), MACHADO; WALLBANK (1997)). With the same purpose other environments such as atmospheric air (dry machining), argon enriched environment and liquid nitrogen (cryogenic machining) are also been employed as alternative cooling technology to improve the machinability of titanium-alloys. Since the gases can alter the tribological conditions existing between two surfaces in contact such as the cutting zone during machining, other environments such as atmospheres, dried air, oxygen, nitrogen, CO_2 and organic compounds such as tetrachloromethane (CCl_4) and ethanol vapour (C_2H_5OH) are also expected to improve the machinability of titanium-alloys. Some special machining techniques including specially designed ledge tools, self-propelled rotary tool (SPRT), ramping technique (taper turning) and hot machining have shown remarkable success in when machining titanium alloys (EZUGWU; BONNEY; YAMANE (2003), EZUGWU; WANG (1997), EZUGWU (2005)).

This thesis on the machining Ti-6Al-4V alloy with various cutting tools and different cooling environments was developed in collaborative program with industrial partners: Rolls-Royce Plc (aero-engine manufacturer), SECO Tools (cutting tool manufacturer) and Pumps and Equipment Ltd (Warwick) who provided the high-pressure coolant delivery system for this study. A comprehensive literature survey on the machinability of aero-engine alloys under various cutting environments as well as the experimental techniques adopted in all stages of the research programme such as turning tests, data acquisition, sample preparation, analysis of the worn tools and machined surfaces, as well as initial machining results are presented in this thesis. An investigation of the machinability of components manufactured with titanium-base, Ti-6Al-4V (or IMI 318), alloy will involve the following:

i) Evaluation of recently developed cutting tools materials (uncoated and coated cemented carbides, Polycrystalline Diamond (PCD) inserts, Cubic Boron Nitride (CBN) and SiC Whiskers Reinforced Al_2O_3 Ceramics) when machining titanium-base, Ti-6Al-4V, alloy at high speed conditions;

ii) Cutting environments (high pressure coolant supplies at pressures of 7 MPa (70 bar), 11 MPa (110 bar) and 20.3 MPa (203 bar), argon enriched environment, and conventional coolant flow;

iii) Validation of the optimum machining conditions achieved on prototype component without compromising its integrity.

1.1 Aims of the thesis

This thesis is geared primarily to achieve a step increase in the machining productivity of a commercially available titanium-base, Ti-6Al-4V, alloy using recently developed cutting tool materials, machining techniques and various cooling media such as conventional coolant flow, high pressure coolant supplies and argon enriched environment. This study is part of the Joint Strike Fighter (JSF) project – a vectored thrust, multi-role combat aircraft designed for conventional take-off and landing or a Navy version which requires Short Take Off/Vertical Landing capability in collaboration with Rolls-Royce plc. The thesis aims primarily towards significant reduction in cost of manufacturing jet engines in the immediate future using modern cutting tool technology and machining techniques.

The literature survey section covers cutting tool materials and the various cutting environments employed in the machining of aero-engine alloys. The objectives of this thesis are listed below:

- Investigation of the effect of various cooling media (high-pressure coolant supply, argon enriched environment and conventional coolant flow) on tool performance when finish turning of titanium-base, Ti-6Al-4V (IMI 318), alloy;
- Investigation of the dominant tool failure modes and wear mechanisms of newly developed cutting tools (uncoated and coated cemented carbides, different grades of Polycrystalline Diamond (PCD), Cubic Boron Nitride (CBN), SiC Whiskers Reinforced Ceramic, and Al_2O_3 and Si_3N_4 base nano-grain ceramic inserts) when finish turning of titanium-base, Ti-6Al-4V (IMI 318), alloy at high speed machining;

- Analysis of the surface finish and surface integrity of machined surfaces as well as run-out of the machined bars;
- Selection of the best combination of cutting tool-cutting environment-cutting conditions to employ in the machining of prototypes/scaled down models of the 3 bearing swivel nozzle.

CHAPTER II

LITERATURE SURVEY

2.1 Historical Background of Machining

At the end of second ice age, more than 370,000 years ago, the mortal remains of a recognizable human were preserved in a cave near Pekin. The presence of flakes of stone and burned bones surrounding him was evidence that fire and tools had been discovered (ARMYTAGE, 1970). Fire enabled him to live in cold countries, prepare food, frighten animals away and lighten the gloom of his caves as well as use it to make pottery and stabilize his life. Tools were no less important. As *homo faber*, man the maker, his first tools were made of stone. By 3000 B.C. the communities cultivating the alluvial plains of the Nile, the Tigris-Euphrates and the Indus valleys were producing foodstuff that they could use labourers to dig canals, employ artisans to manufacture tools and support merchants who bought other produce. They used sails to propel boats, oxen to draw ploughs, wheels to bear carriages and metals to fabricate tools and facilitate arduous manual operations. The beginning of civilization among people in Egypt (early third millennium B.C.) coincided with mining. These mines were worked by slaves, obtained by war. Workers often used hammers and wedges, bones and horns. At the beginning of the 2^{nd} century before Christ, a greek called Ctesibius compressed air to work a gun, built a water clock and a water organ sprayed fire through a hose. Hero of Alexandria, in the 1^{st} century B.C., constructed pneumatic devices like water organs and ingenious toys of all kinds, including a steam turbine called an aeolipile. He gave an account of five simple machines which become the basis of early technology: the wedge, the pulley, the lever, the wheel and axle, and the endless screw. Metals obtained at that time includes gold, silver, iron, lead, and later copper and tin were used in various ways. Ethiopian kings bound their prisoners with gold chains. By about 1350 B.C. it is known that

Argonatus raided Colchis in Georgia looking for gold. Silver was used for handles on shields (ARMYTAGE, 1970).

Machine tools, screw-cutting lathe and pumping plants were first described by Galileo´s disciple in 1579, professor Jacques Besson (Orleans), in his *Theâtre des Instruments Mathematiques et Méchaniques*. However, it was only from 18th century that great technical advances in machine tools began. The early developments were laying the base for industrial development. At the beginning of the 18th century, wood was the dominant workpiece material and the machining of metal was very limited and quite crude. By about 1740, the power revolution in Britain, and the development of the steam engine, led to the development of superior engineering materials like, cast iron, wrought iron, bronze and brass which were relatively easy to machine with tools materials available in that time: the carbon tools steels hardened and tempered by blacksmiths (TRENT; WRIGHT, 2000). There were early planning and milling machines as well as lathes that could perform threading. The introduction of the cross-slide on a lathe represented a great progress, meaning that tools did not need to be held by hand, they could be secured in a tool-post instead. Machining operation was very slow at the beginning of the 19th century, one example being the shapping of one and half square metres of an iron surface taking all of one working day. The cutting depth and the length of stroke were set and the shapping machine was left to run. The development of workshops and their machinery was extensive in Europe and in America during 19th century. They were mainly stimulated by the armament industry, navigation and railway industries. On the American continent, arms makers led the progress and developed machines and introduced manufacturing based on interchangeable parts and standardised measurements. The turret lathe was introduced as a major quick-change of tools and turret lathes and automatic screw machines were widely in operation by the end of the 19th century in industrialised countries (AB SANDVIK COROMANT, 1994).

From the 1860s, the expanding economy promoted increase in productivity. With further development of new metals and alloys (considered more difficult to machine) like steel for instance, even the best carbon steel tools were pushed to their functional limits, thus becoming insufficient for manufacturers' needs, constraining production speed and hampering efficiency. It was at this stage that emphasis was shifted from the development of basic machine tools to cutting tool materials which could withstand the severe conditions in metal cutting i.e. tool materials which could cut at higher cutting conditions. However, by the end of the 19th century both labour and capital costs of machining increased significantly. Reducing

costs by accelerating and automating the cutting process became necessary. Machine tools with manual control have became uneconomical as the required output rises, and the need to design and produce advanced machines became indispensable. At the same time, advances in technology led to developments in metal cutting field. Production of machine tools in order to maximise the utilisation of each generation of the cutting tool materials has been created. Semi-automatic and automatic machines became available. Additionally, the engineering and economic requirements of the performance of machined components were constantly changing and becoming more demanding. Technical problems necessitated a more realistic appraisal of mechanical engineering design problems. The designer must critically examine his selection of material design products, strength properties, processing operations, and means for securing adequate material inspection (ASME HANDBOOK, 1965).

In the 20^{th} century the introduction of automatic machines, computer numerically controlled (CNC) machines and transfer machines allowed better tool efficiency to be achieved. Subsequently the development of the jet engine by Great Britain, United States and German, forced mechanical and metallurgical engineers to work towards the improvement and/or development of tool materials capable of withstanding the demands imposed by the new materials. Optimisation of shape and geometry of tools, as well as changing the properties of cutting tools by manipulation of chemical composition have been made to prolong tool life at higher cutting speeds; development of new coolants and lubricants ensured to improve surface finish and higher rates of metal removal. Advances in materials science enabled the development of novel materials that can operate under aggressive environments such as severe conditions of stress, high temperature and corrosion. Aluminium-base alloys, magnesium-base alloys, high-alloy steels, nickel-base and titanium-base alloys and other metal matrix composites are examples of these materials currently in use. They led to the evolution of new cutting tool materials capable of providing long tool life, high stock removal rates and greater component accuracy and integrity.

2.2 Overview of Aerospace Alloys

Living in the modern society will involve the use of manufactured items such as telephones for communication, cars and aeroplanes for transportation, etc. It therefore becomes unavoidable to stop the changes or trends taking place in the modern world. There is a need to adjust to this situation, particularly in cases where demand for better quality and

reliability are critical factors that have led companies to design the process technology and to ensure that the system is flexible, controllable, and as efficient as possible in order to remain competitive in the global market place (DE GARMO; BLACK; KOHSER, 1999). In this context, rapid advances in aircraft and space vehicles have created a need for the development of many new materials to withstand extreme temperatures, high stresses and unusual environments. Aircraft and space vehicle structures operate at elevated temperatures and stresses than formerly served by aluminium and magnesium alloys. High strength steels, high temperature alloys, refractory alloys, beryllium, and plastics are materials in common use in the aerospace industry. Most of the aerospace alloys are susceptible to surface alterations or damage during machining, hence extreme care must be exercised to maintain surface integrity of machined components (FIELD, 1968). Apart from continuous efforts to improve engine performance, weight reduction and manufacturing costs also come into play, indeed increasingly so. The best preparation for the intense competitive pricing in the aerospace industry is by reducing overall manufacturing cost (MILLER, 1996).

2.2.1 Aero-Engine Alloys

The aero-engines, also called gas turbine engines or jet engines, are responsible for propelling most modern passenger and military aircrafts. An aero-engine consists of an inlet, compressor, shaft, burner and nozzle as are shown in Figures 2.1 (a) and (b) (BENSON (2002), ROLLS-ROYCE PLC (2003)). High performance, light weigh, low life cycle cost are the main requirements for aero-engines in addition to the need for increasing their thrust-to-weight ratio (T/W). A way to increase this performance is by increasing turbine inlet temperature (TIT). The TIT increased significantly from the 1980's onwards. Figure 2.2 shows the trend in turbine inlet temperature in aero-engines (OHNABE et al., 1999). Figure 2.3 shows that some improvements in the performance of aero-engine alloys can be associated with ability of the materials designer to provide the engineer with materials that can withstand high temperatures conditions (BENSON, 2002). Figure 2.4 shows the maximum service temperature chart to help with identification of new possibilities for materials development (LOVATT; SHERCLIFF, 2002).

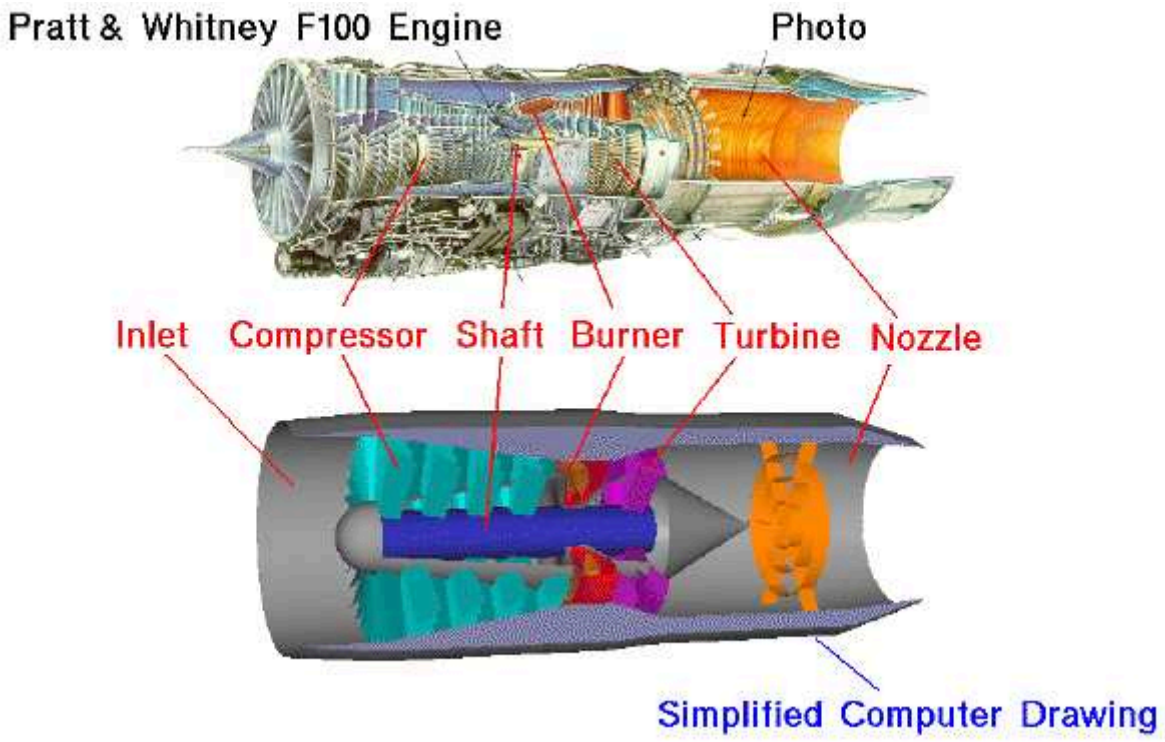

(a)

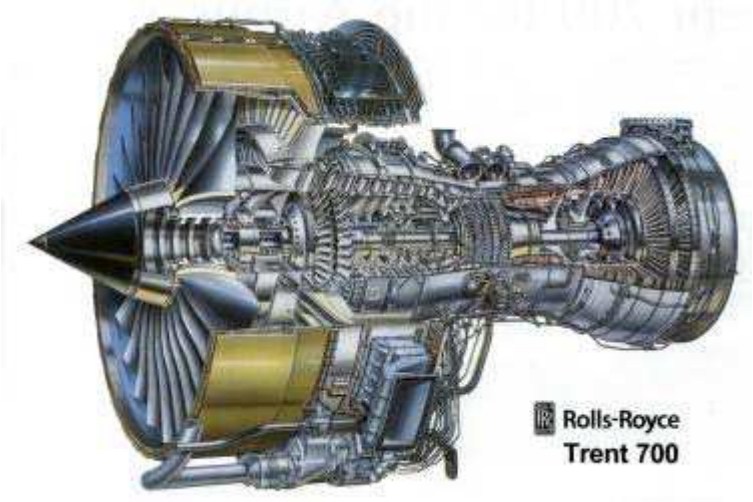

(b)

Figure 2.1 - (a) A typical jet engine and its main parts (Pratt and Whitney F100 jet engine) (BENSON, 2002); (b) typical jet engine (Trent 700) manufactured by Rolls-Royce plc (ROLLS-ROYCE PLC, 2003).

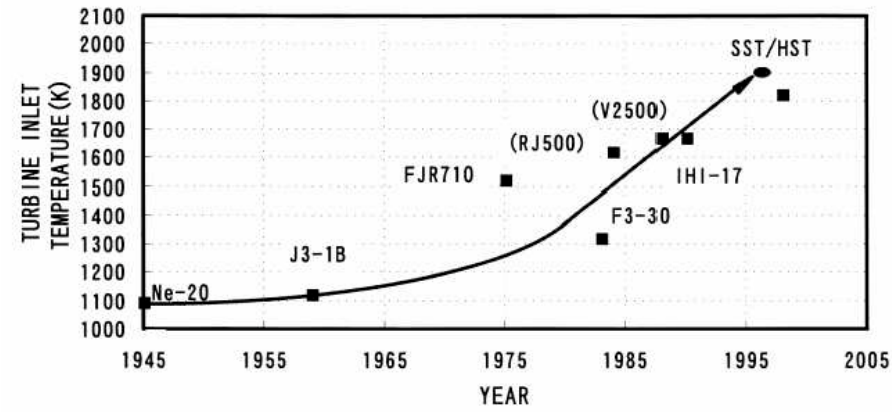

Figure 2.2 - Trends in turbine inlet temperature in areo-engines (OHNABE et al., 1999).

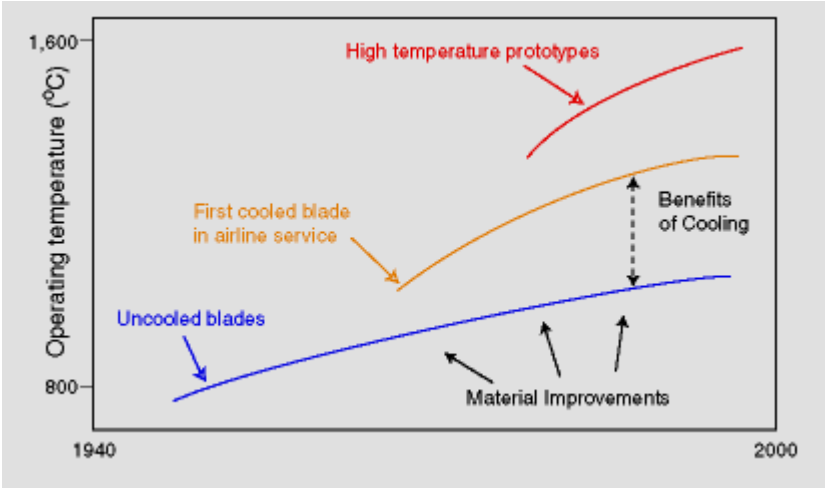

Figure 2.3 - Improvements in aero-engine performance (BENSON, 2002).

Carbon composites have been used in the aero-engine industry since the 1970s in relatively smaller quantities. They are currently attracting more attention due to their improved properties and manufacturing processes. Figure 2.5 shows trend of materials usage in typical aero-engines. Increasing demand for titanium and nickel-base alloys up till the end of the 20th century is clearly illustrated, highlighting their dominant and competitive use in the manufacture of aerospace engines (MILLER, 1996).

Materials employed in the aerospace industry can be grouped into different categories according to their nominal composition, Table 2.1 (FIELD, 1968). General areas of application of various categories of materials used on the aerospace industry are described in Table 2.2 (FIELD, 1968).

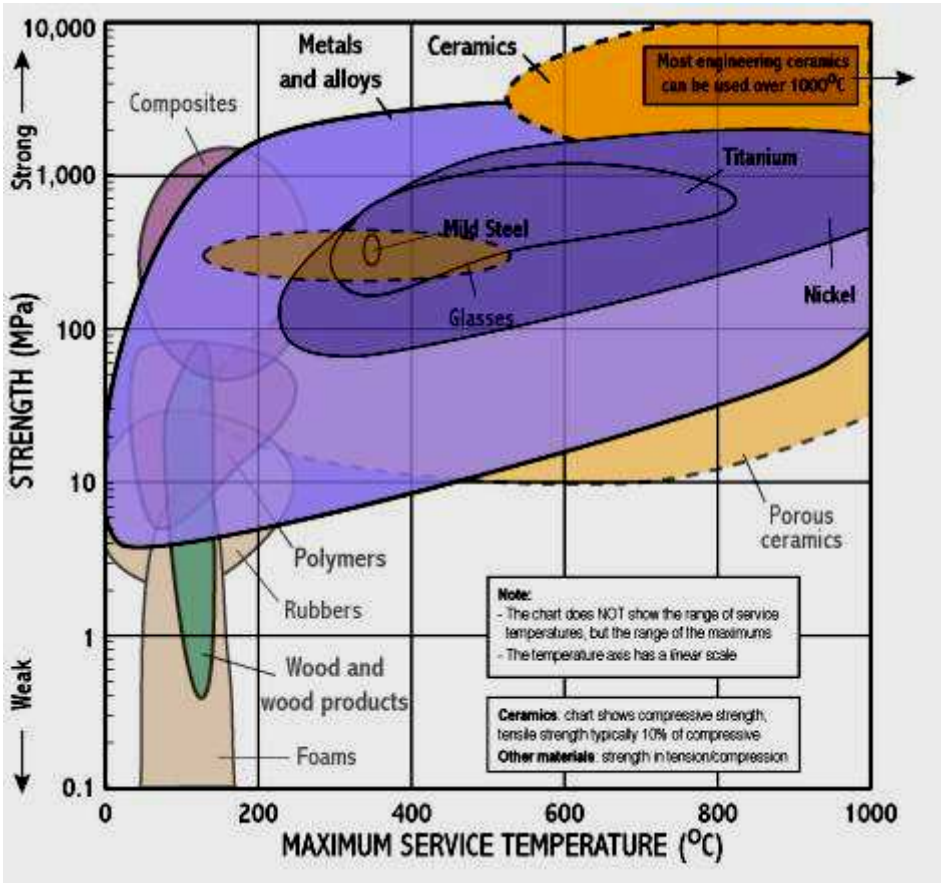

Figure 2.4 - Maximum service temperature of various materials (LOVATT; SHERCLIFF, 2002).

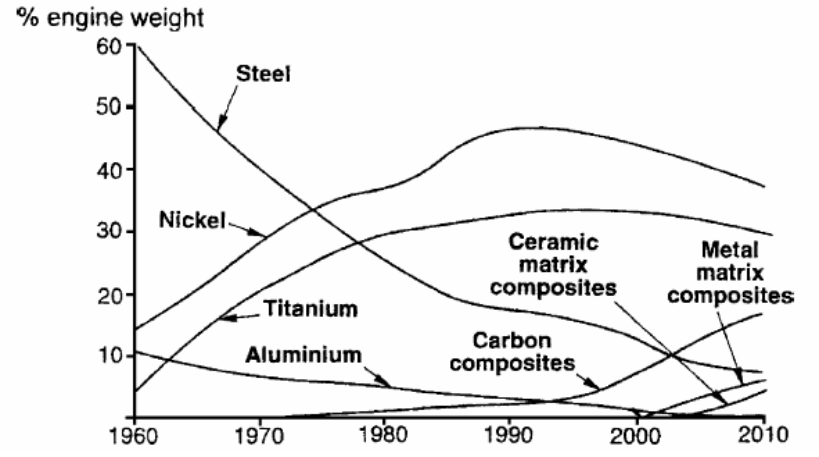

Figure 2.5 - Trend of materials usage in aero-engines (MILLER, 1996).

Table 2.1 - Classification of aerospace materials (FIELD, 1968).

Type of material	Designation	Nominal composition
Aluminium alloy	2024	Al-4.5Cu-1.5Mg
Austenitic stainless steels	302	Fe-18Cr-9Ni
	321	Fe-18Cr-11Ni
Martensitic stainless steel	410	Fe-12Cr
Precipitation-hardening stainless steels	17-7 PH	Fe-17Cr-7Ni-1Al
	17-4 PH	Fe-16.5Cr-4Ni-4Cu
High-strength steels	4340	Fe-0.8Cr-1.8Ni-0.4C
	H-11	Fe-5.25Cr-1.35Mo-0.5V-0.37C
	D6AC	Fe-1Cr-0.5Ni-1Mo-0.46C
	18% Ni maraging steel	Fe-18Cr-8.5Co-3.25Mo
Nickel-base high-temperature alloys	Inconel 718	Ni-19Cr-3Mo-5.2Cb-0.8Ti-0.6Al-18Fe
	Udimet 500	Ni-18Cr-16Co-4Mo-2.8Ti-2.8Al
	Rene 41	Ni-19Cr-11Co-10Mo-3.1Ti-1.5Al
	Waspaloy	Ni-19.5Cr-13.5Co-4.2Mo-3Ti-1.2Al-2Fe
Cobalt-base high temperature alloys	HS-25	Co-20Cr-10Ni-15W-3Fe
Iron-base high temperature alloy	A-286	Fe-15Cr-26Ni-1.2Mo-2Ti
Titanium alloys	Ti-6Al-4V	Ti-6Al-4V
	(IMI 318)	
	Ti-8Al-1Mo-1V	Ti-8Al-1Mo-1V
	Ti-3Al-13V-11Cr	Ti-3Al-13V-11Cr
Pure tungsten	Unalloyed tungsten	W plus trace elements
Molybdenum alloy	TZM	Mo-0.5Ti-0.07Zr
Columbium alloy	Columbium D31	Cb-10Mo-10Ti
Tantalum alloy	Ta-10W	Ta-10W
Beryllium	I-400	Be-4.25BeO
Composite and plastics	Fibre reinforced plastics	-----

Table 2.2 - Application of aerospace alloys (FIELD, 1968).

Material	Application
Austenitic stainless steel	Compressor rings and housings, wing panels, cryogenic vessels
Martensitic stainless steel	Compressor blades, disks and rings and
Precipitation-hardening stainless steels	spars, struts, fittings, fasteners, wing panels,
High-strength steels	Compressors disks, airplane spars, rocket motor cases, longerons, struts, bulkheads, landing gear, fitting
Nickel-or colbalt-base high-temperature alloys	Turbine disks, turbine blades
Titanium alloys	Airplane spars, wing skins and panels, longerons, struts, bulkheads, fasteners, rocket motor cases
Refractory alloys	Space propulsion structures, nozzles and nozzles inserts
Beryllium	Compressors disks and blades, re-entry capsules, guidance systems
Composites and plastics	Nose cones, thermal barriers, heat shields, ablative components, compressor blades, rocket motor cases

2.3 Superalloys

The origin of the term “Superalloy” refers to “Heat Resisting Alloys” or “High Temperature Alloys”. The nomenclature “superalloy” became popular in the late 1940s, after Word War II, to describe a group of alloys developed for use in turbo superchargers and aircraft turbine engines which operated at elevated temperature service in severe corrosive environments where relatively severe mechanical stressing is encountered and where surface stability frequently is required. These alloys, usually based on Group VIII A elements, consist of various formulations made from the following elements: nickel, iron, cobalt and chromium, as well as lesser amounts of niobium, tantalum, titanium, tungsten, molybdenum and aluminium. The most important properties of the superalloys are long-time strength at temperatures above 650 ºC (1200 ºF) and resistance to hot corrosion and erosion (ASM INTERNATIONAL, 1988).

Many alloys are used at elevated temperatures and must be able to withstand the deteriorating effect of the service atmosphere, as well as possess sufficient strength for the design condition and have adequate stability to withstand damaging metallurgical structural

changes at operating temperature. For use at moderate temperatures (< 540 ºC) and moderate stress, the 12% Cr corrosion-resistant steels are satisfactory. A group containing chromium and molybdenum and/or carbide formers and/or cobalt or nickel, the so-called super 12% Cr steels, have been used where conditions of higher stress and moderate temperature are required. As the temperature is increased, under conditions of low stress, higher chromium steels, either the ferritic corrosion-resistant or the austenitic stainless steels containing nickel as well as chromium, or nickel-chromium alloys are employed. For very high operating temperatures, there is increasing interest in the refractory metals of Groups V (vanadium, niobium, and tantalum) and VI (chromium, molybdenum and tungsten) as well as ceramics. The refractory metals, however, exhibit very poor oxidation resistance, and their use is generally restricted to non-oxidizing environments. Because of low toughness for most structural applications, ceramic materials have limited use. The high-temperature applications of superalloys are extensive, including components for aircraft, chemical plant equipment and petrochemical equipment.

2.3.1 Titanium Superalloys in the Aerospace Industry

Although all superalloys materials play a significant role in Aerospace industry, nickel-base and titanium alloys are the major materials used due to their improved properties. In this thesis the emphasis will be placed on the machinability of titanium-base, Ti-6Al-4V, alloy.

Wilhelm J. Kroll, in the late 1930s, was the person responsible for development of a safe and economical method of production of titanium (ASM HANDBOOK, 1998). Initially, Kroll´s process involved reduction of titanium tetrachloride (TiCl4) with sodium and calcium. Later magnesium was utilized in an inert gas atmosphere. Research continued through World War II and by the late 1940s, with definition of physical and mechanical properties as well as alloying characteristics, that titanium really gained industrial and academic importance.

Titanium is encountered in two crystallographic forms. At room temperature, unalloyed (commercially pure) titanium has a hexagonal close-packed (hcp) structure referred to as alpha (α) phase. At 883 ^{o}C (1621 ºF), titanium undergoes an allotropic transformation from hcp to a body-centred cubic (bcc) structure known as beta (β) phase, which remains stable to the melting point. The manipulation of these crystallographic variations through alloying additions and thermomechanical processing is the basis for the development of a wide range of alloys and properties. These phases also provide a convenient way to categorise titanium mill products (ASM HANDBOOK, 1998). Based on these phases, titanium alloys can be

categorised into four main groups namely alpha (α), near alpha, alpha + beta and beta (β) based on their atomic crystal structure. The alloying elements can be categorised according to their effect on the stability of the α- and β-phases. Those that raise the transformation temperature are known as α-stabilisers (Al, O, N and Ga) and those that decrease the transformation temperature are called β-stabilisers (Mo, V, W and Ta). Cu, Mn, Fe, Ni, Co and H are also β-stabilisers but form the eutectoid (BHADESHIA, 2003). Al is a very effective α-strengthening element at ambient and elevated temperatures up to 550ºC and its low density is an additional advantage. The residual elements (or impurities) such as C, N, Si and Fe raise the strength and lower the ductility of titanium products. Basically, O and Fe contents determine strength levels of commercially pure titanium. In higher strength grades, O and Fe are intentionally added to the residual amounts already in the sponge to provide extra strength. On the other hand, C and N usually are held to minimum residual levels to avoid embrittlement. When good ductility and toughness are required, the extra-low interstitial (ELI) grades are recommended (ASM HANDBOOK, 1998). Table 2.3 contains the chemical composition by weight of commercially available pure-titanium and titanium-base alloys (ASM HANDBOOK, 1998). Detailed description of titanium alloys and their properties have been reported elsewhere (ASM HANDBOOK (1998), BOYER (1996), EZUGWU; WANG, 1997).

- Alpha alloy: represents the group of the commercially pure titanium alloy grade with oxygen and iron as the primary alloying elements; Alpha alloys generally have creep resistance superior to β alloys, and are preferred for high-temperature applications. The absence of a ductile-to-brittle transition, a feature of β-alloys, makes α-alloys suitable for cryogenic applications. Materials of this group are characterised by satisfactory strength, toughness and weldabillity, but poorer forgeability than β-alloys. A single phase α-alloy, Ti 5-$2\frac{1}{2}$(Ti-AL-$2\frac{1}{2}$Sn) is still available commercially besides commercially-pure titanium;
- Near alpha alloy: contain large percentage of α-stabilisers and small amount of β -stabilisers like molybdenum and vanadium. Typical alloys in this group include Ti-3Al-2.5 V (Ti-3-2.5), Ti-8Al-1Mo-1V (Ti-8-1-1) and Ti-6Al-2Sn-4Zr-2Mo (Ti-6-2-4-2S). These alloys have mainly used at operating temperatures between 400 to 520^{o}C EZUGWU; WANG (1997);

- Alpha + beta alloy: this is a mixture of α- and β-phases and may contain between 10 and 50% β-phases at room temperature. The most common α + β alloys are Ti-6Al-4V (Ti-6-4 or IMI 318), Ti-6Al-2Sn-4Zr-6Mo (Ti-6-2-4-6) and Ti-6Al-2Sn alloys. The properties of these alloys can be controlled through heat treatment, which is used to adjust the amounts and types of β-phase element. A good combination of their properties ensure better operations within the temperature range of 315-400^{o}C (ASM HANDBOOK (1998). Solution treatment followed by aging at 480 to 650 ºC (900 to 1200 ºF) precipitates α and β in a matrix of retained or transformed β-phase;
- Beta alloy: these are referred to as high hardenability titanium alloys due to the β-stabilisers, represented by Ti-15V-3Cr-3Al-3Sn (Ti-15-3), Timetal 21S (Ti-15Mo-2.7Nb-3Al-0.2Si), Ti-3Al-8V-6Cr-4Mo-4Zr and Ti-10V-2Fe-3Al alloys. As stated earlier, the transition elements present in these group such as Mo, V and Nb tend to decrease the temperature of the α- to β-phase transition and thus promote development of the bcc β-phase. They have excellent forgeability over a wider range of forging temperatures than α-alloys (ASM HANDBOOK, 1998). They also exhibit high stress corrosion resistance, can be heat-treated to high strengths and offer fabrication advantages, particularly for producing sheets, owing to their cold rolling capabilities. Some β-alloys, such as Ti-10-2-3 and β-C, have excellent fatigue properties while others such as Ti-15-3 have, in general, poor fatigue properties relative to their strengths.

Table 2.3 - Nominal chemical composition (wt.%) of various commercially available pure-titanium and titanium-base alloys (BOYER, 1996).

Product Specification		C	H	O	N	Fe	Al	Sn	Zr	Mo	Others
Pure titanium	JIS class 1	…	0.015	0.15	0.05	0.20	…	…	…	…	…
	JIS class 2	…	0.015	0.20	0.05	0.25	…	…	…	…	…
	JIS class 3	…	0.015	0.30	0.07	0.30	…	…	…	…	…
	DIN 3.7025	0.08	0.013	0.10	0.05	0.20	…	…	…	…	…
	DIN 3.7035	0.08	0.013	0.20	0.06	0.25	…	…	…	…	…
	DIN 3.7055	0.10	0.013	0.25	0.06	0.35	…	…	…	…	…
	GOST BT1-00	0.05	0.008	0.10	0.04	0.20	…	…	…	…	…
	ASTM grade 12 (UNS R53400)	0.10	0.015	0.25	0.03	0.30	…	…	…	…	…
Titanium base alloys	Ti-2.5Cu	0.08	0.01	0.2	0.05	0.2	…	…	…	…	2.0-3.0Cu
	Ti-5Al-2.5Sn (DIN 17851)	0.08	0.02	0.2	0.05	0.5	4.0-6.0	2.0-3.0	…	…	...
	Ti-5Al-2.5Sn- ELI (AMS 4909)	0.05	0.0125	0.2	0.035	0.25	4.5-5.75	2.0-3.0	…	…	O + Fé=0.32, 0.005Y
	Ti-8Al-1V-1Mo (MIL-R-81588)	0.035	0.005	0.12	0.015	0.20	7.35-8.35	…	…	0.75-1.25	0.75-1.25V
	Ti-6242	0.05	0.0125	0.15	0.05	0.25					0.1Si, 0.005Y
	Ti-679	0.04	0.008	0.17	0.04	0.12	2.25	11	5	1	0.2Si
	Ti-6Al-2Sn-1.5Zr-1Mo	...	...	...	...	...	6	2	1.5	1	0.35Bi, 0.1Si
	IMI 829	...	...	...	...	...	5.5	3.5	3	0.25	1Nb, 0.3Si
	Ti-6Al-4V (IMI 318)	0.08	0.01	0.2	0.05	5.5-6.75	5.5-6.75	...	...	...	3.5-4.5V 0.005Y
	Ti-6Al-4-ELI (AMS 4907)	0.08	0.0125	0.13	0.05	0.25	5.5-6.75	...	...	...	3.5-4.5V
	Ti-6Al-6V-2Sn	0.05	0.015	0.20	0.04	0.35-1.0	6	2	...	...	0.75Cu, 6V
	Ti6246	0.04	0.0125	0.15	0.04	0.15	6	2	4	6	...
	IMI 679	...	…	…	…	…	2	11	4	1	0.25Si
	Ti-13V-11Cr-3Al (MIL-T-9047)	0.05	0.025	0.17	0.05	0.35	2.5-3.5	...	...	...	12.5-14.5V, 10-12Cr
	Ti-8Mo-8V-2Fe-3Al	0.05	0.15	0.16	0.05	1.6-2.4	2.6-3.4	...	...	7.5-8.5	7.5-8.5V
	Ti-10V-2Fe-3Al	0.05	0.015	0.13	0.05	1.6-2.5	2.5-3.5	...	...	...	9.25-10.75V
	Transage 175	0.08	0.015	0.15	0.05	0.20	2.2-3.2	6.5-7.5	1.5-2.5	…	12-14V

Titanium alloys possess high strengths, high strength-to-weight ratio relative to other materials such as steel (60% density of steel) and high compatibility with composite structure which can often bridge the properties gap between aluminium and steel alloys, providing many of the desirable properties of each. For example, titanium like aluminium is non-magnetic and has good heat-transfer properties (despite its relatively low thermal

conductivity). Thermal expansion coefficient of titanium alloys, ranging from about 9 to 11 ppm $^{o}C^{-1}$, is slightly lower than that of most steels and less than half that of aluminium (ASM HANDBOOK, 1998). Titanium could also replace aluminium when operating temperature exceeds about 130ºC, the normal maximum operating temperature for conventional aluminium (BOYER, 1996). Other important characteristics of titanium alloys depend on the class of alloy and the morphology of the alpha constituents. In the near alpha and alpha-beta alloys, the variations in the alpha morphology are achieved with different heat treatments. Titanium alloys have high-temperature strength that is associated with the alpha and near-alpha alloys. However, when creep strength is not a factor in an elevated-temperature application, the short time elevated-temperature tensile strengths of beta alloys have a distinct advantage.

Excellent corrosion resistance is another important property of titanium alloys. Although titanium is a highly reactive metal, it also has an extremely high affinity for oxygen and thus forms a very stable and highly adherent protective oxide film on its surface. This oxide film forms spontaneously and instantly when fresh metal surfaces are exposed to air and/or moisture. In addition to its passive behaviour, titanium is non-toxic and biologically compatible, making it useful in applications ranging from chemical processing equipment to surgical implants and prosthetic devices (ASM HANDBOOK, 1998). Its corrosion resistance is such that corrosion protective coatings of paint are not required. Typical applications in very corrosive environments which dictate the use of titanium to provide high structural durability are the floor structure under the galleys and lavatories. Titanium alloys are also predominantly used within medical and aerospace industries.

In biomedical applications, the effectiveness and reliability of titanium implants in human body are essential requirements because, once they are installed, they cannot readily be maintained or replaced. The natural selection of titanium for implantation is determined by a combination of most favourable characteristics including immunity to corrosion, biocompatibility, strength, low modulus and density and the capacity for joining with bone and other tissue – osseointegration. The mechanical and physical properties of titanium alloys combine to provide implants which are highly damage tolerant. A titanium implant has a stiffness of less than half that of stainless steel or cobalt chrome, therefore reducing the effects of weight shielding. Most metals in body fluids and tissue are found in stable organic complexes. Titanium is judged to be completely inert and immune to corrosion by all body fluids and tissue and is thus wholly biocompatible. Typical application of titanium in

biomedical area are**:** dental implants, bone and joint replacement, maxilla and cranium/facial treatments, external prostheses, cardiovascular devices and surgical instruments (plates, pins and hipjoints) (TIG, 2002). Figure 2.6 (a) shows typical medical/dental applications of titanium alloys (TIG, 2002).

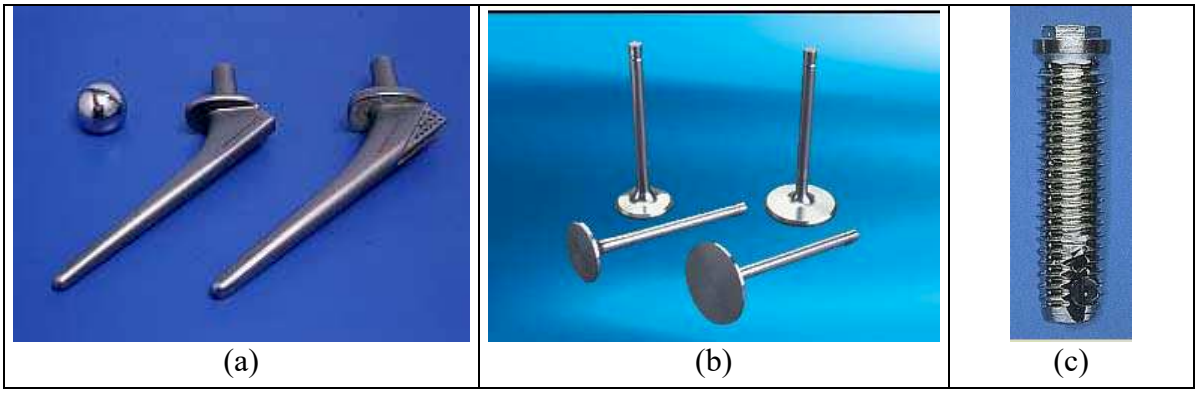

(a) (b) (c)

Figure 2.6 - Typical applications of titanium: (a) modular femoral components (prostheses manufactured in titanium-base, Ti-6Al-4V, alloy, (b) valves and (c) screw (TIG, 2002).

Titanium industry market is mainly shared by commercial and military jet aircraft. Its dependence on the aerospace industry, which is cyclical in nature, resulted in several setbacks (Figure 2.7).

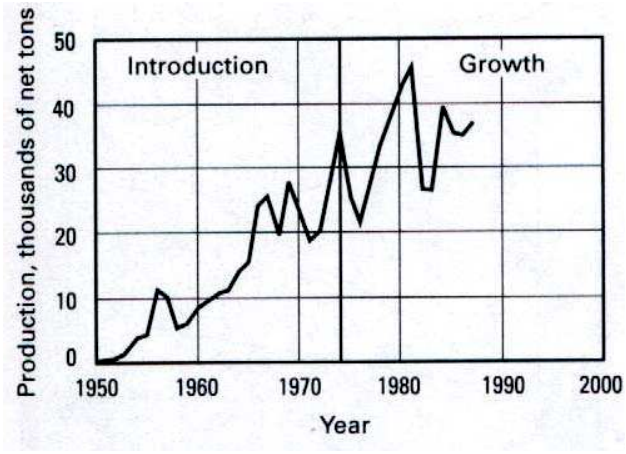

Figure 2.7 - Phases of titanium product life cycle in the U.S. (ASM HANDBOOK, 1998).

This Figure shows the rapid growth of the U.S. titanium industry as well as the phases of titanium product life cycle. Despite continued development of new alloys and product forms, titanium has moved rapidly through its product life cycle to maturity in the aircraft

industry. Titanium is still in growth stage in applications where corrosion resistant is required, such as the marine and biomedical industries. Due to their low strength-to-weight ratio, tensile strength up to 1200 MPa and capability of operating at temperatures from sub zero to 900°C (ASM HANDBOOK, 1998), titanium alloys are widely used for highly loaded aerospace components that operate at low to moderately elevated temperatures, including both airframe (fittings, bolts, wing boxes, fuselage frames an panels, brake assemblies, hydraulic tubing etc) and aero-engine components (discs, blades, shafts, afterburner cowlings, bolts, hot-air ducts casings from the front fan to the last stage of the high pressure compressor, and at the rear end of the engine for lightly loaded fabrications such as plug and nozzle assemblies). Polymer matrix composite (PMC) compatibility has also becoming an important issue with higher utilization of composite structure on aircraft. The titanium is galvanically compatible with the carbon fibres in the composites, whereas aluminium (and low alloy steels) and carbon generate a significant galvanic potential. The selection of titanium for this application is related to the critically of the structure. There are corrosion protection systems which are used to isolate aluminium from carbon composites to preclude the corrosion problem, but the integrity of the coating over the life of the airframe must be taken into account (BOYER, 1996).

Other applications of titanium alloys are in the automotive industry (valve and suspension assemblies, cam belt wheels, steering gear, connecting rods, drive shafts, crankshafts, high strength fasteners) (Figure 2.6 (b) and (c)); construction/architecture (facing and roofing, concrete reinforcement, monument refurbishment); chemical processing (storage tanks, pumps, frames, pressurized reactors, piping and tubing); marine equipment (deep-sea pressure hulls, submarines, submarine ball valves, data logging equipment, lifeboat parts, cathodic protection anodes); machine tools (flexible tube connections, protective tubing, instrumentation and control equipment); cutting implements (scissors, pliers, knives) and consumer products (jewellery, watches, camera shutters, bicycle frames, tennis rackets, horse shoes, target pistols).

The most widely used titanium alloy is the Ti-6Al-4V alpha-beta alloy. This alloy was first introduced in 1954 and nowadays accounts for about 60% of the total titanium production. It is processed to provide mill-annealed or β-annealed structures and is sometimes solution treated and aged. Ti-6Al-4V is extensively used in the aerospace industry, in all mill product forms, for airframe structural components (80%-90%) and other applications requiring strength at temperatures up to 315ºC, because of its outstanding strength-to-weight

ratio relative to other materials (BOYER (1996), ASM HANDBOOK (1998)). Other applications are for high-strength prosthetic implants and chemical-processing equipment. Its tensile strength can reach up to 1100 MPa (ASM HANDBOOK, 1998). Ti-6Al-4V-ELI (extra-low interstitial) alloy possesses reduced interstitial impurities, which improves ductility and toughness. This grade is designed for cryogenic applications and fracture-critical aerospace applications. Ti-6Al-4V alloy has limited section size hardenability hence is most common used in the annealed condition. This alloy is very forgiving with variations in fabrication operations, despite its relatively poor room-temperature shaping and forming characteristics when compared to steel and aluminium. It also has useful creep resistance up to 300ºC and excellent fatigue strength and fair weldability (ASM HANDBOOK, 1998). As a basis for comparison, some of important properties of Ti-6Al-4V alloy and of AISI 1045 steel are given in Table 2.4(MACHADO; WALLBANK, 1990).

Table 2.4 - Properties of Ti-6Al-4V alloy compared with a medium carbon steel, AISI 1045 (MACHADO; WALLBANK, 1990).

Material	Tensile Strength (MPa)	Yield Strength (MPa)	Thermal conductivity ($W\ m^{-1}\ K^{-1}$)	Specific heat at 20-100ºC ($J\ kg^{-1}\ K^{-1}$	Hardness (HV)	Density ($g\ cm^{-3}$)	Elongation (%)	Reduction in area (%)	Modulus of elasticity tension (GPa)
Ti6Al4V annealed bar	895	825	7.3	580	340	4.43	10	20	110
Ti6Al4V solution treated and aged bar	1035	965	7.5	…	360	…	8	20	…
AISI 1045 cold drawn	625	530	50.7	486	179	7.84	12	35	207

Other titanium alloys are designed for particular application areas. They are: Ti-5Al-2Sn-2Zr-4Mo-4Cr (Ti-17) and Ti-6Al-2Sn-4Zr-6Mo designed for high strength in heavy sections at elevated temperatures; Ti-6242S, IMI 829 and Ti-6242 designed for creep resistance; Ti-6Al-2Nb-1Ta-1Mo and Ti-6Al-4V-ELI designed to resist stress corrosion in aqueous salt solutions and for high fracture toughness; Ti-5Al-2.5Sn and the grade ELI designed for weldability and cryogenic applications, respectively; Ti-6Al-6V-2Sn, Ti-10V-

2Fe-3Al designed for high strength at low-to-moderate temperatures (ASM HANDBOOK, 1998).

Due to the expensive cost of titanium alloys, relative to other metals, owing to the complexity of the extraction process, difficulty of melting and problems during fabrication and machining, integrated researches have been established in many countries to improve the machinability of titanium alloys. Success in the machining of aerospace alloys, especially titanium alloys, will depend on the correct selection of cutting tool (s), cutting environment and appropriate cutting conditions for each machining operation (NORTH, 1986).

2.4 Machining Operations

Machining can be defined as a process in which parts with desired shape, size and finish are obtained by removing unnecessary or excess material in form of swarf or chips (GHOSH; MALLIK, 1986). Machining process is perhaps the most versatile manufacturing process. Figure 2.8 illustrates schematically the main components involved in a conventional machining operation (cylindrical machining or turning). It is common to use the term “metal cutting” to refer to the machining process. Modern metal cutting produces many chips and controlled chip formation is a prerequisite for any operation of metal removed (WATERS, 2000).

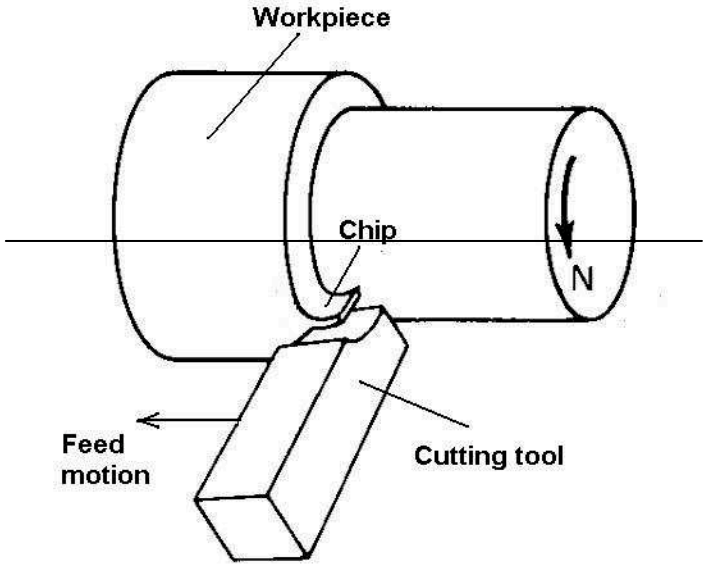

Figure 2.8 - Metal cutting diagram (WATERS, 2000).

Machine tools are generally designed for specific machining operations based on features that are mainly related to how the relative motions are generated and on the cutting tools employed. According to the British Standard Institution Publication (BRITISH STANDARD, 1972), the important motions in machining are:

1. Primary Motion: also referred to as cutting motion. It is responsible for the cutting action between the tool and the workpiece;
2. Secondary Motion: this motion is responsible for gradually feeding the uncut portion, and thus also known as feed motion. This in addition to the primary motion, leads to repeated or continuous chip removal and the creation of a machined surface with the desired characteristics. This motion may proceed continuously or by steps;
3. Resultant Motion: motion resulting from simultaneous primary and secondary motion.

2.4.1 Terminology used in Metal Cutting

The following useful terminologies are used to describe metal cutting operations (BRITISH STANDARD, 1972) and illustrated in Figure 2.9 (KALPAKJIAN; SCHMID, 2000):

- Cutting Speed (V): is defined as the rate at which the surface of workpiece being machined moves across the cutting edge of the tool and measured in metres per minute (m min^{-1}). The following formula, Equation (2.1), is used to calculate the cutting speed:

$$V = \frac{\pi \times d \times n}{1000} \tag{2.1}$$

Where d is the diameter of the workpiece material

n is the spindle speed expressed in revolutions per minute (rev min^{-1});

- Feed Rate (f): is defined as the distance that the tool travels in an axial direction during each revolution of the workpiece material and expressed in millimetres per revolution (mm rev^{-1});
- Depth of Cut or width of cut (DOC or w): is defined as the thickness of the unwanted material removed from the workpiece in the radial direction and expressed in millimetres (mm);
- Work Surface: the surface on the workpiece to be removed by machining operation;

- Machined Surface: the desired surface formed on the workpiece which is produced by the action of the cutting tool;
- Transient Surface: the part of the surface of the workpiece which is formed by the cutting edge and removed during the following cutting revolution or stroke of the tool or workpiece material;
- Metal Removal Rate (MRR): this is the product of the cutting speed, feed rate and the depth of cut, and is a parameter often used to determine the efficiency of a machining process given by the Equation (2.2). It is expressed in cm3 min-1:
- MRR = V× f × DOC • (2.2)
- Tool Life Line (L): is the product of the cutting speed and tool life (T). This is the parameter that can determine the optimum cutting speed when machining at a given feed rate and depth of cut. The tool life line is calculated by the Equation (2.3) and is expressed in metres (m):

$$L = VxT \quad (2.3)$$

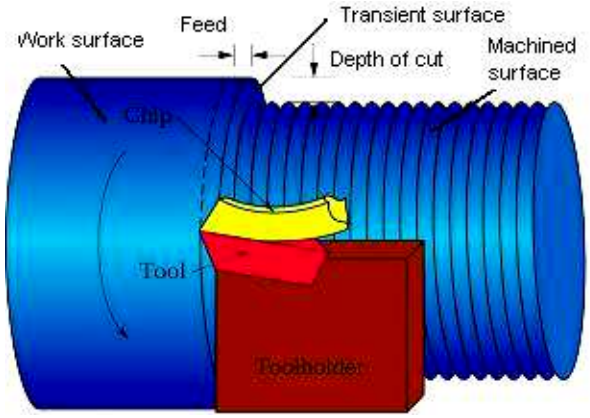

Figure 2.9 - Basic machining operation and important parameters (KALPAKJIAN; SCHMID, 2000).

Cutting tools that can be used in machining are classified into three groups:

1. Single-Point Tools: these are cutting tools that have one cutting part and one shank as illustrated in Figures 2.10 (a). Although these tools have traditionally been produced from solid tool-steel bars, they have been largely replaced by carbide or other indexable inserts of various shapes and sizes, as shown in Figure 2.10 (b). Turning operation is probably the most common of all the machining processes. It is

defined as the process for generating external surfaces (BOOTHROYD; KNIGHT (1989), KALPAKJIAN; SCHMID (2000)). The workpiece material in the form of a cylindrical bar is held in the chuck of a lathe and rotated about the axis of symmetry while the cutting tool is held in a tool post and moved with a feed motion parallel to the workpiece axis (Figure 2.11). Single point tools can also be used in other cutting operations such as shaping, boring, trepanning and threading (BOOTHROYD; KNIGHT, 1989).

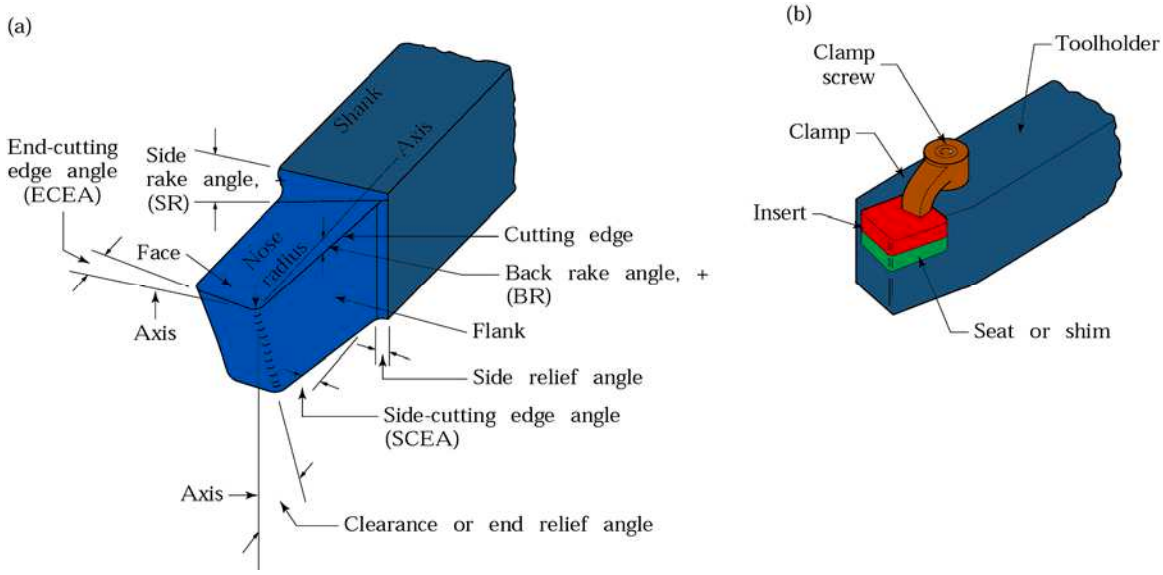

Figure 2.10 - Schematic illustration of typical single-point cutting tool with the tool angles (KALPAKJIAN; SCHMID, 2000).

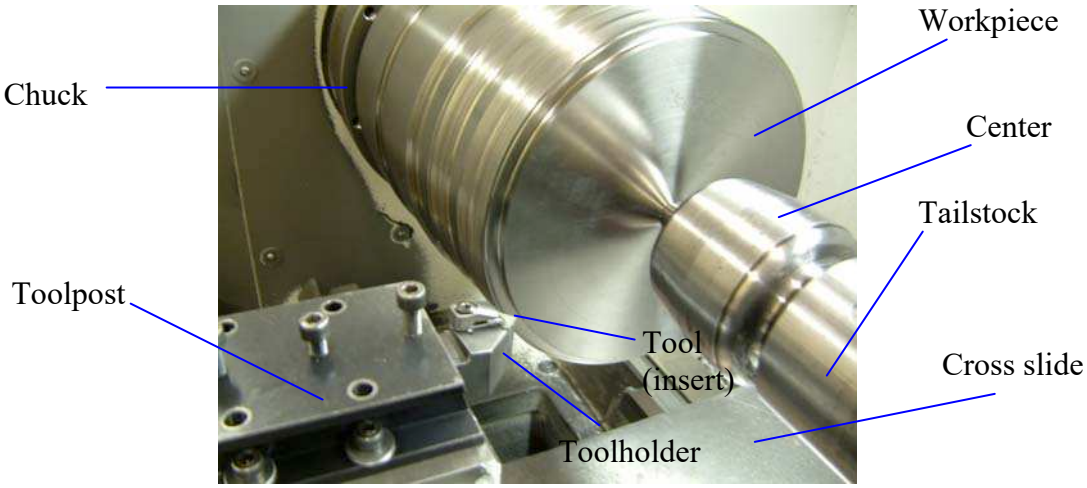

Figure 2.11 - Workpiece-tool-machine system for turning operation.

2. Multi-Point Tools: are cutting tools that have a more than one cutting part and they are secured to a common body such as drills, milling cutters, reamers, etc. The majority of multipoint tools are intended to be rotated and have either a taper or parallel shank for holding purposes or a bore through which a spindle can be inserted. Milling is the most common operation using muilti-points tools. Unlike turning operation, with the standard method of milling the tool rotates on its own axis, in a fixed position, and the workpiece is brought into contact with this rotating tool. The workpiece is then moved in the required direction to carry out the machining process (Figure 2.12). Other cutting operations that use multi-point tools are drilling, reaming, tapping, broaching and sawing (BOOTHROYD; KNIGHT, 1989);

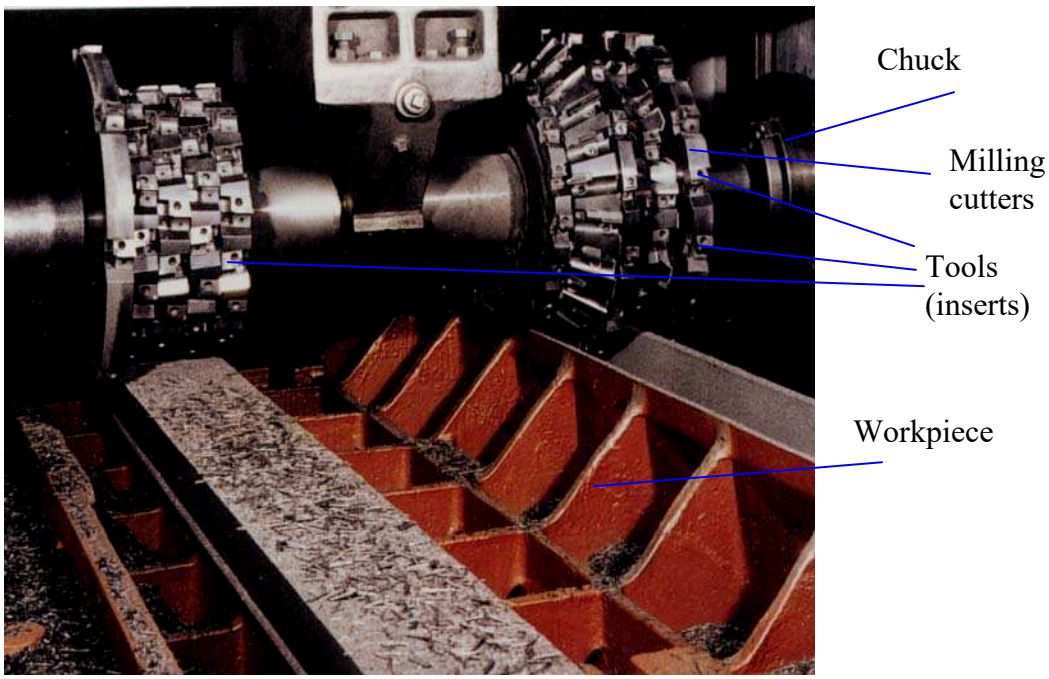

Figure 2.12 - Form-milling operation with gangs of side and face milling cutters (AB SANDVIK COROMANT, 1994).

3. Abrasive Wheels: these are cutting tools with a large number of small cutting parts that are randomly shaped and oriented. The machining process that uses abrasive wheels as a cutting tool is termed abrasive machining. The most common abrasive machining process is grinding where the abrasives are bonded to the shape of a wheel (or grinding wheels) which rotates at a high speed. Grinding wheels consist of individual grains (each grain is considered as small cutting part) of very hard

material (usually silicon carbide or aluminum oxide) bonded in the form required. Typical shape of abrasive wheels are cylindrical, disc-shaped, or cup shaped. The other finishing operations using abrasives are honing and lapping (GHOSH; MALLIK, 1986).

2.4.2 Nomenclature of Cutting Tools

In this Section more emphasis will be placed on nomenclature of single-point cutting tools. Figures 2.9 and 2.10 (a) show the general terms used for single-point cutting tools.

The part of the tool engaged in the cutting process is characterised by the rake and flank faces.

- Rake Face: the surface or face of the tool over which the chip flows during the machining process;
- Flank Face: the surface of the tool in contact with the freshly cut surface of the workpiece. The part of the flank which intersects the rake face to form the cutting edge is termed major flank. The remaining part of the flank, which is not actually engaged in cutting and intersects the rake face, is called the minor flank or minor clearance face (See Figure 2.10 (a)).

In order to prevent interference and rubbing of the freshly cut surfaces against the tool, clearance angles are provided on both the flank faces. The one on the major flank face is called the clearance angle and the one on the minor flank face is called the end clearance angle. In order to strengthen the cutting wedge a radius is always provided at the point where both the flank faces meet. This is called the nose radius.

System of planes are generally used to better define and specify the angles of a cutting tool. If one point on the cutting edge is selected and a reference system of planes is located in this point. The two major systems of planes are known as "*tool-in-hand-system*" and "*tool-in-use-system*" (Figure 2.13) (BOOTHROYD; KNIGHT, 1989). The former is used to define the geometry of the tool for its manufacture and measurement, while the later is used to specify the geometry of the cutting tool when it is performing a cutting operation. Other detailed definitions can be found elsewhere (BOOTHROYD; KNIGHT (1989), BRITISH STANDARD (1972)).

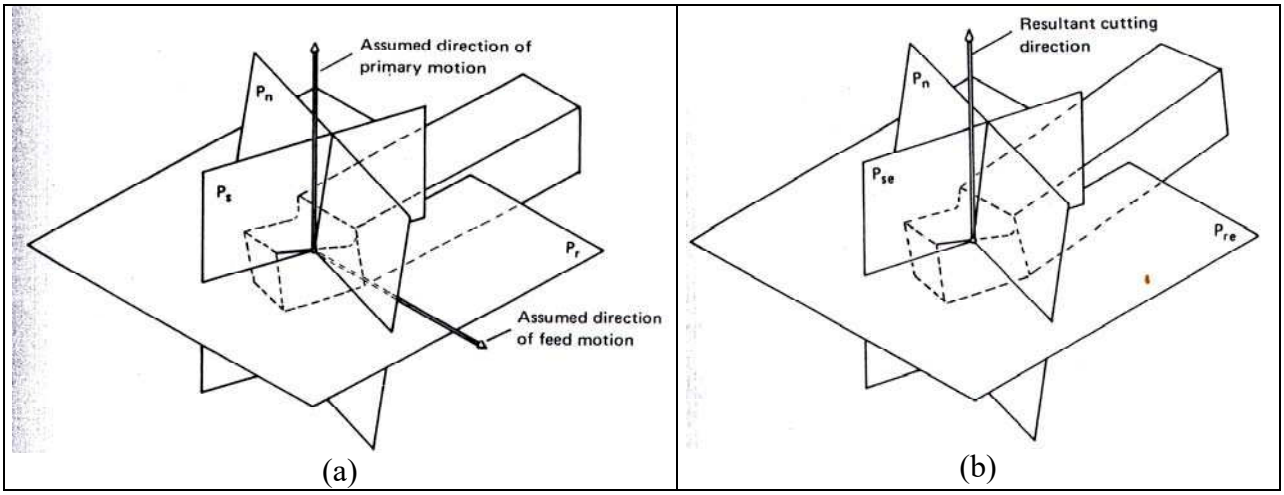

Pn: cutting edge normal plane
Ps: tool cutting edge plane
Pr: tool reference plane

Ps: working cutting edge plane
Pr: working reference plane

Figure 2.13 - Cutting tool planes: (a) *"tool-in-hand"* planes and (b) *"tool-in-use"* planes (BOOTHROYD; KNIGHT, 1989).

Angles derived from "*tool-in-hand-system*" are called "*tool angles*" and angles derived from the "*tool-in-use-system"* are known as "*working angles*". These angles are showed in Figure 2.14 and listed below:

- Tool cutting edge angle (k_r);
- Tool minor cutting edge angle (k'_r);
- Tool included angle (ε_r);
- Tool cutting edge inclination angle (λ_s);
- Tool normal rake angle (γ_n);
- Tool normal clearance angle (α_n);
- Tool normal wedge angle (β_n).

In the suffix after the symbol of the angles of "*tool-in-hand"* planes (Figure 2.13) represents the plane of the system in which the angle is measured. The suffix 'r' refers to the plane Pr (tool reference plane) that is parallel to the tool base. The suffix 's' refers to the plane Ps (tool cutting edge plane), which is tangential to the cutting edge and perpendicular to the Pr plane. The suffix 'n' refers to the plane Pn (cutting edge normal plane), which is perpendicular to the cutting edge. For the "*tool-in-use"* planes the suffix 're' refers to the

plane Pre (working reference plane) which is perpendicular to the resultant cutting direction; the suffix ‘se’ refers to the plane Pse (working cutting edge plane) which is tangential to the cutting edge and perpendicular to the working reference plane Pre and the suffix ‘n’ refers to the plane Pn (cutting edge normal plane), which is perpendicular to the cutting edge.

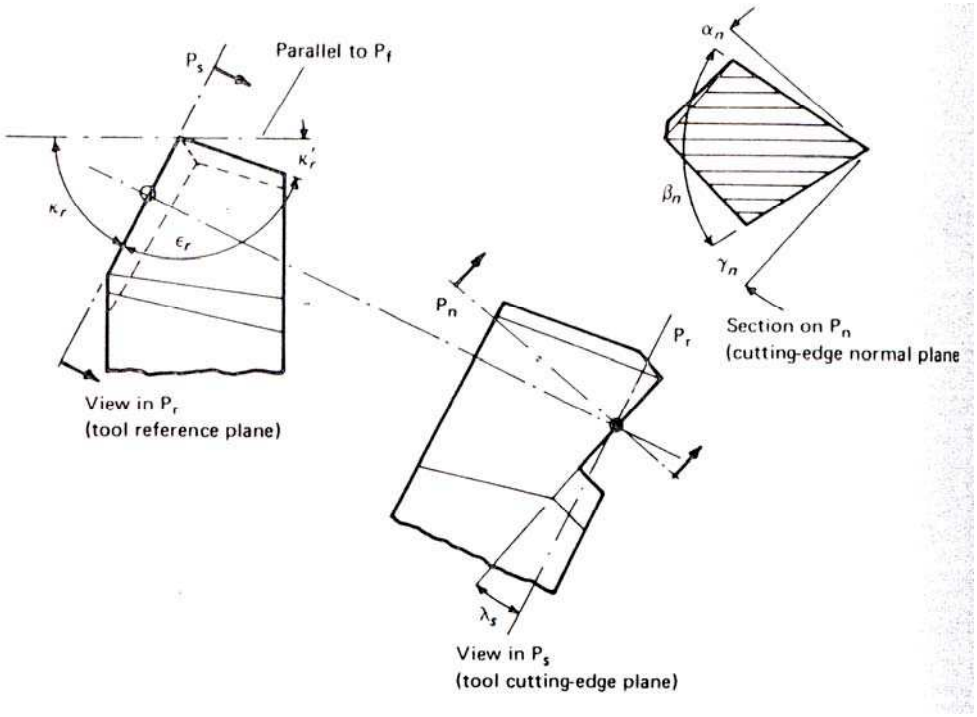

Figure 2.14 - Tool angles for a single-point tool according to the ISO: tool cutting edge angle (k_r), tool minor cutting edge angle (k'_r), tool included angle (ε_r), tool cutting edge inclination angle (λ_s), tool normal rake angle (γ_n), tool normal clearance angle (α_n) and tool normal wedge angle (β_n) (BOOTHROYD; KNIGHT, 1989).

.

2.5 Chip Formation Process

The understanding of the metal cutting process is much about the behaviour of various types of metals during deformation to produce chips. Many parameters in metal cutting, such as tool wear, friction between the tool rake face and the chip, cutting forces, temperature, surface finish, machined surface integrity and machining power are related to the process of chip formation. In this context, understanding the mechanisms and process of chip formation is essential as the fundamental knowledge can help in resolving practical problems (XIE; BAYOUMI; ZBIB, 1996) as well as in optimising cutting conditions to increase the production rate which will further reduce the production costs. The type of chips produced

during metal cutting depends on the material being machined and the cutting conditions employed.

Metal cutting is a process of removing a thin layer from the surface of a workpiece material by driving a wedge shaped tool asymmetrically into it. During this process two new surfaces are generated and the thin layer of material, termed chip or swarf undergoes deformation throughout its volume. The chip impinges on the tool rake face while moving in a direction away from the direction of motion of the workpiece. The chip then separates from the workpiece via shear deformation occurring along the shear plane.

The chip formation can be explained considering the "klmn" volume of metal travelling against the direction of the tool edge (Figure 2.15). As this volume of material passes through the primary shear zone (boundary between the unsheared work material and the body of the chip), it deforms plastically to a new shape "pqrs". As shearing continues, the volume (chip) slides across the rake face of the tool and then it is forced to change direction, experiencing a curvature and eventually curling. When the strain in the chip reaches a critical value, the chip fractures and the process begins over again (SHAW, 1984). This region, the interface between the tool and the chip on the rake face, is termed secondary shear zone. The chip is thicker than the actual depth of layer to be removed (underformed chip thickness or depth of cut, t_1), i.e., t_2 (actual chip thickness) > t_1 and the chip is correspondingly shorter. Also, the chip velocity (V_c) is, in the same proportion, smaller than the cutting speed V, i.e, $V > V_c$. With the purpose of simplification, the primary shear zone is assumed to be a plane, as illustrated in Figure 2.16 (THE METALS HANDBOOK, 1989). The shear angle, denoted by ϕ (schematically illustrated in Figures 2.15 and 2.16), is the angle between the shear plane and the direction of cutting and can be determined by direct measurement of t_1 and t_2 given by the Equation (2.4):

$$\tan\phi = \frac{r \times \cos\alpha}{1 - r \times sin\alpha} \tag{2.4}$$

Where r (the chip thickness ratio) = t_1/t_2, with r << 1, and α: tool rake angle.

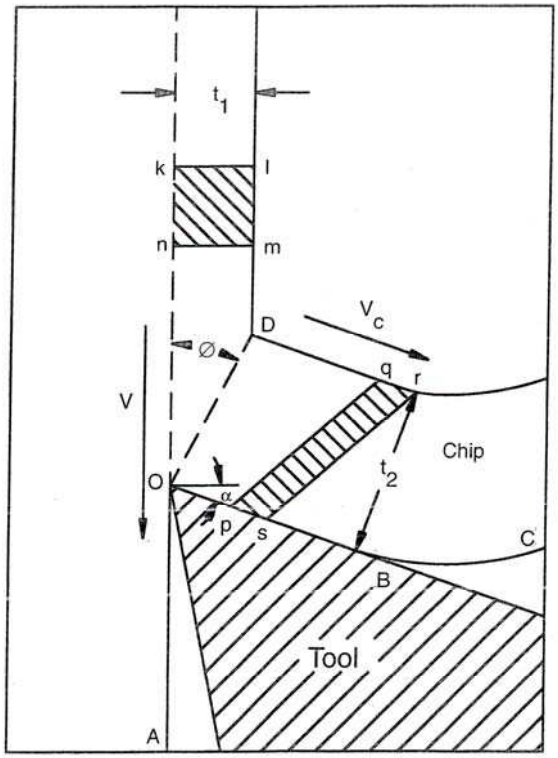

Figure 2.15 - Metal cutting diagram - the chip formation (TRENT; WRIGHT, 2000).

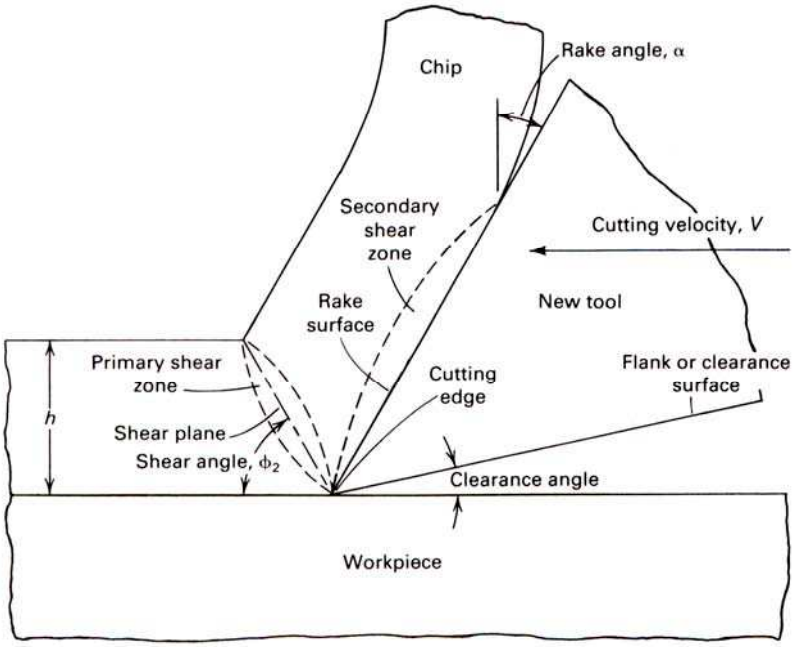

Figure 2.16 - Metal cutting diagram illustrating the primary and secondary shear zones (THE METALS HANDBOOK, 1989).

The shear strain within the primary shear zone is influenced by the value of the shear plane angle and has a significant effect on the chip form. Small shear plane angle means high strain and vice-versa. If the chip thickness ratio is big, the shear plane angle is small and the chip moves away slowly (e.g. for aluminium), while a large shear plane means a thin, high-velocity chip (e.g. for steel) (TRENT; WRIGHT, 2000). A higher strain rate favours the formation of discontinuous chips while lower strain rate produce continuous chips as the shear thickness of element ("klmn" volume of metal) is bigger. Because higher shear strain rate occurs at very short time interval, which does not allow the metal to recover from the strain, chip fractures into discontinuous chips. It is known that high energy is consumed in the secondary shear zone as a consequence of a resistance to chip motion. This resistance to chip motion reduces the shear plane angle and extends the length of the primary shear zone and vice-versa (WRIGHT; BAGHI; CHOW, 1982). The shear plane angle, ϕ, and thus the chip thickness ratio, r, therefore depend on the work material, the tool material, the tool geometry (mainly of tool rake face) and the cutting conditions. In order to determine the value of the shear plane angle (ϕ), Ernst & Merchant (1940) assumed the position of the shear plane would be take up such a value as to reduce the work done in cutting to a minimum, or in order words a value such that the shear stress acting upon the primary shear plane would be a maximum. The resulting expression is given by the Equation (2.5) (BOOTHROYD; KNIGHT, 1989):

$$2\phi + \rho - \alpha = ar\cot(k) \tag{2.5}$$

Where ϕ = shear plane angle; α = tool rake angle; k = constant for the work material, which is related to change of the shear strength with the compressive strength and therefore changes from material to material.

ρ = angle of chip friction, which can be calculated by the Equation (2.6):

$$\mu = \tan(\rho) = \frac{F}{N} \tag{2.6}$$

Where μ is the coefficient of friction, F is the force required to initiate or continue sliding and N is the force normal to the interface at which sliding takes place.

2.6 Classes of Chips

As commented in Section 2.5, the type of chip produced during metal cutting is mainly associated to the properties of the material being machined and the cutting conditions

employed. Based on these parameters, chips can be basically grouped into four classes (TRENT; WRIGHT (2000), BOOTHROYD; KNIGHT (1989)):

a) Continuous chips: These are usually formed when cutting ductile metals and alloys that do not fracture on the shear plane (TRENT; WRIGHT, 2000) such as aluminium, low alloys steels and copper. This chip can also be generated when machining single phase materials or multi-phase materials at high cutting speed and with tools that have larger rake angles (positive rake angles). Figure 2.17 (a) shows the schematic representation of this chip type. In the process of cutting, highly distorted crystals in the chip are sheared off from the parent metal in the shear zone with very large amounts of shear strain, remaining in a homogeneous form and not fragmenting. Continuous chips are undesirable because they usually wrap themselves around the workpiece or get tangled around the tool holder, thus adversely affecting the surface finish generated and/or causing tool damage. In some cases machining has to be interrupted in order to clear them away. Cutting tools with chip breakers can be used to intermittently break the long continuous chips into pieces so that machining does not need to be interrupted. Continuous chips may adopt many shapes – straight, tangled or with different types of helix;

b) Continuous chips with built-up-edge (BUE): They are a variation of the continuous chips observed at the chip-tool interface when cutting a certain group of materials (those with two phases in their structures) at lower cutting speeds (Figure 2.17 (b)). BUE formation involves work hardening and crack initiation/propagation when particles of the workpiece material weld to the rake face of the tool during machining**.** The BUE is a dynamic structure that consists of successive layers of material from workpiece which are gradually deposited on the tool rake face (tip of the tool), Figure 2.15 (b). As the deposition becomes larger it displaces the chip from direct contact with the tool. When the size of the BUE reaches a certain value, at which the resolved shear stress is high enough to shift the shear zone into the BUE, parts of its structure is carried away on the work surface or on the underside of the chip. Detailed information on BUE formation is available elsewhere in (TRENT; WRIGHT (2000), MACHADO; WALLBANK (1990)). The occurrence of BUE is an important factor that affects surface finish and tool wear;

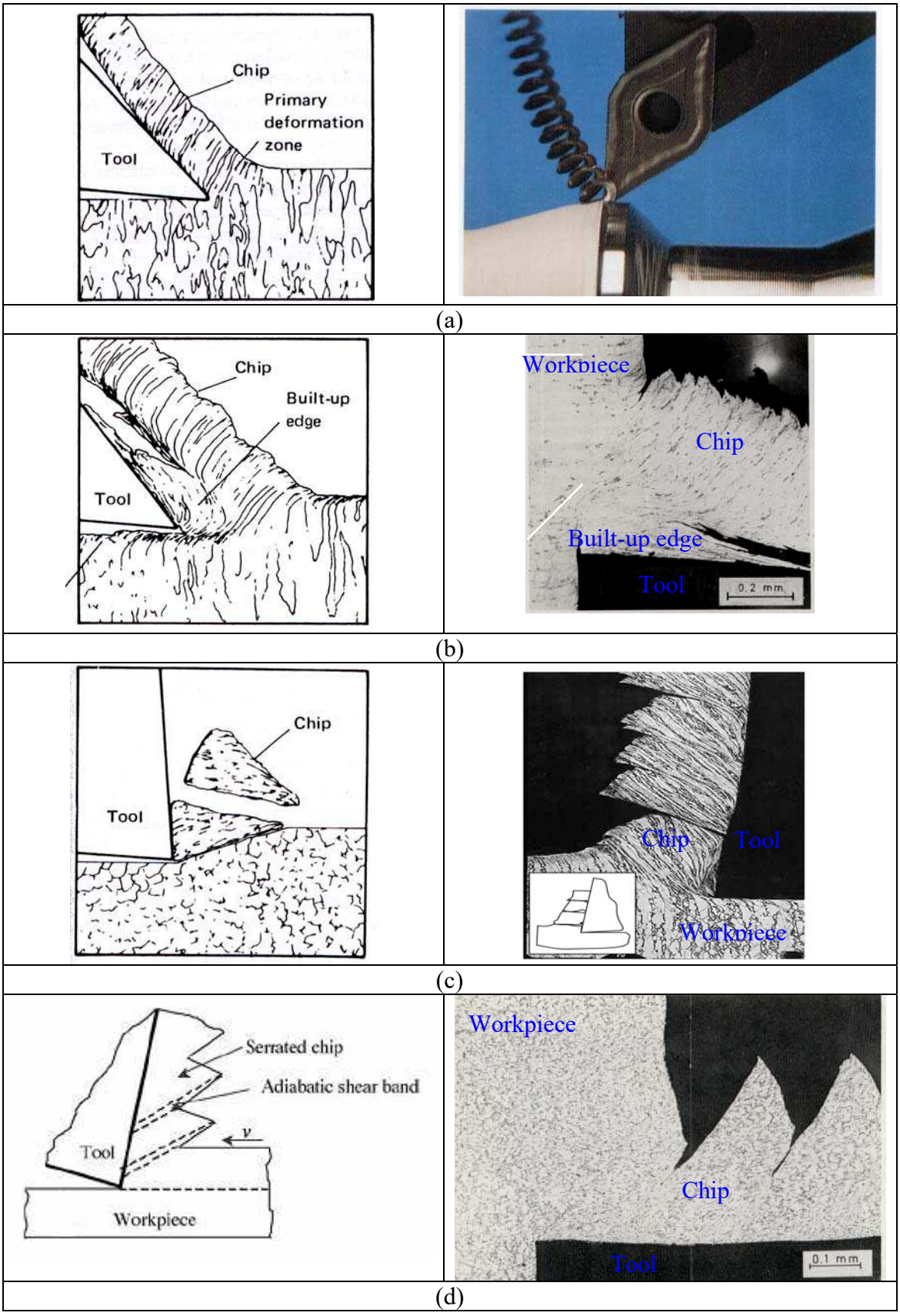

Figure 2.17 - Classes of chips: (a) Continuous chip, (b) Continuous chip with BUE, (c) Discontinuous chip, (d) Serrated chips (TRENT; WRIGHT (2000), MACHADO; WALLBANK (1990), KALPAKJIAN; SCHMID (2000)).

c) Discontinuous chips: These are usually produced when machining brittle materials containing inclusions and impurities at low or high cutting speeds with large depth of cut and using tools with small rake angles. Impurities and hard particles increase the possibility of crack propagation in the material while bigger depth of cut increases the chances of cutting through such defective regions resulting in generation of discontinuous chips. The chips are produced when the work material is not able to sustain large amounts of severe strain without fracture (Figure 2.17 (c)). With increasing cutting speed the chip tends to become more continuous because it is more difficult for contaminants to penetrate at the interface and reduce the constraining force;

d) Serrated chips: Also designated as segmented chips or "saw toothed chips" and described as chips with variation in thickness. The strain involved here is confined to narrow bands between segments with very little deformation within these segments. Adiabatic shear may occur during chip formation, particularly when machining materials exhibiting poor thermal conductivity and high strength that decreases abruptly with temperature such as titanium alloys. In this case serrated chip forms due to unstable adiabatic shear. Komanduri and Brown (1981) proposed that a mechanism of instability in the primary shear zone is based on the behaviour of certain polycrystalline metals at large strains under combined shear and compression, exhibiting negative shear stress-shear strain characteristics and involving microcracking. Serrated chips have saw tooth like appearance as illustrated in Figure 2.17 (d). Tool wear is adversely affected by the formation of serrated chips.

2.7 Forces in Metal Cutting

The understanding of the forces acting on the cutting tool and the study of their behaviour are of vital importance in the design and manufacture of machine tools and their components as well as in optimising tool design and controlling the surface finish and surface integrity of machined components. The cutting forces also act as a machinability index.

The cutting force can be defined as the force exerted by the tool cutting edge on the workpiece material to promote chip shearing. The relative motion between the workpiece material and the cutting tool is responsible for generation of this force. Component forces in a machining process can be resolved into three components in an orthogonal reference system usually involving the machine tool coordinate system (Figure 2.18 (a)). These three components forces are represented by cutting force (F_c), feed force (F_f) and the radial force (F_r) (also called the thrust force). The cutting force is usually the largest force acting on the tool rake face in direction of the cutting velocity. Feed force acts parallel to the direction of the tool feed. The radial force acts to push the tool away from the workpiece in the radial direction. This force is usually the smallest of the force components in semi-orthogonal cutting and, for purposes of analysis of cutting forces in simple turning, it is usually ignored (DE GARMO; BLACK; KOHSER, 1999). Forces acting in metal cutting are generally measured with dynamometer which is a force-platform device that incorporates piezo-electric load cells.

The magnitude of component forces during a machining operation are mainly dependent to the work material and the cutting speed, feed rate, depth of cut, tool geometry, tool material, wear conditions of the tool and cutting fluids employed. The maximum compressive stress acts on the cutting edge and reduces to zero when approaching the end of the tool-chip contact zone. Turning materials which produce discontinuous chips tend to produce lower forces due to the shorter tool-chip contact length. During machining of materials with high strength, large forces are required due to the higher stresses on the shear plane which subsequently result in large amount of heat generated in the cutting zone. With the increase in heat the yield strength of the tool material falls rapidly (TRENT; WRIGHT, 2000). The large forces combined with high cutting temperature will also accelerate wear at the cutting edge during machining. Another factor which has important influences in cutting forces is the cutting speed. An increase in cutting speed increases the shear plane angle, this helps to generate thinner chips resulting in reduced tool-chip contact length, thereby causing a drop in cutting forces (JAWAID, 1982). Increase in cutting speed also increases the cutting temperature (TRENT; WRIGHT, 2000). The rise in temperature promotes the softening of work material, and thus a reduction in the shear strength on the shear plane. Reduction in shear strength leads to a decrease in the component forces. Component forces increases as the tool is worn out because the area of contact at the clearance face increases as the wear at the flank face progresses.

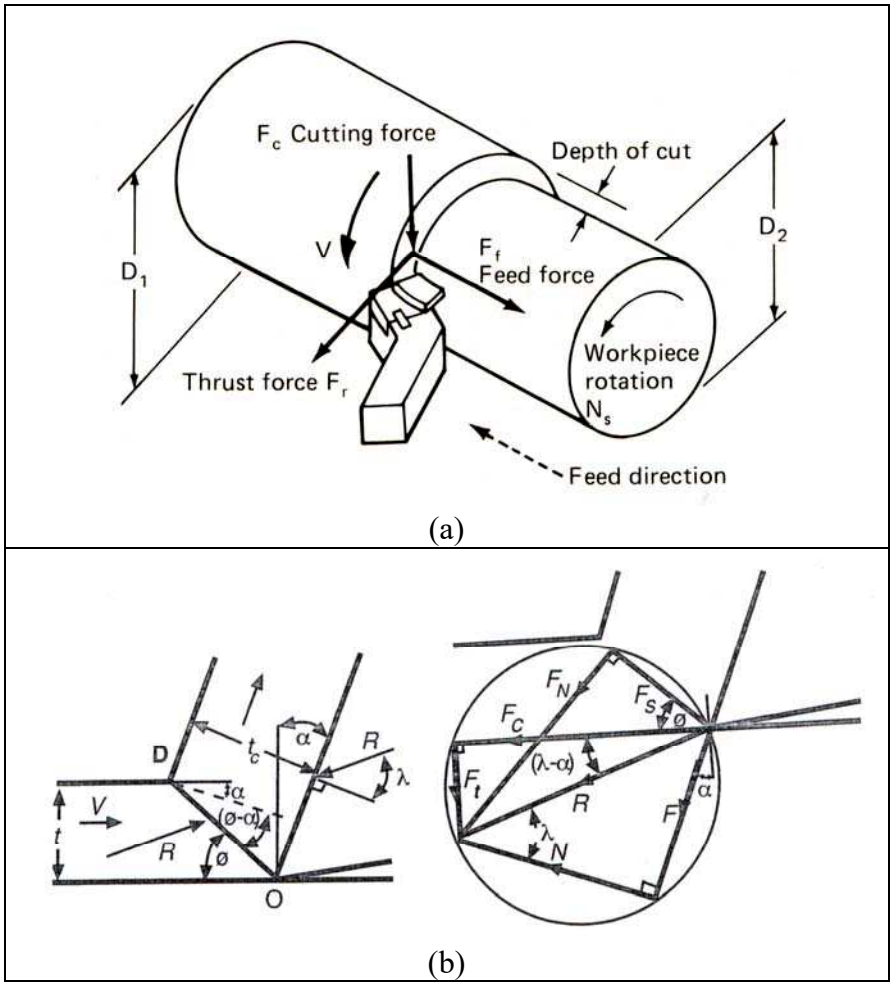

Figure 2.18 - Cutting forces a) Three components forces acting on the cutting tool (DE GARMO; BLACK; KOHSER, 1999) and b) Merchant´s circle (TRENT; WRIGHT, 2000).

Cutting tool geometry, especially the rake angle, also affects the component forces during machining. Tools with larger rake angles require lower cutting and feed forces and reduces the strength of the tool edge due to reduction of the included angle. Tools with negative rake angles are stronger because the higher included angle. Cutting fluids/lubricants can also influence the cutting forces acting to prevent seizure between the tool and workpiece material at lower speed conditions, thus reducing forces acting on the tool.

2.8 Stress and Strain Distribution in Machining

2.8.1 Stress Distribution

Determination of forces also helps to work out the stresses encountered by the tool during the cutting process. Assuming a uniform material distribution on the shear plane and at the tool-chip interface, forces can be resolved into normal and shear forces (stress) and calculated using the following expressions, Equations (2.7) and (2.8) (TRENT; WRIGHT, 2000):

Normal stress: $$\sigma = \frac{F_N}{A_S} \tag{2.7}$$

Shear stress: $$\tau = \frac{F_S}{A_S} \tag{2.8}$$

Where F_N and F_S are the normal and tangential forces acting on the shear plane respectively (Figure 2.18 (b)).

A_S is the area of the shear plane. In orthogonal cutting, it is calculate by the Equation (2.9):

$$A_S = \frac{f \times DOC}{sin\phi} \tag{2.9}$$

Where f is the undeformed chip thickness (feed), DOC is the depth of cut and ϕ = shear plane angle.

Therefore, the force required to form the chip depends on the shear yield strength of the work material under the cutting conditions and the area of the shear plane. The normal stress on the shear plane has no effect on the magnitude of the shear stress and decreases with increasing rake angle. The shear stress on the shear plane is independent of the rake face. The forces increase in direct proportion to increments in the feed rate and depth of cut, the two major variables under the control of the machine tool operator. For a zero-degree rake angle tool, the shear plane may vary from a maximum of approximately 45º to a minimum of 5º or even less (TRENT; WRIGHT, 2000).

According to Zorev (1963), on the rake face the compressive stress has a parabolic distribution, being zero where the chip loses contact with the tool and having a maximum value at the cutting edge, (Figure 2.19) and can be calculated by the Equation 2.10) (BOOTHROYD; KNIGHT, 1989):

$$\sigma_c = q \times x^y \tag{2.10}$$

Where x is the distance from the point where the chip loses contact with the tool, q and y are constants.

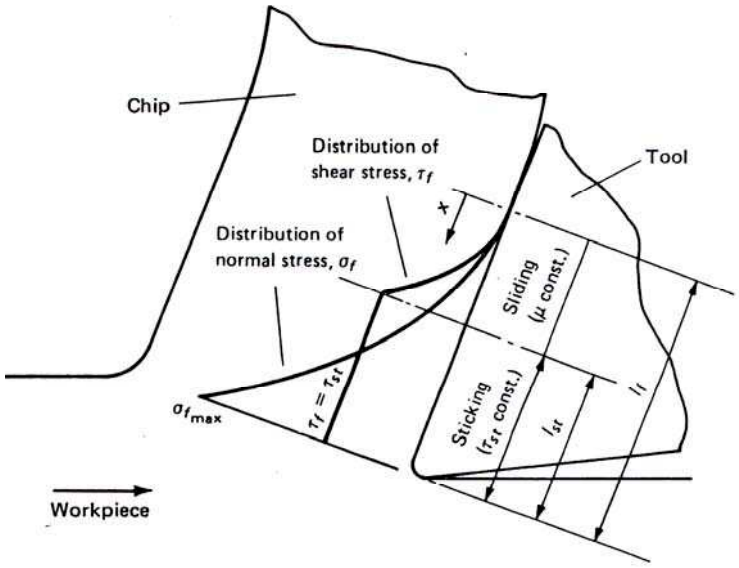

Figure 2.19 - The Zorev´s model of stress distribution on the rake face of a cutting tool in orthogonal cutting where σ_{fmax}= maximum normal stress, σ_f = normal stress, τ_f = shear stress, τ_{st} = shear strength of chip material in the sticking region (BOOTHROYD; KNIGHT, 1989).

Analysis of the stress distribution also showed that the shear stress is constant at the sticking region and equal to the shear strength of the work material. This stress drops to zero at the sliding region where the chip loses contact with the tool. When the stress is very high the tool is deformed downwards towards the clearance face. This form of deformation increases tool forces, and thus accelerating wear processes and consequently reducing tool life. Stress distribution also varies with the work material due to the frictional coefficient between chip and tool and the deformation characteristics of the work material (KATO; YAMAGUSHI; YAMADA (1972), CHILDS; MAHDI (1989)). As the cutting speed is raised, the temperature rises and the yield stress of the tool reduces. These tend to weaken the tool material resulting deformation.

2.8.2 Strain Distribution

Strain in machining is generally related to the shear strain at the primary shear plane (Figure 2.20) and calculated by the expression (Equation 2.11):

$$\delta = \frac{\Delta S}{\Delta Y} = \frac{\cos(\gamma)}{sin(\phi)x\cos(\phi - \gamma)} \tag{2.11}$$

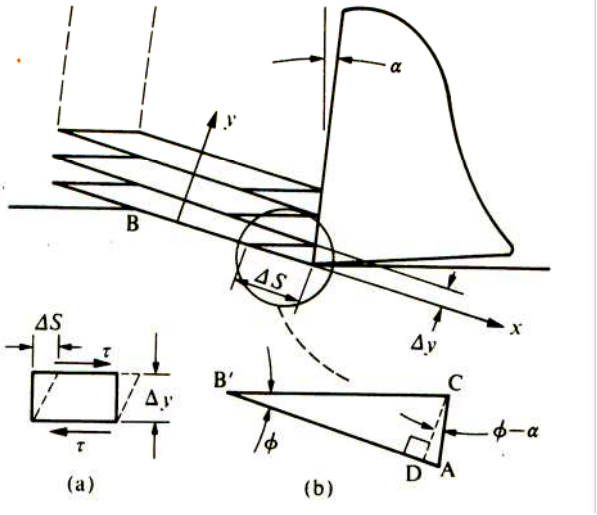

Figure 2.20 - The shear strain in the shear plane (SHAW, 1984).

When the chip thickness ratio is near to unity, i.e., the chip is thin, the shear strain is usually around 2. As this factor increases shear strain value may reach 5 or even greater (TRENT, 1988a). In the particular case of a serrated chip with adiabatic thermoplastic shear, the amount of strain in the flow zone is much higher than the strain in the primary shear plane. The ability of metals and their alloys to withstand such strains in the flow zone (zone of extremely intense shear formed on chip-tool interface) without fracture is attributed to the very compressive stresses in this region which inhibit the initiation of cracks, and cause the re-welding of such small cracks as may be started or already existed in the work material before machining (TRENT; WRIGHT, 2000). Serrated chips are mainly generated when machining titanium and its alloys. When machining such material the shear strain is around 8 within the shear bands and 1.3 within the segments, on the basis of metallographic observations (TURLEY; DOYLE; RAMALINGAM, 1982). Furthermore, the strain rate in the shear plane is up to 1000 s^{-1}, which is considered high (SHAW, 1984). Figure 2.17 (d) illustrates an adiabatic shear band.

A model of shear strain within the flow zone in the primary shear plane was proposed by Trent and Wright (2000). In this model the amount of shear strain increases with the distance from the body of the chip-flow zone interface to the tool rake face. Theoretically, the amount of shear strain becomes infinite at the tool face but laminar flow cannot be considered

as persisting closer to the tool surface than a few microns due to the surface roughness of the tools.

2.9 Heat Generation During Machining Operation

When a material is deformed elastically, some energy is spent to increase its strain energy, which is returned during unloading. For plastic deformation this is different. Here most of the energy used for shearing the workpiece is converted into heat. In a machining operation practically all of the energy involved is consumed either in plastic deformation or in friction. These essentially end up as thermal energy, heat (GHOSH; MALLIK, 1986). A small portion of the remaining energy is retained in the system as elastic energy while the rest is used for generation of new surface area.

There are three zones where the heat is generated during machining as shown in Figure 2.21 and listed below:

i) The primary shear zone, where significant deformation occurs. A large portion of the heat generated in this zone goes to the chip and the rest is conducted into the workpiece and raises its temperature, some times causing dimensional alteration of the workpiece;

ii) The secondary shear zone (the tool-chip interface). The heat generated in this zone is due to the sliding motion of the chip on the rake surface of the tool and is responsible for the rise in tool temperature. In this zone the chip also takes away the major portion of the heat.

iii) The workpiece-clearance face interface zone. The heat generated in this zone is due to friction of the work material against the flank face of the tool. This zone is considered less important, unless a very small clearance angle is used or the tool is severely worn. When sharp tools are employed, the contribution of this heat source zone is negligible GHOSH; MALLIK, 1986).

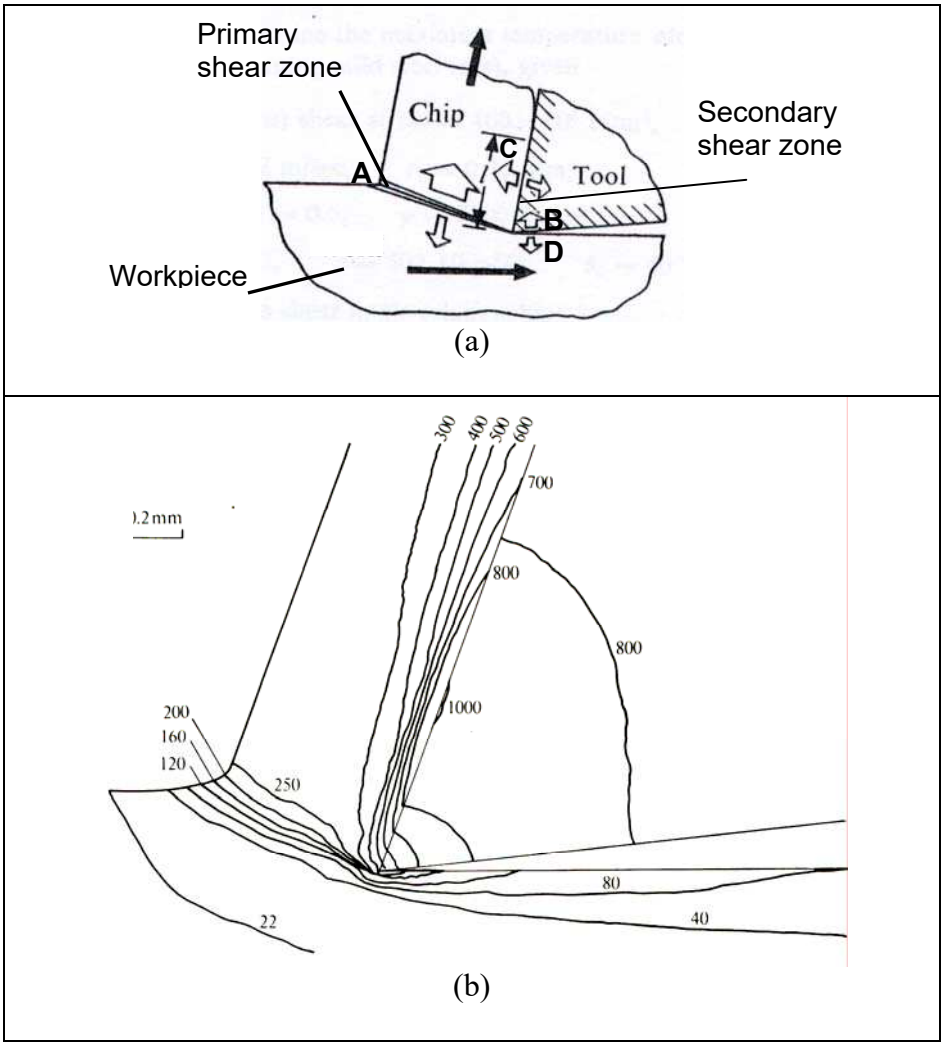

Figure 2.21 - Zones of heat generation during machining: (a) schematic diagram, (b) isothermal lines for dry orthogonal cutting of free machining steel with carbide tool ($\alpha = 20^{o}$) obtained from a finite element technique, at a cutting speed of 155.4 m min^{-1} and a feed rate of 0.274 mm rev^{-1} [adapted from SHAW (1984)]

2.9.1 Effect of Cutting Parameters on temperature generated during machining

Temperature influences the cutting action in several important ways, including (BEDDOES; BIBBY, 1999):

- Altering the properties of the machined surface;
- Causing dimensional changes to the work material and adversely affecting dimensional accuracy of machined component;
- Adversely affecting the strength, hardness and wear resistance of the cutting tool.

The strength and thermal conductivity of the work and tool materials influence the maximum temperature during machining. Increasing feed rate, cutting speed and depth of cut all influence also have significant effect on the cutting temperature, according to the relation given by the Equation (2.12):

$$T_M \ \alpha \ V^a \times f^b \times DOC^c \tag{2.12}$$

Where T_M is the mean cutting temperature, V is the cutting speed, f is the feed rate, DOC is the depth of cut and a, b and c are constants (a > b > c).

Reduction in hardness and wear resistance of the tool with increasing temperature is the major factor that adversely affects tool life. An increase in the metal removal rate leads to a proportional increase in temperature on the cutting tool. This has a direct influence on tool wear and tool life. The tool temperature may not be a critical problem during machining of low strength and low melting point materials such as aluminium and magnesium. However, when ferrous and other high strength materials such as cast iron, steel, nickel and titanium alloys are machined, temperature rises with the speed and the tool strength decreases, leading to a faster wear and consequent tool failure (TRENT; WRIGHT, 2000). Although machining at a high speed is desirable, for higher productivity, the faster tool wear due to the high temperature generated at the cutting zone will establish a limit to the practical cutting speed for each tool-work material pair. Different work materials, during machining, generate different amounts and patterns of heat. For example, the point of maximum temperature when machining titanium alloys is located at the tool rake face and on the flank face when machining nickel alloys (JAWAID, 1982).

When machining materials with high strength, large forces are required due to the higher stresses on the shear plane, leading to large amount of heat generation in the cutting zone. The large forces combine with high cutting temperatures generated will also accelerate failure of the cutting edge during machining An increase in cutting speed increases the cutting temperature (GHOSH; MALLIK (1986), BOOTHROYD; KNIGHT (1989)), consequently encouraging softening of the work material (TRENT; WRIGHT, 2000).

Some considerations regarding metallurgical parameters influencing temperature during machining were enumerated by Trent (1988b):

- The melting point of the main element of the work material. The higher the melting point the higher will be the temperature at the tool-work material interface for any cutting speed;

- Alloying elements which strengthen a metal promotes increase in temperature at the tool-work material interface at any metal removal rate;
- Introduction of phases into the work material that easily form sheared interface layers. They act reducing temperature.

2.9.2 Heat Generation and cutting temperature when machining titanium alloy

The understanding of heat generation process and temperature behaviour in machining of titanium alloys plays an important role in distribution of cutting tool temperature. The high temperatures generated close to the cutting edge of the tool are the principal reasons for the rapid tool wear commonly observed (TRENT; WRIGHT, 2000). In comparison with steel, the heat capacity of titanium and its alloys is much reduced. The consequence is that a considerably greater portion of heat that is generated during cutting enters into the tool because it cannot be removed with the fast flowing chip or bed into the work material due to the low thermal conductivity of titanium alloys, about 37% and 86% lower than the thermal conductivity of Inconel 718 alloy and AISI 1045 steel, respectively (MANTLE; ASPINWALL, 1998). About 80% and 50% of the heat generated is absorbed in the tool when machining titanium-base, Ti-6Al-4V, alloy and Ck 45 (AISI 1045) steel respectively (KONIG, 1979), as illustrated in Figure 2.22. When machining a titanium alloy at a cutting speed of about 30 m min^{-1} the temperature developed at the cutting edge of a carbide tool is about 704ºC, while for steel the temperature is about 538ºC (ZLATIN; FIELD, 1973). The influence of cutting speed on temperature generated when machining commercially pure titanium and various titanium alloys with cemented carbide (K10 grade) was investigated by Motonishi et al. (1987) (Figure 2.23). Increase in cutting speed resulted in higher cutting temperature. The cutting temperature of Ti-6Al-4V alloy was about 200ºC higher than pure titanium, S45C.

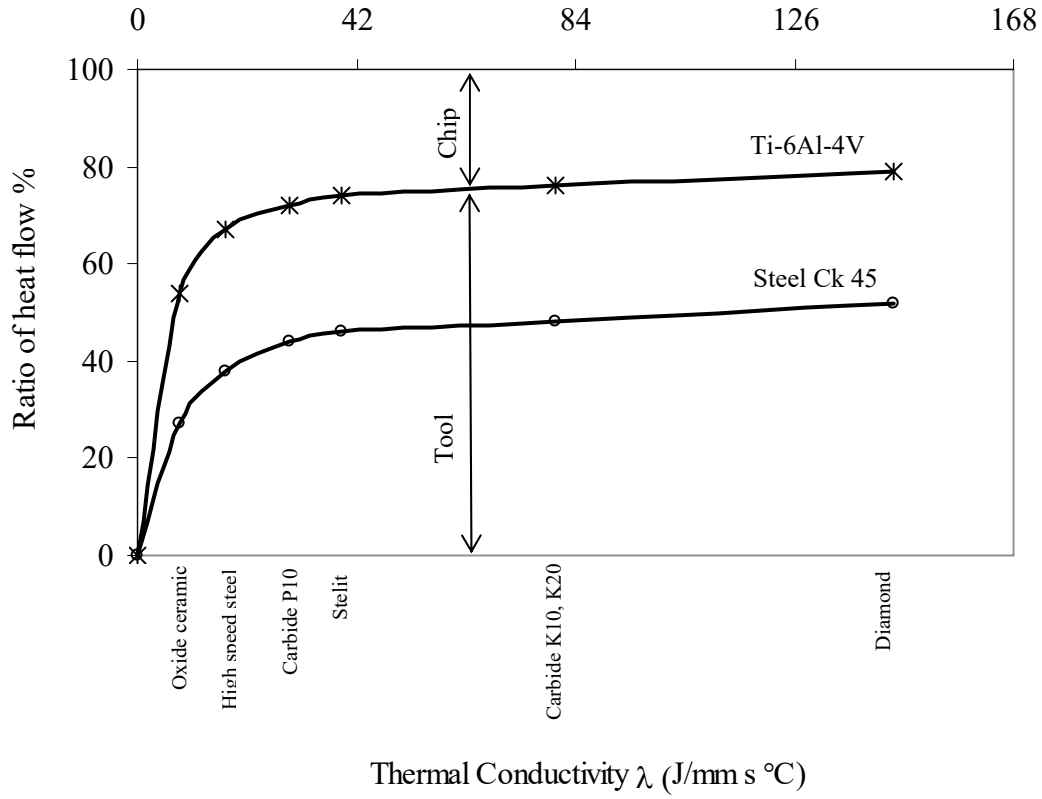

Figure 2.22 - Distribution of thermal load when machining titanium-base, Ti-6Al-4V and Ck 45 (AISI 1045) steel [adapted from KONIG (1979)].

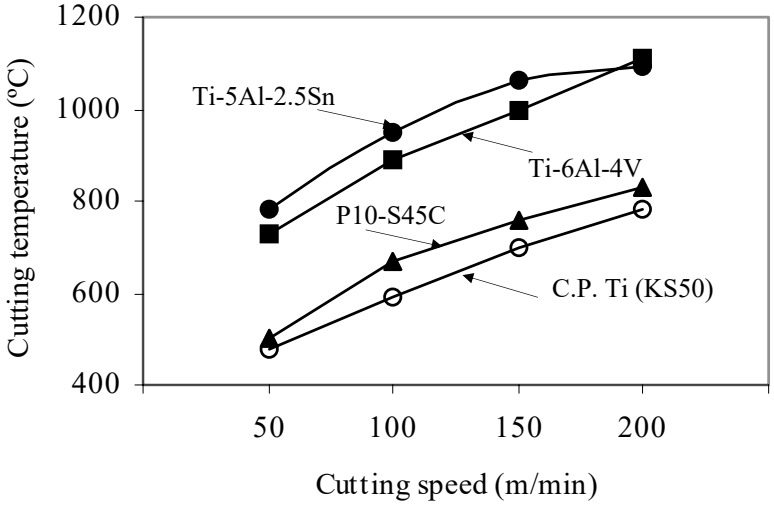

Figure 2.23 - Influence of cutting speed on the cutting temperature when machining titanium and its alloys [adapted from MOTONISHI et al. (1987)].

2.10 Tool Failure Modes

During machining, as the work material is cut, the tool edge degrades away causing a gradually alteration of tool shape, consequently affecting dimension, tolerance and the quality of machined part and associated reduction of the efficiency of the machining process. In metal cutting, progressive wear occurs on both the rake and the clearance faces of cutting tools. The type of tool wear depends on tool geometry, tool and work material and their physical, mechanical and chemical properties as well as cutting parameters and machining environment employed. Figure 2.24 shows diagrammatically typical tool failure modes (DEARNLEY; TRENT, 1985):

a) Flank wear
b) Rake face wear (crater wear)
c) Notch wear
d) Cutting edge chipping

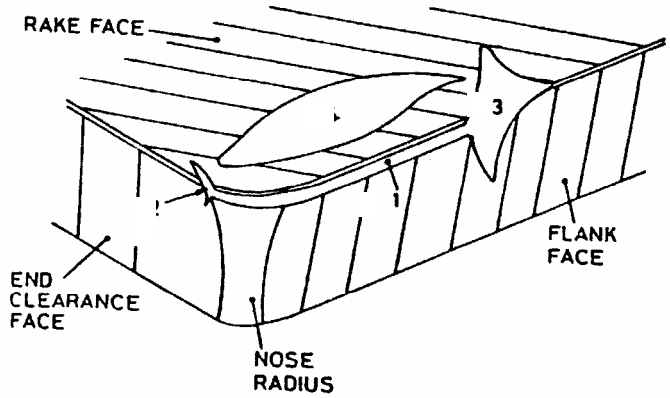

A: Flank wear; B: Rake face wear (crater wear); C: Notch wear; D: Cutting edge chipping
Figure 2.24 - Regions of wear on a cutting tool (DEARNLEY; TRENT, 1985).

a) Flank wear occurs at the flank face of the tool as the newly formed surface rubs against of the clearance face of the tool causing adhesive and/or abrasive wear which is enhanced by the rise in temperature during machining. The friction action causes the loss of relief angle on the clearance face of the tool, thereby resulting in wear. In general, the flank wear rate is high at the beginning of the cut, but decreases as the wear land (VB) reaches a critical value. As the cutting time progresses a second

critical value is reached. Further machining results in a rapid increase in flank wear rate. Machado (1990) observed that maximum flank wear (VB_{max}) was the predominant form of wear when machining titanium-base, Ti-6Al-4V alloy, with uncoated cemented carbides under conventional and high pressure coolant supplies. It was also observed that a layer of work material was always bonded to the tool, on the wear land and can some times be thicker, especially when machining with conventional coolant flow. Motonishi et al. (1987) reported that flank wear on carbide tools after machining titanium alloys is associated with fluctuations of cutting force caused by the serrated chips;

b) Rake face wear (crater) is generally associated with high temperatures generated at the chip-tool interface and occurs on the rake face of a tool due to a combination of diffusion and adhesion as the chip moves over the rake face of the tool. The maximum depth of the crater usually occurs near the midpoint of the contact length between the chip and the rake face, where the temperature is believed to be at a maximum. Excessive crater wear alters the geometry of the cutting edge and can adversely affect chip formation and weaken the tool because of the decrease in its yield strength (AB SANDVIK COROMANT, 1994). It was reported that during machining of titanium-base, Ti-6Al-4V alloy, with cemented carbides a shallow crater was initially formed on the rake face of the tool and a little flank wear was produced along the whole extension of the depth of cut (MACHADO, 1990). Additionally, the crater was formed close to the cutting edge and joining the flank wear;

c) Notch wear or groove formation occurs as a result of sliding wear when machining work materials which have their surfaces strained hardened from previous cuts or work hardened due to coolant effects and/or fluctuating temperature. Leading edge notching is a major problem when machining titanium and aluminium alloys (hardening by precipitation of γ’ phase) (RICHARDS; ASPINWALL, 1989). Stress concentration towards the unmachined surface due to the stress gradient and the presence of a burr at the edge of the freshly machined surface as well as the cut surface also contribute to the notch formation. Jawaid (1982) suggested that notching generally takes place under sliding conditions and disappears at cutting conditions where seizure takes place. It was also reported that the presence of different machining environments, such as gases like air, argon and nitrogen,

influence notch wear rate when machining nickel-base alloys with ceramic tool materials. Notching at the depth of cut was the predominant form of wear observed when machining nickel-base, Inconel 901 alloy, with various grades of carbides (MACHADO, 1990);

d) Cutting edge chipping is the process of plucking of small pieces of tool particles at the cutting edge of the tool. The chipped off particles can be small or large fragments. Unlike wear, chipping is not a gradual process. It occurs on a random and unpredictable manner and alters the geometry of the tool edge. Chipping is associated with mechanical shock due to impact, particularly in interrupted cutting. Excessive wear for the tool such as flank wear, crater wear and notching will increase cutting forces and weaken the tool. The presence of thermal cracks generated in interrupted cutting due to the thermal cycling can also lead to the generation of chipping and sudden failure of the cutting tool. High feed rates and depth of cut can also cause chipping. Chipping was observed when machining with tool materials with inadequate fracture toughness such as ceramic tools and finishing grades of tungsten carbide containing less than 3% weight of cobalt (SHAW, 1984).

2.11 Tool Wear Mechanisms

The understanding of the wear mechanisms of tools in metal cutting has great importance for improvement and development of better tool materials and designs in order to minimise tool wear. Detailed research into tool failure modes has suggested that wear in metal cutting is attributed to the following wear mechanisms schematically illustrated in Figure 2.25 and listed below (TRENT; WRIGHT, 2000):

a) Attrition wear
b) Abrasion wear
c) Diffusion wear
d) Plastic deformation

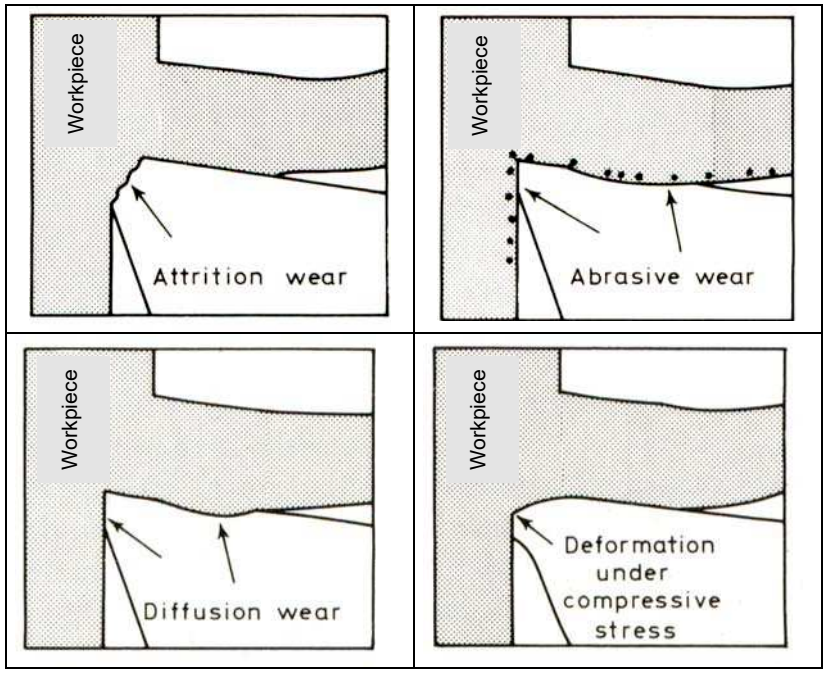

Figure 2.25 - The main wear mechanisms on a cutting tool [adapted from (TRENT; WRIGHT, 2000)].

a) Attrition wear is also known as adhesive wear and is a mechanism that occurs at relatively low cutting speeds which changes the geometry of the tool by mechanical detachment of small particles from tool surface which are carried away by the work material. Attrition wear is more related to the irregular flow of the chip as it passes the cutting edge and the ability of the tool to withstand the tearing action resulting from uneven flow under conditions of sliding. The high compressive stresses acting at the tool-workpiece interface causes adhesion at the asperity. Fragments of the work material are torn and carried along the tool edge. As the rubbing action of the tool against the workpiece continues the welded material breaks away carrying with it particles of the tool material. This is a process that involves random removal of whole grain or small fragments of the tool material resulting in rapid tool wear. The aspect of worn tool surface is uneven and nibbled away (TRENT; WRIGHT, 2000). The factors that influence and promote attrition wear are low speeds and feed rates, lack of rigidity of the machine tool, vibration and the formation of built-up-edge;
b) Abrasion wear involves the loss of tool material by a hard particles trapped between the tool and the work material. The particles could be dislodged tool materials, fragments of built-up-edge or hard carbides and oxides already existing in the workpiece. The high compressive stresses acting at the tool-workpiece interface

keep trapped hard particles between the machined surface and the tool. As the tool rubs over the machined surface, the particles plough through the tool removing material at the flank face. Abrasive wear at the rake face of the tool is due to sliding action of hard particles located at the under side of the chip as it passes over the rake face of the tool;

c) Diffusion wear involves exchange of atoms between the tool and work material at the tool-workpiece and the tool-chip interfaces. It is a mechanism that occurs at elevated temperatures. Other factors that influence the rate of diffusion tool wear are metallurgical relationship between the work material and the tool material (solubility). The feature characteristic of diffusion wear is the smoothness of the worn surface;

d) Plastic deformation occurs as a result of gradual crack growth caused by thermal shocks and compressive stresses acting on the rake face of the tool. Since there is no lost of tool material during plastic deformation, it is not considered a physical wear process. This process is more likely to occur at high feed rates or when machining materials with poor machinability characteristics like superalloys and certain steels that generate high temperatures and compressive stress which may lead to sudden fracture. Increase in localised stress and temperature can accelerate wear on the flank face or tool nose leading to the subsequent fracture.

2.12 Titanium Machinability

The initial studies on the machining of titanium alloys, the tool wear guidelines and the chip formation process, started around the 1950s in the United States and in France (COOK (1953), COLWELL; TRUCKENMILLER (1953), SIEKMANN (1955)). Titanium alloys are attractive material to designers in the aerospace industry because of their unique combination of strength and lightness despite their low thermal conductivity that concentrates heat generated during cutting at the cutting edge (YANG, 1970). They also exhibit high chemical reactivity, tendency to form adiabatic shears bands and/or rapid work hardening during machining (KOMANDURI; BROWN (1981), TURLEY; DOYLE; RAMALINGAM (1982), SHAW (1967), CHILD; DALTON (1968), KOMANDURI; VON TURKOVICH (1981)). These pose considerable problems in manufacturing hence titanium alloys have poor

machinability (FIELD (1968), EZUGWU; BONNEY; YAMANE (2003), EZUGWU; WANG (1997), HONG; MARKUS; JEONG (2001), MACHADO; WALLBANK (1990), DEARNLEY; GREARSON (1986), ZLATIN; FIELD (1973), MOTONISHI et al. (1987), DEARNLEY; TRENT (1985), MACHADO (1990), COOK (1953), COLWELL; TRUCKENMILLER (1953), SIEKMANN (1955), YANG (1970), SHAW (1967), CHILD; DALTON (1968), KOMANDURI; LEE (1984), JAWAID; CHE-HARON; ABDULLAH (1999), HONG; DING; JEONG (2001), EZUGWU; OLAJIRE; WANG (2002), VENUGOPAL et al. (2003)) and are referred to as difficult-to-machine materials. Machinability can be described as how easily a material can be cut to the desire shape (surface finish and tolerance) with respect to the tooling and machining processes involved. Efforts to improve the high temperature properties of titanium alloys usually impair their machinability (BOYER, 1996). Other factors and output variable such as tool life, quality of machined surfaces (surface texture, surface integrity and form tolerances), chip shape, component forces and power consumed during the machining operation are the main parameters that determine the machinability of a material. Reasons for the relatively poor machinability of titanium alloys have been discussed elsewhere and summarised below (FIELD (1968), SECO TOOLS (2002a), EZUGWU; BONNEY; YAMANE (2003), EZUGWU; BONNEY; YAMANE (2003), EZUGWU; WANG (1997), HONG; MARKUS; JEONG (2001), LOVATT; SHERCLIFF (2002), MACHADO; WALLBANK (1990), DEARNLEY; GREARSON (1986), ZLATIN; FIELD (1973), MOTONISHI et al. (1987), DEARNLEY; TRENT (1985), MACHADO (1990), COOK (1953), COLWELL; TRUCKENMILLER (1953), SIEKMANN (1955), YANG (1970), SHAW (1967), CHILD; DALTON (1968), KOMANDURI; LEE (1984), JAWAID; CHE-HARON; ABDULLAH (1999), HONG; DING; JEONG (2001), EZUGWU; OLAJIRE; WANG (2002), VENUGOPAL et al. (2003), OLOFSON (1965), CATT; MILWAIN (1968), LE MAITRE (1970), ZLATIN; CHRISTOPHER (1973), ZLATIN; CHRISTOPHER (1974), TURLEY (1981), LÓPEZ DE LACALLE et al. (2000)):

1. Resistance to plastic deformation needed to form chips due to the high strength of titanium alloys that is maintained at elevated temperatures during machining;
2. High "coefficient of friction" at the tool-chip interface;
3. Generation of thin chips with reduced contact area with the cutting tool. This is responsible for the generation of high stresses on the rake face of the tool during machining;

4. Chip formation by adiabatic or catastrophic thermoplastic shear process. The instability in the process of chip forming results in serrated (or segmented) chip;
5. Low modulus of elasticity of titanium alloys, which decreases quickly even at moderate temperatures can lead to chatter, deflection and unwanted rubbing of the tool to the freshly generated surfaces as well as bending of parts with thin walls and with lack of precision in their finish;
6. High rate of work-hardening of titanium alloys;
7. High chemical reactivity of titanium at elevated temperatures (> 550ºC) with most tool materials available and their consequent welding by adhesion onto the cutting tool during machining leads to excessive chipping and/or premature tool failure and poor surface finish;
8. The tendency of titanium alloys to ignite during machining at higher speed conditions due to the high temperatures generated;
9. The variations in the cutting and in the axial components of the cutting strength, cause chatter phenomena hence the need to have an stiff machine tool.

All these factors operating separately or in combination can cause rapid wear, chipping or even catastrophic failure of the cutting tools.

2.13 Tool Materials for Machining Titanium Alloys

The machining system comprises of the cutting tool, the workpiece and the machine tool. The cutting tool is the most critical in terms of machining productivity, therefore selection of the right cutting tool material for a specific application is of crucial importance. Other factors that contribute to the continuous development of cutting tool materials is the development of new materials (generally with decreasing machinability) and the increasing use of automated and numerically-controlled machine tools linked with systems which require higher degree of reliability and predictability of cutting tools employed. Regarding to tool cost, the cheapest tool material is not always considered the most economical nor is the most expensive tool the best for a specific machining operation. The best tool material is one that will maximise the efficiency and ensure accuracy at the lowest cost, in other words, the one that will satisfy the requirements of a specific workpiece material (OKEKE, 1999).

It is known that cutting tool materials encounter severe thermal and mechanical shocks when in machining titanium alloys. The combination of high temperature, high stresses, strong chemical reactivity of titanium, formation process of catastrophic shear (irregular) chips generated at and/or close to the cutting edge influence the wear rate and hence tool life. Flank wear, nose wear, crater wear, notching, chipping and catastrophic failure are the typical failure modes observed when machining titanium alloys. High Speed Steel (HSS) tool, coated and uncoated cemented carbides, ceramic tools and ultra-hard materials such as polycrystalline diamond and cubic boron nitride tools are the commercially available cutting tool materials for machining of difficult-to-machine materials. High Speed Steel (HSS) tools were widely used in earlier studies (DEARNLEY; GREARSON (1986), ZLATIN; FIELD (1973), COLWELL; TRUCKENMILLER (1953), YANG (1970), CATT; MILWAIN (1968), ZLATIN; CHRISTOPHER (1973)) on the machining processes of titanium at low cutting speeds because of their limitations and lower cost relative to carbides. Although they are still being used (KIM et al. (2001), SUN (1992)) for machining of titanium alloys at lower cutting speeds conditions, their application have became reduced since cemented carbide tools have proved their superiority in all machining processes of titanium alloys relative to competing tool materials. Uncoated straight grade of cemented carbide (WC-Co) tools are the most suitable for machining of titanium alloys due to their improved performance in terms of tool wear and lower cost relative to other commercially available tool materials (ZLATIN; FIELD (1973), JAWAID; CHE-HARON; ABDULLAH (1999), ZLATIN; CHRISTOPHER (1973), ZLATIN; CHRISTOPHER (1974), KONIG (1979)). Inferior performance of coated carbides tools (in terms of tool life) has been reported in many studies compared to uncoated carbide grade tools when machining titanium alloys (CHRISTOPHER (1973), (KONIG (1979). Recent developments in coating technology seem to demonstrate only negligible improvement in machining titanium alloys. However, developments in advanced cutting tool materials such as super-abrasive family, including PCD and CBN tools, have expanded the application of these tools for the high speed machining of hard materials such as hardened steels and titanium alloys despite their high cost (SHAW (1984), SECO TOOLS (2002b). Some studies worldwide (SECO TOOLS (2002a), LEE (1981), HARTUNG; KRAMER (1982), BHAUMIK; DIVAKAR; SINGH (1995), ZOYA; KRISHNAMURTHY (2000), NABHANI (2001a), MACHADO et al. (2004), MAGALHÃES; FERREIRA (2004)) have reported the superiority of PCD tools in terms of wear rate and hence longer tool life, when machining of titanium alloys**.** Recent studies have reported that CBN tools can be used for

machining titanium alloys at higher cutting speeds despite the high reactivity of titanium alloys with the tool materials (SECO TOOLS (2002a), HONG; MARKUS; JEONG (2001), LEE (1981), HARTUNG; KRAMER (1982), BHAUMIK; DIVAKAR; SINGH (1995), ZOYA; KRISHNAMURTHY (2000), NABHANI (2001a). Although ceramic tools have been used for machining titanium alloys in several studies (YANG (1970), KONIG (1979), LEE (1981), KOMANDURI (1989), LI; LOW (1994), KLOCKE; FRITSCH; GERSCHWILER (2002), KOMANDURI; REED JR (1983)), they are not recommended for machining titanium alloys because of their poor performance due to excessive wear rates as a result of the poor thermal conductivity, relatively low fracture toughness and high reactivity with titanium alloys (DEARNLEY; GREARSON, 1986).

2.13.1 Tool Materials Requirements

Tool selection process must be in accordance with the specification of the material to be cut and cutting parameters. Since cutting tools used for machining titanium generally present accelerated wear, due to extreme thermal and mechanical stresses close to the cutting edge, an ideal cutting tool for machining titanium should possess the following requirements (EZUGWU; WANG (1997), TRENT; WRIGHT (2000)):

i) hot hardness to maintain a sharp and consistent cutting edge at elevated temperature and ability to withstand the high stress involved during machining;
ii) high resistance to abrasion wear in order to avoid alteration tool geometry caused by the rubbing action;
iii) chemical inertness to minimise the tendency to react with titanium and chemical stability to prevent the formation of a built-up edge;
iv) good thermal conductivity to minimise thermal gradients and thermal shocks;
v) high fracture toughness, which allows the insert to absorb forces and shock loads during machining. If an insert is not sufficiently tough, then induced shock load alone can lead to premature fracture of the cutting edge during machining;
vi) good fatigue resistance to withstand the chip segmentation process;
vii) high compressive, tensile and shear strength.

Szeszulski et al. (1990) consider wear resistance, chemical inertness and toughness the main factors affecting the performance of cutting tools when machining aerospace alloys. The reduction of hot hardness at elevated temperature conditions lead to the weakening of the inter-particle bond strength and the consequent acceleration of tool wear. Table 2.5

(KRAMER, 1987) shows the softening temperature of commercially available cutting tool materials while Figure 2.26 illustrates the influence of temperature on hardness of some cutting tool materials used for machining aerospace alloys (ALMOND, 1981).

Table 2.5 - Softening points of tool materials (KRAMER, 1987).

Tool material	Softening point temperature (°C)
High Speed steel	600
Cemented Carbide (WC)	1100
Aluminium Oxide (Al_2O_3)	1400
Cubic Boron Nitride (CBN)	1500
Diamond	1500

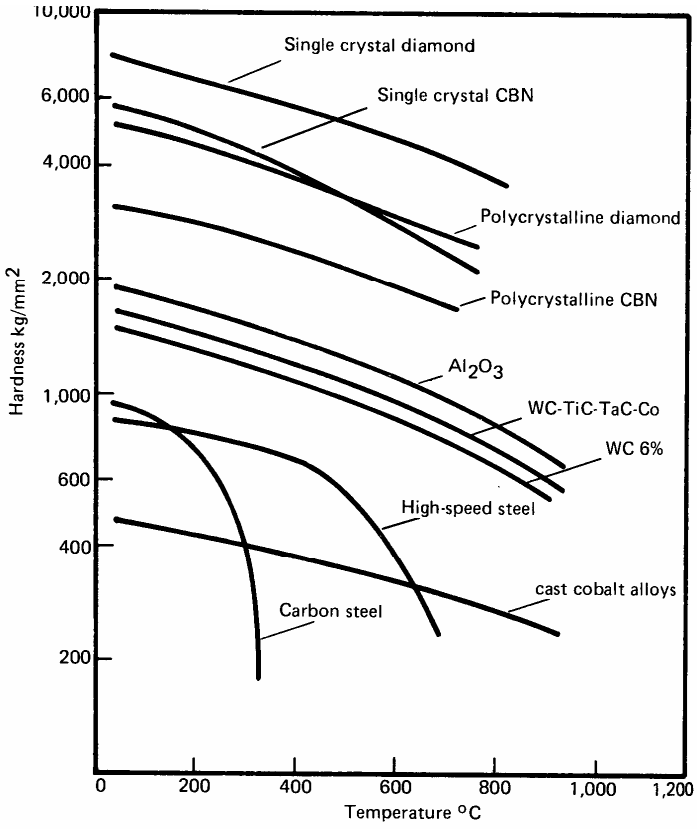

Figure 2.26 - Influence of temperature on hot hardness of some tool materials (ALMOND, 1981).

2.13.2 High Speed Steel (HSS) Tools

High Speed Steel (HSS) tool material was introduced by Taylor and White in 1906. The chemical composition of initial HSS tool was: 0.67% C, 18.1% W, 5.47% Cr, 0.11% Mn,

0.29% V and Fe (balance), under proper heat treatment (TRENT; WRIGHT, 2000). The advent of this allowed increase in metal removal rates and cutting speed up to 30 m min^{-1} could be achieved when machining steel. This increase in cutting speed represented up to 6 times those achieved with carbon steels and low/medium alloy steels (most common cutting tool materials employed in the 19^{th} century). Subsequently a grade containing 18% W, 4% Cr and 1% V was established and generally referred as the 18-4-1 or T grade. The room temperature hardness of HSS tools is of the order of 850 HV (TRENT; WRIGHT, 2000). There are several compositions of high speed steels in the market but three major grades can be easily distinguished: the T-grade, M-grade and T/M grade (EDWARDS, 1993). The tungsten grades of T series HSS tools contain 12-20% W with Cr, V and Co as principal elements. These grades have a relatively wide hardness range and lower tendency to descarburize, but they can readily acquire coarse-grained carbide particles resulting in lower toughness. Molybdenum (Mo) based HSS tools (M series) were developed in the 1930´s and are widely used because of the scarcity of tungsten. The Mo grades contains 3.5-10% Mo with Cr, V, W and Co as alloying elements which tend to combine with carbon to form very strongly bonded carbides with compositions such as $Fe_3(W,Mo)_3C$ and V_4C_3 (TRENT; WRIGHT, 2000). The M-series HSS tools are tougher than the corresponding T-series HSS tools. They are more widely used for drills and end mills. Increasing the Co content increases the toughness but reduces hardness and therefore wear resistance of tool (BOOTHROYD; KNIGHT (1989), EDWARDS (1993)). The third grade contains Co and can be either a T or M series of HSS tools materials.

HSS tools can be employed in most of the common types of cutting tools including single-point turning tools, milling cutters, taps, drills, reamers, thread cutting dies, gear cutters, broaches, hobs and saws. Probably less the 10% of all turning applications are carried out using HSS tools as the cutting tool material. The major area of application is drilling which accounts for 80% of all drilling operations followed by milling (40% of the total milling cutter market) (EDWARDS, 1993). These tools are also employed in the machining of easy to cut materials and in operations where complex shaped tooling is involved. 350 HV is often considered to be the maximum hardness of the workpiece which can be cut with HSS tools. These materials generally are available in form of solid tools or in shape of inserts, both could easily be reground when worn out. Various processes such as nitriding, carburising, ion implantation and peening are used to optimise their properties.

High speed steel tools can be produced by three different processes: cast, wrought and sintered (using powder metallurgy technique). Great progress was made in the 1970s with the production of:

i) Coated HSS tools: layers of TiN, TiC, HfN and Al2O3 can be applied to the HSS tools by either CVD (Chemical Vapour Deposition) or PVD (Physical Vapour Deposition). High temperatures (up to 1000ºC) are required in the CVD process and that may cause metallurgical changes to the parent HSS metal. The PVD process operates at relatively lower temperature (500ºC to 600ºC) compared to CVD process, making it more suitable for HSS tools (NEUMEYER; DULIS, 1976);
ii) Sintered HSS tools: powder metallurgy provide a microstructure consisting of a uniform distribution of carbides throughout the matrix. As result, a substantial increase in toughness can be achieved, ensuring for machining operations involving impact and vibration. A HSS TiN coated indexable insert tooling was recently designed for turning and parting operations. The substrate of the insert is powder metallurgy HSS that ensured incorporation of sintered in chip breaker grooves (NEUMEYER; DULIS, 1976).

The main advantages of using HSS tools are their high toughness relative to commercially available cutting tools and reasonable cost and easy availability. Major drawbacks of HSS tools include: hardness reduction at elevated temperature, limited wear resistance and greater tendency for adhesion of the chip to the tool.

Generally purpose HSS tools grades suitable for machining of titanium alloys are the M1, M2, M7 and M10 grades (THE METALS HANDBOOK, 1989). However, best results are generally obtained with more highly alloyed grades including T5, T15, M33 and the M40 series. It was found that cutting speeds of 14 to 17 m min^{-1} are reasonable for turning Ti-6Al-4V alloy at a feed rate of 0.25 mm rev^{-1} and at a depth of cut of 0.25 mm (THE METALS HANDBOOK, 1989). The authors also reported that a M42 grade of HSS tool provided better tool life than M2 or T15 grades. In other work a high energy electron beam was employed to alloy the surface of M42 HSS tools with various boride powders including WB and MoB in turning of both commercially pure titanium and Ti-6Al-4V alloy. It was reported that 35% increase in cutting speed could be obtained with boride alloyed HSS tools compared with unalloyed plain HSS tools (SUN, 1992). The authors also reported that below the cutting speed limit the tool life of HSS tools increased by more than 7 times by electron beam

alloying with borides. This improvement was attributed to the lower flank and crater wear and the higher hardness of the alloyed tools. Konig (1979) employed S18-1-2-10 HSS grade tools in machining of Ti-6Al-4V alloy and reported that cutting speed achieved was much lower than that used with cemented carbides (grade P) due to the rapid loss of hardness at elevated temperatures above 600ºC. Similar performance was found when a M42 HSS grade and cemented carbide tools were utilised in the experiments of Zlatin and Field (1973). Different tool materials tend to have different responses to different wear mechanisms when machining titanium alloys. The rapid loss of their hardness at elevated temperatures above 600ºC subjects HSS tools to severe plastic deformation, which accelerate the rate of wear.

2.13.3 Cemented Carbide Tools

The introduction of cemented carbide tools in the early 1920s, in West Germany, by Shroter led to a significant improvement in cutting speed capability and productivity due to an unique combination of properties such as good wear resistance, strength and toughness. Further development of cemented carbides began in the USA, Austria, Sweden and other countries (TRENT; WRIGHT (2000), EDWARDS (1993), KALISH (1978), MARI; GONSETH (1993)). Cemented carbides tools are produced by powder metallurgy technique that involves the bonding of the tungsten carbide (56-93%WC) particles by a metal binder cobalt (Co). Pure WC is comparatively brittle and Co is tough. The melting point of Co is over 1400ºC, but there is WC-Co eutectic at about 1300ºC that facilitates liquid-phase sintering. As a result of this, a strongly bonded, virtually 100% dense material is formed KALISH (1978). A combination of these materials results in a compromise between wear resistance and shock resistance according to the amount of Co used. Two factors affect the properties of cemented carbide (WC-Co) (EDWARDS, 1993):

i) The Co content: increase in the Co content increases the toughness of a carbide but reduces its hardness and therefore its wear resistance (BOOTHROYD; KNIGHT, 1989). Reduction of Co content reduces the toughness and increases the wear resistance by increasing the hardness of a cemented carbide. Co content (in weight percent) for cutting purposes generally ranges from 5% to 12%;
ii) The grain size of the WC: fine grain WC increases the hardness and therefore the wear resistance for the wear resistance for a given Co content. Grain sizes of WC ranges from around 0.5-5.0 μm (EDWARDS, 1993).

It has been reported (DEARNLEY; GREARSON (1986), LEE (1981), KOMANDURI; REED JR (1983)) that hot compressive strength of cemented carbides depends on a combination of the Co binder concentration and the WC particle size. The binding metal (Co) easily dissolves in titanium thus carbides containing only small amounts of cobalt should be used. Cemented carbides grades with low cobalt content and a fine grain size were found to perform better than grades with higher cobalt content and/or a larger grain size when turning titanium alloys (DEARNLEY; GREARSON, 1986). However, a lower Co content leads to reduced rigidity of the cutting edge. These authors reported that the most favourable compromise between a limited Co content and adequate rigidity of the cutting edge for machining titanium is found in the carbides of the ISO grades K10 to K20. The grain size of carbides tools affects their wear resistance. Mari and Gonseth (1993) reported that the fine grain size (1.0 μm) of straight cemented carbides provided better resistance to deformation than the coarse grain size (3.1 μm) below 800ºC (Figure 2.27).

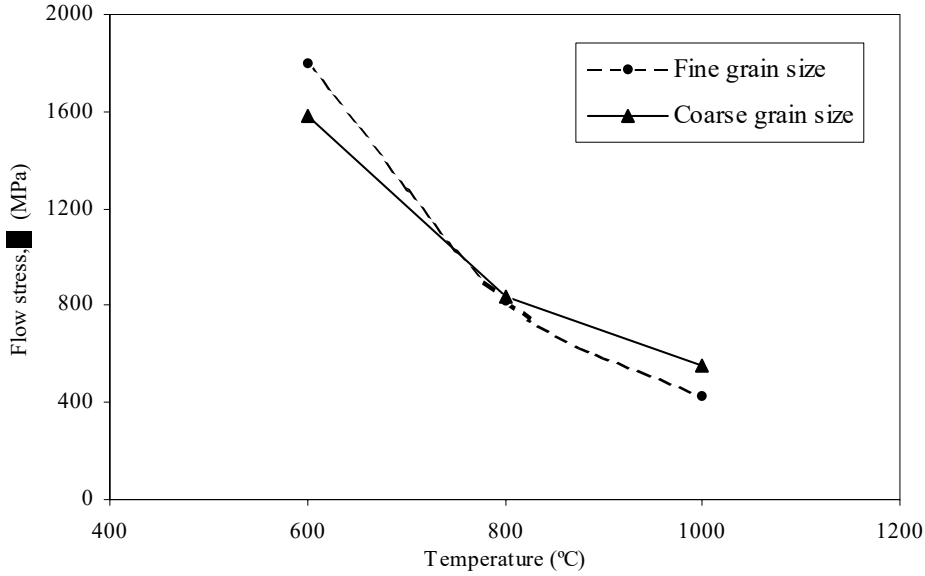

Figure 2.27 - Flow stress measured at 0.6% strain during three point bending tests at a constant strain rate in WC-11wt.%Co (MARI; GONSETH, 1993)

.

In contrast, the coarse grain size carbides showed a higher resistance to deformation at higher temperature. Recent studies (JAWAID; CHE-HARON; ABDULLAH (1999), CHE-HARON (2001)) were carried out to evaluate the performance of different grain sizes of substrate of K10 straight uncoated carbide tools in machining of titanium, Ti-6242, alloy

under dry conditions at cutting speeds up to 100 m min^{-1} and a constant feed rate of 0.25 mm/rev. They reported that lower flank wear rate of the tools hence longer tool life is due to the grain size of 1.0 μm compared to the finer grain size of 0.68 μm (Figure 2.28). The authors attributed the greater wear rate of the finer grain size tools to increased solubility of WC in titanium alloys as the surface area of tool particles exposed to solution wear increased.

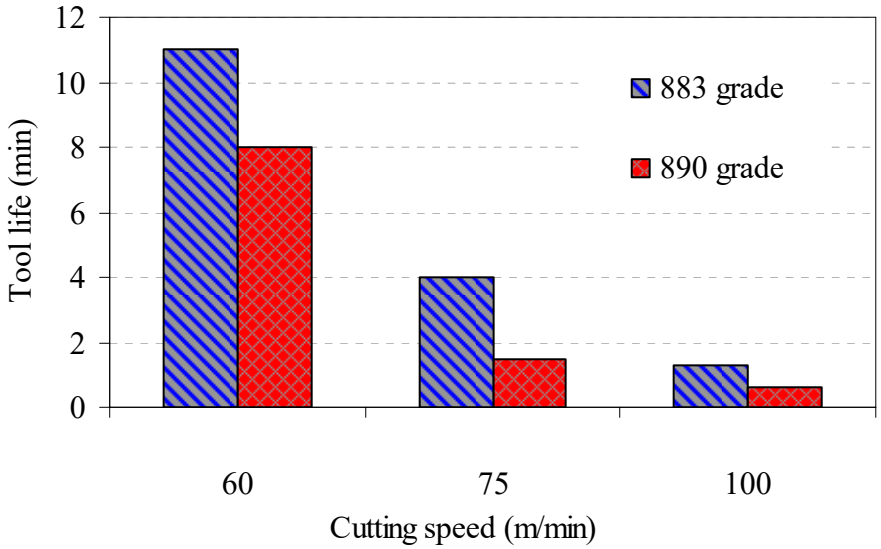

Figure 2.28 - Tool live when turning Ti-6242 alloy with mixed uncoated carbide tools with different grain sizes of substrates at a constant feed rate of 0.25 mm/rev: 0.68 μm (890 grade) and 1.0 μm (883 grade) [adapted from JAWAID; CHE-HARON; ABDULLAH (1999)].

Carbide tools can be classified into six classes, according to ISO specifications which is based on workpiece materials to be machined (INTERNATIONAL STANDARD, 2004):

1. P class: this is the class recommended for machining materials that produces long continuous swarf: all grades of steel and cast steel except stainless steels with and austenitic structure;
2. M class: this is recommended for machining stainless austenitic and austenitic/ferritic steel and cast steel;
3. K class: this is mainly employed in machining of cast irons, such as grey cast iron, cast iron with spheroidal graphite and malleable cast iron;
4. N class: this is recommended for machining aluminium and other non-ferrous metals and non-metallic materials;

5. S class: this is the class recommended for machining difficult-to-machine materials, including heat-resistant special alloys based on iron, nickel and cobalt, titanium and titanium alloys;
6. H class: this class is recommended for machining hardened steel, hardened cast iron materials and chilled cast iron.

Within each class of cemented carbides there are various categories (i.e. P01, P10, P20, P30, P40, P50 and P05, P15 to P45), which are used for different machining operations. Grades P01, M01, K01, N01, S01 and H01 are specific for precision finishing operations because of increased wear resistance requirement under high speeds conditions. Grades P20, M20, K20, N20, S20 and H20 are used for general purpose while P50, M40, K40, N30, S30 and H30 grades are recommended for roughing conditions due to increased toughness under higher feed rates conditions.

Cemented carbides have a different designation in the USA, which will depend on the type of work material to be machined. They can be categorised into two major divisions: C1 to C4 and C5 to C8. The former are suitable for machining cast iron, non-ferrous alloys and non-metallic materials (non-steel materials) while grades C5 to C8 are suitable for machining carbon steels and alloy steels.

Cemented carbides tools for machining applications are divided into two groups: uncoated and coated carbides.

2.13.3.1 Uncoated Carbide Tools

The uncoated cemented carbides cutting tools are commonly used for all machining processes of titanium alloys due to their improved performance in terms of tool wear and lower cost relative to other tool materials. Two categories of uncoated carbide tools are available for machining applications: straight and mixed grade carbides.

i) WC/Co carbides (straight grades): these grades are the original grades of cemented carbides. The usual composition of the straight grade carbides is 94%WC and 6% Co. In general, the best results in machining titanium alloys have been obtained with the C-2 grades, represented by ISO K20 (DEARNLEY; GREARSON (1986), ZLATIN; FIELD (1973), JAWAID; CHE-HARON; ABDULLAH (1999), ZLATIN; CHRISTOPHER (1973), TRUCKS (1987)). However, satisfactory tool lives (< 20 min) in turning titanium alloys were also obtained with ISO K10

uncoated straight carbides at cutting speeds below 60 m min^{-1} (DEARNLEY; GREARSON (1986), ZLATIN; FIELD (1973), (KOMANDURI; REED JR (1983). Satisfactory tool lives were also obtained with ISO K10 uncoated straight carbide tools when machining titanium alloys at cutting speeds of 60 m min^{-1} and 122 m min^{-1} with feed rate of 0.125 mm rev^{-1} and depth of cut of 1.25 mm (HARTUNG; KRAMER, 1982). All these authors reported that flank wear was stable and did not contribute to tool failure until crater wear weakens the edge and plastic deformation of the cutting edge accelerates wear at the tool flank. K10 uncoated straight carbides were also employed in turning of several grades of titanium alloys at a relatively high cutting speed of 100 m min^{-1}, feed rate of 0.1 mm rev^{-1} and depth of cut of 0.5 mm (MOTONISHI et al., 1987). Recent studies have employed K10 uncoated straight carbides in turning of titanium alloys at relatively high cutting speeds ranging from 63 to 150 m min^{-1} (EZUGWU; OLAJIRE; WANG (2002), EZUGWU et al. (2004), EZUGWU et al. (2005), KONIG (1979), MACHADO et al. (2004), MAGALHÃES; FERREIRA (2004), KITAGAWA; KUBO, MAEKAWA (1997)). In most of these studies, the authors observed that tool failure were due to adhesion and diffusion-dissolution wear mechanism on the rake face, and attrition wear mechanisms on the flank face. Plastic deformation on tool nose was responsible for tool rejection of uncoated straight carbides when machining Ti-6Al-4V alloy at speeds in excess of 60 m min^{-1} under conventional coolant supply (KONIG, 1979). Titanium reacts with most cutting tool materials at elevated temperatures (> 550ºC) during machining (MOTONISHI et al. (1987), KONIG (1979), HARTUNG; KRAMER (1982), BROOKES; JAMES; NABHANI (1998)). Figure 2.29 shows crater wear rates of various cutting tool materials when machining titanium alloys at a speed of 61 m min^{-1} for 10 minutes. At such high temperature conditions titanium atoms diffuse into the carbide tool material and react chemically with carbon present in the tool to form an interlayer of titanium carbide (TiC) (KONIG (1979), HARTUNG; KRAMER (1982)) which bonds strongly to both the tool and the chip to form a saturated seizure zone, consequently, minimising diffusion wear mechanism as the reaction is halted. The separation of the welded junction results in tool material being carried away by the fast flowing chip. At lower speed conditions chemical interactions between the carbide tool and titanium alloy is insignificant and wear is

caused mainly by mechanical and thermal fatigue as well as micro-fractures or defects that may be present in the tool (EZUGWU; BONNEY; YAMANE, 2003). Brookes, James and Nabhani (1998) utilised a quasi-static contact method in their experiments to determine the temperature at which adhesion and welding developed at the cutting zone that generated when machining titanium alloys with coated carbide and CBN tools. They reported that the critical temperatures were 740ºC and 900ºC, for the carbide and CBN tool materials, respectively, and the nominal contact pressures developed were approximately 0.23 GPa and 0.146 GPa in these particular cases. It was also reported that fracture generally initiated in the bulk of the harder tool material, rather than in the workpiece at the welded junction interface. Figure 2.30 shows a SEM micrograph of exposed mixed carbide substrate after fracture of the welded junction (NABHANI, 2001b). Uncoated straight cemented carbide tools can also fail by abrasion wear mechanism as result of the chipped hard particles flowing between the tool´s flank face and the newly machined surface (BROOKES; JAMES; NABHANI, 1998). Figure 2.31 shows an enlarged view of the flank face of a worn uncoated straight carbide tool that experienced abrasion by carbide grains after turning of a titanium base, Ti-6242, alloy under dry condition (JAWAID; CHE-HARON; ABDULLAH, 1999);

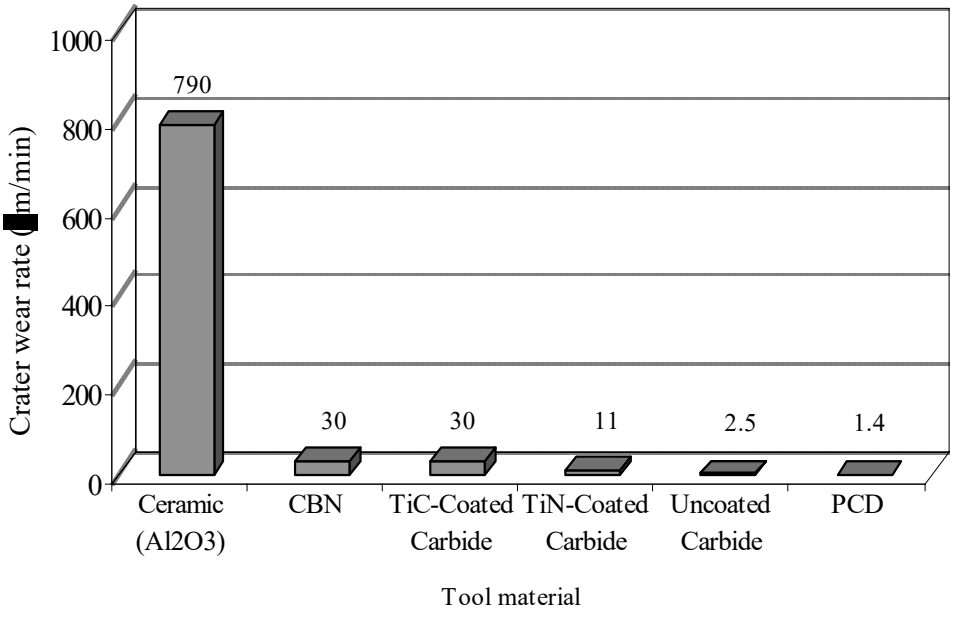

Figure 2.29 - Average crater wear rates of various tool materials in turning of Ti-6Al-4V alloy at a cutting speed of 61 m min^{-1} for 10 minutes [adapted from HARTUNG; KRAMER (1982]

.

Figure 2.30 - SEM micrograph of exposed mixed cemented carbide substrate after fracture of the welded junction (NABHANI, 2001b).

Figure 2.31 - Flank face of a worn uncoated straight carbide tool showing abrasion by carbide grains after turning titanium base, Ti-6242, alloy under dry condition (JAWAID; CHE-HARON; ABDULLAH, 1999).

Mixed carbides (alloyed uncoated carbides grades): these grades have TiC, TaC or NbC and other rare-earth elements such as ruthenium (Ru) added to the base composition of the straight grade (WC-Co). Examples of typical compounds are WC/TiC/Co, WC/(Ta,Nb)C/Co, WC/TiC/Ta(Nb)C/Co. Uncoated straight cemented carbides are the strongest and most wear resistant but are subject to rapid cratering, especially when machining steels. TiC and TaC are

harder than WC and its inclusion improves the crater wear resistance of carbides (BOOTHROYD; KNIGHT, 1989)) but have the disadvantage of lower strength. TiC usual composition ranges from 5-25% by weight. The proportion of TiC added depends on the cutting speed required. An increase in TiC composition generally reduces the toughness of the carbide. Finishing operations generally are carried out at higher speeds for economic metal removal. High speeds will cause cutting temperatures to increase and cratering will be more pronounced. In this case high TiC content is required. When roughing operations are required at lower cutting speeds conditions less TiC is required. TaC addition increases the hot hardness of the tool, thus preventing plastic deformation of the cutting edge during machining at high speed conditions. Mixed grade of carbides containing TiC (4% to 8%), Ta (Nb)C in the range of 5% to 10% and Co (6% to 9%), with hardness range of 1450-1650 HV is also recommended for machining superalloys. Due to the higher cost of TaC, it is often diluted with up to 50% niobium carbide (NbC) without detracting from the performance of the cemented carbide compound. WC/TiC/Ta(Nb)C/Co or Co-Ru cemented carbides can be utilised for machining steels, where higher temperatures and high pressures are generated at the cutting zone as result of a combination of high chemical instability and high temperature properties. Ru can be substituted for the Co and increase in toughness, tool life and cutting performance is achieved without alteration in hardness and other properties. Adhesion diffusion-dissolution, attrition and plastic deformation wear mechanisms are responsible for tool failure when machining with mixed uncoated cemented carbide tools. Figure 2.32 shows the evidence of attrition wear and adhesion of the chips onto the nose of a worn mixed ((Ta,Nb)C) uncoated cemented carbide tool after machining Ti-6Al-4V alloy under conventional coolant supply at a speed of 100 m min^{-1}, a feed rate of 0.15 mm rev^{-1} and a depth of cut of 0.5 mm (EZUGWU et al., 2005).

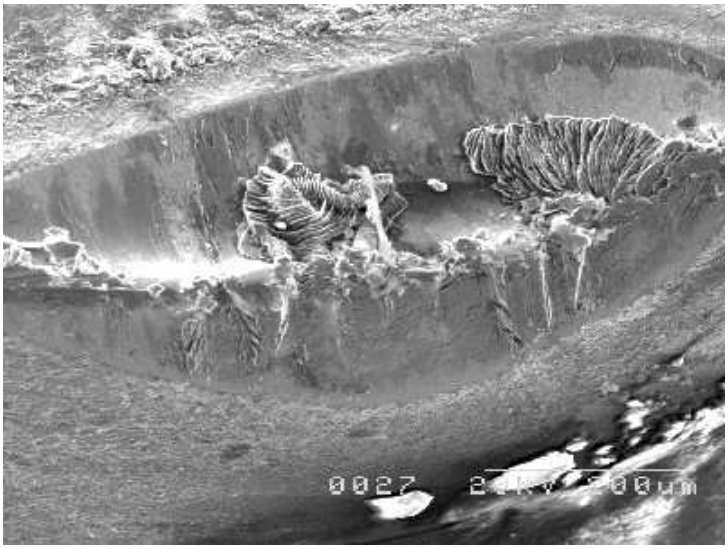

Figure 2.32 - Evidence of adhesion of the chips on the nose of a mixed ((Ta,Nb)C) uncoated (steel cutting grade) tool after machining Ti-6Al-4V alloy under conventional coolant supply at a speed of 100 m min^{-1}, a feed rate of 0.15 mm rev^{-1} and a depth of cut of 0.5 mm (EZUGWU et al., 2005).

2.13.3.2 Coated Carbide Tools

Coatings are used in cutting tools to provide improved lubrication at the tool-chip and tool-workpiece interfaces, reduce friction and consequently lower temperatures at the cutting edge. From a functional standpoint, chemical stability, hot hardness, and good adhesion to the substrate are essential. Optimum coating thickness, fine microstructure, and compressive residual stresses can further enhance coating performance (PRENGEL; PFOUTS; SANTHANAN, 1998). Coatings must have a great resistance to wear in many aspects, retaining their hardness when they are hot and reducing their affinity with the materials to be machined. Additionally, coatings should possess low thermal conductivity to transfer less heat to the substrate and low friction coefficient (LÓPEZ DE LACALLE et al., 2000). Other very important characteristic that coatings must offer is a sharp and consistent cutting edge at elevated temperature generated during machining, thus the coating should have the least possible tendency to diffusion bond to the workpiece material (KLAPHAAK, 1987)

The most common group of coated tools consist of various combinations of titanium nitride (TiN), titanium carbide (TiC), tantalum carbide (TaC), vanadium carbide (VC), titanium carbonitride (TiCN), aluminium oxide (Al_2O_3), hafnium nitride (HfN), hafnium carbide (HfC), zirconium nitride (ZrN) and chrome nitride (CrN) deposited in a single or multilayer manner onto cemented carbides substrates. More recently new coatings with

improved properties have been introduced, including, titanium zirconium nitride (TiZrN), titanium aluminium nitride (TiAlN), molybdenum carbide (Mo_2C), titanium diboride (TiB_2), cubic boron nitride (CBN) and diamond-like coatings. These coatings are deposited on the substrate either by the lower temperature (300-600ºC) Physical Vapour Deposition (PVD) or higher temperature (600-1000ºC) Chemical Vapour Deposition (CVD) coating techniques. Coatings deposited by CVD technique can vary in thickness from 5 to 20 μm, whereas PVD coatings thickness are usually less than 5 μm. Diamond coatings can be deposited by CVD techniques such as hot filament, microwave plasma and plasma torch methods at higher temperature ranging from 700-1000ºC. Their coatings are generally in the range of 20-40 μm (PRENGEL; PFOUTS; SANTHANAN, 1998).

When machining titanium alloys, tools wear out due to the high chemical reactivity with titanium (HARTUNG; KRAMER (1982), BROOKES; JAMES; NABHANI (1998)). Thus, the coatings should have high resistance to wear and high chemical stability to produce a chemical barrier against heat, between the tool and the chip. Both TiC and TiAlN coatings exhibit these properties. TiN is not a hard material, it provides a very low friction ratio in tool cutting edges and greater resistance to crater wear (TURLEY, 1981). TiN is an even better diffusion barrier than TiC but the latter has better abrasion resistance (EDWARDS, 1993). TiC also improves hot hardness but, however, reduces fracture toughness. Layers of Al_2O_3, TiN and TaC can be combined. The outer layers of TiN provide a low friction and chemically inert surface for a new tool. As the TiN wears through, the additional wear resistant layer of Al_2O_3 is exposed (JAWAID, 1982). Al_2O_3 coating can be either deposited by CVD or PVD techniques. CVD Al_2O_3 coating is most chemically stable of all hard coatings at all temperatures, thus providing improved resistance to crater wear. CVD Al_2O_3 coating is very effective for the high-speed machining ferrous materials whereas PVD Al_2O_3 coatings are soft and unstable (PRENGEL; PFOUTS; SANTHANAN, 1998). The low thermal conductivity of Al_2O_3 coatings at high temperatures tends to concentrate the heat in the chips rather than the tools. TaC addition increases the hot hardness of the tool, thus preventing plastic deformation of the cutting edge at higher speed conditions. Hafnium nitride (HfN) coatings have high hardness and chemical stability at elevated temperatures and a coefficient of thermal expansion close to that of WC. These coatings have good resistance to abrasion wear, cratering, and flank wear. TiB_2 is an emergent coating material exhibiting high hardness and chemical inertness (PRENGEL; PFOUTS; SANTHANAN, 1998) deposited by CVD technique. CBN coatings are chemically inert to hot iron, steel and oxidizing environments.

During oxidation, a thin layer of boron oxide is formed. This oxide provides chemical stability to the coating, making them suitable for machining hard ferrous metals (50-65 HRC), gray cast iron, high temperature alloys, and sintered powdered metals. CBN coatings also have good adhesion to carbide substrate. Their thickness is generally restricted to 0.2-0.5 μm. Diamond-like coatings have very high hardness, low friction coefficient, high thermal conductivity and low thermal expansion coefficient. However, diamond has high affinity with elements from group IVA to group VIIA of the periodic table what limits diamond coated tools for machining non-ferrous alloys containing abrasive second-phase particles (i.e. aluminium-silicon alloys) and for machining non-metallic materials that not react with carbon (i.e. metal-matrix composites and fibre-reinforced plastics. Typical failure/wear modes for diamond tools are combinations of oxidation, diffusion, micro-chipping and gross fractures (PRENGEL; PFOUTS; SANTHANAN, 1998).

Coated carbides are currently employed in machining of titanium alloys at cutting speeds similar to those for uncoated carbides, in the range of 56 to 150 m min^{-1} (EZUGWU; OLAJIRE; WANG (2002), VENUGOPAL et al. (2003), LÓPEZ DE LACALLE et al. (2000), NABHANI (2001a), NABHANI (2001b), FITZSIMMONS; SARIN (2001)). Flank and nose wears are the predominant failure modes when machining titanium alloys with coated cemented carbide tools. Figure 2.33 shows typical flank wear plots for coated cemented carbide tools when machining titanium alloy. When machining titanium alloys, multilayer (TiC/TiCN/TiN) coatings of a mixed cemented carbide tool were rapidly removed from cemented carbide substrate by adhesion wear mechanism taking place at the cutting edge (Figure 2.34) (NABHANI, 2001b). The high adhesive forces are likely to result in the plucking of hard particles from the tool. Thus erosion of the coating layer (s) exposes the carbide substrate to extreme temperature at the cutting edge, consequently increasing crater wear depth. A similar process of attrition and grooving wear can also develop on the flank face, leading to deterioration in the machined surface. Ultimately, the combination of the crater and flank wear undermine the integrity of the cutting edge leading to catastrophic failure in extreme cases (NABHANI, 2001b). Adhesion wear mechanism also occurred in tools coated with HfN when machining Ti-6Al-4V alloy (KONIG, 1979). Coatings of TiN, TiC, Al_2O_3 and HfN on both the rake and flank faces worn more rapidly than uncoated straight grade carbides by either dissolution-diffusion or attrition wear mechanisms. Coatings of TiB_2 and CBN tools were more resistant than others. In a recent study, Venugopal et al. (2003) employed coated (TiB_2) cemented carbide tools (P30 grade) in machining titanium

base, Ti-5Al-5Mo-2Sn-V, alloy under dry and cryogenic environments and reported that the TiB_2 coating did not provide any benefit in all conditions tested. The TiB_2 coating was removed by abrasion and attrition in both the rake and flank faces. They attributed this to fluctuation of cutting forces during machining and the poor adhesion of the coating. Lee (1981) carried out a study of performance of cooper-cooper iodide coating layers deposited to a straight cemented carbide tools when machining titanium base, Ti-6Al-4V, alloy and reported that increase in tool life was obtained when coated carbide tool was employed. The author also reported that the coating was effective in improving seizure resistance, but the ultimate performance of the coated tool was limited by the poor abrasion resistance of the coating. Iodine is a lubricant additive for titanium in extreme pressure applications but has an extremely corrosive characteristic, whereas cooper bonds well to cemented carbide tool without affecting its surface. Cooper-iodide compound is one of more stable metal iodides. Other study of evaluation of the performance of coated cemented carbide tools in turning Ti-6Al-4V alloy was carried out by Walter, Skelly and Minnear (1993). In their studies cutting edges of straight grade cemented carbides tools were implanted with halogen elements (chlorine (Cl), fluorine (F), bromine (Br), iodine (I), sulphur (S)) and metallic elements ((indium) In, gallium (Ga) and tin (Sn)) by ion beam process to dose levels of $2x10^{16}$ to 510^{16} ions cm^{-2}. These elements were expected to diffuse from the tool as a gas to react with the workpiece material at high temperatures achieved during machining to provide a lubricant film at the tool-workpiece. Improved tool life was obtained with both of halogen and metallic implants. Chlorine and indium-implanted tools exhibited the best performance in terms of tool life (tool life was increased by a factor of two). Additionally, the amount of titanium sticking to the tool was reduced with coated-implanted tools compared to uncoated tools. The best performance of chlorine implant was due to it reacting most readily with titanium, thus providing the best lubrication to prevent or reduce sticking of titanium to the cutting edge of the tool, leading to further failure of the tool. Since indium is insoluble in cobalt, so that at least part of the indium would be present as liquid globules in the cobalt to supply liquid metal to the interface during machining. This liquid metal would lubricate the interface by preventing the sticking of titanium to the tool (WALTER; SKELLY; MINNEAR, 1993).

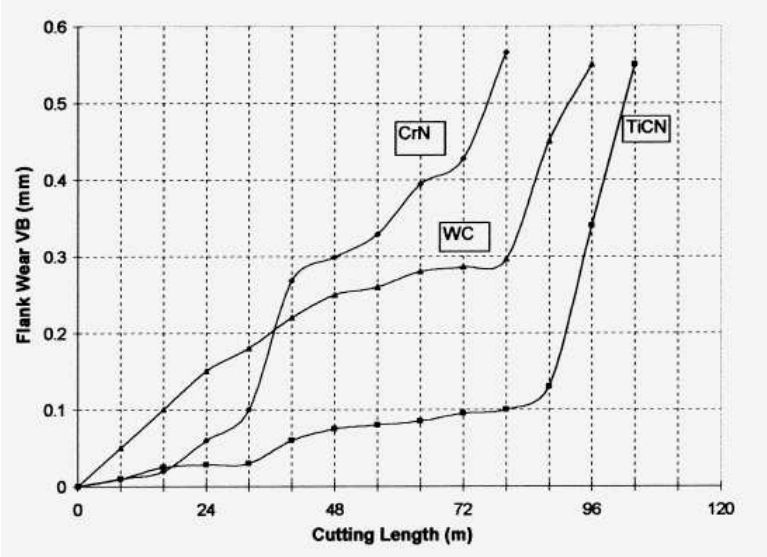

Figure 2.33 - Flank wear curves when machining Ti-6Al-4V alloy with coated (CrN and TiCN) and a straight uncoated carbide tools (TURLEY, 1981).

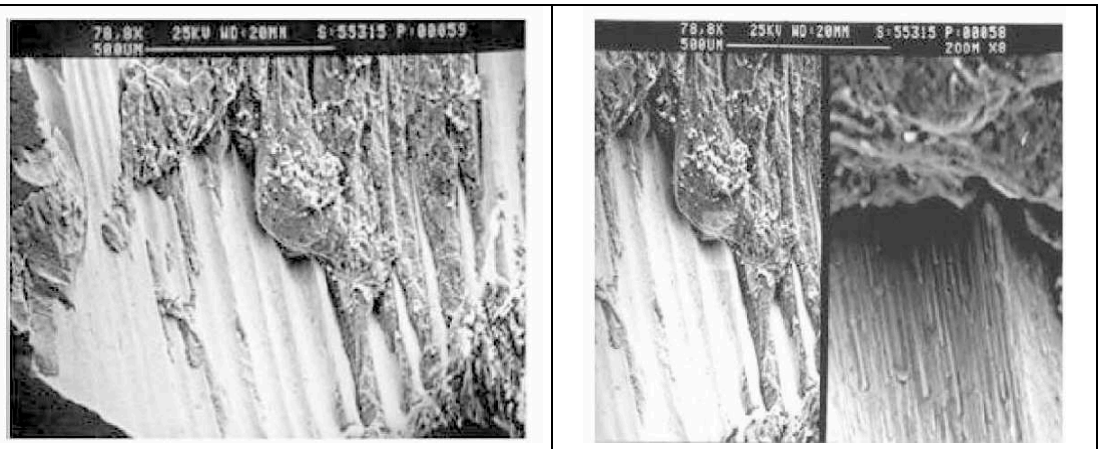

Figure 2.34 - Worn surface of a multilayer (TiC/TiCN/TiN) coated mixed cemented carbide tool showing remains of adherent metal layer (a) and enlarged view of the crater wear showing smooth ridges with fine scoring in direction of chip flow (b) after machining titanium base, Ti-5Al-4Mo-(2-2.5)Sn-(6-7)Si alloy (NABHANI, 2001b).

The coating deposition technique influences tool performance as the bonding strength of the coating to the substrate varies with the processing technique employed. The flank wear rate of multilayered CVD coated (TiCN + Al_2O_3) tools were found to be lower than that of the single layered PVD coated (TiN) tools when milling Ti-6Al-4V alloy with tools between the speed range of 55-100 m min^{-1} and feed rate of 0.1-0.15 mm per tooth (JAWAID; SHARIF;

KOKSAL, 2000). The authors reported that these tools experienced excessive chipping at the cutting edge and chipping and/or flaking on the rake face. The single PVD coated (TiN) layer experienced higher flank wear rate. Additionally, it was observed that coating delamination, adhesion of work material, attrition, diffusion, plastic deformation and thermal cracks were the operating wear mechanisms of these tools (Figure 2.35). Delamination of the coatings can be caused by either chemical reaction and/or crack propagation at the substrate interface, which could be due to the difference in the thermal coefficient of expansion between the coating matrix and the substrate (KONIG (1979), HARTUNG; KRAMER (1982)).

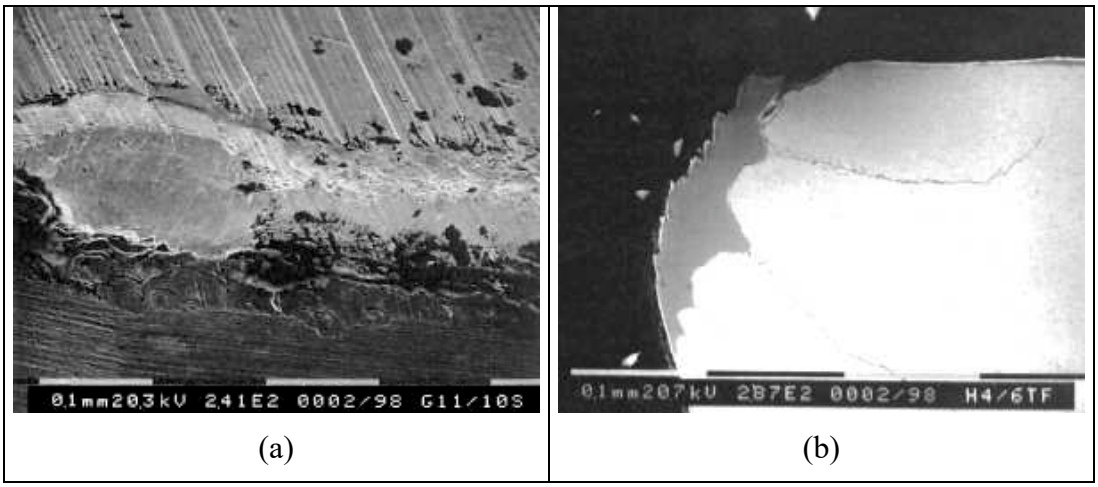

(a) (b)

Figure 2.35 - Coating delamination of PVD coated (TiN) carbide tool, grinding marks and adhered material observed after 10 s (a) and adhesion of work material onto the flank face, plastic deformation and cracks at the cutting edge after 20 s; (b) after face milling Ti-6Al-4V alloy at cutting speeds of 100 m min^{-1} and 50 m min^{-1} and feed rates of 0.15 mm per tooth and 0.1 mm per tooth, respectively (JAWAID; SHARIF; KOKSAL, 2000).

2.13.4 Ultrahard (Superabrasive) Tool Materials

The term ultrahard, or alternatively superabrasive, tool materials refer to those tool materials which possess a hardness of at least 3500 HV room temperature (ALMOND, 1981), and encompasses diamond (both natural and synthetic) – also known as polycrystalline diamond (PCD)) and cubic boron nitride (CBN). Throughout the 1990´s there has been considerable growth in the use of PCD and CBN and polycrystalline cubic boron nitride (PCBN) cutting tools. The automotive, aerospace and woodworking industries in particular benefit from the higher levels of productivity, precision and consistency in manufacturing that

PCD and CBN/PCBN cutting tools can deliver (COOK; BOSSOM, 2000). These materials currently have a well-established market and their properties and performance under severe working conditions are generally considered to be outstanding and highly competitive.

2.13.4.1 Polycrystalline Diamond (PCD)Tools

Natural diamond is the hardest material known with hardness ranging from 6500-12000 HV. The properties of diamonds which are suitable for cutting tool materials include low coefficient of friction, high thermal conductivity, non-adherence to most materials, ability to form a sharp cleavage edge and high abrasion wear resistance ensuring that their cutting edge is maintained throughout most of their useful life. Low compressibility and thermal expansion provide dimensional stability, assuring the maintenance of close tolerances and the generation of high surface finish. However, due to its extreme brittleness, natural diamond is prone to premature failure as well as being very difficult to shape into cutting tools. Machining with diamond cutting tools is generally carried out at high speed and low feed rate conditions to prevent catastrophic failure. Another drawback of sintered diamond is its high chemical reactivity with ferrous materials at elevated temperatures and to revert, at high temperature (about 700ºC), to graphite and/or to oxidise in air (DE GARMO; BLACK; KOHSER, 1999).

Diamond was successfully synthesised in 1958 (EDWARDS, 1993) by subjecting carbon (graphite) to very high temperatures (1500ºC) and ultrahigh pressures (6000 MPa) in the presence of a catalyst or solvent metal (manganese, iron, cobalt, nickel, palladium, platinum and their alloys). This produces fine diamond particles (grain size 1-30 μm), which are then fused together at the appropriate sintering conditions of pressure and temperature to produce polycrystalline diamond. PCD became available as cutting tool material in the mid 1970s. The manufacturing route is basically the same as the used to produce diamond grit, however the temperature and pressure involved are not as high.

Polycrystalline diamond (PCD) tools consist of a thin layer (about 0.5-1.5 mm) of fine grained diamond particles sintered together and metallurgically bonded to a tungsten carbide (WC) substrate which provides adequate toughness and strength. The sintered diamond tools are then finished to shape, size and accuracy by laser cutting and grinding. Typical properties of PCD are: hardness from 7000 to 10000HV, fracture toughness of approximately 8 MPa $m^{0.5}$ and thermal conductivity around 600 $Wm^{-1}K^{-1}$. The main limitation of PCD tools is that they are not generally suitable for machining ferrous metals due to low chemical stability at

elevated temperatures. Diamond reverts to graphite if exposed to temperatures greater than 750ºC for periods longer than 1 minute. Problems of degradation are such that it is not recommended for the machining of ferrous alloys and special care must be taken during brazing. PCD tools are mainly used for machining abrasive non-metallic materials (such as carbon, ceramics, graphite, fibreglass and its composites, reinforced plastic and rubber), non-ferrous metals (such as aluminium alloys, brass, bronze, cooper, zinc and their alloys) and tungsten carbides. PCD tools are widely used for milling, turning, boring, threading and other operations in the mass production of many aluminium alloys, including free machining aluminium alloys and high silicon aluminium alloys because the very long tool life without regrinding can reduce costs (TRENT; WRIGHT, 2000).

PCD grades are usually differentiated by their diamond particle size. Increasing grain size increases abrasion resistance and decreasing grain size increases edge quality (under comparable conditions). Coarse grain size PCD grade is recommended for machining under harsh conditions. Medium and fine grain size PCD grades are recommended for machining under moderately harsh conditions because their resistance is a less important factor and factors such as edge quality/surface finish must be considered. However, Cook and Bossom (2000) carried out a study of evaluation of performance of various PCD grades in milling ceramic impregnated layer and reported that relationship between the PCD grain size and its abrasion wear resistance is not linear (Figure 2.36) and that tool life dropped if the grain size is in excess of 25 μm. When using an ultra coarse grain size of 75 μm, the tool life obtained was considerably lower than those obtained with coarse and medium grain sizes. Similar results were obtained by BAI et al. (2004) in their study evaluating the effects of diamond grain size (2-75 μm) on flank wear of PCD tools when machining laminated flooring with Al_2O_3 overlay. The authors reported that smallest flank wear occurred on the tool with 25 μm grain size. In both studies, the worst performance of ultra coarse grain size was attributed to increased brittleness and rougher cutting edge of coarse grain size, which make them break or abrade, adversely affecting overall performance.

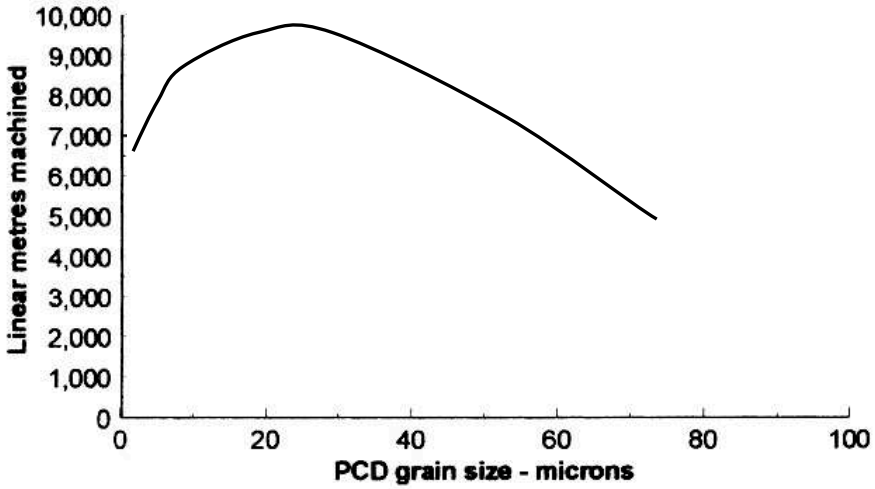

Figure 2.36 - The performance of various grades of PCD tools when milling ceramic impregnated surface of a flooring board (HPL) (COOK; BOSSOM, 2000).

There have been some reports that PCD tools were successfully used for machining titanium base alloys (SECO TOOLS (2002a), LEE (1981), HARTUNG; KRAMER (1982), BHAUMIK; DIVAKAR; SINGH (1995), ZOYA; KRISHNAMURTHY (2000), NABHANI (2001a), MACHADO et al. (2004), MAGALHÃES; FERREIRA (2004), (NABHANI, 2001b)) despite their higher cost, over 8900% higher than cemented carbides (SECO TOOLS, 2002b). A recent study (MACHADO et al., 2004) on evaluation of various cutting tools in finish turning of titanium, Ti-6Al-4V, alloy at high cutting speeds of 110 to 500 m min^{-1} reported that PCD tools gave the longest tool life compared to cemented carbides, CBN and ceramic tool materials. A speed of 175 m min^{-1} was reported as the optimum speed to machine titanium under conventional coolant flow. Superior performance of PCD tools in terms of tool life and surface finish generated relative to CBN and carbide tools was also reported by Nabhani (2001b) when machining titanium base, TA48, alloy at a cutting speed of 75 m min^{-1}, a feed rate of 0.25 mm rev^{-1} and a depth of cut of 1.0 mm under dry condition. The longer tool life recorded with PCD tools was attributed to interdiffusion of titanium and carbon taking place at the interface tool-workpiece, which resulted in the formation of a titanium carbide layer on the rake face of the tool. There was a workpiece layer adhering to the substrate of PCD tool which prevented further diffusion of the tool material into the chip (Figure 2.37). Nabhani (2001b) also reported that the critical interfacial temperature for adhesion to occur when machining titanium alloy with PCD is 760ºC and the nominal pressure is about 0.142 GPa whereas for carbides the temperature is 740ºC and pressure of

0.23 GPa. Dearnley and Grearson (1986) reported that the solubility limit of the tool material in the workpiece is the main factor involved in the dissolution-diffusion process, which determines the magnitude of the concentration gradient in the shear zone, and hence the diffusion flux. This phenomenon was also confirmed by Hartung and Kramer (1982), suggesting that the wear rate of tool materials which maintains a stable reaction layer is limited by the diffusion rate of tool constituents from the tool-chip interface. At equilibrium, this flux will be equal to the diffusion flux of tool constituents through the reaction layer. These authors found that PCD and uncoated cemented carbide tools showed evidence of the formation of stable reaction layer, and were the most wear resistant materials compared to coated cemented carbide and CBN tool materials when machining Ti-6Al-4V alloy.

Figure 2.37 - Formation of strongly adherent layer on the rake face of a PCD tool after machining titanium base, Ti-5Al-4Mo-2Sn-6Si alloy under dry condition (NABHANI, 2001b).

2.13.4.2 Cubic Boron Nitride (CBN) Tools

Cubic boron nitride (CBN) is the hardest material next to diamond (4000 - 6000 HV). CBN is not a naturally occurring compound. The synthesis of CBN from hexagonal boron nitride (HBN) was first announced in 1957 following developments on the synthesis of diamond. CBN powder is manufactured by subjecting HBN to extremely high pressure (6000 MPa) and high temperature (around 1400ºC). CBN can be monocrystalline or polycrystalline and is used for cutting metal when cemented carbide becomes limited in the cutting speeds that can be employed. Table 2.6 shows the mechanical and physical properties and capital cost of a typical high concentration CBN/PCBN tool compared with other cutting

tool materials mentioned previously (ABRÃO, 1995). It can be seen that CBN/PCBN tools retain hardness at high temperatures of 1000ºC with very good fracture toughness, properties that combine with its relatively low solubility in iron to enable CBN/PCBN to machine hard ferrous alloys and some cobalt and nickel superalloys faster than other tool materials. CBN is also employed in machining ferrous materials of hardness of 450 HV or above (tool steels, case hardened steel, chilled cast iron) and high temperature alloys (nickel or cobalt base) of 340 HV and above (RICHARDS; ASPINWALL (1989), WATERS (2000)). The cost of a CBN is about 6500% higher that of a carbide tool (SECO TOOLS, 2002b). Its use has been restricted to finish machining operations in order to effectively compete with grinding which is an expensive process for generating complex surface. Commercial CBN tool blanks/inserts are available in two major grades, namely: CBN_{-H} (High CBN content) and CBN_{-L} (Low CBN content). The CBN_{-H} grade is generally harder and has higher fracture toughness. The CBN_{-L} grade contains in addition to CBN either titanium carbide (TiC) or titanium nitride (TiN) to offer high wear resistance, with reduced fracture toughness. It is generally recognized that low CBN content tools have longer life than those of high CBN content tools in machining of difficult-to-machine materials, especially titanium alloys, due to the ability of the lower CBN content grades to retain their cutting edge for longer period (RICHARDS; ASPINWALL (1989), WATERS (2000), HUANG; LIANG (2003)). In addition to CBN content, the performance of CBN tools depends on the microstructure of binder phase, manufacturing process employed and method of grinding the tool geometry. CBN tools also differ by types of structure: the solid type (indexable insert type) and the layered type (brazeable blank type). The former consists of polycrystalline compact only, whereas the later comprises a layer of polycrystalline CBN in WC substrate.

Notching, chipping and premature tool failure are the dominant failures modes of CBN tools due to their brittle nature. Premature failure of CBN tools can be attributed to the fracturing of the unsupported cutting edge caused by attrition wear (BHAUMIK; DIVAKAR; SINGH, 1995). Recent studies have reported that CBN tools can be used for machining high temperature superalloys, especially titanium-alloys, at a higher cutting speeds (up to 350 m min^{-1}) despite the high reactivity of titanium-alloys with the tool materials in addition to their relatively high cost (SECO TOOLS (2002a), HONG; MARKUS; JEONG (2001), HARTUNG; KRAMER (1982), BHAUMIK; DIVAKAR; SINGH (1995), ZOYA; KRISHNAMURTHY (2000), NABHANI (2001a)). Owing to their high hardness and high melting point, CBN tools can withstand the heat and pressure developed during cutting

without compromising surface integrity of the machined component because of their ability to maintain a sharp cutting edge for longer period (SECO TOOLS, 2002a). Kramer (1987) reported that CBN tools retain their strength at temperatures in excess of 1100ºC while cemented carbide tools encounter plastic deformation at this temperature range. This temperature is also that in which titanium can react with nitrogen in the CBN when interatomic diffusion of titanium and CBN accelerate significantly. This process was confirmed by Nabhani (2001a) when machining titanium-base, Ti-5Al-4Mo-(2-2.5)Sn-(6-7)Si, alloy with CBN and PCD tools where the cutting edge of the tool was bonded to the underside of the chip as shown in Figures 2.38 (a) and (b). CBN tools are recommended for finish machining of titanium alloys at a speed of about 150 m min^{-1} and a depth of cut in excess of 0.5 mm (SECO TOOLS, 2002a).

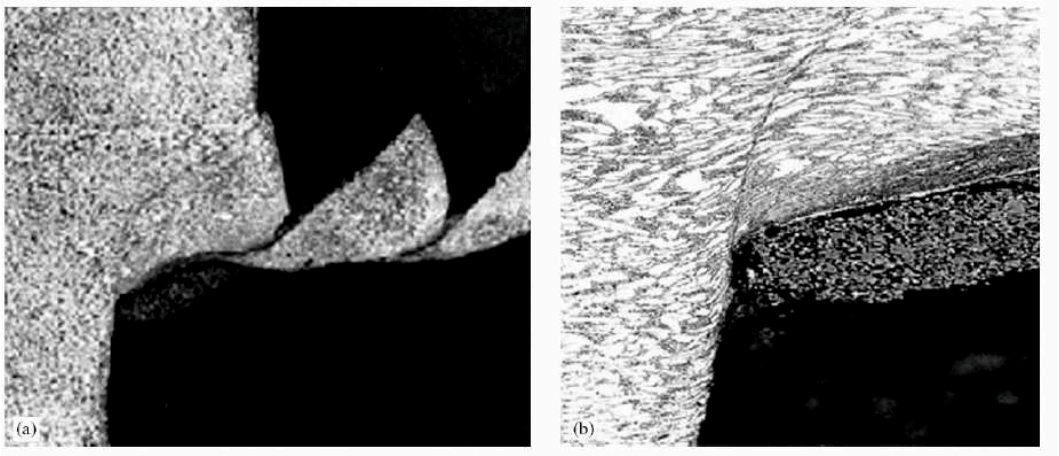

(a) (b)

Figure 2.38 - (a) Section through ‘quick-stop’ specimen showing part of CBN tool adhering to underside of chip (100x), (b) close-up view of Fig. 2.38(a) (200x) (NABHANI, 2001a).

Cutting speed plays an important role in the performance of CBN tools. Increase in cutting speed leads to increase in cutting temperature as well as increasing the intensity of chemical interaction between the tool and the workpiece materials, which subsequently affects tool life. As the cutting temperature increases, seizure of the chip occurs everywhere on the tool face. This forms an adherent layer which becomes saturated with tool particles and serves as a diffusion boundary layer, thus reducing the rate of transport of tool materials into the chip and consequently the wear rate. Since the diffusivity rate increase exponentially with temperature, further increase in cutting speed beyond the speed for minimum wear produces rapid increase in the wear rate. In a study carried out by Dearnley and Grearson (1986) on the

machinability of titanium base, Ti-6Al-4V, alloy with various cutting tool materials, it was reported that CBN tools showed high wear rates with rake and flank surfaces smoothly worn at cutting speeds in excess of 100 m min^{-1}, hence they were not considered suitable for practical application. At cutting speeds lower than 100 m min^{-1} crater wear was irregular, suggesting attrition, and the wear rates exceeded those observed with uncoated straight grade carbides. In other study on evaluation of performance of CBN tools in machining of titanium alloy, Zoya and Krishnamurthy (2000) reported that the occurrence of the increased temperature depends on the cutting speed employed. They also reported that the increase in wear rate occurred around 700ºC, indicating the critical temperature constraining the performance of CBN tools when machining titanium alloys. When machining at a relatively low speed of 150 m min^{-1}, a feed rate of 0.05 mm rev^{-1} and a depth of cut of 0.5 mm, tool wear was associated with localized chipping of the cutting edge (Figure 2.39 (a)), possibly due to tool-tip oscillations. With increase in cutting speed and consequently increase in cutting temperature, cutting tool experienced crater wear and severe nose wear (Figure 2.39(b)). Outstanding performance of wurtzite boron nitride (wBN)-CBN composite cutting tools relative to PCD and cemented carbide tools was observed when machining titanium-base, Ti-6Al-4V, alloy at a cutting speed of 75 m min^{-1}, a feed rate of 0.1 mm rev^{-1} and a depth of cut of 0.5 mm (BHAUMIK; DIVAKAR; SINGH, 1995). This was attributed to a stable interface layer formed on the composite tools, which protected the rake face as well as helped in easy shearing of the work material. This layer also inhibits further diffusion and dissolution, thereby preventing the chip from adhering to the tool and consequently reducing the rate of wear. Brookes; James and Nabhani (1998) found that CBN tools showed lower wear rate and provided better surface finish than coated carbide tools when machining titanium, Ti-5Al-4Mo-(2-2.5)Sn-(6-7)Si, alloy at high cutting speeds. They attributed this in part to the relatively low solubility of boron and also to their higher hardness and melting temperature. Satisfactory tool life and surface finish have been reported when dry machining titanium-base, Ti-5Al-4Mo-(2-2.5)Sn-(6-7)Si, alloy with ultra-hard materials (PCD, CBN) and coated carbide tools at a cutting speed of 75 m min^{-1}, a feed rate of 0.25 mm rev^{-1} and a depth of cut of 1.0 mm (NABHANI, 2001a). Average flank wear was the dominant failure mode. These results show that ultra-hard tool materials can be used in dry machining of titanium alloys at lower speeds and at relatively lower feed rates. Despite encouraging performance of CBN tools, their application in dry machining of titanium alloys is still questionable due to their higher cost compared to carbides and ceramic tools.

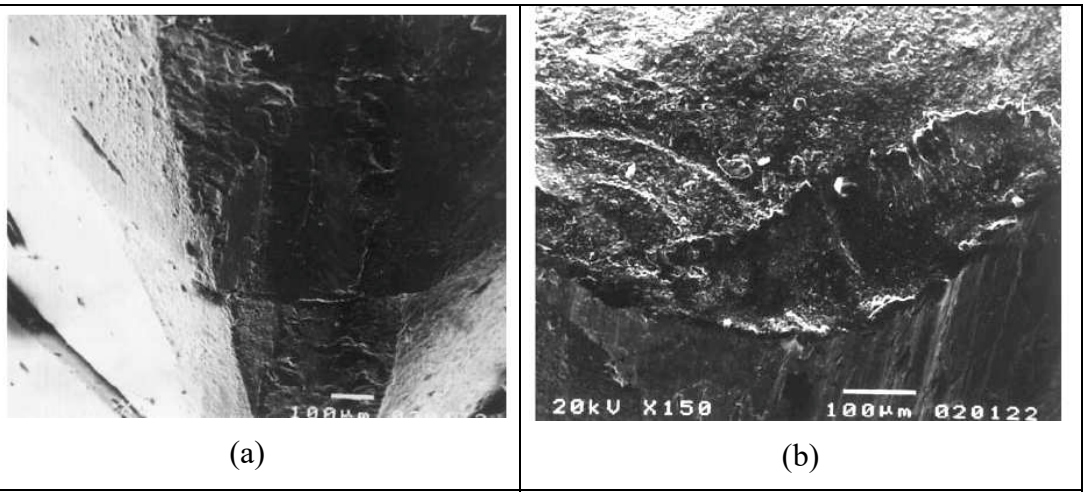

(a) (b)

Figure 2.39 - (a) A typical scanning electron micrographs of worn-out edges: (a) cutting temperature of 734ºC, (b) cutting temperature of 900ºC (ZOYA; KRISHNAMURTHY, 2000).

2.13.5 Ceramic Tools

Although ceramic tool materials were in use thousands of years ago it was not before the early 20th century that they became important again. During and after Second World War, the scarcity of tungsten, and later the development of stronger alloys, compelled material scientists to improve the mechanical properties of ceramic cutting tools by varying the manufacturing routes and trying different additives. The brittleness of ceramic tool materials, coupled with insufficient rigidity and lack of power within the machine tool, hindered their application and usage during their early development. However, these problems have been overcome by developing new advanced ceramics and more powerful, rigid and stable machine tools. Ceramic tools are hard and can retain their hardness at elevated temperature conditions generated when machining at high speed conditions. They also exhibit better chemical inertness and oxidation resistance than cemented carbides. However, the inadequate fracture toughness of ceramic tools relative to HSS tools and cemented carbides is the major disadvantage in their use. This makes them susceptible to mechanical and thermal shock during machining (NORTH, 1986). Ceramics have high melting point and the absence of a secondary binder phase, like carbides, prevents them from softening under high speeds conditions (CHAKORABORTY; RAY; BHADURI, 2000). Ceramic cutting tools are mainly classified into two groups:

a) Alumina-base (Al_2O_3) ceramics (pure oxide, mixed oxides and silicon carbide (SiC) whisker reinforced alumina ceramics);

b) Silicon nitride-base (Si_3N_4) ceramics.

2.13.5.1 Pure Oxide Ceramics

The pure oxide (Al_2O_3) are composed of fine Al_2O_3 grains which are sintered (EZUGWU; WALLBANK, 1987). They possess high hardness, good wear resistance and excellent chemical stability but they lack toughness. The toughness of alumina-base ceramics has been improved by the addition of zirconium oxide (ZrO_2) because of its phase transformation characteristics without affecting their wear resistance. Typical applications of pure oxide ceramics are both finishing and rough cutting of cast materials. However, pure oxide ceramic tools have not been effective in machining aerospace alloys due to their poor thermal shock resistance and low fracture toughness at elevated temperatures.

2.13.5.2 Mixed Oxide Ceramics

The mixed oxide ceramics are obtained by the addition of high percentages of TiB_2 or TiC and/or TiN particles to the pure Al_2O_3 ceramic. Depending on the manufacturer, mixtures of Al_2O_3 with selected additives may be either compacted isostatically, followed by sintering at high temperature, or the powders sintered at high temperature under pressure (LI; LOW, 1994). Magnesium oxide is often added to pure Al_2O_3 ceramic in small amounts to inhibit grain growth during sintering. Additional additives may consist of small amounts of other materials such as chromium oxide, titanium oxide, nickel oxide or refractory metal carbides (WHITNEY, 1983). The purpose of these additives is to achieve certain properties in the tool, particularly increased mechanical strength. Mixed oxide ceramics generally possess improved fracture toughness, hardness and thermal shock resistance (EDWARDS, 1993). The addition of TiC to alumina makes the material more difficult to sinter and so hot pressing is generally employed (RICHARDS; ASPINWALL, 1989); TiC improves hot hardness but, however, reduces fracture toughness. The use of TiN enables the material to be cold pressed and sintered. Introduction of TiC makes the material to be black in colour whilst the Al_2O_3 + TiN is dark brown. These modified alumina ceramics are variously known as “mixed”, “black” or “hot pressed” ceramics. The mixed ceramics are not only thermally tougher but have better retention of the hardness level at elevated temperatures relative to the pure oxide ceramics. The main disadvantage in their use is that the mechanical toughness is inferior to that of the pure oxide ceramics (RICHARDS; ASPINWALL, 1989).

2.13.5.3 Whisker Reinforced Alumina Ceramics

Whisker reinforced (Al_2O_3 + SiC_w) ceramic tools consist of the basic alumina matrix strengthened mechanically with at least 25 wt.% fibres of silicon carbide (SiC_w) (LI; LOW, 1994). The main advantage of the whisker reinforcement is to improve the strength and toughness of the compact through maximising its crack deflection and whisker pull-out mechanisms at elevated temperature condition. This tool grade also possesses low thermal expansion coefficient and high thermal conductivity. The combination of these two factors improves thermal shock resistance of the whisker reinforced alumina ceramics compared to non-reinforced alumina ceramics.

2.13.5.4 Silicon Nitride-base Ceramics

Silicon nitride-base (Si_3N_4) ceramics tools has long been recognised as the toughest ceramic materials. Improvement in hardness, abrasive wear resistance and chemical inertness have produced a material suitable for cutting tools. These cutting tools are manufactured by sintering Si_3N_4 crystals with an inter-granular glass phase of SiO_2 in the presence of Al_2O_3, yttria (Y_2O_3) and magnesium oxide (MgO). There are two forms of Si_3N_4 base ceramic tools for machining purposes: α- Si_3N_4 and β'- Si_3N_4. The α- Si_3N_4 is produced by nitriding of silicon at temperatures up to 1300ºC with small amounts of Y_2O_3 and higher aluminium content (CSELLE; BARIMANI, 1995). The β'- Si_3N_4 is a covalent solid which contains negligible amount of oxygen. It was initially produced by hot pressing at pressure in the range of 7.6 to 17.8 MPa and a temperature in the range of 1650 to 1775ºC, until a density of at least $3.25x10^3$ kg m^{-3} is obtained (LI; LOW, 1994). Their properties can differ for each individual grade depending on its composition, processing route and to a larger extent on the type and quantity of the intergranular phase (RICHARDS; ASPINWALL, 1989). One of most important Si_3N_4 base ceramic is the silicon aluminium oxynitride (also referred to SIALON). SIALON ceramic is the result of substitution of oxygen (O^{2-}) by nitrogen (N^{3+}) in the β'- Si_3N_4 crystal provided that aluminium (Al^{3+}) is simultaneously substituted for silicon (Si^{4+}) to maintain a charge neutrality. This material has the same crystal structure as β'- Si_3N_4, and similar physical properties, but better chemical properties because of the chemical substitution (LI; LOW, 1994). SIALON possesses excellent thermal shock resistance due to their low thermal expansion coefficient as well as high thermal conductivity, so that the stresses between hot and cool parts of a cutting tool insert are minimised, giving good thermal shock resistance (MOMPER (1987), RICHARDS; ASPINWALL (1989)). The relatively high

fracture toughness of Si_3N_4 base ceramic tools is attributed to a fine microstructure containing elongated grains and the fact that cracks are controlled by the pulling out of grains form the matrix. This property make them suitable for rough machining of nickel-base alloys at higher speed conditions as well as rough turning of grey cast iron with strong interruptions of cut, rough milling of grey cast iron and turning of materials having a high nickel content (MOMPER (1987), RICHARDS; ASPINWALL (1989)).

Although ceramic tools have been used for machining of titanium alloys in several studies (DEARNLEY; GREARSON (1986), LEE (1981), KOMANDURI (1989), LI; LOW (1994), KLOCKE; FRITSCH; GERSCHWILER (2002), KOMANDURI; REED JR (1983)) they are not commercially recommended for machining titanium alloys because of their poor performance due to excessive wear rates as a result of the poor thermal conductivity, relatively low fracture toughness and high reactivity with titanium alloys (Figure 2.29) (HARTUNG; KRAMER, 1982). Lower tool lives (< 30 seconds) were recorded when machining titanium-base, Ti-6Al-4V, alloy with various grades of ceramics (SIALON, Al_2O_3 + TiC and Al_2O_3+30ZrO_2) at a cutting speed of 75 m min^{-1} compared with cemented carbide tools (DEARNLEY; GREARSON, 1986). It was reported from this study that all the ceramics exhibited severe notching at depth of cut and the cutting edges of most ceramics revealed smoothly worn rake faces as a result of a dissolution-diffusion and attrition wear mechanisms. SIALON was the most resistant to rake face wear. Smooth and irregular/uneven worn surfaces were observed, but it was, however, prone to severe notching and crater wear, thus not reliable in machining of titanium alloys. Poor performance of SIALON tool was also confirmed by Komanduri and Reed (KOMANDURI; REED JR, 1983) during a study of evaluation of various grades and geometries of cemented carbides and SIALON tools for machining titanium alloys at cutting speeds up to 183 m min^{-1} (Figure 2.40). They reported that the SIALON tools failed almost instantaneously (in less than 15 seconds) with high localised flank wear and cratering, which was followed by notching and catastrophic failure, thus not suitable for machining titanium alloy. Lee (1981) reported that less than one minute tool life was recorded when a pure oxide alumina-base and zirconium-base (Al_2O_3+ZrO_2) alumina ceramics were utilised for machining titanium alloy at a cutting speeds in excess of 122 m min^{-1}. The author attributed the poor performance of ceramic tools to their poor thermal shock resistance and low strength. Other study employed pure oxide alumina-base and SiC whisker reinforced ceramic cutting tools in machining of Ti-6Al-4V alloy at cutting speeds up to 600 min^{-1}, feed rate of 0.1 mm rev^{-1} and depth of cut of 1.0 mm (KLOCKE;

FRITSCH; GERSCHWILER, 2002). The longest tool life of 4 minutes was recorded when a cutting speed of 15 m min^{-1} was employed, suggesting that these tools are not suitable for machining titanium alloys. All the tools were subjected to notch wear, flank wear and crater wear.

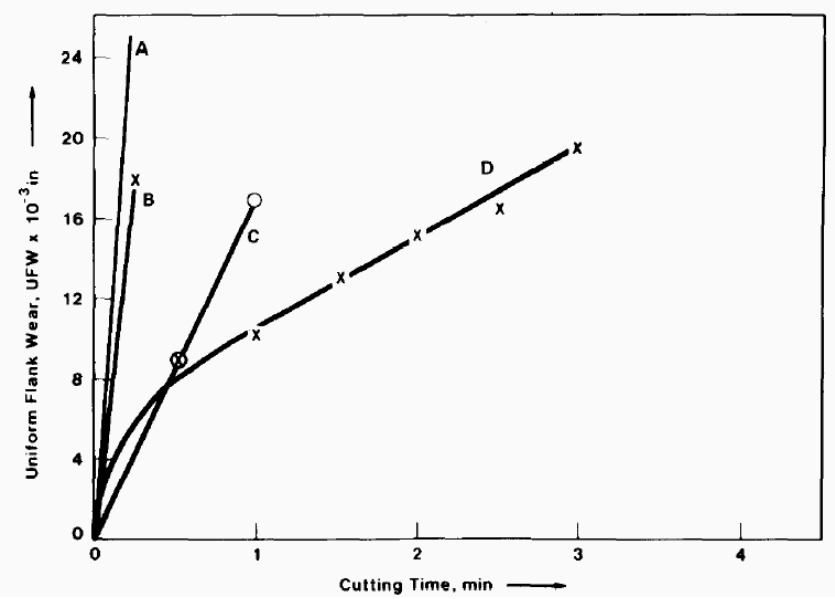

Figure 2.40 - Variation in uniform flank wear with cutting time for the turning of Ti-6Al-4V (hardness, 36 HRC), showing reduced tool wear with the new geometry (cutting speed, 122 m min^{-1}; feed rate, 0.23 mm rev^{-1} unless otherwise indicated; depth of cut, 1.52 mm; tool SNG432 (SCEA, 15º): curve A, SIALON (Kyon 2000) with clearance angles of 17º (localised wear, 0.889 mm; edge fracture; crater) and 5º (localized wear, 1.321 mm; fracture; crater); curve B, SIALON (Kyon 2000) with a clearance angle of 5º and a feed rate of 0.127 mm rev^{-1}; curves C and D, cemented carbide (Carboloy grade 999) with clearance angles of 5º and 17º, respectively (KOMANDURI; REED JR, 1983).

2.13.5.5 Nano-grain Ceramic

Performance of ceramic tools during machining depends on their physical, mechanical and chemical properties (NORTH, 1986). Although conventional micron-grain size ceramic tools did not show encouraging performance when machining titanium alloys, advances in nano-technology have generally led to improved mechanical properties of cutting tools, especially ceramics.

Mechanical properties, such as the hardness, strength and density are related to the size and morphology of the grain and pore as well as the distribution of impurities in the tool

substrate. The use of finer grained substrate generally produced densely packed compact tools after sintering. The fracture modes of ceramics vary with the grain size, which in turn affect the fracture toughness. Increasing the pore size and inter-granular porosity tends to reduce fracture toughness. Wear resistant capabilities of ceramic cutting tool materials are also associated with their grain size. Nano-grain ceramic cutting tool materials have been developed to further enhance their machining performance. The fine grained ceramics also called nano-ceramic possess high specific area, improved thermal shock resistance, improved hardness and superplastic behaviour as well as low thermal expansion coefficient ($4.5x10^{-6}$ $^{o}C^{-1}$) (VAβEN; STÖVER, 1999). Powdered nano-ceramics is defined as a material where the major phase (or at least one constituent) has a grain size in the nanometer range (Figure 2.41) (VAβEN; STÖVER, 1999).

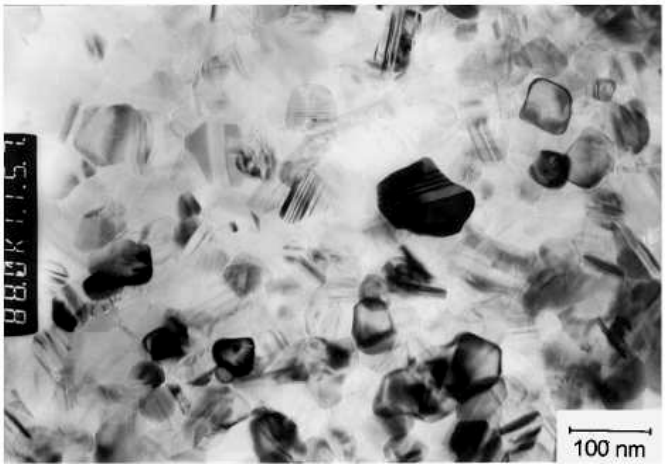

Figure 2.41 - TEM micrograph of HIPed (Hot Isostatic Pressing) nanophase SiC sample with a density of 97% TD (Theoretical density) (VAβEN; STÖVER, 1999).

Powdered nano-ceramics have good formability properties due to their superplasticity behaviour and hence can be formed in complex geometry. Superplasticity is defined by the ability of polycrystalline solids to exhibit exceptionally high levels of elongation in tensile deformation (XIE; MITOMO; ZHAN, 2000). The properties of nano-ceramics to a greater extent depend on the processing technique employed. Despite the fact that nano-ceramics and conventional ceramics generally have the same composition, the production process of the former require high temperature and pressure for efficient sintering in order to reduce the number of agglomerates in their powders, thus ensuring a denser phase powder than conventional ceramics (ZHANG; ZHU; HU, 1996). The sintering pressures can exceed 8 GPa and temperature in excess of 1000ºC. The density of nano-ceramic powder has significant

influence on the mechanical properties such as ductility at low temperature, superplasticity at elevated temperatures and hardness. It is therefore anticipated that this technique will produce cutting tools with improved wear resistance, hardness and toughness relative to conventional ceramics (VAβEN; STÖVER, 1999). Kear et al. (2001) compared the abrasive wear resistance between micron and nano-grained ceramic particles of TiO_2 and concluded that the latter presented about 10% more wear resistance than the former. They also observed a reduction of about 50% in the friction coefficient, surface roughness (R_a) between 20-50 nm, the development of surface plasticity and improved toughness for the nano-grained TiO_2. Bhaduri and Bhaduri (1997) also investigated the toughness behaviour of Al_2O_3-ZrO_2 nano-ceramic and observed a slight drop in hardness with improved toughness in relation to conventional ceramics. The improved hardness observed with reduction in grain size of SiC nano-ceramics (VAβEN; STÖVER, 1999) was attributed to lesser of porosities within the phases with higher density of particles. Furthermore, they observed an excellent thermal shock resistance in materials such as SiC/C-composites with a SiC matrix grain size lower than 200 nm, in spite of the low thermal conductivity relative to conventional ceramics. Kim (1994) verified that increasing the pore size and inter-granular porosity lead to reduction of fracture toughness in ceramic tools. Ezugwu; Bonney and Olajire (2002) observed that micron grain whisker reinforced alumina ceramic tool out performed the nano-grain ceramic tools grades (Al_2O_3 and Si_3N_4) at cutting speed range of 230-270 m min^{-1}, feed rate range of 0.125-0.15 mm rev^{-1} under conventional coolant flow when machining Inconel 718. Silicon nitride (Si_3N_4) base nano-ceramic also gave the worst performance in terms of tool life due to high nose wear rates attributed to the softening of tool materials and consequent weakening of their bond strength when machining at higher speed conditions. A very interesting fact is that nano-grain ceramic tools are more stable in terms of recorded tool life when machining at higher cutting speeds in excess of 230 m min^{-1} and at a feed rate of 0.125 mm rev^{-1}.

2.14 Cutting Fluids

There are many ways to ensure effective and efficient metal cutting. The use of a cutting fluid is one the options and when properly chosen and applied, can be successful. Cutting fluids are used to minimise problems associated with the high temperature and high stresses at the cutting edge of the tool during machining. The main functions of cutting fluids are lubrication, cooling and less important, to clear the swarf away from the cutting area. It is

important to understand how cutting fluids work as lubricants as well as coolants. As a lubricant the cutting fluid works to reduce friction between the tool and the workpiece material, consequently reducing the seizure region. Therefore, its effectiveness depends on its ability of penetrating the chip-tool interface and to form a thin layer in the shortest available time, either by chemical attack or physical adsorption, with lower shear strength than the strength of the material in the interface. In fact, lubricant can only be effective in the sliding zone because the cutting fluid whether in liquid or gaseous form, is unable to gain access to the seizure zone (MACHADO; WALLBANK, 1994). As a coolant the cutting fluids reduces the temperature generated at the tool-workpiece and tool-chip interfaces both by its cooling action and by reducing the heat generated during machining (MACHADO (1990), SALES; DINIZ; MACHADO (2001), BONNEY (2004)). Despite attempts to eliminate the use of cutting fluids in machining operations, when properly applied, they can either increase the rate of production or reduce the total cost per part by ensuring possible the use of higher cutting speeds, higher feed rates and bigger depths of cut (KATO; YAMAGUSHI; YAMADA, 1972). Effective application of cutting fluids can also prolong tool life, thereby reducing the number of tool changes, increase dimensional accuracy as well as improve surface of the machined components (DA SILVA et al., 2001) and decrease the amount of power consumed. The coolant is drawn into the tool-chip and tool-workpiece interfaces by capillary action of the interlocking network of surface asperities. The size of these asperities requires that cutting fluids should have smaller molecular size and good surface tension characteristics. The boundary lubrication at the tool-workpiece interface reduces the welding tendency, thus reducing the rate of wear of the cutting tool. Temperature reduction also leads to a decrease in tool wear rate. This occurs because, first, the tool material is harder and so more resistant to abrasion wear at lower temperatures, and secondly, the diffusion rate of constituents in the tool material is less at lower temperatures. Opposing these two effects, a reduction in the temperature of the workpiece will increase its shear flow stress so that the cutting force and power consumption may be increased to some extent. Under certain conditions this can lead to a decrease in tool life. Built-up-edge can be reduced or completely eliminated by machining with cutting fluids (EL BARADIE, 1996). Since the dual role of cutting fluids is reduction of the cutting temperature (cooling action) and reduction of the heat generated by friction, the use of cutting fluids can lead to reduction of cracks in the cutting tool as well as reduce plucking of tool particles during machining (MACHADO, 1990). The cutting fluid can intermittently penetrate the flank and rake faces of the tool thereby inducing

temperature fluctuation during machining. Due to the elevated cutting temperatures and periodic penetration of cutting fluid to the cutting interfaces, the cutting tool can be subjected to continuous expansion and contraction during machining. Therefore, a cutting tool with a good thermal conductivity and low thermal expansion coefficient can minimise thermal damages by minimising temperature fluctuation at the cutting edge of the tool (EZUGWU; BONNEY; YAMANE, 2003).

When choosing a cutting fluid it is important to optimise the beneficial effects and minimise the harmful effects. In this context, the following properties are desirable in a cutting fluid (MACHADO (1990), DA SILVA et al. (2001), EL BARADIE (1996), FRAZIER (1974)):

- Good lubricant;
- High heat absorption capacity;
- It must not emit toxic fumes;
- Harmless to the lubricating system of the machine tool;
- Harmless to the workpiece surface;
- It should be not be a fire hazard of fume due to increased temperature;
- It must be economical and must remain chemically and physically stable for a long period;
- It should maintain a moderately mild or non-existing odor.

2.14.1 Classification of Cutting Fluids

There are several ways of classifying cutting fluids and there is no standard to establish one of them within the industries. Most of the cutting fluids fall into one of the three categories listed below (BONNEY (2004), EL BARADIE (1996), FRAZIER (1974)):

1. Water based cutting fluids:
    a) Water;
    b) Emulsions (soluble oil);
    c) Chemical solutions (or synthetic fluids);
2. Neat Oils:
    a) Mineral oils;
    b) Fatty oils;
    c) Composed oils;
    d) Extreme pressure oils (EP);

e) Multiple use oils.

3. Gases

Water is the best coolant and it is expected to give the best performance due to its high specific heat, high latent heat of vaporisation and greater turbulence (NAGPAL; SHARMA, 1973). It is, however, a poor lubricant. Because of its high corrosion ability in ferrous materials, it is practically ignored as a cutting fluid.

Soluble oils as the emulsions are bi-phase composites of mineral oils, additives (emulsifiers) and corrosion inhibitors dispersed in water in proportion that varies from 1:10 to 1:100. Additives are usually soaps, acid sludges, saponified phenol and saponified napthenic acids which act to decrease the surface tension forming a stable monomolecular layer in the oil-water interface. Therefore these additives provide the formation of small particles of oil, which can result in transparent emulsions. The stability of the emulsions is related to the development of an electrical layer in the oil-water interface. Repulsive forces among particles of the same charge avoid their coalescence. To avoid the bad effects from water of these emulsions, anticorrosive additives, like sodium nitrite, are used. Since emulsifiers are susceptible to bacterial attack, biocides are also in the formulation to discourage bacterial growth. They must not be toxic and harmful to the human skin. Emulsifiable mineral oils have the desirable characteristics of a good rust inhibition and adequate lubricity for the ordinary cutting applications. The EP and antiwear additives that increase the lubrication properties are the same used in neat oils. However, the use of chlorine in cutting fluids has being restricted due to the harm it causes to the environment and to human health. Sulphur and calcium based additives are being used instead. Both animal and vegetable grease can also be used to enhance lubrication properties.

Cutting fluids can also be produced by chemical (synthetic) and semi-chemical (semi-synthetic) solutions. Synthetic fluids do not have oil in their composition. They are chemical solutions consisting of inorganic and/or other materials dissolved in water and containing no mineral oil. They are based on chemical substances that go into these fluids including amines and nitrites for corrosion inhibitors, nitrates for nitrite stabilization, phosphates and borates for water softening, soaps and wetting agents for lubrication and reduction of surface tension, phosphorus, chlorine and sulphur compounds for chemical lubrication, glycols as blending agents and humectants, and germicides to control the growth of bacteria. The semi-synthetic fluids also known as microemulsions are essentially a combination of chemical fluids and emulsifiable oils in water. These fluids are actually performed chemical emulsions that

contain only a small amount of emulsified mineral oil, about 5% to 30% of the base fluid, which has been added o form a translucent, stable emulsion of small droplet size. They are considered cleaner, with better rust and rancidity control than emusifialbe oils. Extreme Pressure (EP) and anticorrosion additives can be incorporated like in the soluble oils and thus making them suitable for moderate and heavy duty machining and grinding operations.

Neat oils are classified into mineral oils, fatty oils and a mixture based on mineral oil and fatty oil or also with additives, generally of extreme pressure (EP) type. The mixture of mineral and fatty oils is formulated by blending straight mineral oil with 10% to 40% fatty oils. The amount of fatty oils used is dependent on the machinability of the material concerned. Additives are added to neat cutting oils because in some machining operations the load carrying properties of straight oil are inadequate for the severe conditions experienced in the cutting zone. Small additions of the fatty oils have the effect of markedly improving anti-friction characteristics under conditions of boundary lubrication when the rubbing faces are so heavily loaded that a straight oil would be unable to keep the faces apart the fatty additives forms a thin and highly tenacious layer of metallic soap, created by chemical activity between the fatty acid molecules and the metal of the tool, the chip and the workpiece. This layer has very low shear strength and continues to lubricate even after the normal oil film has broken down. The use of these oils as cutting fluids has decreased due to the high cost, fire risks, inefficiency in high cutting speed, low cooling ability, smoke formation and high risk to the human health when compared to water based cutting fluids. Extreme pressure (EP) additives are added to cutting fluids used for machining operations where cutting forces are particularly high, such as tapping and broaching, or for operations performed with heavy feeds. EP additives provide a tougher, more stable form of lubrication at the chip-tool interface. These additives include sulphur, chlorine or phosphorus compounds that react at high temperatures in the cutting zones to form metallic sulphates, chlorides and phosphides.

Gaseous lubricants appear very attractive when the cutting fluid penetration problem is considered. Operations which are performed dry are actually carried out using air as cutting fluid because of its very effective boundary lubrication property. However, as a coolant air is not recommended for machining applications because all gases have relatively poor cooling ability compared to liquids (EL BARADIE, 1996). Detailed information about gaseous lubricant in machining will be given in Section 2.15.6.

Table 2.6 - Tool materials properties and cost (ABRÃO, 1995).

Tool material / Property	High speed steel (M2)	Cemented carbide (M20)	White alumina	Mixed alumina	Whisker reinforced alumina	Silicon nitride-based	CBN/PCBN	Natural diamond	PCD
Typical composition*	0.85wt%C 4wt%Cr 5wt%Mo 6.5wt%W 2wt%V	89.5wt%WC 10wt%Co 0.5wt%other	90-95% Al_2O_3 5-10%ZrO_2	Al_2O_3 30% TiC 5-10%ZrO_2	75% Al_2O_3 25% SiC	77% Si_3N_4 13% Al_2O_3 10% Y_2O_3	98% CBN 2%AlB_2/AlN	-	PCD 2-8% Co
Density (g cm^{-3})	7.85	14.5	3.8 - 4.0	4.3	3.7	3.2	3.1	3.5	3.4
Hardness at RT (HV)	850	1600	1700	1900	2000	1600	4000	10000	8000-10000
Hardness at 1000ºC (HV)	n.a.	≈400	650	800	900	900	≈1800	n.a.	n.a.
Fracture toughness (Mpa $m^{0.5}$)	17	13	1.9	2	8	6	10	3.4	7.9
Thermal conductivity (Wm^{-1} $ºC^{-1}$)	37	85	8 - 10	12 - 18	32	23	100	900	560
Young´s modulus (kN mm^{-2})	250	580	380	420	390	300	680	964	841
Coefficient of thermal expansion ($x10^{-6}K^{-1}$)	12	5.5	8.5	8	6.4	3.2	4.9	1.5 - 4.8	3.8
Approximate cost per edge ♠ (£)	40.3 (bar 25x25 x200 mm)	0.34	0.46	0.6	2.5	1.25	40-60	125-140	30-50

* by volume unless otherwise stated

♠ cost refers to ISO SNGN 120416 inserts

2.14.2 Directions of Application of Cutting Fluids

Cutting fluids are generally directed to the cutting regions where heat is generated though nozzle (external) combined with different directions such as between the workpiece and the chip, between the tool and the chip, between the workpiece and tool, under flooding or “overhead flood cooling” and through the tool (internal)**,** Figure 2.42. Which way that is best will depend on the cutting process and workpiece material. Problems with nozzle holders and positioning of the jet have to be considered if an external jet is used. Factors such as tool layout and tool path have severe limiting impact on the use of an external nozzle (DAHLMAN, 2000). The internal application of the jet is suitable for some cutting processes e.g. drilling and milling. The application of coolant can cause a change in the distribution and location of the peak temperature region in the tool. This change is directly linked to the effect of coolant on chip curl and tool wear (DAHLMAN (2000), SEAH; LI; LEE (1995)). Shaw (1984) found that when the flow is directed from A it can affect the chip curl and chip tool contact length and thus the location of the point of maximum temperature on the rake face of the tool. If the point of maximum temperature is brought close to the cutting edge the effect of applying the flow direction A will be detrimental. Pigott and Colwell (1952) found that tool wear was reduced when very high velocity jet of fluid was applied through direction C. Smart and Trent (1974) also carried out a study on the influence of cutting fluids and the directions of fluid application on temperature distribution in the cutting tool when machining iron and nickel and reported that applying coolant from direction C was the most effective of all directions.

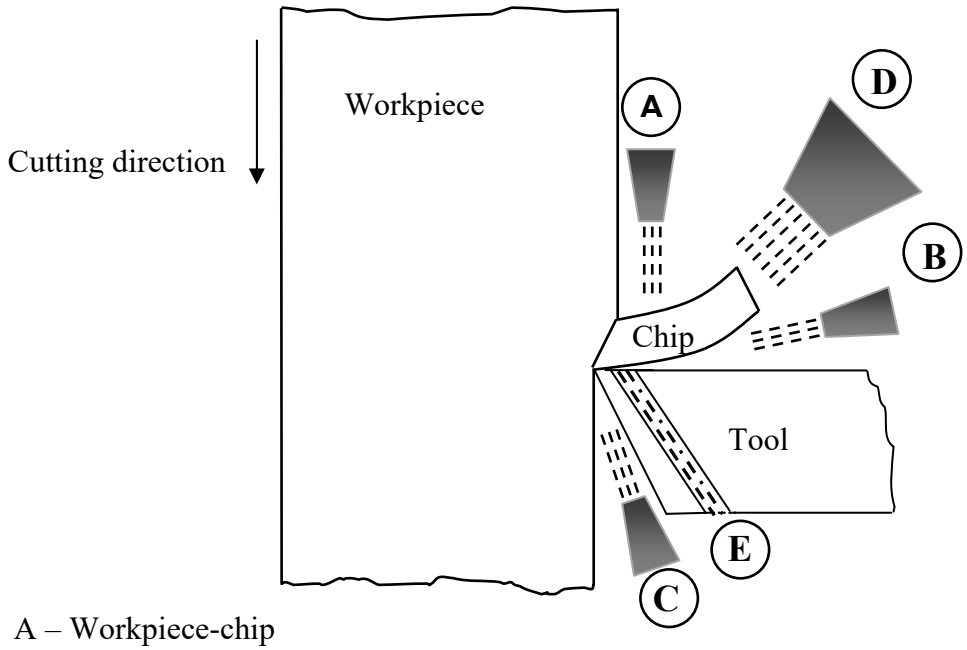

A – Workpiece-chip
B – Tool-chip
C – Workpiece-tool
D – Overhead
E – Internal channel in the tool

Figure 2.42 - Schematic illustration of the possible directions of application of cutting fluids.

Kovacevic; Cherukuthota and Mazurkiewicz (1995) carried out a study to evaluate the performance of three different methods of application of waterjet to the tool-chip interface (through a hole in the tool rake face) through an external nozzle and conventional cooling (overhead) technique in milling stainless steel. They reported that longer tool life, reduction in cutting forces and better chip form were obtained when the jet was applied through an external nozzle toward the area between the rake face and the chip (B direction in Figure 2.42) compared to the jet directed through a hole in the tool rake face (position E) and overhead (position A). Outstanding performance in drilling of Ti-6Al-4V alloy with high-pressure internal cooling was obtained compared with external cooling (LÓPEZ DE LACALLE et al., 2000). Dahlman (2000) found that external application of the jet is suitable for turning operations whereas the jet applied through internal channels in the tool can be more favourable for milling operations. A recent work employing different directions (A, B and C) of application of cutting fluid and different tool geometry in grooving of titanium alloy was carried out by Norihiko and Akio (1998). They found that by applying the cutting fluid from B and C directions simultaneously the grooving performance was improved with the prevention of the adhesion between chip and rake face of the tool as well as the great

reduction of the adhesion on the tool side flank. Conversely, Seah; Li and Lee (1995) found that tool life drastically decreased by application of water-soluble cutting fluid (flowrate of 2.5-3 l min^{-1}) from A direction (Figure 2.42) relative to dry condition when turning AISI 1045 and AISI 4340 with uncoated cemented carbides at cutting speeds up to 190 m min^{-1}. The authors also reported that one effect of the coolant was to slightly increase the crater wear and to shift the position of the crater wear nearer to the tool tip. This causes the tool cutting point to become much weaker.

2.15 Cutting Environments and Techniques Employed when Machining Titanium Alloys

Increased productivity in the manufacturing industry can be achieved by reduction in both non-machining and/or machining time. It is estimated that the cost of an inactive machine is almost the same cost as that of machine used in production. Prevention of this idle time must therefore be given priority (LI; LOW (1994), DAHLMAN (2000)). One common reason for unwanted idle time is the machine operator stopping the machine to clear the chips away as well as to index the cutting tool. The in-put variables of the machining system which generally have influence on machinability of titanium alloys are cutting speed, feed rate, depth of cut, cutting tool and tool geometry, machining environment and the machine tool itself. Tool life and chip shape depends on the in-put variables of the machining system. Reduction of the idle time will depend on a combination of the best machining parameters. However, this combination is not easy to achieve, especially when machining titanium-alloys with characteristics that impair machinability such as low thermal conductivity that consequently increases temperature generated at the tool-workpiece interface, adversely affecting tool life. Since the main in-put variables (cutting speed, feed rate, depth of cut and cutting tool) for a particular machining operation have been chosen previously, the correct choice of cutting environment or atmosphere as well as the suitable technique for machining any material is a decisive factor in order to achieve higher production rates and/or lower manufacturing cost (s).

Attempts have been made to control the high temperature at the cutting zone when machining titanium alloys with cutting fluids using conventional coolant flow. High pressure coolant delivered to the tool cutting edge can provide adequate cooling at the tool-workpiece interface and ensure effective chip segmentation and removal chip from the cutting area

during machining. Other cooling technique, like the minimum quantity lubrication (MQL) has shown considerably improvement in the machinability of aerospace alloys compared to conventional coolant flow (BRINKSMEIER et al., 1999). Although there are still few information about the use of MQL technique in machining titanium-alloys, some encouraging results have been reported in comparison to conventional coolant technique. Although increase in productivity has been obtained using high pressure coolant delivery relative to conventional methods of coolant delivery when machining titanium and nickel-base alloys at relatively lower speed conditions, other environments such as atmospheric air (dry machining), argon enriched environment and liquid nitrogen (cryogenic machining) have been developed as alternative cooling technology to improve the machinability of titanium-alloys due to ecological and economic considerations of the use of cutting fluids. Other environments such as dry air, oxygen, nitrogen, CO_2 and organic compounds such as tetrachloromethane (CCl_4) and ethanol vapour (C_2H_5OH) are also expected to improve the machinability of titanium-alloys by improving the characteristics of the tribological processes present at the tool-workpiece interface and at the same time eliminate environmental damages as well as minimizing some serious problems regarding the health and safety of operators (DA SILVA; BIANCHI (2000), SOKOVIC; MIJANOVIC (2001)).

Despite the poor machinability of superalloys, especially titanium and nickel-base alloys, some special machining techniques including specially designed ledge tools, self-propelled rotary tool (SPRT), ramping technique (taper turning) and hot machining have shown remarkable success in their machining. All of these machining techniques have been used to retard tool wear and consequently prolonging tool life when machining superalloys. As temperature plays a major part in tool failure during machining, it would be reasonable to minimise or even eliminating the temperature generated at the tool-workpiece and tool-chip interfaces. However, for some reasons, the special techniques seem to be not popularised.

2.15.1 Dry Machining

Research activities have mainly concentrated on optimising manufacturing technologies by development of tools with improved properties, by modification/adaptation of tool geometries as well as optimisation of cutting conditions in order to enhance machining productivity (TONSHOFF et al., 1998). In addition to that, ecological regulations and economical considerations have emphasised the need for more dry machining or environmentally clean metal cutting processes. Despite the use of cutting fluid in nearly all

machining, the technology of dry machining is still being applied for special machining operations. The handling, maintenance, recycling and disposal of coolant usually involve significant costs.

In a machining process, new surfaces are cleaved from the workpiece through the removal of material in the form of chips which demands a large consumption of energy. The mechanical energy necessary for the machining operation is transformed into heat. As a result high temperatures, pressures and severe thermal/frictional actions occur at the tool edge in the cutting zone. The greater the energy consumption, the more severe the thermal/frictional actions, consequently accelerating tool wear and making the metal cutting process more inefficient in terms of tool life, dimensional accuracy and material removal rate (KOVACEVIC; CHERUKUTHOTA; MAZURKIEWICZ, 1995). Therefore, the efficiency of the metal cutting process depends to a large extent on the effectiveness of the tribological condition provided for specific material-cutting tool interaction. Unfortunately, conventional cutting fluids cause environmental and health problems. Process-generated pollution in machining has been mainly coming from waste cutting fluids. The cutting fluids disposal became important environmental and economical issues to be considered by machining industry because of the high cost of disposal. The current attention to the environmental impacts of machining processes by government regulations has been forcing manufacturers to reduce or eliminate the amount of wastes (ÇAKIR; KIYAK; ALTAN, 2004). Therefore, dry machining has become a reliable choice in machining of some materials. Decision for dry machining must therefore be made on a case-by-case basis. It is known that these factors are more pronounced especially in dry machining of titanium alloys, thus more wear-resistant cutting tool materials that possess higher hot hardness as well as powerful and rigid machine tools are required (GRAHAM, 2000). The lowest tool lives were obtained with high-speed steel (HSS) and uncoated carbide tools in dry milling of titanium-base, Ti-6Al-4V, alloy compared to minimum quantity of lubrication (MQL) technique and conventional flooding at a cutting speed of 210 m min^{-1}, feed per tooth f_z = 0.08 mm, width of cut a_p = 5 mm and depth of cut a_e = 2 mm (BRINKSMEIER et al., 1999).

Some researches have shown that dry machining can be applied in some materials with coated tools (TONSHOFF et al. (1998), NABHANI (2001a)). Coatings, generally with thickness between 2 and 18 μm, can control temperature fluctuation by inhibiting heat transfer from the cutting zone to the insert or tool. Multilayer PVD coatings with few nanometers thick also have been used (GRAHAM, 2000). The coating acts as a heat barrier, because it has

a much lower thermal conductivity than the tool substrate and the workpiece material. Coated cutting tools, therefore, absorb less heat and can tolerate higher cutting temperatures, permitting the use of more aggressive cutting parameters in both turning and milling without sacrificing tool life. PVD coating of titanium aluminium nitride (TiAlN) are harder, thermally stable and chemically more wear-resistant than TiN coating and have performed better in dry machining at higher speed condition when machining difficult-to-machine materials (GRAHAM, 2000). The better performance of TiAlN coating it attributed to the amorphous aluminium-oxide film that forms at the chip-tool interface when some of the aluminium at the coating surface oxidise at high temperatures. A recent study on the performance of oxygen-rich TiAlON coating of WC-carbides in dry drilling of tempered steel showed that the best wear resistance was found for seven-layered films with alternating interlayers of TiAlN and TiAlON (TONSHOFF et al., 1998). There was no beneficial effect of TiC/TiC-N/TiN coating deposited in tungsten carbide substrate inserts in dry machining of titanium-base, Ti-4Al-8V, alloy at a surface speed of 75 m min^{-1}, a feed rate of 0.25 mm rev^{-1} and a depth of cut of 1.0 mm (ZOYA; KRISHNAMURTHY, 2000). The coating layers were rapidly eroded by a process of adhesive wear, leaving the tungsten carbide substrate vulnerable to cratering. Deformed carbide particles were also observed to be carried off by the underside of the chip, demonstrating the intimacy and strength of the bond between the workpiece and the tool. CVD coating process can be used for depositing a layer of aluminium oxide, the most heat and oxidation resistant coating known. Aluminium oxide (Al_2O_3) is a poor heat conductor and insulates the tool from the heat generated during chip formation, forcing it to flow into the chip. Al_2O_3 is therefore an excellent CVD coating for most dry turning operations performed with carbide substrate. It also protects the substrate at high cutting speeds and is regarded as the best coating material in terms of abrasion and crater wear resistance.

Dry machining of hardened steels has been performed very well using polycrystalline cubic boron nitride (PCBN) and ceramic cutting tools. It is believed that concentrating heat in the cutting zone will reduce the workpiece shear strength, therefore, lowering cutting forces. Pure alumina oxide ceramics (Al_2O_3 + ZrO_2) are also recommendable to this application because of their lower thermal conductivity (ÁVILA; ABRÃO, 2001).

There have been many attempts on dry machining of titanium alloys with conventional and advanced cutting tool materials. These studies have so far provided little improvement in terms of tool life and surface integrity of machined surfaces. However, recent publications have reported the possibility of dry machining of hard materials with ultra-hard cutting tools

such as PCD and CBN. The use of ultra-hard cutting tools for prolonging tool life when machining titanium alloys at relatively high cutting speeds has not been required because titanium alloys are believed to readily ignite at these conditions. PCBN and PCD cutting tools have, however, been used to machine titanium alloys at lower speed conditions (up to 70 m/min). Owing of their high hardness and high melting point, CBN tools can withstand the heat and pressure developed during cutting. According to Seco Tools (2002a), surface integrity of components machined can generally be maintained due to the ability of CBN tool to maintain a sharp edge even when it has witnessed significant wear. Nabhani (2001a) reported satisfactory tool life and surface finish when dry machining titanium-base, Ti-4Al-8V, alloy with ultra-hard materials (PCD, CBN) and coated carbide tools at a surface speed of 75 m min^{-1}, a feed rate of 0.25 mm rev^{-1} and a depth of cut of 1.0 mm. Average flank wear was the predominant failure mode. Ultra-hard materials are suitable for finish machining of titanium alloys at a cutting speed of about 150 m min^{-1} and a depth of cut over 0.5 mm (SECO TOOLS, 2002a). According to this study, PCD tools performed better than CBN and cemented carbide tools, in terms of wear rate and with over 250% improvement in tool life, when dry turning Ti-base, Ti-6Al-4V, alloy at a speed of 75 m min^{-1}, a feed rate of 0.25 mm rev^{-1} and a depth of cut of 1.0 mm. These results show that ultra-hard tool materials can be used in dry machining of titanium alloys at lower cutting speeds and at relatively lower feed rates. Despite the encouraging performance of ultra-hard tool materials, their application in dry machining of aerospace alloys is still questionable due to their higher cost compared to carbide tools. Improvement in recorded tool life is not sufficient to compensate for their high cost, consequently their use in dry machining is not economical. For instance, the price per cutting edge of a PCD insert is about 22.5 times higher than a carbide insert (SECO TOOLS, 2002b).

Besides titanium alloys, materials like austenitic stainless steel, high-temperature alloys like nickel alloys and hardened steel demand alternative machining environments (DALHMAN; KAMINSKI, 1999). The most commonly used environments for machining aerospace alloys are with conventional coolant supply, high and ultra high pressure coolant supplies, which generally delivers coolants in variable quantities. Others include atmospheres containing nitrogen, CO_2, argon, ethanol vapour and pure oxygen can also be used singly or in combination with high pressure coolant delivery systems in machining applications.

2.15.2 Conventional Coolant Supply

Conventional coolant supply technology is the most employed technique to deliver cutting fluid to the cutting zone during machining, especially when machining titanium alloys, despite the trend towards dry cutting and "ecological" (minimum quantity of lubrication) machining. Other terms such as flooding, conventional cooling and flood application can also be encountered in the literature to refer to the conventional coolant supply technique. The cutting fluid is pumped through a flexible pipe to a nozzle, which can be adjusted to direct the stream of the fluid to the desired point. The flow is supplied with little (< 0.3 MPa) or no static pressure but at abundant flow rate (generally lower than 10 $l\ min^{-1}$) to ensure complete coverage of the cutting area (SECO TOOLS, 2002b). This can be achieved by using large piping with a relief valve in the system and by removing restrictions to get maximum nozzle flow at low pressure (MACHADO, 1990). Typical directions of application of cutting fluids when using conventional method are through directions A (workpiece-chip interface), B (tool-chip interface), D (flooding or "overhead") as illustrated in Figure 2.42. Conventional coolant flow technique is effective when machining at lower speed conditions when temperatures at the cutting zone are relatively low. At higher speed conditions, the cutting fluid has negligible access to the tool-workpiece or the tool-chip interfaces which are under seizure condition. The high temperature generated close to the tool edge during machining generally causes vaporisation of the cutting fluid (BONNEY, 2004).

When using cutting fluids in machining, the coolant flow rate should also be taken into consideration. It is believed that by increasing the flow rate and the heat transfer rate heat dissipation at the chip-tool-workpiece interfaces also improves as more quantity of fluid is delivered to the cutting area. Tool life increased by up to 2 folds when the flow rate of emulsion oil was increased from 1.7 to 6.8 $l\ min^{-1}$ during turning of titanium-base, Ti-6Al-4V, alloy (MANTLE; ASPINWALL, 1998). However, in some cases, this cooling effect does not represent advantage in machining. As the heat generated during the machining is transferred to the workpiece, tool, chip and cutting fluid, more attention should be focused on the cutting tool. Subjecting the workpiece to continuous cooling will mean that more energy is required for material removal. High cutting forces therefore becomes inevitable thus a more heat resistant cutting tool is required.

2.15.3 High Pressure and Ultra High Pressure Coolant Supplies

An interesting alternative to conventional coolant supply is the high pressure supply technique. High pressure coolant supply which delivers coolant to the cutting environment has been used for some time to improve the machinability of materials, particularly aerospace alloys. Its credibility had been investigated over the last 50 years and, although practically all high pressure systems tested have produced benefits to the machining processes, they were not adopted as a commercial process in the past because of equipment cost and also the fact that low speed machining was the preferred mode of production as machine tools were not capable of high speed machining applications (BONNEY, 2004). Today higher production rate is the basic principle in industry and the most economic means of achieving this is through the use of high pressure coolant technique. The term “ultra high pressure” is currently used for coolant pressures in excess of 30 MPa. Cutting fluids can be delivered under high pressure supply to very close to the critical point on the secondary shear zone (B and E directions – Figure 2.42 as well as on the workpiece-tool interface (C direction). Figure 2.43 shows a schematic illustration of a toolholder used to deliver coolant at high pressure through an internal channel that reaches the cutting tool in the B direction (SECO TOOLS, 2002b).

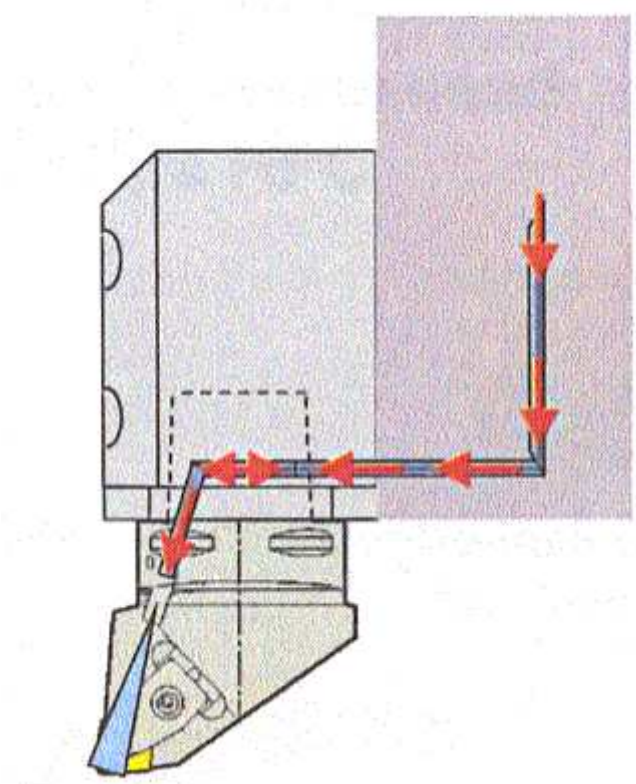

Figure 2.43 - Schematic illustration of a tool holder used for machining under high pressure coolant supply (SECO TOOLS, 2002b).

In addition to ensuring cooling at high speed conditions, the coolant under high pressure can also act as a chip-breaker. Producing snarled chips during machining operations may cause problems such as exposing the operator to imminent danger and damage to the workpiece. This can also hinder the use of advanced manufacturing techniques (unattended machining, for instance) as well as hindering access of the cutting fluid to the cutting zone and associated disposal problems that alternately increase machine tool downtime during production. The high/ultra high pressure coolant jet, generally within the range 0.5 – 360 MPa, is directed via a specially designed orifice in the tool-holder to the region where the chip breaks contact with the tool. A hydraulic wedge is created at the tool-workpiece interface which allows the coolant jet to penetrate the interface deeply with a speed beyond that necessary even for very high speed machining. This action reduces the tool-chip contact length/area and also changes the chip flow direction. A resulting force acting upon the chip is created from the pressure in the fluid wedge. The cantilever effect on the chip is dependant on the pressure distribution. The position of the resulting force can be changed by altering the jet hit position along the cutting width, Figure 2.44 (a) (DAHLMAN, 2000). From this approximation of the pressure distribution in orthogonal cutting, the jet is directed at the middle point of the cutting width and it is assumed that maximum pressure peak occurs just at the jet hit position. At longitudinal turning when the nose radius is engaged, the pressure build up will differ from orthogonal turning. The pressure distribution form cannot be Gaussian since the workpiece helps sustaining a pressure level at the side (DAHLMAN, 2000), see Figure 2.44 (b). The shape and size of the pressure distribution enable control of the chip form and flow direction (DAHLMAN (2000), DALHMAN; KAMINSKI (1999), KAMINSKI; DAHLMAN (1999)). Additionally, the temperature gradient is reduced by penetration of the high-energy jet into the tool-chip interface and consequently eliminating the seizure effect (MAZURKIEWICZ; KUBALA; CHOW, 1989), thereby providing adequate lubrication at the tool-chip interface with a significant reduction in friction (EZUGWU; BONNEY; YAMANE, 2003). These combined with high velocity coolant flow causes the breakage of the chips into very small segments. Because the tool-chip contact time is shorter, the tool is less susceptible to dissolution wear caused by chemical reaction with newly generated chips, especially titanium-alloy chips (LINDEKE; SCHOENIG; KHAN, 1991).

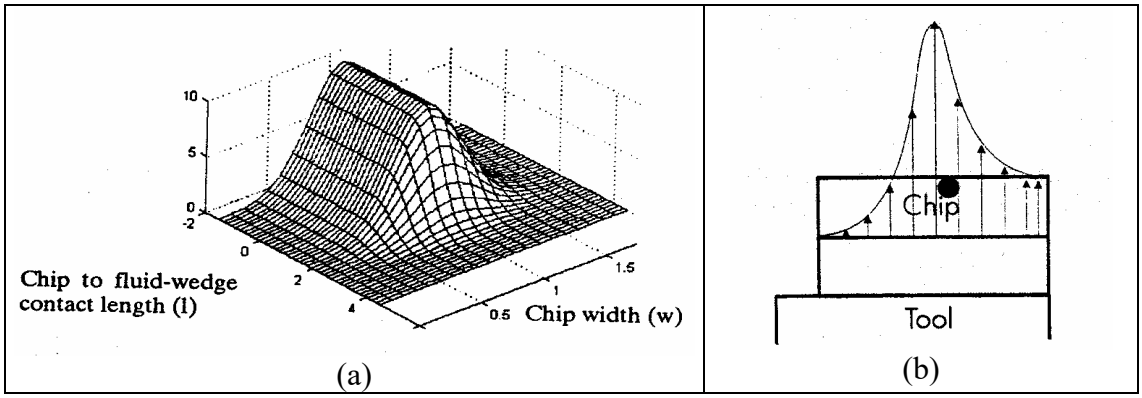

Figure 2.44 - Pressure distribution from the jet momentum action on the chip. (a) Cutting in tube with single straight edge; (b) pressure distribution (2D) at longitudinal turning (DAHLMAN, 2000).

The efficiency of high pressure coolant technique is strongly dependent upon the jet pressure levels (DAHLMAN, 2000). Pigott and Colwell (1952) carried out a series of tests using various jet pressures from 0.17 to 4.14 MPa in machining of SAE 1020, SAE 3150, AISI 3140 steels. They surprisingly found that when the jet pressure exceeded 2.76 MPa the tool life started decreasing. This phenomenon was attributed to an optimum jet-pressure or critical limit as a result of the critical boiling action of the coolant at the tool edge since it was possible to sweep the tool surface faster by the higher jet speed, thus lowering the rate of boiling and cutting down heat transfer which presumably may vary with tool/work material combination as well as cutting conditions. Nagpal and Sharma (1973) carried out various tests similar to those of Pigott and Colwell in order to investigate the optimum jet pressure varying from 0.34 to 3.4 MPa when machining a medium carbon steel with four different cutting fluids. The pressure of 1.34 MPa was the optimum jet pressure achieved by these researchers when using three different oils and it appeared to have a relationship with the total heat generated during machining. However, when using soluble oil the optimum jet pressure was found to be strongly dependent on the feed rate. Kishi et al. (1975) also investigated the influence of high pressure coolant technique on machinability parameters such as cutting forces, cutting temperature and surface roughness when machining pure aluminium, nickel-base, Nimonic 80A, alloy and various grades of steels using four different soluble oils as cutting fluids. The jet was directed from B position (Figure 2.42) and jet pressure varied from 0.3 to 3.9 MPa. They reported that cutting forces, cutting temperature and surface finish all decrease from a zero value of pressure up to a certain value and were either saturated or

reached a critical point and that increased slightly thereafter. Additionally, it was found that cutting fluid composition as well as their effects on lubrication and cooling were mutually related and influenced the machinability of all workpiece materials tested with an increase in jet pressure. The authors explained that the reason why these parameters reach a constant value and increase again was due to the permeation depth of cutting fluid into the cutting zone. As the jet pressure increases cutting fluids can be introduced deeply into the tool-chip interface and thus the effects of lubrication and cooling are sufficiently obtained. However, the permeation depth for cutting fluid to be introduced reaches a constant value and it can not be introduced more deeply than this depth because of high hydrostatic stresses at the tool-chip interface, even if the jet pressure is increased. The formation of vaporised films in the cutting zone decreases remarkably under constant jet permeation depth conditions. Consequently, cutting force and other parameters are minimised in such jet pressure. When the jet pressure is increased, the amount of the thick vaporised films to give the lubricant effect will reduce gradually and instead thin vaporised films will exist in the cutting zone between the tool and the chip. Consequently, as frictional force increases, cutting temperature and cutting force increases gradually with increase of jet pressure. Recently Kovacevic; Cherukuthota and Mazurkiewicz (1995) also investigated the performance of two different methods of application of high pressure water jet cooling/lubrication with jet pressure varying up to 200 MPa in milling stainless steel. In all of the cases the authors observed that when water pressure reached a certain optimum value, a further increase in water pressure was not found to be very beneficial in further improving machining performance. The authors suggested that this could be due to the fact that a high pressure waterjet after penetrating to a certain depth into the tool-chip interface is not capable of penetrating any deeper, hence overcoming the high contact pressures at the tool-chip interface. Bonney (2004) carried out a recent study of high speed machining of Inconel 718 with ceramic and coated carbide tools at cutting speeds up to 60 m min^{-1} and feed rates varying from 0.1 to 0.3 mm rev^{-1} under various high pressure coolant supplies with jet pressures of 11 MPa, 15 MPa and 20.3 MPa. He reported that 15 MPa was the optimum jet pressure for machining with coated carbide tools at speeds lower than 30 m min^{-1} and a feed rate of 0.25 mm rev^{-1}, whereas the jet pressure of 11 MPa was the optimum pressure for machining with the same tool materials in all cutting speed tested and a feed rate lower than 0.25 mm rev^{-1}. From this study it is clear that optimum jet pressure is interdependent of the cutting parameters employed, especially the feed rate.

Another relevant factor that must be considered when using high or ultra high pressure coolant delivery is the cooling jet power. Tool wear increased with an increase in the maximum jet power up to 12kW when machining Ti-base, Ti-6Al-4V, alloy with carbide tools at a speed of 150 m min^{-1}, feed rate of 0.18 mm rev^{-1} and depth of cut of 1.5 mm**.** Crater wear occurred with further increase in the jet power. Chips produced when machining at a jet power lower than 3kW were not completely serrated (VIGNEAU, 1997). Besides the correct choice of coolant pressure, other important factors that can improve the efficiency of coolant delivery at high pressure must be considered such as jet properties and shape of the nozzle.

As the coherence and stability of the jet are associated with chip-control, a reduction in the jet velocity leads to a decrease in momentum power at the impact position. Therefore, a stable pressure build-up at the chip-tool interface is necessary for utilising the effect of the jet in the best possible way. A free jet beam in the air is exposed to drag reduction. The longer the travelling distance in air the more the jet beam deteriorates. In some applications long travelling distances is, however, necessary due to design of tools and other external conditions. It is recommended to keep the distance from the nozzle to the impact position at a reasonable level, preferably no longer than 50 mm (NAGPAL; SHARMA, 1973).

The shape of the nozzle forming the jet is important for several reasons:

- Microscopic imperfections present in worn nozzles cause turbulence and cavitation (NAGPAL; SHARMA, 1973), thereby influencing the boundary layer of the jet. This accelerates deterioration of the jet produced from a worn nozzle than from a new one. This action tends to increase turbulence, leading to loss of jet coherence;
- The nozzle geometry should be adapted to each cutting application and can depend on some factors such as pressure, available flow and tooling;
- Wide rectangular nozzles can cover the cutting edge with one jet. The same coverage can be achieved with more than one round nozzle.

The use of high pressure coolant supply in machining applications was earlier reported in the 1950s by Pigott and Colwell (1952) and later on by Field (1968). From that time until the end of 1980´s few studies (NAGPAL; SHARMA (1973), KISHI et al. (1975), SHARMA; RICE; SALMON (1971), MAZURKIEWICZ; KUBALA; CHOW (1989)) were encountered in the literature. However, it was through the 90´s decade that number of studies employing high pressure coolant technique in machining applications was rapidly increased (MACHADO (1990), GETTELMAN (1991), LINDEKE et al. (1991), WERTHEIM et al.

(1992), KOVACEVIC; CHERUKUTHOTA; MAZURKIEWICZ (1995), NORIHIKO; VIGNEAU (1997), AKIO (1998), BRINKSMEIER et al. (1999), CRAFOORD et al. (1999), DALHMAN; KAMINSKI (1999), EZUGWU; WANG; MACHADO (1999), KAMINSKI; DAHLMAN (1999), SOKOVIC; MIJANOVIC (2001). More recently other many researches (DAHLMAN (2000), KAMINSKI; ALVELID (2000), LÓPEZ DE LACALLE et al. (2000), KLOCKE; RAHMAN; SENTHIL KUMAR; CHOUDHURY (2000), FRITSCH; GERSCHWILER (2002), BONNEY (2004), DAHLMAN; ESCURSELL (2004), MACHADO et al. (2004), MAGALHÃES; FERREIRA (2004)) have been carried out with use of high pressure coolant technique in various machining operations. These studies generally reported increased productivity when compared to the conventional methods of coolant delivery. Reduction of temperature in the cutting zone, increase in tool life (up to 5 folds), lower cutting forces, less vibration levels as well as better surface integrity and closer tolerances of the machined components are major benefits of machining under high pressure coolant supplies. A 3 fold increase in cutting speed have been reported when machining titanium-base, Ti-6Al-4V, alloy with carbide tools under high pressure water jet assistance (HPWJA) relative to conventional flooding (VIGNEAU, 1997). Using HPWJA of 4kW and 12 kW, over 3 and 5 folds increase in tool lives were recorded, respectively, compared to conventional coolant flow. Over 300% increase in tool life was achieved using a high jet pressure of 14.5 MPa in machining Ti-6Al-4V alloy with uncoated carbides at a cutting speed of 60 m min^{-1}, a feed rate of 0.25 mm rev^{-1} and a depth of cut of 2.5 mm compared to conventional coolant flow (MACHADO, 1990). The same author also reported that high pressure coolant supply showed much success as a chip-breaker and marginal gain in tool life due to the high rate of notch wear of the ceramic cutting tool employed when machining the Inconel 901. A recent study of the effect of high pressure coolant flow at a pressure of 14 MPa in face milling of Ti-base, Ti-6Al-4V, alloy with cemented carbide tools reported a 2.5 times increase in tool life than when machining with conventional coolant flow (KLOCKE; FRITSCH; GERSCHWILER, 2002). Studies carried out at 15 MPa and 30 MPa jet pressures reported about 50% increase in cutting speed when machining titanium alloys at a higher jet pressure of 30 MPa relative to conventional coolant flow (SECO TOOLS, 2002a). It has also been reported that machining under high pressure coolant supply did not lead to a significant reduction in cutting forces despite the small change in the chip-tool contact length (EZUGWU; PASHBY (1990), CRAFOORD et al. (1999)). A more recent study (BONNEY, 2004), has shown that high jet pressures of 11MPa and 15 MPa gave about 42% and 71%

increase in tool lives respectively when machining Inconel 718 with ceramics compared to conventional coolant at a speed of 250 m min^{-1} and a feed rate of 0.2 mm rev^{-1}. With coated carbide tools it was reported that up to 518%, 647% and 740% improvement in tool lives was achieved using jet pressures of 11 MPa, 15 MPa and 20.3 MPa, respectively under a cutting speed of 50 m min^{-1} and a feed rate of 0.3 mm rev^{-1}. Other recent study (MACHADO et al., 2004) was carried out to evaluate the influence of the use of high jet pressure technique in tool life of various cutting tools materials when high speed machining of Ti-6Al-4V alloy. It was reported that up to 3 folds increase in tool life was achieved when a jet pressure of 20.3 MPa with uncoated cemented carbide inserts at a cutting speed of 110 m min^{-1} and feed rate of 0.15 mm rev^{-1} compared to conventional coolant supply. When PCD tools were employed at a cutting speed of 175 m min^{-1}, the gain in tool life was about 21 folds.

Another consideration regarding the use of high pressure system is that machine tools must be built with very efficient leak-proofing in order to contain the coolant in the machine and it must also have a mist extractor capable of filtering all the fumes and sprays produced in the machining environment to avoid harming the operator.

2.15.4 Minimum Quantity Lubrication (MQL)

A machining technique called minimum quantity lubrication (MQL) or minimum quantity cutting fluid application (MQCFA) is a viable alternative to improving the characteristics of the tribological processes present at the tool-workpiece interface in order to improve the machinability of materials and at the same time eliminate environmental damages as well as minimizing some problems associated with the health and safety of operators (DA SILVA; BIANCHI (2000), LI et al. (2000), MACHADO; WALLBANK (1997), SOKOVIC; MIJANOVIC (2001)). Using the same principle of high pressure coolant supply, this technique consists of applying a small amount of the highly efficient coolant/lubricant which is pulverised in compressed air stream to the cutting zone at a flow rate often below 100 ml h^{-1} (SECO TOOLS (2002a), LEE (1981)) compared to 120000-720000 ml h^{-1} (2-12 *l* min^{-1}) generally employed in conventional coolant flow. This is why this technique is considered a “clean cutting process”. MQL also contributes to lowering machining costs as low quantity of cutting fluid is utilised.

Improvement in machining performance can be achieved when sufficient amount of cutting fluid gain access to the chip-tool interface (GRAHAM, 2000). Machining with MQL reduces temperature generated at the cutting zone mainly due to the cooling effect of the

compressed air jet and partially due to absorption of heat by the cooling and lubrication functions of cutting fluids**.** The fine spray of oil during the process of lubrication of the cutting zone is also vaporised by the high temperature generated. This small quantity of oil, most of the time, is sufficient to substantially reduce friction and to avoid the adhesion of the chip on the tool. Cooling by convection itself is rather low. MQL technique just delivers the lubricant to the tool-chip and tool-workpiece interfaces while conventional coolant system floods the entire cutting region. In order to achieve best performance of the MQL technique, the nozzle geometry must be taken in consideration. In a machining process, good atomisation is necessary to provide adequate wetting of the work area. Due to exposure to aerosols (generally consisting of hazardous substances), which offers high risks to human health, care must be taken when using MQL.

There are limited studies on MQL technique for machining titanium alloys. A recent study on the use of this technique in milling of titanium alloy with uncoated carbide and high-speed steel (HSS) tools in three different environments (dry condition, conventional coolant flooding and MQL technique) at a feed per tooth f_z = 0.08 mm, width of cut a_p = 5 mm, depth of cut a_e = 2 mm and cutting speeds up to 210 m min^{-1} (BRINKSMEIER et al., 1999). The MQL technique gave moderate performance when machining with uncoated carbide tools. When HSS tools were used with MQL technique at a cutting speed of 80 m min^{-1}, tool lives increased by about 32% and 800% compared to conventional coolant flooding and dry condition, respectively. Despite the high and randomised surface roughness values obtained, encouraging tool life was recorded with the MQL technique at a flow rate of 10 ml h^{-1} compared to dry machining and conventional flooding when turning AISI 52100 hardened steel with a CBN tool at various cutting speeds (NOVASKI; DÖRR, 1999). The use of MQL technique can also contribute to reduce machining problems such as pressure welding of chips to the cutting edge, the main cause of tool failure when milling titanium alloys with high speed steels (HSS) tools. Improved surface finish of the machined components was obtained when machining with MQL (EZUGWU; BONNEY; YAMANE, 2003). A two fold increase in tool life was obtained when milling aerospace alloy steels with coated carbide tools using MQL technique compared to dry machining (DINIZ; FERREIRA; FILHO, 2003). Another benefit of this technique is that it can easily be mounted on to existing machine tools at relatively low cost. Although MQL technique has been promising, its application in general machining operations of titanium alloys is unknown and still requires further studies.

2.15.5 Cryogenic Machining

The past two decades have witnessed an increase in research investigating the effect of lower temperatures in the thermal treatment of steels, particularly in HSS cutting tools (SMOL'NIKOV; KOSSOVICH (1980), POPANDOPULO; ZHUKOVA (1980), TSEITLIN (1980), ZHMUD' (1980)). Initial tests consist of subjecting the materials to sub-zero temperatures varying from –100ºC to –80ºC for a period of 1 hour. Currently, these temperatures can be as low as – 196ºC (DA SILVA; MACHADO; DE SOUZA, 2001). This is referred to as sub-zero cooling or cryogenic treatment. The main purpose of this treatment is to enhance alteration of the microstructure of the material such as transforming the austenite content present in steels into martensite and precipitation of the fine carbide particles, consequently altering the tribological mechanisms to improve its machinability. Up to 25% improvement in the performance of M2 HSS tools cryogenically treated has been reported when drilling AISI 8640 steel at a cutting speed of 40 m min^{-1} (DA SILVA; MACHADO; DE SOUZA, 2001). However, unsatisfactory results were recorded when milling the same workpiece material with coated M2 HSS tools cryogenically treated. With technological advances, it is possible to extend the cryogenic principles to the machining of titanium alloys as another alternative to improving their machinability, using liquid nitrogen and carbon dioxide (CO_2) as the main refrigerants.

Liquid nitrogen (LN2) is often used as coolant because of its higher capacity to absorb heat than liquefied CO_2, its relatively low cost and also the fact that LN2 does not harm the environment. Temperatures in the region of 1100ºC are generated when machining Ti-6Al-4V alloy (KONIG (1979), MOTONISHI et al. (1987)). This promotes the softening of the cutting tool material and consequently accelerates tool wear. Application of LN2 to the tool cutting edge leads to rapid increase in the hardness of the tool, thus retarding tool wear and extending tool life (MAZURKIEWICZ; KUBALA; CHOW, 1989). Therefore, cryogenic machining is an efficient way of maintaining the temperature at the cutting interface to well below the softening temperature of the cutting tool material in addition to being environmentally safe relative to conventional emulsion cooling. This method consists of delivering LN2 via nozzles directed to the tool rake face to the flank face or simultaneously to both faces as is illustrated in Figure 2.45 (HONG; DING; JEONG, 2001).

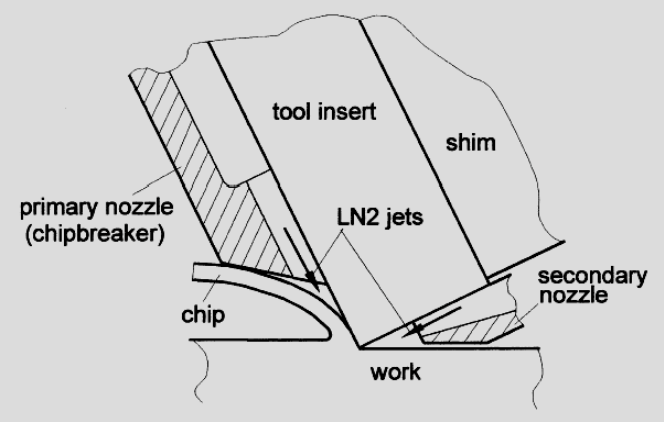

Figure 2.45 - Schematic illustration of nozzle orientation for localized LN2 delivery (HONG; DING; JEONG, 2001).

Figure 2.46 (MAZURKIEWICZ; KUBALA; CHOW, 1989) clearly illustrates the cryogenic cooling concept using an insert with an obstruction type chip breaker. In this schematic diagram liquid nitrogen (LN2) is released trough a nozzle between the chip breaker and the tool rake face. The chip breaker helps to lift the chip to permit LN2 to reach and cool the tool-chip interface. Unlike conventional flood cooling, the chip does not block the flow of LN2. Thus, LN2 absorbs the heat, evaporates quickly and forms a fluid/gas cushion in the tool-chip interface that acts as a lubricant (HONG; DING; JEONG, 2001). As a result of this, the coefficient of friction is reduced consequently reducing both crater and flank wear rates. An auxiliary nozzle can be used to deliver LN2 to the tool flank surface to minimise the appreciable flank wear on the tool when machining titanium alloys. Figure 2.47 shows a picture of the tool assembly, nozzles and LN2 flowing out of the nozzle. However, there is an undesirable phenomena associated with LN2 delivery itself which causes formation of ice on the channel of the jet flow. This can block the coolant circulatory system, adversely affecting the cryogenic machining process. A recent comparative study of the wear rates of cemented carbide tools using LN2 and conventional cooling when machining titanium-base, Ti-6Al-4V, alloy at a cutting speed of 132 m min^{-1}, feed rate of 0.2 mm rev^{-1} and a depth of cut of 1.0 mm showed a five fold increase in flank wear for tools subjected to the conventional cooling (WANG; RAJURKAR, 2000).

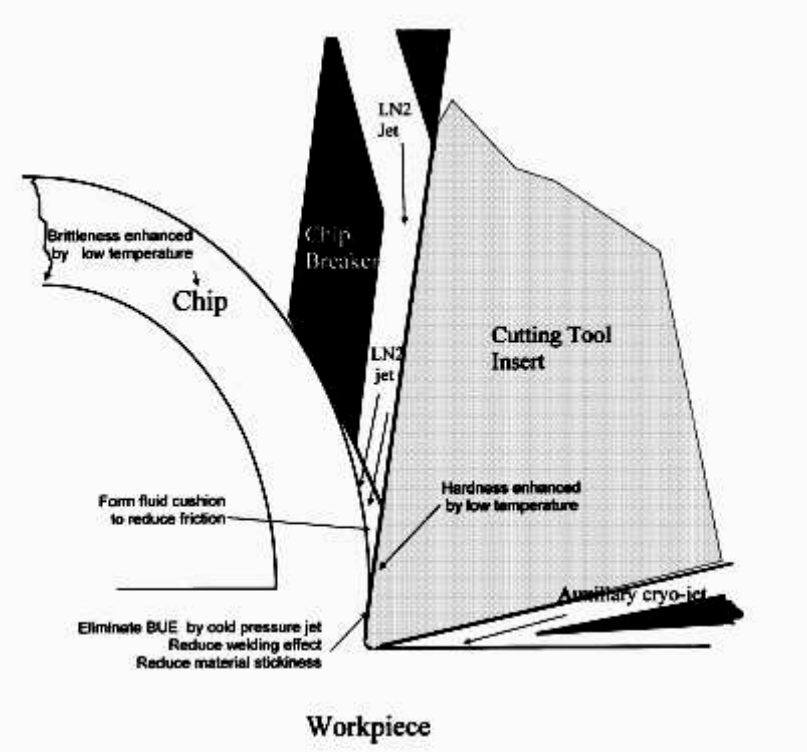

Figure 2.46 - A schematic representation of the cryogenic cooling concepts (MAZURKIEWICZ; KUBALA; CHOW, 1989).

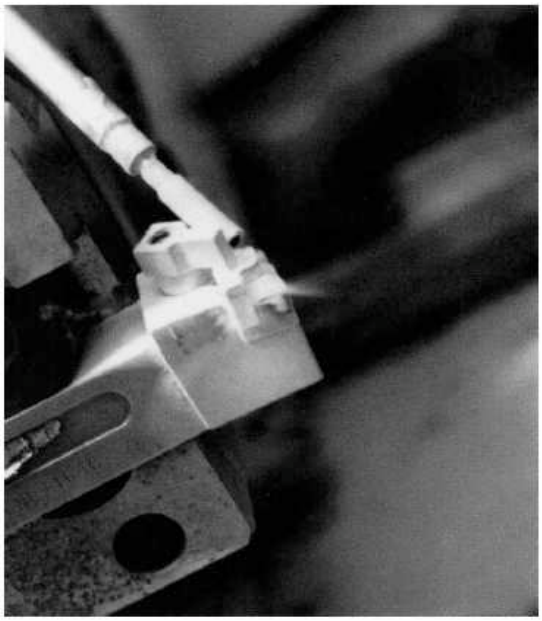

Figure 2.47 -The tool assembly, nozzles and LN2 flowing out of the nozzle (MAZURKIEWICZ; KUBALA; CHOW, 1989).

Yankoff developed an equipment by which carbon dioxide gas (CO_2) combined with water-based fluid was directed across the cutting insert at the tool-chip interface (CRAFOORD et al., 1999). Being a combination of high pressure coolant delivery and cryogenic principles, expanding and cold CO_2 gas jet at temperature of -73ºC cause breakage of the stringiest and softest steel chips into very small segments. The gas/fluid stream also kept the cutting insert cool to the touch, even after machining at high speeds and feed rates. This system was patented under the name of "Flojet" in 1986. Both CO_2 gas and water-based fluid emerges from separate lines from a small nozzle under the cutting tool. They are then mixed in the chamber. Further details on this equipment can be obtained elsewhere (CRAFOORD et al., 1999). A probable question is why they did not use high-pressure fluid alone? The answer is based on the heat generation during machining. Both the high pressure system and the cutting process generate heat. During machining, the water-based fluid soon warms up with subsequent evaporation that reduces its heat absorption capability. The excellent cooling capability of the CO_2 gas can keep the fluid, cutting tool and workpiece at room temperatures or even lower. The thermal expansion of the work material therefore remains unaffected, hence longer tool life can be achieved and the need for a fluid refrigeration system is eliminated.

2.15.6 Other Atmospheres

It has been reported from the literature that some gases have replaced cutting fluids in machining when cutting fluid penetration problem is considered as well as to prevent oxidation of the workpiece and the chips (EL BARADIE, 1996). Various results were given such as lower cutting forces and better surface finish. It was noted that the general information was brief and based on very limited studies. Although these studies have been carried out on the use of gases such as argon, dried air, oxygen, nitrogen, helium, CO_2 and ethanol vapour as additional methods to improve machinability of aerospace alloys, many information on the experimental procedures (specification, methodology and equipment) are still unclarified. It is known that the principles underlying the chemical processes of these gases can alter the tribological conditions existing between two surfaces in contact (MISHINA, 1992), such as the cutting zone during machining (JAWAID (1982), (KHAMSEHZADEH (1991)). Thus the effects of gases on the friction and wear of metals must be considered and extended to machining operations. These gases to a greater extent are reactive with tool materials and newly generated machined surfaces.

Since these principles can be employed to improve machining productivity, many studies were prompted to investigate the existing wear pattern between different materials using the pin-on-disk testing apparatus which has already been used to study coatings for some time. For instance, the friction coefficient of tungsten lowered by hydrogen**,** while argon and nitrogen do not affect wear of nickel (MISHINA, 1992). Titanium and iron have a high chemisorption activity for oxygen but have no (or very little) chemisorption activity for nitrogen. “Chemisorption” refers to chemical adsorption where the particles stick to the surface by forming a chemical bond and tend to find sites that maximize their coordination number with the substrate (ATKINS, 1990). Results of an investigation between the relationship of pin-on-disk testing apparatus and machining tests with tungsten-carbide-base tools in the presence of nitrogen jet flow show that tool wear can be reduced by reducing the oxygen concentration in the atmosphere at the tool-workpiece interface (TENNENHOUSE; RUNKLE, 1987).

A major factor hindering the machinability of titanium alloys is their tendency to react with most cutting tool materials, thereby encouraging solution wear during machining. Machining in an inert environment, such in argon-enriched environment, is envisaged to minimize chemical reaction at the tool-chip and tool-workpiece interfaces when machining commercially available titanium alloys at higher cutting conditions. Argon has been mainly employed in welding to protect welds against oxidation, as well as reducing fume emissions during welding, and in other operations that demand a non-oxidizing atmosphere without nitrogen. The use of argon in machining environment has not been fully explored as it is a novel approach with limited investigation (JAWAID, 1982). It was reported that argon tends to enhance tool wear rate when machining austempered ductile iron with various ceramic cutting tools in the presence of argon and in air enriched atmosphere (MASUDA et al., 1994). A more recent study (EZUGWU et al., 2005) was carried out to evaluate of the effect of argon-enriched environment compared to conventional cooling environment in high speed turning of titanium-base, Ti-6Al-4V, alloy with uncoated cemented carbide tools. The argon gas was delivered to the cutting zone (B direction from Figure 2.42) through a hose at a constant flow rate of 12 l min^{-1}. Higher nose wear rate and, consequently, lower tool life was achieved in the presence of argon compared to conventional coolant supply. This was attributed to the poor thermal conductivity of the argon as well as the poor lubrication characteristics, which tend to concentrate more heat at the cutting region, thus weakening the strength of the cutting tools and accelerating the tool wear. Its poor lubricant characteristics

was also responsible for increasing friction at the cutting interfaces during machining and an increase in cutting forces required for efficient shearing of the workpiece (EZUGWU et al., 2005).

During machining operation the cutting edge generates a freshly cut surface. It is known that the newly generated surface is highly reactive and chemically combines with the atmosphere. An oxide film is rapidly formed on the new surface when machining in an oxygen environment (considered as an active atmosphere). This phenomenon is referred to as "gettering" (KHAMSEHZADEH, 1991). A deoxidised surface layer may enhance the diffusion-attrition wear process as this can result in a surface which generally is very susceptible to bonding. When machining in the presence of oxygen enriched atmosphere, enough oxygen will help to suppress potential bonding. Tool materials with high affinity to oxygen may become oxidised. These phenomena tend to hinder notch formation by lowering forces locally, thus encouraging longer tool life (OKEKE, 1999). It has also been reported that affinity of the Ti and Cr to oxygen has enabled them to form oxides which subsequently prevented the erosion of the beta prime crystals when machining nickel-base, Inconel 901, alloy with SiC whisker reinforced Al_2O_3 ceramic tools at high speed (150-215 m min^{-1}) conditions in oxygen, nitrogen and argon enriched environments. However, when machining in presence of argon and nitrogen enriched atmospheres, severe notching and shorter tool lives were obtained. These can be attributed to the absence of oxygen from the vicinity of the cut and consequently higher bonding forces leading to easier "pullout". Other research states that cutting force behaviour will depend on particular workpiece-cutting tool combination used in the presence of an oxygen atmosphere at pressures greater than 100 Pa (DOYLE; HORNE, 1980).

Çakir; Kiyak and Altan (2004) in a recent study of the effects of applications of gases such as nitrogen, oxygen and carbon dioxide, as well as cutting fluids and dry condition in turning of AISI 1040 steel with cemented carbides reported that lower cutting forces and better surface finish were achieved with application of all the gases compared to dry and wet conditions. Carbon dioxide gas gave the best cooling effect and provided lower friction coefficient and the lowest cutting force and thrust force than oxygen and nitrogen. Applications of gases provided higher shear angle values. The reason for better surface finish in gas applications, instead of wet machining, was due probably to the low penetration and worse lubrication effects than cooling (ÇAKIR; KIYAK; ALTAN, 2004).

CCl_4 has a good lubricant property at low cutting speeds. Ethanoic acid belongs to the family of organic fatty acids, which generally form successful boundary lubricant with longer carbon chains in conventional sliding tests. Its action involves the formation of a layer of low shear strength metal soap. Ethanethiol can be chemically active because of sulphur in its compositon. The organic alcohols such as ethanol in liquid phase are generally not attractive as boundary lubricants and are also considered to be inferior cutting lubricants because they can normally only adsorb physically on to metal surfaces (WAKABAYASHI; WILLIAMS; HUTCHINGS, 1992). Based on the above properties and the possibility of success of these gases in machining applications, a recent study (WAKABAYASHI; WILLIAMS; HUTCHINGS, 1992) was carried out to evaluate the performance of organic compounds as gaseous lubricants such as amino ethane ($C_2H_5NH_2$), ethane (C_2H_6), ethanol (C_2H_5OH), ethanethiol (C_2H_5SH), ethanoic acid (CH_3COOH) and tetrachloromethane (CCl_4) as well as air and vacuum in orthogonal cutting of an aerospace aluminium alloy (2014A). The effectiveness of gaseous lubricants on the cutting process was measured by the friction coefficient. The authors reported that with exception of ethane, the presence of any of the organic gases provided reduction of friction coefficient. The ranking order for effectiveness of machining environments was as follows: CCl_4, C_2H_5OH, C_2H_5SH, $C_2H_5NH_2$, CH_3COOH, C_2H_6, vacuum and air. The best performance of vapour tetrachloromethane (CCl_4) environment was attributed to its improved lubrication, which decreased the tool-chip contact length as well as minimised adhesion wear mechanism between the chip and the tool. Higher friction coefficient and cutting forces were observed when machining in the presence of air compared to vacuum condition. Ethanol (C_2H_5OH), which a liquid phase is not a very effective cutting lubricant, can, however, produce a marginally lower friction coefficient in the vapour phase.

2.15.7 Ledge Cutting Tools

Ledge cutting tools were developed by the General Electric Company (KOMANDURI; LEE (1984), DEARNLEY; TRENT (1985)) and characterised by a thin cutting edge (0.38 to 1.27 mm) that overhangs a small distance (0.38 to 1.27 mm) equal to the desired depth of cut. The optimum thickness will depend on the material to be machined, the cutting conditions and the flank wear tolerable. The advantage of these tools is that they have a restricted clearance face which will limit the maximum flank wear of the tool. As cutting proceeds, they first achieve maximum flank wear and then the length of the overhang wears back without further

development in flank wear due to a restricted clearance face. These characteristics allow the tools to perform for a long period of time as tool life is not limited by amount of flank wear but by the size of the tool edge (KOMANDURI; LEE, 1984). It was reported that a significant improve in tool life (30 min) was achieved when a ledge tool was employed in turning titanium-base, Ti-6Al-4V, alloy with inserts prepared from various grades of uncoated cemented carbides with 0.8 mm overhang x 1 mm thick x 12.7 wide at cutting speed of 600 m min^{-1} (KOMANDURI; LEE, 1984). This cutting speed was up to 5 times higher than conventional cutting speeds for machining titanium alloys. Figure 2.48 shows a ledge tool schematically. Because of its restricted geometry these tools are applicable only to straight cuts in turning, facing, boring, face milling and some peripheral milling operations. Another limitation of the ledge tool is the depth of cut which must be equal to or less than the width of the ledge overhang.

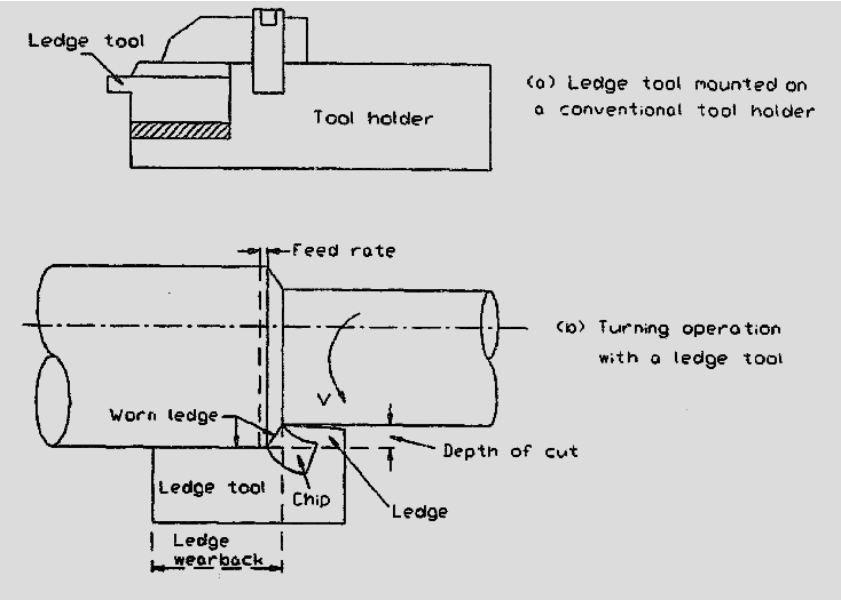

Figure 2.48 - Ledge tool (after KOMANDURY; LEE, 1984))

2.15.8 Rotary Tools

The rotary cutting tool concept has a long history. Rotary cutting tools are in the form circular discs that rotate about their central axis and the principal difference between rotary cutting and conventional cutting is the movement of the cutting edge in addition to the main cutting and feed motion (Figure 2.49). The rotation of cutting edge is the main advantage of rotary cutting tools when compared with traditional cutting tools as is causes a portion of the

tool cutting edge to be heated only for a very short time interval followed by a long rest period which permits the conduction of thermal energy, associated with the cutting process, away from the cutting zone (WANG; EZUGWU; GUPTA (1998), EZUGWU; OLAJIRE; WANG (2002)). Tool wear, in this case, is distributed uniformly across the entire round shaped cutting edge.

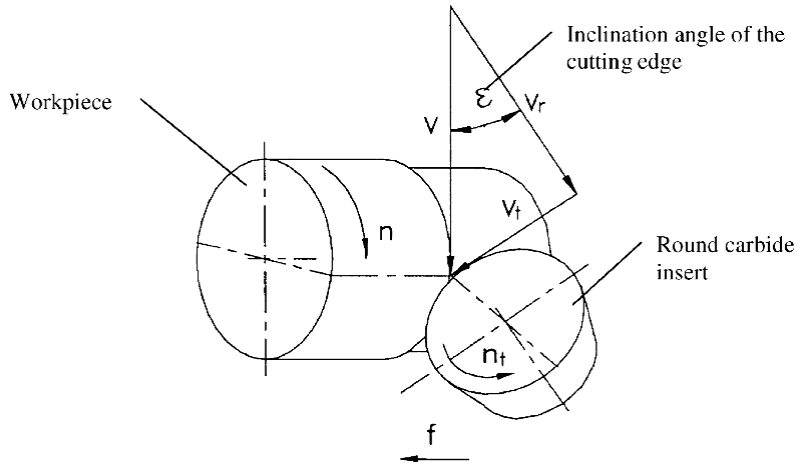

Figure 2.49 - Schematic representation of principle of rotary cutting action (WANG; EZUGWU; GUPTA, 1998).

The cutting tool rotation is affected either by an external driver, in which case the tool will be known as a driven rotary tool (DRT), or by the self-propelled action (SPRT) of the cutting forces exerted on the tool through adjustment of its axis at an inclination with respect to the cutting velocity (WANG; EZUGWU; GUPTA, 1998) . About 60 folds and 4 folds improvement in tool life were obtained (EZUGWU; OLAJIRE; WANG (2002), LEI; LIU (2002)) when machining titanium-base, Ti-6Al-4V, and nickel-base, 718, alloys respectively at high speed conditions with DRT compared to conventional single point turning with round uncoated carbide inserts The outstanding performance of SPRT can be attributed to the very low flank wear rate as a result of reduced amount of work done in deformation and friction at the primary shear zone and on the rake face, respectively, as well as the improved heat transfer from the cutting zone due to rotation of the tool edge during machining process. Additionally, SPRT lower cutting forces, up to 20%, than those obtained under conventional turning with round inserts. Other advantage of using the SPRT relative to the conventional turning is that machined surface is less affected by the thermal damage with better surface finish and compressive residual stresses (WANG, 1997). Reduction in inclination angle

improved values of surface finish when machining Ti-6Al-4V alloy with the SPRT compared to conventional turning operation (WANG; EZUGWU; GUPTA, 1998). However, a SPRT needs to have a large inclination angle for its insert to be able to rotate and its rotational speeds depends on machining conditions. This disadvantage limits the surface finish it can achieve and render it extremely difficult to optimise the process for longer tool life, good surface finish and high material removal rate (LEI; LIU, 2002). The limitations of this technique are that it can only be used at low depth of cuts, generation of more errors than a stationary cutting edge, developing of chatter due to the large tool radius and poor stiffness of the rotary system and difficulty in producing components with complex geometry. More details of the rotary cutting tool technique can be obtained elsewhere (ARMAREGO; KARRI; SMITH (1994), EZUGWU; WANG (1997), WANG (1997), WANG; EZUGWU; GUPTA (1998), EZUGWU; OLAJIRE; WANG (2002), LEI; LIU (2002), KISHAWY; WILCOX (2003)).

2.15.9 Ramping Technique

A typical problem encountered in the machining of super-alloys such as nickel and titanium-base alloys is the development of notch wear (in “V” form) at the tool nose and/or depth of cut region. Notch wear is formed by mechanical and chemical actions between the cutting tool and the work material during machining. As the notch wear generally grows on a random and unpredictable basis, high stress are concentrated at the cutting edge making it prone to catastrophic failure with further machining. Ramping (or taper turning) technique was developed to minimise or even eliminate notching when machining mainly nickel-base alloys. This technique consists of varying the depth of cut during the machining in order to distribute the concentration of notch wear along of cutting edge. The depth of cut line is shifted gradually along the flank face from a minimum to a maximum value and vice-versa, thus shifting the notch wear along the entire flank face of tool (EZUGWU; BONNEY; YAMANE, 2003). This leads to the generation of a uniform flank wear on the cutting edge thus preventing premature tool fracture, initiated by the otherwise severe notching which may have been generated, thereby improving tool performance (BONNEY, 2004). High speed machining trials on nickel-base alloys, such as Inconel 718 and Incoloy 901 alloys, showed that notching on the tool materials was suppressed by employing ramping technique (BALAZINSKI; LITWIN; FORTIN, 1993). A recent study (BONNEY, 2004) reported that ramping technique induced high cyclic loading on ceramic tools when turning Inconel 718

alloy, which consequently contributed to development of chipping process and in some cases flaking on the rake face tools. However, the author observed that notching was completely eliminated in most of cases when machining with coated cemented carbide tools.

2.15.10 Hot Machining / Hybrid Machining

Hot machining process has attracted considerable attention in the machining of difficult-to-machine materials such as high manganese steel, nickel and titanium-base alloys. These materials generally possess high tensile strength and resistance to wear which impair their machinability. Hot machining principle is based on the heating of workpiece material during machining. It has been reported that machining by softening of the workpiece through heating process can be more effective than strengthening the cutting tool in terms of improving machinability of those materials. For machining it is necessary to choose the best method to heat the material ideally. The wrong selection of heating method can induce undesirable structural changes in the workpiece and increases the cost. In the researches there are several heating methods, which are used for heating the workpiece. Furnace, gas torch, induction coil, carbon arc, plasma arc and electrical resistance were the mostly employed methods in previous studies (SHAW, 1984). Some of these methods have still been used and different heating methods have been introduced in machining recently (MADHAVULU; AHMED (1994), BARNES; PASHBY; MOK (1995), RICE; SALMON; ADVANI (1996), PRASAD; VIGNEAU (1997), SESHACHARYULY (1998), ÖZLER; ÍNAN; ÖZEL (2001), TOSUN; ÖZLER (2002), AMIN; YANTI; EIDA (2003)). CO_2 atmosphere was used in turning and milling of nickel-base, Inconel 718, alloy with ceramics and carbide tools at a feed rate of 0.18 mm rev^{-1}, depth of cut of 1.5 mm and cutting speeds up to 350 m min^{-1} (VIGNEAU, 1997). This process was referred to as the laser-assisted machining (LAM), where a CO_2 gas jet is directed to the cutting edge at 6kW. Laser-assisted machining uses a laser beam focused on the work material just in front of the cutting tool. The laser beams extends over the entire depth of cut and is positioned and adjusted to soften the material on the shear plane without allowing appreciable laser energy to flow into the tool (SHAW, 1984). This technique reduced tool wear rate and cutting forces by about 30% and 20-50% respectively when machining with ceramic tools, while accelerated tool wear rate was achieved with carbides tools. Similar results limited the use of LAM when machining titanium-base, Ti-6Al-4V, alloy with carbide tools (VIGNEAU, 1997). Barnes; Pashby and Mok (1995) also employed the LAM technique and conventional machining during turning of an aluminium/silicon carbide

MMC with coated cemented carbides at cutting speeds up to 90 m min^{-1}. The material was preheated at temperatures in the range of 200ºC-400ºC. Tool wear rate increased with increasing workpiece temperature. The main reason for the detrimental effect of pre-heating technique on the MMC machinability was found to be a shift in the stability range of the built-up-edge to lower cutting speeds. The increase in flank wear with increasing pre-heat temperature was attributed to a reduction in the protection provided to the flank face by the built-up-edge. On the other hand, pre-heating the workpiece was beneficial in reducing both the cutting forces and shear yield stress on the primary shear plane. Drawbacks of laser beam heating method are regard its low efficiency and high cost as very high power lasers are required.

The process of plasma-assisted hot machining process for turning operations utilises a high temperature plasma arc in the range of 16,000ºC to 30,000ºC to provide a controlled source of localised heat which softens only that small portion of the work material removed by the cutting tool in the form of chip retaining the metallurgical features of the remaining portions (MADHAVULU; AHMED, 1994). A plasma arc consists of a high velocity, high temperature stream of ionised gas capable of supporting a high-current, low-voltage electric arc. A plasma torch produces this phenomenon by having a tungsten electrode centrally placed within a water cooled copper nozzle. A gas stream is fed down the annulus between these, the gas being ionised by a high frequency discharge between the cooper nozzle and the central electrode. This is followed by a low-current pilot arc and then by a high-current main arc. The arc characteristics and reliability of arc striking are improved with the balanced geometry of the nozzle orifice. Madhavulu and Ahmed (1994) carried out a comparative study of a plasma-assisted hot machining and conventional process in turning various grades of steels with cemented carbides. They reported that up 2 folds improvement in tool life and 1.8 times gain in metal removal rate were obtained using hot machining process. Additionally lower power consumption was obtained in the hot machining process relative to conventional machining process.

Hot machining technique was evaluated by Özler; Ínan and Özel (2001) compared to conventional technique during machining of austenitic manganese steel. They utilised heating temperatures ranging from 200 to 600ºC. The flame was generated by a torch containing a mixture of liquid petroleum gas and oxygen. Figure 2.50 shows the schematic representation of a hot machining technique design used in their experiments. Longer tool lives were achieved when the hot machining technique was employed compared to conventional

machining. The tool wear rate decreased with increase in heating temperature due to the reduction in resistance of the workpiece material to shearing. The longest tool lives were obtained when a heating temperature of 600ºC was used. In other study carried out by Tosun and Özler (2002) liquid petroleum gas (70% propane and 30% butane) flame was used to heat the workpiece (heating temperatures ranging from 200 to 600ºC) during a turning operation of austenitic manganese steel with M20 sintered carbide tools. Artificial neural networks and regression analysis method were also employed using experimental data to predict tool life. Tool life increased with increase in heating temperature. 400ºC was the optimum heating temperature because of the microstructure of the workpiece obtained and the cost.

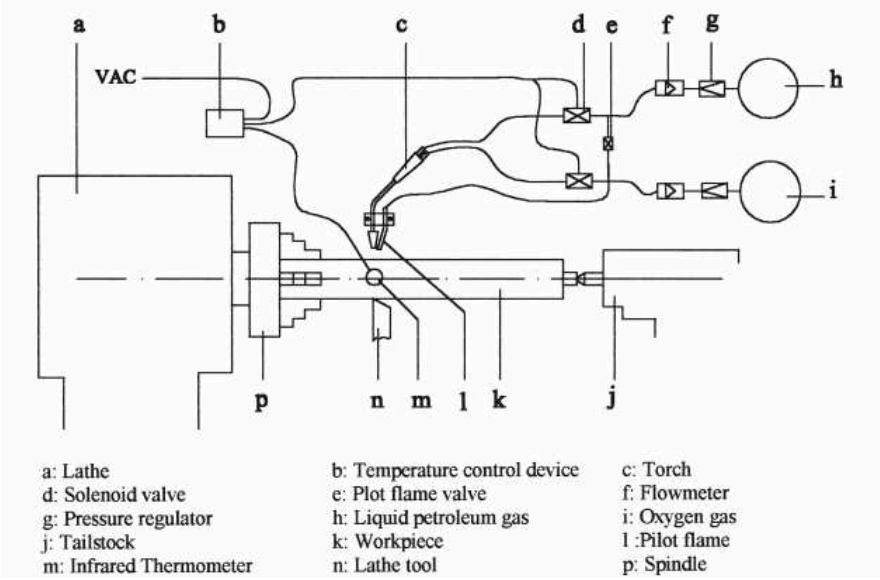

Figure 2.50 - Schematic representation of a hot machining technique design (ÖZLER; ÍNAN; ÖZEL, 2001).

Amin; Yanti and Eida (2003) investigated the effect of hot machining process using oxy-acetylene flame on chatter and tool performance during turning of AISI 1040 steel and reported that chatter was substantially reduced with lower tool wear rate and better surface finish using hot machining process. They also reported that diffusion was the predominant wear mechanism when turning with hot machining process whereas attrition and diffusion were predominant without preheating.

2.16 Surface Integrity

The term surface integrity refers to the control of both surface topography (and geometry) and metallurgical alteration below the surface obtained after machining with respect to the base material. In other words surface integrity determines the quality of the machined surfaces. Temperature generated at the cutting interface during machining generally induces residual stresses (tensile or compressive), can promote metallurgical alterations, surface plastic deformation of the work material as well as influence tool wear. Cutting tools with high wear lands promote severe plastic deformation tearing and cracking of workpiece surfaces (BONNEY, 2004). Control of the surface integrity, therefore, is a key factor in enhancing the function and reliability of a component in order to give the most suitable condition for long life, fatigue performance, safety of individuals and maximum efficiency at minimum cost (MACHADO (1990), BONNEY (2004)). The surface integrity is evaluated either by the surface finish/surface texture and subsurface changes.

2.16.1 Surface Finish and Texture

Surface finish and surface texture are concerned with the geometric irregularities and the quality of the surface. It consists of roughness, waviness, lays and flaws Figure 2.51 (KALISH (1978), DROZDA; WICK (1983), SCHAFFER (1988), KALPAKJIAN; SCHMID (2000)).

i) Roughness is the finer random irregularities which usually result from the inherent action of the cutting process, as feed marks, instead of from the machine. The mean height or depth of irregularities is measured in a relative small length called “roughness sampling length” or “cut-off”. Ideal surface roughness is caused by the given tool shape and the feed rate;
ii) Waviness is the wider spaced repetitive deviation that may be attributed to the characteristics of the machine tool, deflection of the workpiece due to cutting loads, defects in the structure of the work material, vibration, chatter and cutting temperature, tool wear and to external environmental factors;
iii) Lays denotes the direction of predominant surface patterns and determined by the production process used. Typical operations that produce pronounced lays are turning, drilling, milling and grinding;

iv) Flaws are characterised as unintentional, unexpected and unwanted interruptions encountered in the typical topography of a component surface. They are mainly caused by inherent defects such as inclusions, blowholes, cracks, scratches, nicks and ridges and also with the presence of the built-up-edge. Flaws can be either formed during the manufacturing of the material or during the machining of the material. Unless otherwise specified the effect of flaws is usually not included in the roughness average measurements.

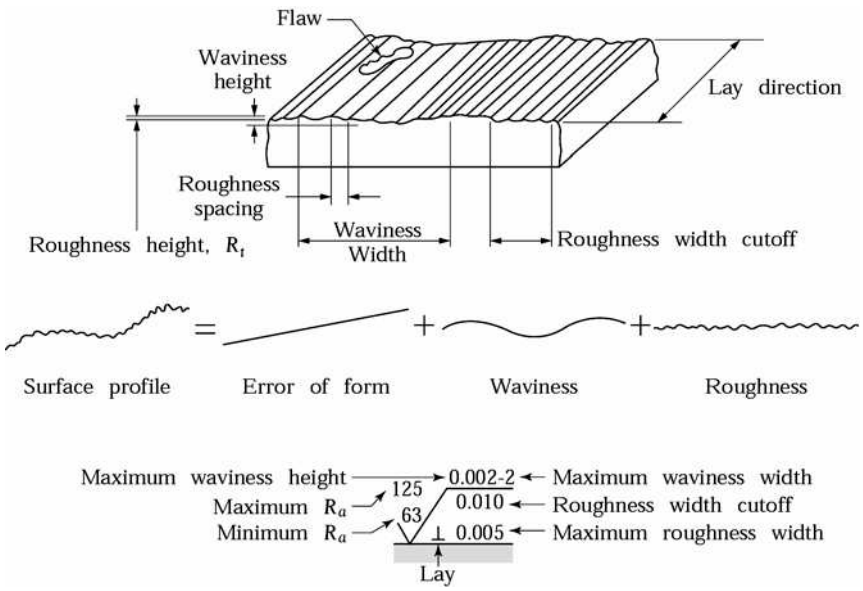

Figure 2.51 - Standard terminology and symbols of the elements of surface texture (μin) (KALPAKJIAN; SCHMID, 2000).

The surface texture is determined by inherent parameters which are classified into three basic categories (SCHAFFER, 1988):

i) Amplitude parameters: they are determined solely by peak height or valley depth or both, of profile deviation, irrespective of their spacing along the surface;
ii) Spacing parameters: these parameters are determined solely by the spacing of profile deviation along the surface;
iii) Hybrid parameters: they are determined by the combination of amplitude and spacing parameters.

The most common method of designating surface roughness is using the arithmetic average parameter, R_a (μm), which belongs to the amplitude category. It is obtained by

measuring the mean deviation of the peaks and valleys from the centreline of a trace, the centreline being established as the line above and below which there is an equal area between the centreline and the surface trace (SHOUCKRY; 1982), as shown in Figure 2.52 and given by the Equation (2.13):

$$R_a = \frac{h_1 + h_2 + h_3 + ... + h_n}{n} \tag{2.13}$$

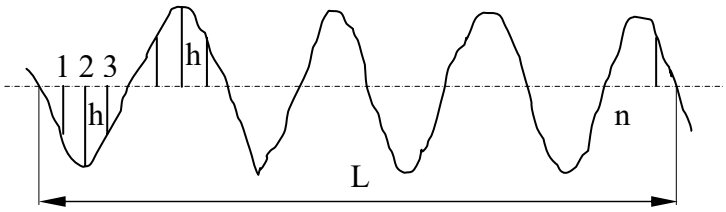

Figure 2.52 - Schematic illustration of the determination of some amplitude parameters of surface texture (SHOUCKRY; 1982).

In turning operation, Ra (μm), parameter can be expressed as a function of the feed rate and nose radius of a tool given by the Equation (2.14) (KALPAKJIAN; SCHMID, 2000):

$$R_a = \frac{0.0321 \times f^2}{r} \tag{2.14}$$

Where f is the feed rate in mm $rev^{-1}$and r is the tool nose radius in mm. This equation is only valid when the feed rate is smaller than the nose radius.

From the equation 2.14 it can be observed that increasing the nose radius improves the surface finish. However, too large a nose radius is not recommendable as it tends to promote chatter during machining. This may occur because the tool-workpiece contact area increases, the shearing stress is decreased, hence higher cutting forces are required for efficient shearing of the workpiece material (BONNEY, 2004). The surface finish can also be improved by decreasing the feed rate. However, reduction in feed rate will decrease the material removal rate and hence implying longer machining time.

The stylus instrument is the most common instruments employed in measurements the surface finish. The stylus, typically with a diamond tip, traverses across the surface at a controlled rate and its vertical movement is converted into an electrical signal by a sensitive

electronic transducer. Modern instruments digitise the electrical signal and store the results in a computer, where statistical analysis can be carried out.

2.16.2 Subsurface Changes

During the machining process of metal removal is created a surface with a layer (extending to a depth of up to 0.25 mm) which can be different from the interior of the workpiece. Various subsurface changes can be encountered in machined components. The subsurface changes consist of several mechanical and metallurgical factors. The main mechanical factors are (FIELD; KAHLES; CAMMET (1972), DROZDA; WICK (1983)):

- Plastic deformation: it is a common microstructural alteration resulting from exceeding the yield point of the material and is normally identified by elongation of grain structure in the direction of flow and also by the increase in hardness level. The extent of plastic deformation is dependent on the cutting conditions employed, tool geometry as well as the properties of workpiece materials. Plastic deformation usually occurs when machining under heavy machining conditions;
- Plastically deformed debris: these are generally fragments of a built-up-edge that has ploughed through the flank surface of the tool and the workpiece which remain attached to the machined surface;
- Microcracking and macrocracking: these are more pronounced when machining brittle materials (such as cast iron and hardened steel). Microcracks are generally detrimental to fatigue and stress corrosion and thus must be avoided. Cracking can occur in the vicinity of untempered martensite, in the region of built-up-edge and during thermal removal processes;
- Residual stress: it is induced into the surface layer as a consequence of the removal of machining load that caused plastic deformation on the material as well as intense localised heating in the surface layer and consequent cooling. The residual stresses introduced by machining are greatly influenced by the wear land developed on the tool surface. They also depend on the cutting force, the distribution of temperature and mechanical stresses during machining operation. Residual stress can be compressive or tensile, low or high, shallow or deep. The tensile stress is detrimental to fatigue strength while the compressive stress is beneficial;
- Microhardness alteration: microhardness distribution is dependent on the machining process and the parameters of that process. The surface hardness can be increased as

a result of formation of untempered martensite or plastic deformation by cold work, i.e., at temperature below the recrystallization temperature. On the other hand, the presence of overtempered martensite will tend to produce surface softening. Microhardness measurements are a powerful tool used to confirm visual alterations and help identify changes in machined components, which are not discernible in a microscopic examination of the surface layer.

In conventional machining the main metallurgical factors are:

- Phase transformation: phase transformation on the surface of the machined component is caused by the intense heating of the surface layer during machining process. When machining steel a very brittle and detrimental untempered martensite can be formed;
- Recrystallization: can occur in any metal whose surface suffer excessive heating and when is plastically deformed during the machining operation. As a consequence the original properties of the materials can be altered.

CHAPTER III

EXPERIMENTAL PROCEDURE

3.1 Introduction

The objective of this work is to investigate the performance of recently developed cutting tool materials (coated and uncoated cemented carbides, polycrystalline diamond (PCD), cubic boron nitride (CBN/PCBN), and ceramics) and various cooling media such as conventional coolant flow, high pressure coolant supplies (7 MPa, 11 MPa and 20.3 MPa) and argon enriched environment at cutting speeds up 500 m min^{-1} in order to provide a step increase in the productivity of finish turning of commercially available titanium-base, Ti-6Al-4V, alloy which is widely used in the aerospace industry. This section describes the equipment, experimental techniques and methodology employed in this study. All the experimental tests carried out in this research as well as sample preparation and analysis of the worn tools and machined surfaces were performed at the laboratories of the Faculty of Engineering, Science & the Built Environment of the London South Bank University. Tool wear, component forces, surface roughness and run-out were recorded and analysed. The surface integrity study was mainly based on the physical and metallographic examination as well as analysis of the microhardness variation of the machined surface and subsurface of the workpiece materials using scanning electron microscope (SEM) and hardness measuring equipment.

3.2 Work Material

The workpiece material used in this investigation is a commercially available alpha-beta titanium-base, Ti-6Al-4V, alloy. The dimension of the Ti-6Al-4V workpiece bar is 300 mm diameter x 300 mm long. The bars were previously homogenised and annealed. The nominal chemical composition and physical properties of the workpiece material are given in Tables 3.1 and 3.2 respectively. Prior to the actual turning tests, the work material bars were trued, centred and cleaned by removing up to 2 mm thickness of material at the top surface of the workpiece in order to eliminate any surface defect that can adversely affect the machining result. Each bar was mounted in the machine tool chuck and supported at the other end by the tailstock to minimise vibration during the machining trials.

Table 3.1 - Nominal chemical composition of Ti-6Al-4V alloy (wt. %)

	Chemical composition (wt. %)								
	Al	V	Fe	O	C	H	N	Y	Ti
Min.	5.50	3.50	0.30	0.14	0.08	0.01	0.03	50 ppm	Balance
Max.	6.75	4.50		0.23					

Table 3.2 - Physical properties of Ti-6Al-4V alloy.

Tensile strength (MPa)	0.2% Proof stress (MPa)	Elongation (%)	Density (g cm^{-3})	Melting point (°C)	Measured hardness (C.I. – 99%)* HV100	Thermal conductivity at 20ºC (W m^{-1} K^{-1})
900-1160	830	8	4.50	1650	Min.= 341 Max. = 363	6.6

* CI: Confidence interval of 99 %, represented by the minimum (Min.) and maximum (Max.) values.

3.3 Machine Tool

All the machining trials were carried out on a Colchester Electronic MASTIFF lathe (Figure 3.1) equipped with a CNC control driven by an 11 kW motor driver which provides a torque of 1411 Nm. The lathe has a variable spindle speed from 16-1800 rpm and a variable feed rate ranging from 0.01 to 5.0 mm rev^{-1}.

Figure 3.1 - Colchester Electronic MASTIFF CNC lathe.

3.4 Cutting Fluid

The cutting fluid used in the machining trials for both conventional and high pressure systems is the HOCUT 3380, manufactured by Houghton, with a concentration of 6%. It is a high lubricity emulsion coolant containing alkanolamine salts of fatty acids and dicyclohexylamine. Additionally, this coolant contains anti-foaming and non splitting properties, making it ideal for high pressure delivery applications. The required concentration of coolant for all the machining trials was prepared by diluting the concentrate with water. The coolant concentration was monitored with a pocket refractometer prior to machining and at various stages of the machining trials. Cutting fluid was applied by flooding or conventional coolant flow (CCF) to the cutting interface (overhead cooling) via a pipe with nozzle diameter of 6 mm at an average flow rate of 2.7 l min^{-1} (conventional method - D

direction (Figure 2.42)) and at a pressure lower than 0.3 MPa (3 bar) with CNC lathe coolant delivery pump system. The distance from the nozzle to the cutting zone was kept at 100 mm.

3.5 High Pressure Unit

The high pressure coolant-jet was delivered by a high powered pumping unit detached from the machine lathe. The high pressure pumping coolant system, Chipblaster (CV26-3000), can operates at maximum load capacity of 22.3 kW, with a tank capacity of 454 *l* and maximum flow rate of 197 *l* min^{-1} and with a maximum output pressure of 21 MPa (210 bar). The Chipblaster has four basic components: a reservoir (tank), a filtration system, an internal high pressure pump and a control unit (Figure 3.2). A dual-filtration system filters the cutting fluid before it enters the unit´s internal reservoir unit. The cutting fluid is pumped from the high pressure pump to a special tool holder (Figure 3.3) which delivers the jet to the region where the chip breaks contact in the tool (tool-chip interface - B direction in Figure 2.42). The tool holder has an external nozzle with diameter of 2 mm and is kept at a distance of 13.5 mm from the cutting zone. Three different high jet-pressures with the flow rates were used in the trials:

- High pressure coolant (HPC) flow of 7 MPa (70 bar) with a flow rate of 16.9 *l* min^{-1} (Figure 3.3);
- High pressure coolant flow of 11 MPa (110 bar) with a flow rate of 18.5 *l* min^{-1}.
- High pressure coolant flow of 20.3 (203 bar) MPa with a flow rate of 24 *l* min^{-1}.

Figure 3.2 - The high pressure pumping coolant system - Chipblaster (CV26-3000).

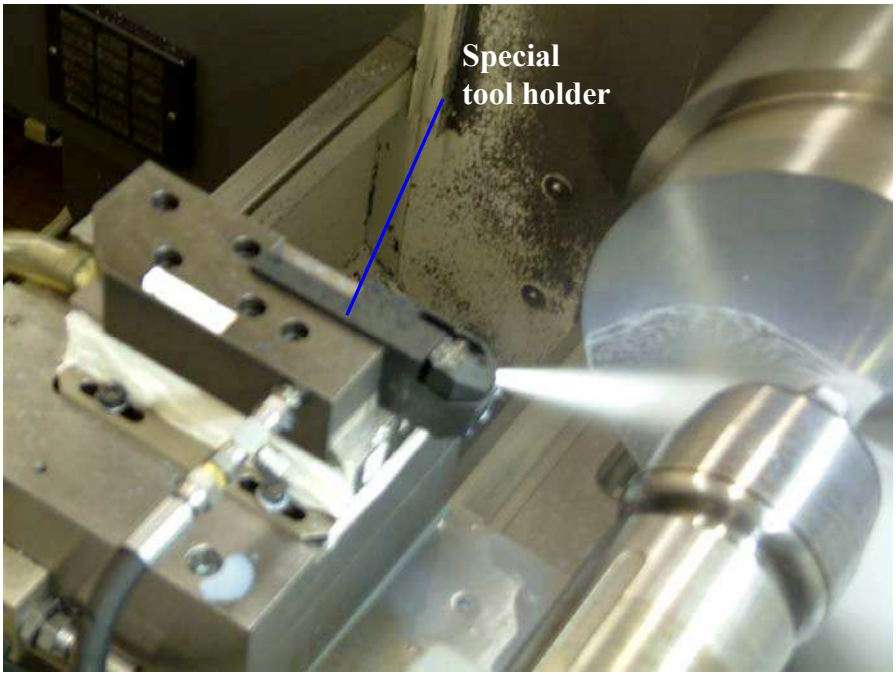

Figure 3.3 - Special tool holder and a cutting fluid jet-pressure of 7 MPa supply.

3.6 Argon Delivery System

The argon gas delivery system consists of an argon cylinder, a valve and a hose which was connected to the same tool holder used in the high pressure cutting fluid delivery system. The cylinder was placed in the back of the machine lathe as shown in Figure 3.4 (a). The argon gas was delivered to the machining environment (tool-chip interface - B direction in Figure 2.42) through a hose connected to a valve (Figure 3.4 (b)) where the flow rate of the gas could be adjusted and supplied to the cutting interface through a nozzle at a constant flow rate of 12 l min^{-1}. Thermal conductivity of argon at a temperature of 300K (27°C) is 0.0177 $Wm^{-1}K^{-1}$.

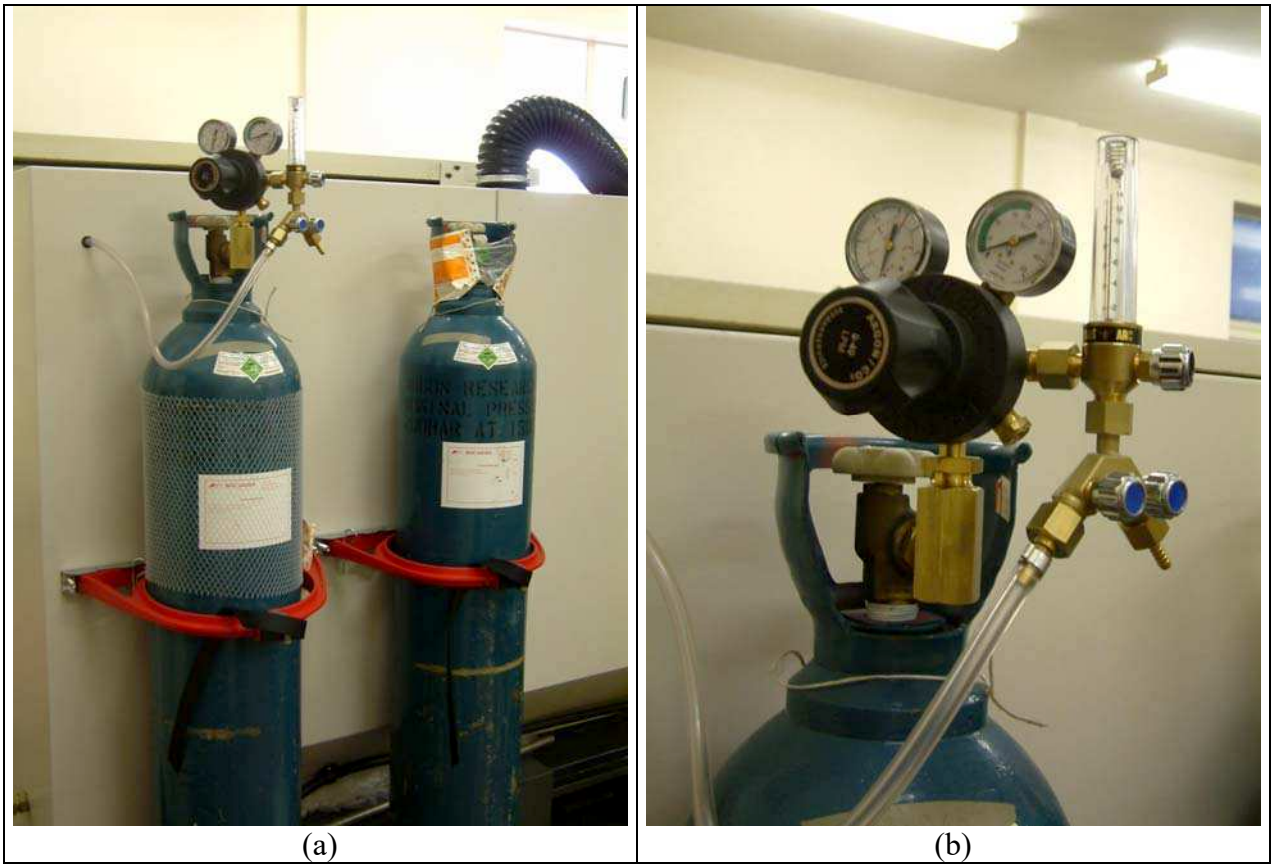

(a) (b)

Figure 3.4 - Argon gas delivery system: (a) cylinder and (b) close-up view of the valve and the hose.

3.7 Tool Material and Machining Procedure

All the cutting tool materials (Figure 3.5) used when machining Ti-6Al-4V alloy were produced by Seco tools, with the exception of the micron-grain size ceramic (provided by NTK tools manufacturer) and nano-grain size ceramics (currently under development). The inserts have 2 different geometries: 80º rhomboid shape and square shape. Rhomboid shape inserts were used when machining Ti-6Al-4V alloy with high pressure cutting fluid supplies. These include: uncoated cemented carbide coded as (T1) 883 and (T2) 890 grades, coated cemented carbide (T3) CP 200 and (T4) CP 250 grades, PCD (grade 20 with two different grain sizes coded as PCD-STD (T5) and PCD-MM (T6), CBN (CBN 10 (T7), PCBN 300 (T8) and PCBN 300-P TiAlN/TiN coated (T9) grades), silicon carbide (SiC_w) whisker reinforced alumina ceramic (WG300) (T10). These insert grades are among the best Seco grades for machining titanium alloys. Only the cemented carbide tools have an integral

obstruction-type chip-breaker on the rake faces. PCD inserts have a nose radius of 1.2 mm whereas all other cutting tools have a nose radius of 0.8 mm. The square shape inserts were used when machining Ti-6Al-4V alloy under conventional coolant supply only. They include: micron-grain size silicon carbide (SiC_w) whisker reinforced alumina ceramic (WG300) (T11) and nano-grain size ceramic inserts Al_2O_3 (mixed alumina) (T12) and Si_3N_4 (silicon nitride based) (T13).

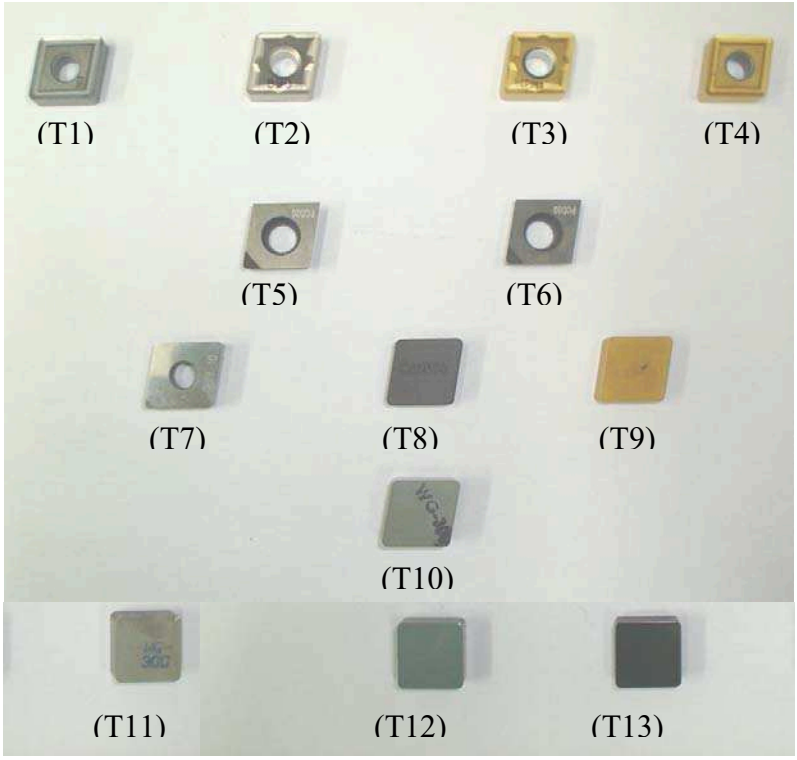

Figure 3.5 - Cutting tools used in the machining trials: uncoated carbides: T1 (883 grade), T2 (890 grade), coated carbides T3 (CP 200), T4 (CP 250 grade); PCD: T5 (20 grade with grain size of 10 μm), T6 (20 grade with grain size < 10 μm); CBN: T7 (10 grade), PCBN: T8 (300 grade), PCBN: T9 (300-P grade); silicon carbide (SiC_w) whisker reinforced alumina ceramic inserts (WG300): T10 (rhomboid shaped) and T11 (square shaped); nano-grain ceramic inserts: T12 (Al_2O_3 grade) and T13 (Si_3N_4 grade).

Table 3.3 gives the chemical and mechanical properties of the all rhomboid shape insert grades and of T11 (SiC_w whisker reinforced alumina ceramic inserts) square shaped cutting tool materials used for the machining trials. The mechanical properties and nominal chemical composition of the nano-grain ceramic inserts are given in Table 3.4. Prior to machining, an insert was checked for any physical damage at the cutting edge with a travelling microscope at a magnification of x20.

Table 3.3 - Specification, chemical and mechanical properties of the cutting tool materials used in the machining trials.

Tool material	Cemented Carbide (K grade)				PCD		Insert CBN	Solid PCBN		Whisker reinforced ceramic	
	Uncoated		Coated								
Tool code	T1	T2	T3	T4	T5	T6	T7	T8	T9	T10	T11
Grade	883	890	CP200	CP250	STD	MM	10	300	300-P	WG300	
ISO designation	CNMG 120412-M1	CNMG 120412-MR3		CNMG 120412-M1	CCMW 120408F-L1		CNGA 120408S-LO	CNMN 120412S		CNGN 120412TN WA1 (rhomboid shaped)	SNMG 120412 (square shaped)
Chemical composition (wt.%)	93.8% WC 6% Co 0.2% (Ta, Nb)C	93.7% WC 6% Co 0.3 Cr_2C_3		93.8% WC 6% Co 0.2% (Ta, Nb)C	Diamond + Co residue		50% CBN 50% TiC ceramic (vol.)	90% CBN 10% Al ceramic (vol.)		70% (Al_2O_3, Y_2O_3, Zr_2O) 30% SiC	
Composition and thickness of coating (wt.%)	-	-	TiAlN (3.5 μm) TiN (0.5 μm		-		-	-	TiAlN (3.5μm) TiN (0.5μm)	-	
Hardness (Knoops) GPa	13 (1760 HV)	1753 (HV)		13 (1760 HV)	50.0		27.5	31.5		94.5 HRA (2000 HV_5)	
Density (g cm^{-3})	14.95	14.92		14.95	4.12	4.31	4.28	3.42		3.7	
Thermal conductivity at 20ºC (W $m^{-1}K^{-1}$)	110	-	-		540	459	44	138		32	
Substrate grain size (μm)	1.0	0.68		1.0	10	<10	2	-	-	Whiskers with 0.5μm of diameter	

Table 3.4 - Mechanical properties and chemical composition (wt%) of nano-ceramic tools material (square shape inserts).

Tool code	Grade	ISO designation	Hardness (HV_5)	Edge toughness (MPa $m^{1/2}$)	Al_2O_3	SiC	Si_3N_4	TiCN	Y_2O_3	ZrO_2
T12	SAZT2	SNMG 120412	1779	10.54	75.0	-	-	20.0	-	5.0
T13	SNCTN1		1670	6.92	4.5	4.5	68.3	18.2	4.5	-

Special tool holders were designed according to ISO designation for each cutting tool material (rhomboid shape inserts) when machining with high pressure coolant (HPC) supply Figures 3.6 (a), (b) and (c). These will enable the cutting fluid to travel from the high pressure unit through its body and to be delivered at high pressure to the region where the chip breaks contact with the tool via a specially designed orifice in its nozzle cap. The specially designed tool holders were also used when machining with conventional coolant flow (CCF). A different holder was employed when machining with square shape inserts (Figure 3.6 (d)). All tool holders have a 25 mm shank. The effective geometry of the rhomboid inserts after rigid clamping in the tool post provide: approach angle of 95°, back rake angle of -6°, side rake angle of -6°, side relief angle of 6° and clearance angle of 6°, whereas the effective geometry of the square inserts is an approach angle of 40°, back rake angle of -5°, side rake angle of 0° and clearance angle of 6°.

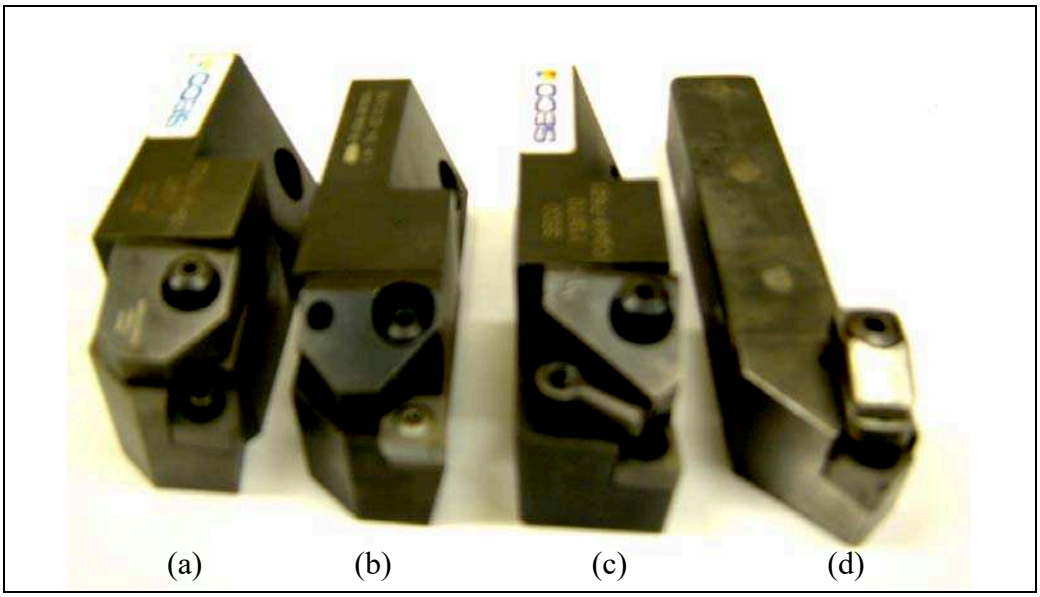

Figure 3.6 - Tool holders used in the machining trials: (a) designation PCLNR2525-M12 used for carbide tools (T1,T2,T3,T4); (b) designation SCLCR2525-M12 used for PCD tools (T5,T6); (c) designation DCLNR2525-M12 used for CBN/PCBN and ceramic tools (T7,T8, T9 and T10); (d) designation MSLNR-252512 used for square tools: micron-grain and nano-grain size ceramics (T11,T12,T13).

3.8 Cutting Conditions

Machining conditions for finish turning of Ti-6Al-4V alloy in this study started with those usually employed in the aerospace industry. A 15 minutes tool life was chosen as the benchmark for establishing acceptable cutting conditions during the turning trials. The initial trials with uncoated cemented carbide (grade 883) tools were aimed at establishing high speed conditions that will consistently achieve 15 minutes tool life under conventional coolant supply, based on the stipulated tool wear rejection criterion: average flank wear, $VB_B \geq 0.3$ mm. The highest speed conditions achieved were used as the baseline conditions for machining with various grades of advanced tools such as PCD, CBN/PCBN and nano-grain ceramic tool materials. A constant feed rate and depth of cut of 0.15 mm rev^{-1} and 0.5 mm respectively were used in all the machining trials. All the experimental trials and their sequence are summarised in Table 3.5. This table shows the tools, machining environments, cutting speed range and output variables investigated in this study. Tools T1, T2, T3, T4, T5, T6, T7, T8, T9 and T10 have rhomboid-shape geometry and were used with conventional and high pressure coolant supplies. The pressure of 7 MPa was employed with uncoated carbide (T1) and PCD (T5) tools in order to investigate the performance of medium pressure in the machinability of Ti-6Al-4V alloy. Argon gas supply was used with uncoated carbide (T1) and coated carbide (T2) tools. Micron-grain size (T11) and nano-grain size (T12, T13) ceramic tools have a square-shaped geometry and were used only with conventional coolant supply. The output variables shown in Table 3.5 and listed below were monitored during the machining trials, except the run-out which was measured at end of tool life when further machining was halted:

i) Tool life (min);
ii) Tool wear (mm);
iii) Component forces (cutting and feed forces (N));
iv) Surface Roughness (R_a - micron);
v) Runout (mm);
vi) Chip form.

Other output variables shown in Table 3.5 such as worn tool micrographs, microhardness measurements, machined surfaces and subsurface examinations were evaluated after each completed machining trial and after sample preparation.

Up to 450 experimental trials were carried out in this study, and it is important to note that replications of experimental trials were performed for some machining conditions. For such cases, average of tool lives was recorded. Additionally, tests were always repeated on occurrence of abnormal and unpredictable tool failure.

Table 3.5 - Summary of the experimental tests carried out when finish turning of Ti-6Al-4V alloy at a constant feed rate and depth of cut of 0.15 mm rev^{-1} and a of 0.5 mm respectively.

Stage	Tool	Machining Environment					Cutting speed (m min^{-1})	Out-put variables									
		CCF	HPC 7 MPa	HPC 11 MPa	HPC 20.3 MPa	Argon		Tool life	Tool wear	Component forces	Worn tools micrographs	Surface roughness	Run-out	Microhardness	Machined surface analysis	Subsurface analysis	Chip photographs
Benchmark trials	T1	X					60,90, 100, 110,120,130		X								
Actual machining trials	T1	X	X	X	X	X	100,110,120, 130	X	X	X	X	X	X	X	X	X	X
	T2,T3	X		X	X		110, 130	X	X	X	X	X	X	X	X	X	
	T4	X		X	X	X	100,110,120, 130	X	X	X	X	X	X	X	X	X	X
	T5	X	X	X	X		140**, 150**, 160**,175, 200,230,250*	X	X	X	X	X	X	X	X	X	X
	T6	X		X	X		140**,150**, 160**, 175, 200*,230*, 250*	X	X	X	X	X	X	X	X	X	X
	T7,T8, T9	X		X	X		150,200*, 250*	X	X	X	X	X	X	X	X	X	X
	T10	X	X	X	X	X	140,200,400, 500	X	X	X	X	X	X	X	X	X	X
	T11, T12, T13	X					110,130,200	X	X	X	X	X	X				X

Keys:

- CCF: Conventional coolant flow delivery system;
- HPC: High pressure coolant delivery system;
- *: Speed identified was not tested under conventional coolant supply;
- **: Speed identified was not tested under high pressure coolant supply(ies);

3.9 Tool Life Criteria

The tool life rejection criteria for finish turning operation employed in this investigation are listed below:

i) Average flank wear, $VB_B \geq 0.3$ mm;

ii) Maximum flank wear, $VB_{Bmax} \geq 0.4$ mm;

iii) Nose wear, $VC \geq 0.3$ mm;

iv) Notching at the depth of cut line, $VN \geq 0.6$ mm;

v) Excessive chipping (flaking) or catastrophic fracture of the cutting edge**;**

vi) Surface roughness value (Ra) ≥ 1.6 μm (Centre line average);

vii) Run-out: 0.1 mm (100 μm)

3.10 Tool Wear Measurement

Tool wear measurement (flank wear, notch wear and nose wear) were carried out at various intervals using a Mitutoyo tool maker´s microscope (Figure 3.7) connected to a digital micrometer XY table with resolution of 0.001 mm at a magnification of x20. The insert is removed from the tool holder and mounted on a small tool makers hand vice placed on the microscope prior to measurement.

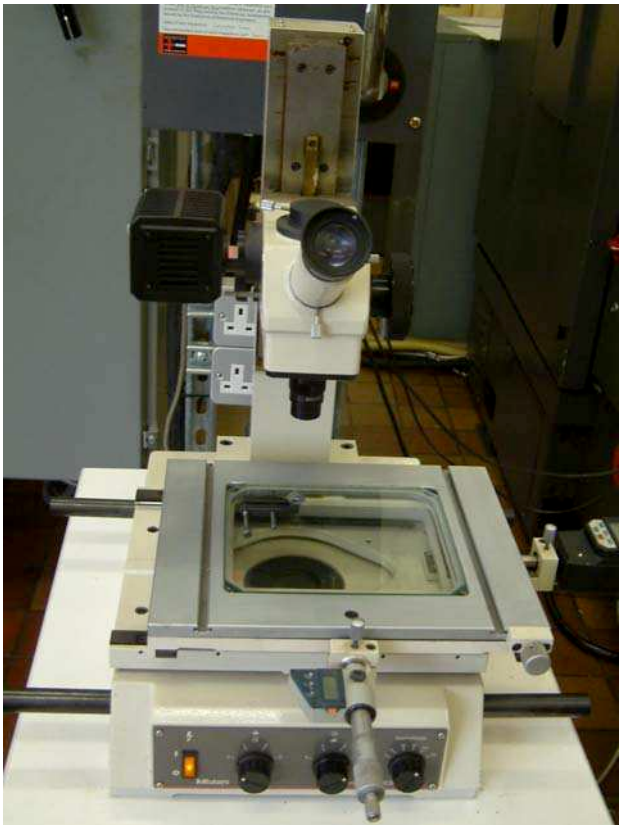

Figure 3.7 - Mitutoyo tool maker´s microscope.

3.11 Component Force Measurement

The component forces (cutting force, F_c and feed force, F_f) generated during the cutting trials were recorded at the start of machining (after one minute machining time when the cutting edge has not undergone pronounced wear) with the aid of a three component Kistler piezoelectric tool post dynamometer. The electric signals generated by the component forces during machining were fed into a charge amplifier connected to the dynamometer (Figure 3.8). This amplifier magnifies the electric signals (voltage) which can be read on a digital oscilloscope. The maximum, minimum, peak-to-peak and average voltage values of the cutting and feed forces were read directly from the screen. These values are converted to mechanical units (Newton) multiplying them by with the charge amplification factor.

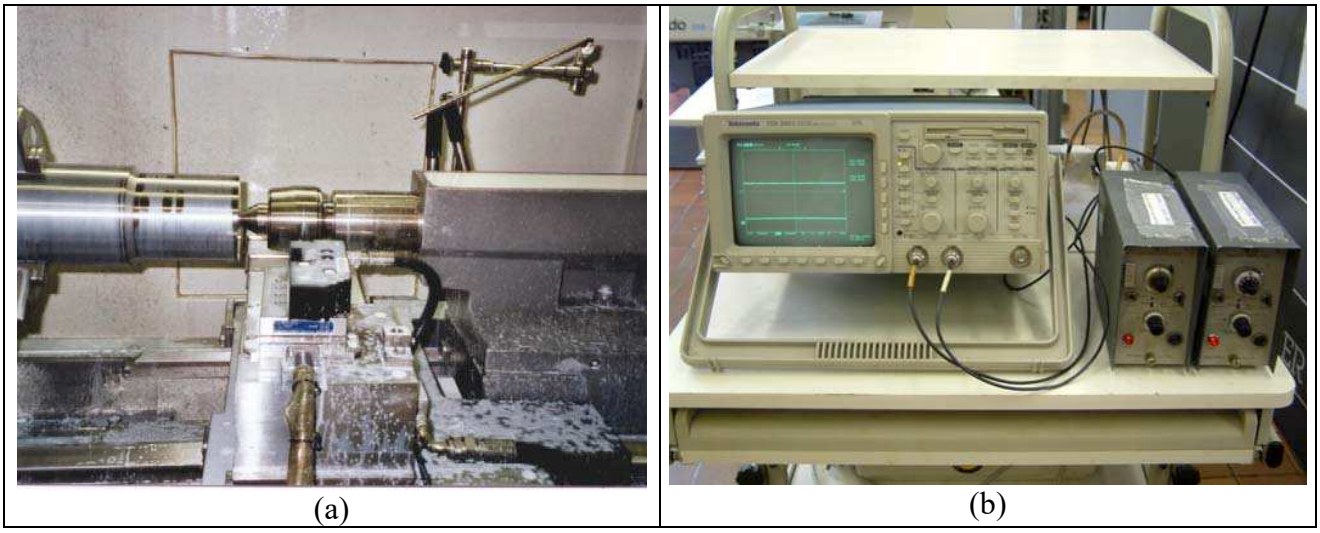

(a) (b)

Figure 3.8 - (a) Kistler dynamometer for capturing forces generated during machining and (b) Oscilloscope with charge amplifier.

3.12 Surface Roughness Measurement

Surface roughness values were recorded after one minute machining time using a Surtronic-10 portable stylus type instrument that traverse over the machined surface (Figure 3.9 (a)). The relative displacement is highly magnified electronically and the results presented as a surface roughness value (Ra) measured in micro metres (μm). The surface roughness value was measured by positioning the instrument perpendicular to the feed marks on the machined surface. The average of three readings at different locations on the workpiece bar represents the surface roughness value of the machined surface. To ensure accuracy of the readings the instrument was calibrated using a standard calibration block prior to use.

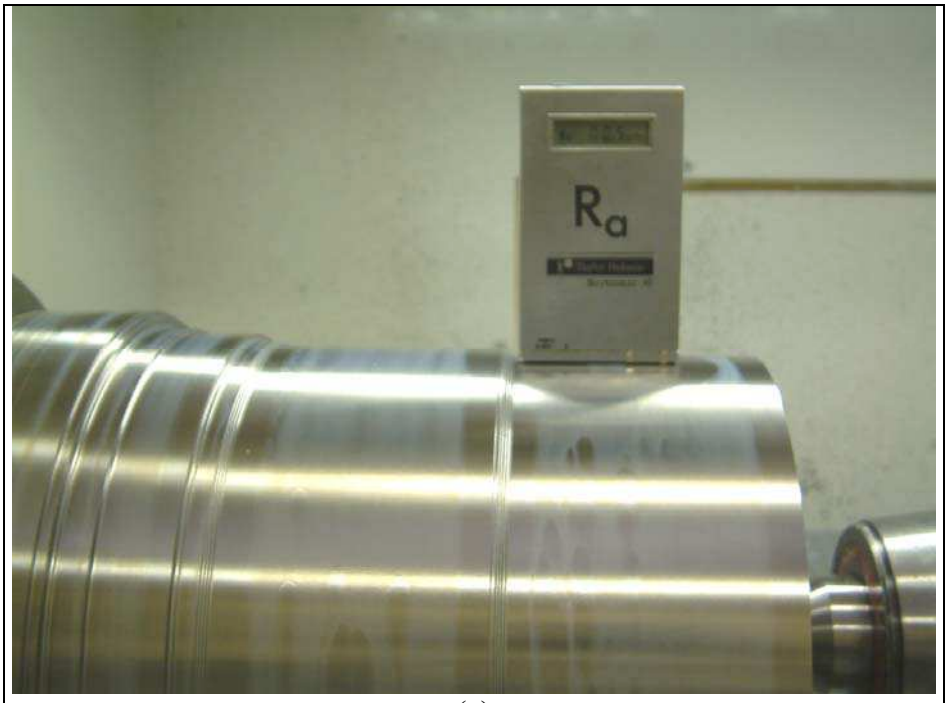

(a)

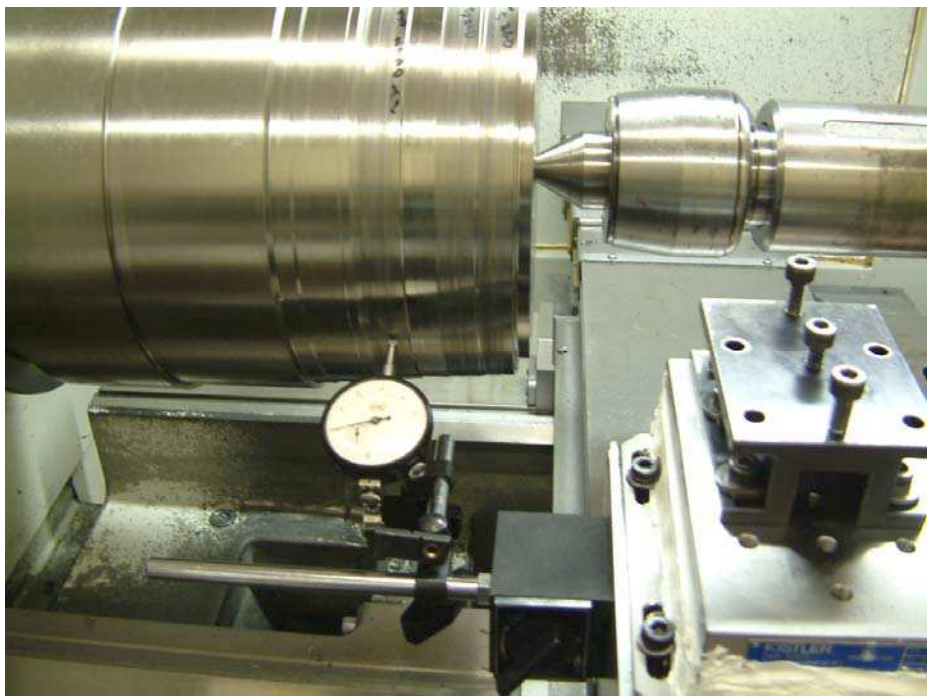

(b)

Figure 3.9: (a) Surtronic-10 portable stylus type used for surface roughness measurement; (b) dial indicator Shockproof – BATY used for run-out measurement.

3.13 Runout Measurement

Run-out measurements are taken at the end of cut using a dial indicator Shockproof – BATY which was placed in the cross slide of the toolholder and pointed towards the workpiece bar as shown in Figure 3.9 (b). A small tension was applied and then the clock was set in the zero position. Finally, the workpiece was rotated to determinate the run-out variation.

3.14 Tool and Workpiece Specimen Preparation

The worn inserts are cleaned in acetone to remove oil stains, dust and adhering work material on the surfaces to be examined. They are mounted on aluminium stubs with sticking carbon glue, prior to examination in the scanning electron microscope (SEM), Hitachi S530, as illustrated in Figure 3.10 (a). The worn surfaces can be viewed in either a three dimensional or two dimensional view from any chosen angle. Relevant images of the worn tools were selected and captured on a computer connected to the SEM. Analysis of these micrographs helps to identify the failure mode(s) of the insert and to formulate possible wear mechanism(s) involved. Additional information on the wear mechanism analysis can be obtained by sectioning the worn region of the cutting tool with a diamond sliting saw which will ensure minimum heat affected zone on the sectioned sample.

For specimens of the machined surfaces, 3 mm thickness was taken from the bars at the end of tool life under various cutting conditions by grooving to a depth of 3 mm and then cutting horizontally with a hand hacksaw. Each sample was further divided into two, one for surface texture examination, and the other for subsurface alterations analysis after fine polishing to 0.25 μm and etching in 3 ml of nitric acid, 6 ml of hydrochloric acid (HCl) and 100 ml of distilled water for 30 seconds in order to reveal the microstructure. The microstructure is examined and photographed with a Nikon metallurgical optical microscope (OPTIHOT-100) with attached camera (Figure 3.10 (b)). Specimens used to examine the surface texture were first cleaned with acetone to remove oil stains and dirt sticking on the surface prior to examination for any physical damage on the machined surfaces in a scanning electron (SEM) microscope at high magnifications.

(a)

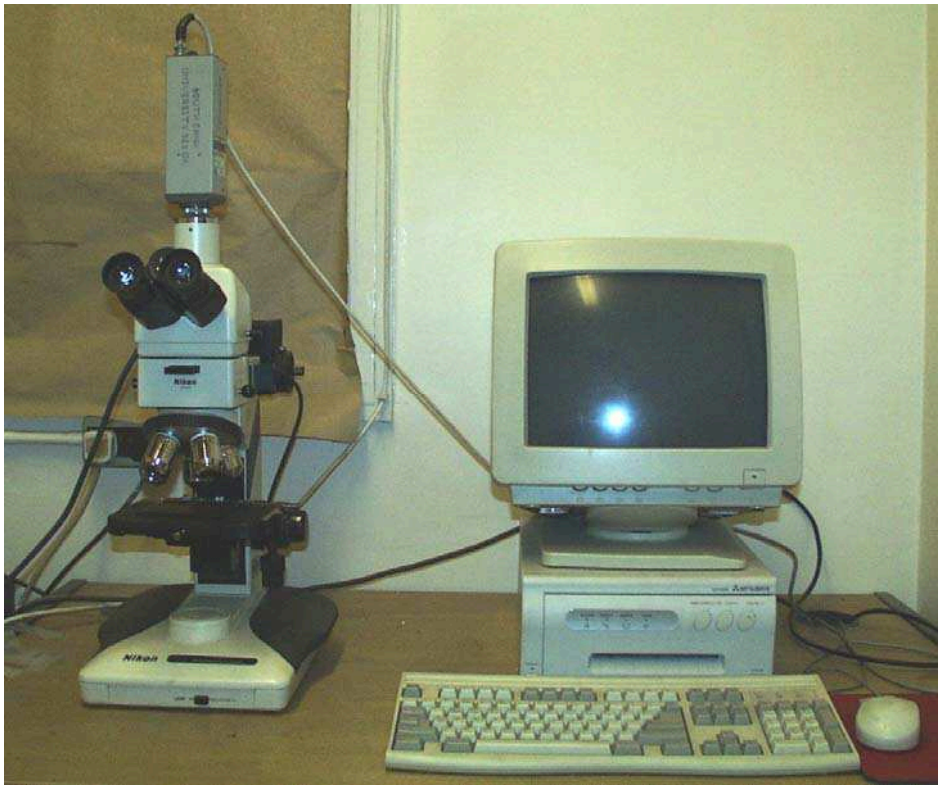

(b)

Figure 3.10 - (a) Hitachi (S530) Scanning Electron Microscope; (b) Nicon Metallurgical Optical Microscope (OPTIPHOT-100) with computerised image system.

All samples used for examination of surface and subsurface alterations were mounted in a mould using conductive phenolic powder (Resin-4 HQ). A Bueler – Automatic Moulding

Machine (Figure 3.11 (a)) was used to mount specimens of the work material and the machined surfaces. An Automatic Grinding/Polishing Equipment – Metaserv 2000 – was used to grind and polish specimens of the workpiece at a speed of 100 rpm (Figure 3.11 (b)). The mounted specimens were polished using a series of silicon carbide papers of decreasing grit/grain sizes (240, 400, 600, 800 and 1200) using water as lubricant. The samples were cleaned in acetone and further polished to 6, 3, 1.0 and 0.25 μm finish on flat plate polishers covered with "NP NAP" cloth impregnated with alumina paste and distilled water as a lubricant. The samples were then examined using optical and electron microscopes at various magnifications.

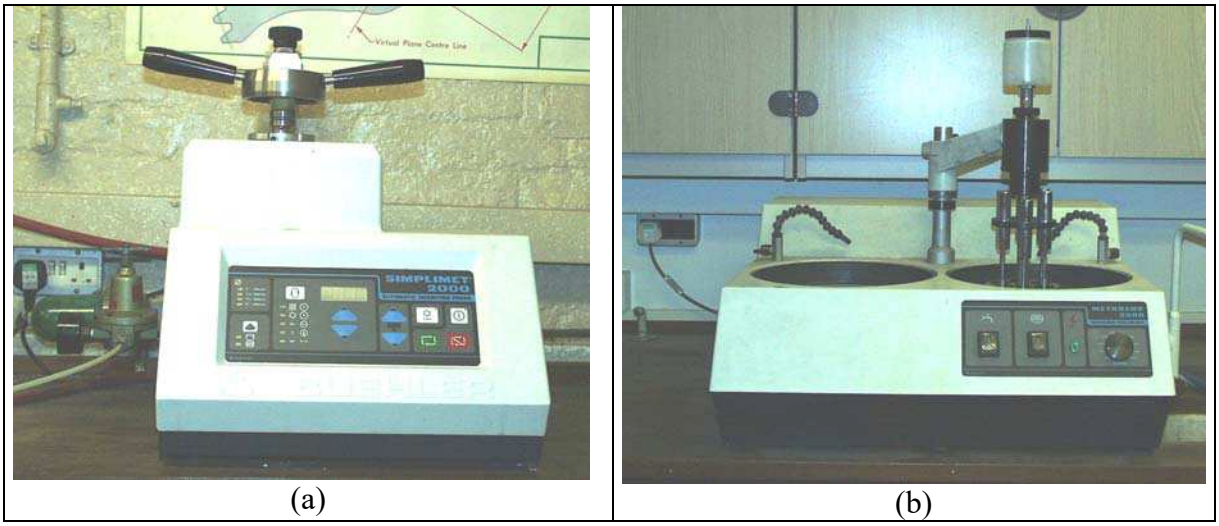

(a) (b)

Figure 3.11 - (a) Buehler Automatic Mounting Press (Simplimet 2000); (b) Automatic Grinding/Polishing Equipment (Metaserv 2000).

3.15 Microhardness Measurements below the Machined Surface

Microhardness of the workpiece samples sectioned after the machining trials were measured using a micro-hardness testing machine, Mitutoyo (MVK – VL), at a magnification of x55 and with an applied load of 0.1 Kgf after polishing the samples to 6μm finish (Figure 3.12). The microhardness of the workpiece sample taken prior to the start of the machining trials is measured at various locations close to the central portion of the sample. This ensures that any effect on the hardness of the workpiece material due to the initial cleaning and sectioning of the sample is kept to a minimum/eliminated. The recorded values were treated

statistically and a confidence interval (C.I.) of 99 % (Table 3.2), represented by the minimum (Min.) and maximum (Max.) Vickers hardness values recorded for the Ti-6Al-4V alloy bars used for the machining trials. The microhardness measurements of the workpiece samples were measured starting from a depth of 0.05 mm below the machined surface up to 2.0 mm.

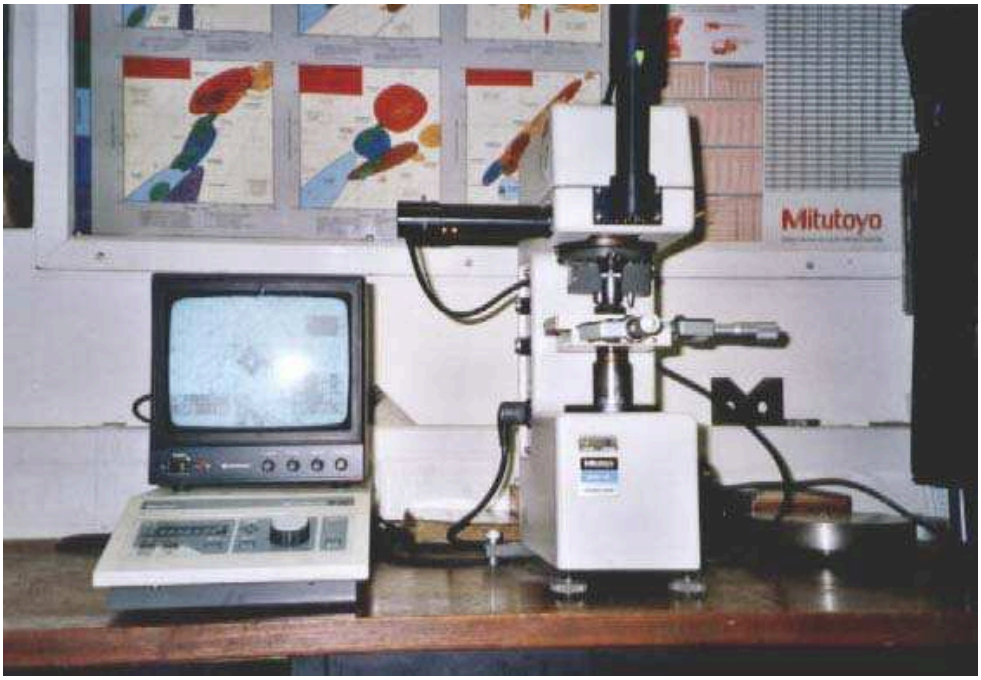

Figure 3.12 -Mitutoyo (MVK – VL) Vickers micro-hardness tester machine.

CHAPTER IV

EXPERIMENTAL RESULTS

4.1 Benchmark trials - Machining of Ti-6Al-4V alloy with Uncoated Carbide (883 grade) inserts

Figure 4.1 shows the average flank wear values recorded when machining with uncoated cemented carbide (grade 883) tools at various cutting speeds under conventional coolant supply, for 15 minutes cutting time. Average flank wear was the dominant tool failure mode when machining Ti-6Al-4V alloy with this insert grade at the conditions investigated in the benchmark trials. Average flank wear, VB_B = 0.3 mm, was, then, the tool life rejection criterion for the benchmark trials. It can be seen that the average flank wear rate increased steadily with increase in cutting speed. Over 1800 % increase in wear was observed by doubling the cutting speed from 60 to 120 m min^{-1}. It can also be observed that at a speed of 120 m min^{-1}, tool wear value is beyond the established rejection criterion of VB_B = 0.3 mm. Therefore, the cutting speed of 100 m min^{-1} was chosen as the baseline cutting speed for the actual machining trials.

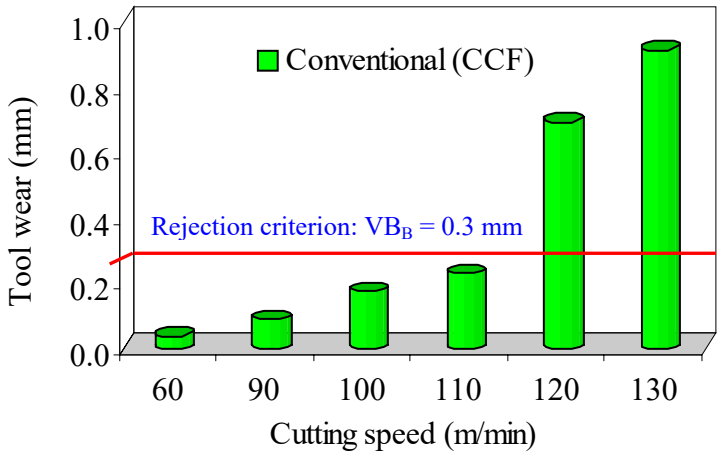

Figure 4.1 - Average flank wear of uncoated carbide (T1) insert at various cutting speeds under conventional coolant supply after 15 minutes machining time (benchmark trials).

4.2 Machining of Ti-6Al-4V alloy with various carbide tool grades (uncoated and coated tools) under various machining environments

4.2.1 Tool Life

Figure 4.2 shows tool life (nose wear, VC ≥ 0.3 mm) recorded when machining Ti-6Al-4V alloy with various grades of cemented carbide (T1, T2, T3, T4) inserts at various cutting speeds and under various machining environments (conventional coolant flow, high pressure coolant supplies of 7 MPa, 11 MPa and 20.3 MPa, and in an argon enriched environment). Tool life of all the insert grades decreased with increasing cutting speed in all machining environments investigated, as expected, due to a reduction in tool-chip and tool-workpiece contact lengths and the consequent increase in both normal and shear stresses at the tool tip (GORCZYCA, 1987). Reduction in tool-chip and tool-workpiece contact areas may also concentrate the high temperature generated to a relatively smaller area as well as shifting the highest temperature region closer to the cutting edge. This phenomenon combines with higher stresses acting at the cutting edge to promote softening of the cutting tool and consequently accelerates tool wear processes, thereby reducing tool life. Tool life generally increased with increasing coolant pressure, especially when machining with the T1 and T4 tool grades.

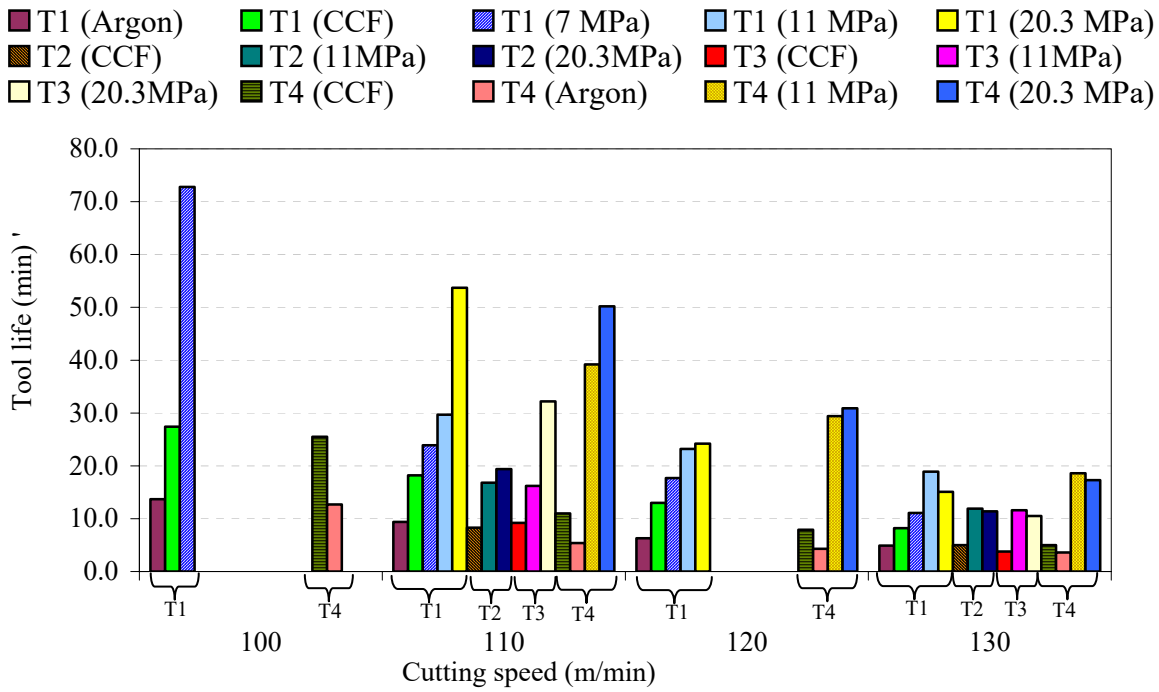

Figure 4.2 - Tool life (nose wear, VC ≥ 0.3 mm) recorded when machining Ti-6Al-4V alloy with different cemented carbide insert grades under conventional coolant flow (CCF), high coolant pressures of 7 MPa, 11 MPa and 20.3 MPa and in argon enriched environment at various speed conditions.

Machining in an argon enriched environment gave the worst performance in terms of tool life relative to conventional and high pressure coolant supplies. It can also be seen in Figure 4.2 that tools T1 (uncoated tool) and T4 (coated tool) with the same substrate composition (Table 3.3) gave the best performance in terms of tool life in all conditions investigated relative to tools T2 (uncoated tool) and T3 (coated tool) with the same substrate composition. In general T4 tool gave the best performance of all the cemented carbide insert grades tested. However, T1 tool outperformed T4 tool when machining under higher coolant pressure of 20.3 MPa at a speed of 110 m min^{-1} and in argon enriched environment. T2 and T3 tools generally exhibited similar performance in terms of tool life at the cutting conditions investigated, except when machining with the highest coolant pressure of 20.3 MPa at a speed of 110 m min^{-1}, where over 65% increase in tool life was achieved with T3 tool. The longest tool life of 73 min was recorded when machining at the lowest speed of 100 m min^{-1} with T1 tool under a coolant pressure of 7 MPa. The second highest tool life was also recorded with T1 tool using the highest pressure supply of 20.3 MPa at a cutting speed of 110 m min^{-1}. T4

tool gave the second best performance, in terms of tool life, relative to T2 and T3 tools when machining in all the machining environments investigated at a lower cutting speed of 110 m min^{-1}. T2 and T3 inserts gave similar performance when machining at a higher cutting speed of 130 m min^{-1}. Figure 4.2 also shows that increasing coolant pressure up to 11 MPa improved tool life for all the carbide tool grades at the highest speed of 130 m min^{-1}. Machining with 20.3 MPa coolant pressure, however, produced slightly lower tool life relative to those obtained with 11MPa coolant pressure at a speed of 130 m min^{-1}, Table 4.1. The highest gains in tool life were achieved when machining with T4 tool at speeds of 110 m min^{-1} and 120 m min^{-1} with 20.3 MPa coolant pressure where 356% and 291% improvement in tool lives were recorded, respectively. Up to 84% and 246% improvement in tool lives were achieved when machining with T1 and T4 tools, respectively, under most aggressive conditions of 130 m min^{-1} using 20.3 MPa coolant pressure. Over 165% improvement in tool life was achieved when machining with T1 tool with 7 MPa coolant pressure relative to conventional coolant supply at the lowest cutting speed of 100 m min^{-1} whereas, at cutting speeds in excess of 100 m min^{-1}, improvement in tool life remained constant (at about 35%). These results show that tool life increased with increasing coolant pressure for all the insert grades investigated. The ranking order for carbide tools in terms of average gain in tool life relative to conventional coolant flow is T4, T3, T2 and T1 (Table 4.1). This also shows that the coolant pressure has a significant effect on tool wear pattern and hence recorded tool life when machining Ti-6Al-4V alloy with carbide tools under finishing conditions.

Figure 4.2 and Table 4.1 also show significant reduction in tool life when machining in an argon enriched environment relative to conventional coolant supply. Average reduction in tool life for T1 and T4 tools are 47 % and 44% respectively. It can also be seen that the uncoated carbide T1 tool outperformed the coated carbide T4 tool when machining with conventional coolant flow and in an argon enriched environment at the cutting conditions investigated. A marginal improvement in tool life of 8% was achieved when machining with T1 tool grade relative to T4 in all the environments tested at the lowest speed of 100 m min^{-1}. Machining with T1 tool at a cutting speed of 110 m min^{-1} produced up to 65% and 74% improvements in tool life with an argon enriched environment and with conventional coolant flow, respectively, compared to T4 grade.

Table 4.1 - Percentage improvement in tool life relative to conventional coolant supply after machining Ti-6Al-4V alloy with different grades of carbides.

Tool	Speed (m min^{-1})	Argon	Coolant pressure (MPa)		
			7	11	20.3
T1	100	-50	165.7	.	.
	110	-48.3	31.3	63.2	195
	120	-51.5	36.1	78.5	86.1
	130	-40.2	35.4	130.5	84.1
T2	110	.	.	102.4	133.7
	130	.	.	138	128
T3	110	.	.	76.1	250
	130	.	.	205.2	176.3
T4	100	-50,2	.	.	.
	110	-50.9	.	256.4	356.4
	120	-45.6	.	272.1	291.1
	130	-28	.	272	246

4.2.2 Tool wear when machining Ti-6Al-4V alloy with various carbide insert grades

Flank wear and nose wear are typical wear patterns observed when machining Ti-6Al-4V alloy with carbide tools. The flank wear rate is generally lower than the nose wear rates. Figure 4.3 shows plots of nose wear rates of different cemented carbide insert grades when machining Ti-6Al-4V alloy under various cutting environments. Machining with carbide tools under finishing conditions showed steady increase in nose wear rate with increasing cutting speed. It can also be seen that nose wear rate generally decreases with increasing coolant pressure. The lowest nose wear rates were recorded when machining with T1 and T4 tools with 11 MPa coolant pressure. Rapid increase in nose wear rate was recorded when machining with T1 and T4 tools at the higher speed conditions of 130 m min^{-1} under conventional coolant flow and in the presence of argon. The highest nose wear rate was recorded when machining Ti-6Al-4V alloy with T4 tool grade in the presence of argon in all cutting conditions investigated. This gave increased nose wear rate of about 38%, 462% and 310% relative to conventional coolant flow, coolant pressures of 11 MPa and 20.3 MPa,

respectively when machining at 130 m min^{-1}. High nose wear rate was also recorded when machining with T1 tool grade in presence of argon at a speed of 130 m min^{-1}. This increase is about 74%, 144%, 479% and 252% relative to conventional coolant flow and coolant pressures of 7 MPa, 11 MPa and 20.3 MPa, respectively. Nose wear rate increased with prolong machining in all the cutting environments tested when machining with the carbide insert grades. At the initial stages of cutting, nose wear was generally uniform for inserts used for machining with high coolant pressures. Further machining accelerated the nose wear as illustrated in Figures 4.4 and 4.5. Figure 4.4 shows a reduction in nose wear with increasing coolant pressure for both T1 and T4 insert grades. The lowest nose wear was recorded when machining with T1 tool with the highest coolant pressure of 20.3 MPa while machining with T4 tool in argon enriched environment gave the highest nose wear. Figure 4.5 shows that the highest and lowest nose wear was recorded with T2 and T3 insert grades at a speed of 110 m min^{-1} using conventional and 20.3 MPa coolant pressure, respectively.

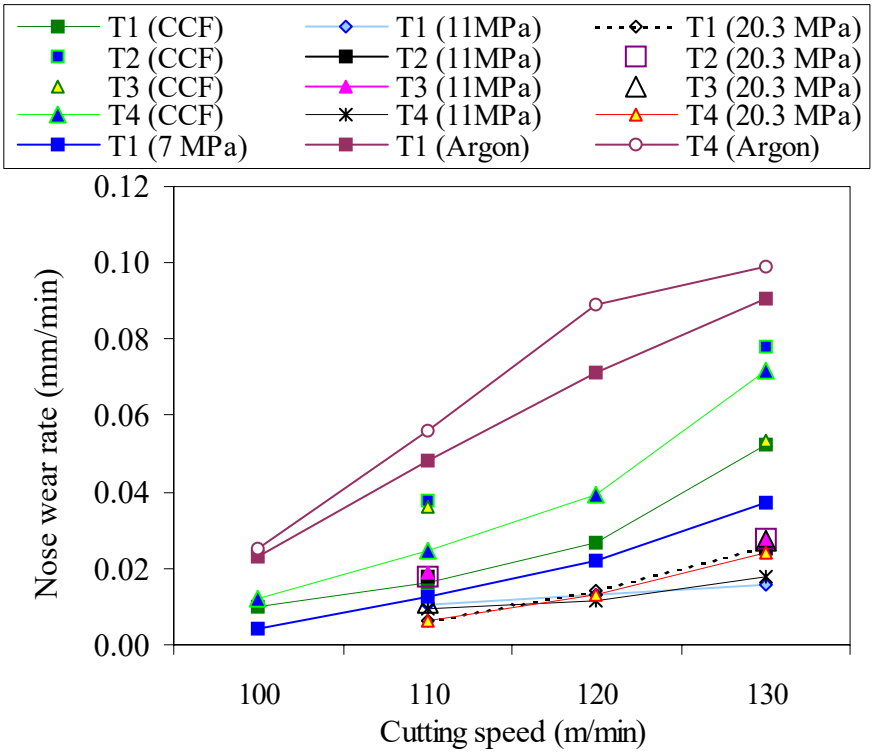

Figure 4.3 - Nose wear rate curves of different cemented carbide insert grades when machining Ti-6Al-4V alloy under conventional coolant flow (CCF), high coolant pressures of 7 MPa, 11 MPa and 20.3 MPa and in argon enriched environment, at a feed rate of 0.15 mm rev^{-1} and a depth of cut of 0.5 mm.

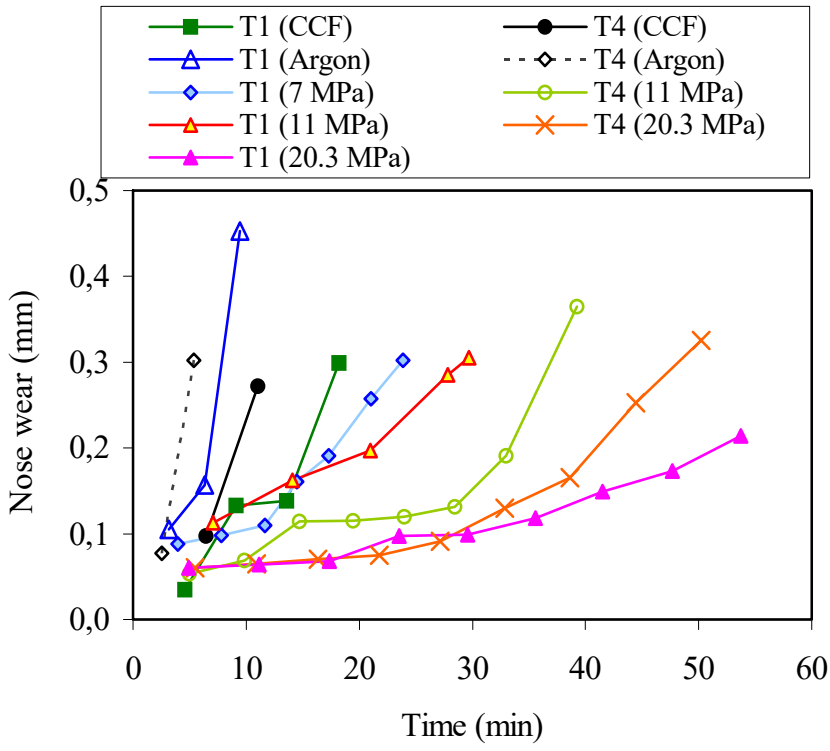

Figure 4.4 - Nose wear curves when finish machining with cemented carbide (T1 and T4) inserts at a cutting speed of 110 m min^{-1}.

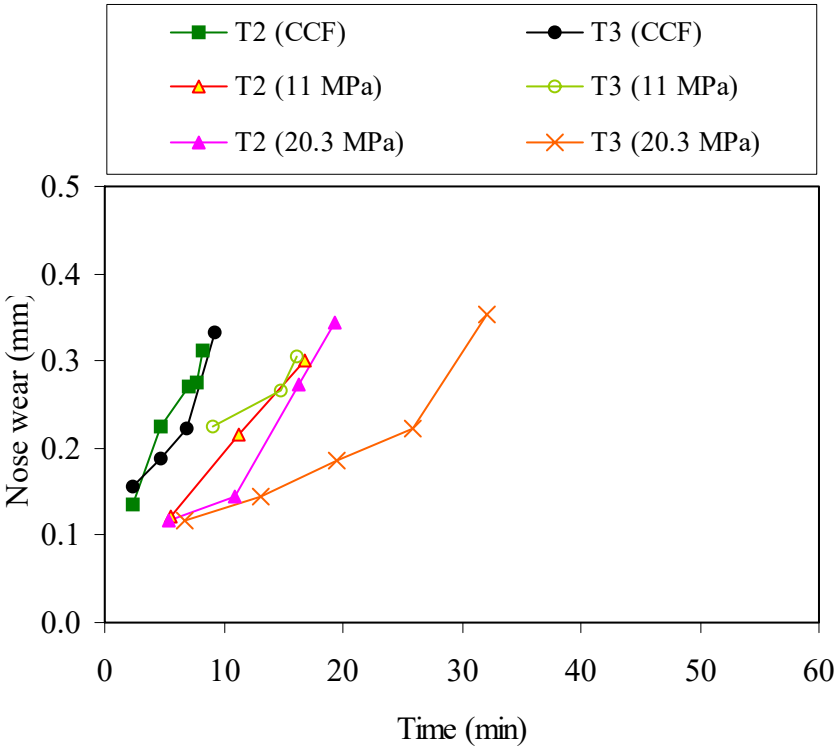

Figure 4.5 - Nose wear curves when finish machining with cemented carbide (T2 and T3) inserts at a cutting speed of 110 m min^{-1}.

Figures 4.6 – 4.10 show worn cutting edges obtained after machining Ti-6Al-4V alloy with T1 tool grade (uncoated carbide tool – 883 grade) under various machining conditions. The T1 grade experienced regular nose wear when machining under conventional coolant flow at the lower speed of 100 m min^{-1} (Figure 4.6 (a)) and more severe nose wear at a speed of 130 m min^{-1} (Figure 4.6 (b)). Figures 4.6 (a) and (b) also illustrate the extent of adhesion of work material to the nose of the worn tool. Figures 4.7 to 4.9 are the micrographs of T1 worn insert after machining with 7 MPa, 11 MPa and 20.3 MPa coolant pressures at cutting speeds of 110 m min^{-1}, 120 m min^{-1} and 130 m min^{-1}, respectively. There is the evidence of adhesion of work material to the tool nose as result of the intermittent contact between the tool and the work material during machining. Flank wear rate when machining under high coolant pressures was generally very low relative to nose wear rate. Figure 4.10 shows a smoothly worn tool with slight cracks on a worn T1 insert after machining in the presence of argon at a speed of 130 m min^{-1}.

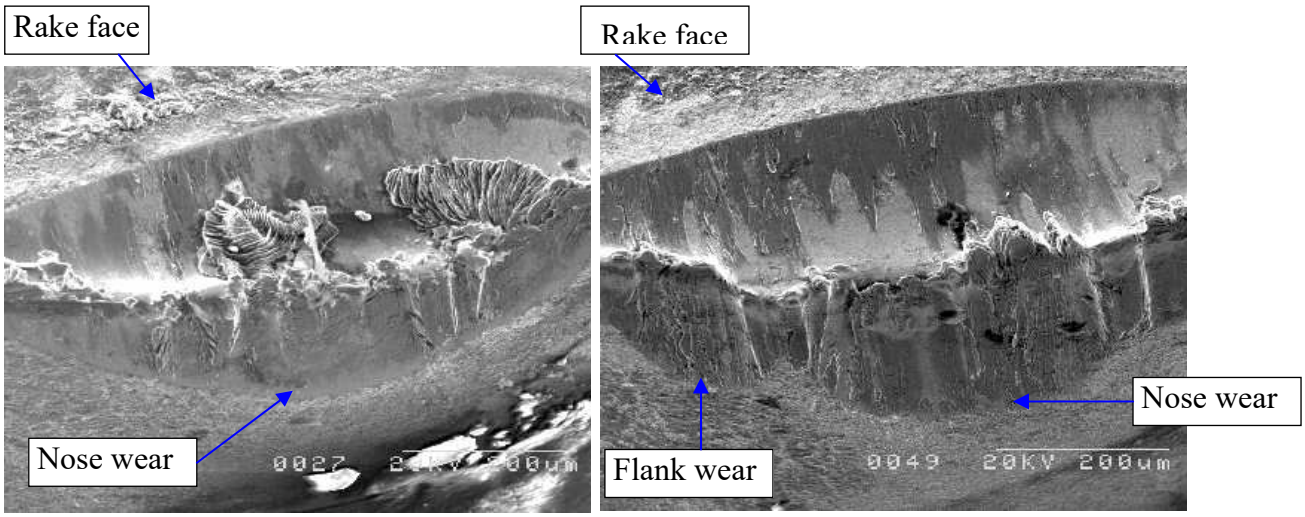

(a) Tool life = 27.4 min (b) Tool life = 8.2 min

Figure 4.6 - Worn T1 insert after machining Ti-6Al-4V alloy with conventional coolant supply at a speed of (a) 100 m min^{-1} and (b) 130 m min^{-1}.

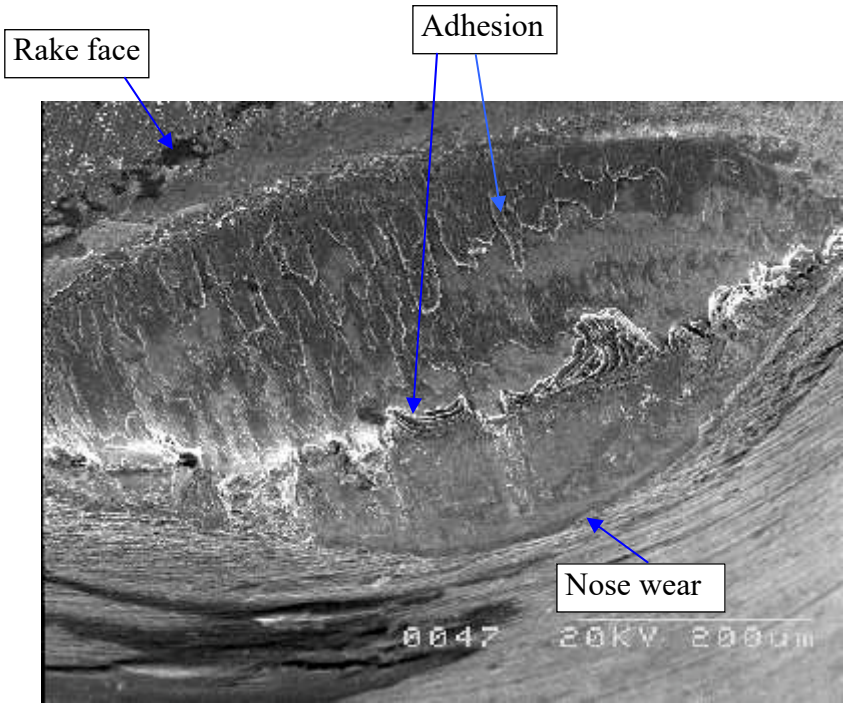

Tool life = 23.9 min

Figure 4.7 - Wear generated at the cutting edge of uncoated carbide T1 insert after machining Ti-6Al-4V alloy with a coolant pressure of 7MPa at a speed of 110 m min^{-1}.

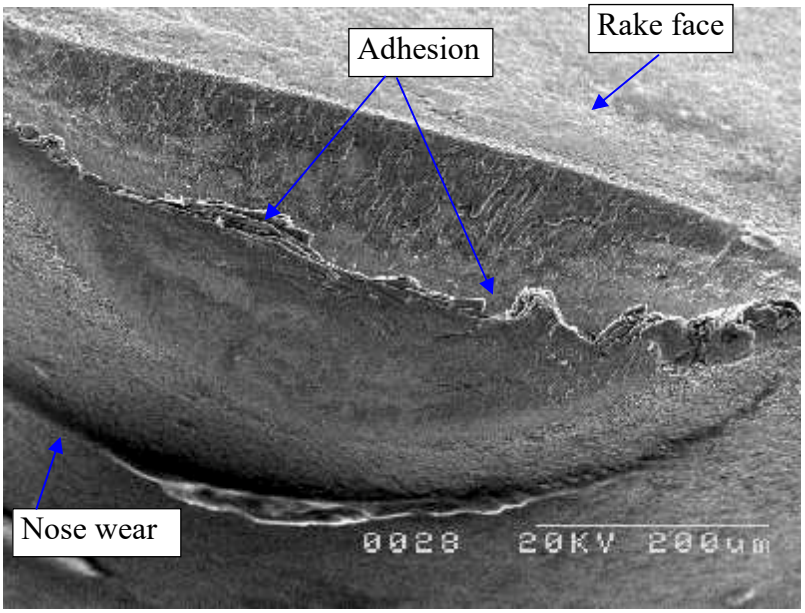

Tool life = 23.2 min

Figure 4.8 -Wear generated at the cutting edge of uncoated carbide T1 insert after machining Ti-6Al-4V alloy with a coolant pressure of 11MPa at a speed of 120 m min^{-1}.

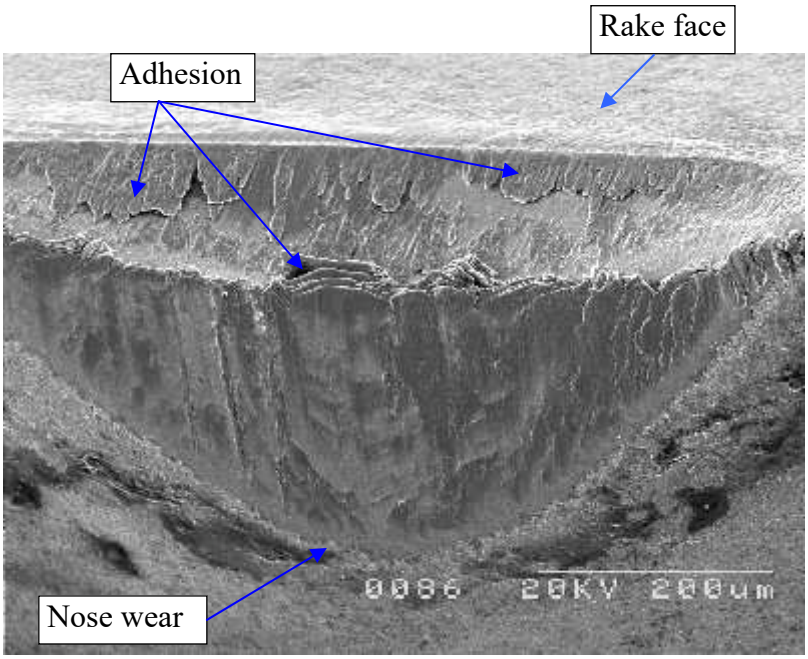

Tool life = 15.1 min

Figure 4.9 - Worn cutting edge of uncoated carbide T1 insert after machining Ti-6Al-4V alloy under a coolant pressure of 20.3 MPa at a speed of 130 m min^{-1}.

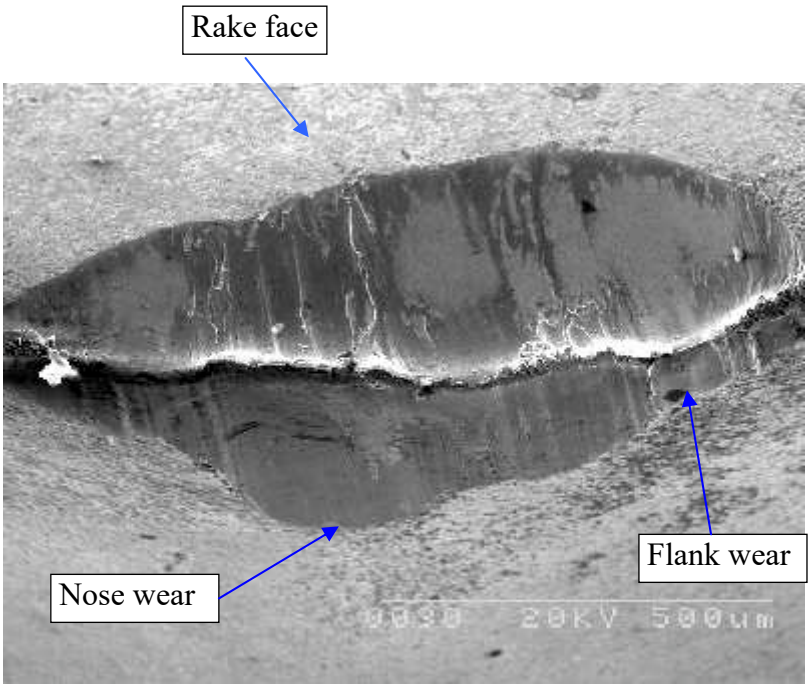

Tool life = 4.9 min

Figure 4.10 - Worn cutting edge of uncoated carbide T1 insert after machining Ti-6Al-4V alloy in argon enriched environment at a speed of 130 m min^{-1}.

Figures 4.11-4.13 are typical micrographs of worn T2 (uncoated carbide tool – 890 grade) inserts after machining Ti-6Al-4V alloy at different cooling and cutting speed conditions. Both flank and nose wears occurred simultaneously at the cutting edge. The flank

wear tend to be displaced towards the nose region with prolonged machining, making only the nose wear responsible for tool rejection. Irregular flank and nose wear patterns were observed across the worn flank face when machining with conventional flow and at the highest coolant pressure of 20.3 MPa at a cutting speed of 130 m min^{-1} (Figure 4.13).

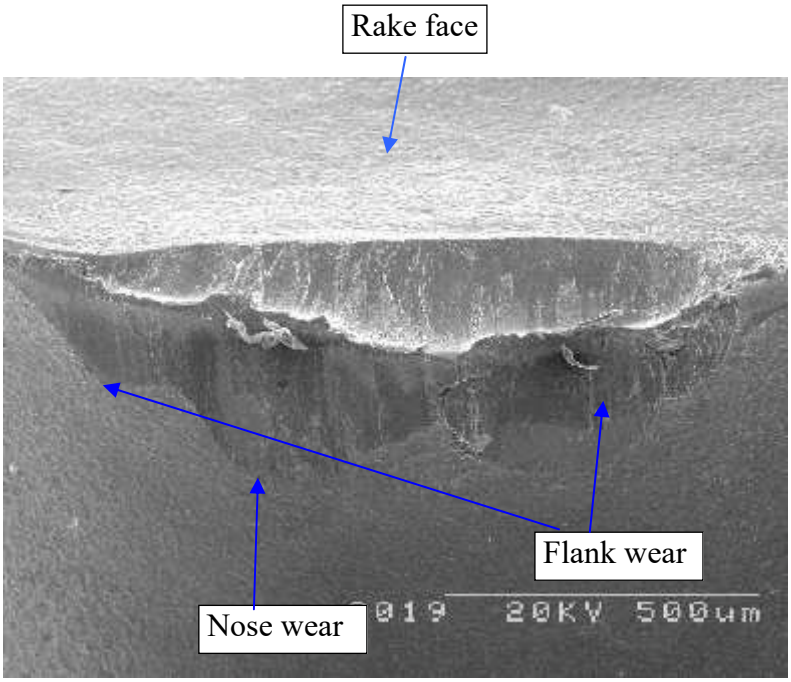

Tool life = 5 min

Figure 4.11 - Flank and nose wears at the cutting edge of uncoated carbide T2 insert grade after machining Ti-6Al-4V alloy under conventional coolant supply at a speed of 130 m min^{-1}, a feed rate of 0.15 mm rev^{-1} and a depth of cut of 0.5 mm.

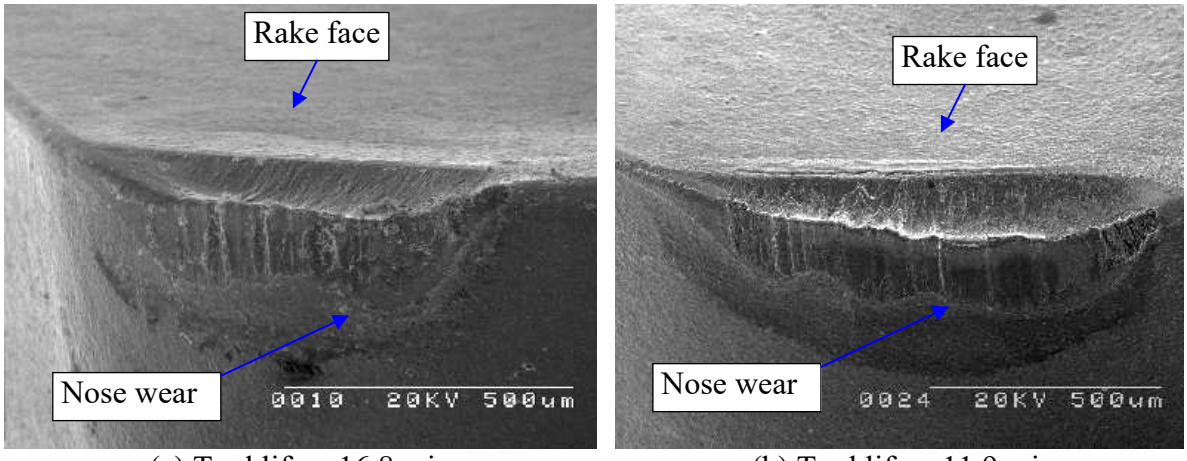

(a) Tool life = 16.8 min (b) Tool life = 11.9 min

Figure 4.12 -Wear generated at the cutting edge of uncoated carbide T2 insert after machining Ti-6Al-4V alloy with a coolant pressure of 11 MPa at a speed of (a) 110 m min^{-1} and (b) 130 m min^{-1}.

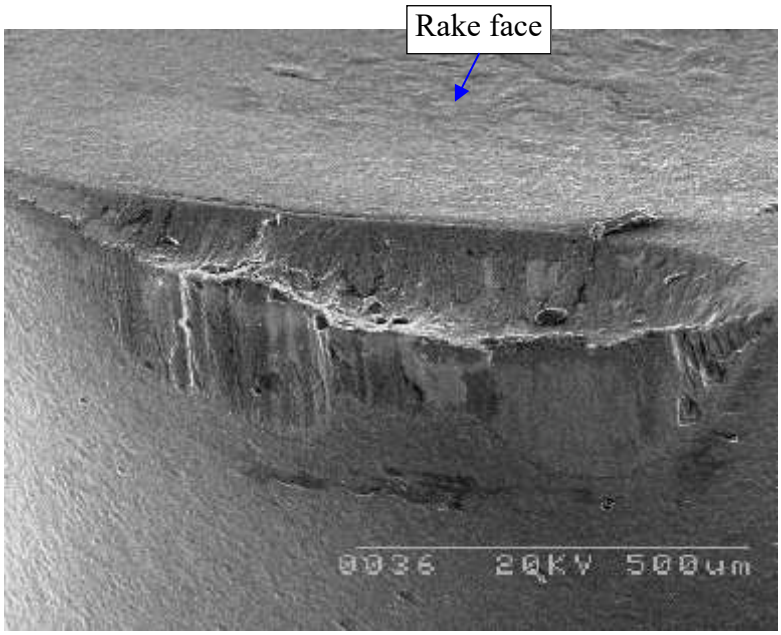

Tool life = 11.4 min

Figure 4.13 - Wear generated at the cutting edge of uncoated carbide T2 insert after machining Ti-6Al-4V alloy with a coolant pressure of 20.3 MPa at a speed of 130 m min^{-1}.

Figures 4.14-4.16 are micrographs of T3 worn tools (coated carbide tool – CP200 grade) after machining Ti-6Al-4V alloy with different coolant pressures and cutting speeds. These figures show that T3 tool grade experienced more severe flank and nose wears in all machining environments tested. Visible grooves were observed on the worn inserts as clearly illustrated in Figures 4.15 and 4.16 (a) and (b).

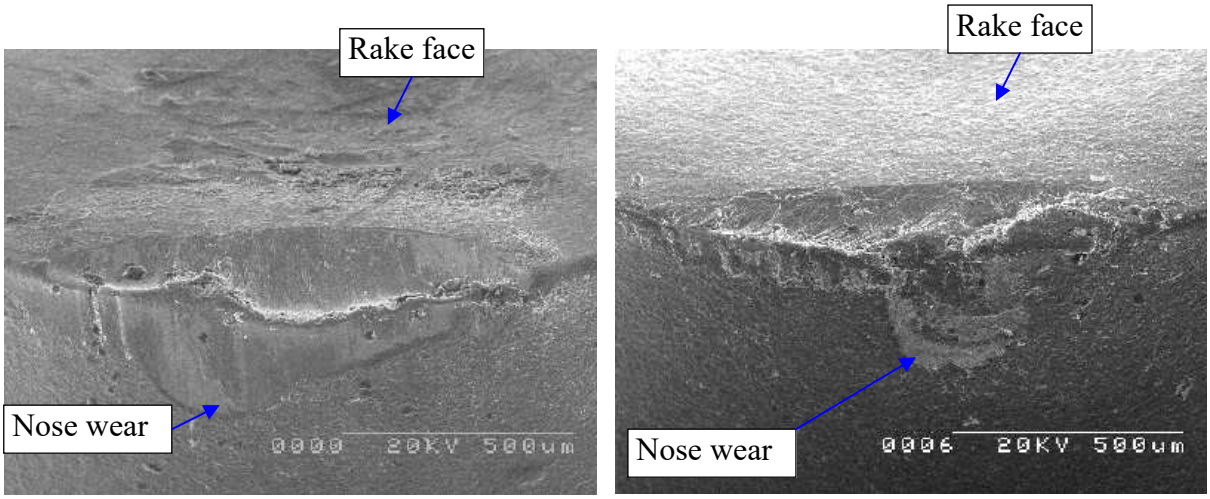

(a) Tool life = 9.2 min (b) Tool life = 3.8 min

Figure 4.14 - Worn cutting edge of T3 coated carbide insert when machining with conventional coolant supply at a speed of (a) 110 m min^{-1} and (b) 130 m min^{-1}.

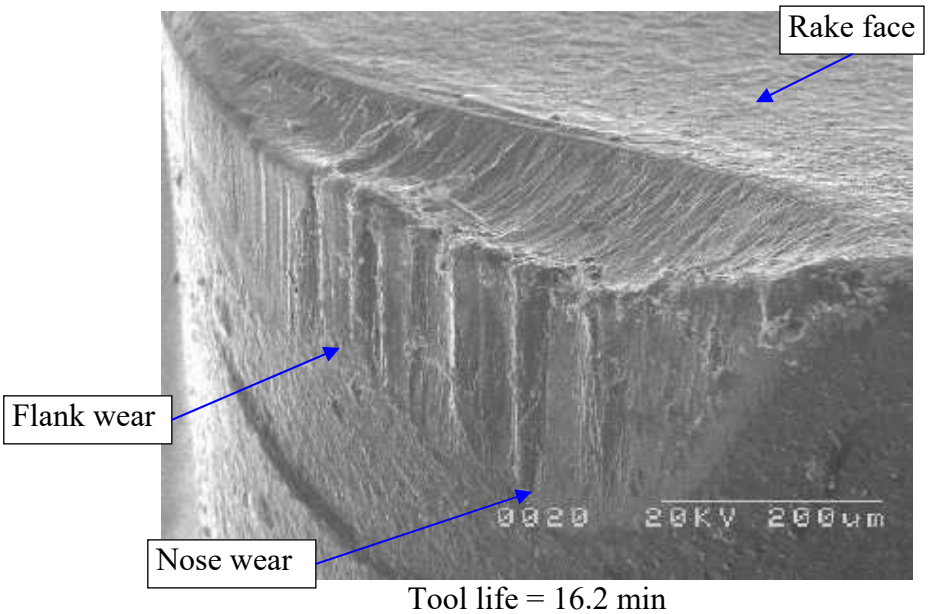

Tool life = 16.2 min

Figure 4.15 - Flank and nose wears a the cutting edge of T3 coated carbide insert after machining Ti-6Al-4V alloy with a coolant pressure of 11 MPa at a speed of 110 m min^{-1}.

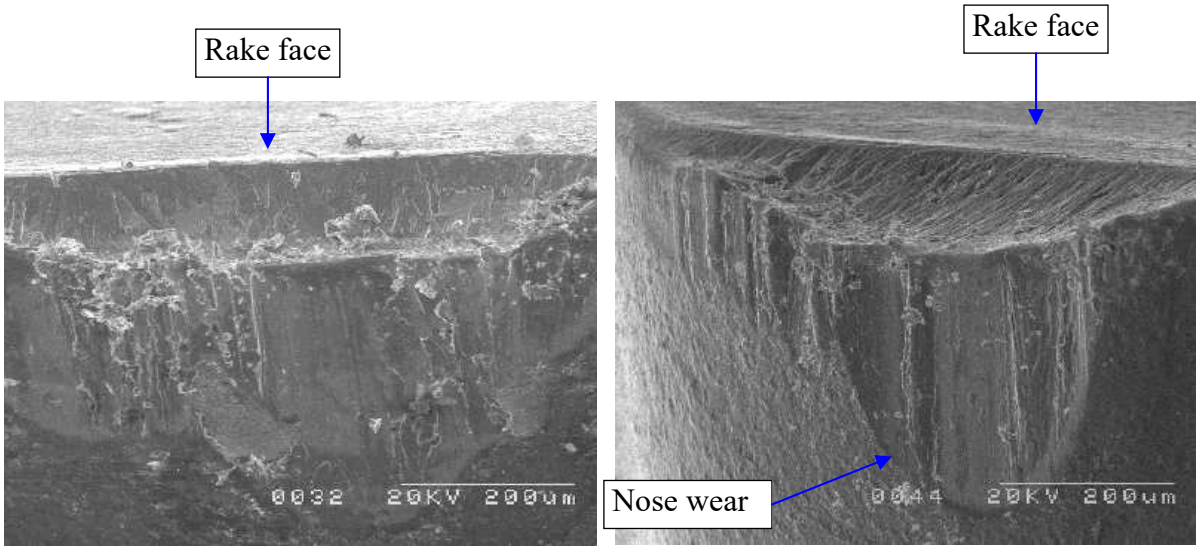

(a) Tool life = 32.2 min (b) Tool life = 10.5 min

Figure 4.16 - Flank and nose wears at the cutting edge of T3 coated carbide insert after machining Ti-6Al-4V alloy with a coolant pressure of 20.3 MPa at a speed of (a) 110 m min^{-1} and (b) 130 m min^{-1}.

Figures 4.17-4.20 are micrographs of T4 worn tools (coated carbide tool – CP250 grade) after machining Ti-6Al-4V alloy with different cooling conditions. Figure 4.17 shows the flank wear spreading along the flank face and displaced towards the nose region. Figure 4.18 is an enlarged view of the worn tool after machining with a coolant pressure of 11 MPa at a cutting speed of 110 m min^{-1} illustrating the extent of adhesion of work material to the tool nose. This was also observed in Figures 4.17 and 4.19 suggesting that high temperatures may be generated at the cutting interfaces during machining. Figure 4.20 (a) shows a

smoothly worn tool obtained after machining in the presence of argon at a speed of 100 m min^{-1} while Figure 4.20 (b) shows that the T4 insert experienced pronounced flank wear and crater wears when machining in an argon enriched environment at a speed of 120 m min^{-1}. These figures also show that the crater wear developed very close to the cutting edge.

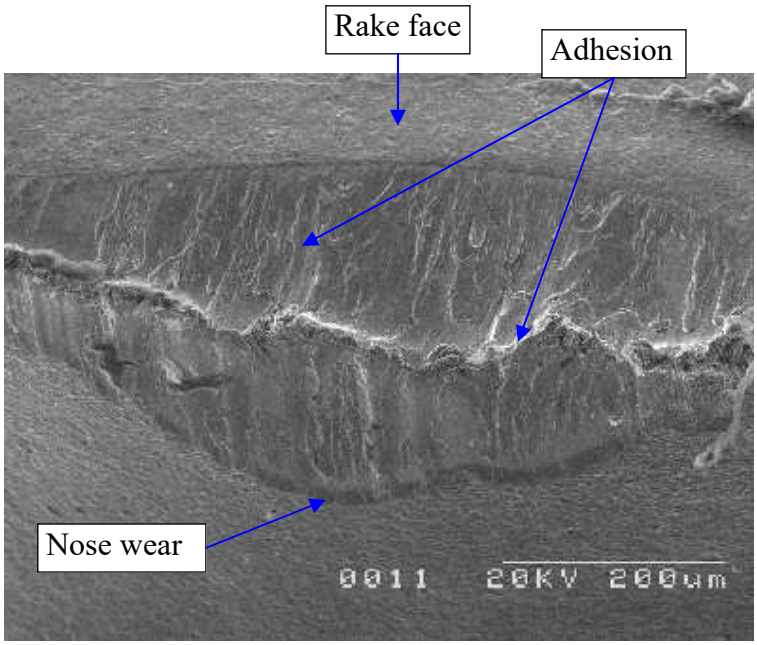

Tool life = 5 min

Figure 4.17 - Worn cutting edge of T4 coated carbide insert after machining Ti-6Al-4V alloy with conventional coolant supply at a speed of 130 m min^{-1}.

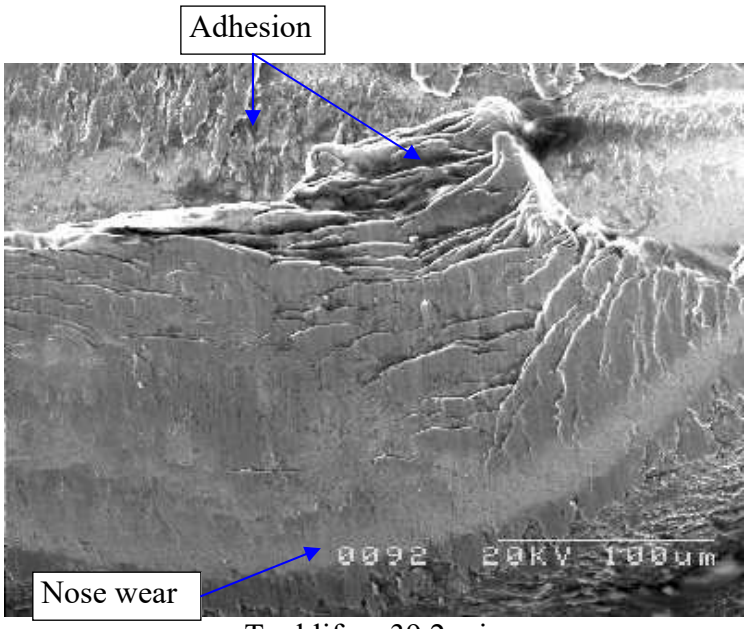

Tool life = 39.2 min

Figure 4.18 - Adhesion of work material on a worn T4 coated carbide insert after machining Ti-6Al-4V alloy with a coolant pressure of 11 MPa at a speed of 110 m min^{-1}.

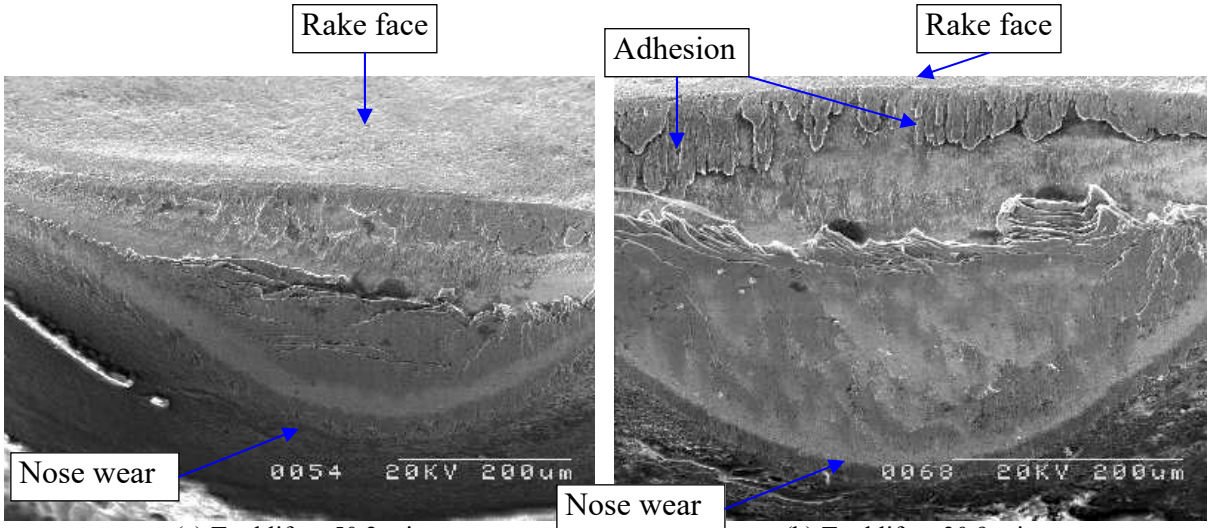

(a) Tool life = 50.2 min (b) Tool life = 30.9 min

Figure 4.19 - Nose wear at the cutting edge of T4 coated carbide insert after machining Ti-6Al-4V alloy with a coolant pressure of 20.3 MPa at a speed of (a) 110 m min^{-1} and (b) 120 m min^{-1}.

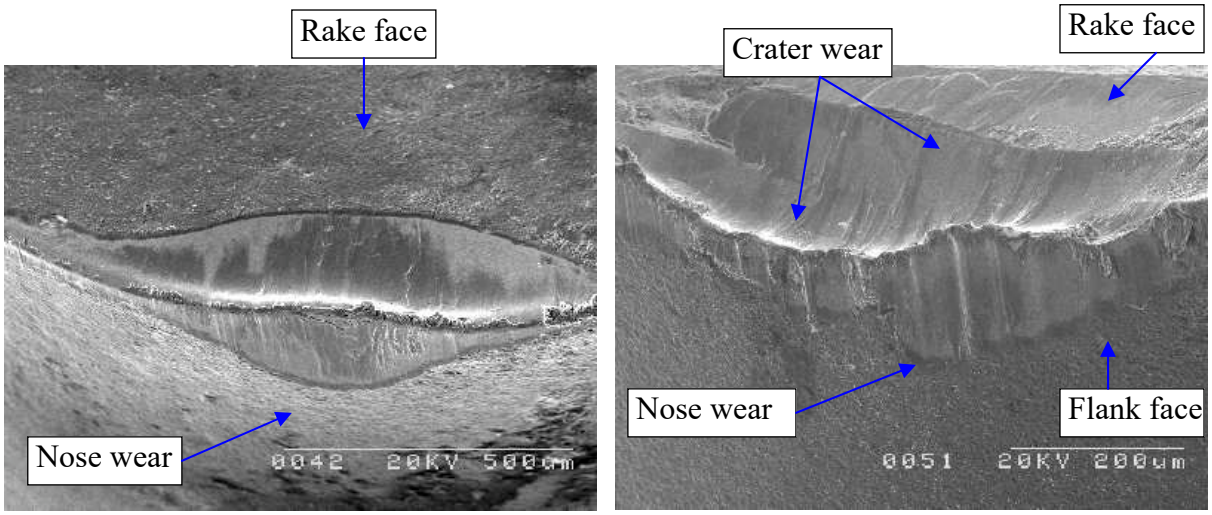

(a) Tool life = 12.7 min (b) Tool life = 4.3 min

Figure 4.20 - Wear at the cutting edge of T4 coated carbide insert after machining Ti-6Al-4V alloy in argon enriched environment at a speed of (a) 100 m min^{-1} and (b) 120 m min^{-1}.

4.2.3 Component forces when machining with various carbide insert grades

Figures 4.21 and 4.22 show variations in cutting and feed forces, respectively, when machining Ti-6Al-4V alloy with different grades of carbide tools under various cutting speeds and machining environments. The component forces were recorded at the beginning of cut when the cutting edge has not undergone pronounced wear. Figure 4.21 suggests that the cutting forces generally decreased with increase in coolant pressure when machining with T1

and T4 insert grades and generally increase with increase in coolant pressure when machining with T2 and T3 insert grades. Figure 4.21 also shows that in general, cutting forces marginally increased with increasing speed when machining with T1 and T2 in all cutting environments tested, unlike T3 and T4 insert grades. Cutting forces recorded with T2 tool grade were generally higher than those recorded with T3 tool in all conditions tested. High cutting forces were generated when machining with T1 and T4 tool grades in argon environment relative to conventional coolant flow.

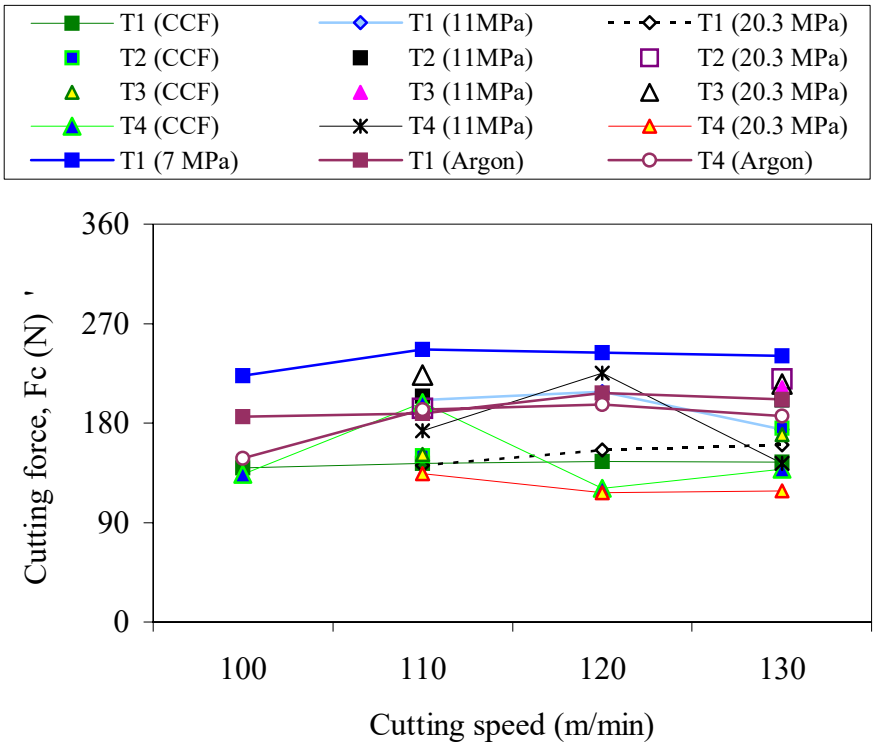

Figure 4.21 - Cutting forces (F*c*) recorded at the beginning of cut when machining Ti-6Al-4V alloy with different cemented carbide grades under various cutting conditions.

Recorded feed forces generally increase marginally with an increase in cutting speed (Figures 4.22). This figure also shows that feed forces increased with an increase in coolant pressure when machining with T1, T2 and T3 tool grades, unlike T4 tool. It can be seen from Figure 4.22 that the highest feed forces were generated when machining with T1 tool grade under a coolant pressure of 7 MPa. Machining with T4 tool grade in the presence of argon provided the lowest feed forces in all conditions tested.

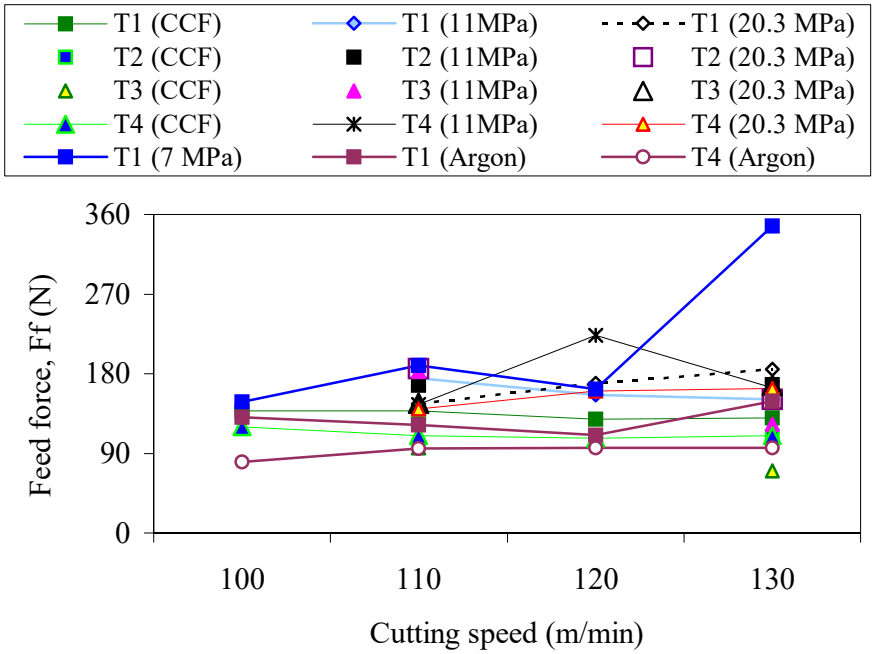

Figure 4.22 - Feed forces (F_f) recorded at the beginning of cut when machining Ti-6Al-4V alloy with different cemented carbide grades under various cutting conditions.

4.2.4 Surfaces roughness and runout deviation when machining with various carbide insert grades

Figure 4.23 and 4.24 show the surface roughness and circular runout deviation values, respectively, recorded when machining Ti-6Al-4V alloy with different grades of carbides at various cutting speeds and under various cutting environments. It can be seen from Figure 4.23 that the surface roughness values recorded in all the conditions investigated varied between 0.3 and 1.0 µm, well below the stipulated rejection criterion of 1.6 µm. This figure, however, shows evidence of deterioration of the surface finish when machining at higher speed conditions.

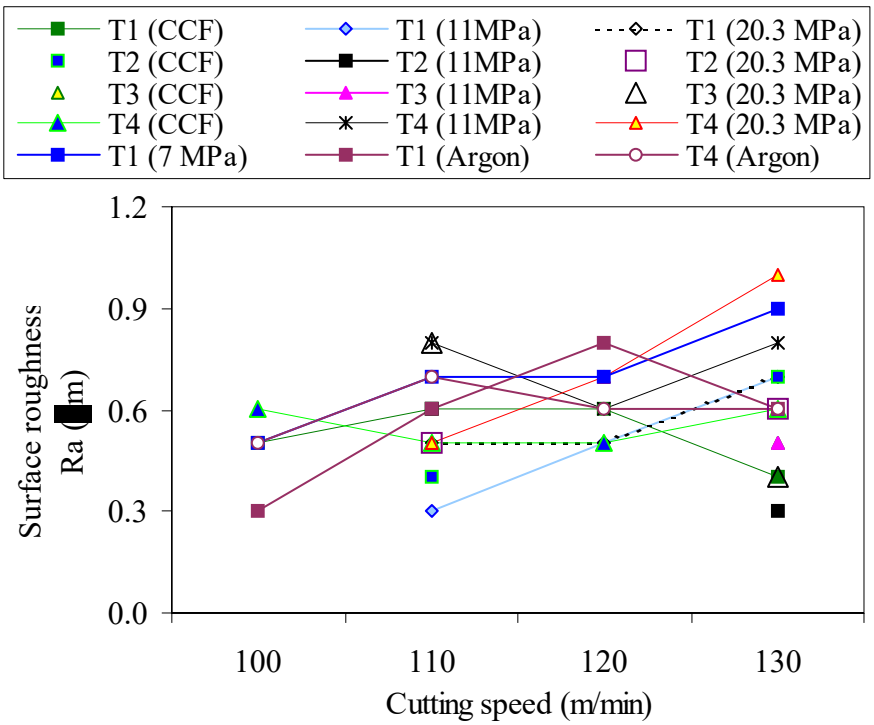

Figure 4.23 - Surface roughness values recorded at the beginning of cut when machining Ti-6Al-4V alloy with different cemented carbide grades under various cutting conditions.

Runout tolerances are used to control the functional relationship of one feature to another or a feature to a datum axis. This tolerance is applicable to rotating parts where the composite surface criterion is based on the part function and design requirements. When dealing with three-dimensional objects, circular runout is defined as the amount that is allowed to deviate from the central axis at one cross section (POLLACK, 1988). Figure 4.24 shows that runout values recorded in all the conditions investigated varies between 2 and 14 µm. These values are far lower than the stipulated rejection criterion value of 100 µm. Machining with T4 tool grade provided lower runout values in all conditions investigated compared to other tool grades. Runout values recorded increased with increasing cutting speed when machining with T2 and T3 insert grades under conventional coolant flow while no variation was observed when machining with T2 and T3 inserts under high coolant pressures.

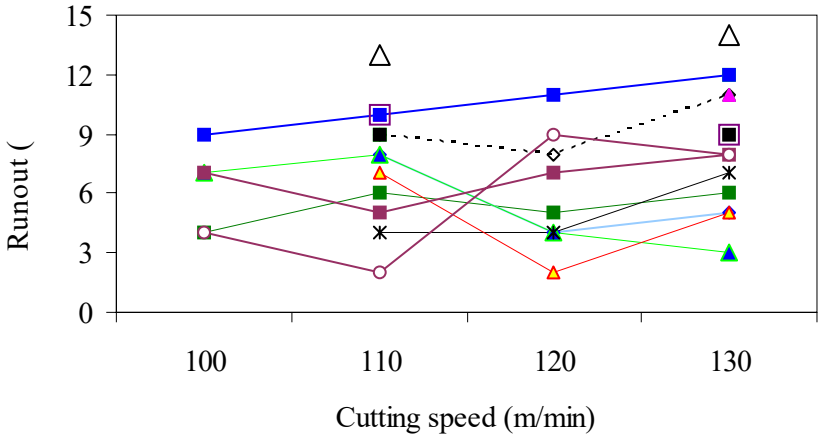
15
12
9
6
3
0
Runout (
100
110
120
130
Cutting speed (m/min)

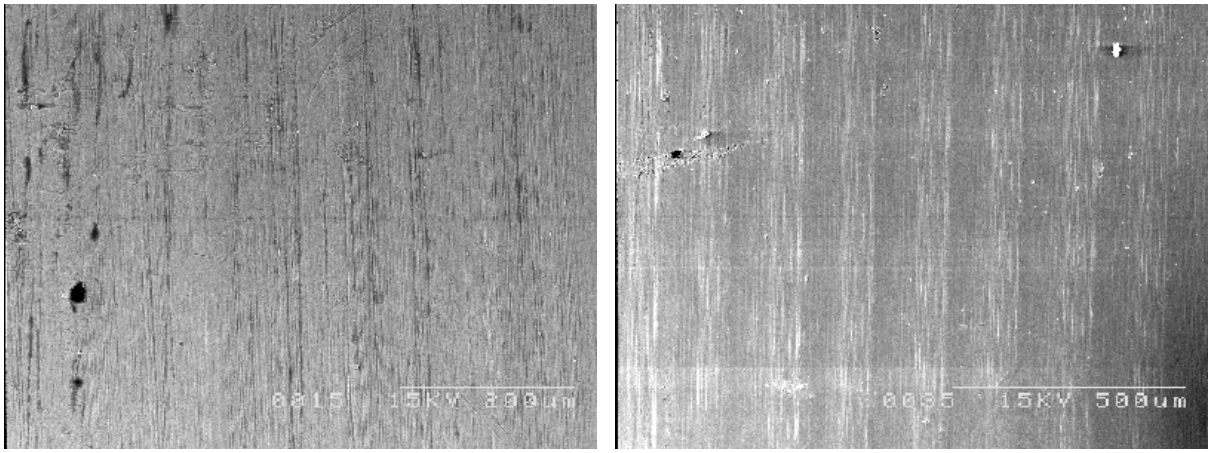

(a) (b)

Figure 4.26 - Surfaces generated after machining with uncoated carbide T1 tool with a coolant pressure of 7 MPa at cutting speeds of (a) 100 m min^{-1} and (b) 130 m min^{-1}.

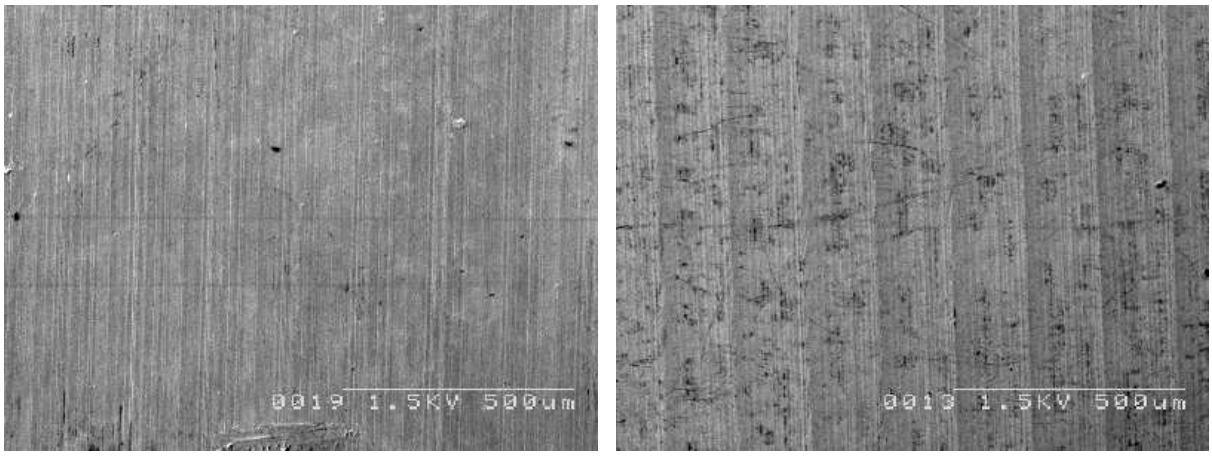

(a) (b)

Figure 4.27 - Surfaces generated after machining with uncoated carbide T1 tool with a coolant pressure of 11 MPa at cutting speeds of (a) 110 m min^{-1} and (b) 120 m min^{-1}.

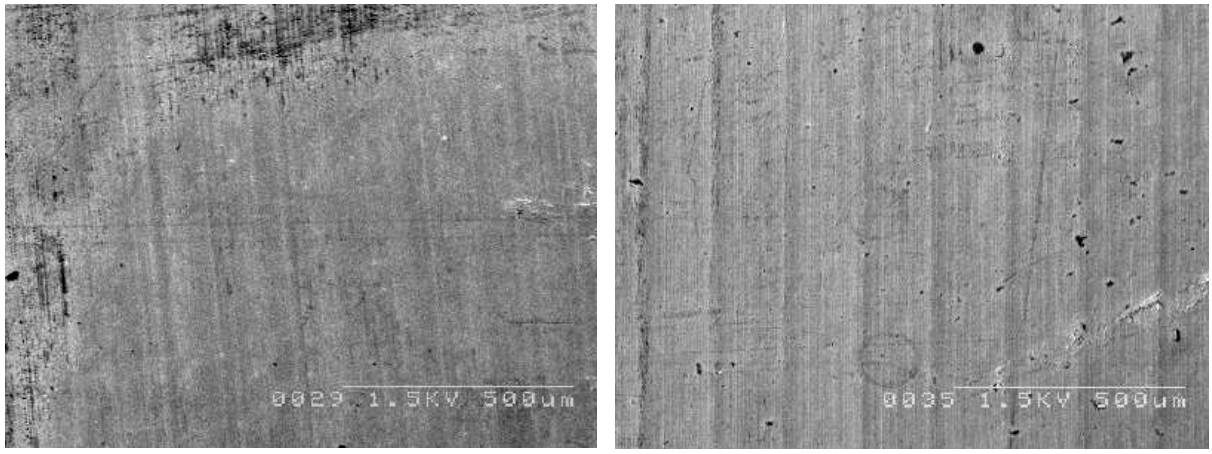

(a) (b)

Figure 4.28 - Surfaces generated after machining with uncoated carbide T1 tool with a coolant pressure of 20.3 MPa at cutting speeds of (a) 120 m min^{-1} and (b) 130 m min^{-1}.

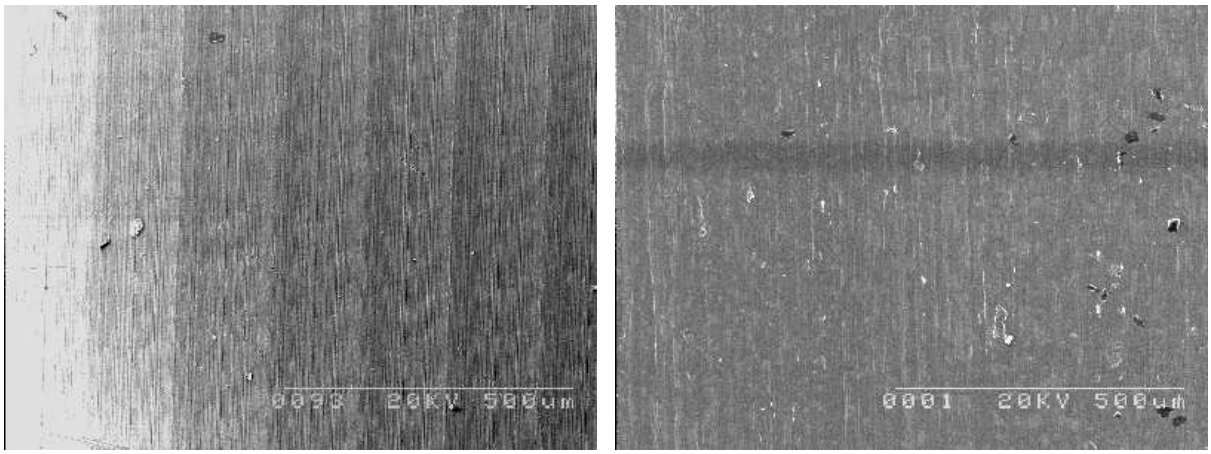

(a) (b)

Figure 4.29 - Surfaces generated after machining with uncoated carbide T1 tool in an argon enriched environment at cutting speeds of (a) 110 m min^{-1} and (b) 120 m min^{-1}.

Figures 4.30 and 4.31 show micrographs of surfaces generated when machining with uncoated carbide (T2) and PVD coated carbide (T3) tool grades under high pressure coolant supplies of 11MPa and 20.3 MPa at a cutting speed of 110 m min^{-1}. There are well-defined uniform feed marks running perpendicular to the direction of relative work-tool motion.

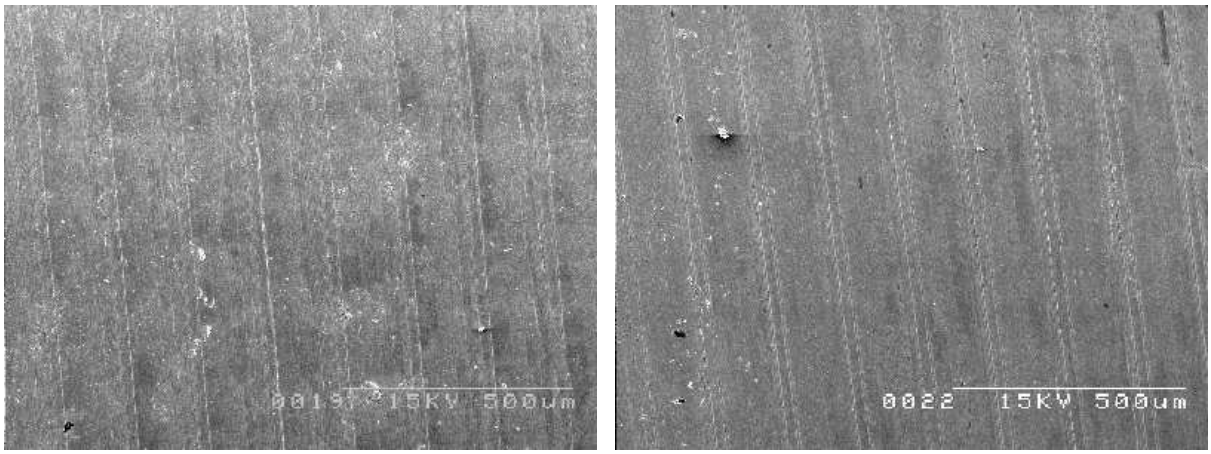

(a) (b)

Figure 4.30 - Surfaces generated after machining with uncoated carbide T2 tool with coolant pressures of (a) 11 MPa and (b) 20.3 MPa at a cutting speed of (a) 110 m min^{-1}.

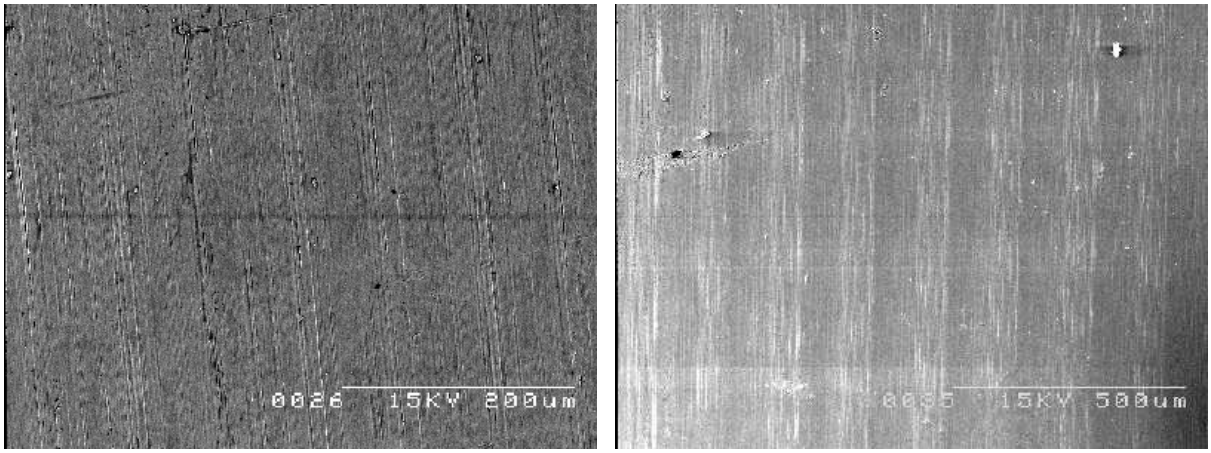

(a) (b)

Figure 4.31 - Surfaces generated after machining with coated carbide T3 tool with coolant pressures of (a) 11 MPa and (b) 20.3 MPa at a cutting speed of 110 m min^{-1}.

Typical surfaces generated when machining with PVD coated carbide (T4) tool grade under various machining environments at a cutting speed of 120 m min^{-1} as shown in Figure 4.32. Well-defined uniform feed marks running perpendicular to the direction of relative work-tool motion with no evidence of plastic flow can be seen. No surface tears and chatter marks were observed after machining Ti-6Al-4V alloy with various cemented carbide tool grades. Generally machining with all the carbide grades under high pressure coolant supplies generated acceptable machined surfaces, conforming to the standard specification established for machined aerospace components (Rolls-Royce CME 5043).

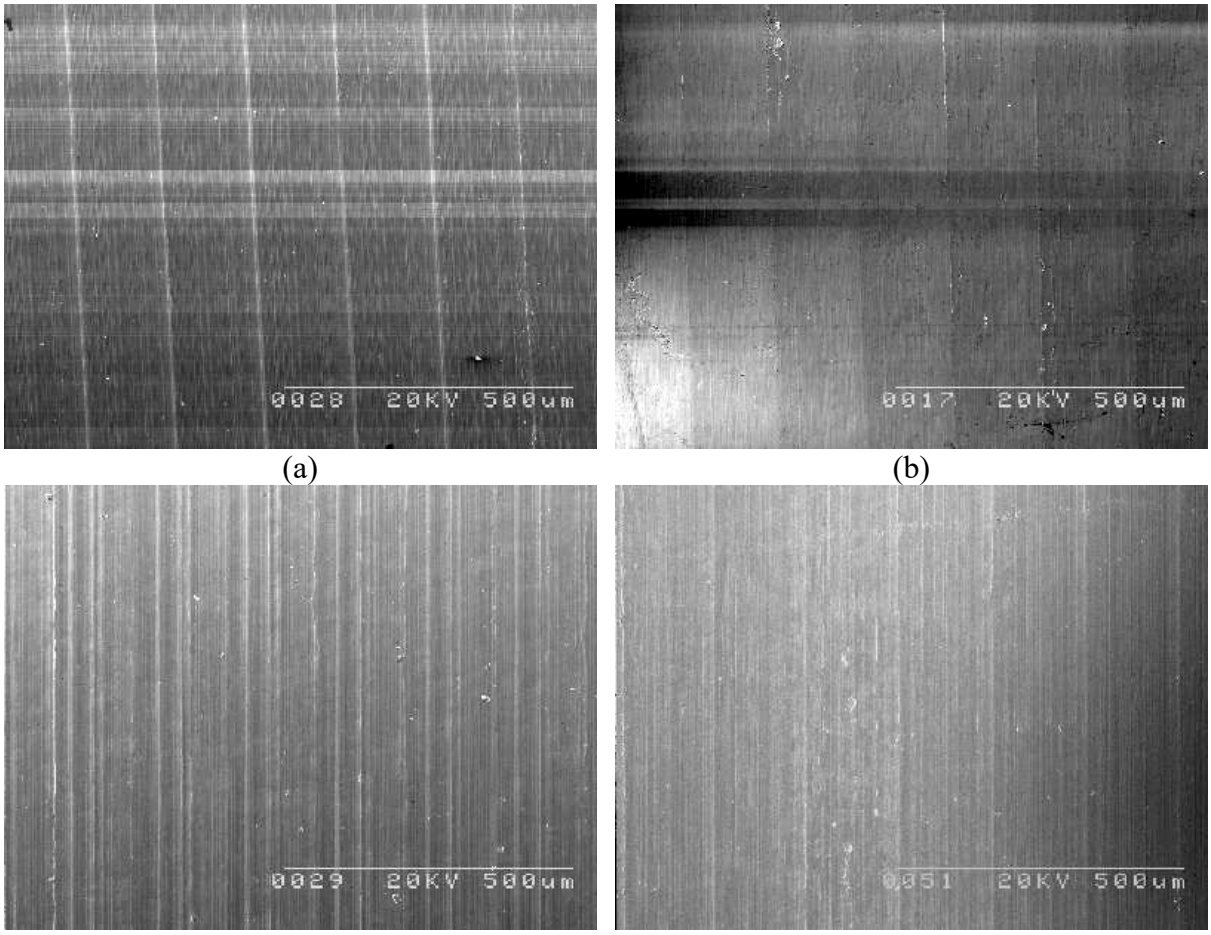

(a) (b)

(c) (d)

Figure 4.32 - Surfaces generated after machining with coated carbide T4 tool with (a) conventional coolant supply, (b) in argon enriched environment, (c) coolant pressure of 11 MPa and (d) 20.3 MPa at a cutting speed of 120 m min^{-1}.

4.2.6 Surface hardness after machining with various carbide tool grades

Figures 4.33-4.42 are plots of the variations of microhardness values recorded from the top of the machined surface up to about 1.5 mm below the machined surface. Note that the range of measured values on the graphs is demarcated by confidence interval (C.I.), represented by the minimum (Min.) and maximum (Max.) Vickers hardness values recorded for Ti-6Al-4V alloy bars prior to machining. This is because the hardness of alloys varies within a range of values. The range (C.I.) is used here instead of the average hardness because it gives a realistic assessment of the material hardness.

Figures 4.33-4.37 are plots of microhardness values of machined surfaces after machining with uncoated carbide T1 tool grade under various machining environments. The plots show relatively low variation in hardness when machining with T1 tool grade with conventional coolant flow at cutting speeds up to 110 m min^{-1} (Figure 4.33). There is, however, evidence of surface hardening beyond the bulk hardness of material at the top surface when machining at speeds in excess of 110 m min^{-1}. Surface hardening up to about 0.4 mm below the machined surfaces of Ti-6Al-4V alloy was observed after machining with uncoated carbide T1 tool grade at a cutting speed of 120 m min^{-1}. Softening of the machined surfaces also occurred, especially, at the higher speed of 130 m min^{-1}. Figure 4.34 shows evidence of softening at the top surface up to about 0.15 below the machined surfaces after machining with T1 tool with a coolant pressure of 7 MPa at speeds of 100 m min^{-1} and 120 m min^{-1}. This figure also shows evidence of surface hardening up to about 0.3 mm below the machined surfaces when machining at a cutting speed of 110 m min^{-1}. Figure 4.35 shows the evidence of softening of machined surfaces after machining with T1 tool with a coolant pressure of 11 MPa at speeds up to 120 m min^{-1}. However, evidence of hardening of the machined surfaces up to about 0.4 mm depth was observed when machining at highest cutting speed of 130 m min^{-1}. Machining with T1 tool grade under the highest coolant pressure of 20.3 MPa gave minimum hardness variation with a uniform distribution of hardness values within the confidence interval of hardness values prior to machining (Figure 4.36). This figure, generally, shows softening of the machined surfaces when machining at all the cutting speeds investigated. Figure 4.37 shows microhardness values of machined surfaces after machining with T1 tool grade in the presence of argon. It can be seen that hardness values are generally distributed within the confidence interval of the hardness values.

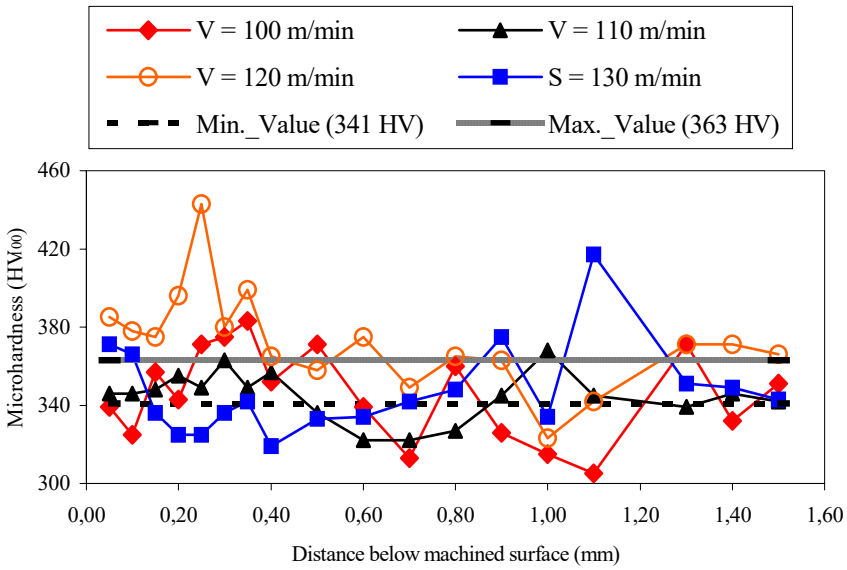

Figure 4.33 - Hardness variation after machining Ti-6Al-4V alloy with uncoated carbide (T1) insert grade with conventional coolant supply.

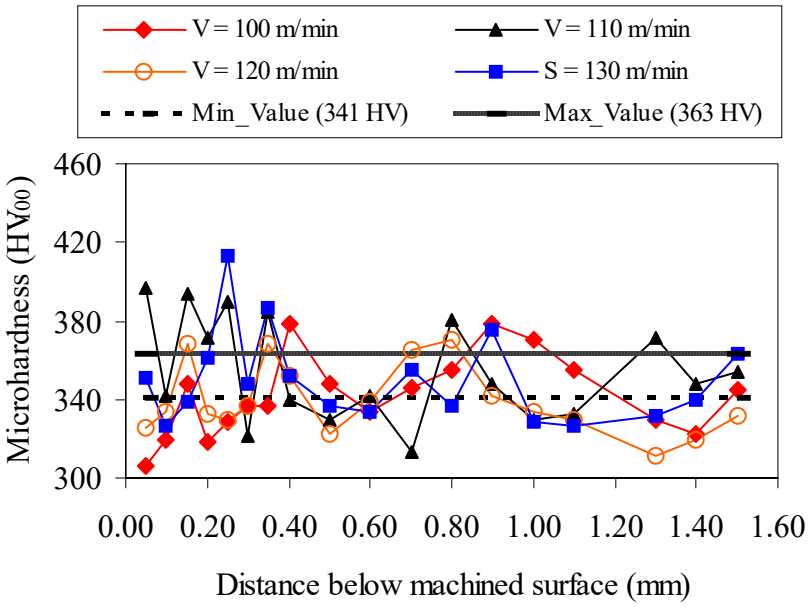

Figure 4.34 - Hardness variation after machining Ti-6Al-4V alloy with uncoated carbide (T1) insert grade with 7 MPa coolant pressure.

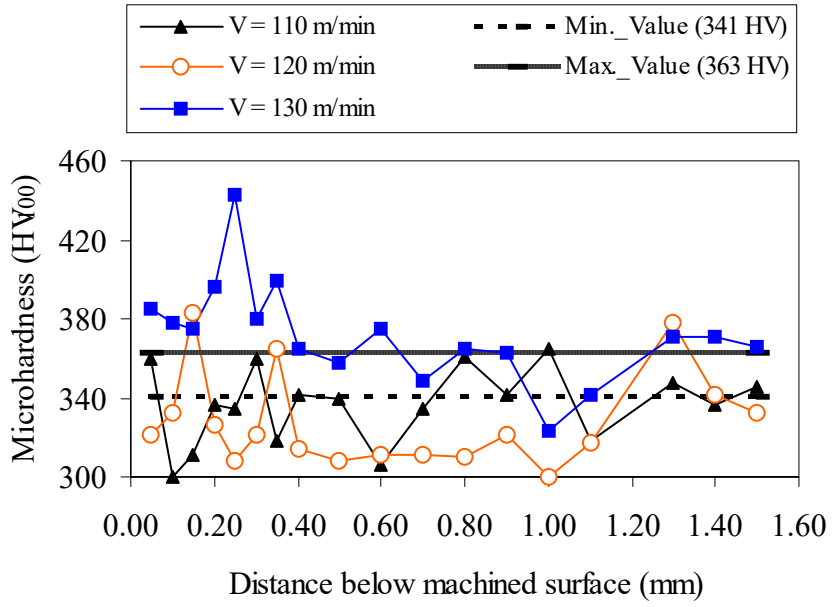

Figure 4.35 - Hardness variation after machining Ti-6Al-4V alloy with uncoated carbide (T1) insert grade with 11MPa coolant pressure.

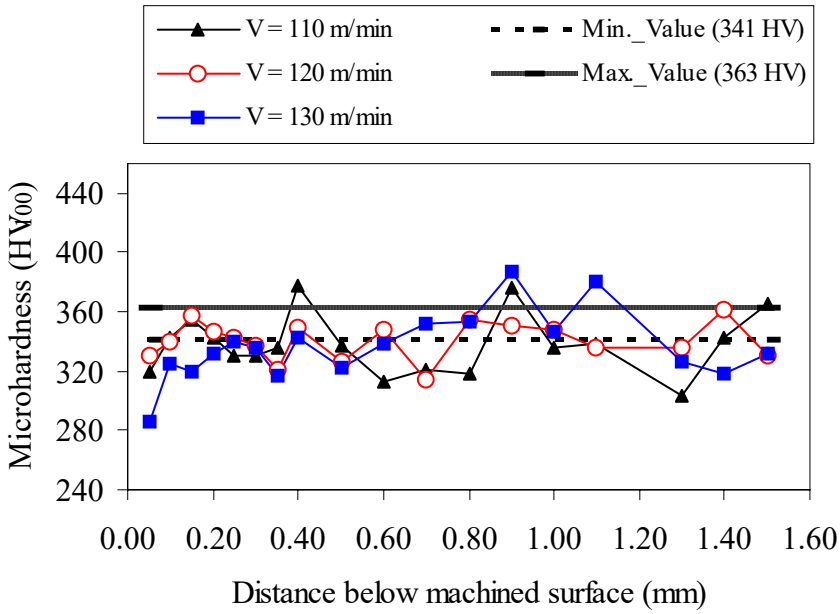

Figure 4.36 - Hardness variation after machining Ti-6Al-4V alloy with uncoated carbide (T1) insert grade under 20.3 MPa coolant pressure.

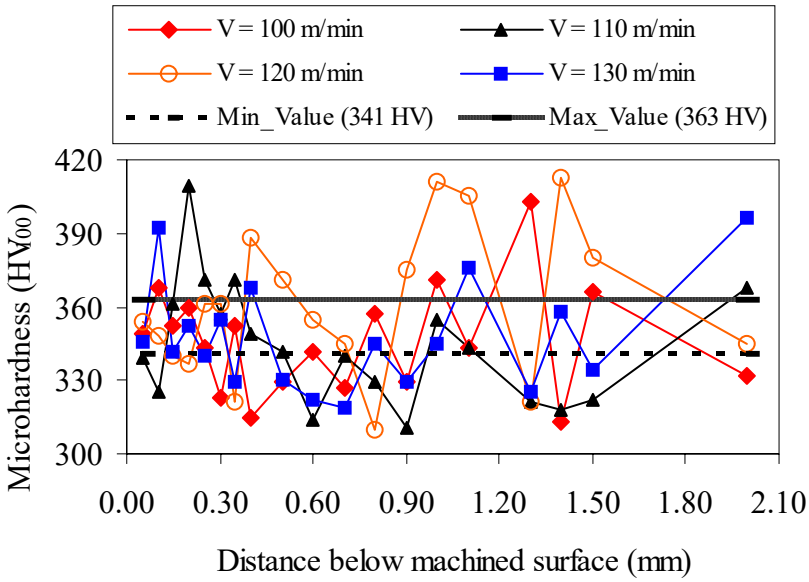

Figure 4.37 - Hardness variation after machining Ti-6Al-4V alloy with uncoated carbide (T1) insert grade in argon-enriched environment.

Figure 4.38 is a plot of the variation of microhardness values recorded at various locations below the machined surfaces after machining with uncoated carbide T2 tool grade using conventional coolant flow and high pressure coolant supplies of 11 MPa and 20.3 MPa. The recorded hardness values are generally distributed within the confidence interval of hardness values of the work material prior to machining. However, Figure 4.38 also shows evidence of surface hardening up to about 0.25 mm below the machined surface when machining with conventional coolant supply at the lowest speed of 100 m min^{-1}. It can also be seen in Figure 4.38 that surface hardness decreased with increasing cutting speed up to about 0.25 mm depth when machining with conventional coolant supply.

Figure 4.39 is a plot of the variation of microhardness values recorded at various locations below the machined surfaces after machining with coated carbide T3 tool grade with conventional coolant flow and high pressure coolant supplies of 11 MPa and 20.3 MPa. It can be seen that the hardness values are uniformly distributed within the confidence interval of the hardness values prior to machining.

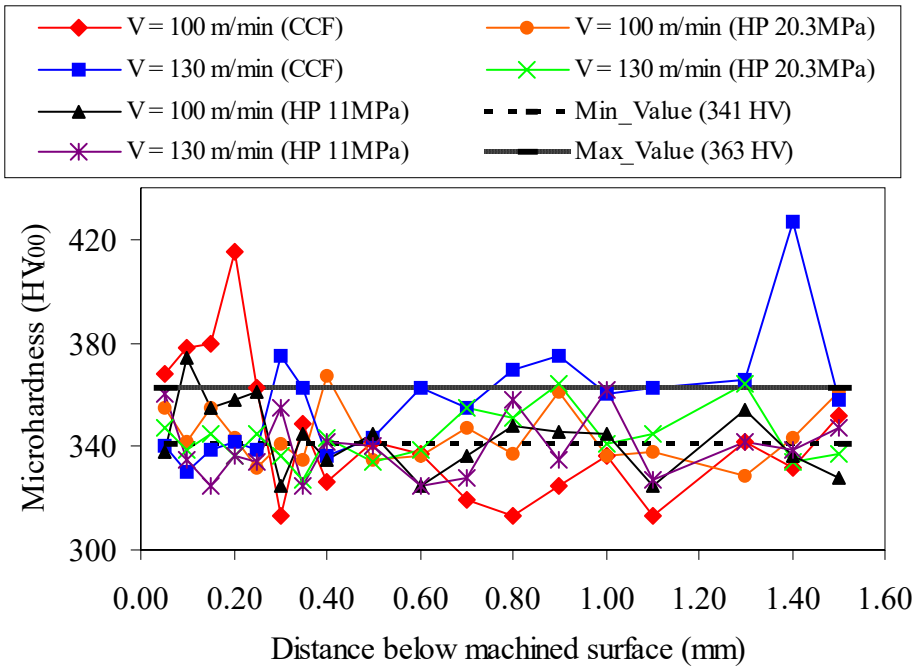

Figure 4.38 - Hardness variation after machining Ti-6Al-4V alloy with uncoated carbide (T2) insert grade under various cutting conditions.

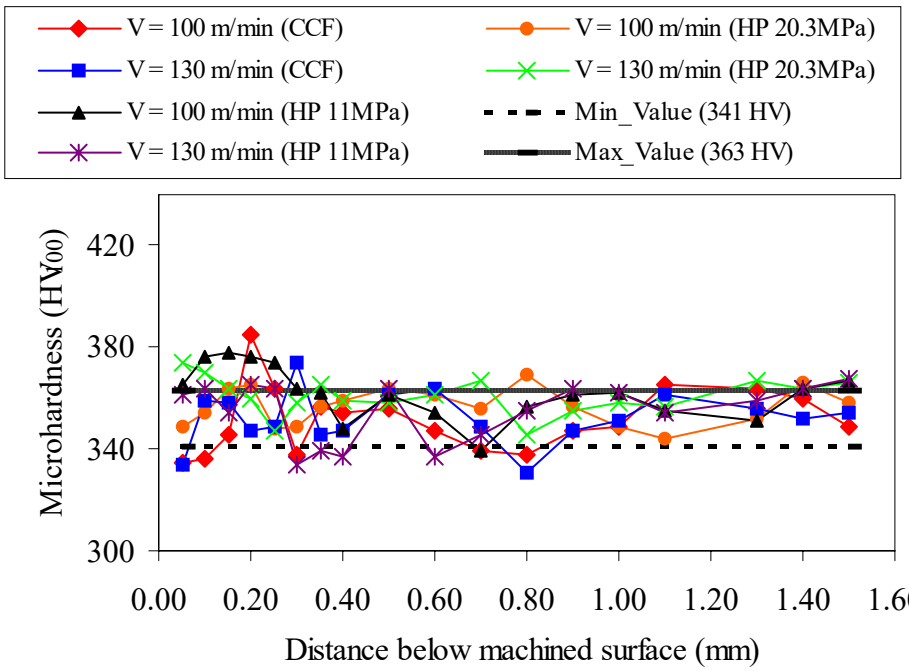

Figure 4.39 - Hardness variation after machining Ti-6Al-4V alloy with coated carbide (T3) insert grade under various cutting conditions.

Figures 4.40-4.42 are plots of microhardness values of machined surfaces after machining with coated carbide T4 tool grade under various machining environments. These figures show that machining with T4 tool grade in all machining environments investigated reduced microhardness of the machined surfaces. This suggests the softening of machined surface up to about 1 mm below the machined surface when machining with conventional coolant flow at all cutting speeds investigated, since all the hardness values recorded are below the minimum hardness values of bulk hardness of the material (Figure 4.40). The least softening depth (235 HV) was recorded when machining at the lowest cutting speed of 100 m min^{-1}. Softening of machined surfaces was also observed when machining under high pressure coolant supplies (Figures 4.41 and 4.42). This softening was more pronounced when machining at the highest cutting speed of 130 m min^{-1}.

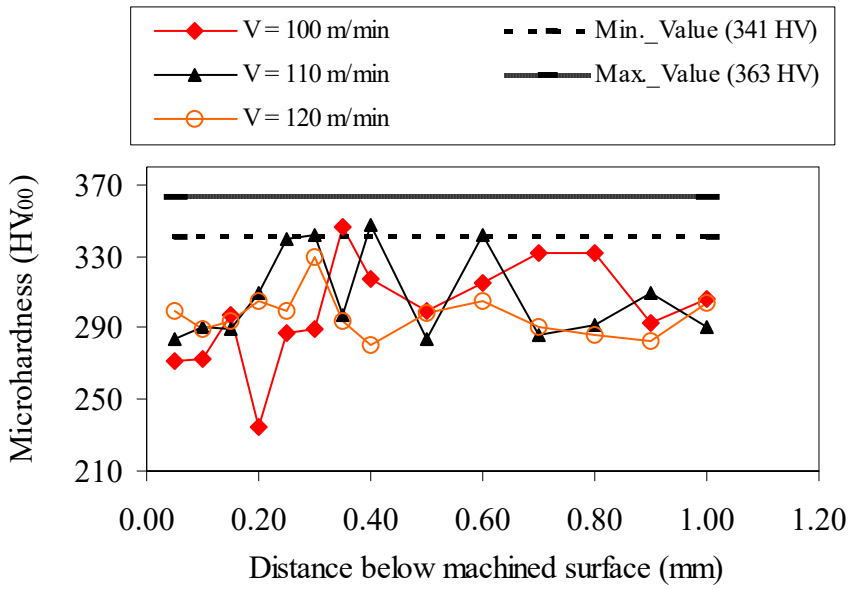

Figure 4.40 - Hardness variation after machining Ti-6Al-4V alloy with coated carbide (T4) insert grade under conventional coolant supply.

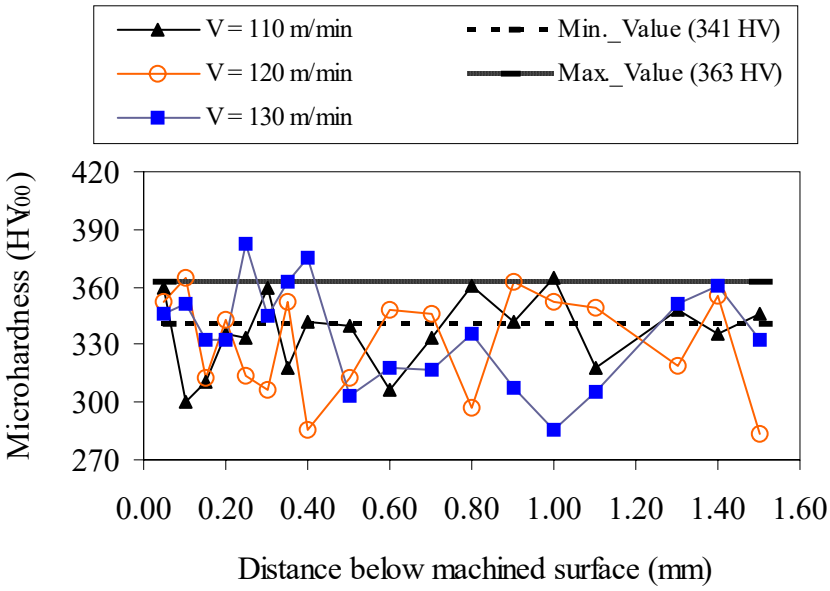

Figure 4.41 - Hardness variation after machining Ti-6Al-4V alloy with coated carbide (T4) insert grade under 11MPa coolant pressure supply.

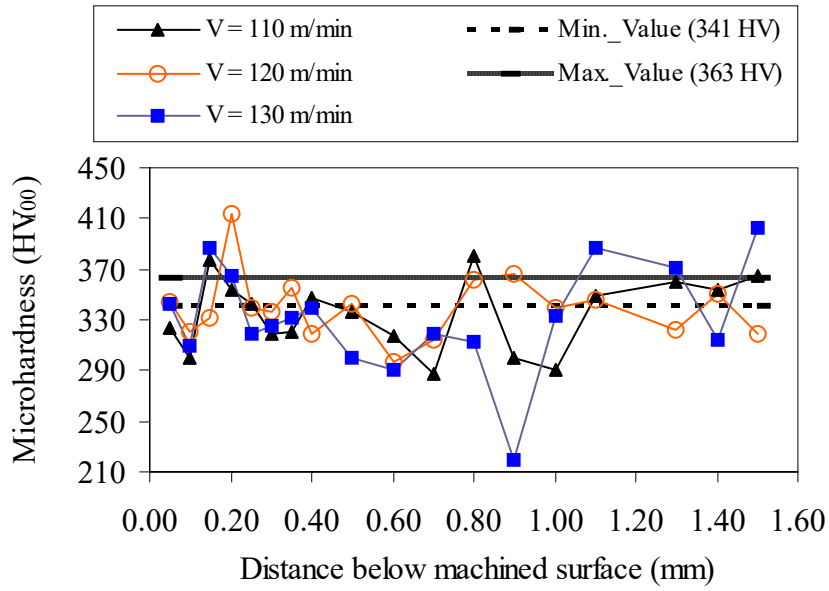

Figure 4.42 - Hardness variation after machining Ti-6Al-4V alloy with coated carbide (T4) insert grade under 20.3 MPa coolant pressure supply.

4.2.7 Subsurface micrographs after machining Ti-6Al-4V alloy with various carbides insert grades

A scanning electron microscope was employed to view etched cross-sections of the machined surfaces in order to detect microstructural alteration and other damages on the machined surfaces. Figures 4.43-4.57 are microstructures of etched machined surfaces of Ti-6Al-4V alloy after machining with different grades of uncoated (T1 and T2) and coated carbide (T3 and T4) inserts under various cutting conditions. All the micrographs exhibit similar characteristics. The well defined grain boundaries are clear evidence that there was no microstructure alteration such as plastic deformation, in the subsurface of machined surfaces.

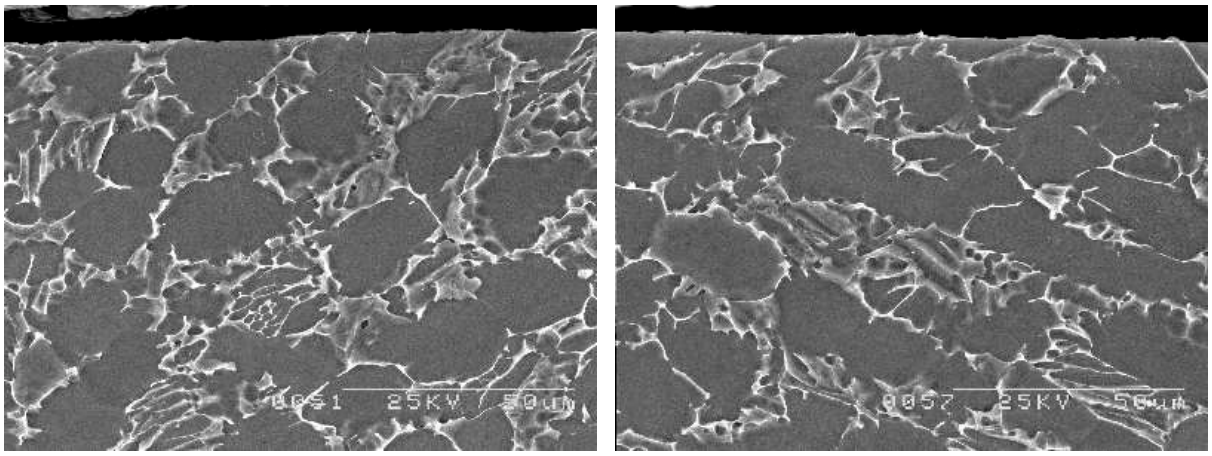

(a) Tool life = 18.2 min (b) Tool life = 8.2 min

Figure 4.43 - Microstructure of Ti-6Al-4V alloy after machining with uncoated carbide T1 insert under conventional coolant supply at cutting speeds of (a) 110 m min^{-1} and (b) 130 m min^{-1}.

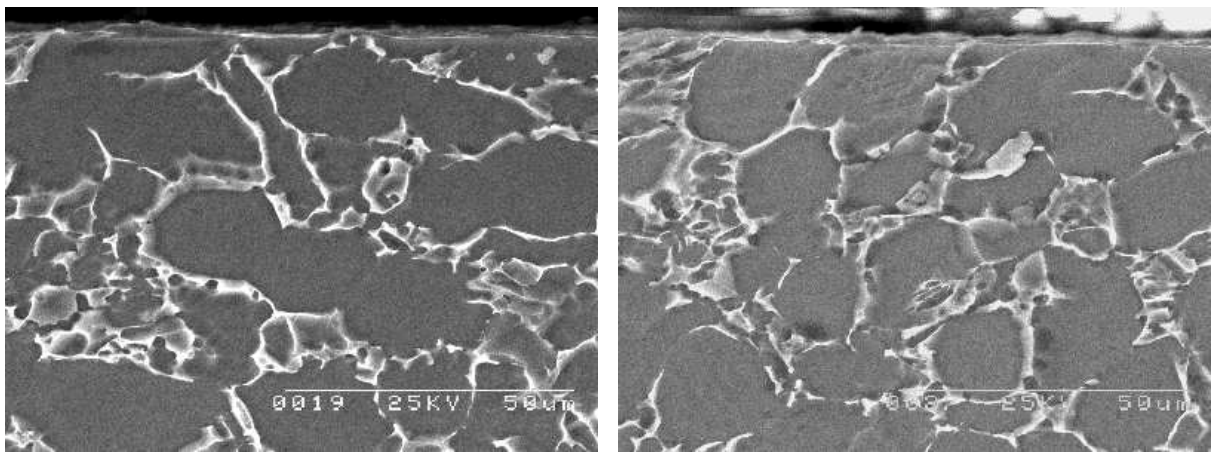

(a) Tool life = 72.8 min (b) Tool life = 17.7 min

Figure 4.44 - Microstructure of Ti-6Al-4V alloy after machining with uncoated carbide T1 insert under a coolant pressure of 7 MPa at cutting speeds of (a) 100 m min^{-1} and (b) 120 m min^{-1}.

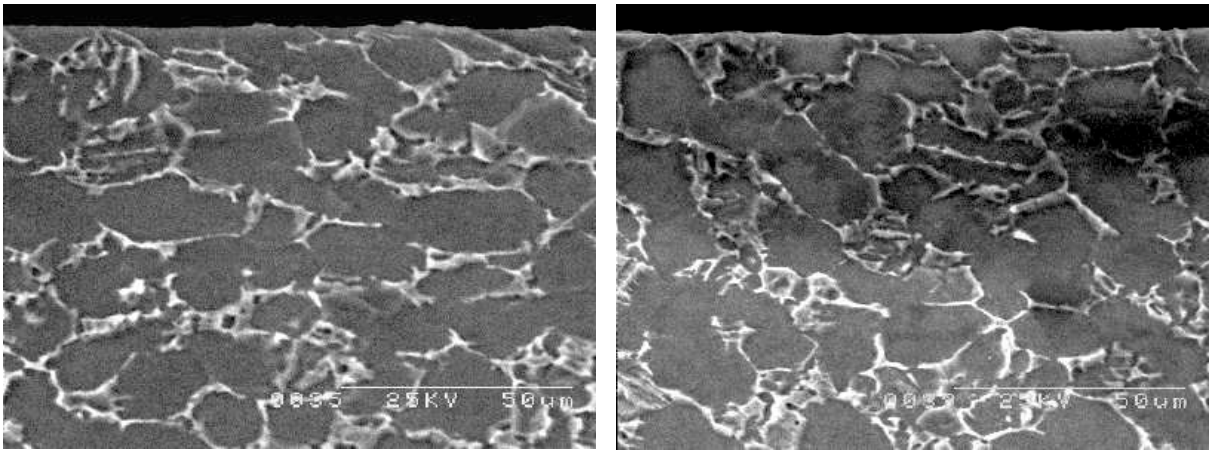

(a) Tool life = 29.7 min (b) Tool life = 23.2 min

Figure 4.45 - Microstructure of Ti-6Al-4V alloy after machining with uncoated carbide T1 insert under a coolant pressure of 11 MPa at cutting speeds of (a) 110 m min^{-1} and (b) 120 m min^{-1}.

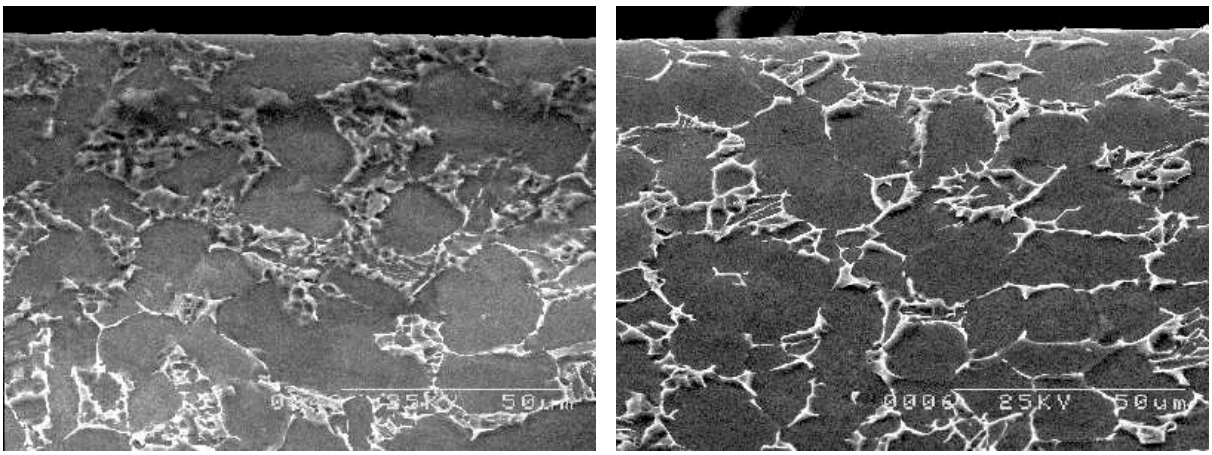

(a) Tool life = 24.2 min (b) Tool life = 15.1 min

Figure 4.46 - Microstructure of Ti-6Al-4V alloy after machining with uncoated carbide T1 insert under a coolant pressure of 20.3 MPa at cutting speeds of (a) 120 m min^{-1} and (b) 130 m min^{-1}.

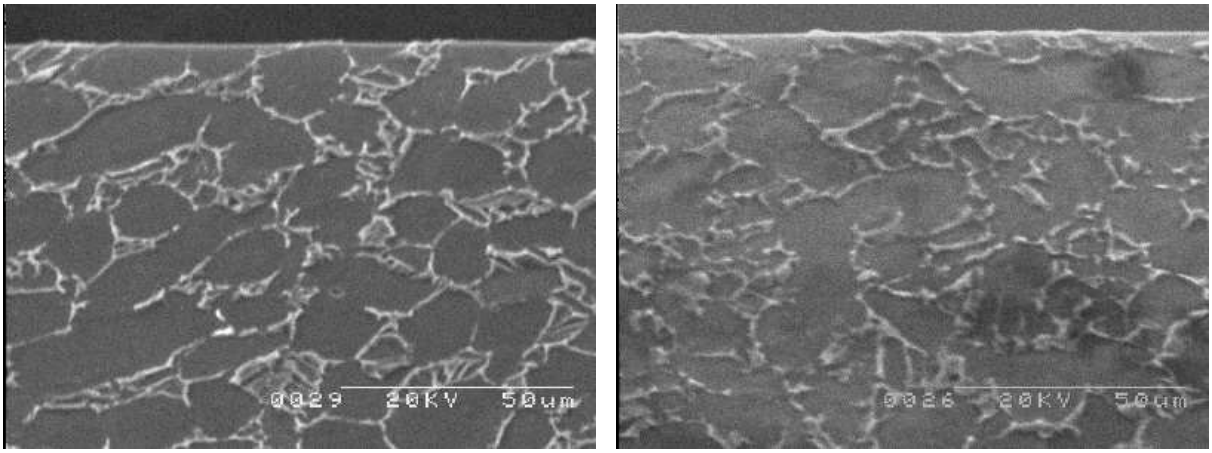

(a) Tool life = 9.4 min (b) Tool life = 6.3 min

Figure 4.47 - Microstructure of Ti-6Al-4V alloy after machining with uncoated carbide T1 inserts in an argon enriched environment at cutting speeds of (a) 110 m min^{-1} and (b) 120 m min^{-1}.

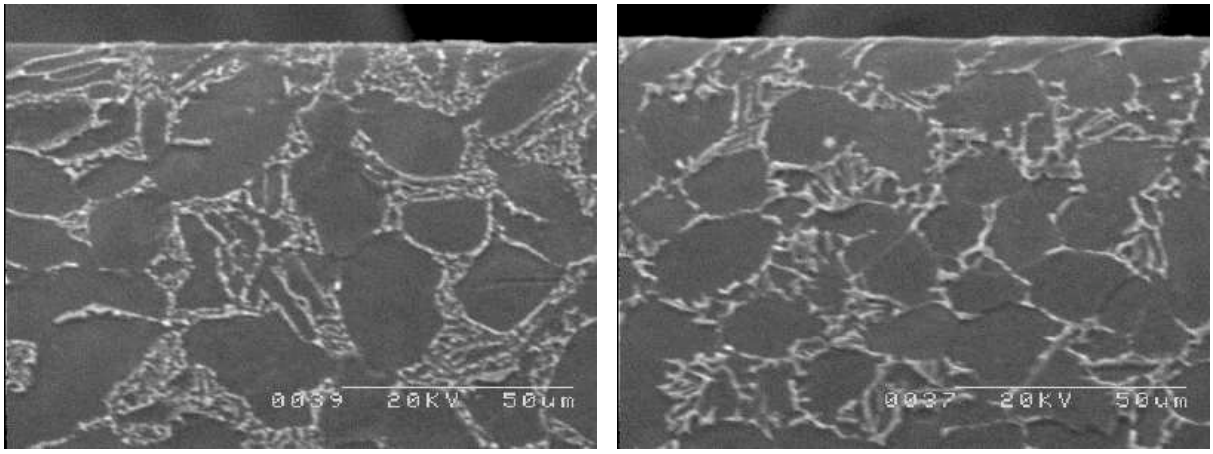

(a) Tool life = 8.3 min (b) Tool life = 5.0 min

Figure 4.48 - Microstructure of Ti-6Al-4V alloy after machining with uncoated carbide T2 inserts with conventional coolant supply at a cutting speed of (a) 110 m min^{-1} and (b) 130 m min^{-1}.

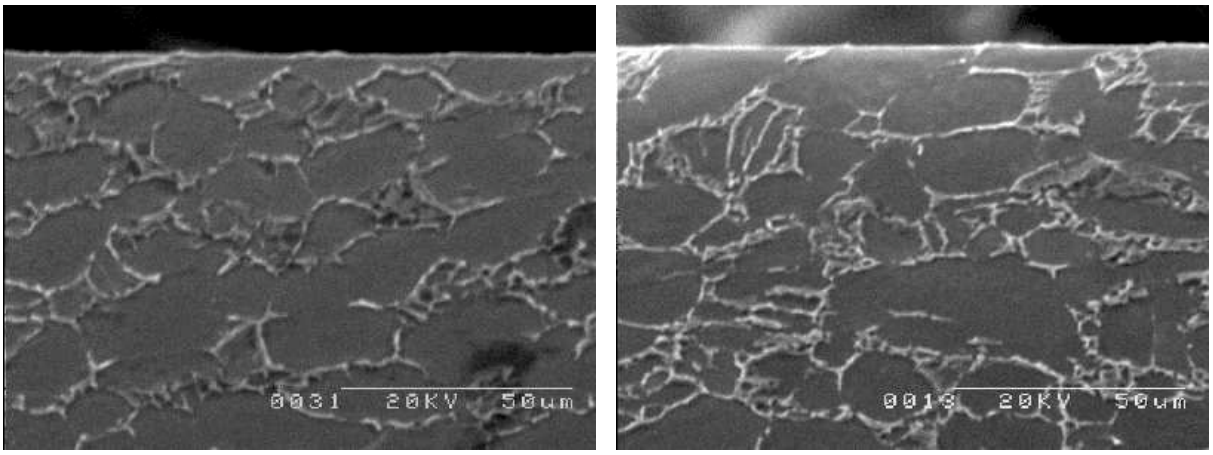

(a) Tool life = 16.8 min (b) Tool life = 11.9 min

Figure 4.49 - Microstructure of Ti-6Al-4V alloy after machining with uncoated carbide T2 inserts with a coolant pressure of 11 MPa at cutting speeds of (a) 110 m min^{-1} and (b) 130 m min^{-1}.

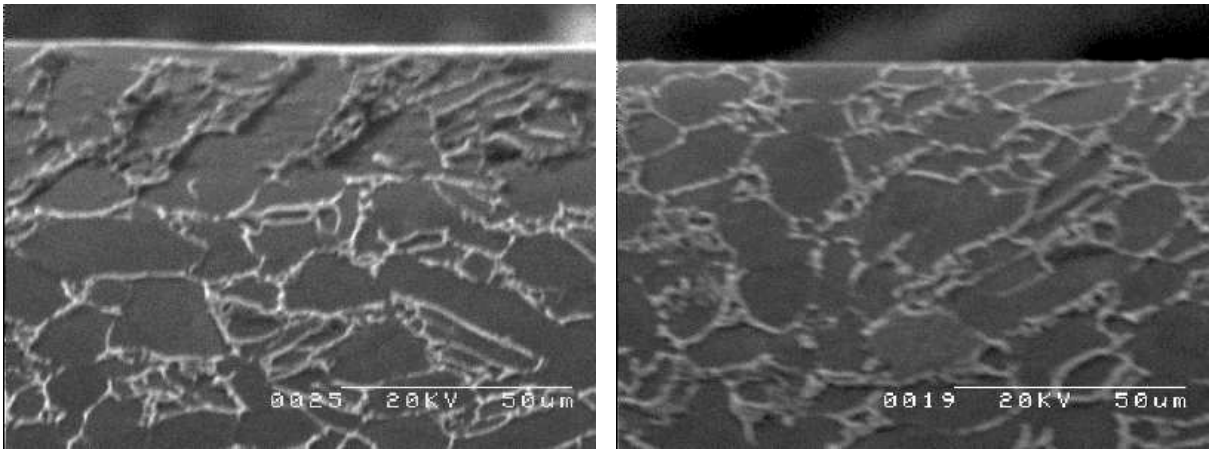

(a) Tool life = 19.4 min (b) Tool life = 11.4 min

Figure 4.50 - Microstructure of Ti-6Al-4V alloy after machining with uncoated carbide T2 tools with a coolant pressure of 20.3 MPa at cutting speeds of (a) 110 m min^{-1} and (b) 130 m min^{-1}.

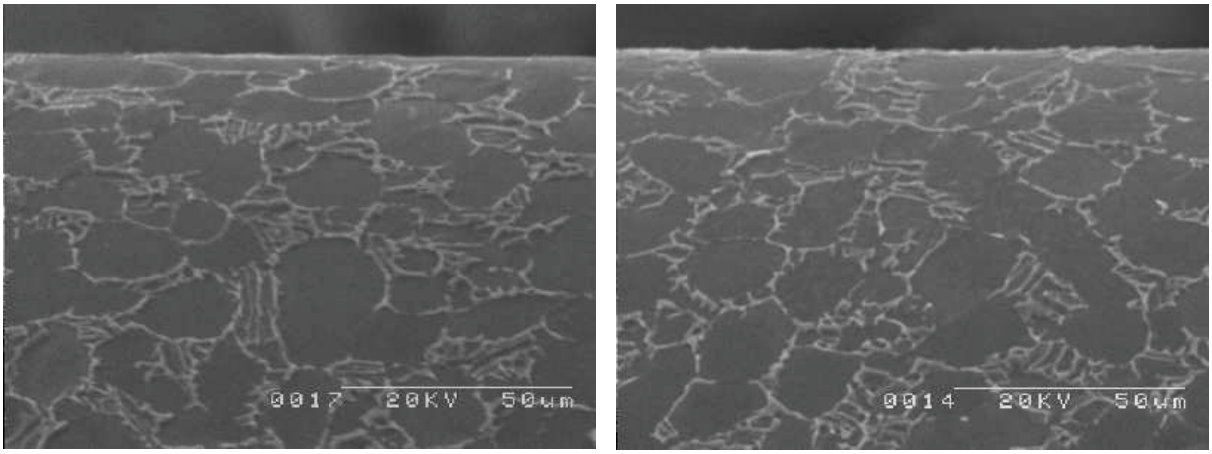

(a) Tool life = 9.2 min (b) Tool life = 3.8 min

Figure 4.51 - Microstructure of Ti-6Al-4V alloy after machining with coated carbide T3 inserts with conventional coolant supply at a cutting speed of (a) 110 m min^{-1} and (b) 130 m min^{-1}.

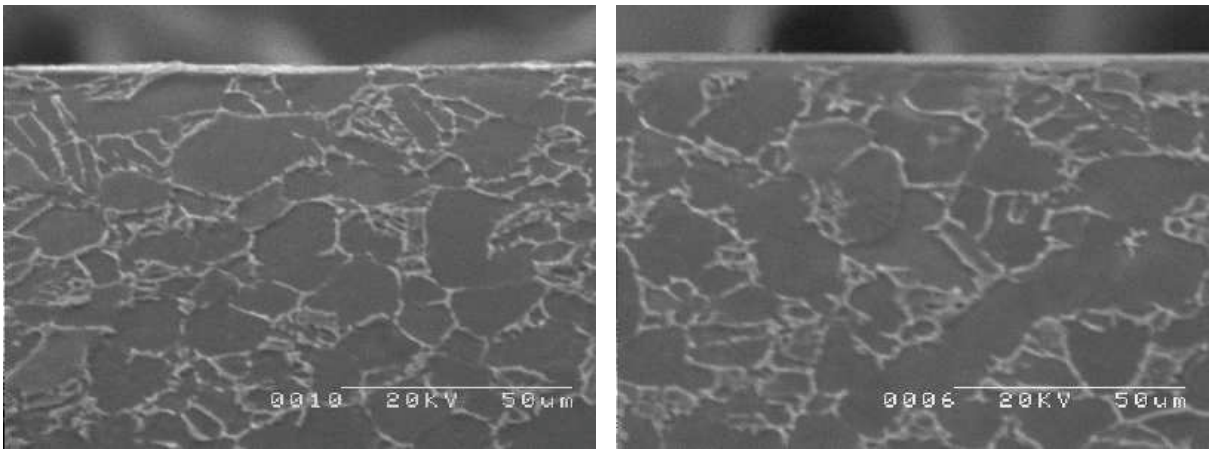

(a) Tool life = 16.2 min (b) Tool life = 11.6 min

Figure 4.52 - Microstructure of Ti-6Al-4V alloy after machining with coated carbide T3 tools with a coolant pressure of 11 MPa at cutting speeds of (a) 110 m min^{-1} and (b) 130 m min^{-1}.

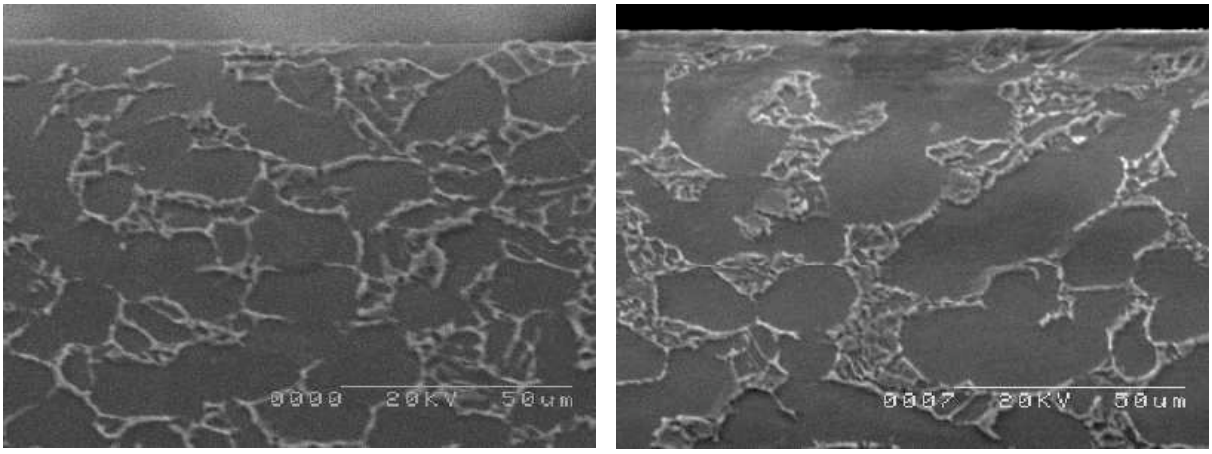

(a) Tool life = 19.4 min (b) Tool life = 11.4 min

Figure 4.53 - Microstructure of Ti-6Al-4V alloy after machining with coated carbide T3 tools with a coolant pressure of 20.3 MPa at cutting speeds of (a) 110 m min^{-1} and (b) 130 m min^{-1}.

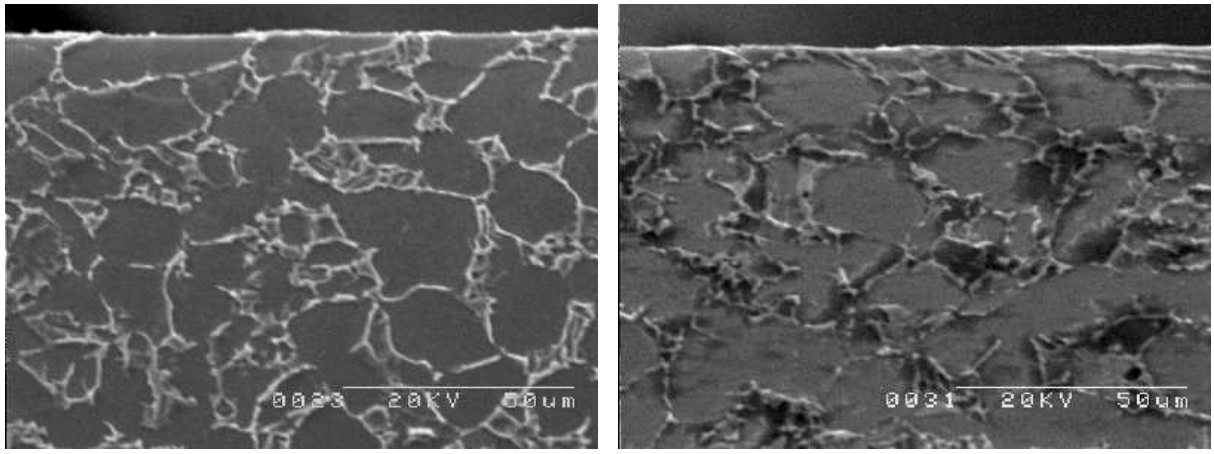

(a) Tool life = 25.5 min (b) Tool life = 7.9 min

Figure 4.54 - Microstructure of Ti-6Al-4V alloy after machining with coated carbide T4 tools with conventional coolant supply at cutting speeds of (a) 100 m min^{-1} and (b) 120 m min^{-1}.

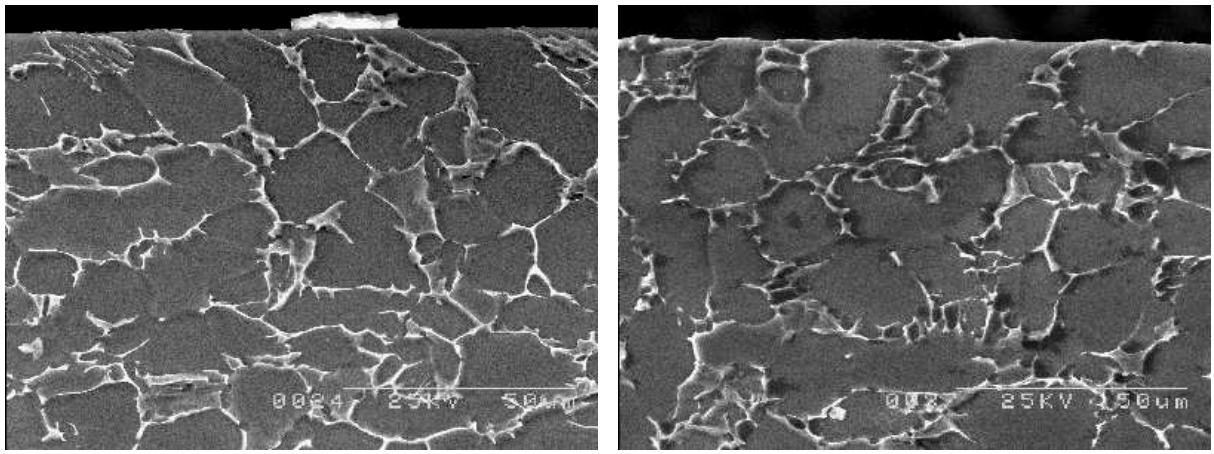

(a) Tool life = 29.4 min (b) Tool life = 18.6 min

Figure 4.55 - Microstructure of Ti-6Al-4V alloy after machining with coated carbide T4 tools with a coolant pressure of 11 MPa at cutting speeds of (a) 120 m min^{-1} and (b) 130 m min^{-1}.

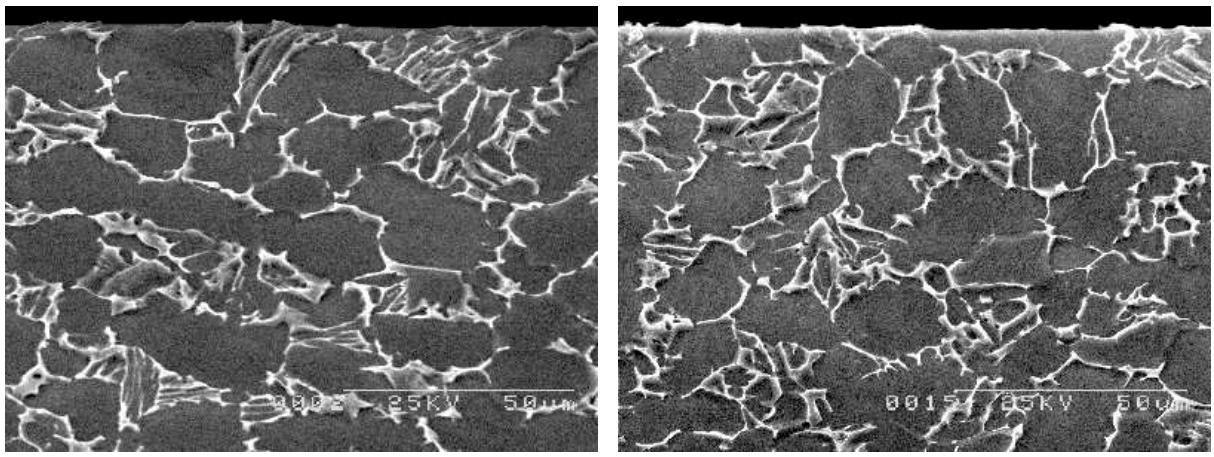

(a) Tool life = 50.2 min (b) Tool life = 17.3 min

Figure 4.56 - Microstructure of Ti-6Al-4V alloy after machining with coated carbide T4 tools with a coolant pressure of 20.3 MPa at cutting speeds of (a) 110 m min^{-1} and (b) 130 m min^{-1}.

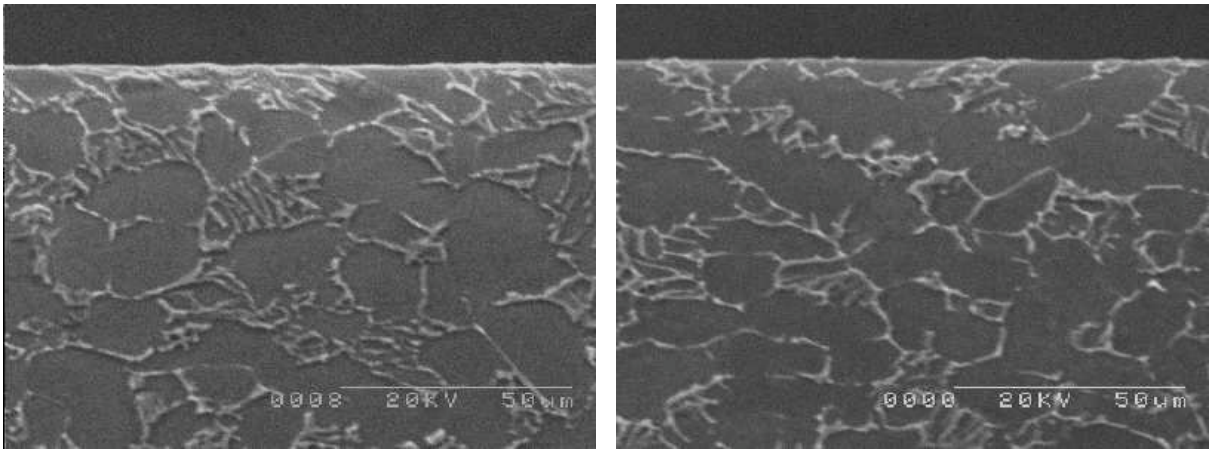

(a) Tool life = 4.3 min (b) Tool life = 3.6 min

Figure 4.57 - Microstructure of Ti-6Al-4V alloy after machining with coated carbide T4 tools in an argon enriched environment at cutting speeds of (a) 120 m min^{-1} and (b) 130 m min^{-1}.

4.2.8 Chips shapes

Figure 4.58 contains samples of chips generated when machining with different grades of uncoated and coated carbide tools (T1,T2,T3 and T4) under various machining conditions. Generally chips produced with all the tools with conventional coolant flow are snarled shapes (Figures 4.58 (a), (b), (f), (h) and (j)). Machining with T1 insert with conventional coolant flow produced long continuous tubular type chips, unlike the small segmented chips produced when machining under high pressure coolant supplies of 11 MPa and 20.3 MPa (Figures 4.58 (d) and (e)). Machining with T1 insert with a coolant pressure of 7 MPa and with T2 insert with high pressure coolant of 11 MPa produced either segmented or snarled type chips. The nature of the chips produced with higher pressure coolant supplies is markedly different from that obtained with conventional coolant flow, as illustrated in Figure 4.58 (c) and (g). Segmented type chips were produced when machining with T4 tool grade under high coolant pressure supplies, similar to those produced with T1 tool grade.

(a) T1 (conventional)
V = 110 m min^{-1}

(b) T1 (argon)
V = 110 m min^{-1}

(c) T1 (7 MPa)
V = 110 m min^{-1}

(d) T1 (11 MPa)
V = 110 m min^{-1}

(e) T1 (20.3 MPa)
V = 120 m min^{-1}

(f) T2 (conventional)
V = 110 m min^{-1}

(g) T2 (HP 11MPa)
V = 110 m min^{-1}

(h) T3 (conventional)
V = 110 m min^{-1}

(i) T3 (20.3 MPa)
V = 110 m min^{-1}

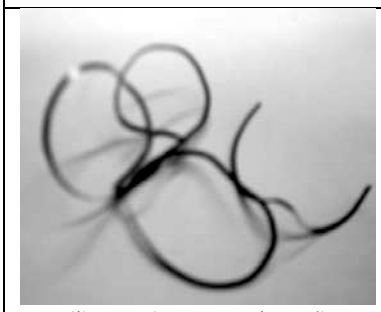

(j) T4 (conventional)
V = 110 m min^{-1}

(k) T4 (argon)
V = 110 m min^{-1}

11 MPa

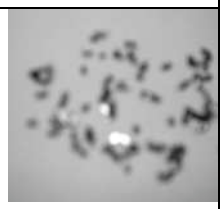

20.3 MPa

(l) T4
V = 110 m min^{-1}

Figure 4.58 - Chips generated when machining Ti-6Al-4V alloy with different carbide tool grades under various cutting conditions: (a) continuous tubular chip; (b), (f), (h) and (k) continuous and snarled chips, (c), (g) and (i) partially segmented chips, (d), (e) and (l) segmented C-shaped chips.

4.3 Machining of Ti-6Al-4V alloy with different grades of PCD tools under various coolant supply pressures

4.3.1. Tool Life

Figure 4.59 shows tool life (nose wear, VC ≥ 0.3 mm) recorded when machining Ti-6Al-4V alloy with the standard (T5) and the multi-modal (T6) grades of PCD inserts at various cutting speeds and at various coolant supply pressures investigated. Tool life of all the PCD insert grades decreased with increase cutting speed in all machining environments investigated due to a reduction in tool-chip and tool-workpiece contact length and the consequent increase in both normal and shear stresses at the tool tip (GORCZYCA, 1987). Lower tool life was recorded when machining with both grades of PCD inserts under conventional coolant flow. Tool life generally increased with increasing in coolant pressure when machining with the larger grain size (T5) grade, unlike lower tool life recorded when machining with the smaller grain size (T6) grade at the highest pressure of 20.3 MPa relative to 11 MPa. Note that high pressure coolant supplies were employed at cutting speeds in excess of 160 m min^{-1}. However, machining with T5 PCD grade with 7MPa coolant pressure gave longer tool life than with conventional coolant flow in all the cutting speeds investigated and with 11 MPa coolant pressure at cutting speeds of 175 and 230 m min^{-1}. This is illustrated in Table 4.2, which provides a summary of the percentage improvement in tool life when machining with T5 and T6 insert grades under various coolant pressures relative to conventional coolant supply. Encouraging tool life of 115 and 97 minutes was recorded when machining with the larger grain size (T5) tool grade at a cutting speed of 175 m min^{-1} under coolant supply pressures of 20.3 MPa and 7 MPa, respectively. These represent over 20 and 17 folds improvement in tool life, respectively, relative to conventional coolant flow. The highest gain in tool life was achieved when machining under most aggressive conditions of 230 m min^{-1} with 7 MPa and 20.3 MPa coolant supplies when over 20 fold improvement in tool life was recorded (Table 4.2). Additionally, improvement in tool life using T5 insert with 11 MPa coolant supply increased with increase in cutting speed.

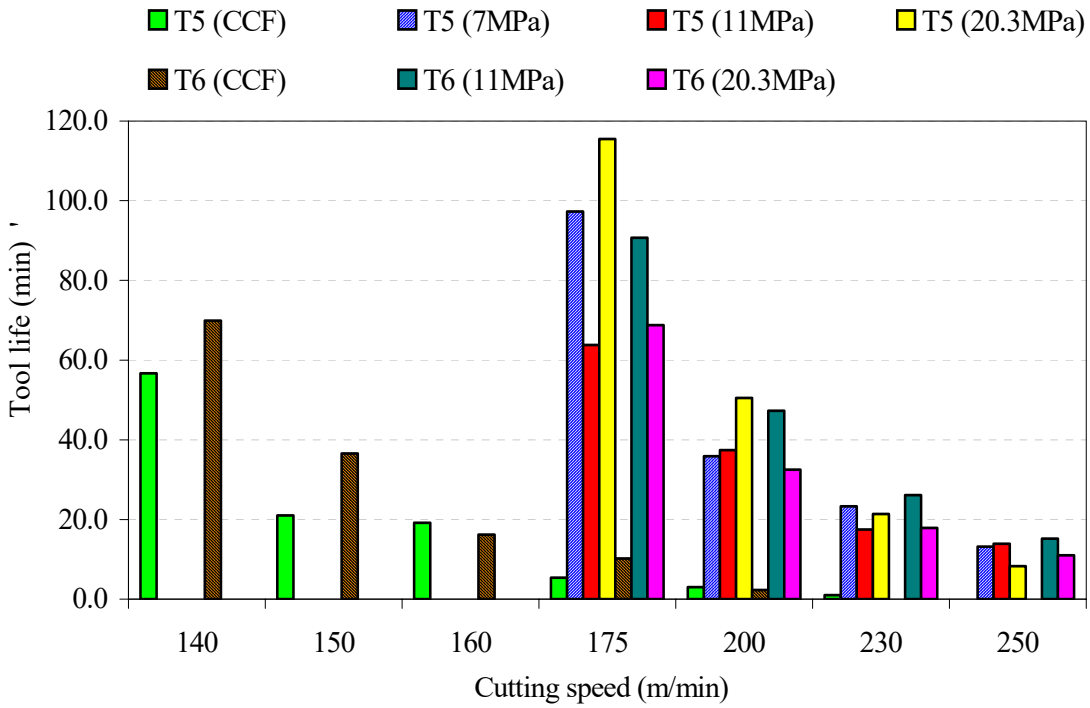

Figure 4.59 - Tool life (nose wear, VC ≥ 0.3 mm) recorded when machining Ti-6Al-4V alloy with PCD-STD (T5) and PCD MM (T6) tool grades with conventional coolant flow (CCF) and high coolant pressures of 7 MPa, 11 MPa and 20.3 MPa at various cutting speed conditions.

Table 4.2 - Percentage improvement in tool life relative to conventional coolant supply after machining Ti-6Al-4V alloy with PCD inserts (STD and MM grades).

Tool	Speed ($m\ min^{-1}$)	Coolant Pressure (MPa)		
		7	11	20.3
T5	175	1701.8	1081.5	2038.9
	200	1096.7	1146.7	1583.3
	230	2230	1650	2040
T6	175	.	879.2	574.5
	200	.	1956.5	1313

It can be also seen from Figure 4.59 that smaller grain size (T6) tool grade exhibited superior performance, in terms of tool life, than T5 tool grade when machining with

conventional coolant flow and at a high pressure coolant supply of 11 MPa at cutting speeds up to 175 m min^{-1} and 250 m min^{-1}, respectively. Over 74% improvement in tool life was achieved with T6 tool grade at a speed of 150 m min^{-1} with conventional coolant flow relative to T5 tool. Over 42% and 26% improvement in tool life were achieved when machining with T6 tool grade at speeds of 175 and 200 m min^{-1} under 11MPa coolant supply compared with T5 insert. Higher tool lives were recorded when machining with T5 tool grade using the highest pressure coolant of 20.3 MPa than with pressure of 11 MPa at cutting speeds up to 230 m min^{-1}. Up to 20 and 13 fold improvement in tool life were recorded when machining with T6 insert under 11 MPa and 20.3 MPa coolant supplies, respectively, relative to conventional coolant flow at a speed of 200 m min^{-1} (Figure 4.59). Machining at a lower speed of 175 m min^{-1} with T6 insert grade under 11 MPa and 20.3 MPa coolant supplies, respectively, gave only about 9 and 6 fold improvement relative to conventional coolant flow. From these results it is clear that coolant pressure has a significant effect on tool wear pattern and hence recorded tool life when machining Ti-6Al-4V alloy with PCD tools under finishing conditions. Additionally, the performance of PCD tools depends on the cutting speed employed. Machining with PCD (T5) tool grade at a speed of 140 m min^{-1} under conventional coolant flow gave up to 6 folds improvement in tool life relative to uncoated carbide (T1) insert after machining at a cutting speed of 130 m min^{-1} (Figure 4.2) and over 10 fold improvement when machining in an argon enriched environment.

4.3.2 Tool wear when machining Ti-6Al-4V alloy with different grades of PCD tools

Flank wear and nose wear are typical wear patterns observed when machining Ti-6Al-4V alloy with PCD inserts. Flank wear rate is generally lower than the nose wear rate, hence nose wear was the predominant failure mode in all the cutting conditions investigated. Figure 4.60 shows typical nose wear rate curves when machining Ti-6Al-4V alloy with T5 and T6 grades of PCD inserts under conventional coolant flow and various coolant pressure supplies. There was a steady increase in nose wear with increasing cutting speed when machining with PCD tools under finishing conditions. Figure 4.60 also shows that there was negligible difference in nose wear rate when machining with both T5 and T6 insert grades at the coolant pressures investigated at higher cutting speeds up to 250 m min^{-1}.

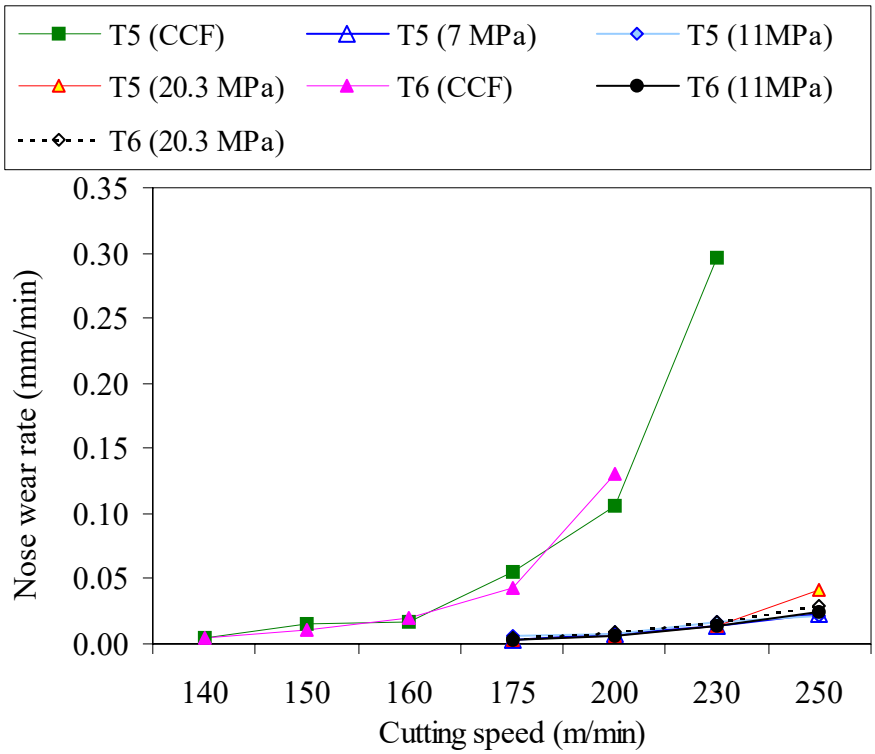

Figure 4.60 - Nose wear rate when machining Ti-6Al-4V alloy with PCD inserts with conventional coolant flow and high coolant pressures of 7 MPa, 11 MPa and 20.3 MPa at various cutting speed conditions.

Nose wear rates increased with prolong machining using both PCD insert grades under all coolant supply pressures employed (Figure 4.61). At the initial stages of cutting, nose wear were generally uniform when machining under high coolant pressures. Further machining rapidly increased wear land. The curves in Figure 4.61 also shows that more severe nose wear was recorded when machining with larger grain size (T5) insert grade under conventional coolant flow unlike the very low, uniform and gradual nose wear rate recorded when machining at the highest pressure coolant supply of 20.3 MPa. Machining with 11 MPa coolant supply pressure, however, gave higher nose wear than with 7 MPa pressure (Figure 4.61). Uniform nose wear with prolong machining, up to 60 min, was observed when machining under 11 MPa pressure. This is increased rapidly after 60 min cutting time until the end of tool life (64 min). Figure 4.61 also shows that higher nose wear occurred when machining with the T5 grade at cutting speed of 175 m min^{-1} under conventional coolant flow relative to the smaller grain size (T6) insert. T5 insert, however, outperformed T6 tool grade in terms of lower nose wear with prolong machining at high coolant pressures.

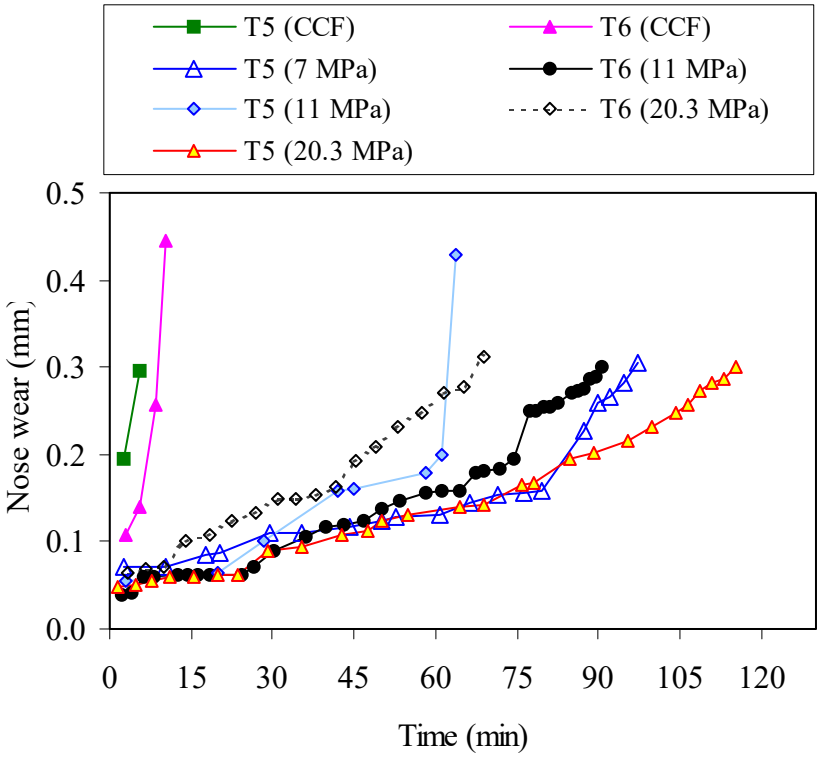

Figure 4.61 - Nose wear when finish machining with PCD-STD (T5) and PCD-MM inserts grades (T6) at a cutting speed of 175 m $m^{-1.}$

Figures 4.62–4.68 show worn PCD tools after finish turning of Ti-6Al-4V alloy at various machining conditions. Figures 4.62 (a) and (b) show the worn cutting edges of a T5 insert after machining at cutting speeds of 140 m min^{-1} and 200 m min^{-1}, respectively, under conventional coolant supply. A uniform nose wear, spreading along the flank face can be observed. Although there was the absence of a well-defined built-up-edge on the worn inserts, the presence of an adherent interfacial layer (adhesion of the workpiece material) on the rake and flank faces of worn T5 and T6 inserts when machining mainly with conventional coolant flow was observed (Figures 4.62). Significant crater wear was observed on both grades of PCD tools when machining with high pressure coolant supplies (Figures 4.63, 4.67 and 4.68). The crater wear usually occurs very close to the cutting edge and joined the notched region at the end of the depth of cut region when machining with T5 insert with 7MPa and 11 MPa pressures at a cutting speed of 175 m min^{-1} (Figures 4.63 (a) and 4.64 (a)). Adhesion of work material can be seen on both the rake and flank faces of the worn T5 insert grade after machining with 7MPa coolant pressure at higher speeds of 175 and 200 m min^{-1} (Figure 4.63 (a) and (b)). Evidence of notching at the depth of cut region can also be seen on the worn T6 insert after machining at a speed of 175 m min^{-1} with conventional coolant flow (Figure 4.66).

In addition to the pronounced crater wear, plucking of PCD tool particles was observed after machining with higher coolant pressures. This process consists of small holes or pockets on the worn tool surface due to mechanical removal of tiny particles from the surface. This process tend to be accelerated at higher coolant pressures and is capable of removing any loose tool material from the rake face with the potential to erode the brittle PCD tool material, thereby exhibiting the characteristic rough texture as illustrated in Figures 4.63-4.68.

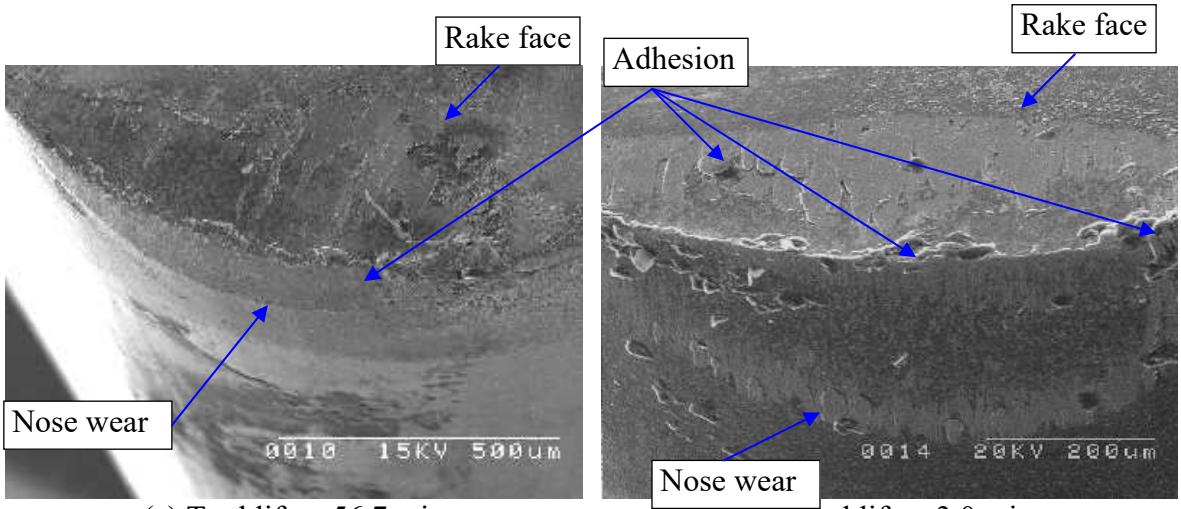

(a) Tool life = 56.7 min (b) Tool life = 3.0 min

Figure 4.62 - Wear observed on T5 insert after machining Ti-6Al-4V alloy with conventional coolant supply at a speed of (a) 140 m min^{-1} and (b) 200 m min^{-1}.

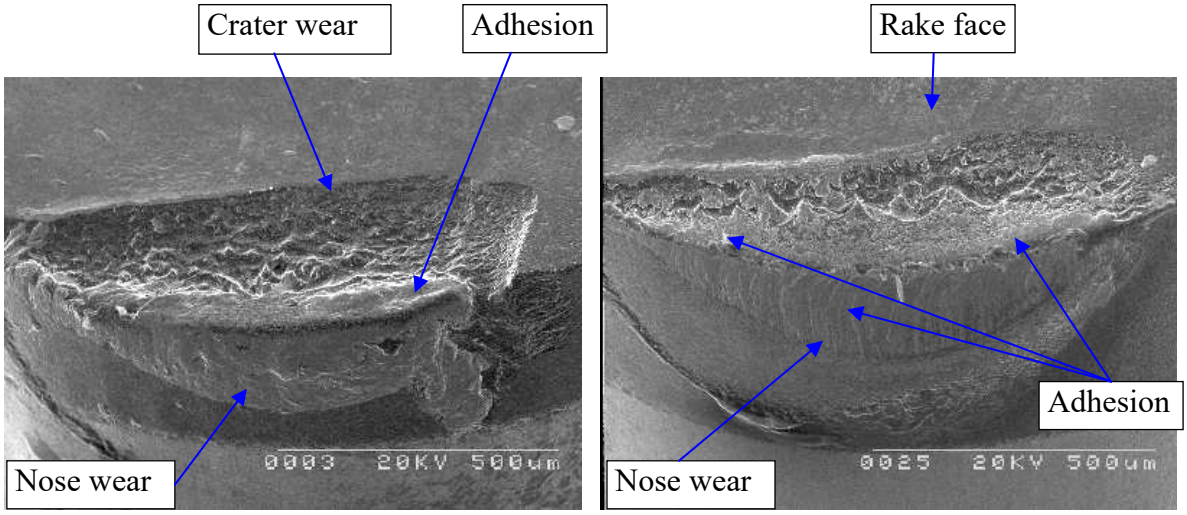

(a) Tool life = 97.3 min (b) Tool life = 23.3 min

Figure 4.63 - Worn T5 insert after machining Ti-6Al-4V alloy with a 7MPa coolant pressure and at a speed of (a) 175 m min^{-1} and (b) 230 m min^{-1}.

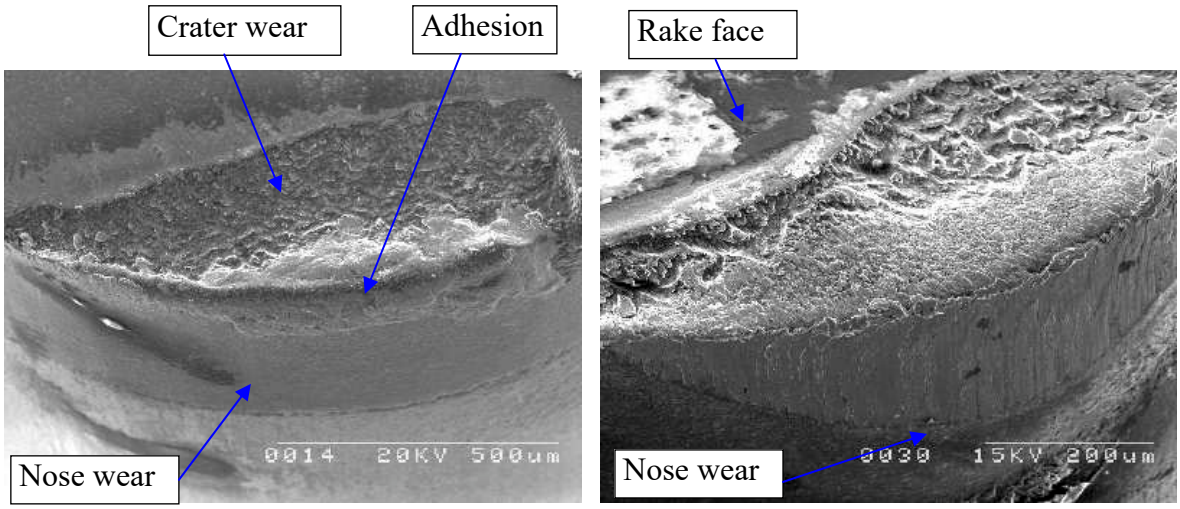

(a) Tool life = 63.8 min (b) Tool life = 17.5 min

Figure 4.64 - Worn T5 insert after machining Ti-6Al-4V alloy with 11 MPa coolant pressure at a speed of (a) 175 m min^{-1} and (b) 230 m min^{-1}.

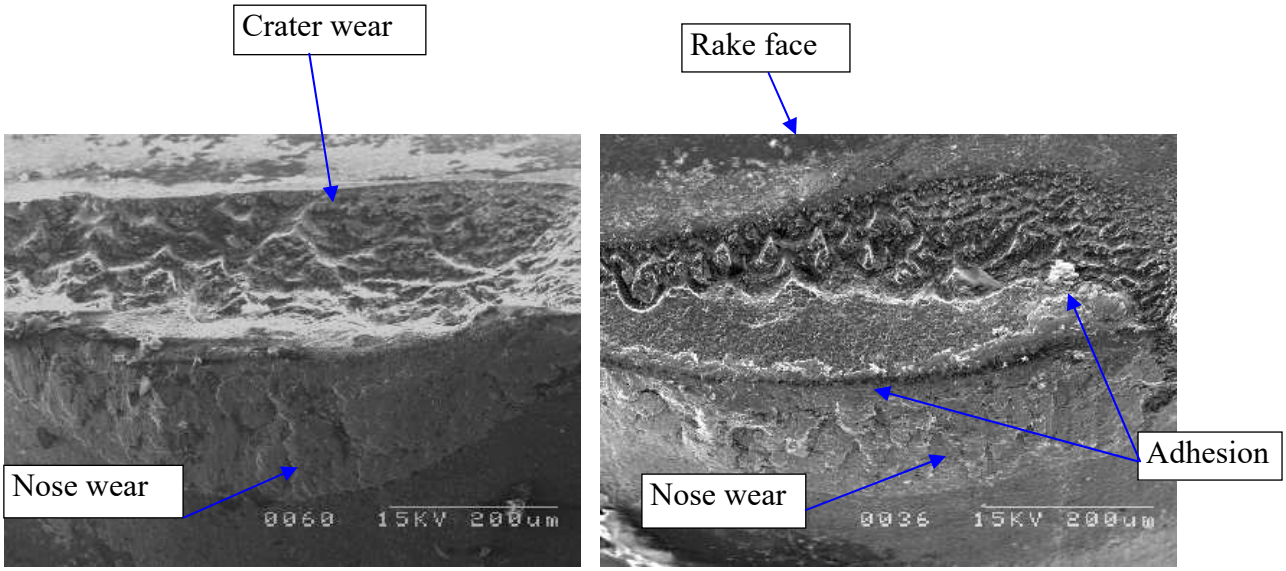

(a) Tool life = 50.5 min (b) Tool life = 8.3 min

Figure 4.65 - Wear observed on a T5 insert after machining Ti-6Al-4V alloy with 20.3 MPa coolant pressure at a speed of (a) 200 m min^{-1} and (b) 250 m min^{-1}.

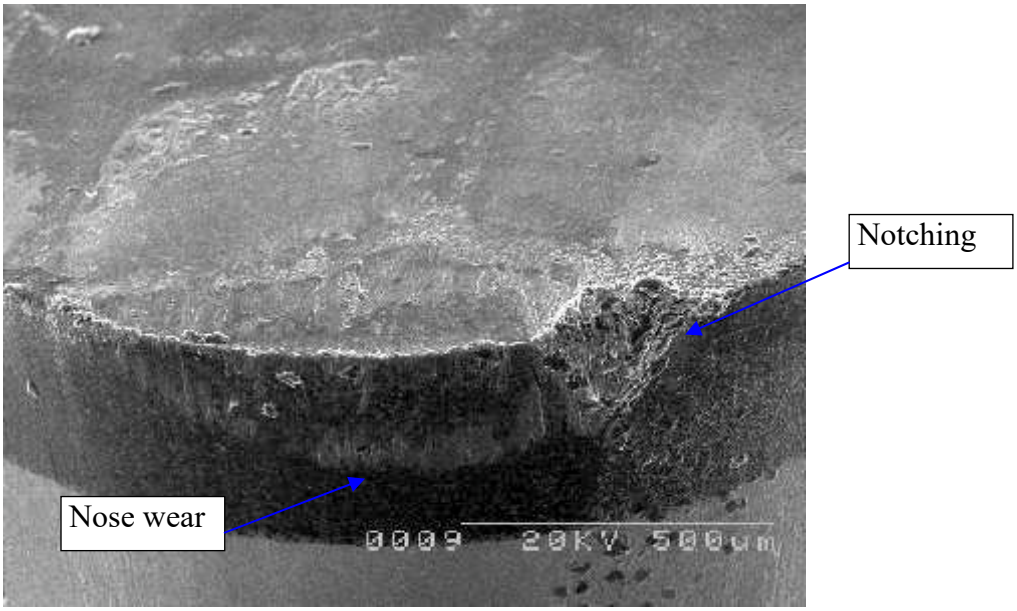

(a) Tool life = 10.2 min

Figure 4.66 - Wear observed on a T6 insert after machining Ti-6Al-4V alloy with conventional coolant supply at a speed of 175 m min^{-1}.

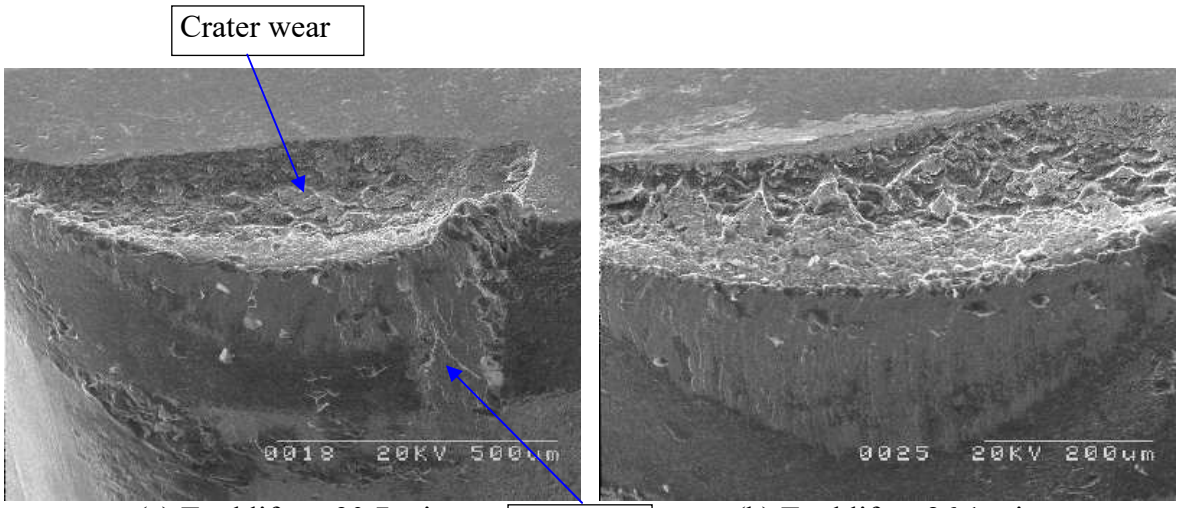

(a) Tool life = 90.7 min (b) Tool life = 26.1 min

Figure 4.67 - Worn T6 insert after machining Ti-6Al-4V alloy with 11MPa coolant pressure at a speed of (a) 175 m min^{-1} and (b) 230 m min^{-1}.

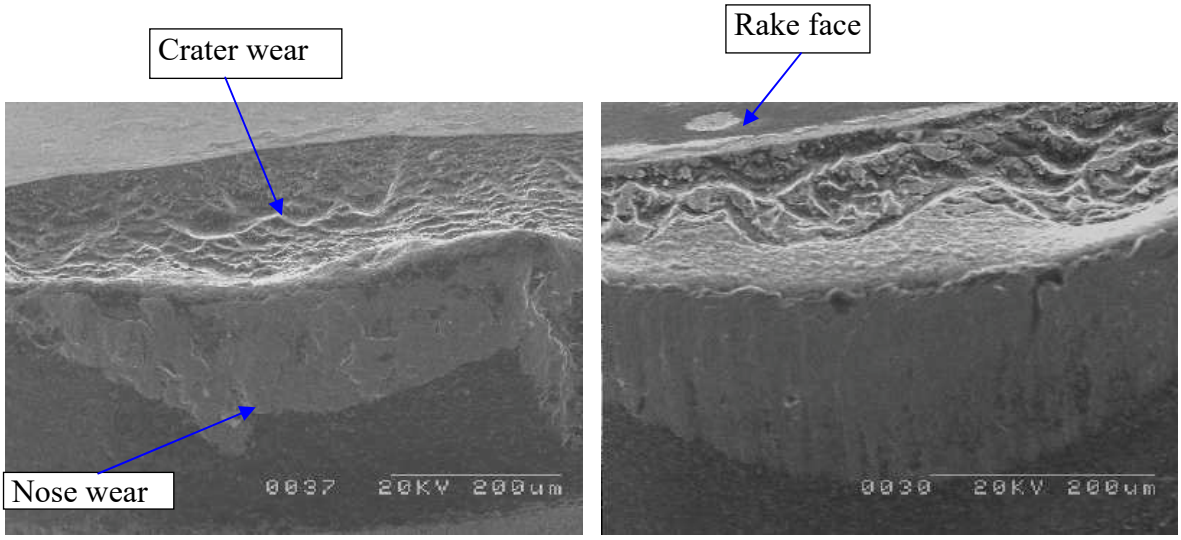

(a) Tool life = 90.7 min (b) Tool life = 26.1 min

Figure 4.68 - Worn T6 insert after machining Ti-6Al-4V alloy with 20.3 MPa coolant pressure at a speed of (a) 175 m min^{-1} and (b) 230 m min^{-1}.

4.3.3 Component forces when machining with different grades of PCD tools

Figures 4.69 and 4.70 show cutting forces and feed forces, respectively, recorded at the beginning of cut when machining Ti-6Al-4V alloy with PCD (T5 and T6) inserts with various cutting speeds and coolant supply pressures. Figure 4.69 shows a norminal variation in cutting forces when machining with PCD tools with all the coolant supply pressures investigated. Cutting forces generally increased with increasing cutting speed when machining with T5 and T6 inserts with conventional coolant supply. It can also be seen from Figure 4.69 that cutting forces generally decreased with increasing coolant pressure, up to 11 MPa, when machining with the larger grain size (T5) tool grade at higher cutting speeds up to 230 m min^{-1}. Machining with the smaller grain size (T6) insert generated lower cutting forces than machining with T5 inserts. Marginal variation in cutting forces was observed when machining with T6 insert with 11 MPa coolant pressure at the cutting speeds investigated. Increase in cutting speed led to a slight reduction in cutting forces under 20.3 MPa coolant supply pressure. Cutting forces generally decrease with increase in coolant pressure when machining with T6 inserts.

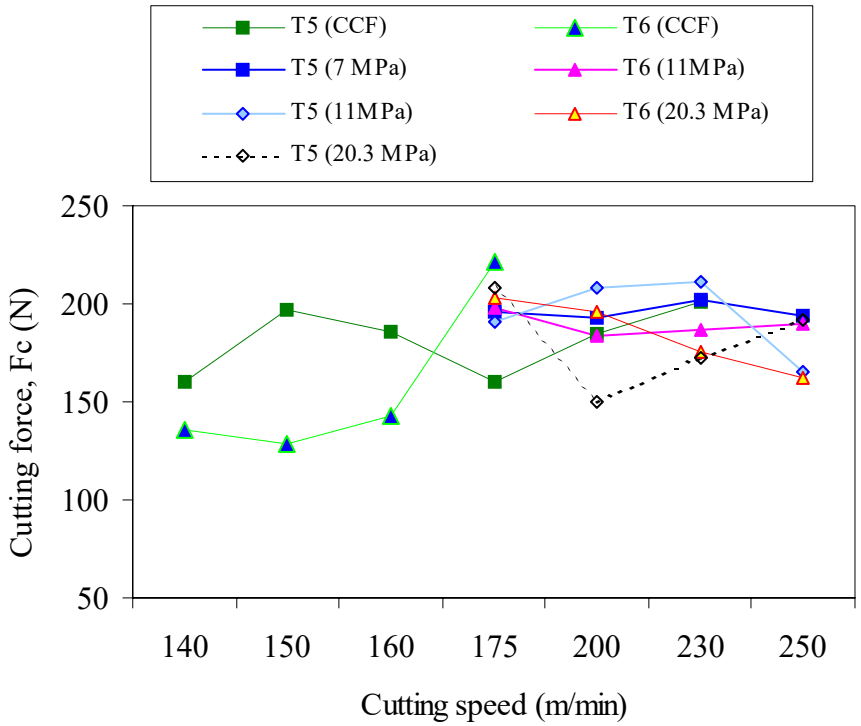

Figure 4.69 - Cutting forces (F*c*) recorded at the beginning of cut when machining Ti-6Al-4V alloy with PCD-STD (T5) and PCD-MM insert grades (T6) at various cutting conditions.

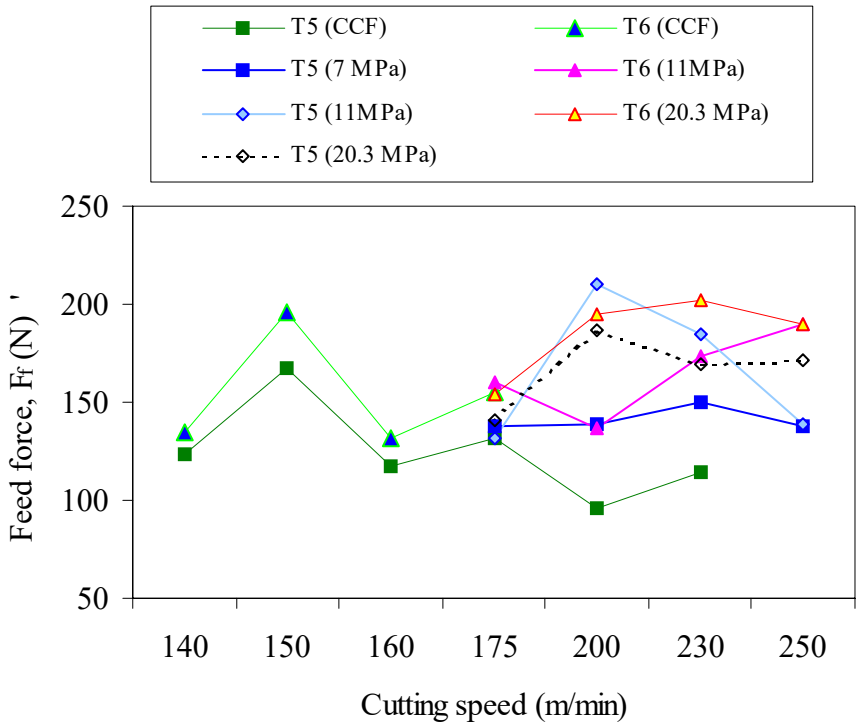

Figure 4.70 - Feed forces (F*f*) recorded at the beginning of cut when machining Ti-6Al-4V alloy with PCD-STD (T5) and PCD-MM insert grades (T6) at various cutting conditions.

Feed forces generated when machining with T5 and T6 inserts were generally lower than cutting forces especially at higher cutting speeds (Figure 4.70). The curves show that feed forces generally decreased with increasing in cutting speed when machining with both T5 and T6 inserts using conventional coolant flow and tend to increase at higher speeds when machining under high coolant pressures. It is interesting to note that the highest feed forces were recorded when machining with T6 insert at the highest coolant supply of 20.3 MPa.

4.3.4 Surfaces roughness and runout when machining with different grades of PCD tools

Figure 4.71 and 4.72 show the surface roughness and runout values, respectively, recorded when machining Ti-6Al-4V alloy with PCD (T5 and T6) inserts at various cutting conditions. Curves in Figure 4.71 show that surface roughness values recorded with PCD tools in all the conditions investigated varies between 0.5 and 2.2 μm. Most of the recorded values are, however, lower than the stipulated rejection criterion of 1.6 μm. Machining with both T5 and T6 insert grades did not produce any significant changes in the surfaces finish generated considering the anticipated scatter. The curves show gradual deterioration of the surface finish with increase in coolant pressure when machining with T5 insert at cutting speeds up to 230 m min^{-1} while increase in coolant pressure improve surface finish generated when machining with T6 insert grade. This figure also shows that good surface finish and norminal variation in surface roughness values were obtained when machining with T5 insert with conventional coolant flow. Machining with T6 insert with a coolant pressure of 11MPa produced the highest surface roughness values at higher speeds in excess of 175 m min^{-1}.

Figure 4.72 are plots of runout values recorded when machining Ti-6Al-4V alloy with T5 and T6 inserts at various cutting conditions. The runout values vary between 2 and 12 μm. These values are far lower than the stipulated rejection criterion value of 100 μm. Generally runout values recorded decreases with increasing cutting speed when machining with both grades of PCD tools. T5 tools gave lower runout values than T6 tools when machining with all coolant supplies at cutting speeds up to 230 m min^{-1}. The least runout value of 2 μm was recorded when machining with T5 insert with high coolant pressure of 20.3 MPa at a cutting speed of 200 m min^{-1}

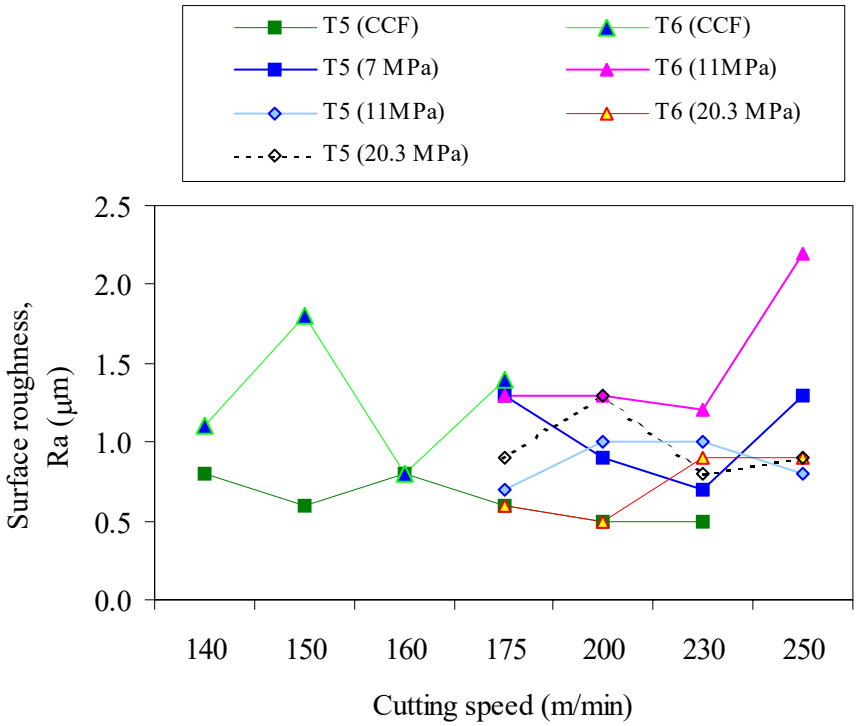

Figure 4.71- Surface roughness values recorded at the beginning of cut when machining Ti-6Al-4V alloy with T5 and T6 inserts at various cutting conditions.

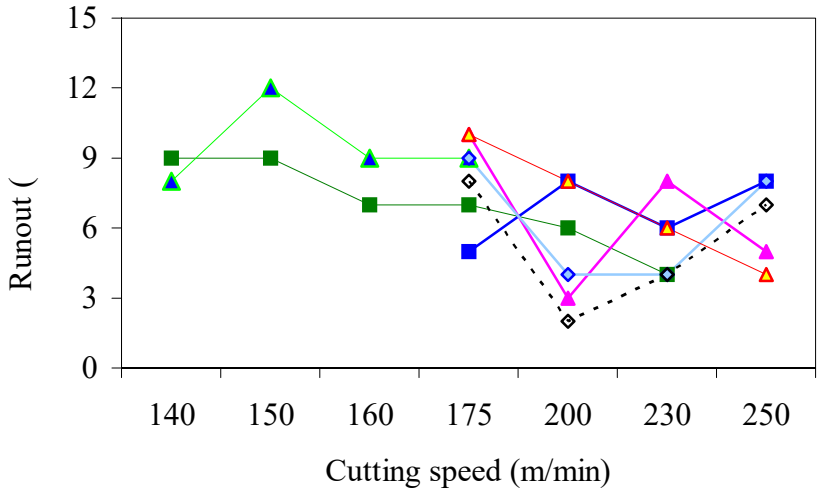

4.3.5 Surface alteration after machining with different grades of PCD tools

Surfaces generated when machining the titanium alloy with PCD (T5 and T6) tools at various cutting speeds and under various coolant supply pressure generally consist of well-defined and uniform feed marks running perpendicular to the direction of relative work-tool motion with no evidence of plastic flow (Figures 4.73-4.79).

Machining with the larger grain size T5 insert with a coolant pressure of 11 MPa did not leave any damage on machined surfaces at all cutting speeds investigated, Figure 4.75. The surface damages observed existed mainly as localised incipient melting of the machined surfaces (Figures 4.73 (a), 4.74 (b), 4.76-4.79) and micro-pits especially when machining with T6 insert using high coolant pressures (Figures 4.78 and 4.79). Most of machined surfaces exhibit evidence of localised incipient melting of the machined surfaces when machining with both grades of PCD tools at the different coolant supplies employed. Distribution of the localised incipient melting of machined surfaces are worse when machining with T5 inserts with the highest coolant pressure of 20.3 MPa (Figure 4.76) and more severe when machining with T6 inserts with coolant supply pressures of 11 MPa and 20.3 MPa (Figures 4.78 and 4.79). The continuity of the feed marks is impaired by the localised incipient melting of the machined surface when machining with T5 insert at a cutting speed of 175 m min^{-1} using conventional coolant flow (Figure 4.73 (a)), at a speed of 200 m min^{-1} under a coolant pressure of 7 MPa (Figure 4.74 (b)) and at the highest coolant pressure of 20.3 MPa. The continuity of the feed marks on machined surfaces was also interrupted by the localised incipient melting of machined surfaces when machining with T6 inserts at all the conditions investigated (Figures 4.77-4.79). Irregular feed marks were observed in some cases when machining with the smaller grain size T6 insert at a cutting speed of 175 m min^{-1} with conventional coolant supply and also with 11 MPa coolant pressure (Figures 4.77 (a) and 4.78 (a), respectively). Generally surfaces generated under all the finishing conditions investigated when machining with both PCD tool grades were free from other damages such as cracking, tearing and rupture that are detrimental to machined components. Therefore, surfaces generated in these trials are acceptable and conform to the standard specification established for machined aerospace components (Rolls-Royce CME 5043).

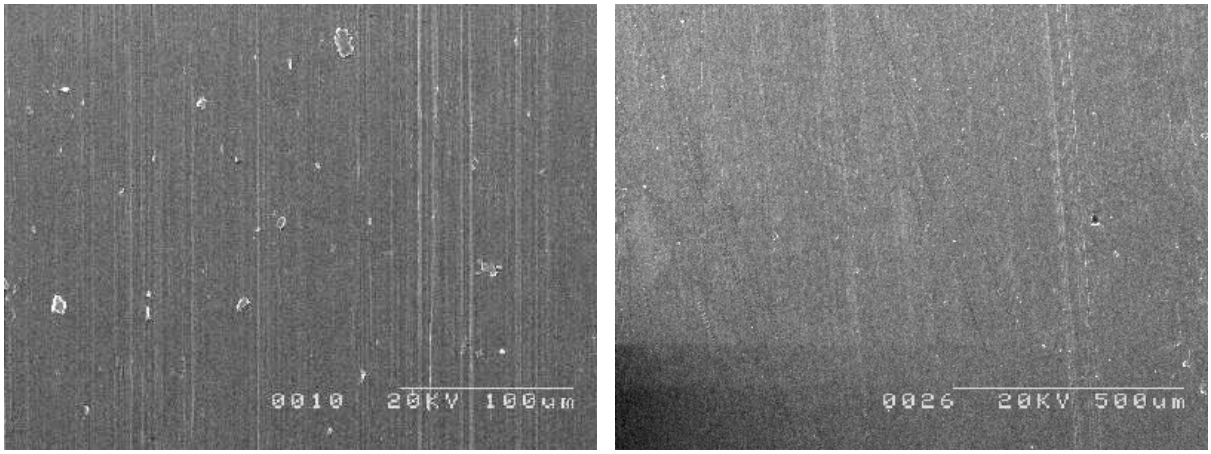

(a) (b)

Figure 4.73 - Surfaces generated after machining with PCD (T5) inserts with conventional coolant supply at a cutting speed of (a) 175 m min^{-1} and (b) 200 m min^{-1}.

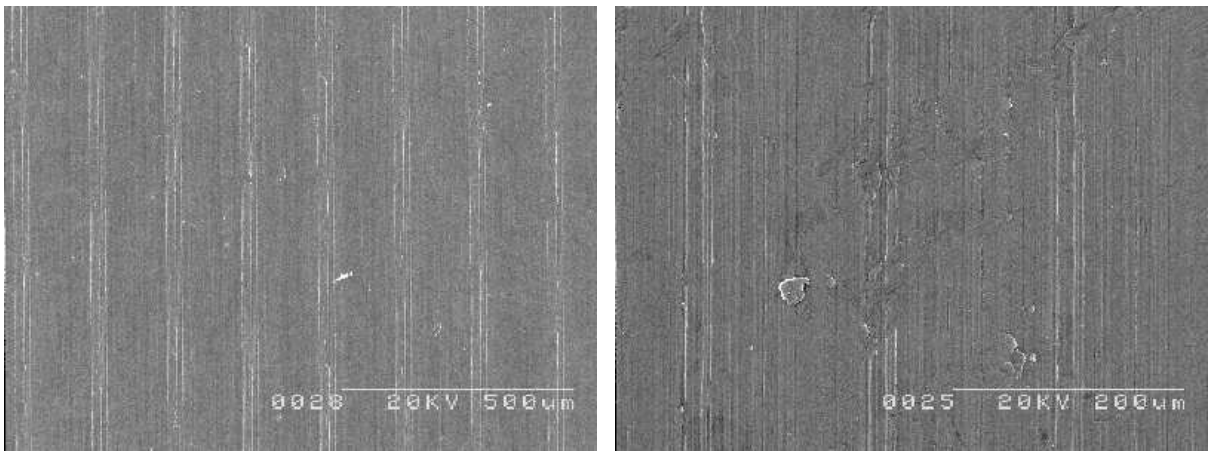

(a) (b)

Figure 4.74 - Surfaces generated after machining with PCD (T5) inserts with a coolant pressure of 7 MPa at a cutting speed of (a) 175 m min^{-1} and (b) 200 m min^{-1}.

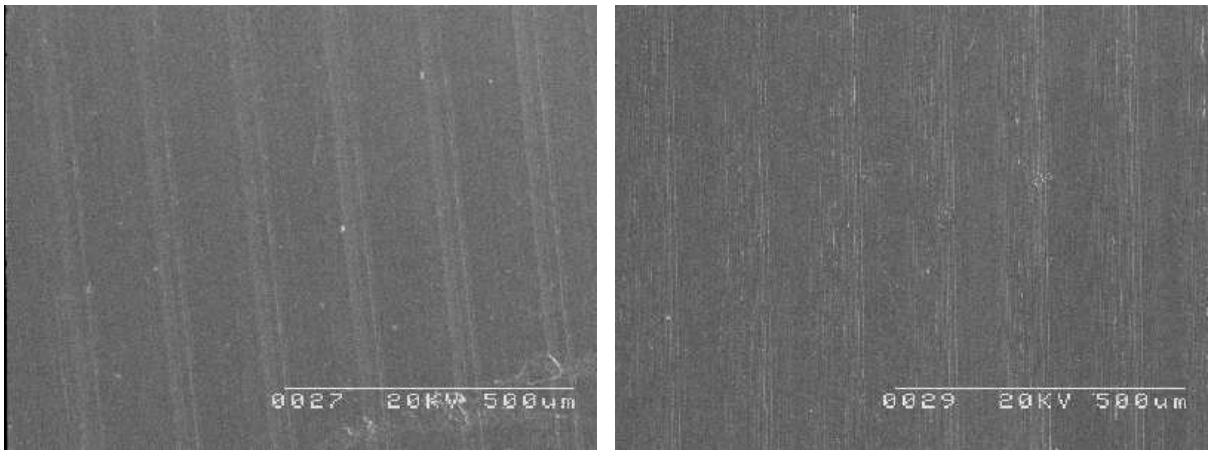

(a) (b)

Figure 4.75 - Surfaces generated after machining with PCD (T5) inserts with a coolant pressure of 11 MPa at a cutting speed of (a) 200 m min^{-1} and (b) 250 m min^{-1}.

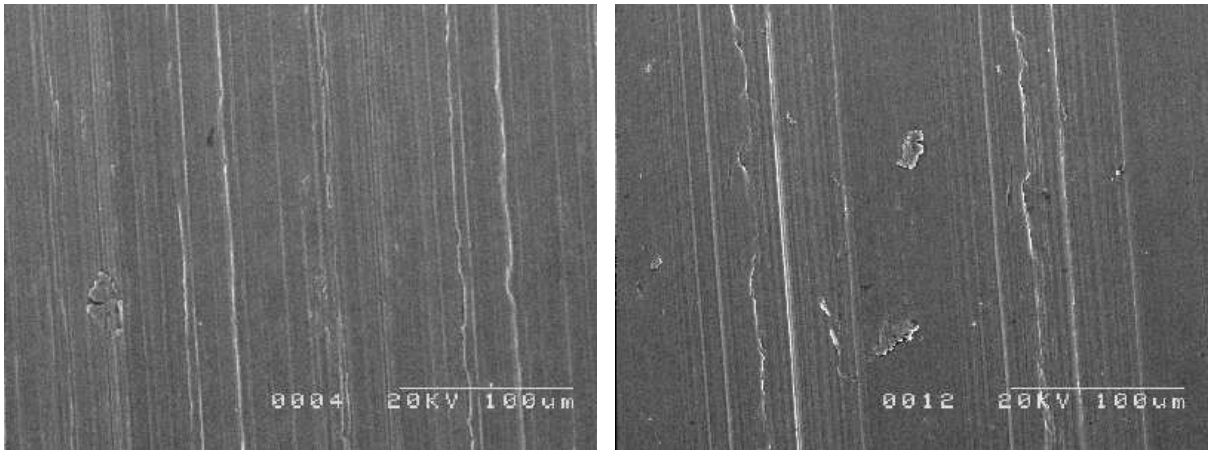

(a) (b)

Figure 4.76 - Surfaces generated after machining with PCD (T5) inserts with a coolant pressure of 20.3 MPa at a cutting speed of (a) 175 m min^{-1} and (b) 200 m min^{-1}.

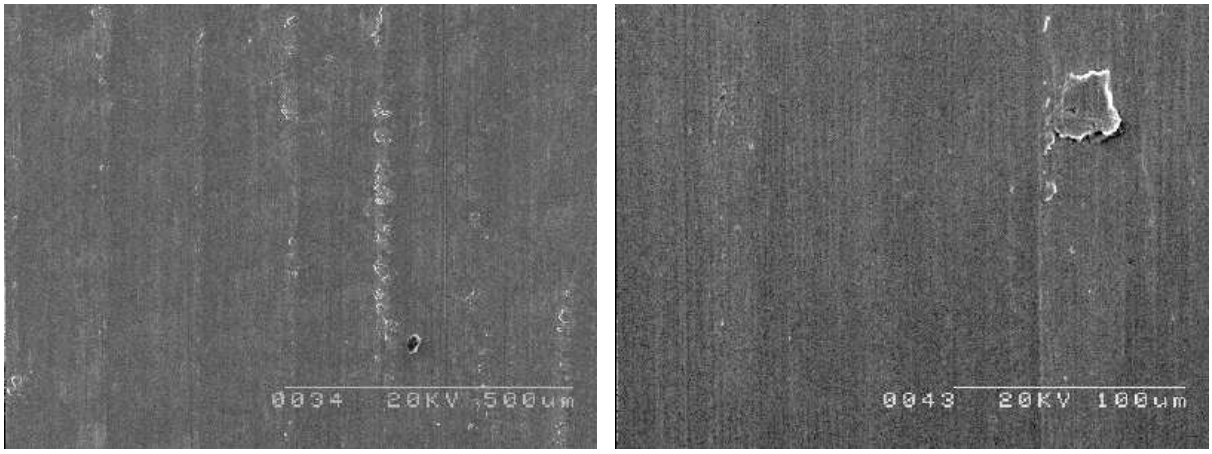

(a) (b)

Figure 4.77 - Surfaces generated after machining with PCD (T6) inserts with conventional coolant supply at a cutting speed of (a) 175 m min^{-1} and (b) 200 m min^{-1}.

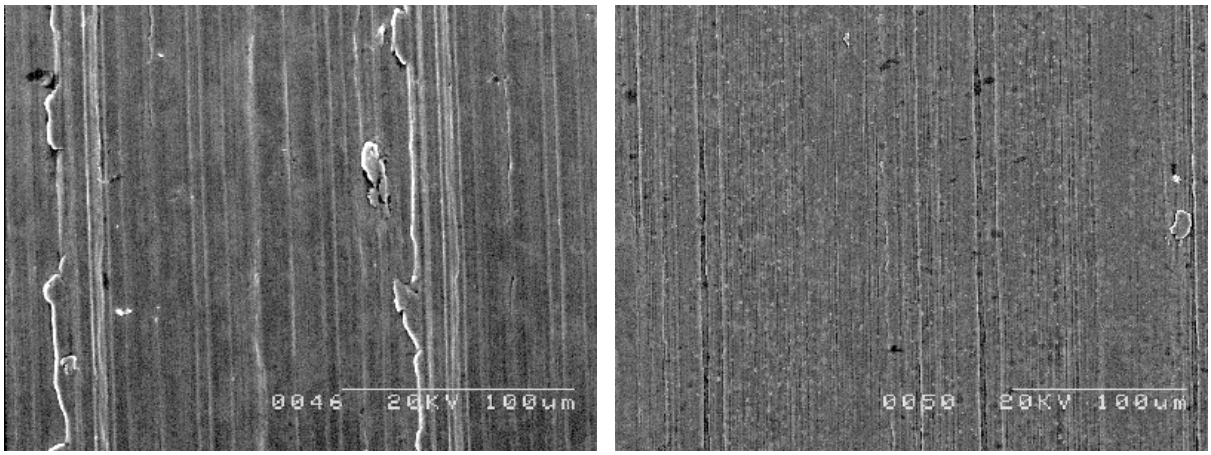

(a) (b)

Figure 4.78 - Surfaces generated after machining with PCD (T6) inserts with a coolant pressure of 11 MPa at a cutting speed of (a) 175 m min^{-1} and (b) 230 m min^{-1}.

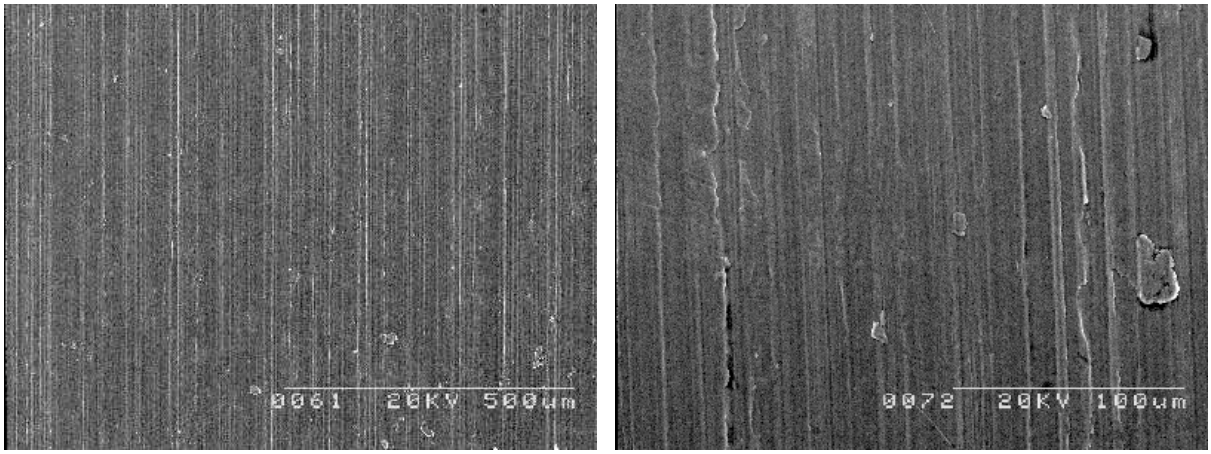

(a) (b)

Figure 4.79 - Surfaces generated after machining with PCD (T6) inserts with a coolant pressure of 20.3 MPa at a cutting speed of (a) 175 m min^{-1} and (b) 200 m min^{-1}.

4.3.6 Surface hardness after machining with different grades of PCD tools

Figures 4.80-4.86 are plots of the variations of microhardness values recorded from the top up to about 1.5 mm below the machined surface after machining with different PCD tools at various cutting speeds and under various coolant supply pressures. The plots indicate that the hardness depth of the machined surface generally increased with increasing in cutting speed when machining with the larger grain size (T5) tools using conventional coolant flow and high coolant pressures supplies up to 11 MPa (Figures 4.80-4.83). A comparison of Figures 4.80 and 4.84 shows that lower hardness values were recorded when machining Ti-6Al-4V with T6 tools.

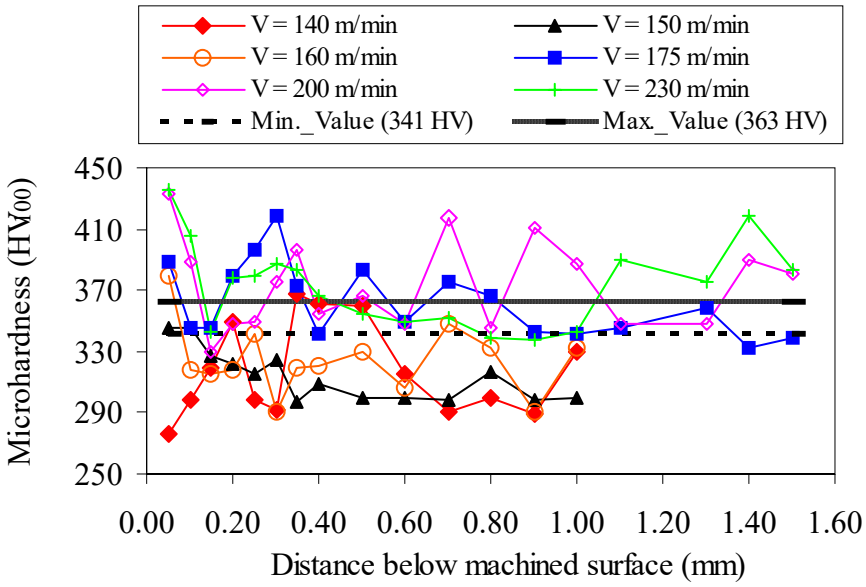

Figure 4.80 - Hardness variation after machining Ti-6Al-4V alloy with PCD (T5) insert with conventional coolant supply.

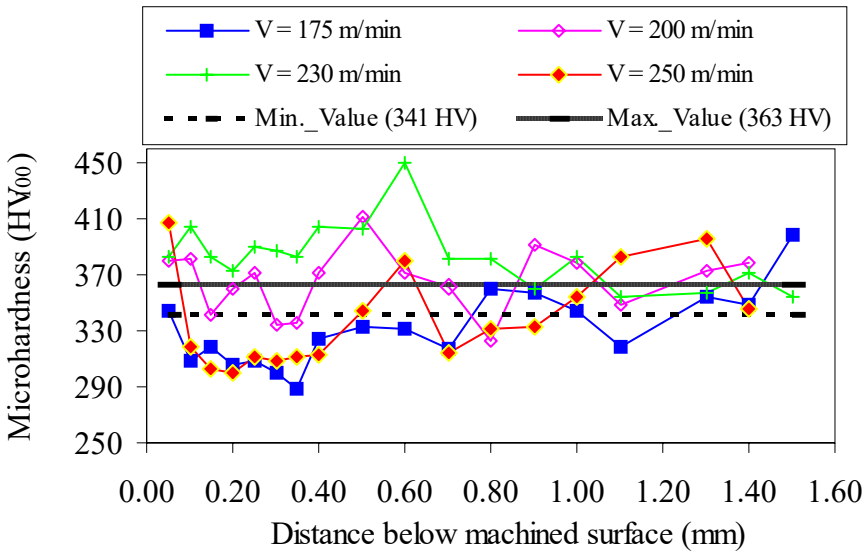

Figure 4.81 - Hardness variation after machining Ti-6Al-4V alloy with PCD (T5) insert with 7 MPa coolant pressure supply.

Analysis of Figures 4.82 and 4.85 suggests that there is considerable softening of the surfaces generated after machining with a 11MPa coolant pressure using both insert grades The use of a higher coolant pressure of 20.3 MPa resulted to pronounced softening when machining with T5 inserts relative to T6 inserts (Figures 4.83 and 4.86).

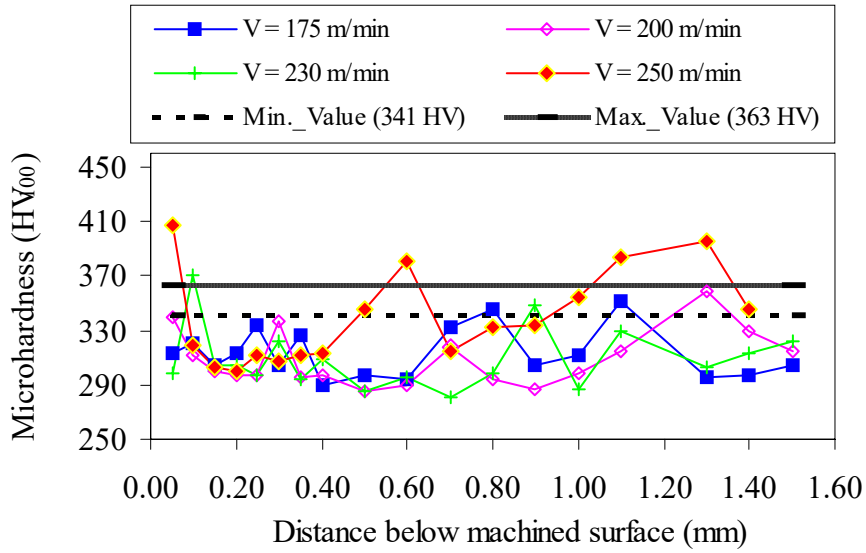

Figure 4.82 - Hardness variation after machining Ti-6Al-4V alloy with PCD (T5) insert with 11 MPa coolant pressure supply.

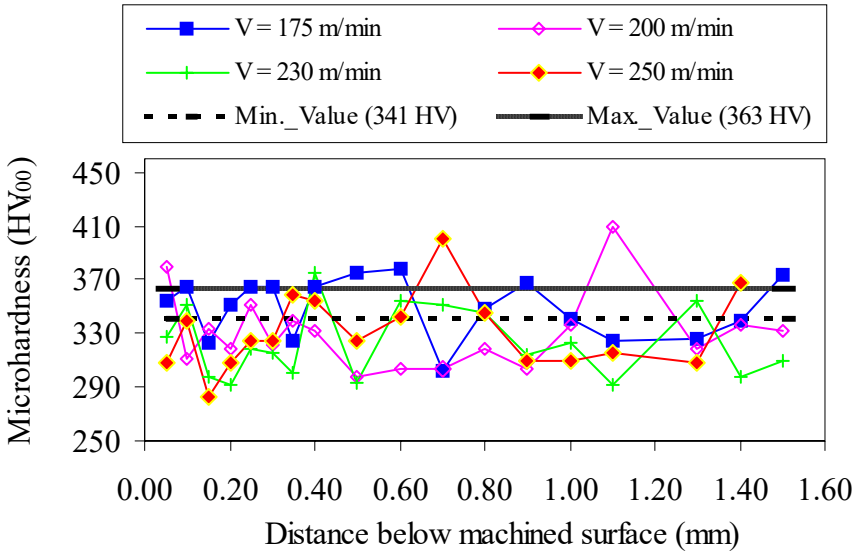

Figure 4.83 - Hardness variation after machining Ti-6Al-4V alloy with PCD (T5) insert with 20.3 MPa coolant pressure supply.

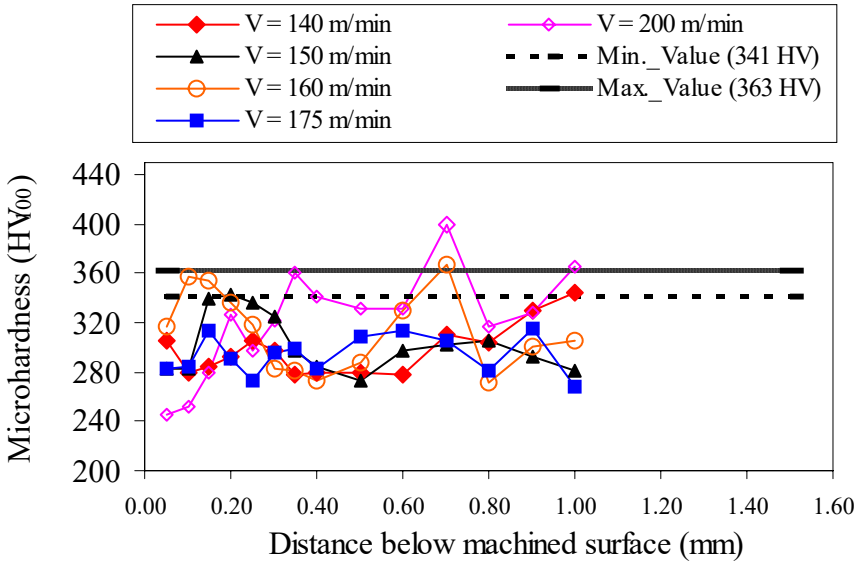

Figure 4.84 - Hardness variation after machining Ti-6Al-4V alloy with PCD (T6) insert with conventional coolant supply.

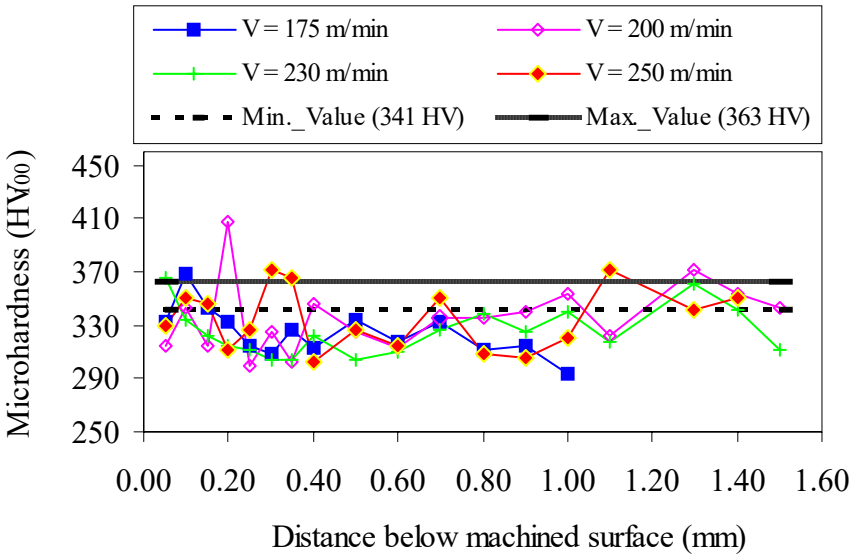

Figure 4.85 - Hardness variation after machining Ti-6Al-4V alloy with PCD (T6) insert with 11 MPa coolant pressure supply.

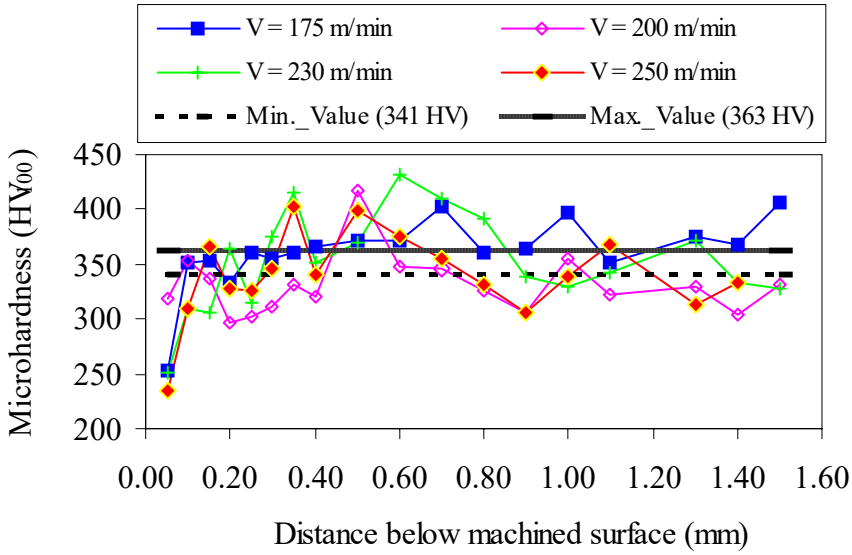

Figure 4.86 - Hardness variation after machining Ti-6Al-4V alloy with PCD (T6) insert with 20.3 MPa coolant pressure supply.

4.3.7 Subsurface alteration after machining Ti-6Al-4V alloy with different grades of PCD tools

Figures 4.87-4.93 are microstructures of etched machined surfaces of Ti-6Al-4V alloy after machining with different PCD (T5 and T6) inserts at the cutting conditions investigated.

These figures show no mechanical damage or microstructural alterations after machining with all the carbide grades at the cutting conditions investigated.

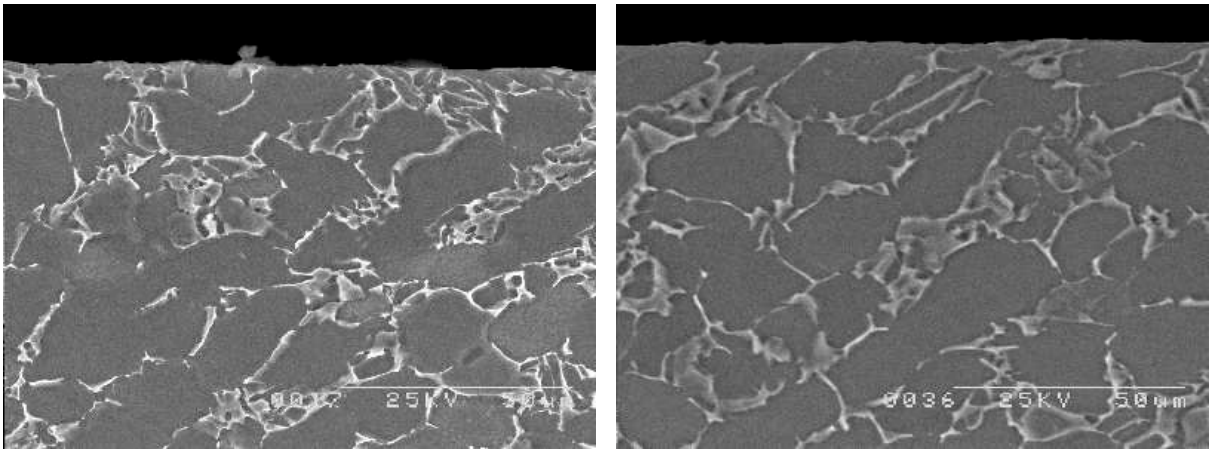

(a) Tool life = 56.7 min (b) Tool life = 1 min

Figure 4.87 - Microstructure of Ti-6Al-4V alloy after machining with PCD (T5) insert with conventional coolant supply at a cutting speed of (a) 140 m min^{-1} and (b) 230 m min^{-1}.

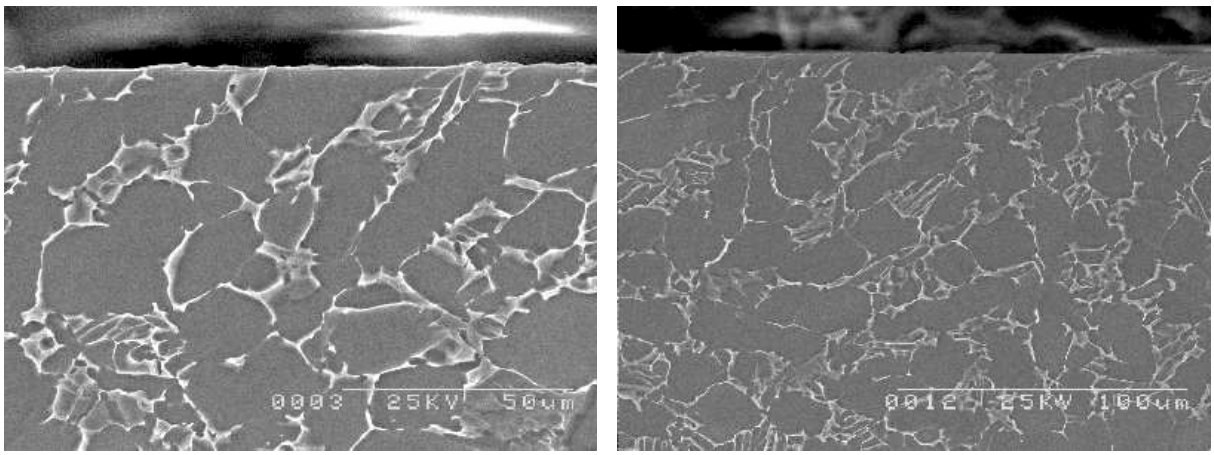

(a) Tool life = 97.3 min (b) Tool life = 13.2 min

Figure 4.88 - Microstructure of Ti-6Al-4V alloy after machining with PCD (T5) insert with a coolant pressure of 7 MPa at a cutting speed of (a) 175 m min^{-1} and (b) 250 m min^{-1}.

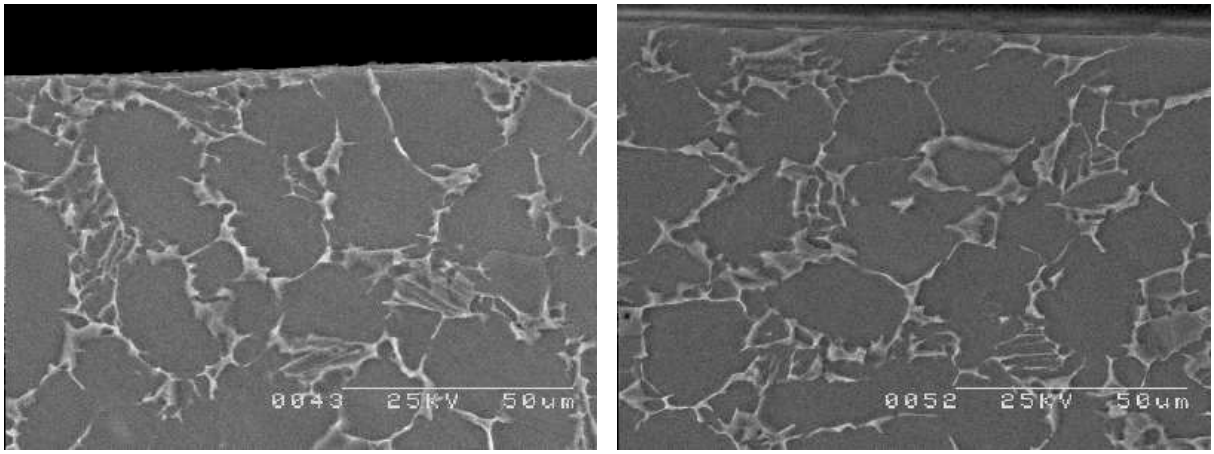

(a) Tool life = 63.8 min (b) Tool life = 17.5 min

Figure 4.89 - Microstructure of Ti-6Al-4V alloy after machining with PCD (T5) insert with a coolant pressure of 11 MPa at a cutting speed of (a) 175 m min^{-1} and (b) 230 m min^{-1}.

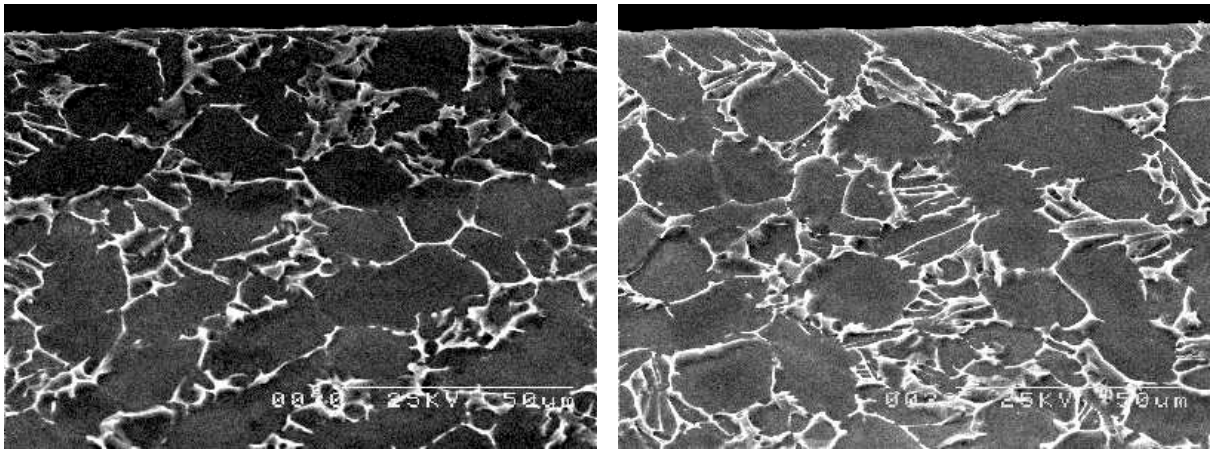

(a) Tool life = 50.5 min (b) Tool life = 21.4 min

Figure 4.90 - Microstructure of Ti-6Al-4V alloy after machining with PCD (T5) insert with a coolant pressure of 20.3 MPa at a cutting speed of (a) 200 m min^{-1} and (b) 230 m min^{-1}.

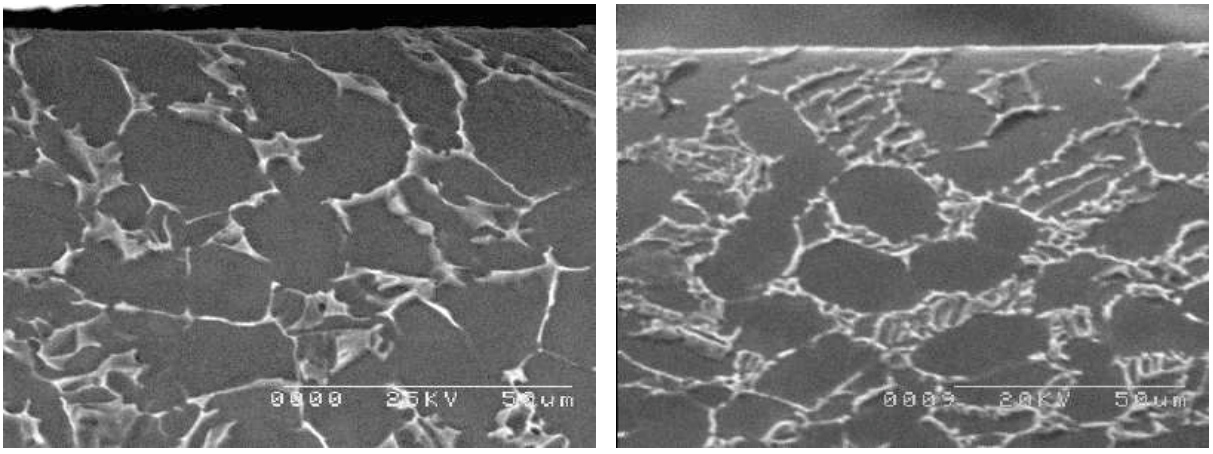

(a) Tool life = 69.9 min (b) Tool life = 2.3 min

Figure 4.91 - Microstructure of Ti-6Al-4V alloy after machining with PCD (T6) insert with conventional coolant supply at a cutting speed of (a) 140 m min^{-1} and (b) 200 m min^{-1}.

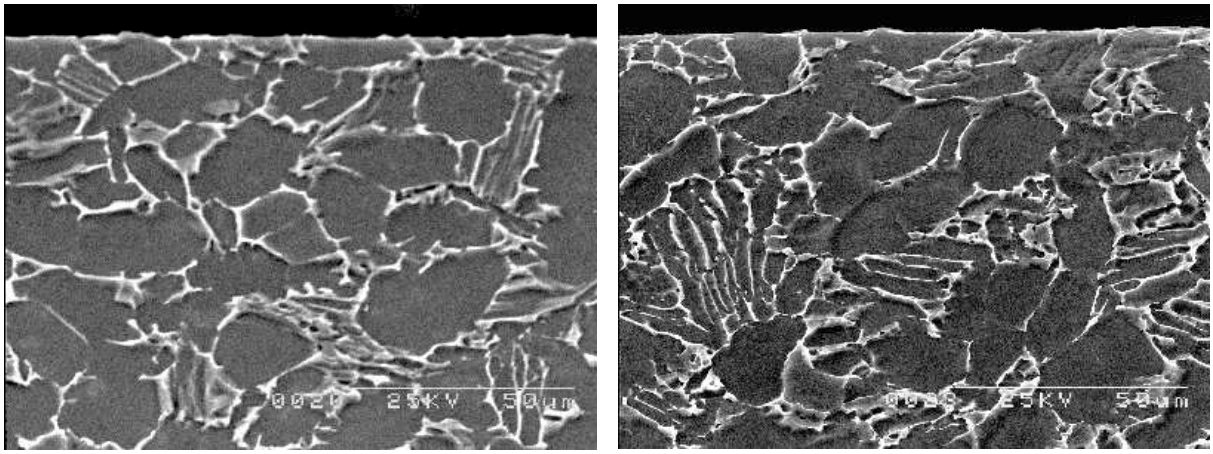

(a) Tool life = 90.7 min (b) Tool life = 26.1 min

Figure 4.92 - Microstructure of Ti-6Al-4V alloy after machining with PCD (T6) insert with a coolant pressure of 11 MPa at a cutting speed of (a) 175 m min^{-1} and (b) 230 m min^{-1}.

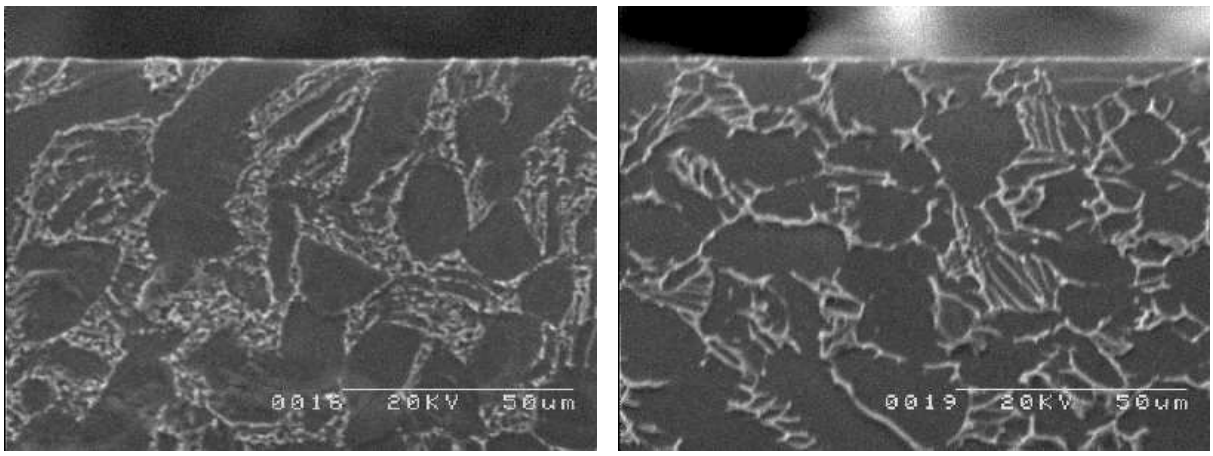

(a) Tool life = 68.8 min (b) Tool life = 17.9 min

Figure 4.93 - Microstructure of Ti-6Al-4V alloy after machining with PCD (T6) insert with a coolant pressure of 20.3 MPa at a cutting speed of (a) 175 m min^{-1} and (b) 230 m min^{-1}.

4.3.8 Chips shapes

Figures 4.94 (a)–(g) show different chips generated when machining with T5 and T6 grades of PCD tools under various cutting conditions. Machining Ti-6Al-4V alloy with the larger grain size (T5) tool grade using conventional coolant flow produced long helical form of chips (Figure 4.94 (a)), whereas T6 insert produced long continuous tubular type chips (Figure 4.94 (e)). Machining with both T5 and T6 inserts with high pressure coolant supplies produced smaller segmented chips (Figures 4.94 (b), (c), (d), (f) and (g)). It is important to note that the nature of swarf produced when machining with high pressure coolant supplies is markedly different to those obtained with conventional coolant flow. Coolant supply at high

pressures tend to enhance chip segmentation as the chip curl radius is reduced significantly, hence maximum coolant pressure is restricted only to a smaller area on the chip.

(a) T5 (conventional)
V = 200 m min^{-1}

(b) T5 (7MPa)
V = 175 m min^{-1}

(c) T5 (11 MPa)
V = 200m min^{-1}

(d) T5 (20.3MPa)
V = 200 m min^{-1}

(e) T6 (Conventional)
V = 140 m min^{-1}

(f) T6 (11 MPa)
V = 175 m min^{-1}

(g) T5 (20.3MPa)
V = 200 m min^{-1}

Figure 4.94 - Chips generated when machining Ti-6Al-4V alloy with different grades of PCD at various cutting conditions: (a): snarled chip; (e): long continuous chip, (b), (c), (d), (f) and (g): segmented C-shaped chips.

4.4 Machining of Ti-6Al-4V alloy with different grades of CBN/PCBN tools under various coolant supply pressures

4.4.1. Tool Life

Figure 4.95 shows tool life (VC ≥ 0.3 mm or VN ≥ 0.6 mm) recorded when machining Ti-6Al-4V alloy with three different grades of CBN (T7) and PCBN (T8 and T9) inserts at

various cutting speeds and with conventional coolant flow and high pressure coolant supplies of 11 MPa and 20.3 MPa. Tool life generally decreased with increasing cutting speed when machining with the lower (50 vol.%) CBN content (T7 grade), unlike when machining with PCBN (T8 and T9) tool grades with higher (90 vol.%) CBN content. Additionally, tool life of the CBN grades generally increased with increasing the coolant pressure, especially when machining with the T7 tool grade at speeds of 150 and 250 m min^{-1}, which was more sensitive to coolant pressure than others. T7 insert gave the best performance, in terms of tool life, at all the conditions investigated. Over 68% and 150% improvement in tool life was recorded when machining with tool T7 grade at a cutting speed of 150 m min^{-1} with the coolant pressure supplies of 11 MPa and 20.3 MPa, respectively, in comparison to conventional coolant flow. However, tool life decreased with increasing the coolant pressure when machining at a cutting speed in excess of 200 m min^{-1}. In general T8 and T9 inserts exhibited similar performance in terms of tool life (generally below 1 min) at the conditions investigated. Figure 4.95 also shows that coating on the T9 insert did not influence tool performance.

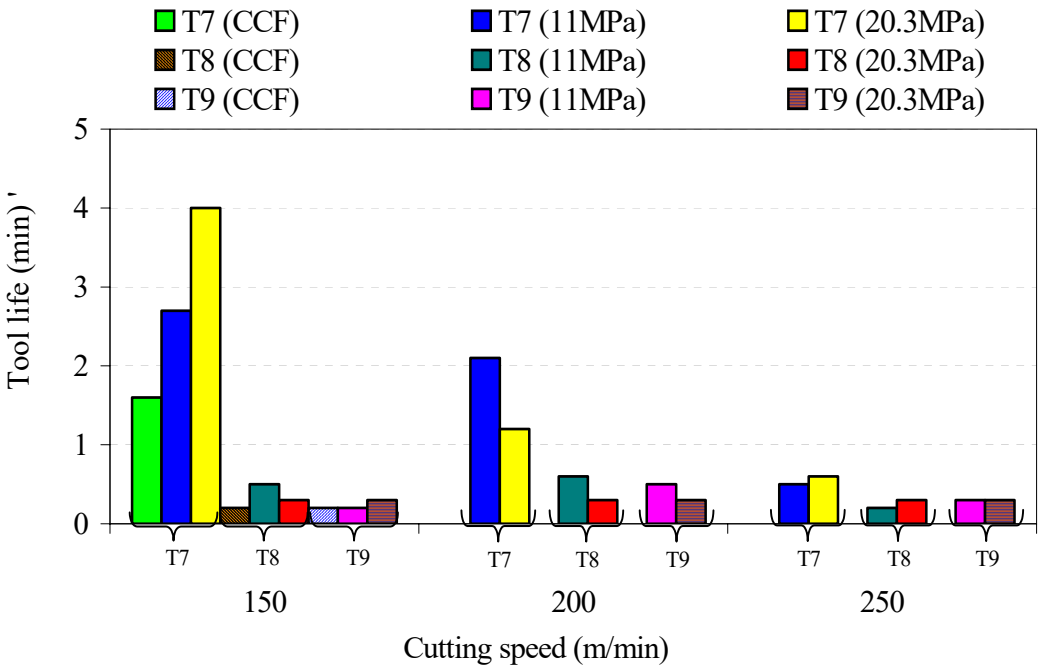

Figure 4.95 - Tool life (VC ≥ 0.3 mm or VN ≥ 0.6 mm) recorded when machining Ti-6Al-4V alloy with different CBN/PCBN tools (T7, T8 and T9) grades with conventional coolant flow (CCF), high coolant pressures of 11 MPa and 20.3 MPa at various cutting speed conditions.

4.4.2 Tool wear when machining Ti-6Al-4V alloy with different grades of CBN/PCBN tools

Figure 4.96 shows tool wear rates when machining Ti-6Al-4V alloy with different CBN/PCBN tool (T7,T8,T9) inserts using conventional coolant flow and high pressure coolant supplies of 11 MPa and 20.3 MPa and at various cutting speeds. It can be seen from the graph that the lower wear rate with regular wear pattern, increasing with increasing cutting speed, was observed when machining with the lower (50 vol.%) CBN content T7 inserts, unlike machining with PCBN (T8 and T9) tool grades, which gave higher wear rates. Nose wear and notching were the dominant failure modes for T7 inserts (Figures 4.97-4.99) whereas notching and chipping were the dominant failure modes for T8 and T9 tools (Figure 4.100). Note that machining trials with CBN/PCBN tool grades using conventional coolant flow were carried out only at a cutting speed of 150 m min^{-1}. Machining under conventional coolant flow gave higher tool wear rates than with high pressure coolant supplies. The least wear rate was recorded when machining with the lower (50 vol.%) CBN content T7 insert using the highest pressure of 20.3 MPa at a cutting speed 150 m min^{-1} whereas the highest wear rate was recorded when machining with T8 tool grade (90 vol.%) PCBN content using conventional coolant flow, Figure 4.96. Figure 4.96 also shows that increasing coolant pressure from 11 to 20.3 MPa did not provide any reduction in wear rate when machining with both T7 andT9 inserts at the conditions investigated. Rapid increase in notch wear rate was recorded when machining with T8 insert using the highest coolant supply pressure of 20.3 MPa at high speeds in excess of 200 m min^{-1}.

Figures 4.97–4.104 show worn CBN/PCBN tools after finish turning of Ti-6Al-4V alloy under various machining conditions. All of these figures clearly show that notching occurred in all the CBN/PCBN tools tested under all the conditions investigated. Chipping of the cutting edge also occurred in most cutting conditions as illustrated in Figures 4.97-4.99, 4.101-4.104. Figures 4.97-4.99 show that, although tool wear rate decreased, machining of Ti-6Al-4V alloy with T7 insert under high pressure coolant supplies did not prevent chipping occurring in comparison with conventional coolant flow.

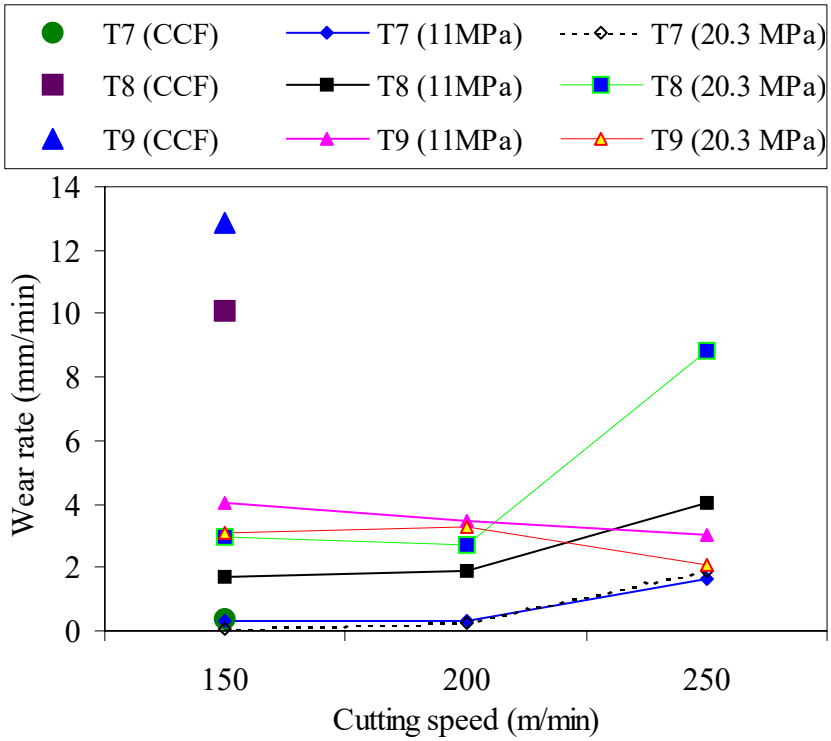

Figure 4.96 - Wear rate curves of different CBN/PCBN tools when machining Ti-6Al-4V alloy with conventional coolant flow and high pressures coolant supplies at various speed conditions.

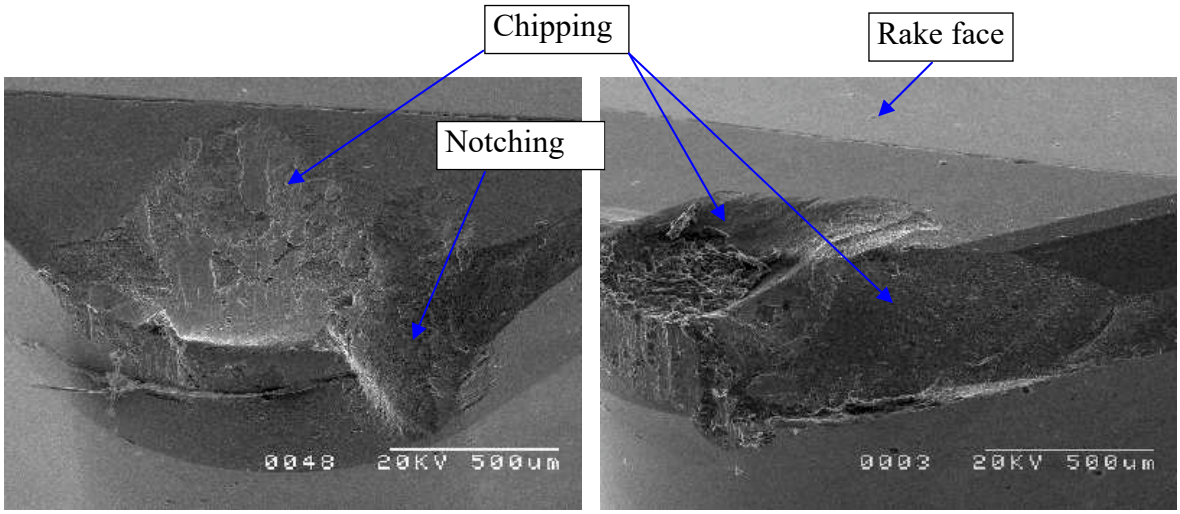

(a) Tool life < 1.6 min (b) Tool life < 0.5 min

Figure 4.97 - Worn PCBN 10 (T7) inserts after machining Ti-6Al-4V alloy using conventional coolant supply at a speed of (a) 150 m min^{-1} and (b) 200 m min^{-1}.

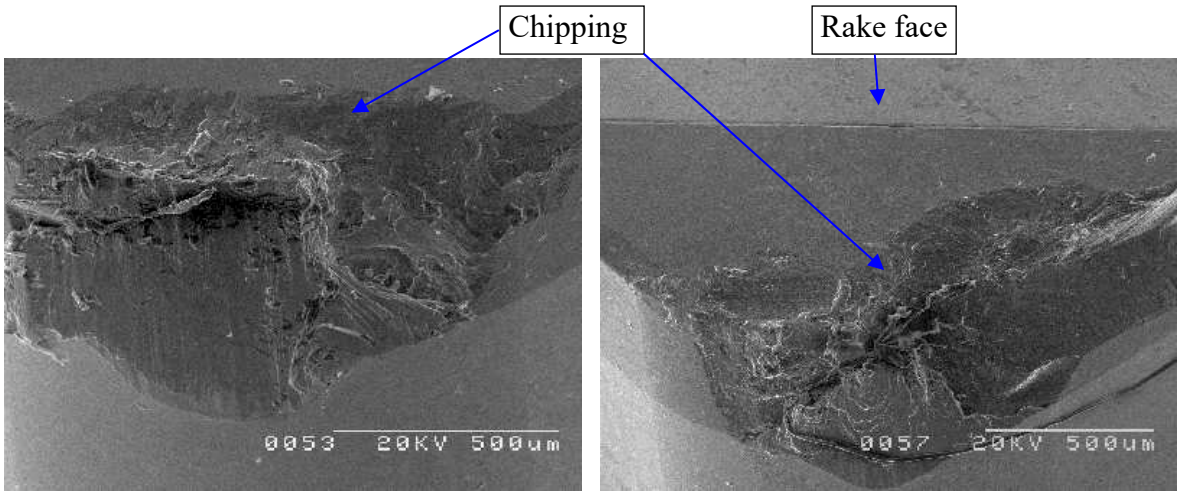

(a) Tool life < 2.7 min (b) Tool life < 1 min

Figure 4.98 - Worn PCBN 10 (T7) inserts after machining Ti-6Al-4V alloy with 11 MPa coolant pressure at a speed of (a) 150 m min^{-1} and (b) 250 m min^{-1}.

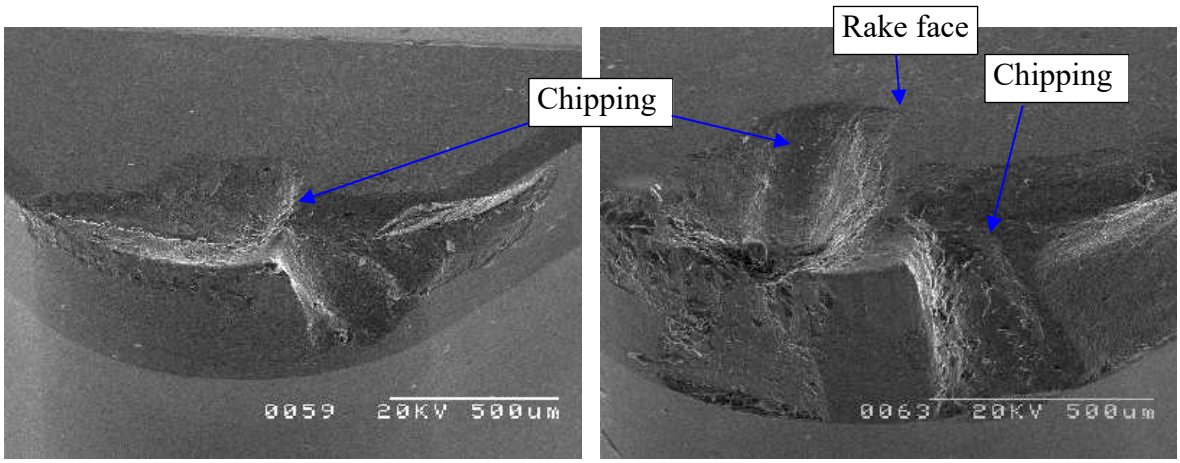

(a) Tool life < 4 min (b) Tool life < 0.6 min

Figure 4.99 - Worn PCBN 10 (T7) inserts after machining Ti-6Al-4V alloy with 20.3 MPa coolant pressure at a speed of (a) 150 m min^{-1} and (b) 250 m min^{-1}.

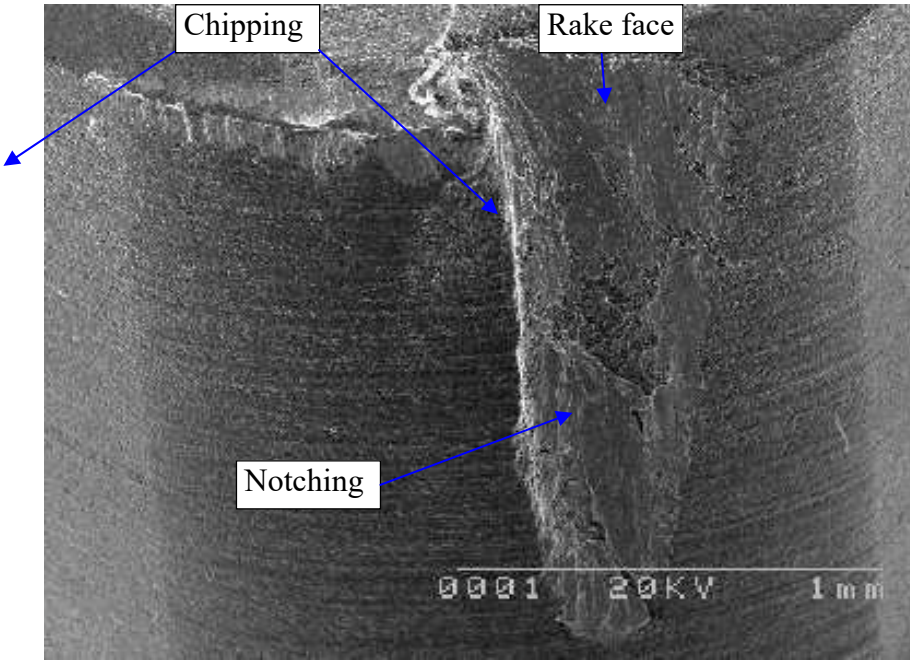

Tool life < 0.2 min

Figure 4.100 - Worn PCBN 300 (T8) inserts after machining Ti-6Al-4V alloy using conventional coolant supply at a speed of 150 m min^{-1}.

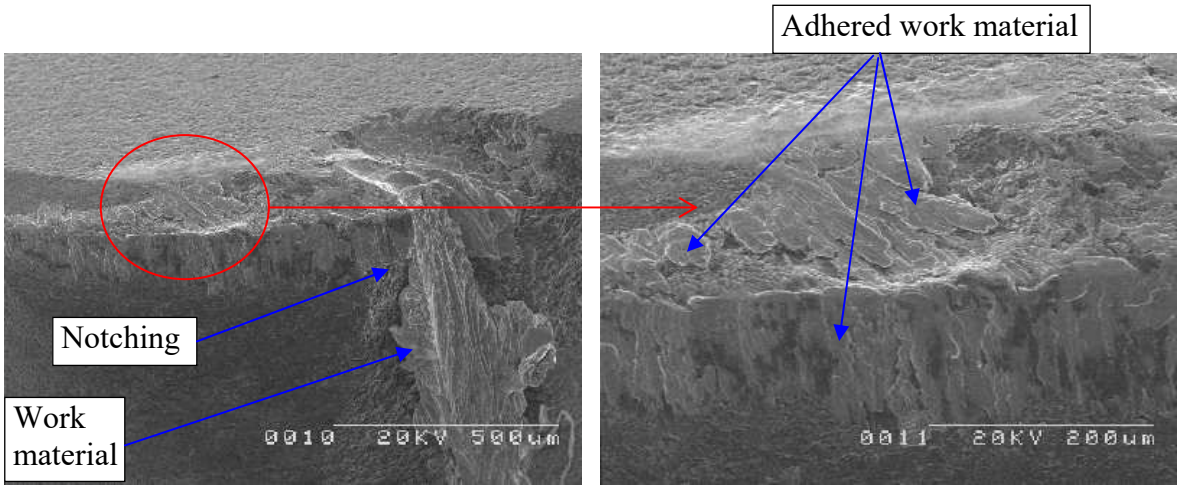

(a) Tool life < 0.5 min (b) Close-up view

Figure 4.101 - (a) Worn PCBN 300 (T8) insert after machining Ti-6Al-4V alloy with 11 MPa coolant pressure at a speed of 150 m min^{-1} and (b) enlarged section of worn surface.

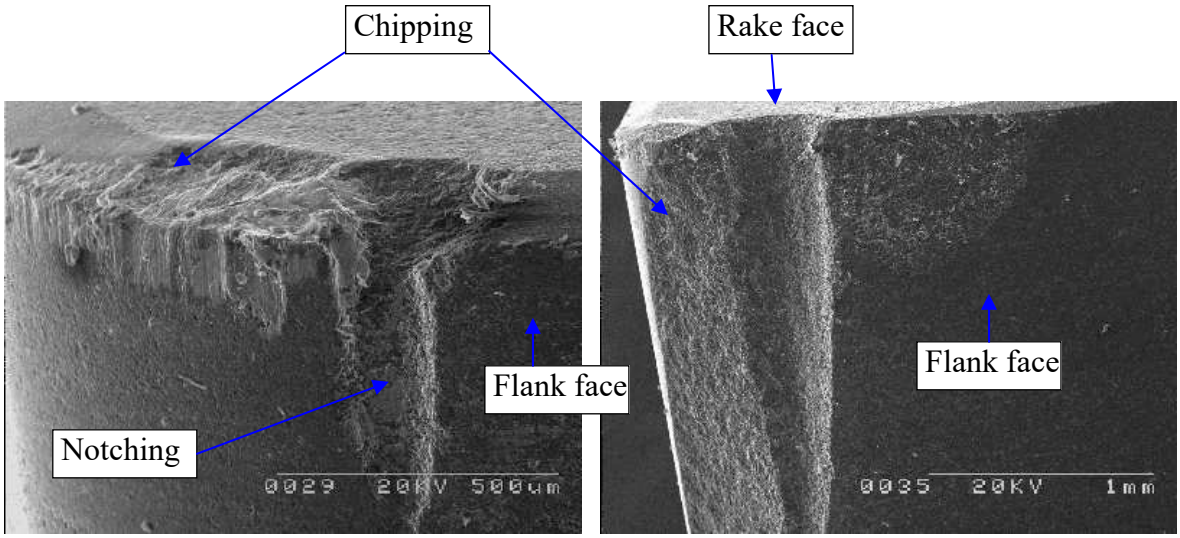

(a) Tool life < 0.3 min (b) Tool life < 0.3 min

Figure 4.102 - Worn PCBN 300 (T8) inserts after machining Ti-6Al-4V alloy with 20.3 MPa coolant pressure at a speed of (a) 200 m min^{-1} and (b) 250 m min^{-1}.

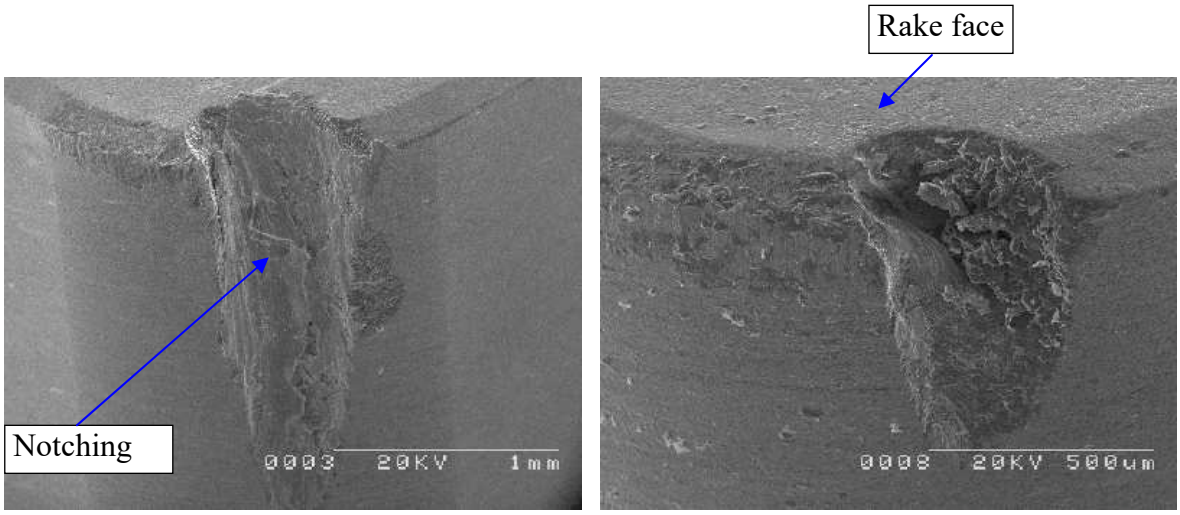

(a) Tool life < 0.2 min (b) Tool life < 0.3 min

Figure 4.103 - Worn PCBN 300-P (T9) inserts after machining Ti-6Al-4V alloy with conventional coolant supply at a speed of (a) 150 m min^{-1} and (b) with 11 MPa coolant pressure at a speed of 250 m min^{-1}.

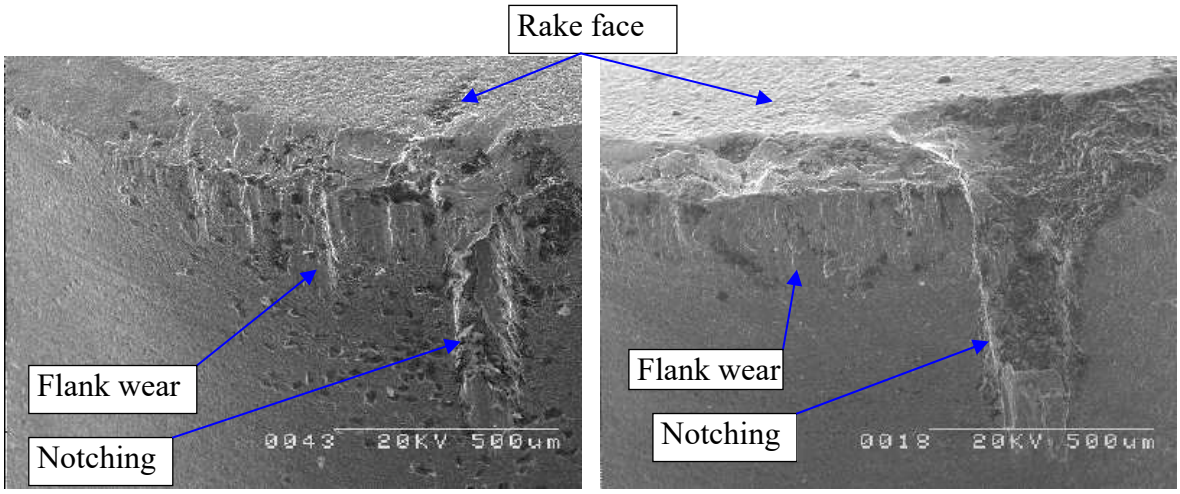

(a) Tool life < 0.3 min (b) Tool life < 0.5 min

Figure 4.104 - Worn PCBN 300-P (T9) inserts after machining Ti-6Al-4V alloy with a 20.3 MPa coolant pressure at a speed of (a) 150 m min^{-1} and (b) 200 m min^{-1}.

4.4.3 Component forces

Figures 4.105 and 4.106 show variations in cutting and feed forces, respectively, recorded at the beginning of cut when machining Ti-6Al-4V alloy with CBN (T7) and PCBN (T8,T9) tools. Figure 4.105 shows that cutting forces generally increase with increase in cutting speed up to 200 m min^{-1} when machining with all the coolant supply pressures investigated. Higher cutting forces were generated when machining with all the CBN/PCBN grades using 11 MPa coolant supply at a cutting speed of 200 m min^{-1}. Figure 4.105 also shows that relatively lower cutting forces were recorded when machining with high pressure coolant supplies at a speed of 250 m min^{-1}. This may be attributed to the severe notching and excessive chipping of the cutting edges as a result of higher temperatures generated at higher speed conditions.

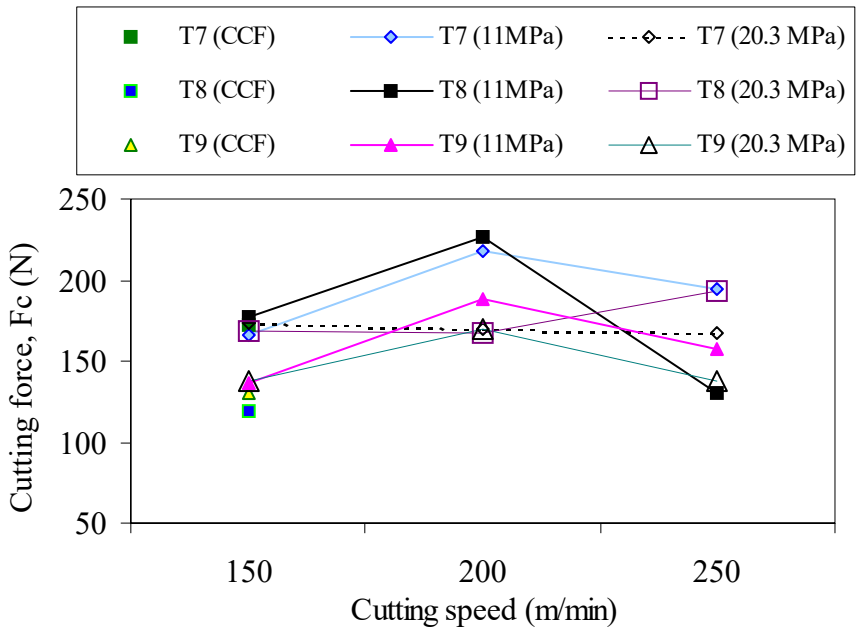

Figure 4.105 - Cutting forces (F*c*) recorded at the beginning of cut when machining Ti-6Al-4V alloy with different CBN/PCBN inserts at various cutting conditions.

Figure 4.106 shows that recorded feed forces were slightly lower than cutting forces at all the cutting conditions investigated. Lower feed forces were generated when machining with conventional coolant flow at the lower cutting speed of 150 m min^{-1} like the cutting forces. Higher feed forces were generated when machining with all the CBN/PCBN insert grades with 11 MPa coolant supply at a cutting speed of 200 m min^{-1}. Feed forces generally increased with increase in cutting speed up to 200 m min^{-1} when machining with all the coolant supply pressures employed.

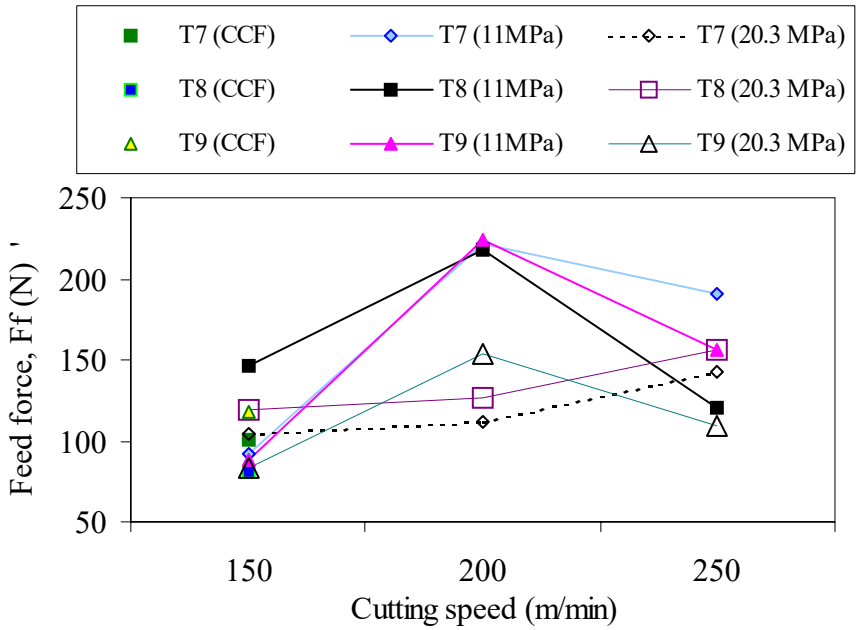

Figure 4.106 - Feed forces (F*f*) recorded at the beginning of cut when machining Ti-6Al-4V alloy with different CBN/PCBN inserts at various cutting conditions.

4.4.4 Surfaces roughness and runout values

Figure 4.107 illustrates the surface roughness values recorded at the end of cut when machining Ti-6Al-4V alloy with CBN/PCBN inserts under various cutting conditions. Higher surface roughness values were recorded when machining with the lower (50 vol.%) CBN content (T7) insert at speeds of 200 m min^{-1} and 250 m min^{-1} using 11 MPa coolant pressure. Surface roughness values increased with increase in cutting speed when machining with T7 tools using 11 MPa coolant pressure. Values recorded when machining with T8 and T9 tools were relatively constant in all the cutting speeds investigated. Figure 4.107 also shows that increase in coolant pressure has negligible effect on the surface roughness values when machining with T8 and T9 tool grades. They varied between 1 and 2 µm.

In general, low runout values well below the stipulated rejection criterion of 100 µm, were recorded when machining Ti-6Al-4V alloy with all the CBN/PCBN tools at the cutting conditions investigated. Figure 4.108 are plots of runout values recorded when machining Ti-6Al-4V alloy with all the CBN/PCBN tools under various coolant supply pressures at a speed of 150 m min^{-1}. The curves show that runout values vary between 5 and 18 µm. Additionally, runout values generally decreased when machining at high pressure coolant supplies. Lower runout values were recorded with the lower (50 vol.%) CBN content (T7) grade than with T8 and T9 insert grades.

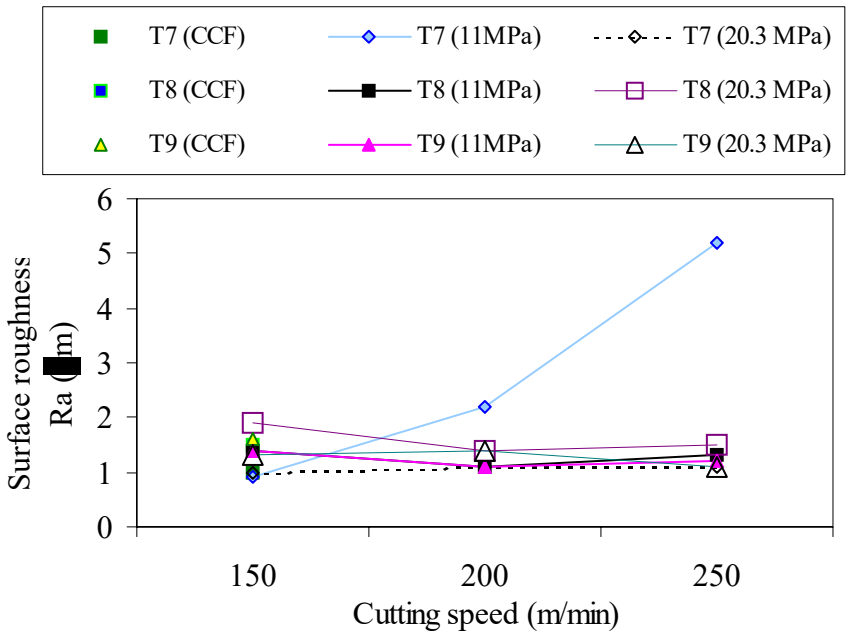

Figure 4.107 - Surface roughness values recorded at the beginning of cut when machining Ti-6Al-4V alloy with CBN/PCBN inserts at various cutting conditions.

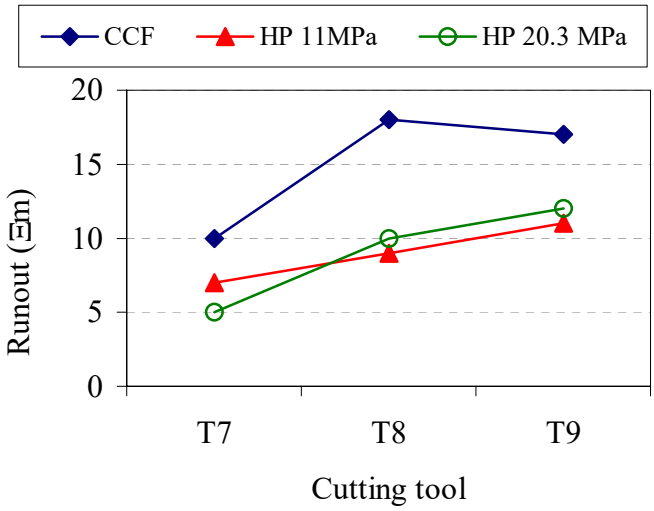

Figure 4.108 – Runout variation recorded at end of cut when machining Ti-6Al-4V alloy with CBN/PCBN inserts using conventional coolant flow and high coolant supply pressures at a speed of 150 m min^{-1}.

4.4.5 Surface hardness and subsurface alteration

Figures 4.109-4.111 are plots of variation of microhardness values with distance below the machined surface of sectioned samples after machining with CBN/PCBN (T7, T8 and T9)

tools with various coolant supply pressures at a cutting speed of 150 m min^{-1}. The plots generally show a regular hardness pattern, i.e. evidence of softening of machined surface up to about 0.15 mm below the top machined surfaces and a uniform distribution of hardness values around the minimum and maximum values of the hardness prior to machining. The plots also suggest that, in general, hardness depth of the machined surface decreased with increasing coolant pressure. Lower microhardness values were recorded when machining with T9 grade under all the coolant supplies.

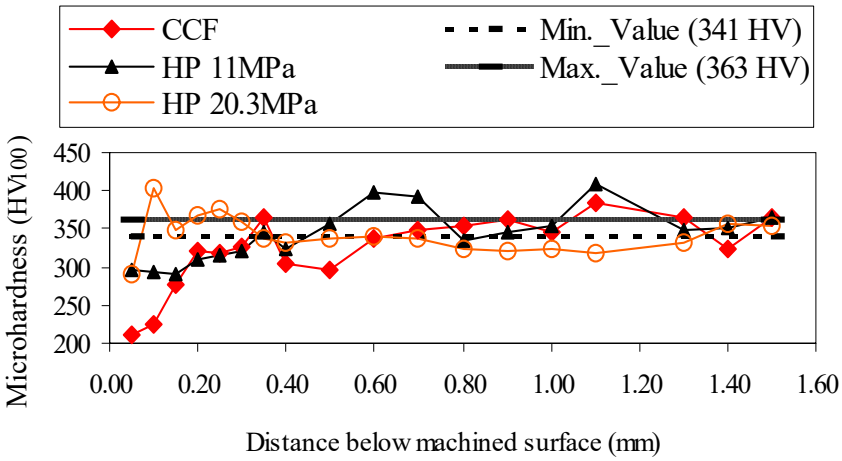

Figure 4.109 - Hardness variation after machining Ti-6Al-4V alloy with PCBN 10 (T7) tools with conventional coolant flow and high coolant supply pressures at a speed of 150 m min^{-1}.

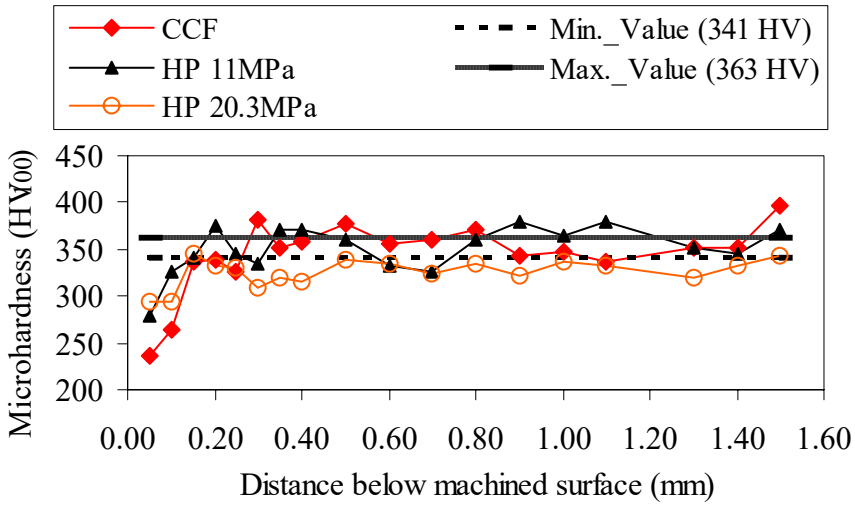

Figure 4.110 - Hardness variation after machining Ti-6Al-4V alloy with PCBN 300 (T8) tools with conventional coolant flow and high coolant supply pressures at a speed of 150 m min^{-1}.

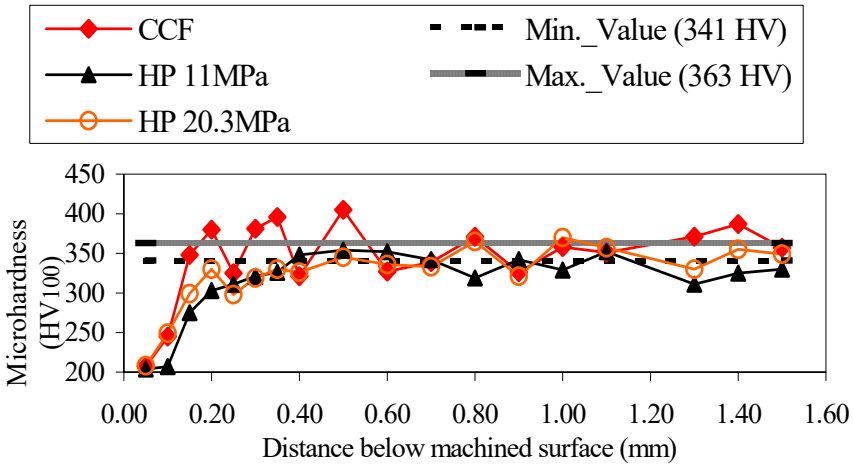

Figure 4.111 - Hardness variation after machining Ti-6Al-4V alloy with PCBN 300-P (T9) tools with conventional coolant flow and high coolant supply pressures at a speed of 150 m min^{-1}.

The microstructure of the etched machined surfaces after machining with CBN/PCBN (T7, T8 and T9) tools using various coolant supply pressures at a cutting speed of 150 m min^{-1} are shown at Figures 4.112-4.114, respectively. These figures exhibit similar characteristics. The well defined grain boundaries show that there is no microstructure alteration in the machined subsurface of the machined surface after machining under the cutting conditions investigated.

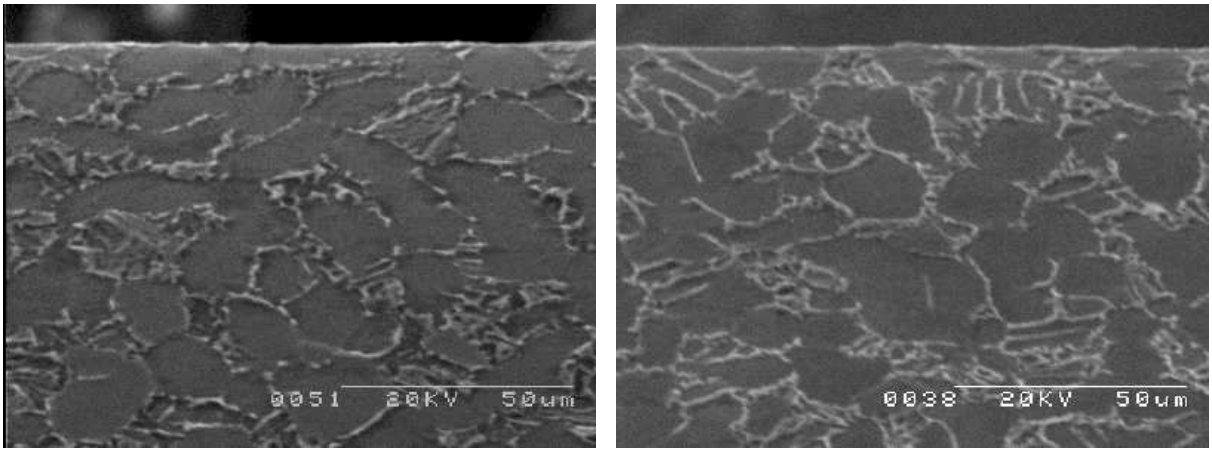

(a) Tool life <1.6 min (b) Tool life < 4 min

Figure 4.112 - Microstructure of Ti-6Al-4V alloy after machining with PCBN 10 (T7) tools with (a) conventional coolant flow and (b) high coolant pressure of 20.3 MPa at a cutting speed of 150 m min^{-1}.

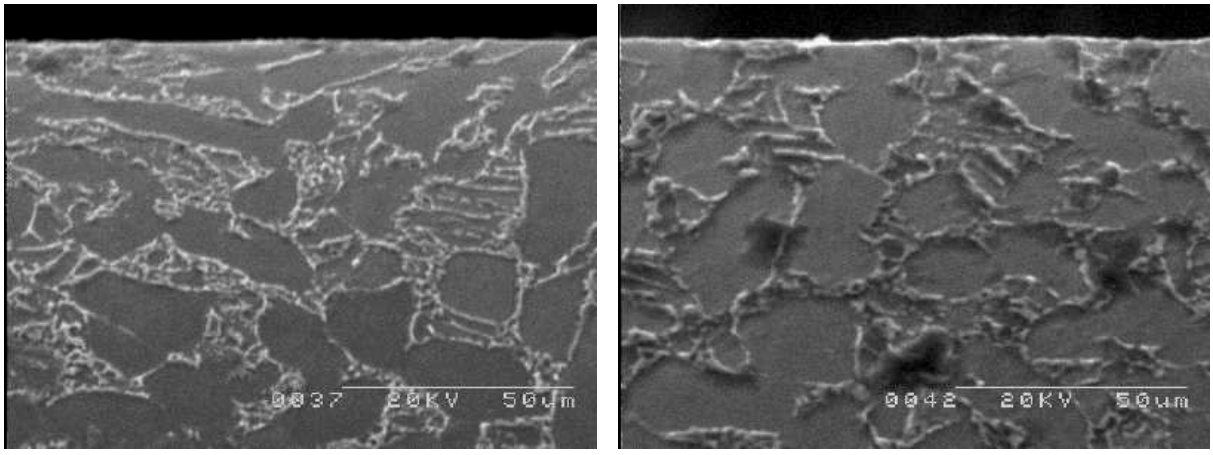

(a) Tool life < 0.5 min (b) Tool life < 0.3 min

Figure 4.113 - Microstructure of Ti-6Al-4V alloy after machining with PCBN 300 (T8) tools at (a) 11 MPa and (b) 20.3 MPa coolant pressure at a cutting speed of 150 m min^{-1}.

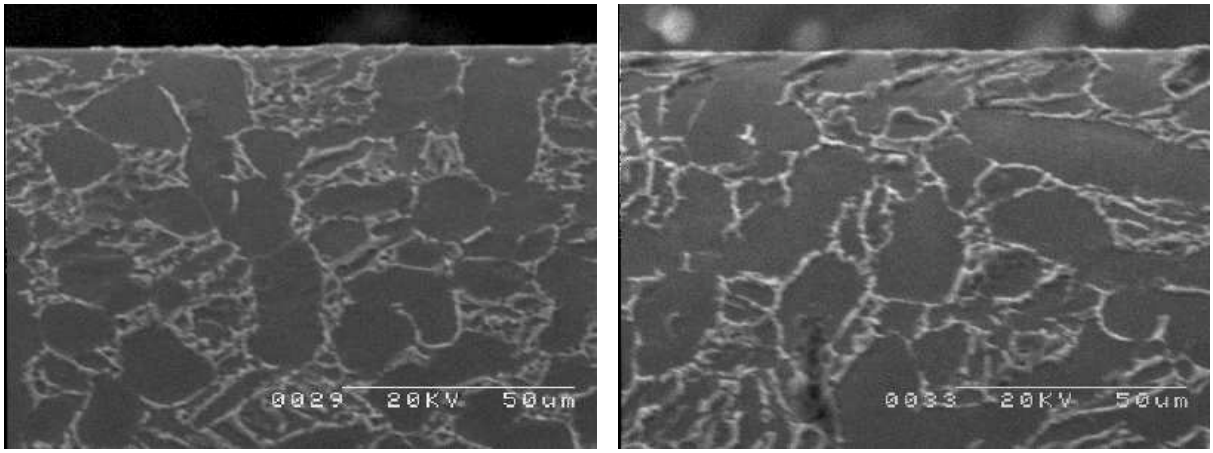

(a) Tool life < 0.2 min (b) Tool life < 0.3 min

Figure 4.114 - Microstructure of Ti-6Al-4V alloy after machining with PCBN 300-P (T9) tools at (a) 11 MPa and (b) 20.3 MPa coolant pressure at a cutting speed of 150 m min^{-1}.

4.4.6 Chips shapes

Figures 4.115 (a)–(g) show different chips generated when machining with CBN/PCBN tools under various coolant supply pressures at a cutting speed of 150 m min^{-1}. These figures show that most of the chips produced during machining Ti-6Al-4V alloy are helical, short and continuous type. These figures also suggest that increasing coolant pressure provided a negligible effect on the nature of swarf produced when machining Ti-6Al-4V alloy with the CBN/PCBN tools. However, machining with the lower (50 vol.%) CBN content (T7) insert

under high pressure coolant supplies produced relatively smaller segmented chips (Figures 4.115 (b)-(c)) compared to T8 and T9 insert grades.

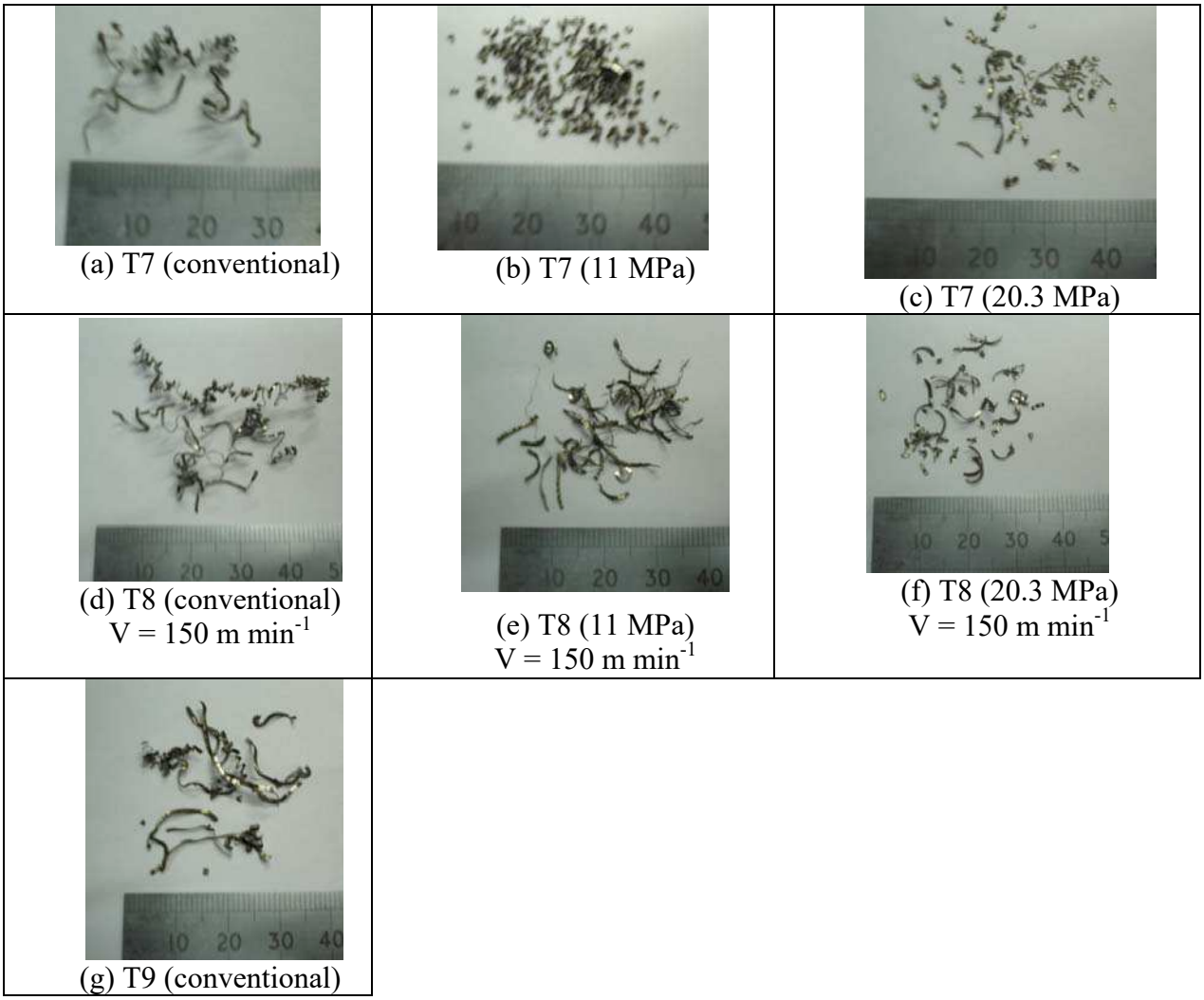

Figure 4.115 - Chips generated when machining Ti-6Al-4V alloy with CBN/PCBN tools with various coolant supplies at a cutting speed of 150 m min^{-1}.

4.5 Machining of Ti-6Al-4V alloy with whisker reinforced ceramic cutting tools under various machining environments

4.5.1. Wear rate and tool life

Figures 4.116 and 4.117 show nose wear rate and tool life, respectively, recorded when machining Ti-6Al-4V alloy with silicon carbide (SiCw) whisker reinforced alumina ceramic - T10 (rhomboid-shaped) and T11 (square-shaped) inserts at various cutting environments.

Note that machining with SiCw ceramic (T10 rhomboid-shaped) inserts with conventional coolant flow was carried out only at a speed of 140 m min^{-1} while machining with SiCw ceramic (T11 square-shaped) inserts were carried out only with conventional coolant flow (CCF) at speeds of 110, 130 and 200 m min^{-1}. Increase in cutting speed generally accelerated tool wear with both T10 and T11 grades of ceramic inserts in all the environments tested, consequently reducing tool life due to a reduction in tool-chip and tool-workpiece contact length and the consequent increase in both normal and shear stresses at the tool tip (GORCZYCA, 1987).

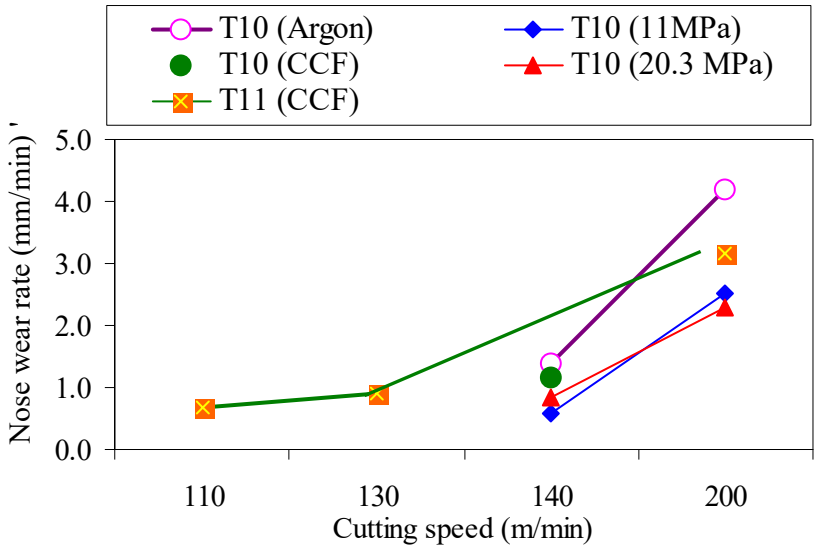

Figure 4.116 - Nose wear curves of silicon carbide (SiCw) whisker reinforced alumina ceramic - rhomboid-shaped (T10) and square-shaped (T11) - inserts after machining Ti-6Al-4V at various cutting conditions.

Figure 4.116 also shows that machining with T10 inserts in the presence of argon gave the highest nose wear rate in all the cutting speeds investigated, hence the worst performance in terms of tool life as illustrated in Figure 4.117 due probably to poor thermal conductivity of argon which tends to accelerate tool wear. Additionally, the poor thermal conductivity of argon can only prevent combustion from taking place during machining and most of the heat generated tends to concentrate at the cutting interface which further accelerates tool wear during machining. It is clear from Figure 4.117 that very low tool life was obtained when machining Ti-6Al-4V alloy with SiCw ceramic (T10 and T11 grades) inserts in all the conditions investigated relative to other cutting tools employed in this study. The longest tool life of 2.7 min was obtained when machining with T10 insert using coolant supply pressure of 11 MPa and at a speed of 140 m min^{-1}. Figures 4.116 and 4.117 also show that machining

under high pressure coolant supplies of 11 MPa and 20.3 MPa resulted to reduced tool wear rate and consequently gave marginal improvement in tool life of T10 grade compared with argon and conventional coolant supply. Machining with 20.3 MPa coolant pressure gave slightly lower tool life than when machining with 11MPa coolant pressure. This can be attributed to the physical phenomenon observed when the critical coolant pressure is exceeded (PIGOTT; COLWELL, 1952). The optimum coolant pressure appears to have a relationship with the total heat generated during machining (NAGPAL; SHARMA, 1973). It can also be seen from Figures 4.116 and 4.117 that machining Ti-6Al-4V alloy with square-shaped ceramic (T11) inserts exhibited inferior performance in terms of tool life than rhomboid-shaped ceramic (T10) inserts in all the conditions investigated.

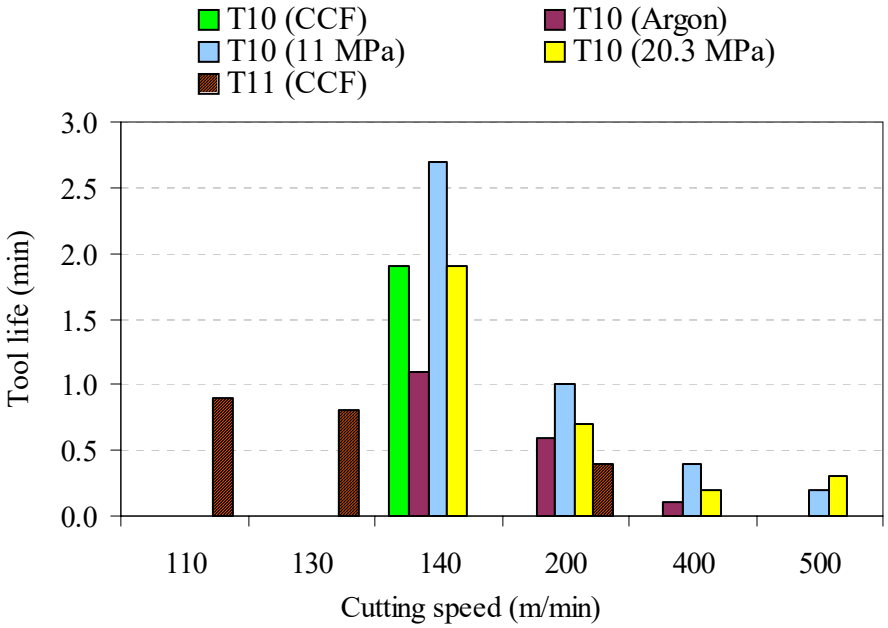

Figure 4.117 - Tool life (nose wear, VC ≥ 0.3 mm or VN ≥ 0.6 mm) recorded when machining Ti-6Al-4V alloy with silicon carbide (SiCw) whisker reinforced alumina ceramic - rhomboid-shaped (T10) and square-shaped (T11) - inserts at various cutting conditions.

Ceramic tools generally exhibit lower fracture toughness than carbides and PCD tools in addition to poor thermal and mechanical shock resistance. Additionally, ceramic tools have high reactivity with titanium alloys. Typical wear patterns observed when machining titanium alloys with ceramic cutting tools are notching and chipping of the cutting edge. Figures 4.118 (a)-(f) and 4.119 (a)-(b) are selected micrographs of worn SiCw reinforced alumina ceramic tools, T10 and T11 grades respectively, after machining Ti-6Al-4V alloy under various cutting conditions. Severe nose wear rate is the dominant failure mode observed when machining with SiCw ceramic tools, especially with T10 insert at lower speed of 140 m min^{-1}

and with T11 insert at lower speed of 130 m min^{-1}, Figures 4.118 and 4.119, respectively. Grooves can be clearly seen on the Figures 4.118 (a)-(f) and 4.119 (a), suggesting that SiCw ceramics tools experienced mechanically related wear mechanism(s) mainly on the flank face, illustrated as parallel ridges on flank faces. Severe chipping was also observed after machining with T11 tool at cutting speed of 200 m min^{-1}, as illustrated in Figure 4.119 (b).

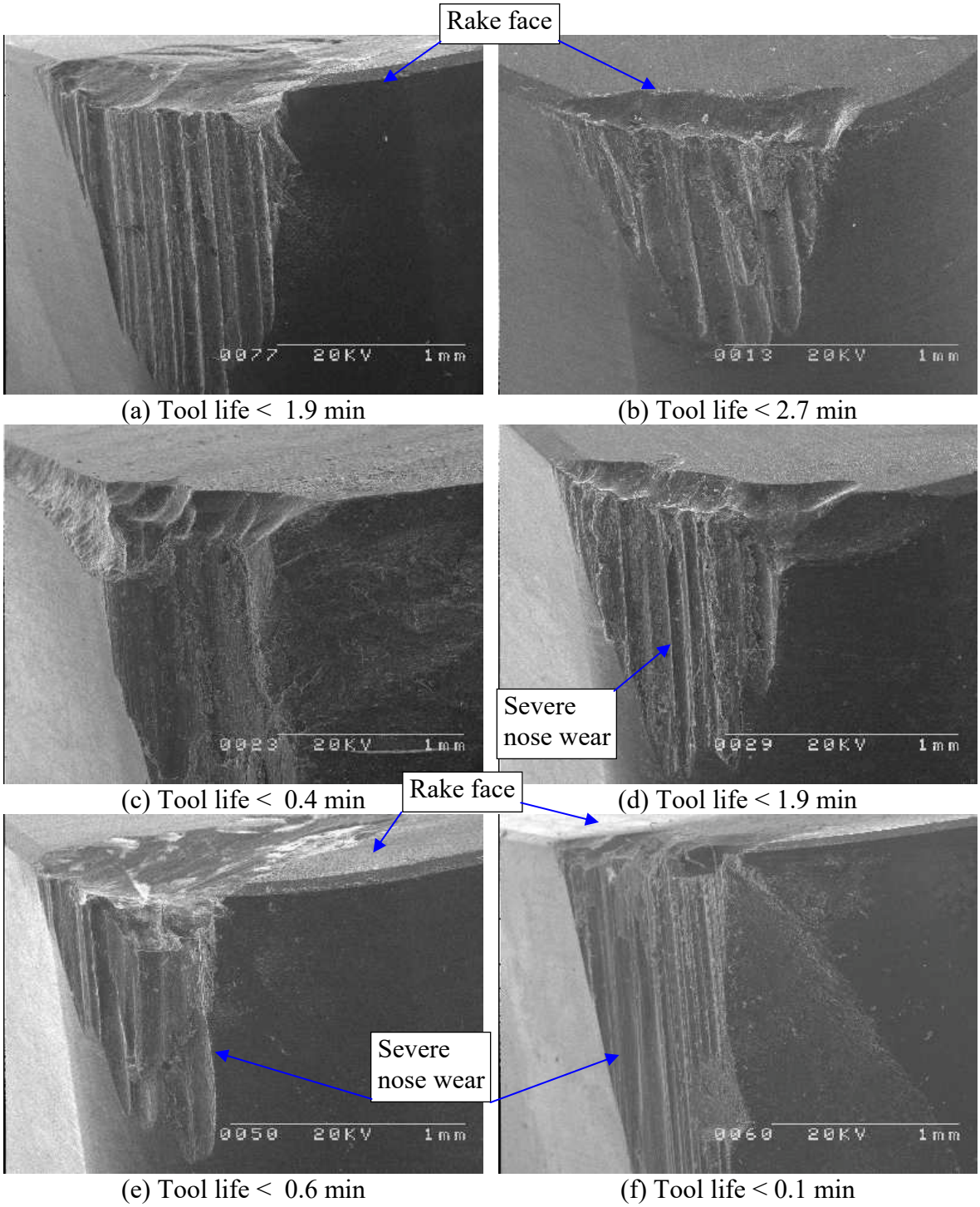

(a) Tool life < 1.9 min (b) Tool life < 2.7 min

(c) Tool life < 0.4 min (d) Tool life < 1.9 min

(e) Tool life < 0.6 min (f) Tool life < 0.1 min

Figure 4.118 - Wear observed on rhomboid-shaped SiCw alumina ceramic (T10 grade) insert after machining Ti-6Al-4V alloy with conventional coolant supply at a speed of (a) 140 m min^{-1}; coolant pressure of 11 MPa at speeds of (b) 140 m min^{-1} and (c) 400 m min^{-1}, coolant pressure of 20.3 MPa at a speed of (d) 140 m min^{-1}, and in an argon enriched environment at speeds of (e) 200 m min^{-1} and (f) 400 m min^{-1}.

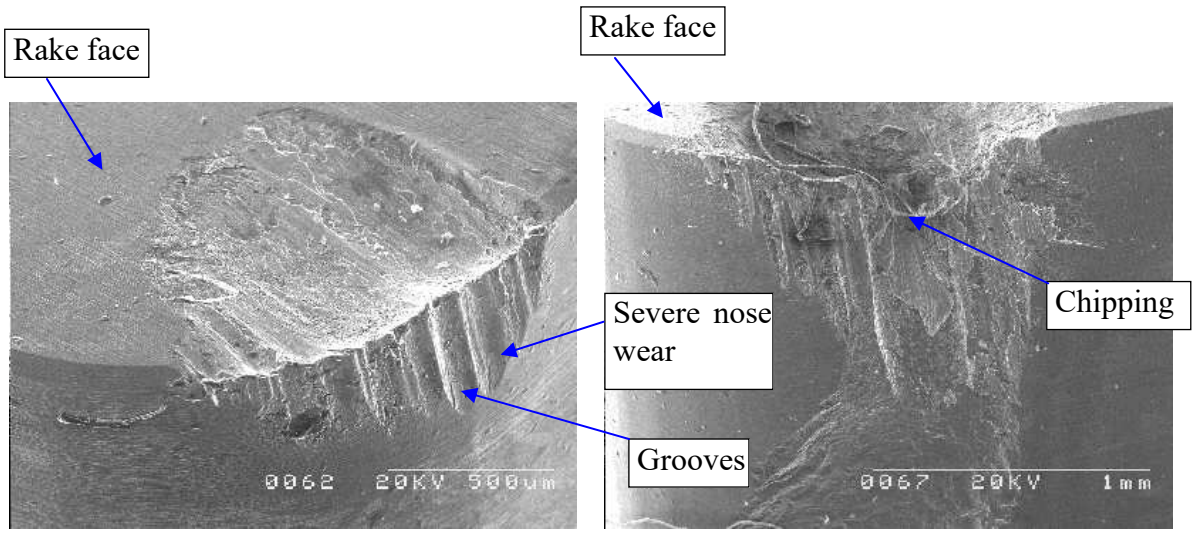

(a) Tool life < 0.8 min (b) Tool life < 0.4 min

Figure 4.119 - Wear observed on square-shaped SiCw alumina ceramic (T11 grade) insert after machining Ti-6Al-4V alloy with conventional coolant supply at speeds of (a): 130 m min^{-1} and (b): 200 m min^{-1}.

4.5.2 Component forces

Figures 4.120 and 4.121 are plots of cutting forces and feed forces, respectively, recorded at the beginning of cut when machining Ti-6Al-4V alloy with SiCw whisker reinforced alumina ceramic (T10 and T11) inserts at various cutting speeds and under various machining environments. Note that cutting and feed forces generated with T10 inserts were recorded only in presence of argon and with high pressure coolant supplies because negligible tool life was generated when machining with conventional coolant flow. This machining time was not enough to record component forces with the methodology employed. It can be seen that recorded cutting forces are higher than feed forces, as expected. Higher cutting forces were generated using T10 insert when machining with high pressure coolant supplies due probably to higher wear rates. Figure 4.120 also shows that cutting forces recorded with T10 insert generally decreased with increasing cutting speed up to a speed of 400 m min^{-1} in all the machining environments, unlike when machining with T11 tool grade with conventional coolant flow. Figure 4.121 also shows that higher feed forces were generated when machining with high pressure coolant supplies. Feed forces generally increased with increasing cutting speed when machining with high pressure coolant supplies and reduced with increase speed when machining in argon environment. The lowest feed forces were recorded when machining in presence of argon.

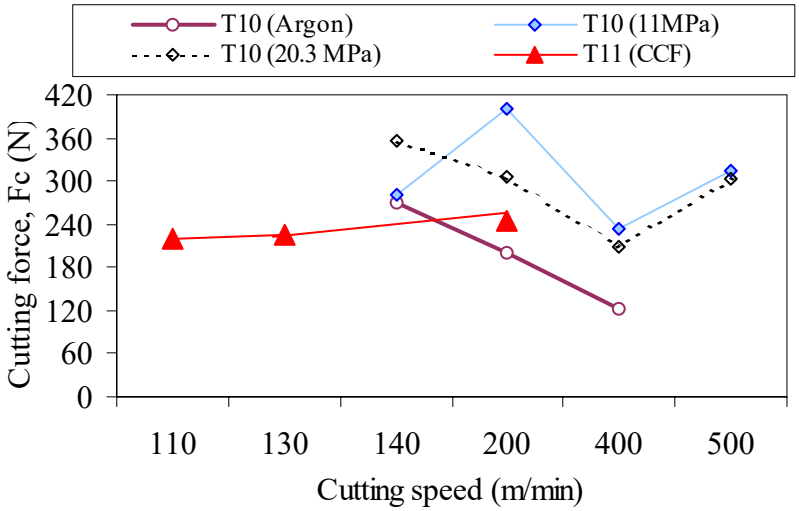

Figure 4.120 - Cutting forces (F*c*) recorded at the beginning of cut when machining Ti-6Al-4V alloy with SiCw alumina ceramic (T10 and T11) inserts at various cutting conditions.

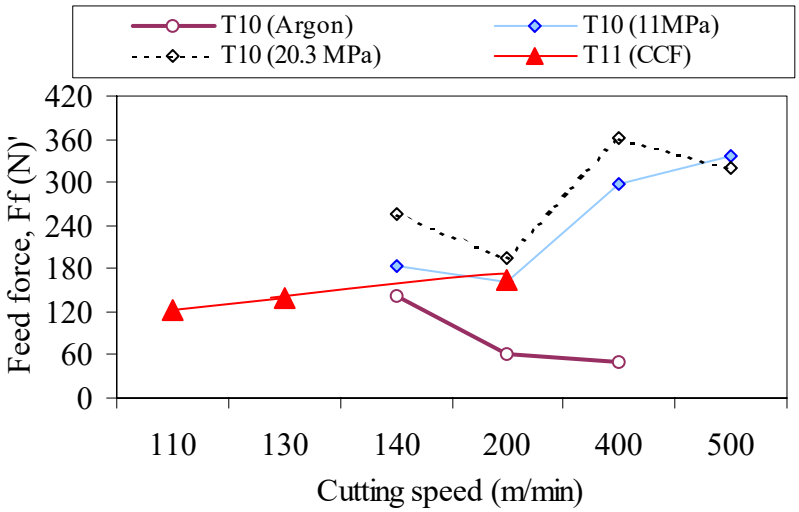

Figure 4.121 - Feed forces (F*f*) recorded at the beginning of cut when machining Ti-6Al-4V alloy with SiCw alumina ceramic inserts (T10 and T11) at various cutting conditions.

4.5.3 Surfaces roughness

Figure 4.122 shows recorded surface roughness values when machining Ti-6Al-4V alloy with SiCw whisker reinforced alumina ceramic (T10 and T11) inserts at various cutting speeds and with T10 inserts with various machining environments. Note that surface roughness obtained when machining under conventional coolant flow and in presence of argon were recorded only at cutting speeds of 140 m min^{-1} and 200 m min^{-1}, respectively, because at other cutting conditions the areas of machined surfaces generated were not enough

to measure surface roughness. It can be seen that surface roughness values recorded when machining with T10 inserts using coolant supply pressures of 11 MPa and 20.3 MPa generally increase with increase in cutting speed up to 400 m min^{-1}. Surface roughness values also increased with increasing in cutting speed when machining with T11 insert using conventional coolant flow. Curves in Figure 4.122 also shows that higher surface roughness values (between 2.1 µm and 5.5 µm) were recorded with conventional coolant flow and high pressure coolant supplies of 11 MPa and 20.3 MPa which are well above the stipulated rejection criterion of 1.6 µm.

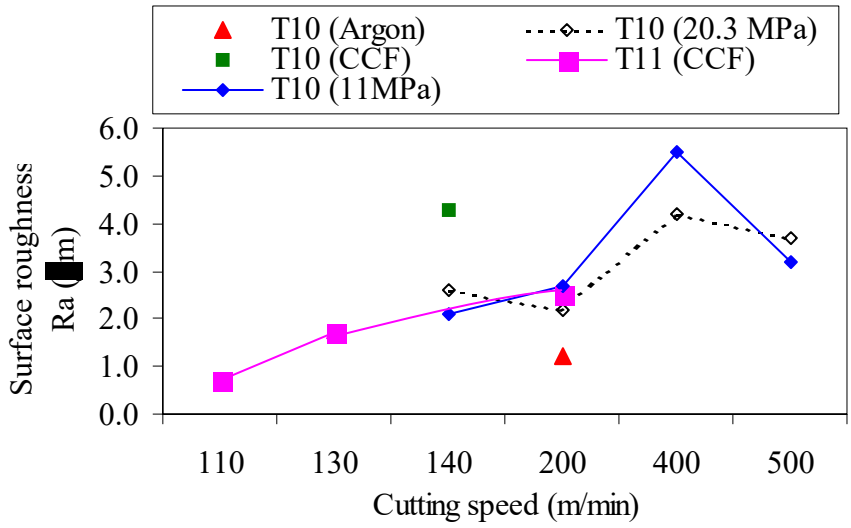

Figure 4.122 - Surface roughness values recorded at the beginning of cut when machining Ti-6Al-4V alloy with SiCw alumina ceramic inserts (T10 and T11) at various cutting conditions.

4.5.4 Surface hardness and subsurface alterations

Figure 4.123 illustrates the variations of microhardness values recorded from the machined surfaces, up to about 1.0 mm below the top surface, after machining with silicon carbide (SiCw) whisker reinforced alumina (T10) ceramic tool using various machining environments and at a cutting speed of 140 m min^{-1}. The plots suggest a softening of the machined surface up to a distance of the about 0.7 mm below the machined surface when machining with conventional coolant supply. The plots also show evidence of hardening when machining with the coolant pressure of 20.3 MPa.

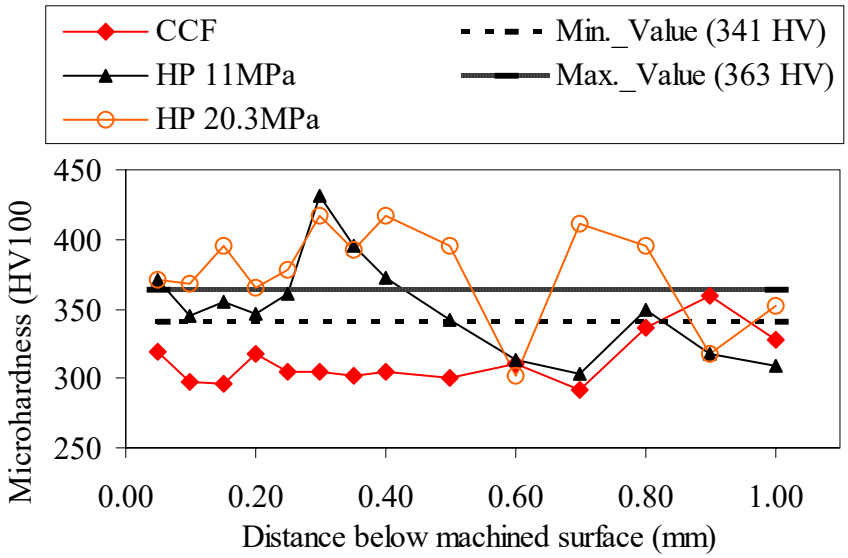

Figure 4.123 - Hardness variation after machining Ti-6Al-4V alloy with rhomboid-shaped SiCw alumina ceramic insert (T10 grade) at various environments and at a speed of 140 m min^{-1}.

Figures 4.124 (a)-(c) are microstructures of etched machined surfaces of Ti-6Al-4V alloy after machining with silicon carbide (SiCw) whisker reinforced alumina (T10) ceramic tool using conventional coolant flow, high pressure coolant supplies of 11 MPa and 20.3 MPa, respectively, at a cutting speed of 140 m min^{-1}. These figures show well defined grain boundaries without microstructure alteration in the machined subsurface of machined surfaces.

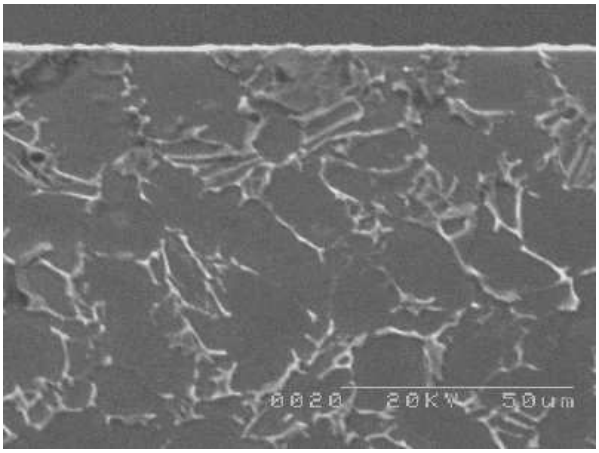

(a) Tool life <1.9 min

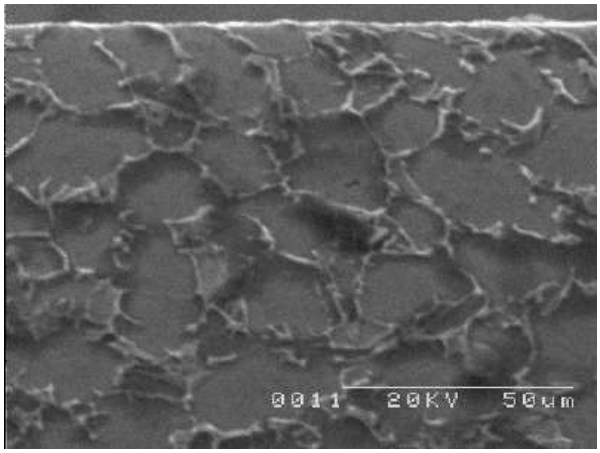

(b) Tool life < 2.7 min

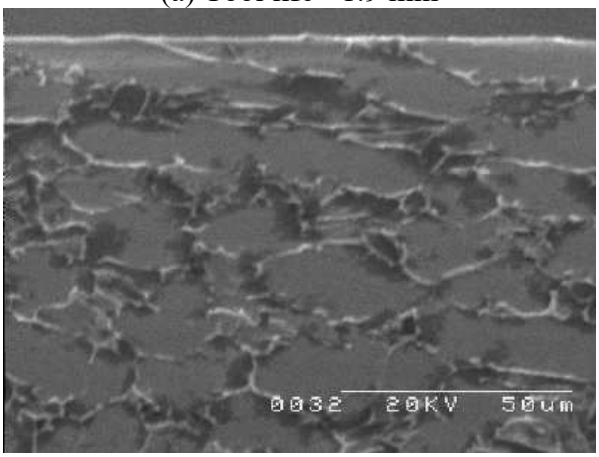

(c) Tool life < 1.9 min

Figure 4.124 - Microstructure of Ti-6Al-4V alloy after machining with SiCw alumina ceramic tool (T10 grade) under: (a) conventional coolant flow, (b) coolant pressure of 11 MPa and (c) coolant pressure of 20.3 MPa at a cutting speed of 140 m min^{-1}.

4.5.5 Chips shapes

Figures 4.125 (a)–(f) show the types of chips generated when machining with SiCw alumina ceramic (T10 and T11) inserts at various cooling environments. Note that Figures 4.125 (a)-(c) show chips produced when machining with T10 insert at a cutting speed of 140 m min^{-1} and Figures 4.125 (d)-(e) show chips produced when machining with T11 insert at cutting speeds of 130 and 200 m min^{-1}, respectively. Three types of chips were produced when machining with various machining environments investigated. Machining with T10 tool with conventional coolant flow and in presence of argon produced snarled type chips (Figures 4.125 (a) and (b), respectively) while either short continuous tubular chips and segmented type chips were produced when machining with high pressure coolant supply of 11 MPa.

Snarled type chips were also produced when machining with T11 insert in all the conditions investigated, as illustrated in Figures 4.125 (d)-(e).

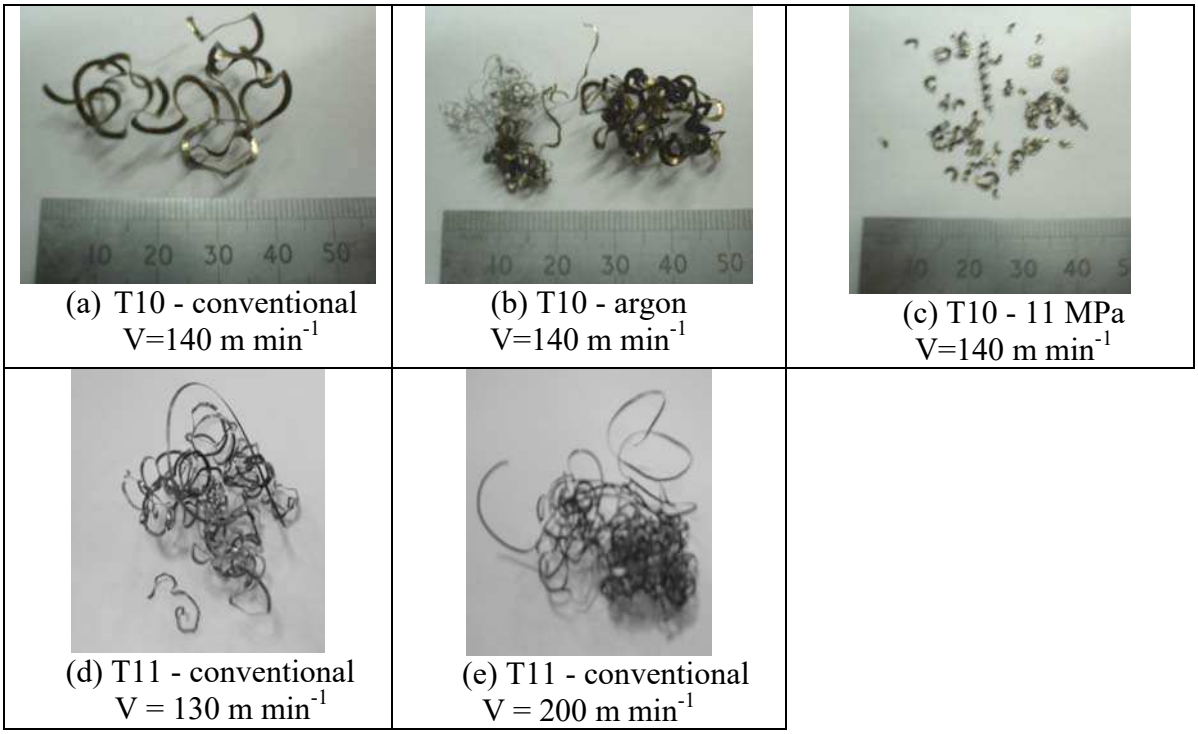

(a) T10 - conventional V=140 m min^{-1}

(b) T10 - argon V=140 m min^{-1}

(c) T10 - 11 MPa V=140 m min^{-1}

(d) T11 - conventional V = 130 m min^{-1}

(e) T11 - conventional V = 200 m min^{-1}

Figure 4.125 - Chips generated when machining Ti-6Al-4V alloy with SiCw alumina ceramic inserts: T10 grade at a cutting speed of 140 m min^{-1} under: (a) conventional coolant flow, (b) argon enriched environment, (c) coolant pressure of 11 MPa; T11 grade with conventional coolant flow at cutting speeds of: (d) 130 m min^{-1} and (e) 200 m min^{-1}.

4.6 Machining of Ti-6Al-4V alloy with Nano-ceramic cutting tools

4.6.1. Wear rate and tool life

Figures 4.126 and 4.127 show notch wear rate and tool life recorded when machining Ti-6Al-4V alloy with nano-grain size (T12 and T13) ceramic tools with conventional coolant flow and at various cutting speeds. Increase in cutting speed generally accelerated tool wear, consequently reducing tool life, as expected, due to a reduction in tool-chip and tool-workpiece contact lengths and the consequent increase in both normal and shear stresses at the tool tip. Machining with the Al_2O_3 base T12 tools gave higher wear rate when machining at a cutting speed of 110 m min^{-1}. The Si_3N_4 base nano-grain T13 tool gave the lowest tool

wear rate. T13 tool, however, gave better tool life at a speed of 130 m min^{-1}. Figure 4.127 shows that the nano-grain size tools gave poor performance, in terms of tool life, compared to other cutting tools (cemented carbides, PCD, and CBN/PCBN tools) when machining Ti-6Al-4V alloy at the conditions employed. It is clear from the machining results that improved properties of the nanoceramic tools have negligible effect on tool performance. This suggests that tool performance is more chemically and/or thermally related.

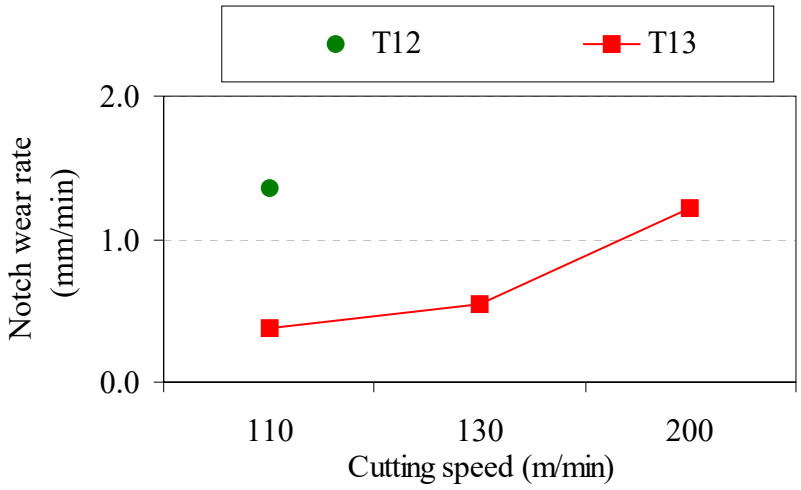

Figure 4.126 - Notch wear rate when machining Ti-6Al-4V alloy with T12 and T13 nano-grain size ceramics tools, Al_2O_3 and Si_3N_4 base respectively, with conventional coolant flow and at various speed conditions

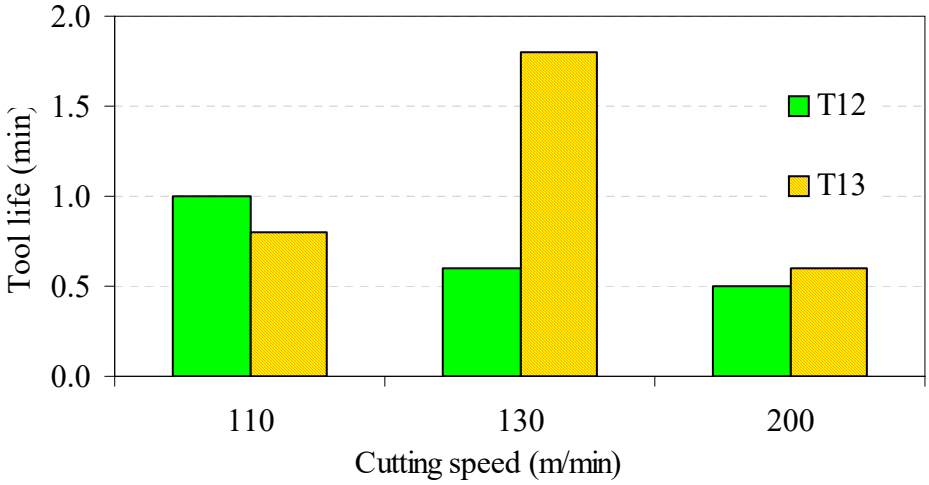

Figure 4.127 - Recorded tool life (VN ≥ 0.6 mm) when machining Ti-6Al-4V alloy with nano-grain size ceramics tools (T12 and T13) with conventional coolant flow and at various cutting speeds.

Figure 4.128 (a)-(d) are typical wear on the worn nano-grain size ceramic tools after machining Ti-6Al-4V alloy using conventional coolant flow at various cutting speeds. Examination of the worn cutting edges revealed irregular/unevenly worn rake faces (Figure 4.128 (a), (b) and (c). Notching which often lead to catastrophic tool failure occurred when machining with the Al_2O_3 base nano-grain T12 tool at speeds in excess of 110 m min^{-1} (Figure 4.128). Severe chipping was also observed after machining with T12 inserts at cutting speed of 200 m min^{-1}, Figure 4.128 (b). This type of wear occurs in a purely random manner and cannot be predicted. Notch wear at the depth of cut can be observed in Figures 4.128 (a) and (d). These appear to be mainly formed by a type of fracture process.

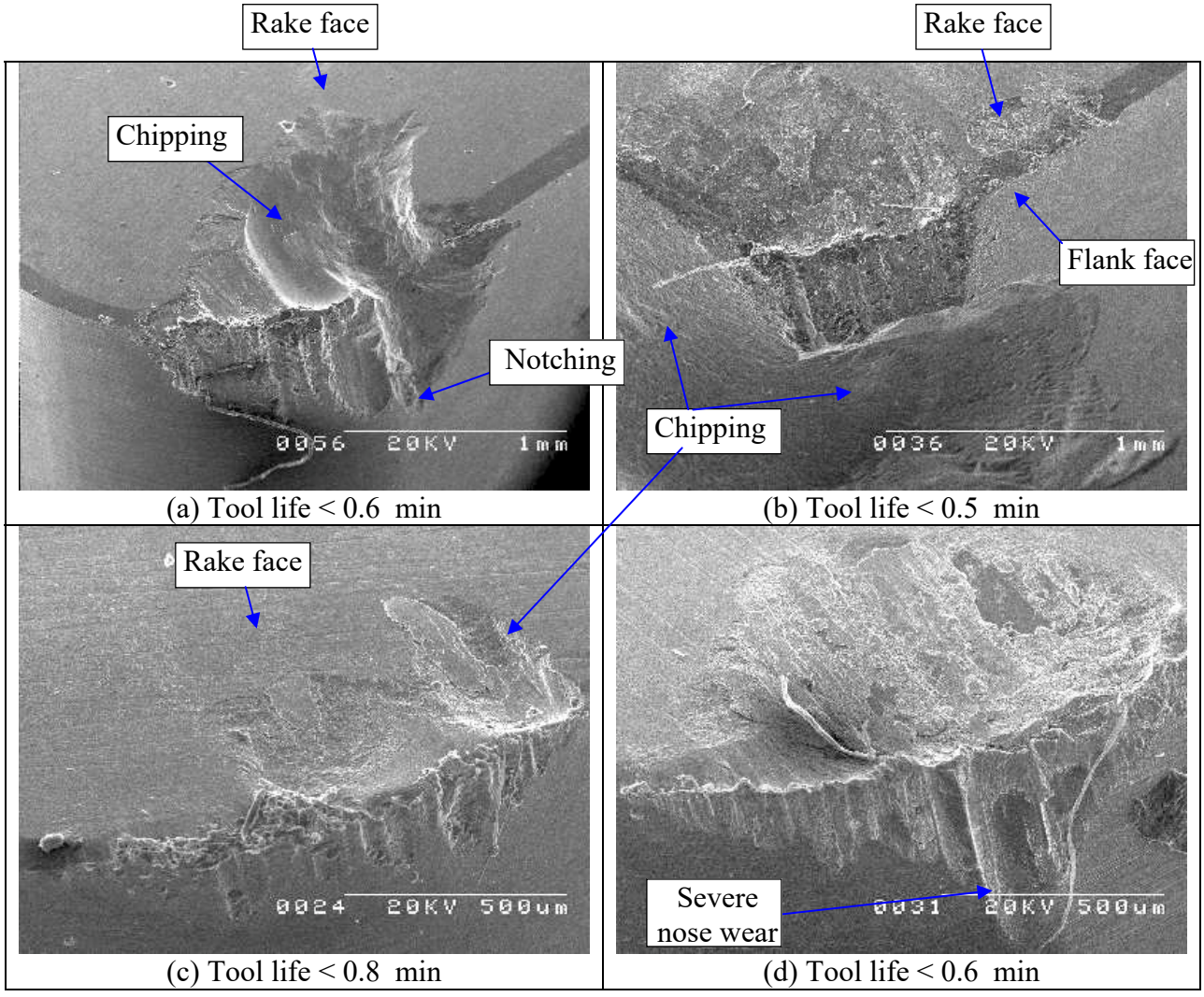

Figure 4.128 - Wear observed on nano-ceramic tools after machining with Ti-6Al-4V alloy at different cutting speeds: T12 (a: 130 m min^{-1}), (b: 200 m min^{-1}); T13 (c: 110 m min^{-1}) and (d: 200 m min^{-1}).

4.6.2 Component forces

Figure 4.129 shows variation of component forces (cutting forces and feed forces) with cutting speed up to 200 m min^{-1} recorded after 30 seconds of machining time when machining Ti-6Al-4V alloy with nano-grain size (T12 and T13) ceramic tools with conventional coolant flow. It is clear from Figure 4.129 that cutting forces generated were higher than feed forces when machining with both grades of ceramic tools in all the conditions investigated. The component forces generated increased with increasing cutting speed. This may be attributed to the very high wear rate of the ceramic tools (Figure 4.128). This tends to increase frictional forces during machining and the consequent loss/blunting of the sharp cutting edge.

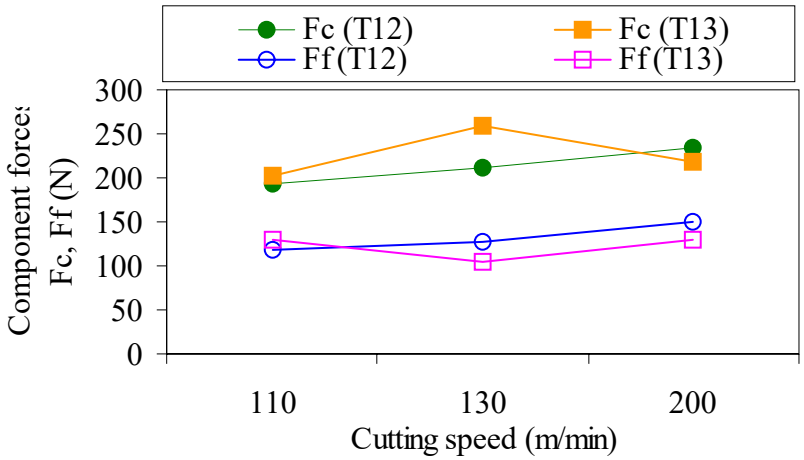

Figure 4.129 - Component forces (cutting forces: F*c* and feed forces: F*f*) recorded at the beginning of cut when machining Ti-6Al-4V alloy with T12 and T13 tools with conventional coolant flow.

4.6.3 Surfaces roughness and runout values

Figure 4.130 and 4.131 are the surface roughness and runout values, respectively, recorded when machining Ti-6Al-4V alloy with nano-grain size (T12 and T13) ceramic tools under conventional coolant flow and at various cutting speeds. Figure 4.130 clearly shows that surface roughness values recorded are above the stipulated rejection criterion of 1.6 µm due to severe wear on the tools. Increase in cutting speed when machining with Si_3N_4 base nano-grain T13 tool grade had a negligible effect on the surface finish generated. Figure 4.130 also shows that high surface roughness values of 12.5 µm and 7.5 µm were recorded when machining with the alumina base nano-ceramic T12 tool at cutting speeds of 130 and 200 m min^{-1}, respectively.

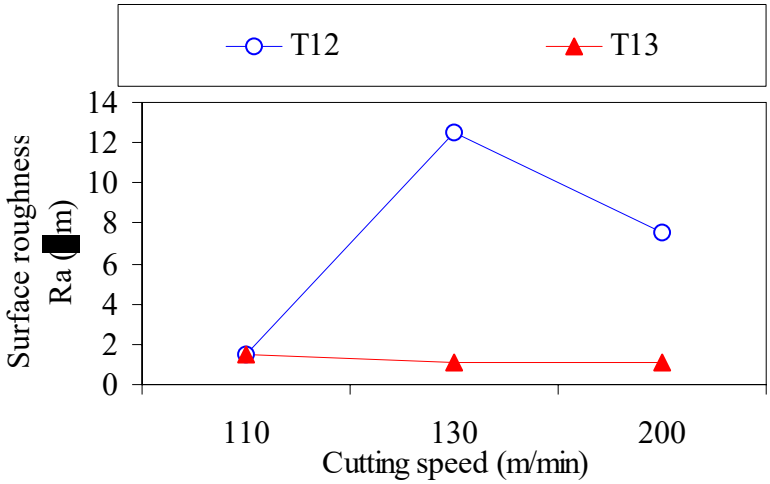

4.130 - Surface roughness values at the beginning of cut when machining Ti-6Al-4V alloy with nano-ceramic (T12 and T13) tools with conventional coolant flow.

Figure 4.131 is a plot of the runout variation with speed when machining with nano-grain size (T12 and T13) ceramic tools under conventional coolant flow. It can be seen that runout values increased with increasing cutting speed for both tool grades investigated. The silicon nitride base (T13) nano-grain size tool gave the lowest runout value of 7μm while the alumina base nano-grain (T12) tool grade gave the highest runout values, rising to 20 μm at the higher speed conditions of 200 m min^{-1}. It should be noted that machining with nano-grain ceramic inserts gave the highest runout values related to other tool grades investigated.

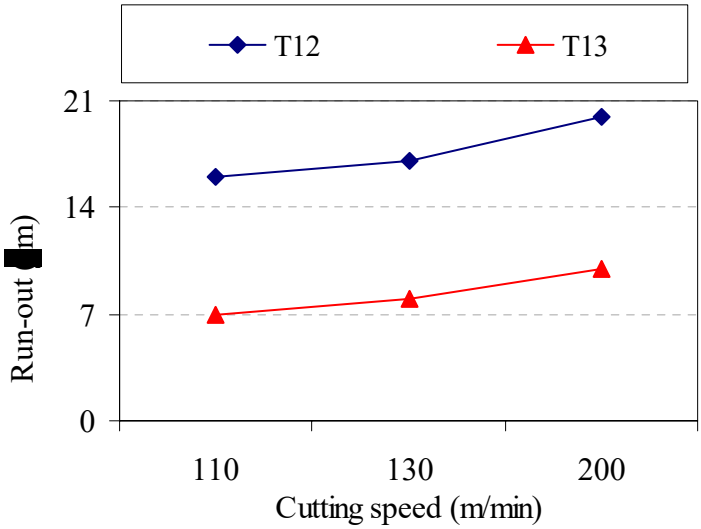

Figure 4.131 – Runout values recorded at the end of cut when machining Ti-6Al-4V alloy cut with nano-ceramic (T12 and T13) tools with conventional coolant flow

4.6.4 Chips shapes

Figures 4.132 (a)–(d) show chips generated when machining with nano-grain size (T12 and T13) ceramic tools with conventional coolant flow and at various cutting speeds. These figures show that machining with nano (T12 and T13) ceramic tool generally produced snarled type chips in all the speed conditions investigated.

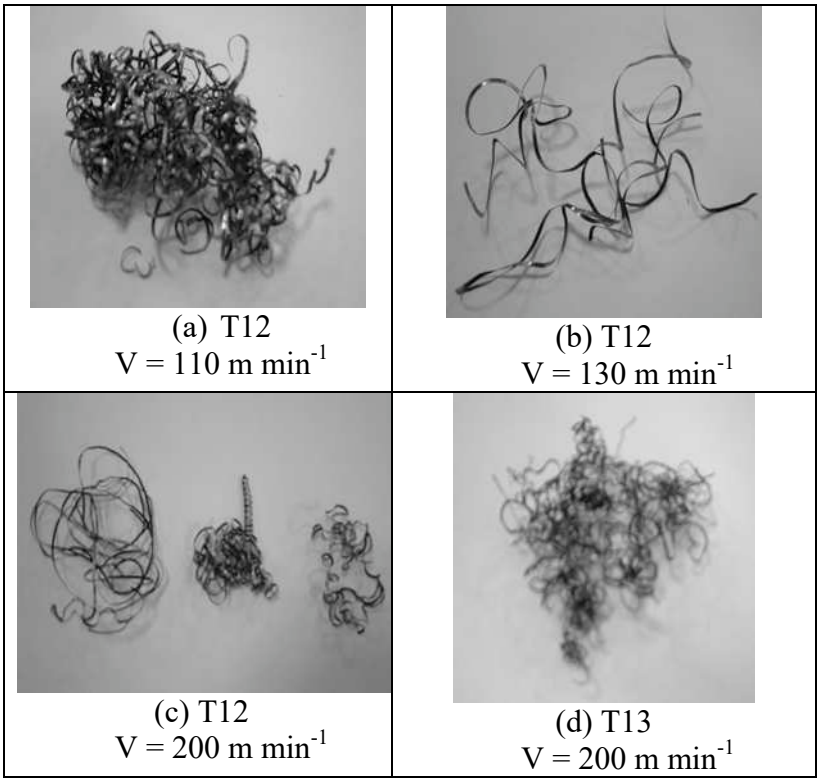

Figure 4.132 - Chips generated when machining Ti-6Al-4V alloy with nano-ceramic tools: T12 (a): 110 m min^{-1}, b: 130 m min^{-1} and c: 200 m min^{-1}); T13 (d: 200 m min^{-1})

CHAPTER V

DISCUSSIONS

5.1 Introduction

As commented previously in Section 1.1 the main objective of this project is to achieve significant reduction in cost of manufacturing jet engines by selecting the best combination of cutting tool; cutting environment; cutting conditions for machining Ti-6Al-4V alloy. This chapter will discuss the experimental results obtained when machining Ti-6Al-4V alloy with various cutting tools (carbides, PCD, CBN and ceramics tool materials) under various machining conditions. Effects of cutting tool material, machining environment such as argon and with cutting fluid delivered at different pressures as well as machining variable such as the cutting speed on the tool life, surface finish and surface damage of the machined workpiece were also investigated.

5.2 Tool performance when machining Ti-6Al-4V alloy with different grades of carbide, PCD, CBN and ceramic tools

5.2.1 Carbides tools

It can be seen from Figures 4.2, 4.59, 4.95, 4.117, 4.127 that increase in cutting speed generally decreased tool life of all the cutting tool materials (T1-T13) investigated in this thesis, as expected, due to a reduction in tool-chip and tool-workpiece contact lengths and the consequent increase in both normal and shear stresses at the tool tip (GORCZYCA, 1987). Reduction in tool-chip and tool-workpiece contact areas also tends to concentrate the high temperature generated to a relatively smaller area as well as shifting the highest temperature

closer to the cutting edge. This phenomenon combines with higher stresses acting at the cutting edge to promote the softening of the cutting tool, and consequently accelerating wear processes and lowering tool life.

Tool life results obtained when machining with cemented carbides (T1,T2,T3,T4) are shown in Figure 4.2. T1 (uncoated grade) and T4 (coated grade) inserts, which have the same substrate composition with slightly coarser grain size and higher hardness than T2 (uncoated grade) and T3 (coated grade) inserts (Table 3.3), gave the best performance in terms of tool life in all conditions investigated relative to T2 and T3 insert grades with the same substrate composition, hardness and substrate grain size. This may be attributed to the substrate grain size and chemical composition. The substrate grain size of T2 and T3 inserts is 0.68 μm, which is smaller than the substrate grain size of T1 and T4 inserts (Table 3.3). As previously stated, hot compressive strength of cemented carbides depends on a combination of the Co binder concentration and the WC particle size (LEE (1981), DEARNLEY; GREARSON (1986), SZESZULSKI; THANGARAJ; WEINNMANN (1990)). The binding metal (Co) easily dissolves in titanium thus carbides containing only small amounts of cobalt should be used. On other hand, a lower Co content leads to reduced toughness/rigidity of the cutting edge. The most favourable compromise between a limited Co content and adequate rigidity of the cutting edge for machining titanium is found in the carbides of the ISO K10 and K20 grades (DEARNLEY; GREARSON, 1986). Influence of grain sizes on wear resistance of carbides tools was investigated by Mari and Gonseth (1993) that attributed the higher resistance to deformation of carbide tool at higher temperature to the coarser grain size. In other studies (JAWAID; CHE-HARON; ABDULLAH (1999), CHE-HARON (2001)) lower flank wear rate of carbide tools, hence longer tool life, is achieved with grain size of 1.0 μm compared to finer grain size of 0.68 μm. The higher wear rate of finer grain size tools was attributed to the increased solubility of WC in titanium alloys as the surface area of tool particles exposed to solution wear increased. The relatively superior performance of T1 and T4 inserts compared to T2 and T3 inserts may also be attributed to presence of tantalum carbide (TaC) in their composition. TaC addition generally improves crater wear resistance and increases the hot hardness of the carbides, thus preventing plastic deformation of the cutting edge when machining at higher speed conditions (BOOTHROYD; KNIGHT, 1989).

Figure 4.2 also shows that T1 tool outperformed T4 tool when machining with conventional coolant flow and in the presence of argon at all the speed conditions investigated. However, T4 insert generally outperformed T1 insert when machining under

high coolant supply pressures up to 20.3 MPa. The relatively inferior performance of T4 tool when machining under conventional coolant flow and in presence of argon can be attributed to the PVD multi-layer (TiAlN /TiN) coating of T4 (Table 3.3) which has its lubrication property suppressed by chemical reactivity with Ti element of the workpiece at the cutting conditions investigated. Titanium is very reactive with most cutting tool materials at elevated temperatures (> 550ºC) during machining (KONIG (1979), HARTUNG; KRAMER (1982), MOTONISHI et al. (1987), BROOKES; JAMES; NABHANI (1998)). Coatings are used in cutting tools to provide improved lubrication at the tool-chip and tool-workpiece interfaces, reduce friction and consequently lower temperatures at the cutting edge. TiN coating is a good diffusion barrier (EDWARDS, 1993) and generally provides a very low friction ratio at the tool the cutting edge and an excellent resistance to crater wear (LÓPEZ DE LACALLE et al., 2000). However, Ti element present in coatings can react chemically with Ti in the workpiece at high cutting temperatures during machining, thereby leading to higher wear rate due to diffusion wear. Difusion wear is a mechanism mainly dependent on temperature rise and involves exchange of atoms between the tool and work material at the tool-workpiece and tool-chip interfaces. It was reported that coatings of TiN, TiC, Al_2O_3 and HfN in carbide tools were worn more rapidly than uncoated straight carbides by either dissolution-diffusion or attrition wear mechanisms when machining Ti-6Al-4V alloy (KONIG, 1979). It has also been reported that multilayer (TiC/TiCN/TiN) coatings of a mixed cemented carbide tool were rapidly removed from cemented carbide substrate by adhesion wear mechanism taking place at the cutting edge (NABHANI, 2001b). The high adhesive forces are likely to result in the plucking of hard particles from the tool. Thus erosion of the coating layer/(s) exposes the carbide substrate to extreme temperature at the tool cutting edge, consequently increasing the crater wear depth.

Results obtained when machining with T4 tool relative to T1 tool show that machining Ti-6Al-4V with high pressure coolant supplies can minimise chemical reaction of TiAlN coatings with workpiece, thus providing improved lubrication at the tool-chip and tool-workpiece interfaces. This phenomenon will minimise dissolution wear, thereby increasing tool life. T2 (uncoated) and T3 (coated) tools, in general, exhibited similar performance in terms of tool life at the cutting conditions investigated, except when machining with the highest coolant pressure of 20.3 MPa and at speed of 110 m min^{-1}, where over 65% increase in tool life was achieved using coated T3 tool. Increasing coolant pressure up to 11 MPa resulted to increased tool life of all the tools at the highest cutting speed of 130 m min^{-1}.

However when machining with 20.3 MPa coolant supply pressure, tool life lowered slightly relative to 11MPa pressure (Figure 4.2 and Table 4.1). Table 4.1 shows that tool life increased with increasing coolant pressure for all the grades of carbide inserts employed. The ranking order for carbide tools in terms of average gain in tool life relative to conventional coolant flow was T4, T3, T2 and T1 (Table 4.1). These results show that the coolant pressure has a significant effect on tool wear pattern hence recorded tool life when machining Ti-6Al-4V alloy with carbide tools under finishing conditions.

When high pressure coolant technique is employed, a hydraulic wedge is created at the tool-workpiece interface which allows the coolant jet to penetrate the interface deeply even at very high speed machining conditions. This action reduces the tool-chip and tool-workpiece contact length/area and also changes the chip flow direction. A resulting force acting upon the chip is created from the pressure in the fluid wedge. Additionally, the temperature gradient is reduced by penetration of the high-energy jet into the tool-chip interface and consequently eliminating the seizure effect (MAZURKIEWICZ; KUBALA; CHOW, 1989). This in turn provides adequate lubrication at the tool-chip interface with a significant reduction in friction (EZUGWU; BONNEY; YAMANE, 2003). These combined with high velocity coolant flow causes the breakage of the chips into very small segments. Because the tool-chip contact time is shorter, the tool is less susceptible to dissolution wear caused by chemical reaction with newly generated chips, especially titanium-alloy chips (LINDEKE; SCHOENIG; KHAN, 1991). Moreover, the efficiency of high pressure coolant technique is dependent upon the jet pressure and cutting speed (PIGOTT; COLWELL (1952), DAHLMAN (2000)). It has been established that machining at any cutting speed, the tool-chip interface temperature initially decreases with an increase in jet pressure up to a critical pressure (or optimum jet-pressure) above which it rises to a relatively constant value for pressures in excess of the critical pressure (SHARMA; RICE; SALMON, 1971) as a result of the critical boiling action of the coolant at the tool edge since it was possible to sweep the tool surface faster by the higher jet speed. This phenomenon lowers the rate of boiling and reducing heat transfer which presumably may vary with tool-work material combination as well as cutting conditions. Additionally, cutting tools operate within a safety temperature zone with minimal tool wear when machining at the critical coolant pressure as thermal stresses are kept to a minimum, thereby prolonging tool life (MACHADO; WALLBANK, 1994). From this explanation, it is clear from Figure 4.2 and Table 4.1 that 20.3 MPa coolant pressure is above the critical pressure for machining Ti-6Al-4V alloy with all carbide tools employed at a cutting speed of

130 m min^{-1}. Critical pressure phenomenon was also reported in the experiments carried out by Nagpal and Sharma (1973), Kishi et al. (1975), Kovacevic; Cherukuthota; Mazurkiewicz (1995), Dahlman (2000) and Bonney (2004). In all of these studies the authors reported that, in general, when coolant pressure reached a certain optimum value, a further increasing in coolant pressure was not found to be beneficial in further improving machining performance. Bonney (2004) also reported that any increase in coolant pressure in certain cases does not improve tool life when machining Inconel 718 at cutting speeds lower than 50 m min^{-1} and a feed rate o 0.25 mm rev^{-1}. Kovacevic; Cherukuthota; Mazurkiewicz (1995) attributed this to the fact that a high pressure water jet after penetrating to a certain depth into the tool-chip interface is not capable of penetrating any deeper, hence overcoming the high contact pressures at the tool-chip interface. This probably explains why proportional and/or further improvement in tool life of carbide tools was not recorded at higher coolant pressure of 20.3 MPa when machining at speeds in excess of 120 m min^{-1}.

Figure 4.2 also shows that machining in an argon enriched environment gave inferior performance in terms of tool life relative to conventional and high pressure coolant supplies when machining Ti-6Al-4V alloy with carbides (T1 and T4). Table 4.1 also shows average reduction in tool life when machining in argon enriched environment relative to conventional coolant supply where 47 % and 44% reduction were obtained with using T1 and T4 tools, respectively. This shows that machining Ti-6Al-4V alloy with carbide tools in an argon enriched environment is still not recommendable because cooling and/or lubrication characteristics of argon gas may be suppressed at the cutting conditions investigated. Additionally, the poor thermal conductivity of argon can only prevent combustion taking place during machining and most of the heat generated tends to concentrate at the cutting interface. This tends to further accelerate tool wear during machining.

5.2.2 PCD tools

Longer tool life was recorded when machining Ti-6Al-4V alloy with PCD (T5 and T6) tools with high coolant supply pressures than with conventional coolant flow (Figure 4.59). This Figure also shows that tool life of the all the PCD tools decreased with increase cutting speed in all machining environments investigated, consequently providing significant reduction in tool life when machining at higher speed conditions. PCD (T5 and T6) tool grades exhibited exceptional performance in terms of tool life when machining Ti-6Al-4V alloy relative to the carbide and other tool materials employed in all the machining conditions

investigated. It has been reported (NABHANI, 2001b) that PCD tools also exhibited outstanding performance relative to carbides and CBN tools when machining titanium TA48 alloy at a cutting speed of 75 m min^{-1}, a feed rate of 0.25 mm rev^{-1} and a depth of cut of 1.0 mm under dry machining conditions. This was probably attributed to the formation of a protective layer of titanium carbide on the rake face of the tool due to inter-diffusion of titanium and carbon atoms at the cutting interface between the work and tool material during machining. The saturated titanium carbide layer adheres to the cutting edge of the PCD tool to prevent further diffusion of the tool material into the chip / work material, thus increasing tool life. Although cemented carbides are also susceptible to the formation of this stable titanium carbide interfacial layer, PCD inserts have higher hot hardness than carbides (Table 3.3) and can therefore maintain consistent cutting edge with prolonged machining at elevated temperature generated in higher speed conditions. Higher thermal conductivity of PCD inserts relative to carbide tools is another relevant factor to be considered. Cutting tool materials with higher thermal conductivity minimise thermal gradients and thermal shocks during machining process because heat generated in the cutting zone can easily be dissipated into the chip and the cooling environment hence the tool maintains it yield stress (EZUGWU; WANG (1997), TRENT; WRIGHT (2000)). This will minimise/prevent the weakening of the tool bond strength, thereby minimising tool wear rate and increasing tool life.

Longer tool life was recorded when machining with T5 tool using a medium coolant supply pressure of 7 MPa relative to conventional coolant flow in all the cutting speeds investigated and also relative to 11 MPa coolant pressure at cutting speeds of 175 and 230 m min^{-1}. This irregular PCD´s tool life behaviour suggests that optimum cutting conditions for machining titanium alloys will depend on the correct combination of several variables such as coolant pressure, grain size of tool and cutting speed. Additionally, coolant pressure employed has a significant effect on tool wear pattern and hence recorded tool life when machining Ti-6Al-4V alloy with PCD tools under finishing conditions, similarly the carbides tools. The best performance of larger grain size (T5) tool when machining Ti-6Al-4V alloy can be achieved using the highest coolant pressure supply of 20.3 MPa at a cutting speed range of 175-230 m min^{-1} whereas the best performance of smaller grain size (T6) tool is achieved when machining with coolant pressures lower than 20.3 MPa and at cutting speeds up to 230 m min^{-1}. High temperatures generated close to the cutting edge of the tool are the principal reasons for the rapid tool wear commonly observed when machining titanium alloys (TRENT; WRIGHT, 2000). About 80% of the heat generated is generally absorbed in the tool

when machining Ti-6Al-4V alloy while the machining of steel it is about 50% (KONIG, 1979). This suggests that the superior performance of T5 tools under the conditions investigated is a result of their higher thermal conductivity compared to T6 tools (Table 3.3) combined with higher heat removal rate provided by the higher coolant flow rate delivered to the cutting zone at a coolant pressure supply of 20.3 MPa. On the other hand, the lower thermal conductivity of T6 tool (459 $Wm^{-1}K^{-1}$ against 540 $Wm^{-1}K^{-1}$) caused more heat to develop at the cutting zone, thus assisting in the softening of the work material. The improved performance of T6 tool may be attributed to its smaller grain size. It has been reported (COOK; BOSSOM (2000), BAI et al. (2004)) that abrasion resistance of PCD tools and consequently tool life increases with increase in grain size. However, this correlation is not linear and tool life can be lowered if a grain size is increased beyond a certain value (COOK; BOSSOM, 2000). This is dependent on the cutting conditions employed. Finally, it is important to state that the outstanding performance, in terms of tool life, exhibited by PCD tools relative to carbides is suppressed by their higher cost (over 8900% higher than cemented carbides) (SECO TOOLS, 2002b).

Regard Costing and Productivity analysis, some benefits of using the High Coolant Pressure Technology in Machining Ti-6Al-4V alloy with carbide and PCD tools were achieved: results of research programme generated a generic technology that can be employed by all industries engaged in superalloy machining. Therefore, the results from machining technology developed in this research programme produced 50% reduction in Cycle times demonstrated on JSF Blisk Turning; 5 fold reduction in consumables. Additionally, about £ 1.5 million capital saving for JSF Factory and £ 1750.00 saving per machined part (based on projected cost rate and reduction in cycle time).

5.2.3 CBN tools

Lower tool life was recorded when machining Ti-6Al-4V alloy with CBN (T7, T8 and T9) inserts (Figure 4.95) relative to the carbide and PCD tools due probably to the high reactivity of titanium alloys with CBN tools (VIGNEAU (1997). Tool life decreased with increasing cutting speed when machining with the lower (50 vol.%) CBN content (T7 grade), unlike when machining with T8 and T9 inserts with higher (90 vol.%) CBN content. T7 insert gave the best performance in terms of tool life among all the CBN tools at all conditions investigated. T8 and T9 inserts in general exhibited similar performance in terms of tool life (generally below 1 min) at the conditions investigated. Additionally, the coating of the T9 tool

did not influence tool performance. The results from Figure 4.95 suggest that the relatively good performance of T7 grade compared to T8 and T9 grades are associated with the lower CBN content of the T7 substrate as well as the high temperature characteristics of the ceramic matrix (Table 3.3). Superior performance in terms of tool life of low CBN content tools relative to those of high CBN content tools when machining difficult-to-machine materials, especially titanium alloys, is attributed to the ability of the lower CBN content grades to retain their cutting edge for longer period (KOMANDURI; REED JR (1983), RICHARDS; ASPINWALL (1989), HUANG; LIANG (2003)). Table 3.3 also shows that the higher CBN contents, T8 and T9, inserts exhibit much higher thermal conductivity than T7 insert ($138Wm^{-1}K^{-1}$ against $44Wm^{-1}K^{-1}$). This can enhance the weakening of the CBN-ceramic bond at higher speed conditions, thereby accelerating tool failure by mechanically related modes such as chipping and notching as illustrated in Figures 4.97-4.104.

Figure 4.95 also shows that tool life of all the CBN inserts generally increased with increasing coolant pressure, especially when machining with the T7 tool at speeds of 150 and 250 m min^{-1}, which are more sensitive to coolant pressure than others. Over 68% and 150% improvement in tool life was recorded when machining with T7 tool at a speed of 150 m min^{-1} with coolant pressures of 11 MPa and 20.3 MPa, respectively, relative to conventional coolant flow. However, tool life decreased with increasing the coolant pressure when machining at higher cutting speeds in excess of 150 m min^{-1}. This tool life pattern can be attributed to the physical phenomenon observed when the critical coolant pressure is exceeded (PIGOTT; COLWELL, 1952). The optimum coolant pressure appears to have a relationship with the total heat generated during machining. A major benefit of coolant delivery at higher pressures is improved access of the coolant to the cutting interface and the subsequent reduction of the cutting temperature, hereby minimising and/or completely eliminating thermally related wear mechanisms (BONNEY, 2004).

5.2.4 Micron-grain ceramic tools

Lower tool life (< 2 min) was recorded when machining Ti-6Al-4V with various grades (T10,T11,T12 and T13) of ceramics tools under various cutting conditions relative to carbides and PCD tools (Figures 4.2, 4.59, 4.117 and 4.127). Ceramic tools generally exhibit lower fracture toughness than carbides as well as poor thermal and mechanical shock resistance. Poor performance of ceramics tools, in terms of wear rate and consequently very low tool life can be attributed to their low thermal conductivity compared to other

commercially available cutting tool materials (Table 3.3) as well as to their relative low fracture toughness and high reactivity with titanium alloys (YANG (1970), (KONIG (1979), LEE (1981), KOMANDURI; REED JR (1983), LI; LOW (1994)). The reduction of hot hardness at elevated temperatures conditions during machining lead to the weakening of the inter-particle bond strength and the consequent acceleration of tool wear (NORTH, 1986). Rhomboid-shaped ceramic (T10) inserts in general outperformed squared-shaped ceramic (T11) inserts when machining at relatively low cutting speeds, (< 200 m min^{-1}), using conventional coolant flow (Figure 4.117). Note that machining with SiCw ceramic (T10) insert under conventional coolant flow was carried out only at a speed of 140 m min^{-1}. Increase in cutting speed generally accelerated tool wear when machining with all ceramic tool grades tested in all the environments investigated due to a reduction in tool-chip and tool-workpiece contact length and the consequent increase in both normal and shear stresses at the tool tip. The reduction in tool-chip and tool-workpiece contact areas also tend to concentrate the high temperature generated to a relatively small area as well as shifting the highest temperature closer to the cutting edge (GORCZYCA, 1987). Machining in presence of argon also gave the highest nose wear rate in all the cutting speeds investigated, hence the worst performance in terms of tool life relative to other cooling environments. This performance may be attributed to poor thermal conductivity of argon which tends to accelerate tool wear. From Figure 4.116 also can be seen that increase in coolant pressure up to 11 MPa lowered tool wear rate, consequently improved tool life, especially at lower speed conditions. Similar to the phenomenon observed when machining with carbides and PCD tools, machining with coolant supply pressure of 20.3 MPa and at cutting speeds up to 400 m min^{-1} gave lower tool life compared to coolant pressure of 11MPa. This can be attributed to the physical phenomenon observed when the critical coolant pressure is exceeded (PIGOTT; COLWELL, 1952), as previously stated. This explains why proportional and/or further improvement in tool life was not recorded when machining Ti-6Al-4V alloy with rhomboid-shaped SiC (T10) ceramic inserts at the highest coolant pressure of 20.3 MPa at the cutting conditions investigated.

5.2.5 Nanoceramic tools

Al_2O_3 base (T12) and Si_3N_4 base (T13) nano-grain ceramic inserts gave the least performance in terms of tool life when machining Ti-6Al-4V alloy under conventional coolant flow (Figures 4.126 and 4.127) relative to cemented carbides, PCD, CBN and

micron-grain ceramic inserts employed in this study. Increase in cutting speed generally lowered tool life, as expected, due to a reduction in tool-chip and tool-workpiece contact lengths and the consequent increase in both normal and shear stresses at the tool tip. It is also clear from the machining results (Figure 4.127) that improved properties of the nanoceramic (T12,T13) insert have negligible effect on tool life relative to commercially available ceramic tools used for machining titanium alloys. This, therefore, suggests that the tool performance of nano-grain ceramic tools is more chemically and/or thermally related. The Si_3N_4 base nano-grain T13 grade gave better performance in terms of tool life and tool wear rate relative to T12 and micron-grain size SiC_w alumina (T11) tools with the same tool geometry, as illustrated in Figure 4.117 and Table 3.3. Although the micron-grain size SiCw alumina (T11) and Al_2O_3 base nano-grain (T13) inserts have theoretically improved edge toughness desired for efficient machining, their relatively poor performance can be associated with their higher hardness and associated brittleness (Table 3.3). The ranking order for the performance of the nanoceramics tools, in terms of tool life, when machining Ti-6Al-4V alloy is T13 and T12.

5.3 Tool failure modes and wear mechanisms when machining Ti-6Al-4V alloy with different grades of carbides, PCD, CBN and ceramic tools

5.3.1 Carbide tools

Adhesion, diffusion-dissolution, attrition and plastic deformation wear mechanisms are typical tool failures of cemented carbide tools (KONIG (1979), HARTUNG; KRAMER (1982), MACHADO; WALLBANK (1990), EZUGWU et al. (2005)). Diffusion wear mechanism generally occurs where high temperature exists at the cutting interfaces. Adhesion wear mechanism frequently occurs when there is chemical affinity between the tool and the work material. High temperature generated at the chip-tool interface is a relevant phenomenon in relation to the tribological system behaviour existing during machining operation. Although attrition wear mechanism is commonly associated to lower cutting speeds, it can also occur in situations where intermittent contact exists at the chip-tool interface. Cemented carbide tools can also fail by abrasion wear mechanism as a result of the chipped off hard particles sandwiched between the tool flank face and the newly machined surface. As the tool rubs over the machined surface, the particles plough through the tool removing material at the flank face (BROOKES; JAMES; NABHANI (1998), TRENT; WRIGHT (2000). This type of

wear mechanism has been reported when turning a titanium base, Ti-6242, alloy under dry condition with carbide tools (JAWAID; CHE-HARON; ABDULLAH, 1999). The poor thermal conductivity of the titanium alloy workpiece encourages the development of maximum temperature closer to the cutting edge than is the case with other metals and alloys. Thus, the formation of a crater in this region undermines the integrity of that cutting edge resulting to fracture and accelerated wear rate (BROOKES; JAMES; NABHANI, 1998).

Typical failure modes observed when machining Ti-6Al-4V alloy with all cemented carbides tools under various cutting conditions are nose wear and flank wear. The flank wear rate is lower than the nose wear rate when machining with all carbide (T1,T2,T3,T4) inserts. Since nose wear is the predominant failure mode observed in all conditions investigated (Figures 4.3-4.5), flank wear curves were omitted in this thesis. This is due to the fact that initial flank wear developed in all conditions investigated during the machining process tend to be displaced towards the nose region with prolonged machining (Figures 4.6, 4.7, 4.10-4.17 and 4.20) and also with increasing cutting speed due to the reduction in the chip-tool and tool-workpiece contact lengths areas (SADIK; LINDSTRÖM, 1995).Concentration of shearing forces at the nose region usually increases the frictional forces and temperature that accelerate wear at the tool nose (BONNEY, 2004). Rapid increase in nose wear occurred when machining with all carbide inserts at speeds in excess of 110 m min^{-1} in the presence of argon and under conventional coolant flow (Figure 4.3). This, therefore, suggests that high pressure coolant supplies are responsible for reduction in temperature at the cutting interface and consequently low wear rates during machining, thereby increasing tool life. In other words, the ability to remove heat from cutting tool increases with increase in coolant pressure. Machado (1990) reported that high pressure coolant system reduces the size of the heat source (reduced contact length) but not the amount of heat generated, hence higher temperatures in a smaller heat affected zone at the tip of the tool would be expected. However, the author reported that the high pressure coolant jet is expected to cause dissipation of the heat more efficiently from the heat affected zone. This suggests that a smaller flow zone produces the same amount of heat. This heat is, however, conducted more efficiently, thereby lowering the cutting temperature. The temperature gradient reduces by penetration of the high-energy jet into the tool-chip interface and consequently eliminating the seizure effect (MAZURKIEWICZ; KUBALA; CHOW, 1989), thereby providing adequate lubrication at the tool-chip interface with a significant reduction in friction (EZUGWU; BONNEY; YAMANE, 2003). These combined with high velocity coolant flow causes breakage of the chips into very

small segments. Because the tool-chip contact time is shorter, the tool is less susceptible to dissolution wear caused by chemical reaction with newly generated chips, especially titanium-alloy chips (LINDEKE; SCHOENIG; KHAN, 1991).

Machining with carbide tools under finishing conditions showed steady increase in nose wear rate with increasing cutting speed (Figure 4.3). Additionally, nose wear rate generally decreases with increasing coolant pressure. This is attributed to the fact that high coolant pressure technique reduces the tool-chip contact length/area and also changes the chip flow direction (as stated previously), thereby providing adequate lubrication at the tool-chip interface with a significant reduction in friction (EZUGWU; BONNEY; YAMANE, 2003). In general, flank wear rate observed when machining under high coolant pressures was very low compared with nose wear rate. The mechanism of wear that will predominate depends on what is happening at the interface during machining. Titanium reacts with most cutting tool materials at elevated temperatures (> 550ºC) during machining (KONIG (1979), (HARTUNG; KRAMER (1982), MOTONISHI et al. (1987), BROOKES; JAMES; NABHANI (1998)). At such high temperature conditions titanium atoms diffuse into the carbide tool material and react chemically with carbon present in the tool to form an interlayer of titanium carbide (TiC) (KONIG (1979), (HARTUNG; KRAMER (1982)) which bonds strongly to both the tool and the chip to form a saturated seizure zone. This action, minimise diffusion wear mechanism by halting the reaction. The separation of the welded junction results in tool material being carried away by the fast flowing chip. Titanium has a strong tendency to adhere to the tool material. Micrographs of worn inserts (Figures 4.6, 4.11 and 4.17) show that adhesion of material was more pronounced when machining with T1, T2 and T4 inserts, respectively, using conventional coolant flow. This suggests that adhesion of work material to the tool nose is minimised when machining with high coolant pressure supplies.

Grain sizes of a tool substrate also affect its wear resistance. Nose wear rates of T2 and T3 inserts were higher than those obtained when machining T1 and T4 inserts in all the conditions investigated (Figure 4.3). Micrographs of T2 and T3 inserts in Figures 4.11 and 4.14 (b) illustrate the irregular wear pattern observed along the flank and rake faces of these tools compared to T1 (Figure 4.6 (b)) and T4 (Figure 4.17) inserts. Inferior performance of T2 and T3 tools may be attributed to their smaller substrate grain size (0.68 μm) compared to substrate grain size of T1 and T4 tools (1μm) (Table 3.3). Similar results were reported in several studies attributed the higher wear rate of finer grain size tools to increased solubility of WC in titanium alloys as the surface area of tool particles exposed to increased solution

wear have been reported (MARI; GONSETH (1993), JAWAID; CHE-HARON; ABDULLAH (1999), CHE-HARON (2001)). Additionally, the presence of TaC in composition of T1 and T4 tools improved their crater wear resistance and increased their hot hardness, thus preventing plastic deformation of the cutting edge to take place during machining at high speed conditions (BOOTHROYD; KNIGHT, 1989).

Evidence of abrasion wear mechanism is shown in Figure 4.12 (a) from the visible groove marks on the worn tool surfaces of T2 tool grade with a coolant pressure of 11MPa and speed of 110 m min^{-1} and T3 tool with high coolant pressures of 11 and 20.3 MPa as illustrated in Figures 4.15 and 4.16, respectively. Grooves are more pronounced in coated carbide T3 insert what suggesting that the wear mechanism is mechanically related and may be generated by hard particles of the tool that have been detached by attrition and rubbed against the flank surface. The erosion of the coating layer exposes the carbide substrate to extreme temperature at the tool cutting edge causing severe grooving and the cratering (NABHANI, 2001a). A similar process of attrition and grooving wear can also develop on the flank face, leading to deterioration in the machined surface. Ultimately, the combination of the crater and flank wear undermines the entire cutting edge and causing pronounced chipping and/or fracture (NABHANI, 2001b). It is important to note that this wear mechanism was not occur when machining with coated carbide T4 inserts. Figures 4.7-4.9 and 4.19 show a typical worn tool showing flank and rake face wears. The uniform flank wear observed may be due to the low wear rate caused by temperature reduction at the cutting interface when machining with high coolant pressures.

The high adhesive forces are likely to result in the plucking of hard particles from the tool. Therefore, erosion of the coating layer (s) exposes the carbide substrate to extreme temperature at the tool cutting edge causing its surface to become grooved and the increasing crater wear. T3 (coated carbide CP200 grade) insert experienced more severe flank and nose wears in all machining environments tested relative to other carbide inserts. Visible grooves were observed on the worn T3 inserts (Figures 4.15 and 4.16 (a) and (b)). Figure 4.20 (b) shows that coated carbide T4 tool experienced severe flank and crater wears very close to the cutting edge, when machining in presence of argon at a speed of 120 m min^{-1}. The high chemical reactivity of the titanium alloys results in excessive tool wear during machining. Figures 4.12 (a), 4.15 and 4.16 (b) also suggest that T2 and T3 tools also experienced appreciable crater wear. This failure mode is generally associated with high temperature generated at the chip-tool interface and occurs on the rake face of a tool due to a combination

of diffusion and adhesion as the chip moves over the rake face of the tool (AB SANDVIK COROMANT (1994), TRENT; WRIGHT (2000)). It was reported that when machining Ti-6Al-4V alloy with cemented carbides a shallow crater was initially formed on the rake face of the tool and a low flank wear was produced along the whole extension of the depth of cut (MACHADO, 1990).

Figures 4.10 and 4.20 (a) show worn tools after machining in the presence of argon with uncoated (T1) and coated carbide (T4) inserts at a speed of 130 m min^{-1} and 100 m min^{-1}, respectively. Examination of these inserts revealed smoothly worn tool with slight cracks and adhesion of work material to the tool nose as a result of the intermittent contact between the tool and the workpiece. This suggests that high temperatures were generated at the cutting interface and that diffusion wear mechanism is dominant under such conditions. The highest nose wear rate recorded when machining with T1 and T4 inserts in the presence of argon can be attributed to the poor thermal conductivity of argon which can only prevent combustion taking place during machining. Most of the heat generated tends to concentrate at the cutting interface, thus weakening the strength of tool and accelerating the tool wear during machining.

5.3.2 PCD tools

Nose wear was the predominant failure mode observed when machining Ti-Al-4V alloy with PCD tools in all the conditions investigated. Nose wear rate increased with increase in cutting speed and with prolong machining using both PCD tools under all the coolant supplies employed. There is a steady increase in nose wear rates on both PCD (T5 and T6) tools at cutting speeds up to 160 m min^{-1} when machining with conventional coolant flow (Figure 4.60). This low wear pattern is observed at cutting speeds up to 250 m min^{-1} when machining with high pressure coolant supplies of 7, 11 and 20.3 MPa. It is clear that the coolant pressure has a significant effect on tool wear and hence recorded tool life when machining Ti-6Al-4V alloy with PCD tools under finishing conditions. Rapid increases in nose wear rate occurred when machining with both PCD (T5 and T6) tools at speeds in excess of 160 m min^{-1} with conventional coolant flow. As observed when machining with carbide tools at a different cutting speed range, this wear pattern shows the ability to remove heat from cutting tool increases with increase in coolant pressure. The strength of the cutting tools is, therefore, expected to increase if a significant reduction in the tool temperature can be achieved, particularly at high temperature regions typical of those encountered when machining

superalloys (MACHADO, 1990). Reduction in temperature can reduce tool wear rate during machining, hence providing longest tool life. Figure 4.60 shows that nose wear rate can be reduced at least by 88% by employing high pressure coolant technique in machining of Ti-6Al-4V alloy with PCD, T5, tool grade at the cutting conditions investigated. Similar percentage reduction in nose wear rate was also observed when machining with T6 insert. Figure 4.61 illustrates the curves of progress of the nose wear *versus* machining time when cutting with both PCD grades at a cutting speed of 175 m min^{-1}. The concentration of the shearing forces at the nose region causes increased frictional forces and temperature that leads to high wear rate at the nose region of the tool (BONNEY, 2004). Machining with conventional coolant flow always provided accelerated nose wear, hence the lower tool life, than with high pressure coolant supplies at the conditions investigated.

Diffusion-dissolution, attrition and plastic deformation are typical wear mechanisms observed when machining titanium alloys with PCD tools. High temperature generated at the chip-tool interface combined with the chemical affinity between the PCD tool and titanium alloys when machining at higher speed conditions lead to significant reduction in tool life. Although attrition wear mechanism is commonly associated to lower cutting speeds, it can also occur in situations where intermittent contact exists at the chip-tool interface. Segmented chips are generated at both lower and higher speed conditions when machining titanium alloys. This phenomenon can enhance the stick-slip process, removing from the rake and flank faces minute amount of tool particles by plucking action, thus accelerating tool wear (MACHADO (1990),(NABHANI (2001b), BONNEY (2004)). The plucking process tend to be accelerated by the application of high pressure coolant supply which is capable of removing any loose tool material from the rake face as well as eroding the brittle PCD tool particles. It has been reported that diffusion is an important wear mechanism in responsible for cratering and it also predominates at the flank face leading to the development of the maximum flank wear on tool (TRENT, 1988b). Additionally, rates of diffusion at the interface normally increase exponentially with temperature. Notch wear is caused by abrasion, mainly at the depth of cut line, of hardened saw tooth like material during machining. Notching can also be accelerated by high temperature generated at the tool edge during machining and subsequent weakening of the bond strength of the tool material. According to Bonney (2004), the initial notch formed during machining usually act as a highly stressed point and tends to accelerate tool wear leading to fracture in the worse case.

Figures 4.62-4.68 show micrographs of the worn PCD tools under various machining conditions. Tool surfaces that may have been subjected to stick-slip action during machining show a characteristic rough texture as illustrated in Figures 4.63-4.65, 4.67 and 4.68. Figure 4.62 suggests that adhesion of work material to the tool nose occurred when machining with PCD tools under conventional coolant flow. Adhesion of work material to the nose of tools may be caused by the intermittent contact between the tool and the workpiece. Notching on was observed when machining with T6 insert under conventional coolant flow at a cutting speed 175 m min^{-1} (Figure 4.67). This may be attributed to the interdiffusion of titanium and carbon at elevated temperature conditions developed during machining (KONIG (1979, HARTUNG; KRAMER (1982), NABHANI (2001b)). The diffusion process results in the formation of titanium carbide layer on the tool, which prevents further diffusion. Although worn rake face of tools employed when machining with high pressure coolant supplies show evidence of a tiny layer of work material on the both rake and flank faces due to high chemical affinity between titanium from the workpiece and carbon from the cutting tool (Figures 4.63-4.65, 4.67 and 4.68), crater wear seems to be more pronounced under these conditions than with conventional coolant flow. This suggests that crater wear increased when machining under high pressure coolant supplies. It has been reported that crater wear of carbide tools increased with the coolant jet power when machining Ti-6Al-4V alloy with carbide tools (VIGNEAU, 1997). It has also been reported that under certain conditions, titanium adheres to the tool and no relative sliding occurs at tool-chip interface. A boundary layer of titanium forms at the interface, and the relative motion between the tool and chip is generated internally by shear within the titanium chip material. This layer will quickly become saturated with tool constituents, limiting the mass transport of tool constituents from the tool surface (HARTUNG; KRAMER, 1982). This would explain why no wear occurred in certain regions of the crater zone of some tools (Figures 4.62 (b), 4.63 (b) and 4.66). Evidence of notching at depth of cut can be seen in the worn T6 tool grade after machining at a speed of 175 m min^{-1} under conventional coolant flow (Figure 4.66). However, this type of wear was absent when machining with high pressure coolant supplies.

5.3.3 CBN tools

Figure 4.96 shows that machining with CBN (T7,T8,T9) inserts gave higher wear rates, hence worse overall performance than carbides and PCD tools. The lower (50 vol.%) CBN content T7 tool grade gave the lowest nose wear rate among the CBN tools investigated.

Cutting speed plays an important role in the performance of CBN tools. Increase in cutting speed leads to further increase in cutting temperature as well as increases in the intensity of chemical interaction between the tool and the work materials which adversely affects tool life. As the cutting temperature increases, seizure of the chip occurs everywhere on the tool face. This forms an adherent layer which becomes saturated with tool particles and serves as a diffusion boundary layer, thus reducing the rate of transport of tool materials into the chip and consequently the wear rate. Since the diffusivity rate increase exponentially with temperature, further increase in cutting speed beyond the speed for minimum wear produces rapid increase in the wear rate.

Nose wear, notching, chipping and premature tool failure are the dominant failure modes encountered when machining with CBN tools due to their brittle nature (Figures 4.97-4.105). Premature failure of CBN tools are generally attributed to the fracturing of the unsupported cutting edge caused by attrition wear (BHAUMIK; DIVAKAR; SINGH, 1995). However, average flank wear was the dominant failure mode when dry machining titanium-base, Ti-5Al-4Mo-(2-2.5)Sn-(6-7)Si, alloy with CBN tools at a cutting speed of 75 m min^{-1}, a feed rate of 0.25 mm rev^{-1} and a depth of cut of 1.0 mm (NABHANI, 2001a). Kramer (1987) reported that CBN tools retain their strength at temperatures in excess of 1100ºC while cemented carbide tools encounter plastic deformation at this temperature range. This temperature is also that in which titanium can react with nitrogen in the CBN insert when interatomic diffusion of titanium and CBN accelerates significantly.

Cutting speed also plays an important role in tools performance of CBN tools. Increase in cutting speed leads to further increase in cutting temperature as well as increases in the intensity of chemical interaction between the tool and the work materials which adversely affects tool life. As the cutting temperature increases, seizure of the chip occurs everywhere on the tool face. This forms an adherent layer which becomes saturated with tool particles and serves as a diffusion boundary layer, thus reducing the rate of transport of tool materials into the chip and consequently the wear rate. Since the diffusivity rate increase exponentially with temperature, further increase in cutting speed beyond the speed for minimum wear produces rapid increase in the wear rate.

CBN insert grades encountered severe notching and chipping of the cutting edges with increase in cutting speed up to 250 m min^{-1} and the consequent increase in cutting temperature. These tend to lower tool life, even when using high pressure coolant supplies (Figures 4.97 (b), 4.98 (b), 4.99 (b), 4.102 (b), 4.103 (b) and 4.104 (b)). The slightly better

performance of T7 grade relative to T8 and T9 grades may be associated with the lower CBN content of the T7 substrate as well as the high temperature characteristics of the ceramic matrix. Table 3.3 shows that the higher CBN content (T8 and T9) tools exhibit much higher thermal conductivity. This can enhance the weakening of the CBN-ceramic bond at higher speed conditions, thereby accelerating tool failure by mechanically related modes such as chipping and notching (Figures 4.97-4.104). Machining under conventional coolant flow gave higher tool wear rates than with high pressure coolant supplies. Tool wear rate generally decreased with increasing in coolant pressure up to 11 MPa, especially when machining with T7 insert (Figure 4.96). However, it can be seen from this figure that increasing coolant pressure from 11 to 20.3 MPa did not provide any appreciable reduction in wear rate when machining with both T7 ant T9 tool grades at the conditions investigated. This can be attributed to the physical phenomenon observed when the critical coolant pressure is exceeded (PIGOTT; COLWELL, 1952). Additionally, high pressure coolant supplies in general did not prevent chipping from taking place. In some cases, CBN tools experienced fracture of cutting edge, especially when machining with T8 grade (Figure 4.102 (b)). Notching was the predominant failure modes present in all the CBN tools tested under all the conditions investigated, followed by chipping of the cutting edge as illustrated in Figures 4.97-4.100, 4.102-4.103 and 4.104 (b). Dearnley and Grearson (1986) reported that CBN tools gave higher wear rate than carbides when machining Ti-6Al-4V alloy at speeds in excess of 100 m min^{-1} and therefore they were not considered suitable for practical application. Other study reported that wear in CBN tools was associated with localized chipping of the cutting edge as a result of tool-tip oscillations (ZOYA; KRISHNAMURTHY, 2000).

Rapid increase in notch wear rate was recorded when machining with T8 tool grade under the highest coolant supply pressure of 20.3 MPa at high speeds in excess of 200 m min^{-1}. Examination of worn CBN (T8 grade) tools revealed adhesion of work material to both the nose and flank faces of tool as a result of the intermittent contact between the tool and the workpiece (Figure 4.101). This figure shows that the thickness of the layer of material stuck on the rake face of higher (90 vol.%) CBN content T8 tool grade may reach huge proportions, even when machining with high pressure coolant supply. If thick layers of work material stuck where the worn area develops, small fragments of it will flow down the flank surface and cause further damage to the tool by attrition (MACHADO, 1990).

5.3.4 Micron-grain ceramic tools

Wear resistance, chemical inertness and toughness are considered main factors affecting the performance of cutting tools when machining aerospace alloys, especially nickel and titanium alloys (SZESZULSKI; THANGARAJ; WEINNMANN, 1990). Any ceramic tool with a potential application for titanium machining must require a good thermal shock resistance (LEE, 1981). Ceramic tool materials generally have three properties which distinguish them from cemented carbides: chemically inert (with ferrous materials), highly resistant to abrasive wear and capable of superior heat dispersal during chip forming process (WHITFIELD, 1988). Silicon carbide (SiCw) whisker reinforced alumina ceramic has silicon-carbide whiskers added to a matrix of aluminium oxide that reinforces the hard and somewhat brittle aluminium oxide, allowing it to better withstand mechanical stresses. The fracture toughness of silicon carbide (SiCw) whisker reinforced alumina ceramic (for instance, WG300 grade) is enhanced by the phenomenon of whisker "pull-out" where the whiskers generally pull out during the fracture process. Additionally, under actual cutting conditions where temperatures at the tool-chip interface may reach over 1000ºC, whisker reinforced alumina ceramic will retain high strength and hardness well beyond the point at which a cemented carbide material has softened, deformed or failed completely (SMITH, 1986). Machining with both (T10 and T11) ceramic inserts gave high nose wear rates, hence lower tool life relative to carbide, PCD and CBN inserts employed in this study (Figure 4.116). Ceramic tools generally exhibit lower fracture toughness than carbides and PCD tools in addition to poor thermal and mechanical shock resistance. Additionally, ceramic tools have high reactivity with titanium alloys (KONIG (1979), LEE (1981), DEARNLEY; GREARSON (1986)). This factor is responsible for the worst performance of ceramic tools relative to other tools. Machining in presence of argon with T10 ceramic tool gave the highest nose wear rate in all the cutting speeds investigated due probably to the poor thermal conductivity of argon which tends to accelerate tool wear. Machining with high pressure coolant supplies of 11 MPa and 20.3 MPa reduced tool wear rate and consequently gave marginal improvement in tool life for T10 grade compared with using argon and conventional coolant flow (Figure 4.116). This may be attributed to the fact that high pressure coolant technique reduces the tool-chip contact length/area and also changes the chip flow direction (as stated previously), thereby providing adequate lubrication at the tool-chip interface with a significant reduction in friction (EZUGWU; BONNEY; YAMANE, 2003). High pressure coolant technique may have reduced tool temperature due to its ability to remove heat from

tool, thereby strengthen them for longer period during machining. Reduction of the temperature can reduce tool wear rate during machining, hence prolonging tool life.

Figures 4.118 and 4.119 are micrographs of worn SiCw reinforced alumina ceramic tools, T10 and T11 grades respectively, after machining Ti-6Al-4V alloy under various cutting conditions. Typical failure modes observed with ceramics tools when machining Ti-6Al-4V alloy are severe notching, chipping and, in some cases, severe nose wear. The rhomboid-shaped (T10) ceramic grade experienced severe abrasive type wear mechanism (Figures 4.118) while the square-shaped ceramic (T11) inserts experienced severe abrasive wear on both the rake and flank faces (Figures 4.119). Abrasion wear mechanism involves the loss of tool material by hard particles sandwiched between the tool and workpiece material. The particles could be dislodged tool materials, fragments of built-up-edge or hard carbides and oxides already existing in the workpiece. The high compressive stresses acting at the tool-workpiece interface keep the trapped hard particles between the machined surface and the tool. As the tool rubs over the machined surface, the particles plough through the tool removing material at the flank face. In some cases this phenomenon lead to chipping of cutting edge and eventually to catastrophic tool failure observed when machining at speeds in excess of 140 m min^{-1} as shown in Figures 4.118 (c) and (f) and 4.119 (b). This type of wear occurs purely on a random manner and cannot be predicted. It has been reported that abrasive wear mechanism in ceramic tools can also be caused by plastic flow of the tool material due to the high temperature conditions encountered at the cutting interface (NORTH (1986), DEARNLEY; GREARSON (1986), LI; LOW (1994), GATTO; IULIANO (1997)). According to Bonney (2004), the laminar chip flow abrades the tool by stretching the contacting plasticised tool layer until necking. This type of abrasion wear generally is recognized by the presence of grooved surfaces as parallel ridges can be seen on the flank face of tool (Figures 4.118 (a), (b), (d), (e) and 4.119 (a)). The formation of ridges on the worn flank face is attributed to seizure between the workpiece and the tool flank face. This type of ridges was also observed on ceramic worn tools when machining Inconel 718 (BONNEY, 2004). Although ceramic tools have high hardness at ambient temperature, plastic behaviour of ceramics is possible at high temperature conditions when hydrostatic conditions occur. This unusual thermo-mechanical property is exhibited by nano-ceramics and is referred to superplasticity, defined as the ability of polycrystalline solids to exhibit exceptionally large elongation in tension (KIM, 1994). SiC particles present in whisker reinforced alumina ceramic tools may be responsible for abrasion wear mechanism that generated severe nose

wear. It is therefore clear from the machining results that improved properties of the silicon carbide (SiCw) whisker reinforced alumina ceramic (T10 and T11) tools have negligible effect on tool performance compared with other commercially available ceramic tools employed in the machining of titanium alloys.

5.3.5 Nano-grain ceramic tools

Machining with nano-grain ceramic (T12 and T13) tools gave high notch wear rate, hence lower tool life, relative to other tool grades employed in this study (Figure 4.126). The Si_3N_4 base nano-grain T13 grade gave the better performance in terms of tool wear rate relative to T12 tool grade when machining Ti-6Al-4V alloy with conventional coolant flow (Figure 4.127). It has been reported that addition of zirconium oxide (ZrO_2) improves the toughness and resistance to fracture of the alumina base tools (BONNEY, 2004). For this reason T12 tool should theoretically exhibit superior performance than T13 tool because of its higher edge toughness and hardness (Table 3.3). However, the results shown in Figures 4.126-4.127 did not confirm this. The relatively poor performance of T12 insert in terms of nose wear rate (tool life) can be associated with their higher hardness with associated brittleness compared to Si_3N_4 base nano-grain T13 grade (Table 3.3). The higher TiCN content in T12 can also be responsible for accelerated and severe notching due to increased affinity of TiC to the titanium workpiece material which often leads to catastrophic tool failure at speeds in excess of 110 m min^{-1} (Figure 4.128). Occurrence of catastrophic failure is often influenced by the stress developed during machining and the toughness property of the tool. Severe chipping was also observed after machining with tools T12 at cutting speed of 200 m min^{-1}, as illustrated in Figures 4.128. This type of wear occurs on a purely random manner and cannot be predicted. According to Khamsehzadeh (1991) the high temperatures generated during machining also promote the development of uneven stress regions on the cutting tool due to varying microstructure which will increase the stress on the ceramic bond. Alumina ceramic tools are more susceptible to catastrophic failure due to their low toughness when machining nickel alloys (KHAMSEHZADEH, 1991). Additionally, it was reported that addition of TiC resulted to increase in toughness of ceramic tools by increasing their thermal conductivity and reduce the possibility of the fracture.

5.4 Components forces when machining Ti-6Al-4V alloy with different grades of carbide, PCD, CBN and ceramic tools

The cutting force can be defined as the force exerted by the tool cutting edge on the workpiece material to promote chip shearing. Cutting force can be resolved into three components in an orthogonal reference system usually involving the machine tool coordinate system (Figure 2.18 (a)). These three components forces are represented by cutting force (F_c), feed force (F_f) and finally the radial force (F_r) also called the thrust force. Cutting force is usually the largest force acting on the tool rake face in direction of the cutting velocity. Feed force acts parallel to the direction of the tool feed. The radial force tends to push the tool away from the workpiece in a radial direction (DE GARMO; BLACK; KOHSER, 1999).

Understanding of the forces acting on the cutting tool and the study of their behaviour are of vital importance in the design and manufacture of machine tools and their components as well as in helping to optimise tool design and controlling the surface finish and surface integrity of machined components. Additionally, excessive forces can induce vibrations which are also detrimental to the quality of the machined components hence they are considered as a machinability index. In this context, more efforts are directed to selecting optimised cutting conditions to prevent vibration during machining. A curious fact is that cutting forces generated during machining can either decrease or increase with increasing speed. An explanation for the first phenomenon is based on the softening of workpiece material as a result of high temperature generated at the cutting interface (LI; LOW, 1994). As a consequence, the shear strength of the workpiece material is lowered and hence lower cutting forces are required at higher speed conditions. On the other hand, cutting forces can also increase with increasing cutting speed when the wear rate of the tool increases due to the softening of tool material, hence higher cutting forces are required when machining at high speed conditions (ZHAN et al., 2000).

Cutting and feed forces can also be influenced by the coolant delivery method, especially when machining under high pressure coolant supplies. There are, therefore, two contrasting tendencies on the cutting forces: (i) they tend to decrease them slightly, due to the marginally shorter sticking zone region produced and (ii) they tend to increase them due to the shear yield strength as a result of the generation of lower temperatures (MACHADO, 1990). In the first case, it is well known that the chip-tool contact length decrease with increase in coolant pressure during machining (PIGOTT; COLWELL (1952), MACHADO (1990),

KOVACEVIC; CHERUKUTHOTA; MAZURKIEWICZ (1995), DAHLMAN (2000)). A hydraulic wedge is created at the tool-workpiece interface that allows the coolant jet to penetrate the interface deeply with a speed beyond that necessary even for very high speed machining. This action reduces the tool-chip contact length/area and also changes the chip flow direction. A resulting force acting upon the chip is created from the pressure in the fluid wedge. In this case, a shorter sticking region is produced as tool-chip contact is decreased, hence cutting forces would be expected to decrease. The second tendency is based on the fact that the yield strength of the work material at the shear zone increases with increase in coolant pressure. This ability to remove heat when increasing coolant supply compared to conventional coolant flow was investigated by Machado (1990) who found a significant reduction of about 175ºC in cutting tool temperature when machining Ti-6Al-4V alloy at a cutting speed of 30 m min^{-1}. In addition to these two tendencies, it has recently been reported that cutting forces can also be influenced by the generation of reactive forces inherent of cutting process under high pressure coolant supplies (BONNEY, 2004). This is illustrated in Figure 5.1. The reactive force is introduced as a result of the coolant jet momentum which tends to push the tool away from the workpiece material. These reactive forces can generate severe vibrations during the cutting process, which is detrimental to the integrity of the machined component. Therefore, it is important to note that, in this study, the reactive forces were not subtracted from cutting and feed forces recorded values using high pressure coolant supplies.

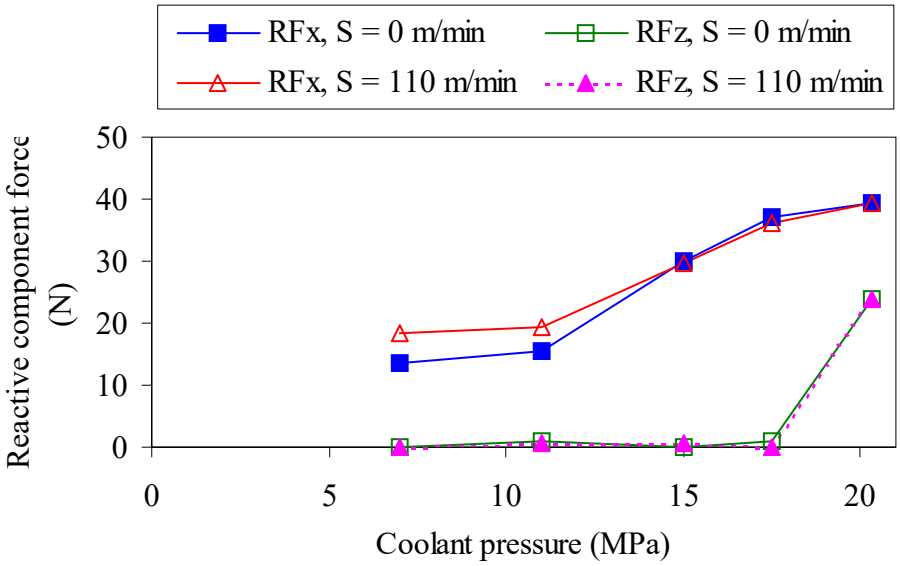

Figure 5.1 - Variation of reactive component forces with coolant pressure supply before machining Ti-6Al-4V alloy.

Figures 4.21 shows that cutting forces generally decrease slightly with increase in coolant pressure when machining with T1 and T4 tool grades whereas the opposite effect is observed when machining with T2 and T3 tool grades. As often reported, higher cutting forces generated with T1 and T4 inserts may be attributed to the reduced chip-tool contact length at high pressure coolant supplies which consequently provided a shorter sticking region. In case of machining with T2 and T3 tool grades, the relative increase in cutting forces with coolant supplies may be due to two possible explanations. Firstly, their smaller grain size relative to T1 and T4 may have reduced their resistance to deformation at higher temperature (MARI; GONSETH, 1993), thus accelerating tool wear rate and consequently requiring higher cutting forces. Secondly, the increased ability to remove heat from the cutting zone with increasing coolant supply, compared to conventional coolant flow may have outweighed the effect of reducing the contact length, thus leading to increase in cutting forces. Figures 4.21 and 4.22 also show that, in general, cutting and feed forces marginally increased with cutting speed when machining with all carbides tools tested. Cutting forces recorded with T2 tool grade were generally higher than those recorded with T3 tool in all conditions tested. This may be attributed to coating of T3 which could have improved lubrication at the cutting interface, hence requiring lower cutting forces. High cutting and feed forces were generated when machining with T1 and T4 tool grades in the presence of argon relative to conventional coolant flow due probably to the poor thermal conductivity of argon which tends to concentrate more heat at the cutting interface. This accelerates tool wear during machining at higher cutting speeds due to the softening of tool material, hence higher cutting forces are required when machining at high speed conditions.

Figures 4.69 and 4.70 show variations in cutting and feed forces, respectively, when machining Ti-6Al-4V alloy with PCD (T5 and T6) tool grades under various cutting speeds and coolant pressures. Although PCD tools were employed at higher speed conditions, comparison of Figures 4.21 and 4.69 show that in general PCD tools generated lower cutting forces than carbides tools and they vary marginally under all the coolant pressures investigated. This can be attributed to the higher hardness of PCD tools (Table 3.3), which tend to retain a sharp and consistent cutting edge with prolong machining at elevated temperature conditions, therefore requiring lower component forces to perform cutting. Cutting forces generally increase with increase in cutting speed when machining with T5 and T6 inserts at lower cutting speeds using conventional coolant supply, contrary to expectation.

However, cutting forces generally decrease with increase in coolant pressure when machining with both T5 and T6 inserts.

Feed forces generated when machining with T5 and T6 inserts are relatively lower than cutting forces, especially at higher speed conditions, as expected. Feed forces generally decrease with increase in cutting speed when machining with both T5 and T6 inserts with conventional coolant flow and increase when machining with high coolant pressures. The highest feed forces were recorded when machining with T6 insert at the highest coolant supply of 20.3 MPa (Figure 4.70). Unlike the cutting forces, feed forces increased with increase in coolant pressure. The higher feed forces recorded at the higher speed conditions may be attributed to the reactive forces introduced as a result of the high coolant pressure. The reactive feed forces measured at the various coolant pressures show that they increase with increasing coolant pressure (Figure 5.1). Figure 5.1 also shows that the reactive forces increased when the workpiece is rotating. According to Bonney (2004) this phenomenon occurs because dynamic forces are introduced which increase with increasing cutting speed for the same mass of workpiece material.

Figures 4.105 and 4.106 show variations in cutting and feed forces, respectively, when machining Ti-6Al-4V alloy with different CBN (T7,T8,T9) inserts with different coolant pressures and at various cutting speeds. Lower cutting and feed forces were generated when machining with conventional coolant flow at a the lowest cutting speed of 150 m min^{-1} whereas higher cutting forces were generated when machining with all the CBN grades with coolant pressure of 11 MPa at a cutting speed of 200 m min^{-1}. This may be attributed to the reactive forces introduced as a result of the coolant pressure especially at higher speed conditions. In general, lower cutting and feed forces were generated when machining with CBN tools relative to carbide and PCD tools. Figure 4.105 also shows that relatively lower cutting and feed forces were also generated when machining with high coolant pressures at speeds in excess of 200 m min^{-1}.

Figures 4.120 and 4.121 show plots of cutting and feed forces, respectively, when machining Ti-6Al-4V alloy with micron-grain size ceramic (T10 and T11) inserts at different cutting speeds and under various machining environments. Higher cutting forces were generated when machining with high coolant pressures compared to argon enriched environment. This can be attributed to the reactive forces inherent of cutting process with high coolant pressures (BONNEY, 2004). Additionally, component forces generated during machining are proportional to stresses at the tool cutting edge. Therefore high compressive

forces at the cutting edge will lead to accelerated tool wear and plastic deformation of the tool edge. These can adversely affect the cutting edge geometry. Prolong machining leads to accelerated tool wear as a result of high cutting edge temperature (Kear et al., 2001). In general cutting forces generated with T10 inserts decreased with increasing cutting speed. Evidence of decreasing cutting forces with increasing cutting speed up to 110 m min^{-1} was reported by Ezugwu et al. (2005) when finish turning Ti-6Al-4V alloy with uncoated carbides in an argon enriched environment. The increase in cutting forces with increasing cutting speed in this case may be attributed to the very high wear rate of the ceramic tools (Figures 4.118 and 4.119). The very high wear rate of ceramics is due to their high reactivity with titanium alloys (LEE (1981), DEARNLEY; GREARSON (1986)) which causes severe notching and chipping of cutting edge. This tends to increase frictional forces during machining and the consequent loss/blunting of the sharp cutting edge. This phenomenon also explains the reason of higher cutting and feed forces generated with ceramics (T10, T11) tool relative to those generated with carbides, PCD and CBN tools.

Machining Ti-6Al-4V alloy with nano-grain size ceramic (T12 and T13) inserts gave high component forces (Figure 4.129). Cutting forces generated during machining are higher than feed forces, as expected. In general component forces increased with increasing in cutting speed. This may be attributed to high chemical reactivity of ceramic with titanium alloys which tends to increase frictional forces during machining and the consequent loss/blunting of the sharp cutting edge. Despite the relative lower component forces generated relative to other cutting tools, nano-grain size ceramics gave the worst performance, suggesting that their superplastic flow temperature is low and inadequate for machining titanium alloys. The very poor performance of nano-ceramic tools when machining Inconel 718 was attributed to this drawback (BONNEY, 2004).

5.5 Surfaces roughness and runout values when machining Ti-6Al-4V alloy with different grades of carbide, PCD, CBN and ceramic tools

Figures 4.23, 4.71, 4.107, 4.122 and 4.130 show the surface roughness recorded when machining Ti-6Al-4V alloy with different cutting tools at various cutting conditions. It is important to note that surface roughness values were recorded after one minute machining time whereas runout deviation measurements were taken at the end of tool life. Surface

roughness values recorded when machining with cemented carbides, PCD and CBN tools (Figures 4.23, 4.71 and 4.107 respectively) were below the stipulated rejection criterion of 1.6 μm for finishing operation, unlike those recorded with ceramic tools (Figures 4.122 and 4.130). The lowest surface roughness values hence improved surface finish were recorded when machining with cemented carbides, especially with T1 tool grade, using high coolant pressures of 11 MPa and 20.3 MPa at cutting speeds up to 120 m min^{-1}, while the highest values were obtained with ceramic T10 tool grade with the various coolant pressures. The better finishes generated with carbide tools relative to other cutting tools may be attributed to their larger nose radius of 1.2 mm (Table 3.3). It has been established (KALPAKJIAN; SCHMID, 2000) that roughness value is closely related to the corner radius and feed rate given by equation $R_a = \frac{0.0321 \times f^2}{r}$ (2.14), where f is the feed rate and r is the tool nose radius (contact radius). According to this equation, the bigger the nose radius the better the surface finish generated. Therefore, better surface finish is generated when machining Ti-6Al-4V with carbides with conventional and high pressure coolant supplies. Additionally, the smooth surface finish generally obtained with carbide inserts when machining under high pressure coolant supplies can be attributed to the formation of segmented chips. Coolant supply at high pressures tend to enhance chip segmentation as the chip curl radius is significantly reduced, hence maximum coolant pressure is restricted only to a smaller area on the chip (MACHADO (1990), DALHMAN; KAMINSKI (1999), KAMINSKI; DAHLMAN (1999), DAHLMAN (2000), BONNEY (2004)). The poor performance of ceramic tools can be attributed to their high chemical reactivity with titanium alloys which tend to produce severe abrasive wear, chipping and consequently leading to a loss of the edge sharpness (Figures 4.118 and 4.119). This adversely affects the surface finish generated during machining (Figures 4.122 and 4.130). Surface finish deteriorates with increase in cutting speed when machining with carbides, CBN and ceramic tools (Figures 4.23, 4.107, 4.122 and 4.130, respectively), unlike when machining with both PCD (T5 and T6) inserts which showed no significant variation in the surface roughness with cutting speed (Figure 4.71). The relatively low nose wear rates generated when machining with PCD tools suggests that they maintained their sharp cutting edge for longer periods. It can, however, be seen in Figure 4.71 that there is gradual deterioration of the surface finish with increase in coolant pressure when machining with larger grain size (T5) insert at cutting speeds up to 230 m min^{-1} whereas a reverse surface roughness pattern was observed when machining with T6 insert. Plots in

Figures 4.23, 4.71 and 4.107 show that finish of the machined surfaces are not adversely affected when machining Ti-6Al-4V with high coolant pressures using carbide, PCD and CBN inserts under the cutting conditions investigated.

Figures 4.24, 4.72, 4.108, 4.131 show runout deviation values recorded when machining Ti-6Al-4V alloy with different cutting tools at various cutting speeds and with different cutting environments. In all cases, the runout values recorded are well below the stipulated rejection criterion of 100 μm. In general runout increased with increase in cutting speed when machining with carbides (T1,T2,T3 and T4) and ceramic (T11,T12 and T13) inserts with conventional coolant flow, unlike PCD (T5 and T6) inserts. The lowest runout values (0.3 μm) were obtained when machining with T4 (carbide) and T5 (PCD) inserts with the highest coolant pressure of 20.3 MPa. Additionally, minimal variation in recorded runout values were also obtained when machining with PCD tools with high coolant pressures (Figure 4.72). This may be attributed to the higher hardness of PCD inserts that ensures more rigidity to the tool-workpiece system during machining and also due to their lower chemical reactivity with titanium relative to other cutting tools, hence providing lower nose wear rates. Consequently, PCD tools can maintain sharp their cutting edge for longer periods, thus ensuring minimal variation in recorded runout values. However, high runout values were obtained when machining with CBN and ceramic tools compared to carbide and PCD tools. Ceramic and CBN tools have high chemical reactivity with titanium alloys and are therefore more susceptible to accelerated tool wear, especially under higher cutting conditions. Reduction of hot hardness at elevated temperatures conditions during machining can lead to the weakening of the inter-particle bond strength and the consequent acceleration of tool wear (NORTH, 1986). Typical tool failure modes observed when machining Ti-6Al-4V alloy with CBN and ceramic tools are chipping of cutting edge, severe notching and eventually catastrophic tool failure (Figures 4.97-104 (b), 4.118 (c), (d) and (f)) and 4.119 (b). These types of wear occur on a purely random manner and cannot be predicted, leading to a loss of the edge sharpness which adversely affects the dimensional tolerance of a machined component.

5.6 Surface generated of Ti-6Al-4V after machining with carbide and PCD tools

Figures 4.25-4.32, 4.73-4.79 show micrographs of surfaces generated when machining Ti-6Al-4V alloy with various grades of carbides and PCD tools. In general the surfaces

generated with carbide tools consist of well-defined uniform feed marks running perpendicular to the direction of relative work-tool motion with no evidence of plastic flow. Irregular feed marks were, however, observed in some cases when machining with the smaller grain size PCD T6 tool grade at a cutting speed of 175 m min^{-1} using conventional coolant supply and also with a coolant pressure of 11 MPa as illustrated in Figures 4.77 (a) and 4.78 (a), respectively. There is the evidence of localised incipient melting of the machined surfaces when machining with uncoated carbide T1 tool grade at a higher cutting speed of 130 m min^{-1} using conventional coolant flow (Figure 4.25 (b)) and with both grades of PCD tools using different coolant supplies employed (Figures 4.73 (a), 4.74 (b), 4.76-4.79). Although distribution of localised incipient melting of machined surface is more severe when machining with T5 and T6 (PCD) tools, especially when machining with the highest coolant pressure supply of 20.3 MPa, no evidence of plastic flow was observed. Presence of small particles (debris) and sometimes surface damages can also be seen on machined surfaces when machining with carbides and PCD inserts using high coolant pressures (Figures 4.27 (a), 4.28, 4.30, 4.31 (b), 432 (a)-(c), 4.75,4.76 and 4.78). This can be attributed to the smaller and fragmented chips generated when machining with high coolant pressures which are thrown out against the workpiece by the high pressure coolant jet. In other cases the surface finish of machined surfaces are not adversely affected when machining Ti-6A-4V alloy under high pressure coolant supplies with carbides and PCD tools, as illustrated in Figures 4.23 and 4.71, for example. Generally surfaces generated under all the finishing conditions investigated when machining with both PCD inserts were free from other damages such as cracking, tearing and rupture that are detrimental to machined components. Therefore, surfaces generated in these trials machined are acceptable and conform to the standard specification established for machined aerospace components - Rolls-Royce CME 5043.

5.7 Surface hardness after machining Ti-6Al-4V alloy with different grades of carbide, PCD, CBN and ceramic tools

The plots of microhardness measurements of the machined cross-sections when machining with carbide (T1,T2,T3,T4) inserts indicate that in general the curves vary randomly around the hardness range (confidence interval) of the workpiece material and most of them below the maximum (Max.) Vickers hardness value recorded for the Ti-6Al-4V alloy

prior to machining (Figures 4.33-4.42). This suggests that there was no considerable surface hardening after machining with carbides at the cutting conditions investigated. Surface hardening up to about 0.4 mm below the machined surfaces of Ti-6Al-4V alloy was observed after machining with uncoated carbide T1 insert at a cutting speed of 120 m min^{-1} using conventional coolant flow. Evidence of surface hardening up to about 0.25 mm below the machined surface was also observed when machining with T2 tool using conventional coolant flow at the lowest speed of 100 m min^{-1}. This may be attributed to severe plastic deformation generated under conventional coolant supply when compressive and shear stresses at the cutting interface become higher than the yield point of the work material due to high wear land and cutting temperature (TRENT (1988b), MACHADO; WALLBANK (1994), DAHLMAN (2000), BONNEY (2004)). Machining with T1 tool using the highest coolant pressure of 20.3 MPa gave minimum hardness variation with a uniform distribution of hardness values within the confidence interval of hardness values (Figure 4.36). Analysis of Figures 4.34-4.37 shows that minimum hardening effect was most accentuated in the following decreasing order: conventional coolant flow, argon enriched, 11 MPa and 20.3 MPa coolant pressures respectively. Recorded results clearly show that increasing coolant pressure generally reduced the hardening effect. Hardening effect in this case is due to high plastic flow rate combining with the heat generation at the primary shear zone. Efficient coolant supplies conditions enhance the access of the coolant to the chip-tool interface and contribute to reducing friction coefficient and the resistance to primary shear zone (SALES (1999), TRENT; WRIGHT (2000), BONNEY (2004)). As a consequence of this, heat generation is decreased, resulting to lower temperatures and plastic flow which minimizes the hardening effect. However, the cutting fluid has negligible access to the tool-workpiece or the tool-chip interfaces which are under seizure condition when machining at higher speed conditions. The high temperature generated close to the tool edge during machining generally causes vaporisation of the cutting fluid (BONNEY, 2004) hence reducing the efficiency of cutting fluid to remove heat from cutting zone. This may explain the softening of the machined surface observed when machining with T1 insert at a relatively high speed of 130 m min^{-1} using conventional coolant flow. Machining with T3 insert in all cutting conditions investigated generated hardness values that are uniformly distributed within the confidence interval with minimum variation of hardness values prior to machining. This, therefore, suggests that T3 inserts has superior performance in terms of minimum hardness variation when machining Ti-4Al-4V relative to other carbide inserts employed. Plots of microhardness

measurements after machining with coated carbide T4 inserts show evidence of softening of machined surface when machining in all the cutting conditions investigated (Figures 4.40-4.42). This softening effect was more pronounced when machining with conventional coolant flow, as all the hardness values recorded are below the minimum hardness values of the titanium workpiece prior to machining (Figure 4.40). This softening phenomenon may be attributed to the over-ageing of titanium alloy at the local surface (CHE-HARON, 2001). There is longer tool-workpiece contact time when machining at lower cutting speeds. The low thermal conductivity of titanium alloy encourages retention of the temperature below the machined surface. Softening of machined surfaces was also observed when machining with T4 insert under high pressure coolant supplies (Figure 4.41 and 4.42) due probably to the higher tempering effect generated when machining at higher cutting conditions. Other cause could be the TiAlN coating of T4 insert. The coating generally acts as a heat barrier, because it has a much lower thermal conductivity than the tool substrate and the workpiece material. This tends to reduce heat dissipation rate from the cutting zone and consequently retaining more heat into the workpiece.

Machining Ti-6Al-4V alloy with PCD T5 and T6 inserts generally gave lower hardness values beneath the machined surfaces compared to when machining with carbide inserts at the conditions investigated (Figures 4.80-4.86). It is important to note that cutting speed range when machining with PCD inserts is 140-250 m min^{-1} whereas the range for carbides is 100-130 m min^{-1}. This suggests that machining with PCD tools can lead to softening of the machined surfaces due to probably to the higher tempering effect caused by the higher temperature generated at higher speed conditions. This result was unexpected because PCD inserts with higher thermal conductivity than carbide inserts (Table 3.3) was supposed to provide higher heat dissipation rate during machining. Increased in cutting speed generally led to increased hardness when machining with the larger grain size PCD (T5) tool under conventional coolant flow and under coolant pressures up to 11 MPa (Figures 4.80-4.83), as expected due to higher temperatures generated at the cutting interface. These Figures also explains minimum variation in hardness values, with uniform distribution of hardness values around the confidence interval, obtained when machining with T5 insert at a speed of 175 m min^{-1} in all the coolant pressures employed. Machining with higher coolant pressures generally gave less dispersion of hardness values, i.e. hardness values relatively within the confidence interval compared to conventional coolant flow (Figures 4.80-4.86). Similar to the phenomenon that occurred when machining with carbide inserts, here efficient coolant

supplies enhance the access of the coolant to the chip-tool interface and contribute to minimise friction and the resistance to primary shear zone (SALES (1999), TRENT; WRIGHT (2000), BONNEY (2004)) thereby ensuring improved heat dissipation from cutting zone.

Machining with CBN (T7, T8 and T9) inserts under various coolant pressures at a cutting speed of 150 m min^{-1} generally gave regular microhardness pattern, i.e. evidence of softening of machined surface up to about 0.15 mm below the top machined surfaces and a uniform distribution of hardness values around the minimum and maximum values of the hardness prior to machining (Figures 4.109-4.111). These values suggest that hardness was not adversely affected when machining with CBN inserts under the cutting conditions investigated. The plots also suggest that, in general, hardness depth of the machined surface decreased with increasing coolant pressure. Again, high pressure coolant technique contributed to reducing friction coefficient and the resistance to primary shear zone (SALES (1999), TRENT; WRIGHT (2000), BONNEY (2004)) thereby ensuring improved heat dissipation from cutting zone. Lower microhardness values were recorded when machining with T9 grade using all the coolant supplies employed. This may be attributed to heat barrier property of the TiAlN coating in T9 inserts (Table 3.3) that may have reduced the heat dissipation rate from cutting zone. This tends to retain more heat in the workpiece leading to the softening of the machined surface.

Machining with silicon carbide (SiCw) whisker reinforced alumina (T10) ceramic inserts generally gave hardness values around the minimum and maximum values of the hardness prior to machining at high coolant pressures while evidence of softening of the machined surface up to a distance of the about 0.7 mm below the machined surface was recorded when machining with conventional coolant supply (Figure 4.123). This may be attributed to two possible hypotheses. The first hypothesis relies on the fact that the high temperature generated close to the tool edge during machining at conventional coolant flow generally causes vaporisation of the cutting fluid (BONNEY, 2004) hence reducing the efficiency of cutting fluid to conduct heat away from cutting zone. The second hypothesis is based on the excellent cooling capability of the high coolant pressure technique that reduces temperature at the cutting zone, thereby minimising the quantity of heat could be conducted into the workpiece.

Additionally, it is important to note that Ti-6Al-4V alloy has two different phases (α- and β phases) which have different hardness values. Therefore, some scattered pattern

observed in results of surface hardness values recorded when machining with carbide, PCD, CBN and ceramic tools at the conditions investigated may be attributed the presence of these phases.

5.8 Subsurface micrographs after machining Ti-6Al-4V alloy with different grades of carbide, PCD, CBN and ceramic tools

All the micrographs of the etched machined surfaces generated after machining with carbide (T1,72,T3,T4) inserts exhibit similar characteristics. The well defined grain boundaries in Figures 4.43-4.57 clearly show that there were no microstructural alterations such as plastic deformation, in the subsurface of the machined surfaces. However, a slight plastic deformation of about 10 μm below the machined surface was observed when machining with T4 tool grade under high pressure coolant supply of 11 MPa at a cutting speed of 120 m min^{-1} (Figure 4.55 (a)). This may be attributed to the combination of low thermal conductivity of titanium alloy with the heat retention characteristics of the coating on T4 insert that can prevent heat developed on a given shear plane from being dissipated. This leads to softening of work material and causing further shear deformation at the same point (SHAW, 1984). Astakhov (1999) defined plasticity of a material as its ability to undergo irreversible plastic deformation when a sufficient external load is applied. The shear deformation introduced by the cutting action creates a new surface layer with different structure and properties than the base material. Plastic deformation generally occurs under a complex non-homogeneous stress, structural changes and a transient temperature field. This is accompanied by five different energy fluxes: release of elastic energy, crack formation, heat flow, mass transfer and movement and multiplication of dislocations of material. The change in properties is due to dislocation of the sub-structure due to residual stresses (induced by the cutting forces and cutting temperatures) and the consequent strengthening of the material. The plastic deformation extends to a few microns below the machined surface (BONNEY, 2004). Machined surfaces produced by conventional machining processes (turning, milling, drilling, reaming, etc) have a tendency to develop compressive residual stress at depth above 50 μm from surface. Additionally, this surface status is hardly dependent on the cutting parameters, tool geometry, tool material and cutting fluid condition. For example, when machining in dry conditions, the residual stresses generated were always tensile at all depths beneath machined

surface whereas when turning with cutting fluids at the same conditions compressive stress were recorded up to 15 μm beneath the machined surface and below this value, the residual stress became tensile (ARUNACHALAM; MANNAN; SPOWAGE (2004a), ARUNACHALAM; MANNAN; SPOWAGE (2004b)). Evidence of plastic deformation at about 20 μm below the machined surface was reported when machining Inconel 718 with coated carbide tools under finishing conditions (BONNEY, 2004). A recent study (CHE-HARON, 2001) reported that a thin layer of disturbed or plastically deformed layer immediately underneath the machined surface was created after finish turning Ti-6Al-4V alloy with uncoated carbide inserts under dry conditions This study also reported that machining with nearly worn or worn tool led to the generation of irregular surface, consisting of tearing and plastically deformed surface as a result of the high temperature developed at the chip-tool interface.

Although machining of the titanium alloy with PCD tools suggested softening of machined surfaces due probably to the high temperature generated when machining at higher speed conditions, they also generated surfaces of Ti-6Al-4V alloy free from mechanical damage or microstructural alterations (Figures 4.87-4.93). This suggest that the higher thermal conductivity of PCD tools relative to other cutting tools employed (Table 3.3) is an essential tool property for efficient machining of titanium alloys since they can increase heat dissipation rate from the cutting zone, thus preventing occurrence of plastic deformation during machining.

The well defined grain boundaries shown in the microstructure of the etched machined surfaces after machining with CBN (T7, T8 and T9) and ceramic (T10) tools (Figures 4.112-4.114 and 4.124 (a)-(c)) evidence that there was no microstructural alteration in the subsurface of machined surfaces after machining at the cutting conditions investigated.

5.9 Chips shapes

Machining with uncoated and coated carbide (T1,T2,T3 and T4) , PCD (T5 and T6), CBN (T7, T8 and T9) and ceramic (T10 and T11) tools generally produced four different forms of chips: long tubular chip-shape when machining with T1 and T6 inserts with conventional coolant flow (Figures 4.58 (a) and 4.94 (e)), snarled chip-shape when machining with T1, T4, T11 inserts in the presence of argon (Figures 4.58 (b) and (k)) and with T2, T3,

T4, T5, T6, T10 inserts under conventional coolant flow (Figures 4.58 (h) and (j), 4.94 (a) and (e), 4.115 (a), (d), (e), (f) and (g), 4.125 (a), (d)-(e).), partially segmented chip-shape when machining with carbide (T2 and T3) inserts at high pressure coolant supplies (Figures 4.58 (c) and (g)) and segmented C-shaped chip when machining with T1, T4, T5, T6, T7 inserts at high coolant pressure supplies (Figures 4.58 (d), (e) and (l), 4.94 (b), (c), (d), (f) and (g))., 4.115 (b) and (c), 4.125 (c)). It has been reported that chip formation process is related to the cutting tool thermal conductivity that alters tool-chip contact length during machining (TRENT; WRIGHT, 2000). Continuous and snarled chips are undesirable because they usually wrap themselves around the workpiece or to get tangled around the tool holder, adversely affecting the surface finish generated and/or causing tool damage. This can also hinder the use of advanced manufacturing techniques (unattended machining, for instance) as well as hindering access of the cutting fluid to the cutting zone and associated disposal problems that ultimately increase machine tool downtime during production. Long continuous and, in some cases, snarled chip shapes produced when machining with carbide tools under conventional coolant flow are in good agreement with the literature (FIELD (1968), KONIG (1979), TURLEY (1981), TRUCKS (1987), BOOTHROYD; KNIGHT (1989), MACHADO (1990), MACHADO; WALLBANK (1990)). Chip-tool interface conditions are the most important factors controlling the rate and the amount of deformation within the heavily deformed areas that will culminate in the catastrophic thermoplastic shear process to form the segments. When machining Ti-6Al-4V with T2, T3, T8 and T9 inserts the high coolant pressure system may have failed to break the chips completely into small segments. They were partially segmented/ribbon type instead. This suggest that there may be a critical chip thickness, smaller than the jet geometry created when machining with T1, T2, T5 and T6 inserts, which is unable to break the swarf. According to Machado (1990), when a very thin chip is forming it has high flexibility due to its higher elasticity. Thus, the bending force imposed by the jet is insufficient to break the chip as was obtained with T1 and T4 inserts (Figures 4.58 (c) and (g)).

Chip segmentation was observed when machining at high coolant pressures with T1, T4, T5, T6, T7 and T10 insert grades. Effective chip segmentation was more visible when machining with carbides (T1 and T4) and PCD (T5 and T6) inserts. This may be attributed to the lesser chemical reactivity of titanium with these tools that promote a more stable chip segmentation process. When a coolant is delivered under high pressure, a hydraulic wedge is created at the tool-workpiece interface which allows the coolant jet to penetrate the interface

deeply with a speed beyond that necessary even for very high speed machining. This tends to lift up the chip after passing through the deformation zone, thereby reducing the tool-chip contact length/area as well as changing the chip flow direction. The cantilever effect on the chip is dependant on the pressure distribution, flow rate and cutting tool. The shape and size of the pressure distribution enable control of the chip form and flow direction (DALHMAN; KAMINSKI (1999), KAMINSKI; DAHLMAN (1999), DAHLMAN (2000)). Additionally, the temperature gradient is reduced by penetration of the high-energy jet into the tool-chip interface, consequently eliminating the seizure effect (MAZURKIEWICZ; KUBALA; CHOW, 1989). This action tends to provide adequate lubrication at the tool-chip interface with a significant reduction in friction (EZUGWU; BONNEY; YAMANE, 2003). These combined with high velocity coolant flow causes the breakage of the chips into very small segments.

CHAPTER VI

CONCLUSIONS

1. High Pressure coolant technology has proven that longer tool life can be obtained when machining difficult-to-machine aerospace alloys (Ti-6Al-4V alloy) with carbide and PCD inserts, hence improving overall machining productivity
2. PCD (T5 and T6) inserts gave the best performance in terms of tool life when machining Ti-6Al-4V alloy compared with carbide tools and other cutting tools employed in all the machining conditions investigated.
3. Coarser grain size carbide (T1 and T4) inserts gave longer tool life than T2 and T3 insert grades in all cutting conditions investigated because the finer grain size tools have increased solubility of WC in the titanium alloy as the surface area of tool particles exposed to solution wear increases. The presence of TaC in the composition of T1 and T4 tools also increase wear resistance when machining the Ti-6Al-4V alloy.
4. T1 inserts outperformed T4 inserts when machining with conventional coolant flow and in the presence of argon at all the speed conditions investigated while T4 inserts generally outperformed T1 inserts when machining with high coolant supply pressures up to 20.3 MPa.
5. T2 (uncoated) and T3 (coated) carbide tools generally exhibited similar performance in terms of tool life at the cutting conditions investigated.
6. Coolant pressure has a significant effect on tool wear and hence recorded tool life when machining Ti-6Al-4V alloy with carbides, PCD and CBN inserts under finishing conditions.
7. High Pressure coolant technology has proven that longer tool life can be obtained when machining difficult-to-machine aerospace alloys (Ti-6Al-4V alloy) with carbide and PCD inserts, hence improving overall machining productivity

8. Encouraging tool life can be achieved when machining Ti-6Al-4V alloy with medium (7 MPa) and high coolant pressures of 11 MPa and 20.3 MPa relative to conventional coolant flow and in argon enriched environment.
9. On average, tool life increased with increasing coolant pressure for all grades of carbide inserts employed. The ranking order for carbide tools in terms average gain in tool life relative to conventional coolant flow is T4, T3, T2 and T1 insert grades.
10. Machining with all carbide tools with 20.3 MPa coolant pressure gave lower tool life than using a lower coolant pressure of 11 MPa at a cutting speed of 130 m min^{-1}. Similar behaviour was observed when machining with PCD tools. This suggests that 20.3 MPa coolant pressure is above the critical pressure for machining Ti-6Al-4V alloy under such conditions, therefore optimum cutting conditions for machining the titanium alloy will depend on the correct combination of several variables such as coolant pressure, tool grain size and cutting speed.
11. Up to 8 folds improvement in tool life were achieved when machining with PCD tools relative to carbide inserts using conventional coolant flow.
12. Up to 20 folds improvement in tool life can be achieved when machining with T5 insert under the most aggressive conditions of 230 m min^{-1} using high pressure coolant supply compared with conventional coolant flow.
13. Up to 3 folds and 5 folds improvement in cutting speed can be achieved when machining with carbide (T1) and PCD (T5) inserts respectively, relative to that currently achieved in the manufacturing environment.
14. Nose and flank wears are the dominant failure modes when machining Ti-6Al-4V alloy with all the cutting tools investigated. However, machining with PCD tools with high coolant pressures can lead to plucking process that can erode the brittle PCD tool particles.
15. Over 88% reduction in tool wear rate can be achieved when machining with PCD (T5) tool grade under high pressure coolant supplies relative to conventional coolant flow at higher cutting speeds in excess of 175 m min^{-1} All the grades of CBN and ceramic inserts gave poor performance when machining Ti-6Al-4V alloy at all the conditions investigated due to accelerated nose wear and, in some cases, severe chipping of the cutting edge.
16. Machining with PCD tools generated lower cutting and feed forces than carbides tools.

17. Surface roughness values recorded when machining the Ti-6Al-4V alloy with carbides and PCD tools are generally below the 1.6 μm rejection criterion for finish turning, whereas higher values were recorded when machining with CBN and ceramics inserts.
18. Surfaces generated when machining with all the cutting tools were generally acceptable and free of physical damages such as tears, laps or cracks in all the conditions investigated.
19. No significant hardness variation occurred on the machined surfaces when machining with carbides, PCD and ceramic tools.
20. No evidence of microstructure alteration was observed in the machined subsurface of Ti-6Al-4V alloy after machining with all the cutting tools employed under the conditions investigated.
21. Machining with PCD, carbide and CBN tools gave effective chips segmentation using high pressure coolant technique (discontinuous C-shape chips were produced).
22. The benefits achieved from these results after employing High Coolant Pressure Technology in Machining Ti-6Al-4V alloy with carbide and PCD tools in the production line are:

a) 50% reduction in Cycle times demonstrated on JSF Blisk Turning

b) 5 fold reduction in consumables

c) £ 1.5 million capital saving for JSF Factory and £ 1750.00 saving per machined part (based on projected cost rate and reduction in cycle time).

CHAPTER VII

RECOMMENDATIONS FOR FURTHER WORK

This research project has shown that a step increase in the machining productivity of a commercially available titanium-base, Ti-6Al-4V, alloy can be achieved using recently developed cutting tool materials as well as using high pressure coolant supplies up to 20.3 MPa (203 bar). It was evident that High Coolant Pressure Technique provided a mechanism of breaking the swarf and outstanding performance when machining the titanium alloy. This is strongly dependent on a cutting tool (especially carbide and PCD inserts), cutting speed range, feed rate and depth of cut employed as well as a given high coolant pressure. Selection of the best combination of cutting tool-speed-coolant pressure has been successfully implemented in the shop-floor by the collaborating industrial partner, resulting in a significant reduction in the cost of manufacturing components of jet engines without compromising their integrity. In this context, determination of an optimum coolant pressure becomes the major aim. However, this requires an exhaustive number of complete tool life tests that are time consuming and costly.

From the results obtained in this study, the following future work are recommended:

1. Variation of other cutting parameters such as feed rate and depth of cut would provide adequate results to establish the optimum coolant pressure (s). Experimental design techniques have been extensively used to reduce the quantity of machining tests through application of statistical tools such as ANOVA method, factorial experiment and Statistic software to determinate the significance of cutting parameters.
2. The use of these tools would reduce the large number of potentially important parameters to those that are more significant since it is not economically practical to perform every possible combination of parameter setting. This would also

contribute to developing of a model that can relate primary cutting conditions: speed, feed rate, depth of cut and coolant pressure.

3. The direction of the coolant jet and nozzle geometry (length, shape, diameter) investigated in several studies (PIGOTT; COLWELL (1952), SMART; TRENT (1974), SHAW (1984), MACHADO (1990), KOVACEVIC; CHERUKUTHOTA; MAZURKIEWICZ (1995), SEAH; LI; LEE (1995), NORIHIKO; AKIO (1998), DAHLMAN (2000), LÓPEZ DE LACALLE et al. (2000)) was found to have influence on the tribological conditions present at the tool-workpiece interface, tool wear, cutting forces when machining various work materials, especially titanium alloys. This suggests that further tests with different directions of application of cutting fluid would be valuable.
4. Results from this thesis suggest that different wear mechanisms occurred when machining with all the cutting tools and cutting conditions employed. X-ray analysis would be an important technique to enable a better investigation and analysis of wear mechanisms and possible interactions between elements from the work material and the cutting tool.

At the time of this investigation few studies were reported about the use of high pressure cooling technology in milling of titanium alloys. Therefore, it will be wise for future research work to exploit this technology in mill

CHAPTER VIII

REFERENCES

AB SANDVIK COROMANT, Modern Metal Cutting – A Practical Handbook, Sandvik Coromant, Technical Editorial dept, First Edition, 1994, Sweden.

ABRÃO, A.M., **The Machining of Annealed and Hardened Steels Using Advanced Ceramic Cutting Tools**, 1995, p. 241. Ph.D. Thesis, The University of Birmingham.

ALMOND, E.A., Towards Improved Tests Based on Fundamental Properties, Proceedings of the International Conference on Improved Performance of Tool Materials, The National Laboratory and the Metals Society, Teddington, Middlesex, April 28-29, 1981, pp. 161-169.

AMIN, A.K.M.N.; YANTI, R.A.R. and EIDA, N.R., Effect of Workpiece Heating Using Oxy-Acetylene Flame on Chattering and Tool Performance during Turning of Steel, **Proceedings of the Advances in Materials and Processing Technologies** (AMPT), Volume I, Dublin City University, Dublin, Republic of Ireland, 8th –11th July, 2003, pp. 791-794.

ARMAREGO, E.J.A.; KARRI, V. and SMITH, A.J.R., Fundamental Studies of Driven and Self-Propelled Rotary Tool Cutting Processes – I. Theoretical Investigation, **International Journal of Machine Tools & Manufacture**, Elsevier Science Ltd., Vol. 34, No. 6, 1994, pp. 785-801.

ARMYTAGE, W.H.G, A Social History of Engineering, Faber and Faber Limited, Third Edition, London, Great Britain, 1970, p. 379.

ARUNACHALAM, R.M.; MANNAN, M.A. and SPOWAGE, A.C., Residual stress and surface roughness when facing age hardened Inconel 718 with CBN and ceramic cutting tools, **International Journal of Machine Tools & Manufacture**, Elsevier Science Ltd., Vol. 44, 2004 (b), pp. 879-887.

ARUNACHALAM, R.M.; MANNAN, M.A. and SPOWAGE, A.C., Surface integrity when machining age hardened Inconel 718 with coated carbide cutting tools, **International Journal of Machine Tools & Manufactur**e, Elsevier Science Ltd., Vol. 44, 2004 (a), pp. 1481-1491.

ASM HANDBOOK, Properties and Selection: Nonferrous Alloys and Special-Purpose Materials, **ASM International**, Introduction to Titanium and Titanium Alloys", Vol. 2, 1998, p. 1328.

ASM INTERNATIONAL, Bradley, F.E., Superalloys – A Technical Guide, **ASM International** – Metals Park, United States of America, 1988, p. 280.

ASME HANDBOOK - HORGER, O.J., Metals Engineering Design, Metals Engineering Handbook Managing Committee of The American Society of Mechanical Engineers, Second Edition, McGraw-Hill Book Company, New York, 1965, p. 632.

ASPINWALL, D.; DEWES, R.; MANTLE, A. and NG, E., HSM takes off in the Aerospace Sector, pp. 1-4. Available at: <www.delcam.com/info/articles/hsm_rollsroyce.htm>. Accessed in 7th. May 2003.

ASTAKHOV, V.P., Metal Cutting Mechanics, CRC Press LCC, 1999, USA, p. 297.

ATKINS, P.W., Physical Chemistry, Fourth Edition, Oxford University Press, 1990, p. 995.

ÁVILA, R.F. and ABRÃO, A.M., The Effect of Cutting Fluids on The Machining of Hardened AISI 4340 Steel, **Journal of Materials Processing Technology**, Elsevier Science B.V., Vol. 119, 2001, pp. 21-26.

BAI, Q.S.; YAO, Y.X.; PHILLIP BEX and ZHANG, G., Study on Wear Mechanisms and Grains Effects of PCD tool in Machining Laminated Flooring, **International Journal of Refractory Metals & Hard Materials**, Elsevier Science Ltd., Vol. 22, 2004, pp. 111-115.

BALAZINSKI, M.; LITWIN, J. and FORTIN, C., Influence of Feed Variation on Tool Wear when Machining Inconel 600, **Transactions of the CSME**, Vol. 17, No. 4A, 1993, pp. 659-669.

BARNES, S.; PASHBY, I.R. and MOK, D.K., The Effect of Workpiece Temperature on the Machinability of an Aluminium/SiC MMC, **Manufacturing Science and Engineering**, MED-Vol.2-1/MH-Vol. 3-1, ASME 1995, pp. 219-228.

BEDDOES, J. and BIBBY, M.J., Principles of Metal Manufacturing Processes, Arnold – Hodder Headline Group, London, Great Britain, 1999, p. 326.

BENSON, T., Gas Turbine Parts, **Glenn Research Center,** p 2, 2002. Available at: <htttp:// www.grc.nasa.gov/WWW/K-12/airplane/turbparts.html>. Accessed in 5th. May 2003.

BHADESHIA, H.K.D.H, Titanium and its alloys, Materials Science & Metallurgy, Part II, Course C9, Alloys, p 11. Available at: <htttp://www.msm.cam.ac.uk/phase-trans/2000/C9/lecture3.pdf>. Accessed in 7th. May 2003.

BHADURI, S. and BHADURI, S.B., Enhanced Low Temperature Toughness of Al_2O_3-ZrO_2 Nano/Nano Composites, **NanoStructured Materials**, Elsevier Science Ltd, Acta Metallurgica Inc, USA, Vol. 8, No.6, 1997, pp. 755-763.

BHAUMIK, S.K.; DIVAKAR, C. and SINGH, A.K., Machining Ti-6Al-4V with wBN-cBN Composite Tool, **Materials & Design**, Elsevier Science Ltd, Vol. 16, No. 4, 1995, pp. 221-226.

BONNEY, J., **High-Speed Machining of Nickel-base, Inconel 718, Alloy with Ceramic and Coated Carbide Cutting Tools using Conventional and High-Pressure Coolant**

Supplies, March 2004, p. 238. Ph.D. Thesis, London South Bank University, London, Great Britain.

BOOTHROYD, G. and KNIGHT, W.A, Fundamentals of Machining and Machine Tools, Second Edition, Marcel Dekker, INC, New York, U.S.A., 1989, p. 542, ISBN: 0-8247-7852-9.

BOYER, R.R., An Overview on the use of Titanium in the Aerospace Industry, **Materials Science and Engineering**, Vol. A213, 1996, pp. 103-114.

BRINKSMEIER, E.; WALTER, A.; JANSSEN, R. and DIERSEN, P., Aspects of Cooling Lubrication Reduction in Machining Advanced Materials, **Proc. Instn. Mech. Engrs**. Vol. 213, Part B, 1999, pp. 769-778.

BRITISH STANDARD, Specification for Single Point Cutting Tools, Part 2, Nomenclature, 1972, BS 1296/2.

BROOKES, C.A.; JAMES, R.D. and NABHANI, F., Wear of Ultra-Hard Cutting Tools in the Machining of Titanium, **1st Int. Conf. On the Behaviour of the Materials in Machining**, Stratford-upon-Avon, Stratford, England, November 1988, p. 8.

ÇAKIR, O.; KIYAK, M. and ALTAN, E., Comparison of Gases Applications to Wet and Dry Cuttings in Turning, **Journal of Materials Processing Technology**, Elsevier Science B.V., Vol. 153-154, 2004, pp. 35-41.

CATT, E.J. and MILWAIN, D., Machining of Titanium Alloys – Part 2: General Machining Behaviour of Titanium, Iron and Steel Institute – ISI, Spe. Rep. No. 94, London, Great Britain, 1968, pp. 143-150.

CHAKORABORTY, A.; RAY, K.K. and BHADURI, S.B., Comparative Wear Behavior of Ceramic and Carbide Tools during High Speed Machining of Steel, **Materials and Manufacturing Processes**, Vol. 15, No. 2, 2000, pp. 269-300.

CHE-HARON, C.H., Tool Life and Surface Integrity in Turning Titanium Alloy, **Journal of Materials Processing Technology**, Elsevier Science B.V., Vol. 118, 2001, pp. 231-237.

CHILD, H.C. and DALTON, A.L., Machining of Titanium Alloys – Part 1: Mettalurgical Factors affecting Machinability, Iron and Steel Institute – ISI, Spe. Rep. No. 94, London, Great Britain, 1968, pp. 139-142.

CHILDS, T.H.C. and MAHDI, M.I., On the Stress Distribution Between the Chip and Tool During Metal Turning, **Annals of CIRP**, Vol. 38, No. 1, 1989, pp. 55-58.

COLWELL, L.V. and TRUCKENMILLER, W.C., Cutting Characteristics of Titanium and its Alloys, **Mechanical Engineering**, Vol. 75, No. 6, June 1953, pp. 466-480.

COOK, M.W. and BOSSOM, P.K., Trends and Recent Developments in the Material Manufacture and Cutting Tool Application of Polycrystalline Diamond and Polycrystilline Cubic Boron Nitride, **International Journal of Refractory Metals & Hard Materials**, Elsevier Science Ltd., Vol. 18, 2000, pp. 147-152.

COOK, N.H., Chip Formation in Machining Titanium, **Proceedings of Symposium on Machining and Grinding of Titanium**, Watertown Arsenal, Watertown 72, Massachusetts, 31 March 1953, pp. 1-7.

CRAFOORD, R.; KAMINSKI, J.; LAGERBERG, S.; LJUNKRONA, O. and WRETLAND, A., Chip Control in Tube Turning using a High-Pressure Water Jet, Proc. Instn. Mech. Engrs, Vol. 213, Part B, 1999, pp.761-767.

CSELLE, T. and BARIMANI, A., Today´s Applications and Future Developments of Coating for Drills and Rotating Cutting Tools, **Surface Coating Technology**, Elsevier Science S.A., Vol. 76-77, 1995, pp. 712-718.

DA SILVA, E.J. and BIANCHI, E.C., Procedimentos–Padrão para o Uso Correto de Fluidos de Corte -[Standard Procedures for the Correct Usage of Cutting Fluids], **Máquinas e Metais Magazine**, Aranda Editora, Brazil, Ano XXXVI, No. 410, 2000, pp. 88-103 [In Portuguese].

DA SILVA, F.J.; MACHADO, A.R. and DE SOUZA JR, A.M., Desempenho de Ferramentas de Aço-Rapido tratatas Criogenicamente [Performance of HSS Cutting Tools treated Cryogenically], I COBEF (**Brazilian Congress of Manufacturing Engineering**), Held at UFPR, Curitiba, PR, Brazil, 02-04 April 2001. [In Portuguese].

DA SILVA, L.R.; COELHO, R.T.; BEZERRA, A.A. and MENDONÇA, W.G., Estudo da Geometria de Corte para Torneamento de Inconel [Study of the cutting geometry for machining Inconel], Magazine Máquinas e Metais, Aranda Editora, Brazil, Ano XXXVII, N. 427, 2001, pp. 32-55. [In Portuguese].

DAHLMAN, P. and ESCURSELL, M., High-Pressure Jet-Assisted Cooling: A New Possibility for Near Net Shape Turning of Descarburized Steel, **International Journal of Machine Tools and Manufacture**, Elsevier Science Ltd, Vol. 44, Issue 1, 2004, pp. 109-115.

DAHLMAN, P., **High Pressure Jet-Assisted Turning – Chip Control and Temperature Reduction**, Sweden, 2000, p. 31. Thesis for the Degree of Licentiate Engineering, Chalmers University of Technology.

DALHMAN, J. and KAMINSKI, J., Aspects on High-Pressure Jet-Assisted Turning, Proceedings of the 10th. American Water Jet Conference, Houston, USA, 1999.

DE GARMO, E.P.; BLACK, J.T. and KOHSER, R.A., Materials and Processes in Manufacturing, Eighth Edition, John Wiley & Sons, Inc., 1999, p. 1259.

DEARNLEY, P.A. and GREARSON, A.N., Evaluation of Principal Wear Mechanisms of Cemented Carbides and Ceramics used for Machining Titanium Alloy IMI 318, **Materials Science and Technology**, Vol. 2, January 1986, pp. 47-58.

DEARNLEY, P.A. and TRENT, E.M., Wear Mechanisms of Coated and Uncoated Carbides, Trans ASME, **Journal of Eng. Materials and Technology**, Vol. 107, January 1985, pp. 68-82.

DINIZ, A.E.; FERREIRA, J.R. and FILHO, F.T., Influence of Refrigeration/Lubrication Condition on SAE 52100 Hardened Steel during at several Cutting Speeds, **International Journal of Machine Tools & Manufacture**, Elsevier Science Ltd., Vol. 43, 2003, pp. 317-326.

DOYLE, E.D. and HORNE, J.G., Adhesion in Metal Cutting: Anomalies associated with Oxygen, **Wear**, Elsevier Science V.B., Vol. 60, 1980, pp. 383-391.

DROZDA, T.J. and WICK, C., Tool and Manufacturing Engineers Handbook – Chapter 1: Principles of Metal-cutting and Machinability, Vol. 1, 4th. Edition,: Machining, SME, 1983, p. 64.

EDWARDS, R., Cutting Tools, The Institute of Materials, The University Press, London, Great Britain, ISBN 0901716480, 1993, p. 200.

EL BARADIE, M.A., Cutting Fluids: Part I. Characterisation, **Journal of Materials Processing Technology**, Elsevier Science S.A.,Vol. 56, 1996, pp. 786-797.

ERNST, H. and MERCHANT, M.E., Chip Formation, Friction and High Quality Machined Surfaces, **Proc. Symp. Surface Treatment of Metals**, Cleveland, 21-25 October 1940, pp. 299-378.

EZUGWU, E.O. and PASHBY, I.R., High Speed Milling of Nickel-based Superalloys, Proceedings of the 7th. Conference of the Irish Manufacturing Committee, Trinity College, Dublin, 29th- 31st August 1990, p. 12.
EZUGWU, E.O. and WALLBANK, J., Manufacture and Properties of Ceramic Cutting Tools: A Review, **Materials Science and Technology**, Vol. 3, 1987, pp. 881-888.

EZUGWU, E.O. and WANG, Z.M., Titanium Alloys and their Machinability – A Review, **Journal of Materials Processing Technology**, Elsevier Science S.A., Vol. 68, 1997, pp. 262-274.

EZUGWU, E.O., Key improvements in the machining of difficult-to-cut aerospace alloys, **International Journal of Machine Tools & Manufacture**, Elsevier Science S.A., Vol. 45, 2005, pp. 1353-1367.

EZUGWU, E.O.; BONNEY, J. and OLAJIRE, K.A., Evaluation of the Machinability of Nickel-Base, Inconel 718, Alloy with Nano-Ceramic Cutting Tools, **Tribology Transactions**, Vol. 45, No. 4, 2002, pp. 506-511.

EZUGWU, E.O.; BONNEY, J. and YAMANE, Y., An Overview of the Machinability of Aeroengine Alloys, **Journal of Materials Processing Technology**, Elsevier Science B.V., Vol. 134, 2003, pp. 233-253.

EZUGWU, E.O.; DA SILVA, R.B.; BONNEY, J. and MACHADO, A.R., The Effect of Argon Enriched Environment in High Speed Machining of Titanium Alloy, **Tribology Transactions, Society of Tribologists and Lubrication Engineers** (STLE), Vol. 48, 2005, pp. 18-23.

EZUGWU, E.O.; FADARE, DA SILVA, R.B.; BONNEY, J. and SHABAZZ NELSON, A., Wear prediction of Uncoated Carbide Tool during High Speed Turning of Ti-6Al-4V alloy using Artificial Neural Network, **Proceedings of Second International Conference on Manufacturing Research** - ICMR 2004, Sheffield Hallam University, 7-9 September 2004, England, U.K., pp. 36-41.

EZUGWU, E.O.; OLAJIRE, K.A. and WANG, Z. M., Wear Evaluation of a Self Propelled Rotary Tool when Machining Titanium, IMI 318, Alloy, Proceedings of the Inst. of Mech. Engineers, Vol. 216, Part B: **Journal Engineering Manufacture**, 2002, pp. 891-897.

EZUGWU, E.O.; WANG, Z.M and MACHADO, A.R., The Machinability of Nickel-Based Alloys: a Review, **Journal of Materials Processing Technology**, Vol. 86, 1999, pp. 1-16.

FIELD, M., Machining Aerospace Alloys, ISI - Spec. Rep., 94, 1968, pp. 151-160.

FIELD, M; KAHLES, J.F and CAMMET, J.T., A Review of Measuring Methods for Surface Integrity, **Annals of CIRP**, Vol. 30, No. 2, 1972, pp. 219-238.

FITZSIMMONS, M. and SARIN, V. K., Developments of CVD WC-Co Coatings, **Surface and Coating Technology**, Elsevier Science B.V., Vol. 137, 2001, pp. 158-163.

FRAZIER, A.D., Cutting Fluid Applications For Today´s Materials, Presented at SME´s Westec Engineering Conference, March 1974, pp. 19-24.

GATTO, A. and IULIANO, L., Advanced Coated Ceramic tools for Machining Superalloys, **International Journal of Machine Tools & Manufacture**, Elsevier Science Ltd., Vol. 37, No. 5, 1997, pp. 591-605.

GETTELMAN, K.M., Bye Bye Bird's Nests, Modern Machine Shop, September 1991, pp. 55-62.

GHOSH, A. and MALLIK, A.K., Manufacturing Science, **Ellis Horwood Series in Mechanical Engineering**, Chichester, England, 1986, p. 433.

GORCZYCA, F.E., Application of Metal Cutting Theory, Industrial Press, New York, U.S.A., 1987, ISBN 0-8311-1176-3.

GRAHAM, D., Dry Out – Cutting Tool Engineering, **Cutting Tool Engineering**, March 2000, pp. 56-65.

HARTUNG, P.D. and KRAMER, B.M., Tool Wear in Titanium Machining, **Annals of the CIRP**, Vol. 31, 31 January 1982, pp. 75-80.

HONG, S. Y.; DING, Y. and JEONG, W., Friction and Cutting Forces in Cryogenic Machining of Ti-6Al-4V, **International Journal of Machine Tools & Manufacture**, Elsevier Science Ltd., Vol. 41, 2001, pp. 2271-2285.

HONG, S. Y.; MARKUS, I. and JEONG, W., New Cooling Approach and Tool Life Improvement in Cryogenic Machining of Ti-6Al-4V, **International Journal of Machine Tools & Manufacture**, Elsevier Science Ltd., Vol. 41, 2001, pp. 2245-2260.

HUANG,Y. and LIANG, S.Y., Cutting Forces Modelling Considering the Effect of Tool Thermal Property – Application to CBN Hard Turning, **International Journal of Machine Tools & Manufacture**, Elsevier Science Ltd., Vol. 43, 2003, pp. 307-315.

INTERNATIONAL STANDARD – ISO 3685, Tool-life testing with single-point turning tools, ISO 3685, Second edition, 1993-11-15, p. 48.

INTERNATIONAL STANDARD - ISO 513, Classification and application of hard cutting materials for metal removal with defined cutting edges – Designation of the main groups and groups of application, ISO 513:2004(E), pp. 1-3.

JAWAID, A., CHE-HARON, C.H. and ABDULLAH, A., Tool Wear Characteristics in Turning of Titanium Alloy Ti-6246, **Journal of Materials Processing Technology**, Elsevier Science S.A., Vol. 92-93, 1999, pp. 329-334.

JAWAID, A., **Syalon Ceramics in Metal Cutting**, 1982, p. 149. Ph.D. Thesis, University of Warwick, Coventry, Great Britain.

JAWAID, A.; SHARIF, S. and KOKSAL, S., Evaluation of Wear Mechanisms of Coated Carbide Tools when Face Milling Titanium Alloy, **Journal of Materials Processing Technology**, Elsevier Science S.A., Vol. 99, 2000, pp. 266-274.

KALISH, H. S., Some Plain Talk about Carbides, American Machinist, Vol. 122, No. 05, May 1978, pp. 95-98.

KALPAKJIAN, S. and SCHMID, S.R., Manufacturing Engineering for Engineering Materials, Fourth Edition, Addison-Wesley Publishing Company, March 2000, p. 1168, ISBN: 0201361310.

KAMINSKI, J. and ALVELID, B., Temperature Reduction in the Cutting Zone in Water-Jet Assisted Turning, **Journal of Materials Processing Technology**, Elsevier Science B.V., Vol. 106, 2000, pp. 68-73.

KAMINSKI, J. and DAHLMAN, P., Chip-Forming Possibilities in High-Pressure Jet Assisted Turning, Proceedings of the International Symposium on New Applications of Water Jet Technology, Ishinomaki, Japan, 1999.

KATO, S.; YAMAGUSHI, K. and YAMADA, M., Stresses Distribution at the Interface Between Tool and Chip in Machining, Transactions of the ASME, **Journal of Engineering for Industry**, Vol. 94, May 1972, pp. 683-689.

KEAR, B.H.; COLAIZZI, J.; MAYO, W.E. and LIAO, S.C., On the Processing of Nanocrystalline and Nanocomposite Ceramics, **Scripta Materialia**, Elsevier Science Ltd., Vol. 44, 2001, pp. 2065-2068.

KHAMSEHZADEH, H., **Behaviour of Ceramic Cutting Tools when Machining Superalloys**, May 1991, p. 124. Ph.D. Thesis, University of Warwick, Coventry, Great Britain.

KIM, S., Material Properties of Ceramic Cutting Tools, Key Engineering Materials, **Trans. Tech. Publications**, Switzerland, Vol. 96, 1994, pp. 33-80.

KIM, S.W.; LEE, D.W.; KANG, M.C. and KIM, J.S., Evaluation of Machinability by Cutting Environments in High-Speed Milling of Difficult-To-Cut Materials, **Journal of Materials Processing Technology**, Elsevier Science B.V., Vol. 111, 2001, pp. 256-260.

KISHAWY, H.A. and WILCOX, J., Tool Wear and Chip Formation during Hard Turning with Self-Propelled Rotary Tools, **International Journal of Machine Tools & Manufacture**, Elsevier Science Ltd., Vol. 43, No. 4, March 2003, pp. 433-439.

KISHI, K.; EDA, H.; FURUSAWA, T. and ICHIDA, Y., Some Aspects for the Cooling and Lubrication Effects by a Jet Infusion Method, Proc. of the JSLE-ASLE, Int. Lub. Conf., Tokyo, Japan, 9th –11th June, 1975, pp. 579-587.

KITAGAWA, T.; KUBO, A. and MAEKAWA, K., Temperature and Wear of Cutting Tools in High-Speed Machining of Inconel 718 and Ti-6Al-6V-2Sn, **Wear**, Elsevier Science S.A., Vol. 202, 1997, pp. 142-148.

KLAPHAAK, D.J., Coated Tools for Machining Aerospace Materials, Ovonic Synthetic Materials Co, **Carbide and Tool Journal**, , Vol. 19, N. 5, September/October, 1987, pp. 14-16.

KLOCKE, F.; FRITSCH, R. and GERSCHWILER, K., Machining Titanium Alloys – A Continuous Challenge in Manufacturing, 5th International Conference on Behaviour of Materials in Machining, Chester - UK, 12-13 November 2002, pp. 251-258.

KOMANDURI, R. and BROWN, R.H., On the Mechanics of Chip Segmentation in Machining, Transactions of the ASME, **Journal of Engineering for Industry**, Vol. 103, February 1981, pp. 33-51.

KOMANDURI, R. and LEE, M., General Electric Company, Corporate Research and Development, 84 CRD 115, May 1984, p. 18.

KOMANDURI, R. and LEE, M., High-Speed Machining of Titanium Alloys with a New Cutting Tool Insert: The Ledge Tool, **The Winter Annual Meeting of ASME**, December 9-14, New Orleans, Louisiana, USA, 1984, pp. 217-229.

KOMANDURI, R. and REED JR, W.R., Evaluation of Carbide Grades and a New Cutting Geometry for Machining Titanium Alloys, **Wear**, Elsevier Sequoia/Printed in Switzerland, Vol. 92, 1983, pp.113-123.

KOMANDURI, R. and VON TURKOVICH, B.F., New Observations on the Mechanism of Chip Formation when Machining Titanium Alloys, **Wear**, Vol. 69, 1981, pp. 179-188.

KOMANDURI, R., Advanced Ceramic Tool Materials for Machining, **Inter. J. Refratory Mat. & Hard Metal**, Vol. 8, 1989, pp. 125-132.

KONIG, W., Applied Research on the Machinability of Titanium and its Alloys, **Proc. 47th Meeting of AGARD** – Structural and Materials Panel, Florence, 26-28 September 1978. AGARD – CP256, London, Great Britain, 1979, pp. 1.1 – 1.10.

KOVACEVIC, R.; CHERUKUTHOTA, C. and MAZURKIEWICZ, M., High Pressure Waterjet Cooling/Lubrication to Improve Machining Efficiency in Milling, **International Journal Machining Tools Manufacturing**, Vol. 35, No. 10, 1995, pp. 1459-1473.

KRAMER, B.M., On Tool Materials for High Speed Machining, **Journal of Engineering for Industry**, Vol 109, May 1987, pp. 87-91.

LE MAITRE, F., Machinability of Titanium and its Alloys, **Society of Manufacturing Engineers**, EM70-101, Deaborn, Michigan, USA, 1970, pp.1-11.

LEE, M., The Failure Characteristics of Cutting Tools Machining Titanium Alloys at High Speed, **Proc. Symp. on Advanced Processing Methods for Titanium**, AIME, Louisville, Kentucky, 13-15 October, 1981, pp. 275-287.

LEI, S. and LIU, W., High-Speed Machining of Titanium Alloys using Driven Rotary Tool, **International Journal of Machine Tools & Manufacture**, Vol. 42, Elsevier Science Ltd., January 2002, pp. 653-661.

LI, M.; EDA, H.; IMAI, T.; NISHIMURA, M.; KAWASAKI, T.; SHIMIZU, J.; YAMAMOTO, T. and ZHOU, L., Development of High Water-content Cutting Fluids with a New Concept Fire Prevention and Environmental Protection, Precision Engineering - **Journal of the International Societies for Precision Engineering and Nanotechnology**, Vol. 24, 2000, pp. 231-236.

LI, S.X. and LOW, I.M., Advanced Ceramics Tools for Machining Application – I, Key Engineering Materials, **Trans. Tech. Publications**, Switzerland – Germany – UK – USA, Vol. 96, 1994, p. 257.

LINDEKE, R.; SCHOENIG, F. and KHAN, A., Cool Your Jets, **Cutting Tool Engineering**, October 1991, pp. 35-37.

LINDEKE, R.R.; SHOENIG, F.C., KHAN, A. K. and HADDAD, J., Machining of α-β Titanium with Ultra High Pressure through the Insert Lubrication/Cooling, **Transactions NAMRI/SME**, 1991, pp. 154-161.

LÓPEZ DE LACALLE, L.N.; PÉREZ, J.; LLORENTE, J.I. and SÁNCHEZ, J.A., Advanced Cutting Conditions for the Milling of Aeronautical Alloys, Journal of Materials Processing Technology, Elsevier Science S.A., Vol. 100, 2000, pp. 1-11.

LÓPEZ DE LACALLE, L.N.; PEREZ-BILBATUA, J.; SÁNCHEZ, J.A.; LLORENTE, J.I.; GUTIÉRREZ, A. and ALBÓNIGA, J., Using High Pressure Coolant in the Drilling and Turning of Low Machinability Alloys, **International Journal Advanced Manufacturing Technology**, Vol. 16, 2000, pp. 85-91.

LOVATT, A. and SHERCLIFF, H., Aero-Engines – Hotter, Stiffer, Stronger, Lighter…Where Does the Aero-Engine Go Next?, University of Cambridge, Department of Engineering, 2002. Available at: <htttp://www-Materials.eng.cam.ac.uk./mpsite/short/OCR/aero/default.html> Accessed in 7th. May 2003.

MACHADO, A.R. and WALLBANK, J., Machining of Titanium and its Alloys, **Proceedings of the Inst. Of Mech. Engineers**, Vol. 204, Part B: Journal Engineering Manufacture, 1990, pp. 53-60.

MACHADO, A.R. and WALLBANK, J., The Effect of Extremely Low Lubricant Volumes in Machining, **Wear**, Elsevier Science S.A., Vol. 210, 1997, pp. 76-82.

MACHADO, A.R. and WALLBANK, J., The Effects of a High-Pressure Coolant Jet on Machining, **Proc. Instn. Mech. Engrs**., Vol. 208, 1994, pp. 29-38.

MACHADO, A.R., **Machining of Ti-6Al-4V and Inconel 901 with a High Pressure Coolant System**, 1990, p. 288. Ph.D. Thesis, University of Warwick, Coventry, Great Britain.

MACHADO, A.R.; DA SILVA, R.B.; EZUGWU, E.O. and BONNEY, J., Fluido de Corte Aplicado à Alta Pressão é a Solução para Usinagem da Liga de Titânio em HSM – [Cutting Fluid Delivered at High Pressure is the Solution for Machining of Titanium Alloys at HSM], Usinagem 2004 [Machining 2004] – Fair and Conference, Held at Expo Center Norte, 27-29 October 2004, Sao Paulo, Brazil, p. 14. [In Portuguese].

MADHAVULU, G. and AHMED B., Hot Machining Process for Improved Metal Removing Rates in Turning Operations, **Journal of Materials Processing Technology**, Elsevier Science B.V., Vol. 44, 1994, pp. 199-206.

MAGALHÃES, C.A. and FERREIRA, J.R., Usinagem por Torneamento em Acabamento da Liga de Titânio 6Al-4V, [Machining 2004] – Fair and Conference, Held at Expo Center Norte, 27-29 October 2004, Sao Paulo, Brazil, p. 18. [In Portuguese].

MANTLE, A.L. and ASPINWALL, D.K., Tool Life and Workpiece Surface Roughness when High Speed Machining a Gamma Titanium Aluminide, Progress of Cutting and Grinding, **Proceedings of the Fourth International Conference on Progress of Cutting and Grinding**, October 5-9, Urumqi and Turpan, China, International Academic Publishers, 1998, pp. 89-94.

MARI, D. and GONSETH, D.R., A New Look at Carbide Tool Life, **Wear**, Elsevier Sequoia, Vol. 165, 1993, pp. 9-17.

MASUDA, M.; SATO, T.; KORI, T. and CHUJO, Y., Cutting Performance and Wear Mechanism of Alumina-based Ceramic Tools when Machining Austempered Ductile Iron, **Wear**, Elsevier Science B.V., Vol. 174, 1994, pp. 147-153.

MAZURKIEWICZ, M.; KUBALA, Z. and CHOW, J., Metal Machining with High-Pressure Water-Jet Cooling Assistance – A New Possibility, J**ournal of Engineering for Industry**, Transactions of the ASME, Vol. 111, 1989, pp. 7-12.

MILLER, S., Advanced Materials mean Advanced Engines, **The Institute of Materials**, Interdisciplinary Science Reviews, Vol. 21, No. 2, 1996, pp. 117-129.

MISHINA, H., Atmospheric Characteristics in Friction and Wear of Metals, **Wear**, Elsevier Science Ltd.,Vol. 152, 1992, pp. 99-110.

MOMPER, F., Flexible Production with Ceramics, Production Engineer, May 1987, pp. 18-19.

MOTONISHI, S.; HARA, Y.; ISODA, S.; ITOH, H.; TSUMORI, Y. and TERADA, Y., Study on Machining of Titanium and its Alloys, Kobelco Technology Review, No. 2, August 1987, pp. 28-31.

NABHANI, F., Machining of Aerospace Titanium Alloys, **Robotics and Computer Integrated Manufacturing**, Elsevier Science Ltd., Vol. 17, 2001 (a), pp. 99-106.

NABHANI, F., Wear Mechanisms of Ultra-Hard Cutting Tools Materials, **Journal of Materials Processing Technology**, Elsevier Science B.V., Vol. 115, 2001 (b), pp. 402-412.

NAGPAL, B.K. and SHARMA, C.S., Cutting Fluids Performance – Part 1 – Optimization of Pressure for "Hi-Jet" Method of Cutting Fluid Application, Transactions of the ASME, **Journal of Engineering for Industry**, August 1973, pp. 881-889.

NEUMEYER, T.A. and DULIS, E.J., P/M Super High Speed Steels – New Generation for Carbides, **Proc. Int. Conf. on Hard Mat. Tool Techn**., Carnegie-Mellon University, Pittisburgh, Pennsylvania, USA, 22-24 June, 1976, pp. 93-100.

NORIHIKO, N. and AKIO, O., Improved Grooving of Beta-Titanium Alloy with Some Trial Techniques, Progress of Cutting and Grinding, **Proceedings of the Fourth International Conference on Progress of Cutting and Grinding**, October 5-9, Urumqi and Turpan, China, International Academic Publishers, 1998, pp. 7-12.

NORTH, B., Ceramic Cutting Tools, SME Technical Paper, **SME**, Dearborn, Michigan, MR 86-451, 1986.

NOVASKI, O. and DÖRR, J., Usinagem quase a Seco [Machining in almost dry condition], Máquinas e Metais Magazine, Aranda Editora, Brazil, Ano XXXVI, No. 406, 1999, pp. 34-41. [In Portuguese]

OHNABE, H.; MASAKI, S.; ONOZUKA, M.; MIYAHARA, K. and SASA, T., Potential Application of Ceramic Matrix Composites to Aero-engine Components, Composites: Part A, Vol. 30, No. 4, 30, Elsevier Science Ltd., 1999, pp. 489-496.

OKEKE, C.I., **Threading and Turning of Aerospace Materials with Coated Carbide Inserts**, 1999, p. 247. Ph.D. Thesis, South Bank University London, London, Great Britain.

OLOFSON, C.T.; GERDS, A.; BOULGER, F.W. and GURKLIS, J.A., Machining of Titanium Alloys, Battele Memorial Institute, Columbus, Ohio, Defense Metals Information Center, February 1965, Cont. AF 33 (615) 1121, DMIC, memo 199, AD 611846.

ÖZLER, L.; ÍNAN, A. and ÖZEL, C., Theoretical and Experimental Determination of Tool Life in Hot Machining of a Austenitic Manganese Steel, **International Journal of Machine Tools & Manufacture**, Elsevier Science Ltd., Vol. 41, 2001, pp. 163-172.

PIGOTT, R.J.S. and COLWELL, A.T., Hi-Jet System for increasing Tool Life, **SAE Quarterly Transaction**, Vol. 6, No. 3, 1952, pp. 547-566.

POLLACK, H.W., Tool Design – Geometric Control, Prentice Hall International, Second Edition, Englewood Cliffs, New Jersey, 1988, pp. 223-235.

POPANDOPULO, A.N. and ZHUKOVA L. T., Transformations in High Speed Steels During Cold Treatment [Translated from Metallovedenie i Termicheskaya Obrabotka Metallov], 1980, No. 10, pp. 9-11.

PRASAD, Y.V.R.K. and SESHACHARYULY, T., Processing Maps for Hot Working of Titanium Alloys, **Materials Science and Engineering**, Elsevier Science S.A., A 243, 1998, pp 82-88.

PRENGEL, H.G.; PFOUTS, W.R. and SANTHANAN, A.T., State of the Art in Hard Coatings for Carbide Cutting Tools, **Surface and Coating Technology**, Elsevier Science B.V., Vol. 102, 1998, pp. 183-190.

RAHMAN, M.; SENTHIL KUMAR, A. and CHOUDHURY, M.R., Identification of Effective Zones for High Pressure Coolant in Milling, **Annals of the CIRP**, Vol. 49, No. 1, 2000, pp. 47-52.

RICE, W.B.; SALMON, R. and ADVANI, A.G., Effects of Cooling and Heating Workpiece and Tool on Chip Formation in Metal Cutting, **International J. Mach. Tool Des. Res.**, Pergamon Press, Great Britain, Vol. 6, 1996, pp. 143-152.

RICHARDS, N. and ASPINWALL, D., Use of Ceramic Tools for Machining Nickel Based Alloys, **International Journal of Machine Tools & Manufacturing**, Elsevier Science B.V., Vol. 29, No. 4, 1989, pp. 575-588.

ROLLS-ROYCE PLC, Product Information - Product Fact Sheets. Available at: <htttp://www.rollsroyce.com/media/prod_info/civil/trent700.htm>. Accessed in 5th. May 2003.

SADIK, M.I. and LINDSTRÖM, B., The Effect of Restricted Contact Length on Tool Performance, **Journal of Materials Processing Technology**, Elsevier Science Ltd., Vol. 48, 1995, pp. 275-282.

SALES, W.F., **Determination of cooling and lubricant characteristics of cutting fluids** (In Portuguese), 1999, 166p. PhD Thesis, Federal University of Uberlândia, Uberlândia, Minas Gerais, Brazil.

SALES, W.F.; DINIZ, A.E. and MACHADO, A.R., Application of Cutting Fluids in Machining Processes, **Journal of the Brazilian Society of Mechanical Sciences**, ABCM, Vol. XXIII, No. 2, 2001, pp. 227-240.

SCHAFFER, G.H., The Many Faces of Surface Texture, American Machinist and Automated Manufacturing", June 1988, pp. 61-68.

SEAH, K.H.W; LI, X. and LEE, K.S., The Effect of Applying Coolant on Tool Wear in Metal Machining, **Journal of Materials Processing Technology**, Elsevier Science S.A., Vol. 48, 1995, pp. 495-501.

SECO TOOLS - "Price and Stockist", Technical Catalogue, Seco Tools AB, Sweden, 2002 (b), p. 420.

SECO TOOLS, Turning Difficult-To-Machine Alloys, Technical Guide, Seco Tools AB, Sweden, 2002 (a), p. 21.

SHARMA, C.S.; RICE, W.B. and SALMON, R., Some Effects of Injecting Cutting Fluids Directly into the Chip-tool Interface, **Journal of Engineering for Industry**, Transactions of the ASME, Vol. 93, May 1971, pp. 441-444.

SHAW, M.C., Metal Cutting Principles, Clarendon Press – Oxford, England, 1984.
SHAW, M.C., The Assessment of Machinability, in Machinability, ISI Spec. Rep. 94, Iron and Steel Institute, London, Great Britain, 1967.

SHOUCKRY, A.S., The Effect of Cutting Conditions on Dimensional Accuracy, **Wear**, Vol. 80, 1982, pp. 197-205.

SIEKMANN, H.J., **Tool Engineering**, Vol. 34, January 1955, pp. 78-82.

SMART, E.F. and TRENT, E.M., Coolants and Cutting Tool Temperatures, **Proc. of. 15th Int MTDR Conf.**, Birmingham, England, September 1974, pp. 187-195.

SMITH, K.H., Whisker Reinforced Ceramic Composite Cutting Tools, Greenleaf Corporation, **Carbide and Tool Journal**, September/October, 1986, pp. 8-11.

SMOL'NIKOV, E.A. and KOSSOVICH G.A., Cold Treatment of Cutting Tools, [Translated from Metallovedenie i Termicheskaya Obrabotka Metallov], 1980, No. 10, pp. 5-7.

SOKOVIC, M. and MIJANOVIC, K., Ecological Aspects of the Cutting Fluids and its Influence on Quantifiable Parameters of the Cutting Processes, **Journal of Materials Processing Technology**, Elsevier Science V.B, Vol. 109, 2001, pp. 181-189.

SUN, Y.; BELL, T.; WISE, M.L.H. and ASPINWALL, K., Evaluation of the Machining Behaviour of Boride Surface Alloyed HSS Tools for Turning Titanium and Its Alloys, Tribology in Metal Cutting and Grinding", **6th joint ImechE/IOP Meeting**, held at the **Institution of Mechanical Engineers** on 10 April 1992, London, Great Britain, pp. 65-72.

SZESZULSKI, K.J.; THANGARAJ, A.R. and WEINNMANN, K.J., On the Cutting Performance of Whisker-Reinforced Ceramics Machining Inconel, Winter Annual Meeting of ASME, **Fundamental Issues in Machining ASME**, Dallas, TX, USA, 1990, pp. 97-13.

TENNENHOUSE, G.J. and RUNKLE, F.D., The Effects of Oxygen on the Wear of Tungsten-Carbide-based Materials, **Wear**, Elsevier Science, Vol. 118, 1987, pp. 365-375.

THE METALS HANDBOOK, Machining, ASM International, Ninth Edition, Vol. 16, 1989.

TIG - Titanium Information Group, Aerospace Alloys and Applications, April 2002. Available at: < htttp://www.titaniuminfogroup.co.uk>. Accessed in 7th. May 2003.

TONSHOFF, K.; KARPUSCHEWSKI, B.; MOHLFELD, A.; LEYENDECKER, T.; ERKENS, G.; FUβ, H.G. and WENKE, R., Performance of oxygen-rich TiAlON coatings

in dry cutting applications, **Surface and Coatings Technology**, Elsevier Science S.A., Vol. 109, 1998, pp. 535-542.

TOSUN, N. and ÖZLER, L., A Study of Tool Life in Hot Machining using Artificial Neural Networks and Regression Analysis Method, **Journal of Materials Processing Technology**, Elsevier Science B.V., Vol. 124, 2002, pp. 99-104.

TRENT, E.M. and WRIGHT, P.K., Metal Cutting, Butterworth-Heinemann, Fourth Edition, 2000, Woburn, USA.

TRENT, E.M., Metal Cutting and the Tribology of Seizure: II- Movement of Work Material over the Tool in Metal Cutting, **Wear**, Vol. 128, 1988 (a), pp. 47-64.

TRENT, E.M., Metal Cutting and the Tribology of Seizure: III – Temperature in Metal Cutting, **Wear**, Vol. 128, 1988 (b), pp. 65-81.

TRUCKS, H.E., Machining Titanium Alloys, Machine and Tool BLUE BOOK, January 1987, pp. 39-41.

TSEITLIN, L.B., Tool Life of High Speed Steel Cutters after Cold Treatment, [Translated from Metallovedenie i Termicheskaya Obrabotka Metallov], 1980, No. 10, pp. 7-9.
TURLEY, D.M., Slow Speed Machining of Titanium, Department of Defence, Materials Research Laboratories, Report WRL-R-833, Commonwealth of Australia, 1981.

TURLEY, D.M.; DOYLE, E.D. and RAMALINGAM, S., Calculation of Shear Strains in Chip Formation in Titanium, **Materials Science and Engineering**, Vol. 55, 1982, pp. 45-48.

VAβEN, R AND STÖVER, D., Processing and Properties of Nanophase Ceramics, **Journal of Materials Processing Technology**, Elsevier Science Ltd, Vol. 92-93, 1999, pp. 77-84.

VENUGOPAL, K.A.; TAWADE, R.; PRASHANTH, P.G. and CHATTOPADHYAY, A.B., Turning of Titanium Alloy with TiB_2-Coated Carbides under Cryogenic Cooling, Proceedings of the Inst. Of Mech. Engineers, Vol. 217, Part B: **Journal Engineering Manufacture**, 2003, pp. 1697-1707.

VIGNEAU, J., Cutting Materials for Machining Superalloys, International CIRP/VDI Conference on Cutting Materials and Tooling, Dusseldorf, 19-20 September, 1997.

VIGNEAU, J., Obtendo Alta Produtividade na Usinagem de Ligas de Titânio e Superligas, [Achieving High Productivity in Machining Titanium Alloys and Superalloys], Máquinas e Metais, Aranda Editora, Ano XXXII, No. 380, 1997, pp. 16-32. [In Portuguese].

WAKABAYASHI, T.; WILLIAMS, J.A. and HUTCHINGS, I.M., The Actions of Gaseous Lubricants in Metal Cutting, Tribology in Metal Cutting and Grinding", **6th joint ImechE/IOP Meeting,** held at the Institution of Mechanical Engineers on 10 April 1992, London, Great Britain, pp.33-40.

WALTER, J.L.; SKELLY, D.W. and MINNEAR, W.P., Ion Implantation of Cobalt-Tungsten Carbide Tools for Machining Titanium, **Wear**, Elsevier Science Sequoia, Vol. 170, 1993, pp. 79-92.

WANG, Z.M, **Machining of Aerospace Superalloys with Coated (PVD and CVD) Carbides and Self-Propelled Rotary Tools**, 1997, p. 202. Ph.D. Thesis, South Bank University, Great Britain.

WANG, Z.M.; EZUGWU, E.O. and GUPTA, A., Evaluation of a Self-Propelled Rotary Tool in the Machining of Aerospace Materials, Tribol. Trans. 41 (2), 1998, pp. 289-295.
WANG, Z.Y. and RAJURKAR, K.P., Cryogenic Machining of Hard-to-Cut Materials, **Wear**, Vol. 239, 2000, pp 168-175.

WATERS, T.F., Fundamentals of Manufacturing for Engineers, UCL Press Limited, London, Great Britain, Reprinted 2000, p. 321, ISBN: 1-85728-338-4 PB.

WERTHEIM, R.; ISCAR LTD.; ROTBERG, J. and BER, A., Influence of High-Pressure Flushing through the Rake Face on the Cutting Tool, **Annals of the CIRP**, Vol. 41, No. 1, 1992, pp. 101-106.

WHITFIELD, G., Advanced ceramics at front of materials technology, GTE Valentine Corporation, **Cutting Tool Engineering**, circle 311, December, 1988, pp. 40-42.
WHITNEY, E.D., Modern Ceramic Cutting Tool Materials, **Powder Metallurgy International**, Vol. 15, No. 4, 1983, pp. 201-205.

WRIGHT, P.K.; BAGHI, A. and CHOW, J.G., Influence of Friction on the Shear Plane Angle in Machining, **Proc. of the 10th North American Manufacturing Conf.**, Mc Master University, Hamilton, Ontario, Canada, 24-25 May 1982, pp. 255-262.

XIE, J.Q.; BAYOUMI, A.E. and ZBIB, H.M., A Study on Shear Banding in Chip Formation of Orthogonal Machining, **Int. J. Mach. Tools Manufact**, Elsevier Science Ltd, Vol. 36, No. 7, 1996, pp. 835-847.
XIE, R.-J.; MITOMO, M. and ZHAN, G.-D., Superplasticity in Fine-Grained Beta-Silicon Nitride Ceramic Containing a Transient Liquid, **Acta Materialia**, Acta Metallurgica Inc. Published by Elsevier Science Ltd,. Vol. 48, 2000, pp. 2049-2058.

YANG, C.T., Machining Titanium Alloys, American Machinist, 14 December, 1970, pp. 59-60.

ZHAN, G.; MITOMO, M.; XIE, R. and KURASHIMA, K., The Deformation Mechanisms of Superplastic Flow in Fine-Grained Beta-Silicon Nitride Ceramics, **Acta Materialia**, Vol. 48, 2000, pp. 2373-2382.

ZHANG, Z.; ZHU, Y. and HU, L, Nanostructured SiC Ceramics Prepared a Nex Process-Crystallization of Interfacial Glass, **NanoStructured Materials**, Elsevier Science Ltd, Acta Metallurgica Inc, USA, Vol. 7, No. 4, 1996, pp. 453-459.

ZHMUD', E.S., Improved Tool Life after Shock Cooling, [Translated from Metallovedenie i i Termicheskaya Obrabotka Metallov], 1980, No. 10, pp. 3-5.

ZLATIN, N. and CHRISTOPHER, J., Proper Application of Carbide in Machining Exotic Materials, Technical Paper, **Society of Manufacturing Engineers**, MR-73-909, 1974, pp.1-15.

ZLATIN, N. and CHRISTOPHER, J., Recommendations for Machining High Strength Steels and Titanium Alloys, Technical Paper, **Society of Manufacturing Engineers**, MR-71-819, 1973, pp.11-20.

ZLATIN, N. and FIELD, M., Procedures and Precautions in Machining Titanium Alloys, **Titanium Science and Technology**, Titanium D73/12249, Vol. 1, 1973, pp. 489-504.

ZOREV, N.N., Interrelationship Between Shear Processes Occurring Along Tool Face and on Shear Plane in Metal Cutting, **International Research in Product Engineering Research Conf.**, September 1963, Pittsburgh, Pensylvania, USA, pp. 42-49.

ZOYA, Z.A. and KRISHNAMURTHY, R., The Performance of CBN Tools in the Machining of Titanium Alloys, **Journal of Materials Processing Technology**, Elsevier Science S.A., Vol. 100, 2000, pp. 80-86.

APPENDIX

LIST OF PUBLICATIONS FROM THIS STUDY

Refereed Journals

1. E.O. Ezugwu, J. Bonney, R.B. Da Silva and Á.R. Machado, Evaluation of the Performance of Different Nano-Ceramic Tool Grades when Machining Nickel-Base, Inconel 718, Alloy, Journal of the Brazilian Society of Mechanical Science & Engineering – ABCM / RBCM. Vol. XXVI, No. 1, January-March 2004, pp. 12-16.
2. E.O. Ezugwu, R.B. Da Silva, J. Bonney and Á.R. Machado, The Effect of Argon Enriched Environment in High Speed Machining of Titanium Alloy, Tribology Transactions – Society of Tribologists and Lubrication Engineers (STLE) – Vol. 48: pp. 18-23, 2005, ISBN: 0569-8197.
3. E.O. Ezugwu, R.B. Da Silva, J. Bonney and Á.R. Machado, Evaluation of the Performance of CBN tools when turning Ti-6Al-4V alloy with high pressure coolant supplies, International Journal of Machine Tool and Manufacture, Vol. 45, July 2005, pp.1009-1014.
4. E.O. Ezugwu, D.A. Fadare, J. Bonney, R.B. Da Silva and W. F. Sales, Modelling of The Correlation between Cutting and Process Parameters in High Speed Machining of Inconel 718 Alloy using Artificial Neural Network, International Journal of Machine Tool and Manufacture, Vol. 45, 2005, pp. 1375-1385, ISBN: 0890-6955.

Refereed Conferences

1. E.O. Ezugwu, J. Bonney, R.B. Da Silva and Á.R. Machado, Evaluation of the Performance of Different Nano-Ceramic Tool Grades when Machining Nickel-Base, Inconel 718, Alloy, Presented at the Second Brazilian Manufacturing Engineering Conference (II COBEF) in Uberlândia-MG, Brazil, May 2003, CD-Rom.
2. E.O. Ezugwu, R.B. Da Silva, J. Bonney and Á.R. Machado, The Effect of Argon Enriched Environment in High Speed Machining of Titanium Alloy, Presented at the Society of Tribologists and Lubrication Engineers, 59th. Annual Meeting & Exhibition, in Toronto, Canada, 17-20 May 2004.
3. E.O. Ezugwu, D.A. Fadare, R.B. Da Silva, J. Bonney and A. Shabazz Nelson, Wear prediction of Uncoated Carbide Tool during High Speed Turning of Ti-6Al-4V alloy using Artificial Neural Network, Proceedings of Second International Conference on Manufacturing Research – ICMR in Sheffield Hallam University, England, pp. 36-41, 7-9 September 2004.
4. E.O. Ezugwu, D.A. Fadare, R.B. Da Silva and J. Bonney, Application of Artificial Neural Networks for Tool Condition Monitoring when Turning Ti-6Al-4V Alloy with High Pressure Coolant Supply, Presented at the 7th. International Conference on Progress of Machining Technology in Zuzhou, China 8-11 December 2004.
5. R.B. Da Silva, E.O. Ezugwu, J. Bonney, Á.R. Machado and A.M. Reis, High Speed Turning of Ti-6Al-4V alloy with Coated Carbides tools in an Argon Enriched Environment, Presented at the 38th. CIRP – International Seminar on Manufacturing System in Florianópolis–SC, Brazil, 16-18 May 2005.
6. R.B. Da Silva, Á.R. Machado, E.O. Ezugwu and J. Bonney, Evaluation of the Machinability of Ti-6Al-4V alloy with (SiCw) Whisker Reinforced Alumina Ceramic Cutting Tool under Various Cooling Environments, Presented at the 18th. International Congress of Mechanical Engineering (COBEM 2005) in Ouro Preto–MG, Brazil, 06-11 November 2005.
7. R.B. Da Silva, Á.R. Machado, E.O. Ezugwu and J. Bonney, Increasing productivity when machining Ti-6Al-4V alloy in HSM under high pressure coolant supply, presented at the Fifth International Conference on High Speed Machining (HSM) in Metz, France,13th.-15th March 2005